THE METEOROLOGICAL MAGAZINE

HER MAJESTY'S STATIONERY OFFICE

January 1987

Met.O.978 No. 1374 Vol. 116

METEOROLOGICAL OFFICE Met.O.978

THE METEOROLOGICAL MAGAZINE

No. 1374, January 1987, Vol. 116

551.586:551.556:612(41-4)

Wind-chill indices — a review

J.C. Dixon and M.J. Prior
Meteorological Office, Bracknell

Summary

A description is given of the background to the formulae most widely used for quantifying the chilling effects of strong winds combined with low temperatures. These are expressed in terms of wind-chill indices (or factors) and wind-chill equivalent (or apparent) temperatures. Their applications are discussed and a wind-chill climatology for various locations in the United Kingdom is presented.

1. Introduction

The term wind-chill is a familiar one that has been used (and occasionally misused) for many years, normally in connection with human comfort, i.e. the common experience that a person will feel colder when the wind is blowing than when it is not. However, it can be applied more generally to indicate enhanced heat loss from objects that are warmer than their surroundings.

Countries regularly experiencing severe winter weather such as Canada and the USA have, for a long time, taken account of the chilling effect of the wind in weather forecasts issued to the general public. It is only recently that wind-chill has been included in media forecasts in the United Kingdom, although forecasts of wind-chill have been issued in the past to farmers in connection with potentially stressful conditions for new-born lambs (Starr 1984). During the winter of 1984/85, and more especially that of 1985/86, wind-chill and wind-chill equivalent temperatures were quoted on television forecasts. This led to the receipt of enquiries by the Meteorological Office Advisory Services Branch and Weather Centres about wind-chill calculations and the situations to which they can be applied. Some enquirers did not realize the limitations of either the concept or its applications.

2. History

An object cools because of radiative, conductive and convective heat losses (plus evaporation if its surface is wet). Convective heat loss varies with wind speed, thus total heat loss from an object is greater when the wind is blowing than when it is not (other things being equal). Work describing this wind-enhanced cooling power of the atmosphere pre-dates the First World War.

A generalized heat-balance equation was produced by Hill (Stone 1943) for the cooling of a dry, heated body by convection and conduction to the air (an equilibrium between incoming and outgoing radiation was assumed) of the following format:

$$H = (a + b\sqrt{v})\,(t_s - t_a)$$

where the notation is as follows:
H = rate of heat loss
a = heat transfer coefficient of conduction
b = heat transfer coefficient of convection
v = wind speed
t_s = surface temperature of object
t_a = ambient air temperature.
Other workers produced various values for the coefficients using instruments such as the katathermometer (an alcohol thermometer with an oversized cylindrical bulb whose rate of cooling from 38 to 35 °C in different meteorological conditions was assumed to be proportional to the rate of human cooling) and the frigorimeter (a nearly solid copper sphere whose temperature was maintained at 37 °C, in various conditions, by electric current — the amount of current needed was assumed to be a measure of the cooling power of the atmosphere).

A first power wind-speed term was introduced into the generalized heat-balance equation by Plummer (1944) and by Siple and Passel (1945). It was Siple (1939) who first used the term 'wind-chill' to describe the wind-enhanced cooling power of the atmosphere while producing a comfort scale for workers and explorers in cold climates, and who promoted its use during work in Antarctica in the 1940s. The Siple–Passel formula is described in detail in Section 3. It became established as the major wind-chill formula, at least in the English-speaking world, mainly because of its ease of calculation. Other formulations based upon the Siple–Passel formula have also been proposed (Court 1948, Lyall 1981).

An entirely new formula was introduced by Steadman, based on the concept of thermal equilibrium, i.e. all heat generated by a body is balanced by heat lost, provided the body is covered by an adequate thickness of clothing (Steadman 1971). The Steadman formula, and its subsequent development (Steadman 1984) is described in detail in Section 4.

Additional factors influencing comfort were considered by Beal (1974). He produced an equation by considering the same heat losses as Steadman plus variables such as age, health, time of food digestion, time of day and psychological effects (e.g. length of darkness, snow and general state of mind). Because it is more complicated, Beal's equation is more difficult to implement.

A further formula, developed by Rodriguez, considers conductive heat transfer from the body core to the skin surface and then convective heat loss from the skin surface to the air (Rodriguez 1980). A fixed body-core temperature is used but the skin temperature is allowed to vary with air temperature and wind speed. However, he did not consider the vaso-constriction process, i.e. when the brain senses reduced skin temperature, blood is diverted from the exterior by the constriction of peripheral blood vessels in order to reduce heat loss. This process maintains the temperature of vital organs (brain, heart and lungs) at 37 °C at the expense of more 'superficial' areas such as hands and feet.

3. The Siple–Passel wind-chill formula

This wind-chill formula was developed from experiments conducted in Antarctica during 1941. Measurements were made of the time required to freeze 250 gm of water in a plastic cylinder (5.7 cm diameter and 15 cm high) in a variety of wind speeds and temperatures. The rate of heat loss was assumed to be proportional to the difference in temperature between the cylinder and the temperature of the surrounding air. Of the 89 separate results obtained, 56 were used to produce the following equation:

$$H = (12.12 + 11.6\sqrt{v} - 1.16\,v)\,(33 - t_a)$$

where the notation is as follows:
H = rate of heat loss (W m^{-2}) (to convert to Kcal m^{-2} h^{-1}, divide by 1.16)
v = wind speed (m s^{-1})
33 = bare-skin temperature (°C)
t_a = ambient air temperature (°C).

The original application of the Siple–Passel formula was to predict conditions likely to produce frost-bite during army exercises. Maps of wind-chill indices for the USA, Canada and, eventually, all continents were produced as a guide to clothing requirements. The formula is still widely used and forms the basis of wind-chill tables and nomograms in numerous textbooks and articles, e.g. Thomas and Boyd (1957), National Oceanic and Atmospheric Administration (1975), Anton (1981) and Schlatter (1981).

4. The Steadman wind-chill formula

This formula is based upon the concept of thermal equilibrium. Steadman assumes that a healthy adult (of height 1.7 m and with a body surface area of 1.7 m^2) whilst walking outdoors at 3 m.p.h. (1.3 m s^{-1}) would generate 188 W m^{-2} of heat. This is offset by heat losses from the body and to maintain thermal equilibrium in a variety of weather conditions, the amount of clothing worn has to be varied. The appropriate amount of clothing, expressed as clothing thickness, is the result obtained from Steadman's formula.

Steadman considered more variables than Siple and Passel and, consequently, the formula is more complex:

$$\begin{aligned}\text{Heat generated} &= \text{Heat lost}\\ &= \text{evaporative loss in breath} && (1)\\ &+ \text{loss due to heating breath} && (2)\\ &+ \text{loss from uncovered skin} && (3)\\ &+ \text{loss from thinly clothed hands and feet} && (4)\\ &+ \text{loss from fully clothed areas} && (5)\end{aligned}$$

$$188 = \underset{(1)}{16.29} + \underset{(2)}{0.22\,(37 - t_a)} + \underset{(3)}{\frac{0.13\,(30 - t_a)}{R_s}} + \underset{(4)}{\frac{0.5\,(30 - t_a)}{0.5 + R_s}} + \underset{(5)}{\frac{3.55\,(33 - t_a)}{R_f + R_s}}$$

where the following notation has been used:
188 = heat generated by a healthy adult walking outdoors and suitably clothed (W m^{-2})
t_a = ambient air temperature (°C)
37 = body-core temperature (°C)
33 = skin temperature adequately covered with clothing (°C)
30 = bare-skin temperature (°C)
R_f = clothing resistance (m^2 s °C cal^{-1})
= clothing thickness divided by thermal conductivity of the clothing

R_s = surface resistance ($m^2\,s\,^\circ C\,cal^{-1}$) $= \dfrac{1}{h_r + h_c}$

h_r = heat transfer coefficient of radiation ($cal\,m^{-2}\,s^{-1}\,^\circ C^{-1}$)

$$= 0.0135 \left\{ 4.0 \left(\frac{t_a + 273}{100} \right)^3 + 0.3 \left(\frac{t_a + 273}{100} \right)^2 \right\}$$

h_c = heat transfer coefficient of convection $= 0.61\,(S^{0.75})$

S = effective wind speed (m.p.h.), i.e. that measured at the conventional height of 10 m above the ground adjusted to represent the wind relative to a person walking at 3 m.p.h.

The effect of the walker's speed on the relative wind speed is only important in light winds, hence two equations exist to calculate the effective wind speed, namely:

$$S = (v_{10}^2 + 10)^{0.5} \text{ if } v_{10} \geqslant 6.4 \text{ m.p.h. } (2.9 \text{ m s}^{-1})$$

$$S = \{v_{10}^2 + 10 + 7(6.4 - v_{10})^{0.5}\}^{0.5} \text{ if } v_{10} < 6.4 \text{ m.p.h.}$$

where v_{10} is the 10 m wind.

An extra term can be incorporated into the heat-balance equation — a heat gain due to the insolation effects on a person in full sunshine. As a heat gain it must be deducted from the heat losses on the right-hand side of the thermal equilibrium equation:

$$\text{additional heat gain due to sunshine} = \alpha\,PG$$

where α, P and G are defined as follows:

α = absorptivity of the skin (or clothing)

P = proportion of the skin (or clothing) effectively receiving normally incident radiation

G = insolation ($cal\,m^{-2}\,s^{-1}$).

Subsequently, Steadman extended his work to cover all air temperatures from −40 °C to +50 °C, wind speeds up to 20 m s^{-1} and humidity effects, i.e. to consider both wind-chill effects and heat-stress effects (Steadman 1984). This new work contains several modifications to his earlier ideas, although these mainly concern heat-stress calculations.

5. Discussion of the Siple–Passel and Steadman formulae

The two most widely used wind-chill formulae in the English-speaking world are the empirical one due to Siple and Passel and the theoretical one due to Steadman. These two formulae approach the subject of wind-chill in different ways.

The Siple–Passel formula is based upon experiments to measure the time taken for water to freeze in a variety of weather conditions, i.e. the stronger the wind blows, the greater will be the convective heat loss and the less the time taken for the water to freeze. Objections have been raised about the observational procedures and the experimental basis (Court 1981, Molnar 1960). These relate particularly to the extrapolation to weather conditions other than those measured and the applicability to heat-generating humans, wearing clothing. It is not really possible to express the effect of the wind on heat loss from a person without referring to the amount of clothing being worn (Burton and Edholm 1955) and so the Siple–Passel formula should be applied to bare-skin areas only.

Steadman, however, bases his theory on the more realistic situation of a fully clothed person walking outdoors. In order to remain in thermal equilibrium in varying weather conditions, the amount of heat lost from a person must not exceed the heat generated, a balance being achieved by wearing appropriate thicknesses of clothing. Steadman's formula considers all forms of heat loss from a person as a whole. However, the 'wind-chill' part of his equation (term 3) can be isolated, and is applicable to bare-skin areas, assumed to be only the face. The output from the equation as a whole is a thickness of clothing (mm) — that which is necessary to maintain thermal equilibrium; the output from the 'wind-chill' part is an amount of heat loss (W m^{-2}).

In Steadman's formula the relationship between heat loss and wind speed is approximately linear and positive (Fig. 1). This contrasts with the Siple–Passel formula where a maximum amount of heat loss is obtained with a wind speed of 25 m s^{-1} (twice the strongest wind speed measured during their experiments) implying that higher wind speeds have little additional effect on heat loss (see Figs 1 and 2). This is not borne out in experiments (Currie 1951). Most tables or nomograms of wind-chill produced using the Siple–Passel formula do not give results for wind speeds greater than about 22 m s^{-1} (43 kn or 49 m.p.h.) because of the inconsistency.

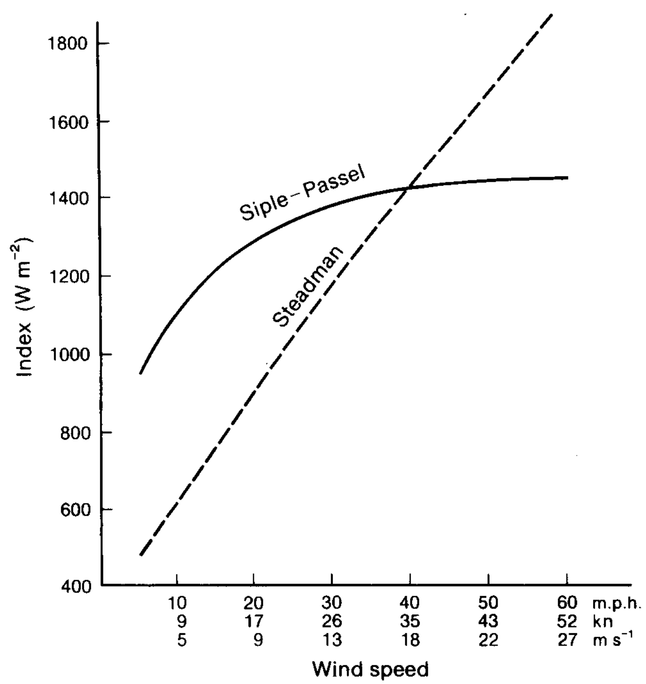

Figure 1. Values of the Siple–Passel and Steadman wind-chill indices for a fixed air temperature of −2 °C at various wind speeds.

The temperature chosen to represent that of bare skin is different in the two formulae. Siple and Passel chose 33 °C to be consistent with the 'clo' unit used for clothing requirements (Gagge *et al.* 1941), but Steadman believed this value to be too high and chose a value of 30 °C (Steadman 1971). However, Rodriguez (1980) stated that if the bare-skin temperature remained at these values (30 or 33 °C) then no discomfort would be felt. One of the major differences between Steadman's 1971 and 1984 work is the calculation of the bare-skin temperature for every occasion, using the body-core temperature of 37 °C and the weather conditions prevailing, i.e. the bare-skin temperature is no longer a fixed value of 30 °C.

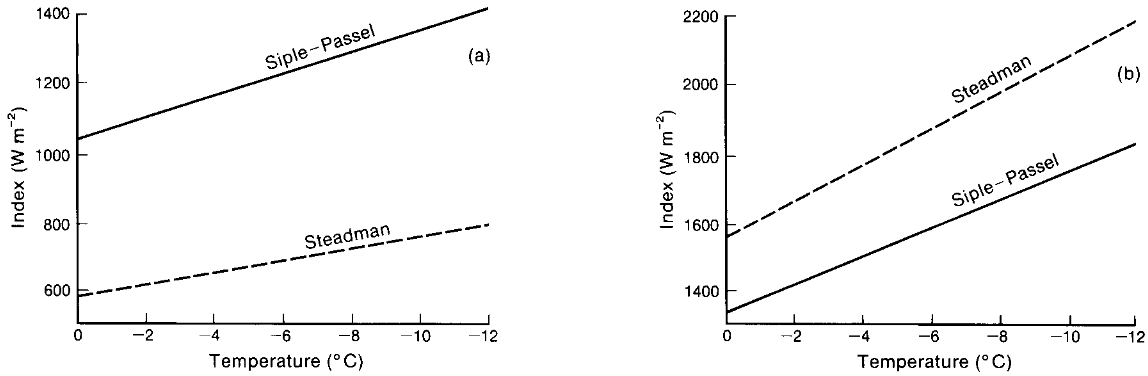

Figure 2. Values of the Siple–Passel and Steadman wind-chill indices at various temperatures for (a) 10 m.p.h. and (b) 50 m.p.h. wind speed.

However, Steadman does not recommend calculating this if the air temperature is less than 0 °C because of the uncertain response of the skin temperature to the vaso-constriction process.

The output from the Siple–Passel equation is a rate of heat loss for each combination of wind speed and temperature. As part of his work on a bioclimatic classification for the USA, Terjung (1966) adopted the sensation categories given in Table I, based upon the development by Siple and Passel of proposals made by Gold (1935).

Table I. *Wind-chill ranges corresponding to the sensation felt by the majority of people (after Terjung 1966). To convert Kcal m^{-2} h^{-1} to cal m^{-2} s^{-1}, divide by 3.6.*

Wind-chill		Sensation felt by majority
W m^{-2}	Kcal m^{-2} h^{-1}	
348–696	300–600	cool
697–929	601–800	very cool
930–1160	801–1000	cold
1161–1390	1001–1200	very cold
1391–1625	1201–1400	bitterly cold
> 1625	> 1400	exposed flesh freezes

However, criticism of the formula has thrown doubt on the absolute values obtained; even though a value of 1625 W m^{-2} calculated from the formula may correspond to conditions when exposed flesh freezes, the rate of heat loss is not necessarily 1625 W m^{-2}. Siple himself recognized the limitations of his formula (and its application to circumstances other than those originally intended) and recommended dropping the units and regarding the results as simply numbers for empirical purposes (Molnar 1960).

6. Wind-chill equivalent temperatures

Wind-chill equations produce values for the rate of heat loss from a body. However, often a more useful product is the wind-chill equivalent temperature. A certain combination of wind speed and temperature is associated with a certain rate of heat loss. The same heat loss may also be produced by combining a reference speed (e.g. a person's walking speed) with a different temperature, known as the wind-chill equivalent temperature or apparent temperature. By using this, the chilling effects of the wind may be expressed in terms of the lower temperature needed to produce the same sensation for a person walking in calm conditions.

The Siple–Passel equivalent temperatures relate to bare skin only and are easy to calculate by rearranging the wind-chill equation given in Section 3.

For wind speed v and air temperature t_a, the wind-chill is H. The equivalent temperature t_e is the air temperature required to give the same wind-chill, but for a given wind speed v_o. The most often quoted value of v_o is 5 m.p.h. (2.6 m s^{-1}), a person's walking speed. Use of this value yields the following expression for t_e in terms of v and t_a:

$$t_e = 33 - \frac{(12.12 + 11.6\sqrt{v} - 1.16v)(33-t_a)}{27.81} .$$

Steadman's equivalent temperatures are based on the thickness of clothing required to insulate 85% of the body surface and to keep the body in thermal equilibrium. These temperatures are difficult to calculate from Steadman's 1971 equation, but in his 1984 paper he gives simplified equations for calculating equivalent temperatures for any combination of air temperature, humidity, wind speed and solar radiation.

The characteristics of the Siple–Passel and Steadman's 1971 wind-chill equations are reflected in the equivalent temperatures given in Tables II and III, e.g. Siple and Passel's formula produces equivalent temperatures that are more sensitive to changes in the lower wind-speed ranges, than those in the higher ranges.

Table II. *Wind-chill equivalent temperatures (°C) using Siple–Passel equation (using a reference wind speed of 5 m.p.h.)*

Wind speed kn	Wind speed m.p.h.	Wind speed m s^{-1}	Air temperature °C 0	−1	−2	−3	−4	−6	−8	−10	−12	−14	−18
4	5	2	0	−1	−2	−3	−4	−6	−8	−10	−12	−14	−18
9	10	5	−6	−7	−8	−9	−11	−12	−14	−17	−20	−22	−26
13	15	7	−9	−11	−12	−13	−14	−16	−19	−22	−24	−28	−32
17	20	9	−12	−13	−14	−16	−18	−19	−22	−25	−28	−31	−35
22	25	11	−14	−15	−16	−18	−19	−21	−24	−28	−31	−34	−38
26	30	13	−15	−16	−18	−19	−21	−23	−26	−29	−33	−36	—
30	35	16	−16	−17	−19	−21	−22	−24	−27	−31	−34	—	—
35	40	18	−17	−18	−20	−22	−23	−25	−28	−32	—	—	—

Table III. *Wind-chill equivalent temperatures (°C) using Steadman's 1971 equation (using a reference wind speed of 5 m.p.h.)*

Wind speed kn	Wind speed m.p.h.	Wind speed m s^{-1}	Air temperature °C 0	−1	−2	−3	−4	−6	−8	−10	−12	−14	−18
4	5	2	0	−1	−2	−3	−4	−6	−8	−10	−12	−14	−18
9	10	5	−3	−4	−5	−6	−7	−9	−11	−13	−16	−18	−22
13	15	7	−4	−6	−7	−8	−10	−11	−14	−17	−19	−22	−26
17	20	9	−6	−8	−9	−11	−12	−13	−17	−19	−22	−25	−30
22	25	11	−8	−9	−11	−13	−14	−16	−19	−22	−25	−28	−33
26	30	13	−10	−11	−13	−14	−16	−17	−21	−24	−28	−31	—
30	35	16	−11	−12	−14	−16	−18	−19	−23	−27	−31	—	—
35	40	18	−12	−14	−16	−17	−19	−21	−25	−29	—	—	—

The two formulae produce different equivalent temperatures for the same combinations of wind speed and temperature, e.g. at −6.0 °C and 9 m s^{-1} the Siple–Passel equivalent temperature is −19 °C, whereas the Steadman (1971) equivalent temperature is −13 °C.

Equivalent temperatures are not quoted when the wind speed is less than the reference walking speed as the equivalent temperature that is calculated is warmer than the air temperature. This unrealistic result does not occur with the equivalent temperatures derived from the Steadman 1984 equation as the reference wind speed adopted is zero, i.e. the full effect of the wind is taken into account. The gain in equivalent temperature due to sunshine is also calculated, plus a humidity increment, although this is small at low temperatures. Tables IV and V give these equivalent temperatures and the sunshine correction. A nomogram has been prepared (Fig. 3) to enable other combinations of wind and temperature to be assessed.

Forecasts of equivalent temperatures are issued regularly in North America where the often harsh winter weather warrants a relevant indication of how cold it will feel outdoors. However, because of differences in people's age, activity, state of health, metabolic rate, etc., not everyone will experience the

Table IV. *Wind-chill equivalent temperatures (°C) using Steadman's 1984 equation – rounded to the nearest 0.5 °C*

Wind speed kn	m.p.h.	m s^{-1}	Air temperature °C 20	18	16	14	12	10	8	6	4	2
4	5	2	19.5	17.5	15.5	13.5	11.5	9.5	7.5	5.0	3.0	1.0
8	9	4	18.0	16.0	14.0	12.0	9.5	7.5	5.0	3.0	1.0	−1.5
12	13	6	17.0	14.5	12.5	10.5	8.0	5.5	3.5	1.0	−1.0	−3.5
16	18	8	16.0	13.5	11.0	9.0	6.5	3.0	2.0	−0.5	−3.0	−5.5
19	22	10	15.0	12.5	10.5	8.0	5.5	3.0	0.5	−2.0	−5.0	−7.0
23	27	12	14.5	12.0	9.5	7.0	4.5	2.0	−1.0	−3.5	−6.0	−8.5
29	33	15	13.5	11.0	8.5	6.0	3.5	0.5	−2.0	−5.0	−7.5	−10.0
39	45	20	12.5	10.0	7.0	4.5	1.5	−1.5	−4.0	−7.0	−10.0	−12.5

kn	m.p.h.	m s^{-1}	0	−5	−10	−15	−20	−25	−30	−35	−40
4	5	2	−1.0	−6.0	−11.0	−16.0	−21.5	−26.5	−31.5	−36.5	−41.5
8	9	4	−3.5	−9.0	−14.5	−20.0	−25.0	−30.5	−36.0	−41.5	−46.5
12	13	6	−6.0	−11.5	−17.5	−23.0	−28.5	−34.0	−40.0	−45.5	−51.0
16	18	8	−8.0	−14.0	−20.0	−25.5	−31.5	−37.5	−43.0	−49.0	−54.5
19	22	10	−9.5	−16.0	−22.0	−28.0	−34.5	−40.0	−46.0	−52.0	−58.0
23	27	12	−11.0	−17.5	−24.0	−30.5	−36.5	−42.5	−49.0	−55.0	−61.0
29	33	15	−13.0	−19.5	−26.5	−33.0	−39.5	−45.5	−52.0	−58.5	−64.5
39	45	20	−15.5	−22.5	−29.5	−36.5	−43.0	−50.0	−56.5	−62.5	−69.5

Table V. *Increase in equivalent temperatures (°C) due to full sunshine (Steadman 1984)*

Temperature °C	Wind speed m s^{-1} 0	2	4	6	8	10	12	15	20
−40	7.2	6.8	5.7	4.7	4.0	3.2	3.0	2.9	2.4
−20	7.4	7.0	5.9	5.0	4.3	3.6	3.4	3.1	2.7
0	7.4	7.0	6.0	5.2	4.5	3.8	3.6	3.4	3.0
20	8.5	8.3	7.4	6.5	5.5	4.6	4.3	3.8	3.3
30	8.3	8.1	7.2	6.6	6.2	5.9	5.6	5.3	4.9

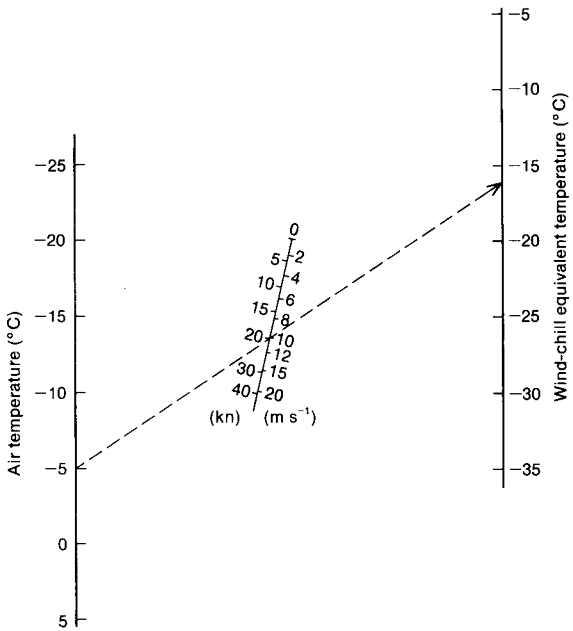

Figure 3. Nomogram for obtaining the wind-chill equivalent temperatures for various combinations of air temperature and wind speed at 10 m (after Steadman 1984). The example shows an equivalent temperature of −16 °C resulting from an air temperature of −5 °C and a wind speed of 20 kn.

same level of discomfort at the same equivalent temperature. No experimental evidence exists to suggest whether Steadman's or Siple and Passel's equivalent temperature is more applicable to the majority of people.

During the winter of 1984/85, weather forecasters in the United Kingdom started quoting equivalent temperatures. The Meteorological Office favours the more realistic approach adopted by Steadman (1984) for assessing wind-chill and uses his equivalent temperatures in forecasts during severe weather.

7. Applications

During and after the cold spell of February 1986, the Meteorological Office received many requests for information about wind-chill for a wide variety of reasons. The subjects that came to the attention of the authors included:

(a) alleged mistreatment of animals,
(b) inadequate heating of office blocks,
(c) interference with outdoor construction (effects both on materials and on operatives),
(d) effects of exposure for soldiers on exercise,
(e) damage to car engines and
(f) damage to crops.

Wind-chill indices do have a role to play for the types of application illustrated by subjects (a) to (d), either in the traditional sense of heat loss from bare skin or simply in terms of a measure of severe weather. For example, when materials need to be maintained at temperatures above that of their surroundings, chilling winds have an adverse effect. Daines (1985) describes how wind can reduce the time available for the compaction of bituminous materials used in road construction and how tables of wind speed versus temperature can be used to assess this effect. Strong cold winds can also increase the energy needed to maintain comfortable temperatures in buildings, particularly those that are poorly insulated or very exposed. Analyses of the frequency of wind-chill indices by wind direction can be used when deciding upon the design and layout of buildings to enable protective measures, e.g. the placing of shelter belts, to be taken (Dodd 1985). These and other applications of wind-chill calculations in the construction industry have already been described by the authors (Dixon and Prior 1986). The enhanced heat loss from young lambs (Starr 1984) is one example of the stress that wind-chill can cause animals, especially when they are wet.

The main misconception about wind-chill is the application of wind-chill equivalent temperatures to unheated, inanimate objects such as machinery, storage tanks or crops. When the wind is blowing, any dry, unheated, inanimate object cannot cool below the ambient air temperature; an object with a wet surface could, of course, cool to somewhat below the ambient air temperature due to evaporative heat loss. However, a heated object, for example a running car engine, will lose heat more quickly by convection when the wind is blowing. Once the engine is switched off and heat is no longer being generated, the engine will quickly cool towards the ambient air temperature as described above, but will be unable to cool below this temperature. Rodriguez (1980) quotes a typical misuse of the wind-chill concept with regard to sales of anti-freeze solution — 'One can be told that although the temperature is going down to −23 °C, one should protect the automobile engine down to −51 °C because of expected high winds'.

For human applications, the wind-chill index has its roots in assessing the comfort of military personnel spending prolonged periods outdoors in harsh climates. Even in the United Kingdom, the decrease of mean temperature with altitude coupled with an increase in mean wind speed leads to severe conditions in many upland areas for significant parts of each winter. Considerable use of such areas is now also made for sport and recreation, and the proper planning of these can be assisted by considering wind-chill indices and the associated clothing requirements (Baldwin and Smithson 1979).

When used as a comfort index for the general public, the great variety of personal circumstances (such as dress, activity and state of health) somewhat lessens the applicability of the wind-chill equivalent temperature to that of a general, although still useful, indicator.

8. Climatology

The spatial and temporal variability of wind-chill in the United Kingdom has been commented upon by Smithson and Baldwin (1978). They presented maps for the months January, April, July and October showing 18-year averages of wind-chill index and of the clothing thickness required to maintain the body in thermal equilibrium, using the work of Steadman. Essentially, these maps relate to altitudes less than about 100 m above mean sea level, since almost all the stations used in the analyses were below this level. The analyses were based upon monthly averages of temperature and wind speed, thus both masking the true range of conditions during a month and introducing problems concerned with the co-variance of wind and temperature over the United Kingdom. To overcome these difficulties, Mumford (1979) proposed an alternative approach using a 5% random sample of 1200 GMT observations over 15 years to produce seasonal maps of both mean and absolute maximum wind-chill, again for lowland Britain. Data from six sites in upland Britain have been processed by Baldwin and Smithson (1979), in terms of the frequency of wind-chill and required clothing thickness.

Several workers have calculated the wind-chill indices during particular cold spells, notably Howe (1962), Lyall (1981) and Giles (1986); the last named has discussed the severe weather at Birmingham in February 1986 in the context of the previous 45 Februarys.

Extensive computer archives of hourly temperature, mean wind speed and mean wind direction are now available for the network of weather observing stations administered by the Meteorological Office.

The more populous parts of the United Kingdom are well represented, with some records spanning 30 years or more. Thus it is now possible to examine hourly mean wind-chill indices and equivalent temperatures easily and over relatively long periods. A standard computer program is available to produce frequency distributions of temperature versus wind speed and a program has been written to calculate wind-chill indices on a monthly or seasonal basis, in terms of 30° wind direction sectors, from either the Siple–Passel or the Steadman (1971) formulae.

Since the wind-chill information given in public weather forecasts relates to low equivalent temperatures, an indication of their frequency in various parts of the United Kingdom will be of interest. Figs 4–10 show frequency distributions for seven stations (see Fig. 18 for their locations) whose hourly data during the 'winters' (October–April) of the years 1965–85 have been analysed in terms of Steadman (1984) equivalent temperatures. Only equivalent temperatures of 0 °C or less were considered, the average proportion of the 'winter' with such values varying typically from about a quarter in southern England (Figs 4 and 5) to about a half in lowland Scotland (Figs 8 and 9) to almost three quarters in the Shetlands (Fig. 10). The distributions suggest that the most frequent winter equivalent temperature is above 0 °C in most parts of the United Kingdom, with one exception being the Shetlands where values as low as −4 °C to −5 °C are common (Fig. 10). It should be noted that almost all the wind speeds used were measured by anemometers with a standard exposure (effective height 10 m), so the values will overestimate wind-chill effects for more sheltered sites in the vicinity, e.g. urban areas, and underestimate them for more exposed locations, e.g. over hills or near coasts. The Steadman equivalent temperature calculation incorporates a wind speed adjustment to 2 m above ground level.

An alternative presentation is given in Figs 11–17, in terms of indices from the 'wind-chill' term in the 1971 Steadman formula that are greater than 500 W m^{-2}. This threshold corresponds roughly to an index of 900 W m^{-2} produced by the Siple–Passel formula, a value associated with the human sensation 'cold' by Terjung (1966). The average proportion of the winter deemed 'cold' or worse varies from about one third in south-east England (Fig. 11) to about three quarters in the Shetlands, where the shape of the frequency distribution again reflects the harsh climate (Fig. 17). At most of the locations the proportion of 'cold' hours is only slightly greater than that for hours with an equivalent temperature 0 °C or less; notable exceptions are Plymouth (Figs 5 and 12) and Stornoway (Figs 9 and 16) where the windy, relatively mild, climate leads to many more hours qualifying when the less rigorous wind-chill index criterion is chosen.

Fig. 18 shows the contributions to the total number of hours with indices above 800 W m^{-2} from each 30 ° wind direction sector at the seven locations. The influence of topography is evident at several locations, with preferred directions for wind-chill corresponding to those from which winter winds are either enhanced by passage over the sea or funnelled by extensive high ground. The London analysis provides an example of high wind-chill associated with directions other than that of the prevailing wind.

More detailed directional information is given in Fig. 19. This indicates the tendency for high wind-chill indices to be associated mainly with cold continental airstreams in south-east Britain but also with stronger, less cold winds of maritime origin over other parts of the country.

The frequency and directional pattern of chilling winds will vary with location and in this respect it is important to bear in mind the local influence, particularly on wind speed, of terrain roughness, altitude and topography.

9. Concluding remarks

Wind-chill indices are a useful way of quantifying the various detrimental effects of chilling winds. The Siple–Passel wind-chill formula still appears to be the most widely used, despite its shortcomings. The Steadman formula considers criteria that are more realistic for people outdoors and consequently the Meteorological Office favours this more theoretically satisfactory approach.

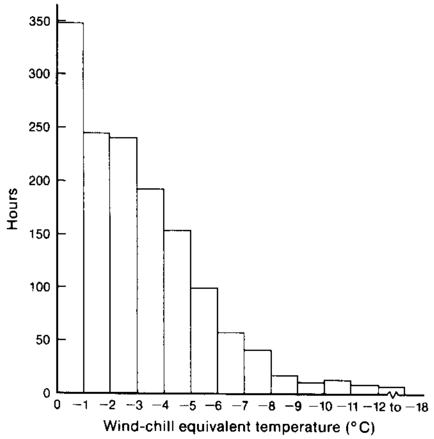

Figure 4. The average number of hours during October–April at London/Heathrow (anemometer effective height 10 m) with Steadman (1984) wind-chill equivalent temperatures in various ranges. The proportion of the period with equivalent temperature 0 °C or less is 28%.

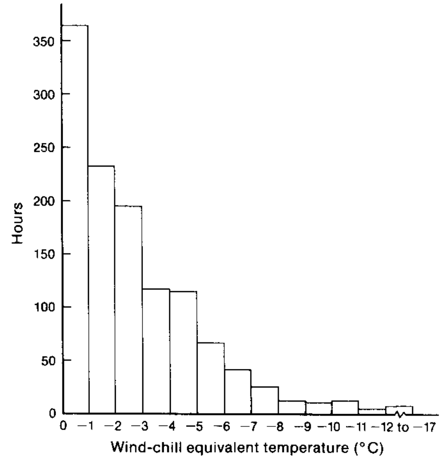

Figure 5. As Fig. 4 but for Plymouth/Mount Batten (anemometer effective height 13 m). The proportion of the period with equivalent temperature 0 °C or less is 24%.

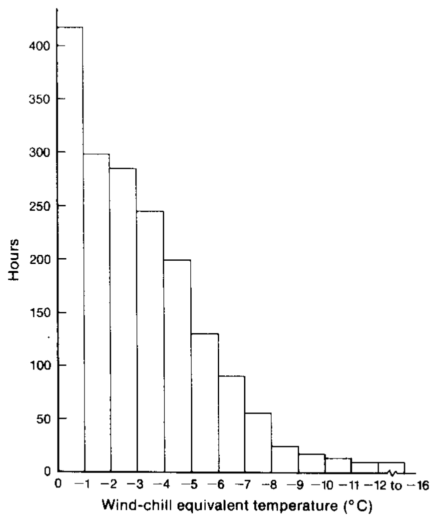

Figure 6. As Fig. 4 but for Manchester/Ringway (anemometer effective height 10 m). The proportion of the period with equivalent temperature 0 °C or less is 35%.

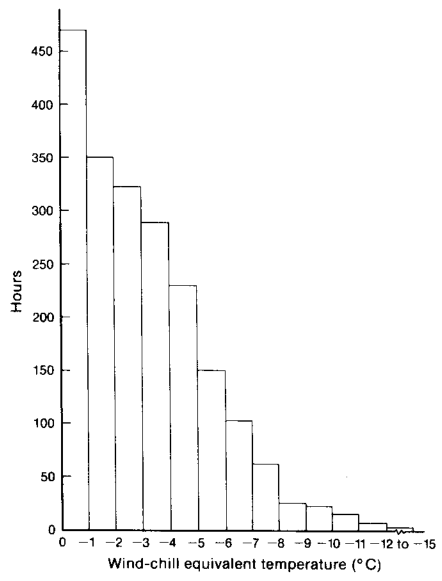

Figure 7. As Fig. 4 but for Belfast/Aldergrove (anemometer effective height 17 m). The proportion of the period with equivalent temperature 0 °C or less is 41%.

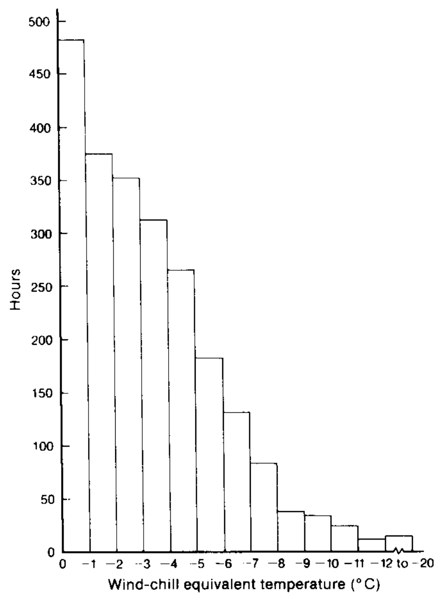

Figure 8. As Fig. 4 but for Edinburgh/Turnhouse (anemometer effective height 10 m). The proportion of the period with equivalent temperature 0 °C or less is 45%.

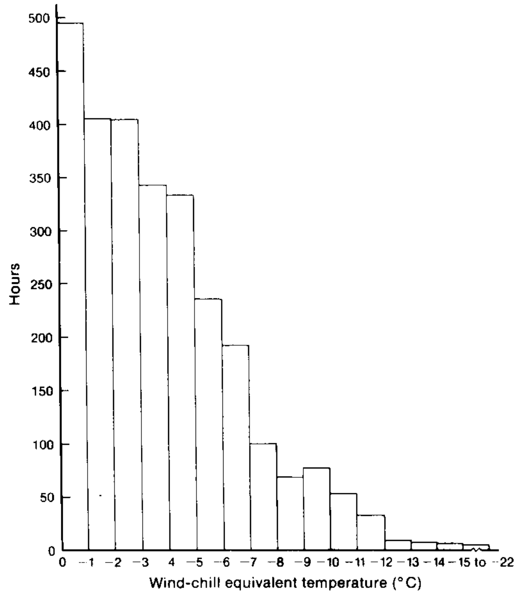

Figure 9. As Fig. 4 but for Stornoway (anemometer effective height 10 m). The proportion of the period with equivalent temperature 0 °C or less is 54%.

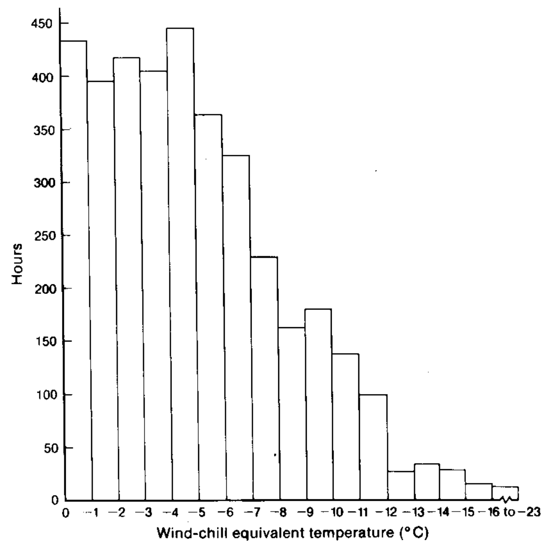

Figure 10. As Fig. 4 but for Lerwick (anemometer effective height 10 m). The proportion of the period with equivalent temperature 0 °C or less is 72%.

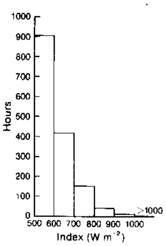

Figure 11. The average number of hours during October–April at London/Heathrow with Steadman (1971) wind-chill indices in various ranges. The proportion of the period with index 500 W m^{-2} or more is 31%.

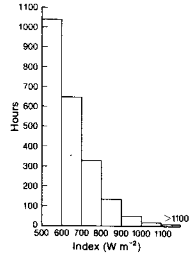

Figure 12. As Fig. 11 but for Plymouth/Mount Batten. The proportion of the period with index 500 W m^{-2} or more is 44%.

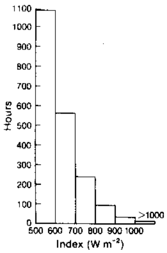

Figure 13. As Fig. 11 but for Manchester/Ringway. The proportion of the period with index 500 W m^{-2} or more is 40%.

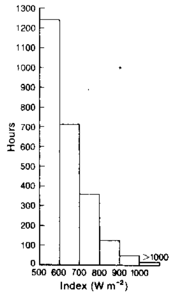

Figure 14. As Fig. 11 but for Belfast/Aldergrove. The proportion of the period with index 500 W m^{-2} or more is 48%.

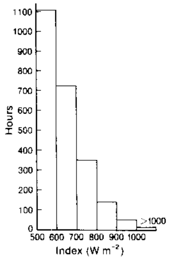

Figure 15. As Fig. 11 but for Edinburgh/Turnhouse. The proportion of the period with index 500 W m^{-2} or more is 47%.

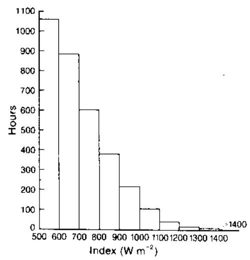

Figure 16. As Fig. 11 but for Stornoway. The proportion of the period with index 500 W m^{-2} or more is 65%.

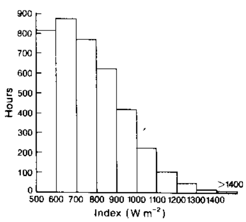

Figure 17. As Fig. 11 but for Lerwick. The proportion of the period with index 500 W m^{-2} or more is 77%.

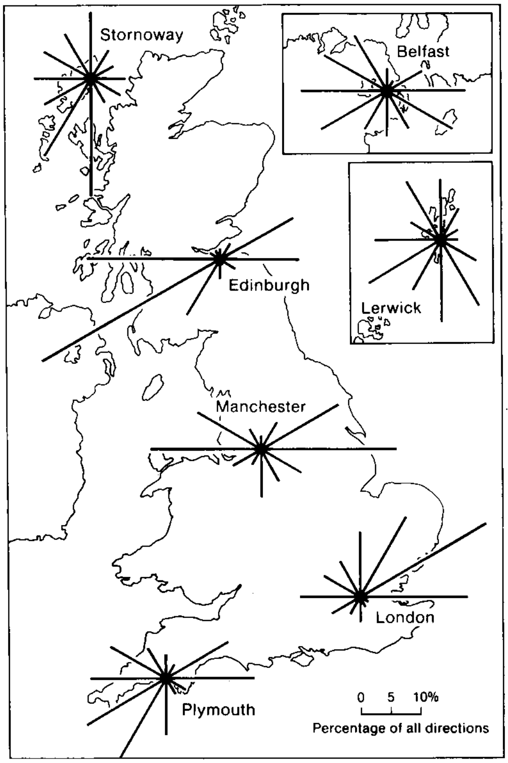

Figure 18. Wind-chill roses of Steadman (1971) indices greater than 800 W m^{-2}.

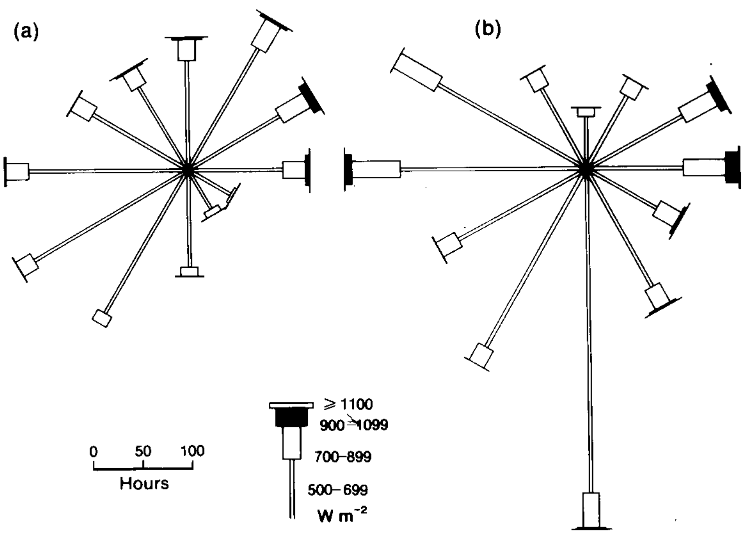

Figure 19. The average number of hours during October–April with Steadman (1971) wind-chill indices in various ranges and by 30° sectors at (a) London/Heathrow and (b) Manchester/Ringway.

It is likely that the demand for wind-chill information (and perhaps for summer-comfort indices as well) will grow, both for operational day-to-day use, and for design and planning purposes. It will be important to bear in mind the circumstances for which the advice is required.

Acknowledgements

The authors would like to thank E.J. Keeble of the Building Research Establishment for stimulating their interest in wind-chill and colleagues in the Advisory Services Branch of the Meteorological Office for their subsequent support and encouragement.

References

Anton, D.J. 1981 Wind chill. *Air Clues*, **35**, 259.
Baldwin, H. and Smithson, P.A. 1979 Wind chill in upland Britain. *Weather*, **34**, 294–306.
Beal, H.T. 1974 An operational windchill index. *Atmosphere*, **12**, 18–30.
Burton, A.C. and Edholm, O.G. 1955 Man in a cold environment. Monographs of the Physiological Society No. 2. London, Arnold.
Court, A. 1948 Wind chill. *Bull Am Meteorol Soc*, **29**, 487–493.
1981 Windchill over 40 years. *In* Fifth Conference on Biometeorology. Boston, American Meteorological Society.
Currie, B.W. 1951 Sensations isopleths on a wind-temperature diagram for winter weather on the Canadian Prairies. *Bull Am Meteorol Soc*, **32**, 371–374.
Daines, M.E. 1985 Cooling of bituminous layers and time available for their compaction. Transport and Road Research Laboratory, Crowthorne, Berkshire. Research Report No. 4.
Dixon, J.C. and Prior, M.J. 1986 Wind-chill indices — their history, calculation and applications in the construction industry. (Unpublished, copy available in the National Meteorological Library, Bracknell.)
Dodd, J. 1985 Landscape development for energy saving. *Construction*, **52**, 6–11.
Gagge, A.P., Burton, A.C. and Bazett, H.C. 1941 A practical system of units for the description of the heat exchange of man with his environment. *Science*, **94**, 428–430.
Giles, B.D. 1986 Exceptionally severe weather: a problem for the DHSS. The situation in February 1986. *Weather*, **41**, 226–229.
Gold, E. 1935 The effect of wind, temperature, humidity and sunshine on the loss of heat of a body at temperature 98 °F. *Q J R Meteorol Soc*, **61**, 316–331.
Howe, G.M. 1962 Windchill, absolute humidity and the cold spell of Christmas 1961. *Weather*, **17**, 349–358.
Lyall, I.T. 1981 Wind-chill in Great Britain during winter 1980–1981. *J Meteorol Trowbridge*, **6**, 253–258.
Molnar, G.W. 1960 An evaluation of wind-chill. *In* Horvath, S.M. (ed); Proceedings of the sixth Conference on Cold Injury. New York, Josiah Macy Foundation.
Mumford, A.M. 1979 Problems of estimating lowland windchill. *Weather*, **34**, 424–429.
National Oceanic and Atmospheric Administration 1975 Wind chill (equivalent temperatures). Environmental Information Summaries C-3.
Plummer, J.H. 1944 Convective heat transfer. Conference on the Principles of Environmental Stress on Soldiers. US Army, Office of the Quartermaster General.
Rodriguez, F. 1980 An engineering view of wind chill. *Heat Transfer Eng*, **2**, 23–27.
Schlatter, T. 1981 Weather Queries? *Weatherwise*, **34**, 266–267.
Siple, P.A. 1939 Adaptation of the explorer to the climate of Antarctica. (Unpublished, thesis held in Clark University, Massachusetts.)
Siple, P.A. and Passel, C.F. 1945 Measurements of dry atmospheric cooling in subfreezing temperatures. *Proc Am Philos Soc*, **89**, 177–199.
Smithson, P.A. and Baldwin, H. 1978 Wind chill in lowland Britain. *Weather*, **33**, 463–474.
Starr, J.R. 1984 Operational forecasting of a 'wind-chill' factor for young lowland lambs. *Meteorol Mag*, **113**, 105–113.
Steadman, R.G. 1971 Indices of wind chill of clothed persons. *J Appl Meteorol*, **10**, 674–683.
1984 A universal scale of apparent temperature. *J Clim and Appl Meteorol*, **23**, 1674–1687.
Stone, R.G. 1943 On the practical evaluation and interpretation of the cooling power in bioclimatology. Harvard University, Blue Hill Observatory, Reprint No. 10.

Terjung, W.H. 1966 Physiologic climates of the conterminous United States: a bioclimatic classification based on man. *Annu Assoc Am Geogr*, **56**, 141–179.

Thomas, M.K. and Boyd, D.W. 1957 Wind chill in northern Canada. *Can Geogr*, **10**, 29–39.

551.509.313:551.515.13

The fine-mesh forecast of severe weather for 25 August 1986

T. Davies

Meteorological Office, Bracknell

Monday 25 August 1986 was a public holiday in England, Wales and Northern Ireland, and the day was notable for the severity of the weather, particularly in areas bordering the Irish Sea. A depression spawned by the remnants of hurricane Charley deepened as it moved into the south-west approaches and brought gale force winds, heavy rain and flooding to many regions. The forecasts produced by the Meteorological Office fine-mesh model during this period were of a high standard and enabled the timely issue of warnings of severe weather. In particular, the wind forecasts were sufficient to deter pleasure craft from venturing out to sea.

The synoptic situations for 24 and 25 August at 12 GMT are shown in Figs 1 and 2. During this 24-hour period the central pressure of the depression fell from 990 mb to 985 mb as it travelled towards south-west Ireland. The corresponding 24-hour fine-mesh forecast valid at 12 GMT 25 August is shown in Fig. 3 where it can be seen that the position and central pressure of the depression compare well with

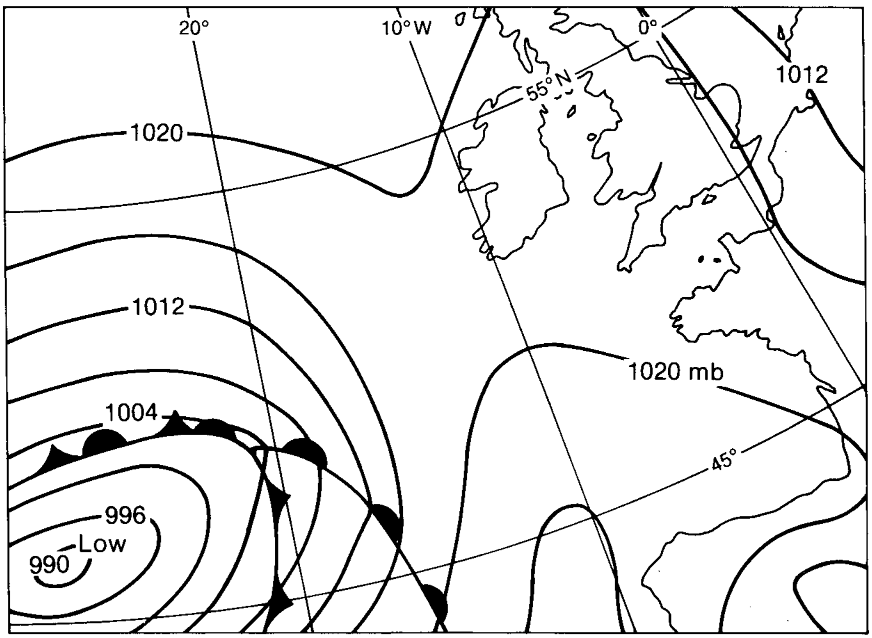

Figure 1. Surface analysis for 12 GMT 24 August 1986.

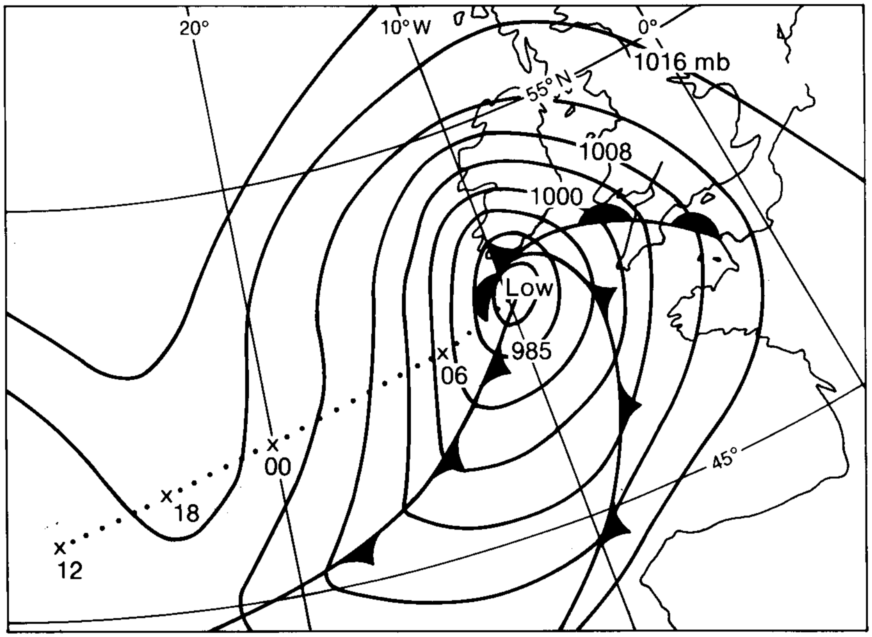

Figure 2. Surface analysis for 12 GMT 25 August 1986. The track of the depression over the previous 24 hours is shown.

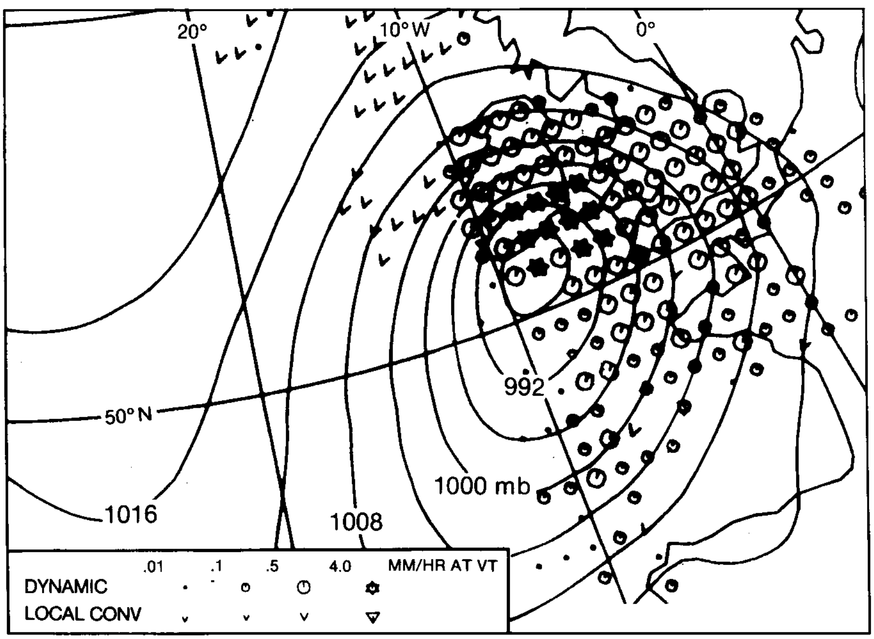

Figure 3. Fine-mesh 24-hour forecast valid for 12 GMT 25 August 1986 showing mean-sea-level pressure and intensity of precipitation.

the analysed values given in Fig. 2. The fine-mesh model had also forecast the heavy rainfall quite accurately. For example, the forecast 24-hour accumulations of rain over parts of the Republic of Ireland were in excess of 90 mm and in South Wales around 50 mm of rain was forecast. These values compare well with reported values considering that the fine-mesh grid points are 75 km apart. For example Dublin Airport reported 68 mm for the 24-hour period starting 06 GMT 25 August and there were reports of flooding in the Republic of Ireland. Flood damage also occurred in South Wales where there was one report of over 80 mm of rain in the 24-hour period starting 09 GMT 25 August.

The subsequent movement of the depression and the spread of the severe weather to northern England were also predicted accurately by the fine-mesh model.

This case clearly illustrates the ability of the fine-mesh model to handle situations which involve the development and spread of severe weather.

551.509.311:551.507.362.2

Bringing the analysis of occluded fronts into the satellite age

K.J. Weston

Department of Meteorology, University of Edinburgh

Summary

Attention is drawn to an inadequacy in the conventional representation of occluded fronts on surface charts. Mature depressions often have a spiral of frontal cloud which, it is suggested, should be represented in the analysis so as to convey more of the information gained from satellite images.

The way in which fronts are shown on surface pressure analyses has changed little since the Norwegian model of the development of a mid-latitude cyclone became well established earlier this century. There has been regular coverage of the earth by meteorological satellites since the 1960s, and the visible and infra-red images which they provide have considerably improved the reliability of surface analyses, especially over data-sparse regions such as the Atlantic Ocean. However, the classical model of the life cycle of an occluding depression appears to inhibit analysts from showing fronts as they really appear; certainly surface analyses could convey more useful information than is often the case. This is particularly true of mature occluded depressions which often have a spiral of cloud and precipitation wound around the depression centre. These cloud spirals are clearly of frontal origin and yet are rarely given such status. The occluded front is usually curtailed (in the classic way!) to the north-west of the low centre. This is best shown by an example — one chosen from many situations which illustrate the same point.

Fig. 1 shows the surface analysis, taken from the *London Weather Centre Daily Weather Summary** for 1200 GMT on 15 August 1985, and selected midday observations of wind and present weather. It shows a depression, with its centre over Northern Ireland, and an occluded front to the north and east. The satellite image, taken at visibile wavelengths by NOAA-9 at 1343 GMT, is shown in Fig. 2. South-west Scotland, north-west England, North Wales and much of the Republic of Ireland are covered by a spiral of dense cloud which gave heavy and continuous precipitation, particularly in western areas. Eskdalemuir, in the Southern Uplands of Scotland, recorded over 20 mm of rain in the

* Meteorological Office; *London Weather Centre Daily Weather Summary* 1200 GMT 15 August 1985.

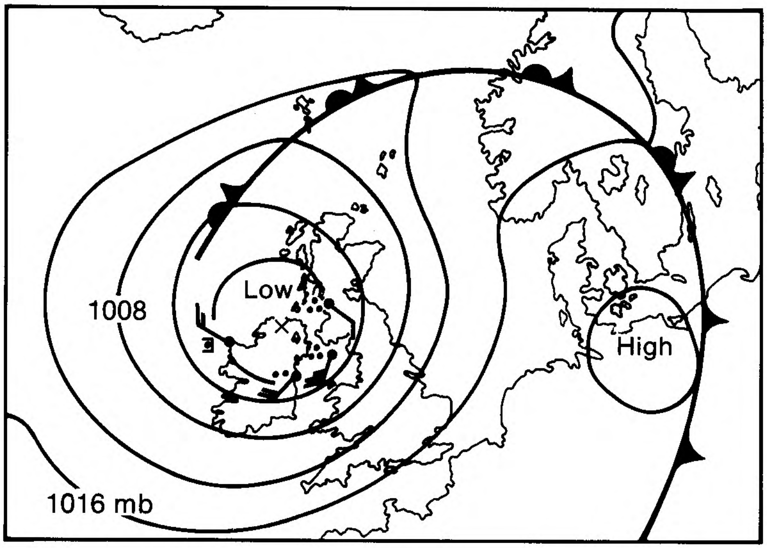

Figure 1. Surface analysis in the vicinity of the British Isles for 1200 GMT on 15 August 1985 taken from the *London Weather Centre Daily Weather Summary*. Also shown are observations of wind and present weather at four stations near the depression centre.

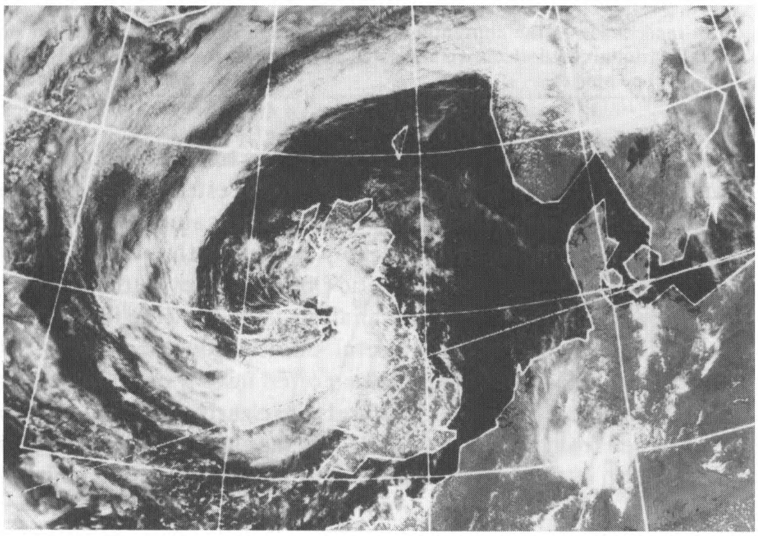

Photograph by courtesy of University of Dundee

Figure 2. Visible (Channel 2) Advanced Very High Resolution Radiometer image from NOAA-9, at 1343 GMT on 15 August 1985.

4 hours following the time of the satellite image. The cloud spiral was prominent in earlier satellite images and yet the cloud and precipitation would be unsuspected from the surface analysis shown in Fig. 1, though one would, of course, expect extensive showery rain. Because this cloud is so clearly of frontal origin, the analysis should convey this information by an extension of the occluded front into the low centre, as shown in Fig. 3. This adaptation is not a large one but is vitally important for those living

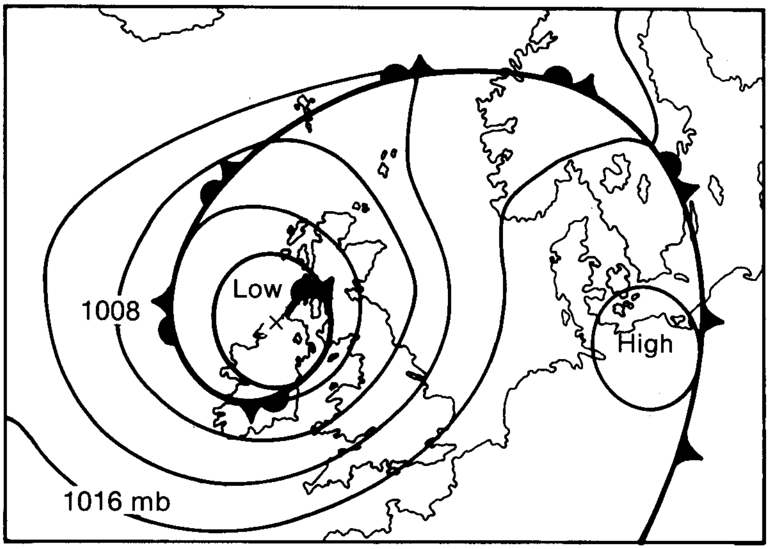

Figure 3. Modified surface analysis for 1200 GMT on 15 August 1985.

in the west of the British Isles and trying to reconcile the surface analysis with the observed weather. This lack of inhibition in drawing occluded fronts should be extended to textbooks showing the life cycle of a depression and, indeed, to the preparation of forecast charts.

551.515.82:551.577.2:551.501.81

Rainfall pattern associated with a split cold front as seen on FRONTIERS*

K.A. Browning

Deputy Director (Physical Research), Meteorological Office, Bracknell

Summary

The radar rainfall pattern associated with a split cold front is used to illustrate the way in which the FRONTIERS display can be used to understand subsynoptic weather systems.

On 5 November 1986, whilst looking over the shoulder of the FRONTIERS operator in the Central Forecasting Office of the Meteorological Office, I saw the interesting radar rainfall pattern shown in Fig. 1 (see Browning (1986) for a description of the FRONTIERS programme); the corresponding surface analysis is shown in Fig. 2. The main feature was a split cold front of the type commonly encountered in the British Isles and described by Browning (1985).

An upper cold front lay from the Humber to the Bristol Channel with the surface cold front in the Irish Sea some 200 km to the north-west. Along the upper cold front there was a band of precipitation extending to medium levels. A combination of visible and infra-red imagery from Meteosat indicated

* FRONTIERS: Forecasting Rain Optimized using New Techniques of Interactively Enhanced Radar and Satellite.

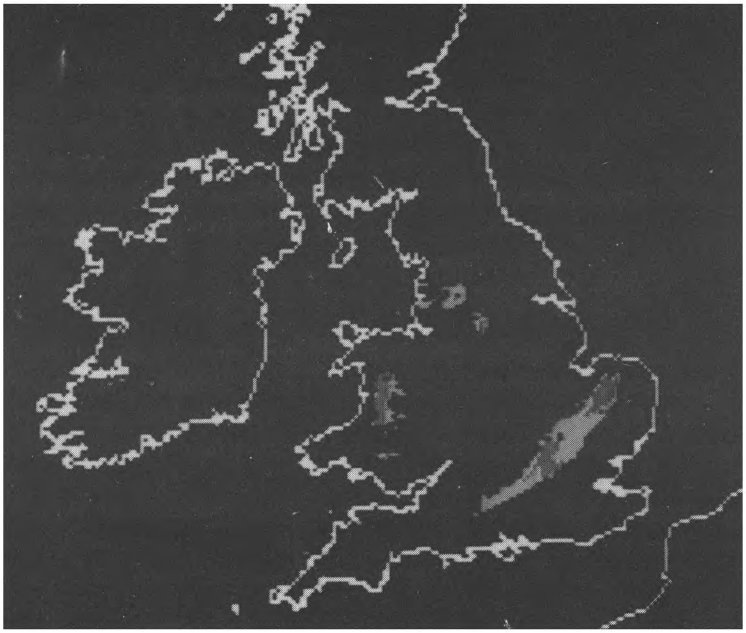

Figure 1. Radar rainfall pattern at 1430 GMT on 5 November 1986 taken from the FRONTIERS display. Light shading < 1 mm h^{-1} and dark shading ≥ 1 mm h^{-1}.

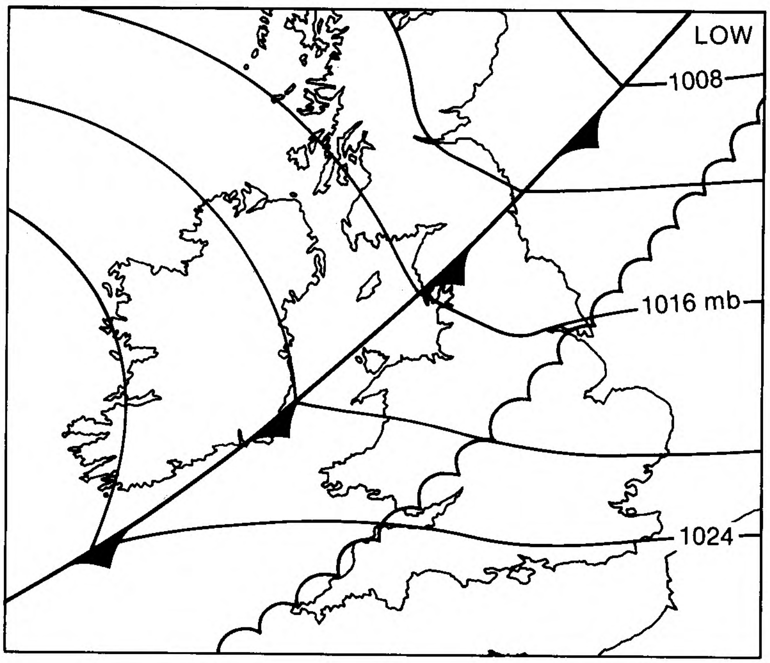

Figure 2. Surface analysis at 1400 GMT on 5 November 1986. The position of the upper cold front as inferred from satellite imagery is shown by a cusped line.

that this precipitation band extended north-eastwards into the North Sea. Between the upper cold front and the surface front there was a shallow moist zone. Satellite infra-red imagery showed the cloud tops in this zone to be no higher than 700 mb. The strong moist west-south-westerly flow at low levels in this zone was generating areas of orographic rain especially over the Welsh hills and the Pennines as shown in Fig. 1. Although patches of drizzle too light to be detected by the radars occurred in some low-lying areas, action replay sequences showed that the main areas of rain in the shallow moist zone remained stationary over the hills — unlike the rain band associated with the upper cold front which travelled rapidly eastwards. An advantage of the FRONTIERS display system is that it enables the operator to compare, replay and otherwise manipulate radar and satellite imagery so that a detailed understanding of subsynoptic weather systems can be built up quickly.

References

Browning, K.A. 1985 Conceptual models of precipitation systems. *Meteorol Mag*, **114**, 293–319.
1986 Weather radar and FRONTIERS. *Weather*, **41**, 9–16.

Reviews

The Bunker climate atlas of the North Atlantic Ocean, Volume 1: Observations, by H.-J. Isemer and L. Hasse. 240 mm × 315 mm, pp. vii + 218, *illus*. Springer-Verlag, Berlin, Heidelberg, New York, Tokyo, 1986. Price DM 275.

The data on which this atlas is based were originally assembled and validated by the late Andrew F. Bunker of the Woods Hole Oceanographic Institution. Bunker, with his co-workers, published several important papers during the mid-1970s on the surface heat budget of the North Atlantic Ocean. However, on his death in 1979 much of his data and results were left in an unpublished state. Isemer and Hasse have obtained Bunker's original computer print-outs, transferred these data to magnetic tape, and used objective analysis techniques, first to reduce the data to a regular grid, and then to draw the charts and graphs contained in this atlas.

This first volume summarizes the basic observations, and these are presented in three formats: firstly as time–latitude diagrams giving the zonally averaged annual variation; secondly as graphs of the mean annual cycle of each variable at 11 characteristic area locations and for the whole North Atlantic; and thirdly, as charts of the monthly and annual means, annual range, and standard deviations. These charts form the major part of the atlas. The variables considered include most of those reported by ships (excluding wave observations): sea surface and air temperature, mixing ratio, relative humidity, air pressure, both total and low cloud cover amounts, and percentage frequency of precipitation reports. The wind field is represented by the mean scalar wind speed, the mean resultant wind velocity vector, the directional steadiness, and the divergence.

A number of the plots tempt one to anticipate the flux data which are to be presented in Volume 2. Charts of the differences in air temperature and in mixing ratio between the air and sea allow one to imagine, for example, the sequence of air-mass transformation as cold, winter-time air from the eastern USA flows out over the Gulf Stream. Although estimating the fluxes from the mean values can be misleading, there are charts of the standard deviations of the thermodynamic variables and the eastward and northward wind components, and it might be possible to estimate, where necessary, a suitable correction factor. That approach, however, would seem a singularly inappropriate use of this atlas since a major feature of Bunker's own work was that he derived the fluxes separately for each individual ship report before performing any averaging. In this respect the atlas will not be complete until Volume 2 is available.

Before the presentation of the graphs and charts, the data set and the analysis techniques are described in a short introductory section. The brief discussion of the accuracy of the data source, the routine reports from the Voluntary Observing Ships, is little more than a warning that errors may exist. Since the authors' stated policy is to leave Bunker's work unchanged as far as possible, they have not applied any corrections to the observations. However, Bunker did apply bias corrections, by adjusting the bulk aerodynamic formulae transfer coefficients, before calculating the fluxes. It will be interesting to see what the authors have chosen for transfer coefficients in calculating the fluxes for presentation in Volume 2. Also briefly summarized in this section is the actual subject of the charts, the climate over the North Atlantic Ocean. Unfortunately, I found that the value of this discussion was diminished by the authors' decision not to quote particular chart numbers. For example, the May sea surface temperature distribution is referred to on page 11 but we are not told that this is chart 10, to be found on page 47. Indeed, a shortcoming of the atlas is that there is no single overall contents list or index. Instead, the contents of each section are hidden away separately (pages 17, 23, and 37), and one is left leafing through the atlas to find a particular chart.

Given that various climatic atlases of the North Atlantic already exist, what then is the value of this particular publication? The authors argue that this atlas is 'unprecedented in the size of the data base and in spatial resolution' and that 'it is based on objective analysis and the most recent understanding of the parameterization of derived quantities such as fluxes of heat and momentum'. The latter argument may apply to Volume 2, but it is not clear that these are the main advantages of Volume 1. Bunker's data set covers the period 1941 to 1972 and was based on the 'TDF-11' data set which has also been used by other authors. The spatial resolution of the data presented is based on a 1-degree grid. However, since these have been derived by interpolating Bunker's results, which were calculated for irregular areas of typical dimensions 2 degrees latitude by 5 degrees longitude, the 1-degree scale data are not, and are not claimed to be, independent. The overall result is that, despite the apparent differences in calculation, comparison of the charts with those in, to take an example, the US Navy *Marine climatic atlas of the world Volume I North Atlantic* (1974 revision), uncovered practically no signficant difference in the isopleths, at least for the random sample which I examined.

Despite the above comments, I believe that this atlas will prove a very important publication. The charts are based on a validated data set for which good documentation is available. Perhaps the most significant factor is that magnetic tapes both of Bunker's results and of the interpolated data are available from the authors. Thus the data set can be used directly as boundary conditions for numerical models. For such usage the wind field is particularly important and it has received especially detailed treatment within the atlas. As a concise summary of the Bunker data set the atlas will receive wide distribution. If, with the increasing emphasis on climate research, this results in an increased use of Bunker's data set it will be no more than a fitting tribute to his efforts. It will also reward the considerable work performed by Isemer and Hasse in making Bunker's results so readily available.

P.K. Taylor

Floodshock: the drowning of planet earth, by A. Milne. 172 mm × 246 mm, pp. 224, *illus*. Alan Sutton Publishing Ltd, Gloucester, 1986. Price £12.95.

The history of the human race contains many unhappy events. Some are undoubtedly of our own making; others represent natural catastrophes in which the efforts of mankind are overwhelmed and belittled by the forces of Nature. Perhaps the most potent threat is that posed by flooding, a view that is put forward in *Floodshock: the drowning of planet earth*. This somewhat disorganized book by Antony Milne, an environmental scientist whose credentials include an involvement with NATO's Committee on the Challenges of Modern Society, would have had more impact had the contents been arranged either chronologically or strictly thematically. Instead, legends concerning a great flood give way to discredited theories about the legends, which in turn precede an account of more acceptable ideas before returning to the legends again. The sea, storms, rivers and dams are the subjects for much of the remainder of the book. The author's aim of alerting the public to the immense destruction that can be accompanied by flooding, a fact that is not generally appreciated in this country, is only partially successful.

Descriptions of some of the world's most devastating water-related incidents commence with the most famous of all floods. The western civilizations are familiar with this through the account in Genesis, but other cultures (such as the Sumerians, Indians and Chinese) recount similar legends. Did it really occur or is it an abstruse piece of theology? Spurred on by the well publicized findings of an archaeological expedition half a century ago at Ur, in Iraq, the book proceeds as if it did and we are led into various theories, some more plausible than others, that might explain the Great Flood. The Biblical explanation of forty days and nights of rain is dismissed as being insufficient; it is also probable that it is an allegory. From the time of Plato to the present day, there seems to have been no shortage of alternative ideas, some of the more recent being the effect of a celestial object passing too close to the earth — the pole shift theory and the melting ice caps theory.

Our attention is then turned from a legendary flood to more recent and better-documented catastrophes in which the sea has played a major part. Nature has extracted a high price for man's desire to create communities in close proximity to the sea, not only altering its average depth but also producing hazards such as surges, tides and tsunami. The tragic consequences are highlighted in selected examples from around the world.

Storms are the subject matter of the next chapter and we learn that it is usually the poorest countries that are most at risk from cyclones and hurricanes. In spite of the Bay of Bengal's history of being a favoured location for devastating cyclones, the loss of life that they cause in that region is still very high. Even when accurate forecasts of impending conditions are broadcast, there is usually nowhere to which the population can flee.

The most ruthless and effective destroyer of life and property is the subject considered next. Rivers have the ability to change quickly from slow, meandering waterways into fast-moving, uncontrollable mixtures of water, rock and debris that can destroy most structures in their path. This devasting power cannot be illustrated more clearly than by considering the reputation of the Hwang Ho (Yellow River) in China to have claimed the lives of more people than any other agent of natural disaster anywhere in the world. Indeed, in just one year, it was responsible for the deaths of seven million people. By comparison, perhaps the best known of Britain's river disasters, that at Lynmouth, Devon in 1952, resulted in 24 deaths. It is entirely probable that the lack of a recent major flooding tragedy in Britain is the reason why the public consider a flood to be 'the least of their worries', even when living in notoriously flood-prone areas. Or could it be because they have faith in our ability to forecast flood-producing conditions sufficiently far in advance for preventive measures to be taken?

In attempting to control rivers or harness their energy, large numbers of dams have been built. Ironically this has led, in several cases, to an increased risk of flooding due to the 'dangerous state of disrepair' of many of them. Recent disasters include the failure of the split-elevation dam at Stava, northern Italy in 1985 which killed 230 people.

Our desire to improve upon the environment in which we find ourselves goes far beyond dam building. In *Floodshock*, the massive Soviet project whereby Siberian rivers will be diverted to irrigate the arid lands of central Asia is described. What are the consequences on global climate of such 'earth-shaping' plans? Of more immediate interest are the climatic implications of deforestation, and Milne argues that this will lead to more floods.

Although aimed at the 'popular' market, the scope of the book is quite large, and various aspects of meteorology, climatology, hydrology, history, geology and astronomy are mentioned. It is well endowed with black-and-white illustrations, and an up-to-date bibliography and comprehensive index complete the book. The diversity of topics has led to some serious errors, for example, a front is described as 'a belt of air of a consistent temperature'. Also, 'ridges of low pressure' are mentioned as are 'jet streams —sometimes known as circumpolar vortexes'. We learn that 'the total mass of humanity now weighs about 180 million tonnes, more than half the total mass of the earth'. And if 'the reason the Sahara receives hardly any rain at all from one year to the next is because the sun burns so fiercely it can actually vaporize any tiny clouds that do appear', why is it that 'the areas of highest rainfall are at the equator'? Additionally, the author's tendency to hyperbolize has apparently gone unchecked and this further detracts from the book from a professional viewpoint. By its very nature, much of the content has appeared elsewhere; nevertheless, the publication of a book solely on the flood hazard is to be welcomed. Time will tell whether the threat of flooding is 'the least of our worries'.

M.S. Shawyer

Cloud investigation by satellite, by R.S. Scorer. 165 mm × 235 mm, *illus.* Ellis Horwood Ltd, Chichester, 1986. Price £39.50.

Professor Scorer is renowned for his classical work on the interpretation of clouds as viewed from the surface of the earth. In his latest book, although the source of the images changes to space-based systems, the philosophy of using them to analyse the dynamics of the atmosphere remains the same. In this approach lies the deep rift between the ubiquitous coffee-table books with their stunning colour pictures and vacuous texts, and this one, in which modest monochromatic images are used to illustrate a tutorial on the mechanics of the atmosphere.

However, the success of even a book such as this, depends upon the quality of its images. Poor visual material could easily obscure a point rather than clarify it. The economic balance between the price of the book and the sumptuosity of its production, and hence the clarity of its images, must have been difficult to achieve. I feel that the publishers have been largely successful. It is true that the images presented do not have the remarkable quality of the originals created at the University of Dundee. However, for the most part, they are clear enough to do the job of illustrating each point made by the author. They are certainly much better than the grubby bits of facsimile paper seen on the benches of our forecasting offices!

Professor Scorer selects most of his material from the images produced by the Advanced Very High Resolution Radiometer situated aboard the TIROS-N series of polar-orbiting satellites. Occasional images from the Ocean Colour Monitor on NIMBUS-7 are also used. The images produced by these instruments have spatial resolutions of about one kilometre, thereby allowing details of even mesoscale weather systems to be studied. One chapter is devoted to the Japanese geostationary satellite Himawari (which means sunflower).

The book is not a systematic treatment of all cloud imagery. Instead, the author has selected a pot-pourri of topics ranging from the traditional meteorology of 'cloud streets and cells' to the more exotic of 'condensation trails'. The satellite images used profusely to illustrate each topic are accompanied by thought-provoking and informative text.

Many of the pictures presented are visually stunning. I enjoyed an image showing cloud streets that were one thousand kilometres long and a few kilometres wide, and go on to merge with extensive cellular cloud. I suspect that this might make salutary viewing for the atmospheric modellers.

My adverse comments are few. Occasionally, more assistance is required to locate within the picture the geographical references of the text. One or two of the images are rather featureless. More importantly, while it is clear that much patient work has gone into a dynamical reconciliation of imagery and observational data, the reader is denied any access to the latter. Figures showing relevant facets of the behaviour of the atmosphere would have been useful.

Professor Scorer does not appreciate the serious uses of colour to enhance satellite images, finding them 'great fun and...popular with the media', a somewhat damning indictment. However, it was John Ruskin (*Stones of Venice* (1851–53)) who noted that 'The purest and most thoughtful minds are those which love colour the most.'

R.J. Allam

Books received

The listing of books under this heading does not preclude a review in the Meteorological Magazine at a later date.

Climate of Antarctica, edited by I.M. Dolgin, translated from Russian by M. Nataraja Pillai (Rotterdam, A.A. Balkema, 1986. Hfl 95.00, US $38.00, £27.50) presents papers read at the All-Union Symposium on the study of the climate of Antarctica during the last 20 years, at which the contributors highlighted the different stages of development of the aerometeorological studies taking place in that region. These papers describe certain new aspects in climatic study, such as the problem of the heat and moisture exchange, the mechanism of atmospheric circulation and the assessment of the relative severity of the climate of different regions of Antarctica, which is examined here for the first time. Other articles include the inflow and outflow of radiational heat energy, new information on the total content of ozone, carbon monoxide and methane in the atmosphere of Antarctica, and the application of statistical methods and computer techniques to the study of the structure of the atmosphere.

The physics of atmospheres, (second edition) by J.T. Houghton, (Cambridge University Press, 1986. £27.00, US $54.50 (hardback), £9.95, US $16.95 (paperback)) is a revision of the first edition of this textbook in order to bring it completely up to date. Several factors have led to vigorous growth in the atmospheric sciences, particularly the availability of powerful computers for detailed modelling, the investigation of the atmospheres of other planets, and techniques of remote sensing. The physical processes governing the structure and circulation of the atmosphere are described. Simple physical models are constructed by applying the principles of classical thermodynamics, radiative transfer and fluid mechanics, together with analytic and numerical techniques. These models are applied to real planetary atmospheres.

Remote sensing for resource development and environmental management, edited by M.C.J. Damen, G. Sicco Smith and H.Th. Verstappen, (Rotterdam, A.A. Balkema, 1986. Hfl 265.00, £82.00) consists of two volumes (with a third promised) containing the proceedings of the seventh international symposium on remote sensing for resources development and environment management, held in August 1986. There are many papers presented under the general headings: visible and infra-red data, microwave data, spectral signatures of objects, renewable and non-renewable resources, hydrology, and human settlement. Many of the latest techniques in different disciplines are discussed in contributions from world-wide authors.

Satellite photograph — 17 October 1986 at 0300 GMT

This picture was taken from the infra-red channel on the NOAA-9 satellite and shows thunderstorms affecting coastal areas of the western Mediterranean, in particular the holiday areas from the Costa Brava to the Costa Blanca, and the Balearic Islands. Highest reported 6-hour rainfall totals in the period from midnight included 51.0 mm at Cap Bear, France (a few kilometres north of the border with Spain). Nearby Perpignan only managed 14.6 mm in the same period. Further south, Alicante recorded 45.0 mm during the previous 6-hour period from 1800 GMT, followed by another 11.0 mm after midnight.

Images such as this can be analysed in detail in the Satellite Meteorology Branch of the Meteorological Office. The infra-red channel indicates the temperature of the surface being viewed and images can be calibrated so that the temperature in °C of a particular spot (or pixel) can be read directly. As an example, the two most northerly large cloud masses, situated over the Costa Brava, were examined. The more northerly one shows a storm at its maximum development with cloud-top temperatures around −60 °C, indicating a height in excess of 40 000 ft (12 000 m). The other cloud mass shows a decaying storm with cirrus streaming away to the north-west with cloud-top temperatures around −54 °C.

The synoptic pattern was not particularly menacing, with relatively low pressure over north Africa and a mainly light easterly flow over the western Mediterranean. The 1000–500 mb thickness pattern showed a weak warm ridge over the area. However, the air within the lower part of this layer was very moist and relatively warm, a recognized precursor to thunderstorm activity. By contrast, the air over Italy was very dry (less than 35% relative humidity at 700 mb compared with over 85% in the thundery area) and the resulting clear conditions allow rivers, lakes and snow-covered mountains to stand out clearly.

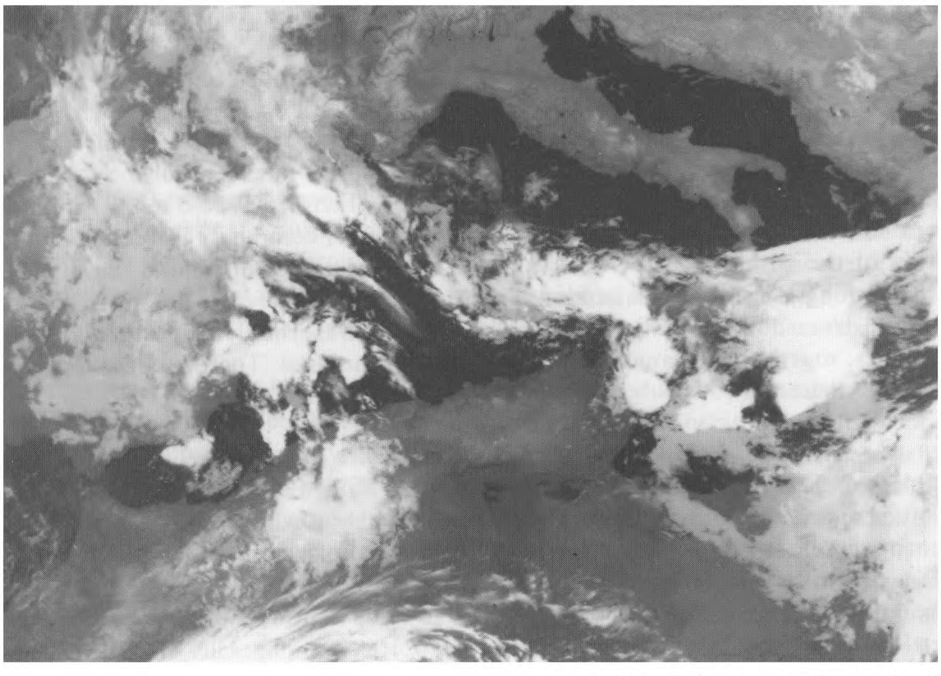

Photograph by courtesy of University of Dundee

Meteorological Magazine

GUIDE TO AUTHORS

Content

Articles on all aspects of meteorology are welcomed, particularly those which describe the results of research in applied meteorology or the development of practical forecasting techniques.

Preparation and submission of articles

Articles for publication and all other communications for the Editor should be addressed to the Director-General, Meteorological Office, London Road, Bracknell, Berkshire RG12 2SZ and marked 'For *Meteorological Magazine*'.

Articles, which must be in English, should be typed, double-spaced with wide margins, on one side only of A4-size paper. Tables, references and figure captions should be typed separately.

Spelling should conform to the preferred spelling in the *Concise Oxford Dictionary*.

References should be made using the Harvard system (author, date) and full details should be given at the end of the text. If a document referred to is unpublished, details must be given of the library where it may be seen. Documents which are not available to enquirers must not be referred to.

Tables should be numbered using roman numerals and provided with headings. We consider vertical and horizontal rules to be unnecessary in a well-designed table; spaces should be used instead.

Mathematical notation should be written with extreme care. Particular care should be taken to differentiate between Greek letters and Roman letters for which they could be mistaken. Double subscripts and superscripts should be avoided, as they are difficult to typeset and difficult to read. Keep notation as simple as possible; this makes typesetting quicker and therefore cheaper, and reduces the possibility of error. Further guidance is given in BS1991: Part 1: 1976 and *Quantities, Units and Symbols* published by the Royal Society.

Illustrations

Diagrams must be supplied either drawn to professional standards or drawn clearly, preferably in ink. They should be about 1½ to 3 times the final printed size and should not contain any unnecessary or irrelevant details. Any symbols and lettering must be large enough to remain legible after reduction. Explanatory text should not appear on the diagram itself but in the caption. Captions should be typed on a separate sheet of paper and should, as far as possible, explain the meanings of the diagrams without the reader having to refer to the text.

Sharp monochrome photographs on glossy paper are preferred: colour prints are acceptable but the use of colour within the magazine is at the Editor's discretion. In either case contrast should be sufficient to ensure satisfactory reproduction.

Units

SI units, or units approved by WMO, should be used.

Copyright

Authors wishing to retain copyright for themselves or for their sponsors should inform the Editor when they submit contributions which will otherwise become UK Crown copyright by right of first publication.

It is the responsibility of authors to obtain clearance for any copyright material they wish to use before submitting it for publication.

Free copies

Three free copies of the magazine are provided for authors of articles published in it. Separate offprints for each article are not provided.

Meteorological Magazine

January 1987

Vol. 116
No. 1374

CONTENTS

Contributions: it is requested that all communications to the Editor and books for review be addressed to the Director-General, Meteorological Office, London Road, Bracknell, Berkshire RG12 2SZ, and marked 'For *Meteorological Magazine*'. Contributors are asked to comply with the guidelines given in the *Guide to authors* which appears on the inside back cover. The responsibility for facts and opinions expressed in the signed articles and letters published in *Meteorological Magazine* rests with their respective authors. Authors wishing to retain copyright for themselves or for their sponsors should inform the Editor when submitting contributions which will otherwise become UK Crown copyright by right of first publication.

Subscriptions: Annual subscription £27.00 including postage; individual copies £2.30 including postage. Applications for postal subscriptions should be made to HMSO, PO Box 276, London SW8 5DT; subscription enquiries 01–211 8667.

Back numbers: Full-size reprints of Vols 1–75 (1866–1940) are available from Johnson Reprint Co. Ltd, 24–28 Oval Road, London NW1 7DX. Complete volumes of *Meteorological Magazine* commencing with volume 54 are available on microfilm from University Microfilms International, 18 Bedford Row, London WC1R 4EJ. Information on microfiche issues is available from Kraus Microfiche, Rte 100, Milwood, NY 10546, USA.

ISBN 0 11 727965 X

ISSN 0026–1149

Printed for HER MAJESTY'S STATIONERY OFFICE
by Delco Printing Co Ltd 12/86 Dd. 739131 C14

THE METEOROLOGICAL MAGAZINE

HER MAJESTY'S STATIONERY OFFICE

February 1987

Met.O.978 No. 1375 Vol. 116

METEOROLOGICAL OFFICE Met.O.978

THE METEOROLOGICAL MAGAZINE

No. 1375, February 1987, Vol. 116

551.509.58:629.7:662.75

Impact of weather forecasts on aviation fuel consumption*

P.W. White

Deputy Director (Dynamical Research), Meteorological Office, Bracknell

Summary

The Meteorological Office has developed a computer-based weather forecasting system for civil aviation that permits the provision of weather forecasts for aircraft anywhere in the world. Information provided by airlines indicates that they are saving an additional £50 million per year through reduced aviation fuel consumption directly related to the improved forecasts.

Civil aviation requires a wide range of weather forecasts from meteorological services. The main types of forecasts are as follows:

(a) Forecasts of route winds, temperatures and weather for flight planning.

(b) Warnings of adverse weather for in-flight operations (e.g. moderate to severe turbulence, icing, thunderstorms, low-level wind shears and cloud covering hill tops) and the handling of aircraft and passengers on the ground (e.g. strong cross-winds, heavy rain and standing water, fog and snow).

(c) Landing forecasts of the weather expected at the destination and at suitable diversions to ensure that sufficient fuel is loaded.

(d) Weather forecasts issued to air traffic control authorities so that they can ensure that a safe distance between aircraft is maintained.

The provision of these services by the Meteorological Office relies upon the forecasts produced by their global, numerical forecasting system. In some cases the computer forecasts are used direct (e.g. for route forecasts) whilst for other services the forecasters have to interpret the computer products before issuing forecasts.

During the last decade there has been a clear and continuous reduction in the error of the forecasts to the extent that, in terms of the correlation of actual and predicted atmospheric changes, forecasts for 3 days ahead are now as accurate as 1-day forecasts were only a decade ago. A particularly marked improvement occurred in 1982 when the present global 15-level forecasting model came into operation; the root-mean-square forecast errors fell by 15% for winds and by about 30% for temperatures. These improvements have had a beneficial effect on the services provided to civil aviation. In particular they have allowed airlines to make considerable savings on aviation fuel consumption.

---

* Taken from a lecture following the presentation of the Royal Society ESSO Award for 1986 to a team from the Meteorological Office.

Aircraft fuel savings can be achieved in a number of ways. The most obvious of these is to use the forecast winds and temperatures for planning the most economical route between the departure and destination airfields, taking advantage of favourable winds and avoiding unfavourable ones. The freedom to choose such tracks only exists over oceanic sectors of the flights; over land the density of air traffic necessitates strict air traffic control and the confinement of air movement to predefined air lanes. Accurate forecast information can, nevertheless, allow airlines to calculate their expected fuel burn over the land flight sectors. By taking on board an appropriate fuel load the aircraft can avoid transporting excessive quantities of fuel, or alternatively avoid making intermediate unscheduled refuelling stops because of unexpected wind conditions.

The principal difficulty in carrying out a survey of fuel savings achieved by airlines is the lack of firm figures that can be used in the calculation. Despite this problem, independent calculations based on the experience of two airlines have been made.

The extent of airline operations can be measured by the amount of revenue tonne kilometres (RTK), defined by the product of the weight conveyed and distance flown on revenue earning flights summed over a year. For the 23 major airlines using forecast data supplied by the Meteorological Office for their flight planning procedures, the total RTK is 80 996 million. Scandinavian Airline Systems (SAS) have a RTK of 1473 million and have reported a fuel saving (directly attributable to the improved forecasts) of 35 kg per hour of flight as an average over all their operations; over a year this saving amounts to £2 million. Assuming that all airlines have the same pattern of operations as SAS, this would imply a total saving by the 23 airlines of £110 million. However a conservative and more realistic estimate of annual saving would probably be about half this figure, say £50 million per year.

British Caledonian Airways estimate that savings on their transatlantic flights have amounted to 2% of fuel used. Since the total annual cost of fuel consumed by airlines for operations over the ocean is about £2000 million, the saving, if extrapolated to apply to all transatlantic flights, is equivalent to £40 million. If savings achieved elsewhere are added to this, a saving of around £50 million per year is obtained once again. The consistency of the two calculations gives some confidence to the estimates.

Fuel savings that may arise from accurate weather forecasts are appreciably smaller than the potential savings from improved aircraft and engine technology (figures as high as 10–20% have been quoted). However, against this must be set the cost of achieving these savings. The 23 airlines mentioned above possess over 2500 aircraft. The cost of replacing these with new technology aircraft would be at least three orders of magnitude greater than a 10-year research programme at the Meteorological Office devoted to improving aviation forecasting. These figures indicate that for civil aviation the meteorological services provide excellent value for money.

The Royal Society Esso Energy Award

The Royal Society Energy Award for 1986 was presented on Monday 13 October 1986 to a team from the Meteorological Office for their development of a world-wide forecasting model providing accurate information on winds and temperatures to the civil aviation industry, so that flight paths and patterns can be selected to use the minimum amount of fuel. It has been estimated that the extra fuel saved as a result of the improved forecasts is worth at least £50 million per annum.

Dr P.W. White, Dr M.J.P. Cullen, Dr A.J. Gadd, Mr C.R. Flood, Dr T.N.Palmer, Mr K.Pollard and Dr G.Shutts received the Award comprising a gold medal and prize of £2000 from Sir George Porter, President of the Royal Society. Photographs of the award winners, the gold medal and the citation are shown opposite.

The Royal Society Esso Energy Award winners with Sir George Porter (President of the Royal Society) and Mr A.W. Forster (Chairman and Chief Executive of ESSO UK plc), left to right: Dr A.J. Gadd, Mr A.W. Forster, Mr C.R. Flood, Dr M.J.P. Cullen, Sir George Porter, Dr P.W. White, Dr T.N. Palmer, Mr K. Pollard and Dr G. Shutts.

Gold medal presented to the winners of the Award.

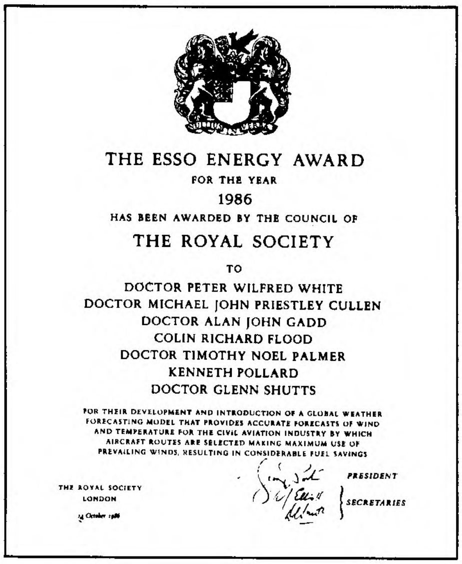

THE ESSO ENERGY AWARD
FOR THE YEAR
1986
HAS BEEN AWARDED BY THE COUNCIL OF
THE ROYAL SOCIETY
TO
DOCTOR PETER WILFRED WHITE
DOCTOR MICHAEL JOHN PRIESTLEY CULLEN
DOCTOR ALAN JOHN GADD
COLIN RICHARD FLOOD
DOCTOR TIMOTHY NOEL PALMER
KENNETH POLLARD
DOCTOR GLENN SHUTTS

FOR THEIR DEVELOPMENT AND INTRODUCTION OF A GLOBAL WEATHER FORECASTING MODEL THAT PROVIDES ACCURATE FORECASTS OF WIND AND TEMPERATURE FOR THE CIVIL AVIATION INDUSTRY BY WHICH AIRCRAFT ROUTES ARE SELECTED MAKING MAXIMUM USE OF PREVAILING WINDS, RESULTING IN CONSIDERABLE FUEL SAVINGS

THE ROYAL SOCIETY
LONDON
14 October 1986

PRESIDENT
SECRETARIES

The citation presented to the winners of the Award.

551.515.81

The mesoscale frontal dynamics project*

S.A. Clough
Meteorological Office, Bracknell

Summary

Cold fronts are among the most important weather features affecting western Europe. In the last 2 years a number of research groups, particularly in the United Kingdom and France, have set up an intensive programme of theoretical and experimental study of the processes occurring in frontal systems. This article describes the scope of this programme, which will culminate in an international field experiment in the autumn of 1987.

1. Introduction

Over the past few years much progress has been made in understanding the physical processes involved in the formation and maintenance of fronts, problems which occupy a major position in mesoscale meteorology and short-term forecasting. The process of frontogenesis occurs as an inevitable consequence of the development of a baroclinic wave and involves a cascade of energy to smaller scales. The primary and secondary processes of baroclinic instability and frontogenesis take place on scales which can loosely be described as synoptic scale and mesoscale. Ageostrophic circulations associated with fronts imply regions of ascent and descent and, in the presence of moisture, the formation of cloud and precipitation follow. The part played by such moist processes is currently a topic of much attention both in numerical weather forecasting and theoretical studies of frontal dynamics. The cloud organization is itself a phenomenon spanning several scales with both mesoscale and small-scale motions being involved, as well as the scales introduced in the microphysics of precipitation growth. Slantwise and upright convection are invoked to distinguish the varying importance of Coriolis and buoyant forces on the mesoscale and smaller scales. The energy cascade progresses to finer scales leading to turbulence and ultimately dissipation, particularly in transition regions like the tropopause, frontal zones and the boundary layer.

Three developments have brought the mesoscale to the forefront of meteorology in recent years. Firstly, advances in computer technology have allowed ever-increasing resolution in numerical prediction models to a point where, even in synoptic-scale forecast models, accurate representation of mesoscale features such as fronts becomes necessary. Secondly, observational techniques, such as dual Doppler radar, VHF radar wind profilers and dropsondes, have been developed to provide a capability for detailed kinematic and thermodynamic measurements on the mesoscale, while routine coverage by weather radar networks and satellites is also improving. Thirdly, advances in the theory of frontogenesis and mesoscale instabilities are showing that the hitherto vague notion of the mesoscale can be better defined from a dynamical viewpoint, so that a proper understanding of these phenomena is beginning to emerge.

Mesoscale meteorology is receiving increased attention world-wide. Notable projects outside Europe include the CYCLonic Extratropical Storms (CYCLES) Project for the study of fronts in the USA, the Cold Fronts Research Programme in Australia, and also the planned Genesis of Atlantic Lows Experiment (GALE) and National STORM Programme in the USA where mesoscale meteorology is being given high priority following a recommendation of the National Academy of Sciences and a series

* This article is a synthesis of reports by the British and French Steering Groups.

of workshops that began in 1977. A sizeable research effort is dedicated to mesoscale problems in Europe also, and it is now timely to bring together this effort in coherently related studies concentrating specifically on cold fronts, particularly active ones. Study of these systems lends itself to such an international collaboration because of the geographical scale necessary to define the synoptic environment and the range of expertise and facilities necessary to understand the complex interplay of processes occurring near cold fronts.

The area centred on the Channel between England and France offers a natural setting for such an experiment, being quite well served by the combination of British and French routine observing networks. As well as the leading contributions to the project from many British and French scientists, it is expected that groups from other western European countries will participate in the project, and such collaboration is welcomed. Groups from the Federal Republic of Germany and Switzerland, for example, have been involved in discussions, and German aircraft, radiosonde and other facilities will be contributing to the field experiment. The British effort, the Mesoscale Frontal Dynamics Project (MFDP), is co-ordinated by a steering group made up of Dr K.A. Browning (Chairman) and Dr P.R. Jonas of the Meteorological Office, and Prof. B.J. Hoskins and Dr A.J. Thorpe of the University of Reading, while Dr J. Testud leads the French team in the parallel FRONT 87 programme.

Active cold fronts like the one illustrated in Fig. 1 are important from several viewpoints. They are ubiquitous features of the weather in north-western Europe, giving a substantial fraction of the precipitation in this area during autumn and winter, and often giving rise to other significant weather such as abrupt changes in wind, temperature, cloud base and visibility. Over the October–December period about two active systems would be expected in a month. The need for monitoring and very-short-range forecasting of systems such as these are two of the reasons for setting up networks of European radars, the integration of which is being considered as part of the COST-72 (European Co-operation in Science and Technology) project.

The specific scientific objectives of the present project are:

(a) To obtain an improved dynamical understanding of synoptic, mesoscale and smaller-scale interactions within systems containing cold fronts, especially active ones.

(b) To acquire mesoscale data sets and use them for the further development of numerical models and the parametrizations in them.

(c) To describe the structure and evolution of mesoscale features in cold fronts, within the full synoptic context, and to derive conceptual models of value in very-short-range forecasting (00–12 h).

It is envisaged that, in the course of the experiment, substantial practical benefit will be derived from the progress made in developing and evaluating new techniques of observation and forecasting. Other scientific objectives will be pursued as far as can be accommodated practicably, e.g. chemical, microphysical or radiative measurements.

On the basis primarily of British and French proposals a composite plan has been developed, detailing the main dedicated resources and their likely deployment. A contribution from the Federal Republic of Germany has also been incorporated into this plan. The project timetable allows a period of 2 years for the necessary logistical development to the experimental phase; during this time the theoretical programme described in Section 2 will be in progress to assess existing theories and models, and provide testable hypotheses for the observational stage described in Section 3.

2. The theoretical programme

The main emphasis of the theoretical programme will be on the general theory of baroclinic instability and frontogenesis from the synoptic scale to the scales of cloud and turbulence, and the influence of

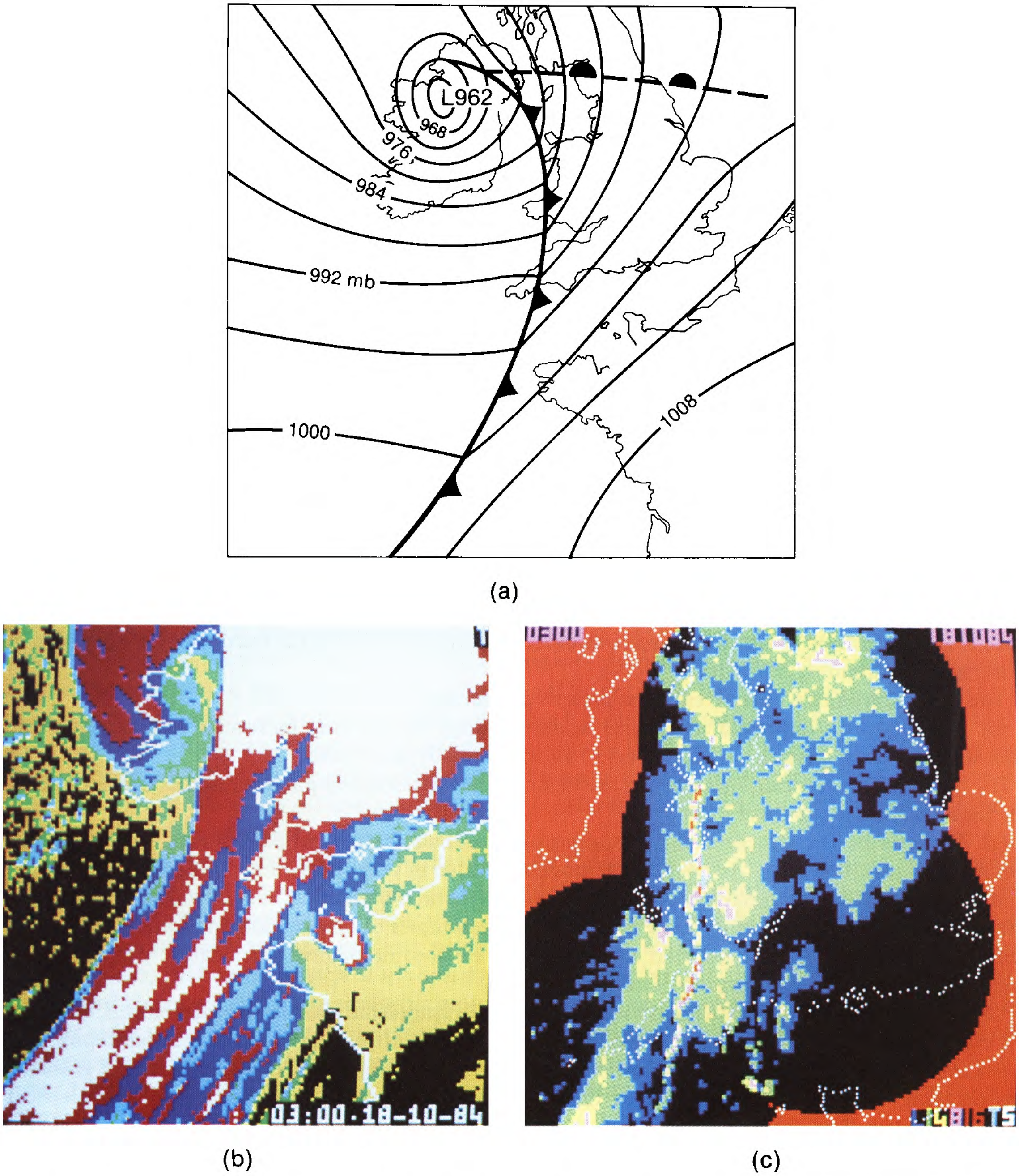

Figure 1. A case of line convection at an active surface cold front on 18 October 1984: (a) surface pressure pattern at 03 GMT, (b) Meteosat infra-red image at 03 GMT: white and red denote high cloud; dark and light blue, medium cloud; green and yellow, low cloud or cold land; black, sea or warm land and (c) radar network observations at 03 GMT: within the network area pink, red and light blue denote heavy rain; yellow and green, moderate rain; dark blue, light rain. The heaviest precipitation occurs at the position of the analysed cold front, while the satellite image shows much of the upper cloud shield behind the surface front.

latent heating and convective structure. Of central importance is the interaction between processes with different scales:

(a) Motion on the synoptic scale can be described by the quasi-geostrophic approximation, which leads to a length scale

$$L \approx NH/f$$

where L and H are the horizontal and vertical length scales, N the Brunt–Väisälä frequency and f the Coriolis parameter. For circulations with scale H corresponding to the depth of the troposphere, $L \approx 1000$ km. Such scales require, for a complete definition, observations at a spacing of less than 300 km.

(b) On the mesoscale, fronts can be described by the semi-geostrophic approximation in which ageostrophic advection is important. Although not directly describable by these equations, moist slantwise convection is believed to occur on a similar scale. Suitable scale analysis suggests that the horizontal scale of mesoscale motion is

$$L \approx U_g/f \approx 100 \text{ km}$$

where U_g is the geostrophic wind. Such scales require observations at a spacing of 20–30 km in the horizontal for their specification. Vertical variations on small scales are often present and observations at 300 m in the vertical may be required to describe slantwise convection adequately.

(c) Smaller-scale processes such as line convection at cold fronts, embedded convective cores within slantwise ascent and gravity waves generated by convection or other processes, generally have $L \approx H \approx 1$ km. Hydrostatic balance is no longer valid for this scale, and observations with horizontal and vertical spacing of not more than a few hundred metres are required to resolve it adequately. On an even smaller scale there are the turbulent processes which provide a cascade of energy that ultimately results in dissipation at the molecular scale.

It is the aim of this project to describe the important interactions between these scales of motion at fronts. For example, phenomena such as rain bands can only occur given an appropriate synoptic environment, while the feedback of such organized convection on the synoptic scale may significantly influence frontal development.

2.1 *Baroclinic instability and frontogenesis*

There have been many studies in two and three dimensions of the life cycle of a baroclinic wave and the consequent frontogenesis but several areas still remain to be clarified, even before moist processes are considered.

Three-dimensional aspects of frontal structure. It is a common occurrence that a quasi two-dimensional cold front approaching north-west Europe will develop a wave on the scale of a few hundred kilometres. This problem was identified by the Bergen school of meteorologists and indeed led to the Norwegian polar front model of cyclogenesis. However, only a limited understanding exists of the dynamics of this process or of the mechanisms leading to differences between fronts distinguished as anafronts or katafronts. It is possible, for example, that wave development is accelerated or indeed is caused by the redistribution of heat and potential vorticity produced by moist and boundary-layer processes. Also it is not clear whether this wave development problem is adequately treated by present operational models. If such a development occurs in the field phase of the project, it would present a valuable opportunity to obtain a three-dimensional observational data base for detailed study.

The interaction of ageostrophic circulations linking upper and lower frontogenesis is also of interest. It is believed that the position of the upper jet core relative to the surface front is of critical importance in providing conditions suitable for the generation and release of convective and potential instability. For example, if the upper jet exit region is to the west of, and aligned along, the surface front it seems possible that upright convection at the surface front may be of limited depth while slantwise convection is enhanced. The mechanism of these processes is an important element in understanding the organization of smaller-scale structures within the synoptic scale.

The concept of geostrophic or other dynamical balance underlies almost all theoretical ideas on synoptic-scale motions, such as Sutcliffe's development theory or the *Q*-vector method. It is of some importance to obtain observational evidence about the extent and nature of departures from the balanced state, particularly in mobile features such as jet streaks. The provision of well-resolved dynamic and thermodynamic fields by the observational programme will be valuable for this purpose.

Role and structure of the boundary layer and frontal discontinuity. In the neighbourhood of an active surface cold front, air parcels undergo large accelerations through flow patterns similar to the schematic of Fig. 2. Frictionally induced ageostrophic flow in the planetary boundary layer is believed to be an important contribution to the gross cross-frontal ageostrophic circulation. In any quantitative account of the frontal dynamics it is thus important to determine the magnitude of the ageostrophic boundary-layer flux and its relation to the boundary-layer structure. The observational programme should provide measurements of the mean boundary-layer flow and turbulent structure. These details will be essential to the diagnosis of numerical models and their boundary-layer schemes.

It is important to describe the role and structure of the boundary layer in the regions where a front is in contact with the surface. Understanding of the disturbed boundary layer, particularly in regions of convection, such as may occur at sharp surface cold fronts, is only at an early stage of development.

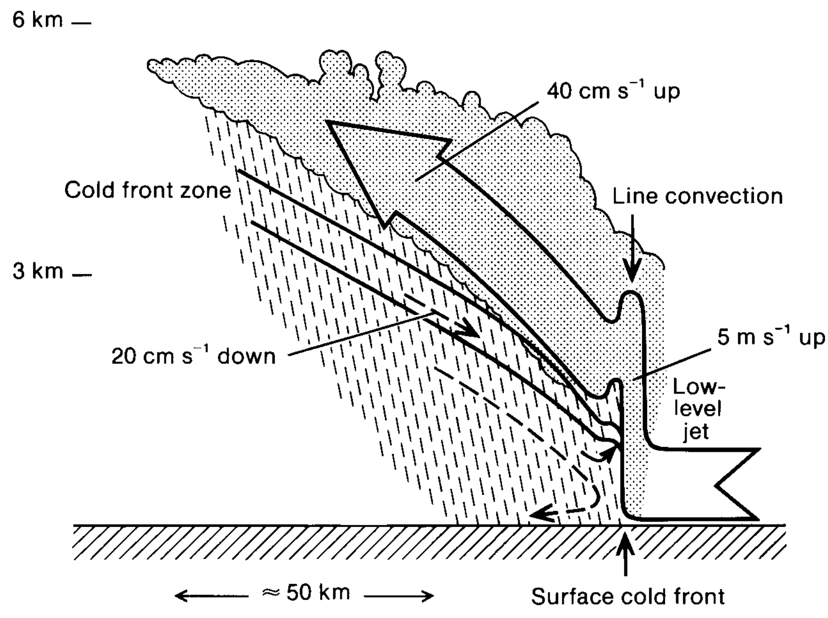

Figure 2. Schematic cross-section of a vigorous cold front (anafront) illustrating the main air flows near the surface front (after Browning 1985).

Further studies using more elaborate boundary-layer theories and models which can be verified against highly resolved wind and temperature data are required.

Frontal theories suggest that a discontinuity will tend to be formed at a boundary, and the modelling of this structure is a challenging problem. As the scale reduces, turbulent stresses and gravity-wave generation become of critical importance and observations may help to decide between differing theories of frontal collapse. Theoretical work is continuing on these problems and it is desirable to observe the process of collapse through *in situ* turbulence measurements in the field programme.

2.2 *Convective structure and the influence of moist processes*

The structure of cloud and precipitation characteristic of active cold frontal zones is indicated in Fig. 3. The role of moist processes is a matter of current research and is a central topic in the project. It is believed that in the frontal zone the synoptic-scale sloped convection of the primary baroclinic wave becomes intensified in moist slantwise convective structures such as rain bands. The scale of such convection is evidently mesoscale (≈ 100 km) and theories and models of moist slantwise convection are producing testable hypotheses for the field experiment.

Upright moist convection (with a scale of about one kilometre) is found embedded within the slantwise convection and at the surface cold front. The pattern of such convection suggests that two-dimensional cloud models with frontal forcing may be able to model these structures, and such research is envisaged. The interaction of slantwise convection, upright convection and synoptic forcing is of major interest, both in the atmosphere and in synoptic or mesoscale model representations.

Several interesting features of the dynamical structure in Fig. 2 are commonly observed: a low-level jet immediately ahead of the front, a nose of cold air resembling a density current and a narrow band (2–5 km) of vigorously precipitating line convection. The dynamics of line convection at active cold fronts is of considerable interest and so theoretical and numerical models of this phenomenon are being developed. A major objective will be to generalize squall-line and line-convection dynamics into a comprehensive theory, consistent with both detailed models and observations.

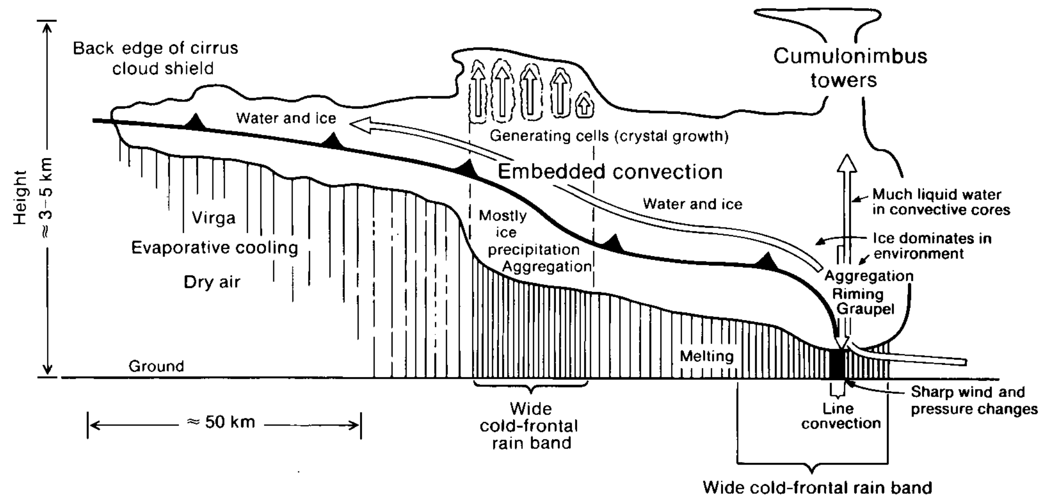

Figure 3. Schematic cross-section of major cloud and precipitation processes in a cold frontal zone (after Matejka *et al.* 1980). The hatched area indicates precipitation, the intensity varying with the density of hatching. Open arrows depict the sense of airflow.

The low-level jet is associated with the warmest air in the depression and some aspects of it have been described in dry baroclinic-wave development simulations. It is, however, also associated with a large moisture flux which is likely to be of considerable importance in the development of convective systems. The strong shears below the jet maximum are likely to be due to boundary-layer frictional processes, the role of which needs further quantifying.

To understand the dynamics of all these phenomena, both convective scale and mesoscale data are necessary to describe both the internal structure of the frontal zone and its environment.

2.3 *Model and diagnostic studies*

As well as the idealized theoretical and numerical model studies described above, a major aim of the project is to apply models of varying scale and sophistication to the observations acquired in the field programme. At this stage not only the earlier theoretical predictions but also methods of assimilating or analysing a large and diverse set of mesoscale data will be subject to test.

Numerical models with resolutions from 1 km to 100 km or more will be run as part of the project. At all scales the primary interest will be in validating and tuning model simulations using observations analysed at a resolution appropriate to the model. Following from such work will come diagnostic studies using simulations to help interpret the observations. For models with resolution coarser than a few kilometres, the availability of coincident fine-scale data and validated high-resolution models will provide opportunities for the development of new parametrizations, notably of such features as slantwise and embedded upright convection which are not represented in current models. The other major area of interest will be in data studies and initialization. Very little is known about the response of mesoscale models to high-resolution data, and it is important to determine what mix of variables to specify to achieve the observed evolution.

Dynamical and conceptual models of fronts have been developed in the last decade and they have not yet been adequately compared with either synoptic observations or operational models, such as the Meteorological Office fine-mesh model. Such a comparison will clarify whether these dynamical and conceptual models provide a good synoptic description of frontal dynamics and thus a guide to the design of more accurate integration schemes for use in operational models.

The representation of frontal dynamics and moist convection in mesoscale operational models is also relevant here. This project will provide a good basis for the necessary diagnostic studies, which the operational environment does not readily allow. For example, the comparison of simulations of fronts in operational and other models where moist processes are artifically suppressed may give some good clues as to the role of these processes in the atmosphere and the working of the physical parametrizations used in the models.

The use of cloud models is also seen as a significant component of the programme. They will be used primarily for the study of features requiring explicit convective or microphysical representations, e.g. line convection and precipitation growth, but they will also provide a useful comparison with results of more extensively parametrized models with lower resolution.

3. The field programme

The scientific problems discussed in the previous section concern a wide range of scales from hundreds of kilometres to metres, and observational study of the processes involved will require a network of measuring systems not only capable of measuring fine scales but also extending over a large area. The present proposal has been formulated to meet these requirements, the location being selected to make optimum use of existing observing stations in an area relatively free of topographic forcing.

Fig. 4 shows the experimental area; a threefold nested structure is envisaged, comprising a zone of intensive small-scale measurements, an inner area and an outer observing area. Throughout the outer region (approximately 1200 km × 1200 km) data from the upper-air network will be used to define the largest scales of motion. By enhancing the standard network somewhat, it is hoped to define the synoptic domain over the outer area every 6 hours with about 300 km resolution. Data from satellites and from the various national weather radar networks will be used to assist in the interpolation between soundings, to fill gaps in relatively data-sparse areas over the sea and to provide continuity in time. Radiosonde coverage with finer resolution of about 150 km is needed in the inner region (approximately 500 km × 500 km). Also in this region additional facilities (including dropsondes, instrumented aircraft

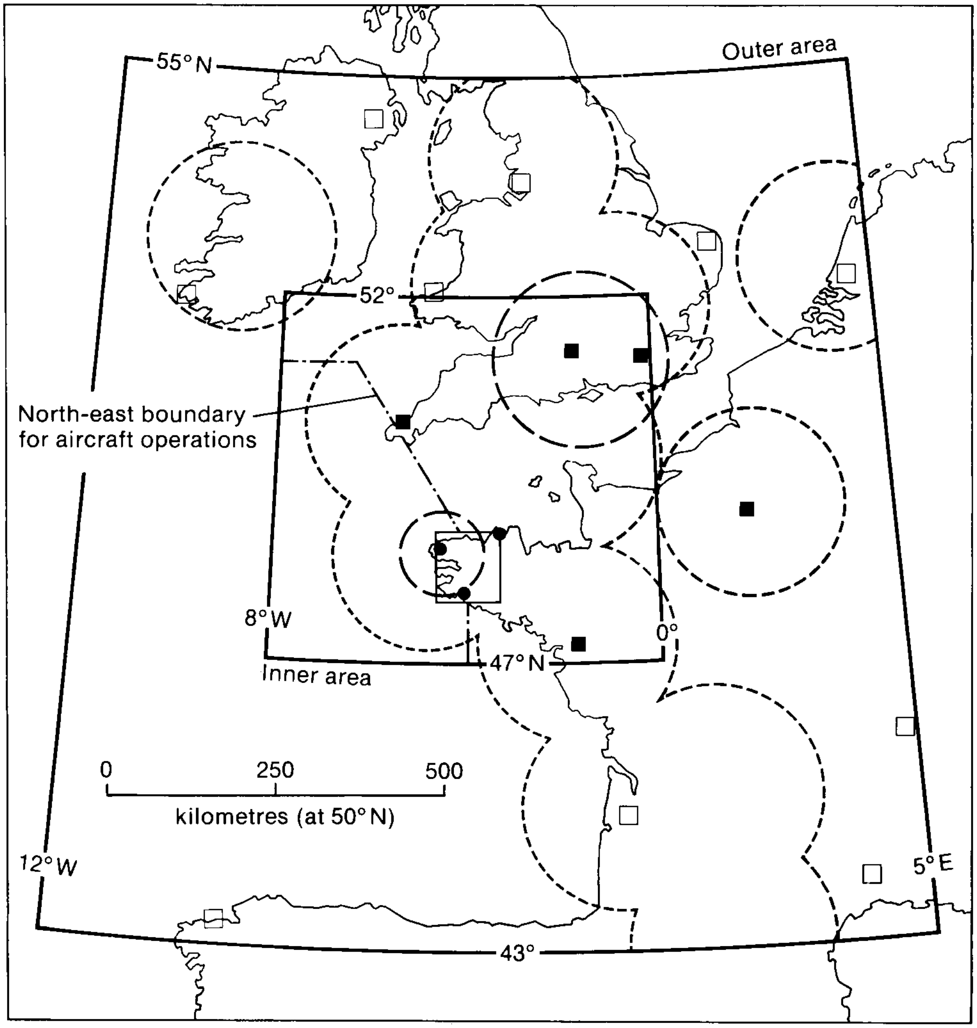

Figure 4. The overall experimental area indicating the main measurement sites and coverage, showing the boundary of the weather radar network coverage (- - - -), boundary of special radar coverage (— —), boxed zone of intensive surface instrumentation in north-west France (——), radiosonde stations reporting at 6-h intervals (□), radiosonde stations reporting at 3-h intervals (■) and mobile radiosonde stations reporting at 1½-h intervals (●).

and ground-based Doppler radar) will also be used to define structure on scales less than 150 km, especially within the intensive instrumentation zone of about 100 km × 100 km based around a dual Doppler radar system.

3.1 *Logistics of the field experiment*

The field phase is planned for autumn 1987, since the period from late September to mid-December appears to offer favourable active frontal cases without some of the adverse operating conditions that might occur in winter. Although individual frontal passages across the outer area are of 1 day's duration it is necessary to have a sufficiently long experimental period to ensure that several active fronts pass through the experimental area during the period.

It is proposed that about six cases of active fronts should be investigated during the 3-month experimental period. A study of frontal systems in the area over recent years has been carried out, and suggests that this number is exceeded in most years. To reduce topographic effects only fronts with a roughly south-west to north-east orientation approaching from the western quadrant will be studied (this is not a severe restriction since most active fronts approach from this direction). At an average frontal speed of 50 km h^{-1} ($\approx$ 15 m s^{-1}) the fronts will cross the outer region in about 24 h. It will therefore be necessary to maintain observations in the outer area for selected periods of about 36 h on each occasion.

Intensive observational periods will be identified at the experimental planning centres (Bracknell in the United Kingdom and Paris in France) 36–48 h in advance, on the basis of numerical forecasts and satellite cloud photographs following consultations with participating groups. The main requirements will be for indications of active fronts with broadly suitable movement and orientation. Based on the expected movement of a front, the period for which additional measurements are required in the outer area will be identified and a first estimate made of the timing of the passage of the front through the inner area. This notification will provide preliminary warning of the need to prepare the intensive observing facilities, to obtain aviation clearances and deploy participating aircraft to suitable bases, and to ensure that essential facilities are fully operational.

At the assumed speed of 50 km h^{-1} the fronts will cross the inner area in about 12 h. Thus it will be possible to provide 12 h notice of the period for which the various national facilities should be deployed in the area. At this time it should be possible to cancel the detailed measurement programme if key facilities are unserviceable or if the front does not behave as expected. It will also be possible, using radar network data and satellite imagery, to provide a more accurate estimate of the frontal movement than that provided earlier. Final decisions on the timing of aircraft flights will be made about 3 h before the expected take-off time. This plan should ensure that those facilities which can provide data for only limited times are fully utilized, though it does not prevent the operation of some facilities for longer periods provided they include the period indicated.

The observational phase will be followed by a period of processing and analysing the large volume of data produced. These data will be exchanged freely among groups actively participating in the project. It will be necessary to ensure that the special data sets are archived in an accessible manner and that the soundings and rainfall records are speedily gathered and combined into convenient data sets. The participating groups will have to agree formats for data exchange. It will be essential to ensure that those groups whose interests are mainly in the interpretation of the observations collaborate closely with those who are active in making the measurements; several groups will be involved in both activities.

3.2 *Outer area measurements*

Radiosondes. Radiosonde stations in the outer area are shown in Fig. 4. In 1987 no permanent weather ship stations will be available within the area, but data from ships of opportunity will occasionally be available through the normal data channels. Where possible, full ascents will be made at 6-h intervals during the intensive operation periods.

Radar network data. The approximate area covered by the various national weather radar networks is also shown in Fig. 4. Data will be available routinely from the network and steps will be taken to ensure that the data obtained during each experimental period are recorded.

Surface observations. Normal synoptic data will be used in the interpretation of frontal weather patterns, etc. Autographic rainfall charts will also be invaluable to support the patterns derived from radar. Additional surface ship observations are also likely to be available at the data-analysis stage.

Satellite data. Maximum use will be made of satellite data both from Meteosat and from polar orbiters. Data from these sources, which should include infra-red and visible imagery, derived winds and temperature retrievals, will not only be invaluable for post-analysis purposes but they will also be essential for the control of the experiment. The data will be made available as near as possible to real time.

3.3 *Inner area measurements*

Some of the data sources which will be used to define the largest scales of motion over the outer area will also be available within the inner area. However, additional sources of data will be used in this area to define the smaller scales of motion, in some cases down to sub-kilometre scales.

Radiosondes. An enhanced radiosonde network is required in the inner area to provide soundings on a scale of about 100 km and to improve the real-time definition of the main frontal region. Soundings to 150 mb will be obtained at 3-h intervals from synoptic stations where possible. In the French component of the experiment this will be achieved by the disposition of three mobile radiosonde stations at Brest, Lannion and Lorient, as shown in Fig. 4. In the UK component the operation of simple radiosonde systems is being investigated to provide some additional partial soundings from Devon or Dorset and Camborne.

Aircraft dropsonde measurements. The British Hercules C-130 aircraft will be capable of producing dropsonde profiles of temperature, humidity and winds below 8 km with horizontal spacing down to about 20 km, though they may only be dropped over the sea (see Fig. 4) or authorized military ranges. Two patterns of dropsondes are planned: a coarse resolution ($\approx$ 100 km) pattern across a front or a finer resolution ($\approx$ 25–30 km) one near surface features of interest. A primary function of these observations is to define the intermediate scales in the environment of the intensive small-scale observations, but isolated radiosonde measurements will also be used to supplement the radiosonde network over the sea in the outer area.

Aircraft in situ observations. Most of the finest scales of observation will be achieved by measurements from aircraft, of which several will be available: the French Piper Aztec, the British C-130 and German Dornier 128. All the aircraft will be equipped to carry out dynamic and thermodynamic measurements, and some will be able to provide information suitable for turbulence studies. The British and French aircraft will also be capable of microphysical observations. The C-130 will be equipped also with chemical measurement facilities and visible, infra-red and microwave radiometers to measure ambient fluxes and to monitor cloud liquid water and precipitation in the column. Such observations might be used for primary studies (e.g. sampling stratospheric intrusions) or secondary experiments.

Radars. As well as the network radars described in Section 3.2, several experimental radars will take part in the experiment. The French Ronsard 5 cm dual Doppler radar facility is a central element of the field programme, with several operating modes in addition to conventional PPI scanning over a 200 km radius. With both radars scanning in successive common planes (the 'COPLAN' mode), high resolution (0.5 km × 0.5 km × 0.25 km) velocity fields can be measured over two areas of 30 km × 30 km, particularly in convective conditions. A vertically-pointing mode provides particle reflectivity and vertical motion with even higher resolution. In more uniform precipitation, mean horizontal and vertical velocities can be evaluated with an effective horizontal scale of about 50 km using an appropriate scanning pattern. The precise siting of this radar facility is yet to be finalized, though it will be in the region around Brest.

The French Rabelais 8 mm Doppler cloud-physics radar, sited near the Ronsard system, should enable the smaller particles in non-precipitating clouds to be detected also, while it is hoped that the UK Chilbolton 10 cm dual polarization radar will be available to provide high resolution three-dimensional fields of precipitation quantity and type within a radius of 200–300 km.

Mesoscale surface network. A network of eight automatic stations will be deployed by the French groups to provide frequent surface measurements over an area. The network's mobile central station is equipped as a forecasting centre with receiving and display facilities for a range of radar, satellite and forecast products, and may provide an appropriate co-ordinating centre for part of the experimental phase. The western and northern French regional networks of automatic stations will provide additional half-hourly surface observations at up to 25 sites.

ST (Stratosphere/Troposphere) radar. A French system of three ST radar units is planned to be sited at Brest, Lannion and Lorient. With a spacing of ≈ 100 km these can produce continuous observations of horizontal and vertical velocities, thus providing much information on small-scale wave structure both in clear air and precipitation conditions. A system of three Doppler sodars at the same sites should provide similar data in the range of 0–500 m above ground level which is not available from the ST radars. It is hoped that a British ST radar will also be available.

Instrumented balloon. It is intended to site a tethered balloon on the Isles of Scilly with instrument packages to measure boundary-layer parameters. The resultant highly resolved observations at several levels in the boundary layer will be of great interest.

4. Conclusions

The range of interactions and scales of importance in frontal systems is of such diversity that a comprehensive view entails resources that are rarely attainable. It is hoped that in the Mesoscale Frontal Dynamics Project the steady progress achieved in observational techniques, numerical modelling and theory in recent years can be consolidated by bringing together the several strands of effort, both in an intensive observational phase and in a period of interrelated theoretical studies. The resulting extension of the present limited data base, as well as the exchange of ideas and testing of theories, should lead to a greater understanding of frontal systems and improved ability to forecast their behaviour.

References

Browning, K.A. 1985 Conceptual models of precipitation systems. *Meteorol Mag*, **114**, 293–319.
Matejka, T.J., Houze, R.A., jun., and Hobbs, P.V. 1980 Microphysics and dynamics of clouds associated with mesoscale rainbands in extratropical cyclones. *Q J R Meteorol Soc*, **106**, 29–56.

551.554:551.515:551.556.1(434.2):629.7

Tornadoes — or microbursts?

J. Malcolm*
Meteorological Office, Royal Air Force Wildenrath

Summary

An aircraft encounter with very severe turbulence, allied to reports of severe damage by tornadoes, is discussed. It is suggested that the damage may not have been caused by tornadoes but by microbursts, such as are described by Fujita (1980).

1. Introduction

On 10 June 1977 I was in a Pembroke aircraft of No. 60 Squadron, Royal Air Force, *en route* from Wildenrath to join Airway R15 west of Norvenich for Florrennes (places mentioned in the text are shown in Fig. 1). A thunderstorm with very severe turbulence was encountered. The following day a German newspaper, the *Erkelenzer Zeitung*, published reports of severe damage, amounting to millions of Deutschmark, caused by tornadoes. The locations of the reported damage are marked (T) in the inset to Fig. 1. This paper discusses these events.

2. The aircraft encounter

At 1320 GMT the Pembroke left Wildenrath and climbed to 8000 ft (approximately 2600 m). I was standing just aft of the crew compartment door and was able to observe the weather and see the flight instruments. During the climb there was 7 oktas of altocumulus and altostratus with a base at about 15 000 ft; the cloud was thick to the south-west and west but thinner towards the east. The visibility was 5–10 km. At 1336 GMT at 50°49′N, 6°20′E broken cumulus and stratocumulus appeared below and there was slight rain at the flight level. We then went into cloud, apparently lowering altocumulus and altostratus, and encountered slight turbulence. At 1337 GMT we entered a severe thunderstorm and experienced very severe turbulence. I was momentarily lifted off the floor and had great difficulty in gaining a passenger seat and securing the seat-belt. The aircrew reported a rate of descent of 4000 ft/min (20 m s^{-1}) followed almost immediately by a rate of ascent, with all power off and the aircraft nose held down, of 2000 ft/min. The ground controller allowed an immediate 180° turn and the aircraft returned to Wildenrath and landed at 1400 GMT, just ahead of the storm. The turbulence was by far the worst that I have ever experienced in more than 1600 hours of meteorological reconnaissance duties and numerous flights as a passenger.

3. Surface events

On 11 June the *Erkelenzer Zeitung* carried reports of severe damage at 1530 h (1330 GMT) at Gerderhahn — 'hardly a house spared by the tornado', 'countless roofs have been torn off houses', 'trees of one metre diameter were uprooted and lay 20 metres away' and 'a farmer found his car ... 15 metres away'. Damage was also reported at Klinkum where 'a sudden tornado caused considerable damage ... to several buildings in an approximately 200 metre long strip', 'trees were uprooted', 'on one farm the roof was torn off the bull shed' and 'one eyewitness reported that balconies flew about 100 metres through the air'. The newspaper reported that similar damage was said to have occurred in Suestersee l and Selfkant after the heavy storm at about 1530 h (1330 GMT); the paper had photographs showing the

* Now on secondment to International Aeradio plc, Bahrain.

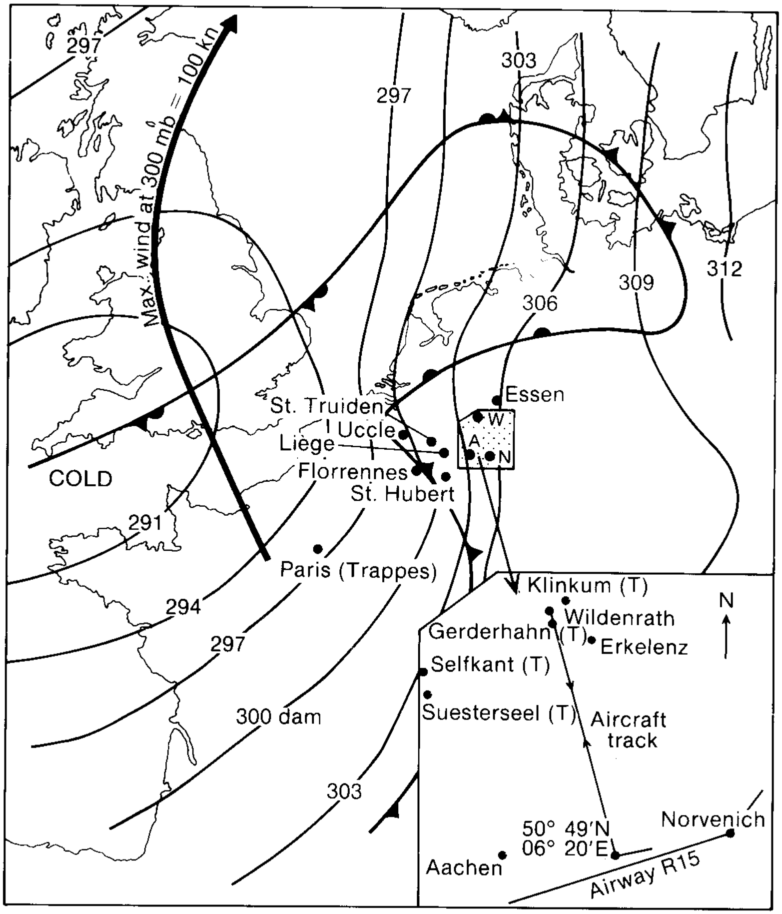

Figure 1. 700 mb analysis for 1200 GMT 10 June 1977 with surface frontal analysis and maximum wind at 300 mb superimposed. Locations of tornado-like damage are marked (T) in the inset.

damage. The Senior Meteorological Officer at RAF Wildenrath reported that two trees had fallen near the main entrance to the airfield.

At 1355 GMT the barogram at Wildenrath recorded a pressure jump of 3 mb. The temperature fell 6 °C and relative humidity rose rapidly from 72% to 96%.

4. Conditions for severe local storms

Roach and Findlater (1983), amplifying the findings of earlier workers, listed the conditions which should be satisfied for severe local storms to form. There should be:

(a) A supply of warm moist air at low levels. The possibility of severe storms should be considered if θ_w exceeds about 15 °C, but cannot be ruled out at lower values.

(b) A great depth of instability.

(c) A large amount of convectively available potential energy, indicated by the excess of surface or low-level wet-bulb potential temperature over the saturation wet-bulb potential temperature in the middle or upper troposphere.

(d) A vertical wind shear in excess of 5 or 6 m s^{-1} km^{-1} throughout the convective layer. The presence of strong directional shear between the surface and the 850 mb level, together with a difference in wind speed in excess of 15 m s^{-1} between these two levels (intense warm advection), is particularly favourable for storm formation.

(e) A trigger action caused by daytime surface heating, low-level convergence, or orographic uplift.

(f) Northward advection of air warmed over Europe, especially Spain, which may form a lid to small-scale convection so that low-level moisture is confined beneath it and high buoyancy can develop before the instability is finally released.

In the next section the synoptic situation on 10 June is examined to see to what extent these conditions were fulfilled.

5. Analysis

At 1200 GMT on 10 June 1977 an open-wave depression, which had moved from the Paris area at approximately 12 m s^{-1} on an average heading of 015° true, was about 80 km north-west of Uccle. The 1200 GMT frontal analysis has been superimposed on the 700 mb analysis in Fig. 1. At 700 mb there was a pool of cold air just off the south-west peninsula of England and a south to south-west flow over the Low Countries, the western part of the Federal Republic of Germany and northern France.

A vertical cross-section for 1200 GMT has been constructed along the line Trappes–St. Hubert–Essen using all available upper-air and surface data (Fig. 2). It shows cloud, wet-bulb potential temperature and the component of wind from 190° true. The aircraft observations were adjusted spatially to 1200 GMT taking the northward movement of the front as 12 m s^{-1}.

From Fig. 2 it can be seen that values of θ_w exceeded 17 °C throughout the warm sector (condition a) and that there was a considerable depth of instability evident in the upper-air soundings, particularly St. Hubert, Uccle and Essen (see Fig. 3), which satisfies condition b. At Uccle the surface $\theta_w = 18$ °C while at 550 mb $\theta_w = 16$ °C (condition c). There was also evidence of strong low-level warm advection; the wind shear between the surface (south-easterly at 5 m s^{-1}) and 850 mb (160° true at 20 m s^{-1} at Uccle) satisfying condition d. Daytime heating was present to assist in the release of the instability (condition e) and the shallow stable layer present between 900 and 880 mb on the Essen ascent may have been sufficient to suppress the instability earlier in the day (condition f).

Thus overall, conditions were favourable for severe storm development. But not all severe storms generate tornadoes. In their research on the linking of severe storms and tornadoes, Fawbush *et al.* (1951) found that the presence of a relatively narrow tongue of warm moist air at low levels was essential to the formation of tornadic storms. They also showed that there must be a band of strong winds aloft between 3000 and 6000 m. In the case under discussion there is such a jet around 3000 m (700 mb) in the region of the frontal wave (Fig. 1). On the vertical cross-section (Fig. 2) the jet is evident and overrides the tongue of high θ_w air at the surface in the warm sector.

In developing a tornado forecasting model, Beebe and Bates (1955) found that a pattern of convergence at low levels surmounted by horizontal divergence aloft is necessary to provide a mechanism for organizing the release of convective energy. They stated that the region of convergence to the left of the low-level jet axis combined with the region of divergence at the right entrance of the upper-level jet was a particularly favourable combination. From Fig. 1 it is evident that on this occasion the storms appear to have developed in such a region.

The conditions would appear to be favourable for tornadic development. However, the evidence from the aircraft behaviour, coupled with the pattern of damage, leaves room for doubt. The surface damage does not readily fit with the expected linear pattern of damage normally associated with a tornado (Smith 1981). The line in this case might reasonably be expected to be normal to the approaching cold

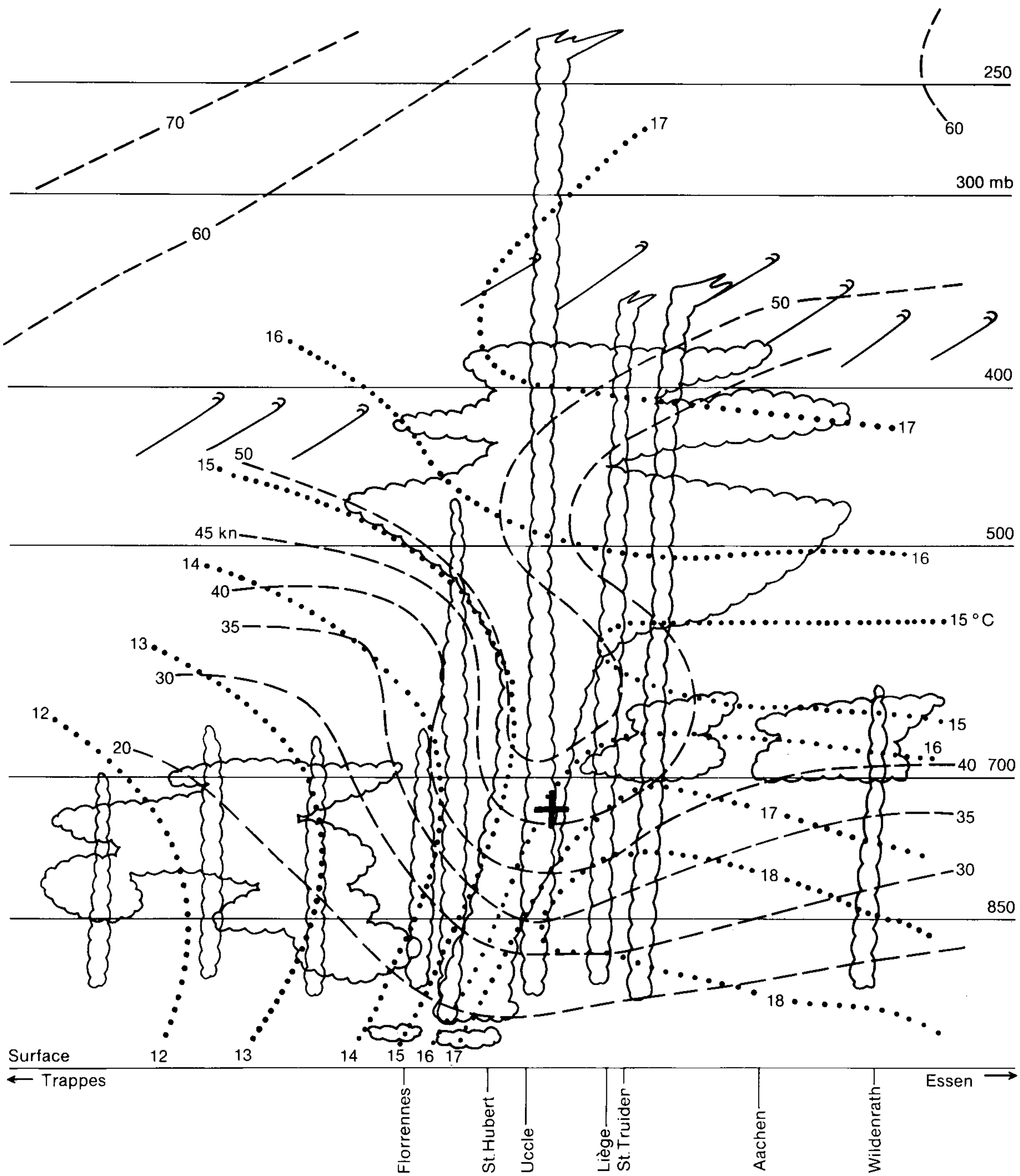

Figure 2. Vertical cross-section for 1200 GMT 10 June 1977, constructed along the line Trappes–St. Hubert–Essen, showing wet-bulb potential temperature (dotted line), component of wind (kn) from 190° true (dashed line) and cloud structure. The frontal surface is more or less coincident with the 15 °C isopleth. The estimated position of the aircraft at the time of encountering the thunderstorm is marked by a cross.

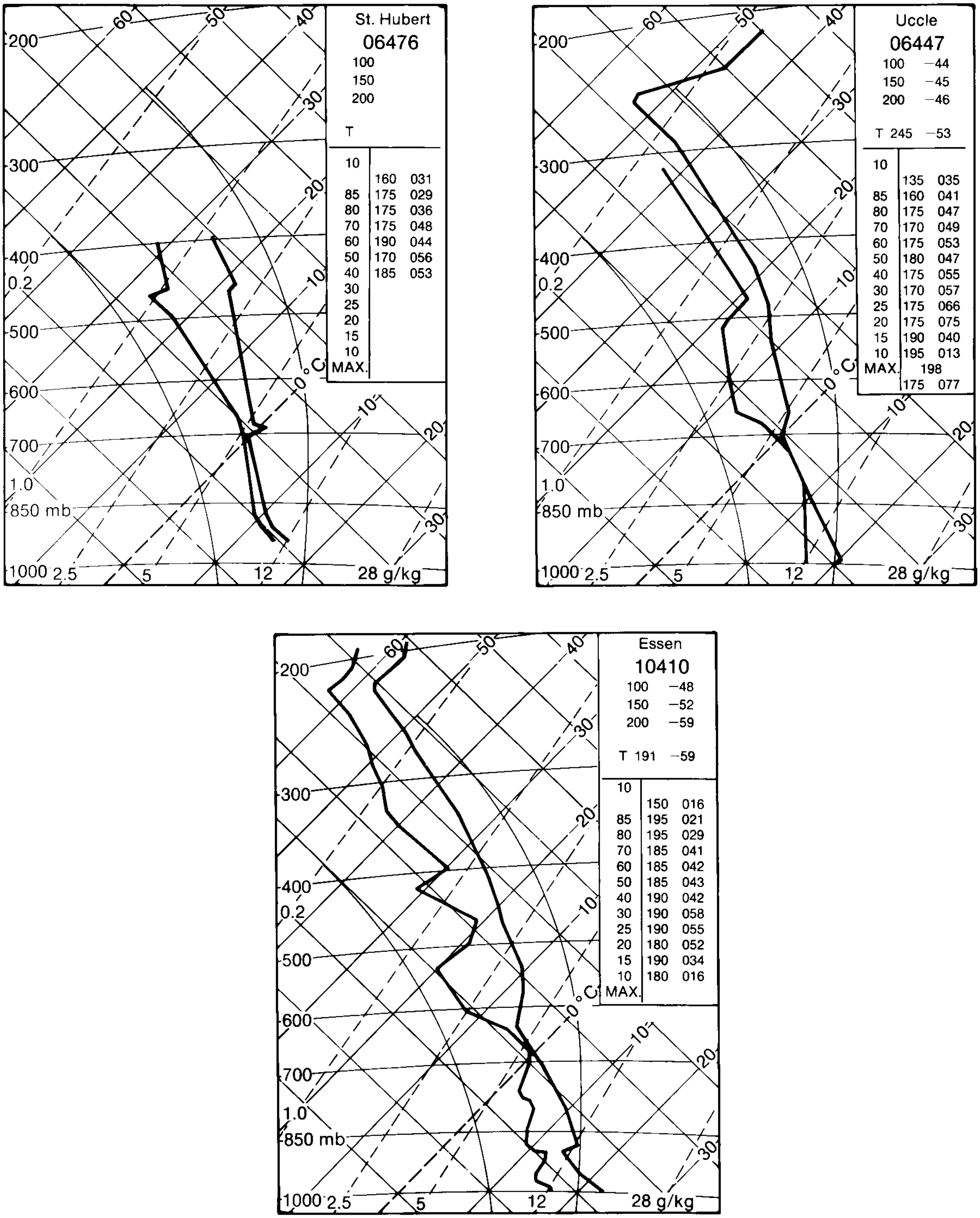

Figure 3. Radiosonde ascents for 1200 GMT 10 June 1977 for St. Hubert, Uccle and Essen.

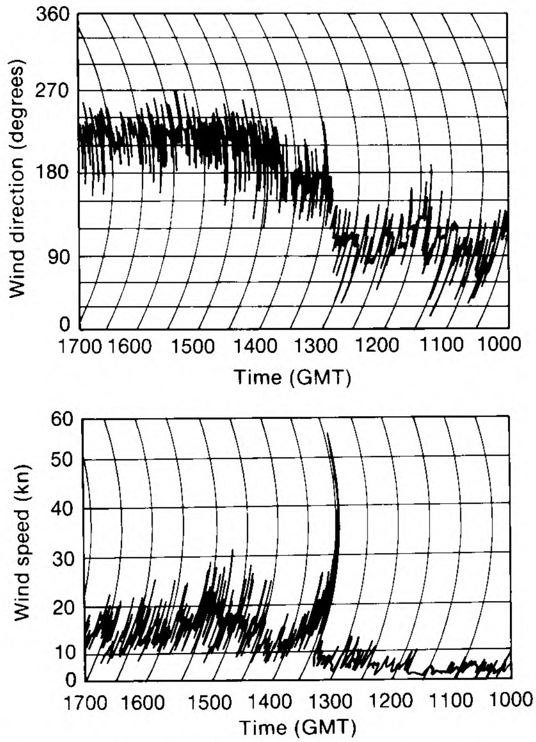

Figure 4. Anemograph traces for Aachen on 10 June 1977.

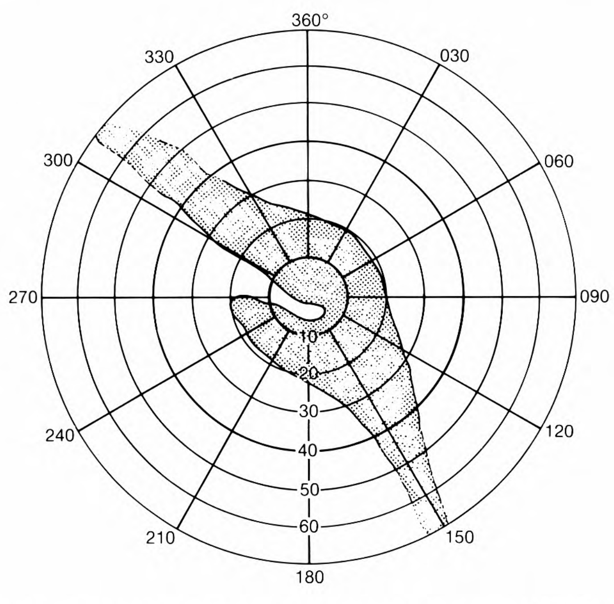

Figure 5. Sketch of the radar display at Wildenrath at 1400 GMT 10 June 1977. Range in nautical miles.

front and indeed Klinkum and Suesterseel/Selfkant lie in such a straight line, but they are some 25 km apart and the damage was reported at both places simultaneously. Such evidence suggests a larger-scale feature than a tornado.

6. Microburst?

Fujita (1978) has defined a downburst as a strong downdraft inducing an outward burst of damaging winds at or near the ground. Such features range in scale from tenths to tens of kilometres. In a later paper Fujita (1980) defined a small-scale downburst (horizontal dimensions of about 5–10 km) as a microburst.

A microburst is defined as having four distinct phases:

(a) Descent.
(b) Contact — the microburst makes contact with the ground.
(c) Outburst — the outflow spreads out violently within a 100–200 m layer above the ground.
(d) Dissipation — the microburst becomes exhausted within a few minutes, but the outflow continues to expand (like a giant smoke ring) but weakening.

Fujita (1978) reports that downburst damage is often highly localized, resembling that of tornadoes, and that even an experienced investigator cannot always identify the nature of the storms without mapping the directions of the damaging winds over a large area. Unfortunately this was not possible in the present case. However, none of the newspaper reports mention debris twisting or whirling. Trees were described as having been uprooted which seems more indicative of winds from a single direction; the newspaper photographs of fallen trees show them snapped off fairly cleanly near the ground, there is no sign of twisting.

Fujita indicated that a microburst is characterized by a single rapid surge and fall of wind speed which is relatively gust free; the anemograph traces for Aachen (Fig. 4) and Wildenrath (not shown) seem to fit this description. He also pointed out that radar reflectivity in and around a strong microburst could be lower than the surrounding area due to rapid evaporation in the descending air. The Senior Meteorological Officer at RAF Wildenrath was in the air traffic control tower as the storm approached. At his request the air traffic radar was being operated in a weather detection mode. No photographic facilities were available but, after the storm had passed, he produced from memory the sketch of the radar display which is shown in Fig. 5. There is a channel in the echo which would fit Fujita's supposition.

7. Conclusions

Considerable tornado-like damage was reported in the Wildenrath area on 10 June 1977 and many of the conditions conducive to tornado development were present. However, in view of the evidence available — the pattern and distribution of damage, the radar echo and the anemograph traces — it is suggested that the damage was caused by microbursts rather than tornadoes.

8. Acknowledgements

This note was developed from an Extension Forecasting Course project at the Meteorological Office College and the assistance of the instructors, Mr Wickham and Mr Spalding, was much appreciated. Thanks are also due to Mr Grant and Mr Findlater (Special Investigations Branch, Meteorological Office), Mr Thomas (RAF Wildenrath) and Herr Rolofs (Deutscher Wetterdienst) for supplying material on which this article was based, and to Mr Drysdale (Lossiemouth High School) for providing full translations of the newspaper reports. Thanks are particularly due to Dr Bennetts (Defence Services Branch, Meteorological Office) who gave a great deal of assistance with the final draft.

References

Beebe, R.G. and Bates, F.C.	1955	A mechanism for assisting in the release of convective instability. *Mon Weather Rev*, **83**, 1–10.
Fawbush, E.J., Miller, R.C. and Starrett, L.G.	1951	An empirical method of forecasting tornado development. *Bull Am Meteorol Soc*, **32**, 1–9.
Fujita, T.T.	1978	Manual of downburst identification for project NIMROD. University of Chicago, Department of geophysical sciences. Satellite and mesometeorology research project, Research Paper No. 156.
	1980	Downbursts and microbursts — an aviation hazard. Boston, American Meteorological Society. 19th conference on radar meteorology, 94–101.
Roach, W.T. and Findlater, J.	1983	An aircraft encounter with a tornado. *Meteorol Mag*, **112**, 29–49.
Smith, E.J.	1981	A Wiltshire tornado, 30 May 1979. *Meteorol Mag*, **110**, 312–323.

551.553.4:551.506.1(41-4)

Wind and the summer of 1985

F.A. Crummay*

Meteorological Office, Bracknell

Summary

Calculations of a windiness index formulated by Smith (1982) for the period 1965–79 have been extended to include an analysis of 1980–5 data. The relative windiness of each season and year (1970–85) is discussed with particular emphasis on the summer of 1985. Finally 1985 is placed in its long-term context using estimated windiness index values for 1881–1980 obtained from pressure fields.

1. Introduction

The need for some quantitative measure to enable a comparison of windiness to be made for months, seasons and years has long been evident. Smith (1982) devised two methods of producing an index to assess relative windiness, one using anemograph records, the other based on surface pressure gradients from six grid points around the British Isles. The latter provides broad, regional values for the United Kingdom and can be used to produce values from 1881 onwards. However, the use of anemograph data, although limited by the relatively short period of reliable data available in machinable form, allows the investigation of relative windiness for specific locations.

Stainer (1986) expressed the view, based on observations in Bristol, that the summer of 1985 was 'exceptionally poor', 'mainly due to the strong wind compounding the below average temperatures and above average rainfall'. The comments referring to temperature and rainfall will not be investigated here. However, using anemograph data, the windiness of the summer of 1985 will be compared with other years having machinable data available and, using Smith's work, a general view of 1985 obtained.

2. Calculation of index values

One of the main requirements for the production of a windiness index from anemograph data is a long record of homogeneous data at a number of stations. In 1981, Smith was limited to 17 stations containing homogeneous data for the period 1965–79, of which three contained some estimated values. A detailed description of the index calculation process is provided by Smith (1982). Briefly, the initial stage consisted of calculating the standardized anomaly of each month's mean speed relative to a long-period (1965–79) monthly average (a standardized anomaly being the difference between the mean speed and the long-period average for a month, divided by the standard deviation of the means of the

* Now at the Tropical Development and Research Institute, London.

month in question). The anomalies were observed to vary across the country in a consistent fashion and, as a result, the United Kingdom was divided into three regions — north, central and south (see Fig. 1) — reflecting the predominantly zonal movement of synoptic-scale features.

The final index consisted of the arithmetic mean of the standardized anomalies over the stations in each region. Annual and seasonal indices were also derived and expressed as a proportion of the standard deviation of the season (year) for the period 1965–79.

Since 1980, three of the original anemograph stations have either closed or can no longer be considered to possess a homogeneous record. Stations from which hourly mean wind speeds were used to produce the long-period (1970–84) monthly average for this study are shown in Fig. 1. Index values have been calculated for each station from 1970–85 together with regional, annual, summer (April–September) and winter (October–March) values.

3. Results

Annual, summer and winter index values for 1970–85 are illustrated in Figs 2–4. In Fig. 2, the annual values obtained by Smith for 1970–80 are also included, both for comparison purposes and to indicate the sensitivity of the technique to the use of different stations and the different period used for the long-term average. The reasonably good agreement between the two sets of values gives confidence in the robustness of the technique.

It is apparent that marked differences do occur between the regions as well as from one year to the next. Considering the annual values in the northern and central regions, 1977 was the windiest in the 16-year sample, but in the southern region 1974 was the windiest. The most important feature of these annual index values, however, is that, for all three regions, 1985 as a whole was less windy than the 1970–84 average. In fact, for the northern region, 1985 was the 'quietest' year in the study period.

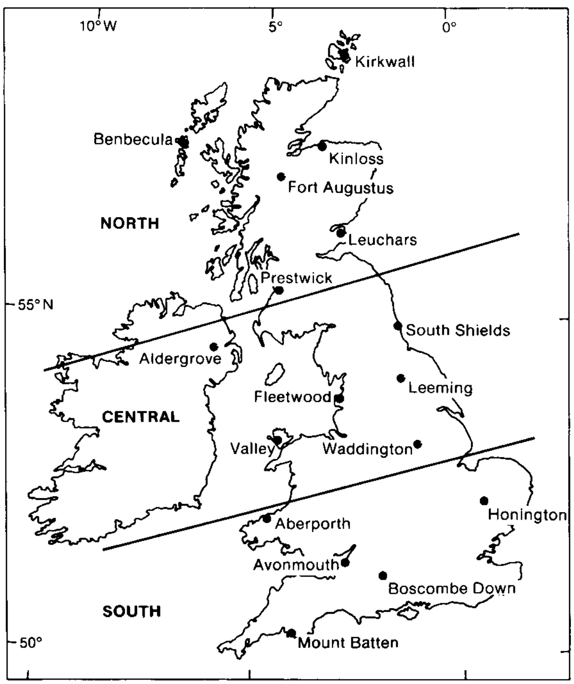

Figure 1. Regions and individual stations used in the calculation of indices.

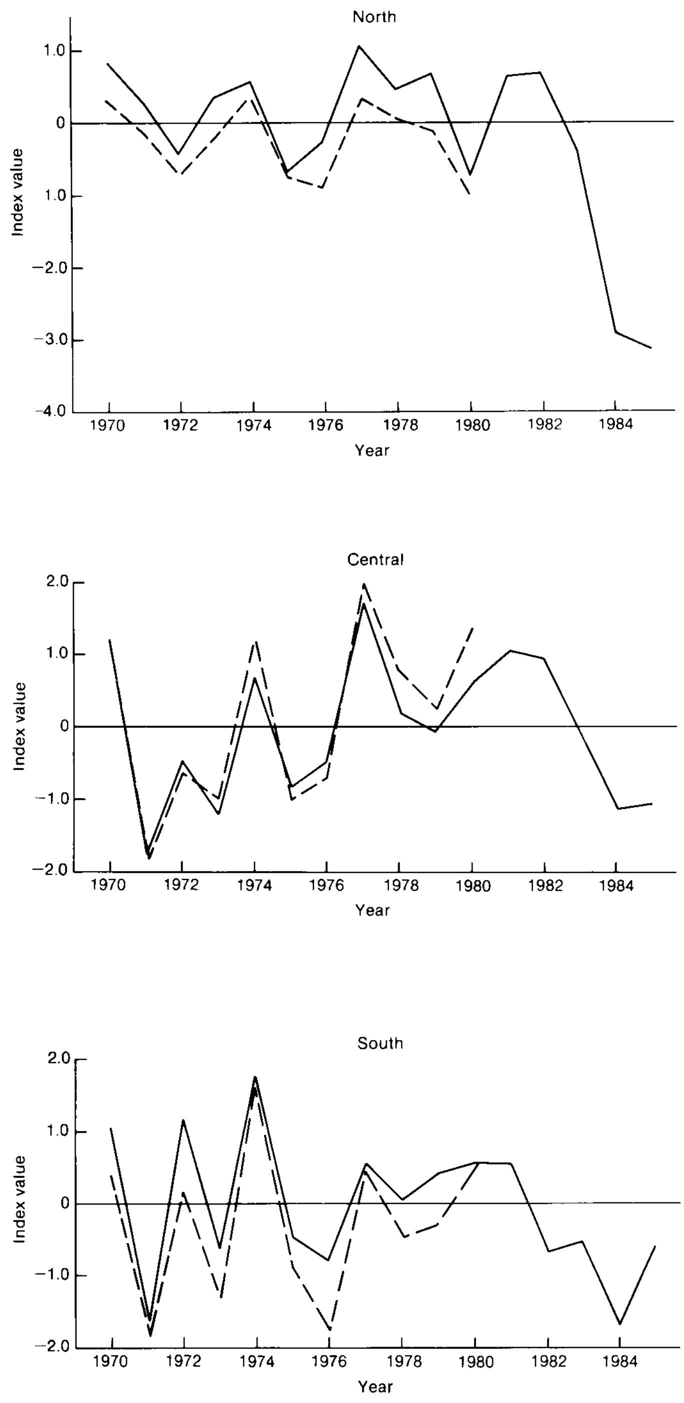

Figure 2. Index values for the year, based on 1970–84 average, for the three regions shown in Fig. 1. Dashed lines show annual values obtained by Smith (1982) based on 1965–79 averages.

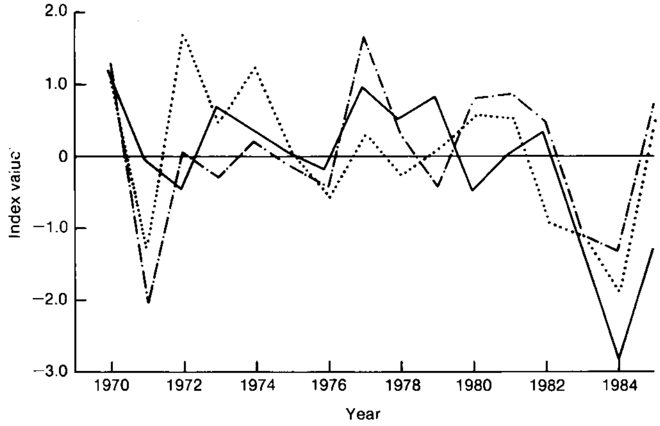

Figure 3. Index values for summer season (April–September), based on 1970–84 average, for the three regions shown in Fig. 1 (—— north, —·— central, ········ south).

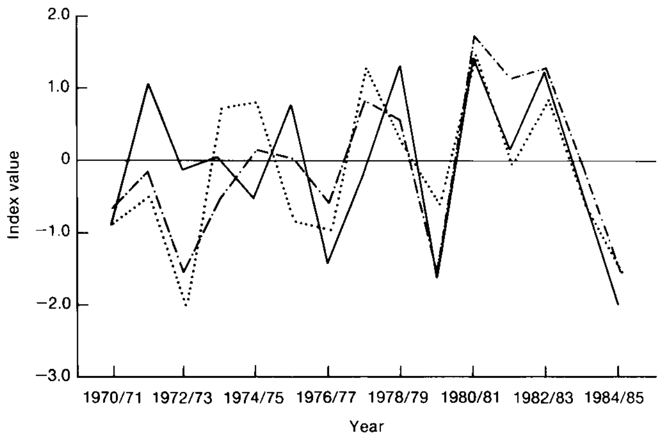

Figure 4. As Fig. 3 but for winter season (October–March).

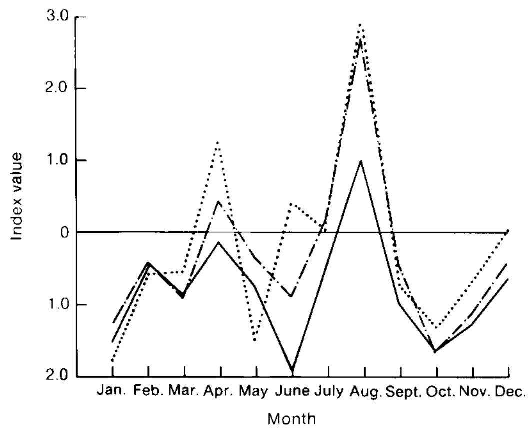

Figure 5. As Fig. 3 but for monthly values during 1985 only.

The positive anomalies during the summer of 1985 over southern and central regions (Fig. 3) indicate that this season could be classed as windy. In contradistinction, the preceding winter for the same regions could be classed as quiet, with large negative anomalies present (Fig. 4). The windiest winter in the study period for all regions occurred in 1980/81 while the calmest was 1972/73 in the south, 1979/80 in the central region and 1984/85 in the north.

Fig. 5 illustrates the monthly index values for all regions in 1985, thus establishing which months were responsible for the high summer index value and those areas most affected. August is clearly the month with the highest index value. In the northern region, only August had higher wind speeds than the 15-year monthly average. In the central region, April was also relatively windy, but for the southern region April, June and August were windier than the 15-year average for each month with July and December approximately average.

Geographical variations in windiness are shown in Figs 6(a) and (b). In Fig. 6(a) the annual index values are illustrated for each of the 17 stations. They indicate that south-west Wales had a windier year in 1985 than the 15-year average and this is further emphasized by the fact that the highest index values for the summer months occurred in Wales, with western coasts in southern and central Britain also relatively windy (Fig. 6(b)).

4. 1985 — the long-term perspective

From a comparison of the 1985 anemograph data and the 15-year averages from 1970–84, it is apparent that the summer months of 1985, particularly August, were relatively windy in southern and western areas despite the fact that as a whole 1985 was quiet. But how representative are these 1970–84 averages of the long-term wind conditions?

Smith (1982), using the surface pressure gradients between six grid points around the British Isles, obtained estimates of the windiness index from 1881 and compared them with those produced using 1965–79 averages. He observed that there was a slight tendency for errors in the estimated values to be greater in summer than in winter months, possibly as a result of the weaker relationship between pressure differences and surface winds at low speeds. In addition, he believed that changes in the analysis of surface pressure in 1972 may have led to lower estimates in the north prior to that date. However, he concluded that since 1968 there had been a high proportion of below average speeds for all regions compared to the 1881–1980 average. This trend has continued in the 1980–5 period.

Corrections for each month were calculated using the 1970–80 values to compensate for the differing averaging periods and stations selected (Table I). This enabled approximate values of the windiness index for 1981–5 (Table II) to be included with the 1881–1980 values and a long-term view of 1985 was obtained using the mean values for each month over all regions. Several features were apparent:

(a) January 1985 was the quietest since January 1881,

(b) October 1985 was the quietest since October 1966,

(c) summer 1984 was quiet with all 6 months recording a negative anomaly when averaged over the three regions (since 1881, this phenomenon has occurred only twice, summer 1971 being the other occasion), and

(d) although August 1985 was windy, a higher index value (i.e. windier month) occurred in August 1961.

5. Conclusions

Although index values for south-west England and Wales indicate that the summer of 1985 was windy, it is obvious that the major contribution came from the month of August thus coinciding with the major holiday period. Northern and central regions had many summer months with index values below

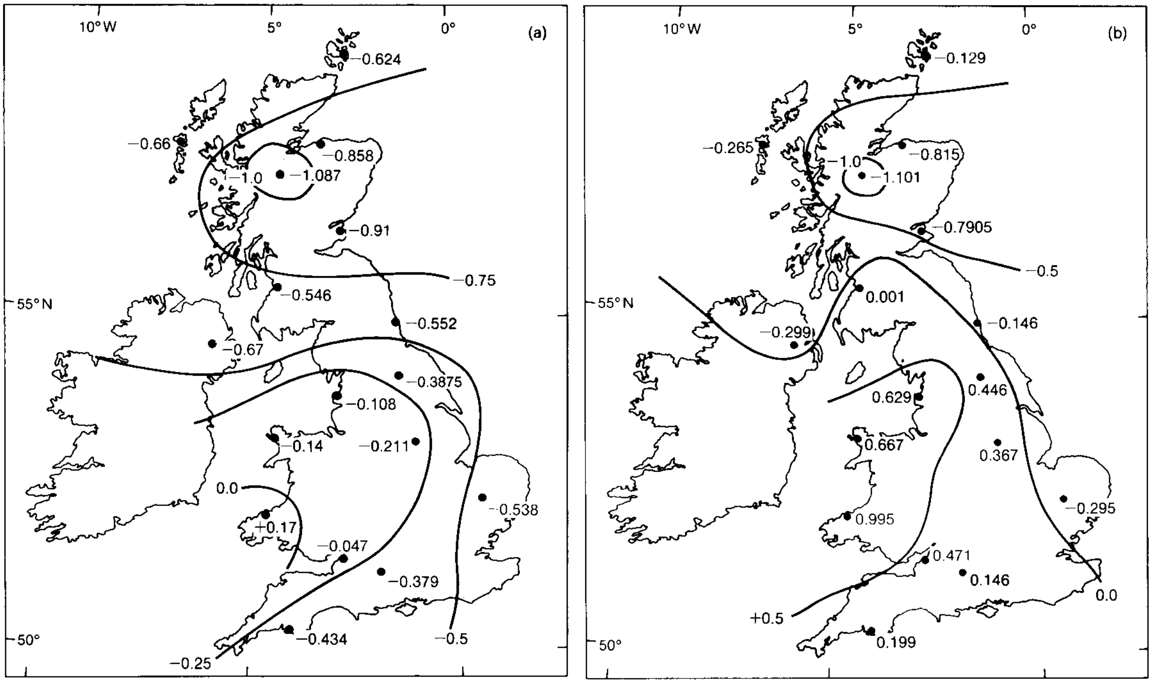

Figure 6. Geographical variations in the index for (a) the year 1985 and (b) the summer of 1985 for the stations shown in Fig. 1.

Table I. *Corrections calculated to compensate for using 1970–84 averages instead of 1965–80 values and for using anemograph data for differing stations. Calculated from data for 1970–80 to produce a national mean value for each month.*

Month	Jan.	Feb.	Mar.	Apr.	May	June	July	Aug.	Sept.	Oct.	Nov.	Dec.
Correction	−0.16	−0.03	0.11	0.35	0.2	0	0.14	0.11	−0.24	−0.27	−0.06	−0.03

Table II. *Monthly indices averaged over the three regions shown in Fig. 1 for the period 1980–5 (values for the period 1881–1980 can be found in Smith (1982))*

Year	Month											
	Jan.	Feb.	Mar.	Apr.	May	June	July	Aug.	Sept.	Oct.	Nov.	Dec.
1980	−1.2	−0.8	−0.3	−0.3	−0.3	0.7*	0.7	0.9	0.7	0.9	0.6*	0.9
1981	0.1	0.6	0.6	−0.6	0.3	1.2	0.4	−0.7	0.2	0.7	0.5	−0.6
1982	−0.3	0.7	0.4	−0.8	−0.4	−0.9	−0.8	1.6	0.2	0.4	0.6	−0.1
1983	1.9	0.2	0.1	−0.9	−0.6	−0.4	−1.8	−1.1	1.0	1.4	−1.6	0.1
1984	1.0	0.1	−1.5	−1.3	−1.7	−0.5	−1.1	−1.2	−0.2	0.5	−0.4	−0.8
1985	−1.4	−0.4	−0.9	0.2	−1.1	−0.8	−0.2	1.9	−0.5	−1.3	−0.9	0.1

* Indicates relatively large regional differences

the 15-year average and, if the mean of the three regions is calculated, the summer as a whole may be described as slightly less windy than average. In addition, since the 1970–84 averaging period is itself characterized by having index values predominantly lower than the 1881–1980 average as calculated by Smith (1982), 1985 may be considered a quiet year.

References

Smith, S.G. 1982 An index of windiness for the United Kingdom. *Meteorol Mag*, **111**, 232–247.

Stainer, D.E. 1986 Summer 1985. (Letter to the editor.) *Weather*, **41**, 167.

Conference report

Computers and Climatic Data, Building Research Establishment, Garston, England, 10–11 June 1986

The Conseil Internationale du Bâtiment (CIB) is an international organization devoted to building research and documentation. It operates through a number of working commissions, one of which (W71, responsible for building climatology) held a 2-day seminar, Computers and Climatic Data, at the Building Research Establishment (BRE) at Garston, England on 10 and 11 June 1986. The seminar was organized by E. Keeble of the Environmental Physics Division at BRE.

Building science applications involving computers and climatic data include estimation of site-specific peak wind loadings, interpretation of energy use, and design to produce buildings which are comfortable and energy efficient.

The size of meteorological data bases and the complexity of a system composed of a building, its occupants and the external environment make computers ideal for investigating the relationship between a building and the weather.

Extreme wind conditions can have a catastrophic effect on buildings and structures like cooling towers, bridges and tower cranes. N. Cook (BRE) demonstrated a computer program (STRONGBLOW) used for calculating wind-gust design data for any UK site and any building height. This program relies on observed wind data received from the Meteorological Office and on-site characteristics supplied by the user, including local topography and surface roughness as a function of both direction and distance. It generates estimates of the 4-, 8- and 16-second gust speeds for a 50-year return period, for 12 equal sectors of the compass. STRONGBLOW is commercially available on microcomputers compatible with IBM personal computers.

Similar methods for calculating wind characteristics were used in interactive programs demonstrated by C. Sacré (Centre Scientifique et Technique du Bâtiment (CSTB), Nantes, France) to estimate the likely output of wind turbines as a function of site characteristics, and by S. Lockley (University of Newcastle upon Tyne) who demonstrated the use of Computer-Aided Design (CAD) graphics to assess exposure to wind-driven rain, which can affect both the fabric and energy use of a building.

The ABACUS computer unit at the University of Strathclyde is a leading UK group working in the field of CAD applied to environmental simulation in buildings. The Environmental Systems Performance (ESP) program is a detailed model capable of providing visual information about many aspects of the performance of a building — down to the transient response of temperatures within the layers of a wall structure, for example. Demonstrating ESP on a Whitechapel MG1 Workstation, J. Clarke (University of Strathclyde) recognized that lack of empathy with computer systems like ESP might be a block to their adoption by designers. He felt that the use of expert scripts giving details about features such as solar shading and overheating, comfort conditions, energy consumption and control-system optimization was the way to develop user output. ABACUS currently has about 90 annual meteorological data bases from Europe and the United Kingdom which can be used with ESP.

Following J. Clarke came P. Martin (Energy Designs and Surveys, Luton) who addressed the problem of providing adequate degree-hour and degree-day data for intermittently occupied buildings. Degree-days give an index, widely used by heating engineers, related to the area accumulated between the external temperature–time graph and a constant temperature (commonly called the base temperature) above which the building does not require heating. Although 15.5 °C is the customary figure, the true base temperature varies with the level of insulation, solar input and casual heat gain. A building's heat requirement should be proportional to the degree-day total. Monthly degree-day data for 17 UK sites are published in the Department of Energy's monthly newspaper *Energy Management* but P. Martin argued that because of holidays and intermittent occupancy this information was not suitable for setting energy targets for schools. He felt that under intermittent occupation a better index would be provided by the degree-hours accumulated during the time the building was actually in use. He illustrated the use of a microcomputer program, TEAM (Targeting, Energy Auditing and Monitoring), which uses temperature data from an electronic module left at a school and energy consumption information provided by utility bills or on-site readings, to decide whether a building is meeting a target energy consumption derived from the historically observed relationship between energy consumption and accumulated degree-hours.

Also in the area of site-specific temperature data, J. Penman (University of Exeter, Energy Study Unit) demonstrated, on a SIRIUS personal computer, a program to predict a site's long-term monthly mean temperature and degree-day figures (to any base temperature) from its geographical co-ordinates and height above sea level. This program relies on polynomial trend surfaces fitted to observed temperature data measured in a particular area. At present this has only been done for the south-west peninsula of the United Kingdom. Other areas could, of course, be analysed. The program gives site-specific information which can be used to estimate average heating requirements, or to correct the published *Energy Management* degree-day data, which for the south-west is measured in Plymouth. The program indicates that sites in Devon and Cornwall may have degree-day totals ranging from about 40% more to 20% less than the Plymouth figures.

Although solar overheating can be a problem, in northern Europe more attention is given to climate as a determinant of space heating requirements. However, at low latitudes the solar input is such that poor design can lead to impossible conditions inside buildings. Other meteorological variables such as temperature, humidity, rain and wind will also influence the type of building structure which produces a comfortable environment in hot climates. Simple guide-lines to good architectural practice in the tropics are provided by the Mahoney Tables, a manual design procedure requiring only monthly values of meteorological variables. However, as with many algorithms in building science, the Mahoney Tables are fairly lengthy to complete and there is an advantage in computerizing them, especially if repeated applications are required as in teaching. This has been done by O.O. Ogunsote (Ahmadu Bello University, Nigeria) whose work was presented by A. Penwarden (BRE).

The problem of shading from direct sunlight has application both in hot climates (to minimize solar gain) and in temperate and cold regions (where maximum solar access will be required in the heating season but shading may be desirable in the summer). The geometry of shading is both complex and variable (because of the sun's seasonal and diurnal movement), and so computers are particularly useful for shading calculations. Two contributions were made on this subject, one from D. Summers (Napier College of Commerce and Technology, Edinburgh) and the other from M. Sattler (Fundação de Ciência e Tecnologia, Porto Alegre, Brazil and University of Sheffield). The first of these was a program (SHADE) developed to predict areas of ground shaded by groups of buildings. This has found application in the Middle East. M. Sattler's program was developed to calculate the shading of buildings and building surfaces by trees as a function of time and season. It was demonstrated as applied to the shading of low-cost housing in Brazil.

The problem of calculating solar inputs was addressed by J. Page (Emeritus Professor at the University of Sheffield) who demonstrated a microcomputer program to calculate solar irradiation and illumination on inclined planes for any geographical location. Meteorological observations generally provide solar data measured on the horizontal plane. Since buildings consist predominantly of vertical planes this ability to go from horizontal to vertical and other orientations is important in calculating solar gains.

The use of shade to provide protection against the sun was illustrated in a series of slides of Italian Renaissance architecture shown by A. Lauritano (University of Palermo) who suggested that transitional spaces between the internal and external environment had been a feature of the architecture of the past and that an abrupt inside/outside interface was a modern characteristic. Transitional spaces could ease the environmental stress on a building envelope and the provision of shade could often provide a comfortable environment outside the building. These ideas were quantified in the computer program ECA (External Climate Assessment). Application of ECA to meteorological data in the Trapani Test Reference Year showed that shade increased, from 40% to 80%, the proportion of time that the external environment was comfortable given sensible choice of clothing. ECA relates individual comfort to the environment through air and mean radiant temperatures, wind velocity, relative humidity, clothing and activity level.

R. Taesler (Swedish Meteorological and Hydrological Institute) described the results of a computer investigation into energy use in housing in an area about 50 km wide around an airfield where meteorological measurements were made. The computer model considered the wind field (which affects air infiltration and surface losses), temperature variation and solar inputs. Variations in energy use of typically 20% were predicted. The orientation of a building with respect to the wind was important and sheltering by surrounding buildings could itself reduce heat losses by 20%, other things being equal. This underlines the importance of shelter to energy efficiency, in northern Europe at least.

It is well known that urban areas are warmer than the surrounding countryside, sometimes by several degrees Celsius. There are several plausible reasons for this, amongst them greater urban albedo, reduced latent heat flux due to rapid urban drainage, heat capacity effects and anthropogenic heat. The relative significance of these factors is, however, uncertain. The analysis of data from the Heat Capacity Mapping Mission (HCMM) satellite, which observes the surface of the earth in the 10.5 to 12.5 micron infra-red atmospheric window from polar orbit, was described by R. Gillies (University of Newcastle upon Tyne) who is investigating the causes of urban heat islands.

Any assessment of climate impact on building energy use requires meteorological data as input. The University of Sheffield, in contract to the UK Science and Engineering Research Council, has been assembling a meteorological data base for UK researchers. This takes hourly data from seven sites, typically over an 8-year period although for one site (Kew) 19 years of data are available. The data cover solar radiation (beam and diffuse), temperature (wet- and dry-bulb), pressure, wind speed and direction, rainfall (amount and duration) and coded weather descriptions. This information can be accessed via the Joint Academic NETwork (JANET) computer network. The development of the data base at Sheffield and an associated data base management system (INFOMET) was described and demonstrated by C. Gibbons.

Statistical descriptions of climatic regimes provide a possible compact alternative to extensive sets of meteorological data. In the second part of his demonstration, C. Sacré (CSTB, Nantes, France) described techniques for simulating cross-correlated sequences of meteorological data as time series described by Markov chains. Seven variables spanning temperature, humidity, wind, solar input and atmospheric pressure were covered.

The formal presentations were followed by a visit on the following day to Milton Keynes Energy Park where the intelligent use of local topography, plant shelter belts and building orientation allowing solar access will contribute to a saving of perhaps 10% in energy use. This is in addition to other savings achieved by energy efficient building design. The principles involved were explored by R. Griffiths, a landscape architect with the Milton Keynes Development Corporation.

The CIB-W71 co-ordinator is V. Torrance (Heriot-Watt University) who, with J. Page (University of Sheffield), shared the chairing of this seminar. The presentations clearly showed the usefulness of computers in fields like building science and climatology which deal with complex systems and large amounts of data. The next CIB-W71 seminar, New Developments in Building Climatology, will be in Moscow in May 1987.

J.M. Penman

Notes and news

IAMAP Scientific Assembly, Reading, 1989

The International Association of Meteorology and Atmospheric Physics (IAMAP) was founded in 1919 and aims to:

(a) promote meteorological research and investigation into all aspects of atmospheric physics, particularly those fields which require international co-operation, and

(b) provide a forum for the discussion of results and trends in research.

IAMAP organizes a Scientific Assembly every 4 years, and the next one will be held at the University of Reading from 31 July to 11 August 1989. The topics to be covered will be decided at the General Assembly of the International Union of Geodesy and Geophysics which takes place in Vancouver during August 1987. It is expected that further information about the IAMAP Scientific Assembly will be available in September 1987 from Ross Reynolds, IAMAP Local Organizing Committee, University of Reading, Department of Meteorology, 2 Earley Gate, Whiteknights, Reading RG6 2AU.

Books received

The listing of books under this heading does not preclude a review in the Meteorological Magazine at a later date.

Contemporary climatology, by A. Henderson-Sellers and P.J. Robinson (Harlow, Longman, 1986. £9.95 (paperback only)) presents a synthesis of contemporary scientific ideas with topics including: local and regional climates, applications of climate information and an analysis of the formulation of climate models with a view to predicting future climates. Its intended readership includes people from other disciplines and without strong scientific background.

Physical fundamentals of remote sensing, by E. Schanda (Berlin, Heidelberg, New York, Tokyo, Springer-Verlag, 1986. DM 48.00) is based on a course presented by the author at the Universities of Bern and Toulouse in recent years. It aims to awaken an appreciation of the physical background of remote sensing and create an awareness of the importance of the interaction between electromagnetic radiation and matter for the optimal use of remote sensing.

An introduction to three-dimensional climate modelling, by W.M. Washington and C.L. Parkinson (Oxford University Press, 1986. £25.00) is a guide to the development and use of computer models of the earth's climate. The book describes the basic theory of climate simulation, including the fundamental equations and relevant numerical techniques for simulating the atmosphere, ocean and sea ice. Results for a variety of past, present and future climates are shown and compared with observations.

Satellite photograph — 12 November 1986 at 1457 GMT

The NOAA-9 visible image indicates a broad zone of thick cloud separating a large complex region of low pressure over the Atlantic from anticyclonic conditions over central Europe. A small northward-moving wave depression (labelled W) that deepened by about 10 mb between 1200 and 1800 GMT is clearly identified by a mass of thick cloud at the rear edge of the frontal cloud band. Vigorous convective cells are observed immediately behind the wave and to the west where cold air is flowing over the warmer sea. In the north-west corner of the picture several vortices are present within the low pressure complex, those along the picture edge being associated with an occluded front.

Considerable cloud detail is present over Europe. The non-fibrous appearance and the length of the shadows indicate that much of the cloud is at medium levels, although an area of fog or low cloud is seen over Belgium. Numerous short lee-wave trains are apparent over the British Isles.

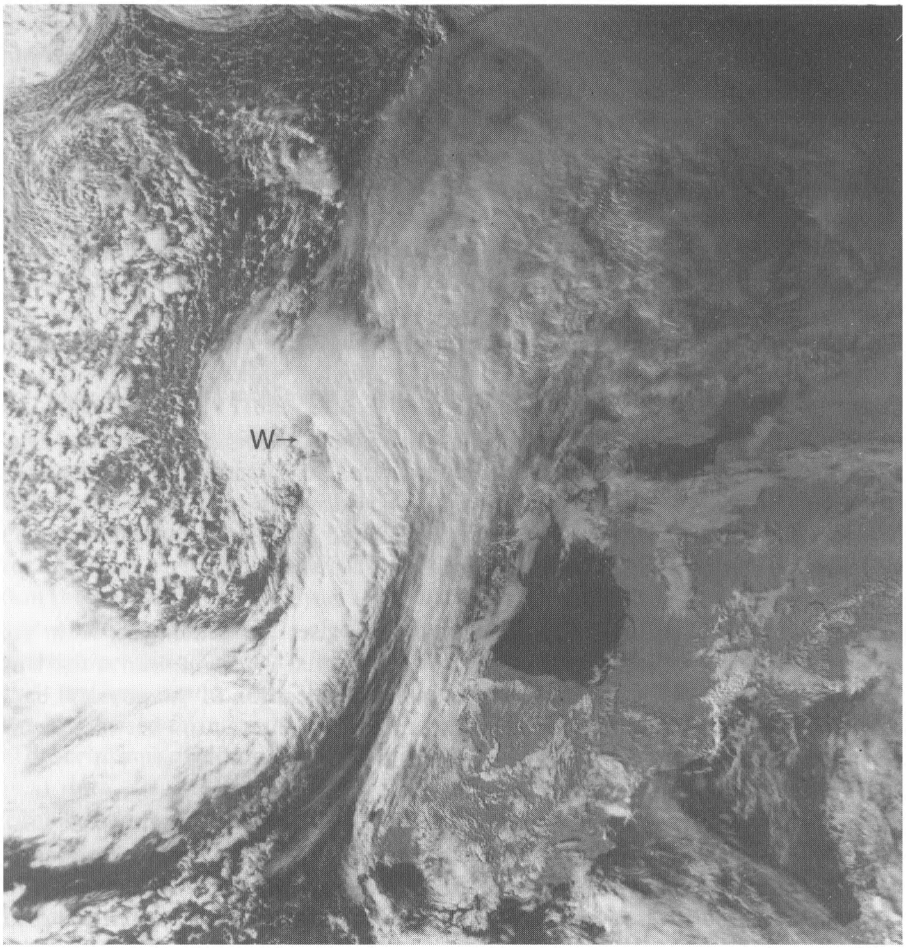

Photograph by courtesy of University of Dundee

Meteorological Magazine

GUIDE TO AUTHORS

Content

Articles on all aspects of meteorology are welcomed, particularly those which describe the results of research in applied meteorology or the development of practical forecasting techniques.

Preparation and submission of articles

Articles for publication and all other communications for the Editor should be addressed to the Director-General, Meteorological Office, London Road, Bracknell, Berkshire RG12 2SZ and marked 'For *Meteorological Magazine*'.

Articles, which must be in English, should be typed, double-spaced with wide margins, on one side only of A4-size paper. Tables, references and figure captions should be typed separately.

Spelling should conform to the preferred spelling in the *Concise Oxford Dictionary*.

References should be made using the Harvard system (author, date) and full details should be given at the end of the text. If a document referred to is unpublished, details must be given of the library where it may be seen. Documents which are not available to enquirers must not be referred to.

Tables should be numbered using roman numerals and provided with headings. We consider vertical and horizontal rules to be unnecessary in a well-designed table; spaces should be used instead.

Mathematical notation should be written with extreme care. Particular care should be taken to differentiate between Greek letters and Roman letters for which they could be mistaken. Double subscripts and superscripts should be avoided, as they are difficult to typeset and difficult to read. Keep notation as simple as possible; this makes typesetting quicker and therefore cheaper, and reduces the possibility of error. Further guidance is given in BS1991: Part 1: 1976 and *Quantities, Units and Symbols* published by the Royal Society.

Illustrations

Diagrams must be supplied either drawn to professional standards or drawn clearly, preferably in ink. They should be about 1½ to 3 times the final printed size and should not contain any unnecessary or irrelevant details. Any symbols and lettering must be large enough to remain legible after reduction. Explanatory text should not appear on the diagram itself but in the caption. Captions should be typed on a separate sheet of paper and should, as far as possible, explain the meanings of the diagrams without the reader having to refer to the text.

Sharp monochrome photographs on glossy paper are preferred: colour prints are acceptable but the use of colour within the magazine is at the Editor's discretion. In either case contrast should be sufficient to ensure satisfactory reproduction.

Units

SI units, or units approved by WMO, should be used.

Copyright

Authors wishing to retain copyright for themselves or for their sponsors should inform the Editor when they submit contributions which will otherwise become UK Crown copyright by right of first publication.

It is the responsibility of authors to obtain clearance for any copyright material they wish to use before submitting it for publication.

Free copies

Three free copies of the magazine are provided for authors of articles published in it. Separate offprints for each article are not provided.

Meteorological Magazine

February 1987

Vol. 116
No. 1375

CONTENTS

Contributions: it is requested that all communications to the Editor and books for review be addressed to the Director-General, Meteorological Office, London Road, Bracknell, Berkshire RG12 2SZ, and marked 'For *Meteorological Magazine*'. Contributors are asked to comply with the guidelines given in the *Guide to authors* which appears on the inside back cover. The responsibility for facts and opinions expressed in the signed articles and letters published in *Meteorological Magazine* rests with their respective authors. Authors wishing to retain copyright for themselves or for their sponsors should inform the Editor when submitting contributions which will otherwise become UK Crown copyright by right of first publication.

Subscriptions: Annual subscription £27.00 including postage; individual copies £2.30 including postage. Applications for postal subscriptions should be made to HMSO, PO Box 276, London SW8 5DT; subscription enquiries 01–211 8667.

Back numbers: Full-size reprints of Vols 1–75 (1866–1940) are available from Johnson Reprint Co. Ltd, 24–28 Oval Road, London NW1 7DX. Complete volumes of *Meteorological Magazine* commencing with volume 54 are available on microfilm from University Microfilms International, 18 Bedford Row, London WC1R 4EJ. Information on microfiche issues is available from Kraus Microfiche, Rte 100, Milwood, NY 10546, USA.

ISBN 0 11 727966 8 ISSN 0026–1149

Printed for HER MAJESTY'S STATIONERY OFFICE
by Delco Printing Co Ltd 2/87 Dd. 739131 C1425

THE METEOROLOGICAL MAGAZINE

HER MAJESTY'S STATIONERY OFFICE

March 1987

Met.O.978 No. 1376 Vol. 116

J/6.

METEOROLOGICAL OFFICE Met.O.978

THE METEOROLOGICAL MAGAZINE

No. 1376, March 1987, Vol. 116

551.513.1:551.558.21

Linear models of stationary planetary waves forced by orography and thermal contrast*

G.J. Shutts
Meteorological Office, Bracknell

Summary

Time-averaged geopotential height maps are dominated by continental-scale long waves forced by orography and land/sea thermal asymmetry. Most of the energy associated with these longitudinal variations is contained in wave numbers 1–3 and extends from the surface to at least the upper stratosphere. Simple quasi-geostrophic theory on a beta-plane can be used to show how planetary waves forced near the surface can propagate to great heights as Rossby waves. Characteristic features of a solution representing the steady response to low-level heating can be identified in observations. These include a westward tilt with height of the wave system, poleward heat transport (particularly near the surface) and a 'whiplash' amplification of the disturbance in the stratosphere.

1. Introduction

By studying the dynamics of large-scale motion systems using linear theory one can effectively regard the weather chart (e.g. 500 mb contour height maps) as an interference pattern (as in wave optics) formed by the superposition of waves of different dynamical origin. Ultra-long wave motion (wavelengths greater than about 6000 km) is particularly amenable to this type of representation since global fields are readily expanded into complete sets of orthogonal functions (e.g. sines/cosines, Legendre functions and Hough functions). For instance, the broad character of the stratospheric circulation is well represented by a Fourier expansion in the zonal direction truncated at wave number 3, though this should not be interpreted as implying that higher wave numbers are dynamically unimportant. The linear approach ignores interactions between waves or between waves and zonally-averaged flow and so must be regarded as a gross approximation. Nevertheless, linearized solutions reveal much about the wave character of dynamical systems and provide a dynamically consistent model against which real data can be interpreted.

In sections 2 and 3 the Rossby wave as a three-dimensional motion system capable of transmitting energy and momentum over great distances in the atmosphere is considered. This involves the derivation of a wave equation for Rossby waves in a uniform westerly flow with constant static stability.

* Lecture note from a series of lectures entitled 'Dynamical Processes in Meteorology' given as part of the 1986 Advanced Lectures (Meteorological Office, 15 September–3 October 1986).

Conditions for wave propagation are established and the direction of energy propagation is linked to the group velocity. In sections 4 and 5 some steady responses of an airstream of uniform speed and direction to sinusoidal orography and fixed diabatic heat sources are obtained as analytical solutions to the quasi-geostrophic equations. The final section contains a comparison of the observed time-mean amplitude and phase of wave number 1 with the thermally-forced response given by the theory.

2. Quasi-geostrophic theory

The quasi-geostrophic vorticity equation on a mid-latitude beta-plane may be written as

$$\frac{\mathrm{D}}{\mathrm{D}t_{\mathrm{H}}}\zeta_{\mathrm{g}} + \beta v_{\mathrm{g}} = \frac{f_0}{\rho_0}\frac{\partial}{\partial z}(\rho_0 w) \qquad \ldots \ldots \ldots \ldots \ldots \ldots \quad (1)$$

where ζ_{g} is the vertical component of the geostrophic vorticity vector, u_{g} and v_{g} are the components of the geostrophic wind, f_0 is a constant mid-latitude Coriolis parameter, β is the mean meridional gradient of the Coriolis parameter, $\rho_0(z)$ is the basic state density field (taken here to be proportional to $\exp(-z/H_0)$ where H_0 is the density scale height) and w is the vertical velocity. Also, the substantial derivative $\mathrm{D}/\mathrm{D}t_{\mathrm{H}}$ is given by

$$\frac{\mathrm{D}}{\mathrm{D}t_{\mathrm{H}}} = \frac{\partial}{\partial t} + u_{\mathrm{g}}\frac{\partial}{\partial x} + v_{\mathrm{g}}\frac{\partial}{\partial y} .$$

The geostrophic wind vector and vorticity are related to the perturbation pressure field p' (defined as the deviation of the pressure from the basic state $p_0(z)$) by

$$(u_{\mathrm{g}}, v_{\mathrm{g}}) = \frac{1}{f_0}\left\{-\frac{\partial}{\partial y}\left(\frac{p'}{\rho_0}\right), \frac{\partial}{\partial x}\left(\frac{p'}{\rho_0}\right)\right\} \qquad \ldots \ldots \ldots \ldots \ldots \quad (2a)$$

$$\zeta_{\mathrm{g}} = \nabla_{\mathrm{H}}^2\left(\frac{p'}{\rho_0 f_0}\right) = \left(\frac{\partial^2}{\partial x^2} + \frac{\partial^2}{\partial y^2}\right)\frac{p'}{\rho_0 f_0} . \qquad \ldots \ldots \ldots \ldots \ldots \quad (2b)$$

The geostrophic wind is approximated by its non-divergent, f-plane equivalent (based on f_0) in quasi-geostrophic theory.

Equation (1) tells us that the relative vorticity ζ_{g} can be changed by meridional advection with the geostrophic wind (βv_{g} term) and by the vertical stretching of planetary vorticity.

The thermodynamic equation may be expressed as

$$\frac{\mathrm{D}}{\mathrm{D}t_{\mathrm{H}}}\left(\frac{\theta'}{\theta_0}\right) + wB = S \qquad \ldots \ldots \ldots \ldots \ldots \ldots \quad (3)$$

where θ' is the perturbation of the potential temperature from a horizontally stratified basic state $\theta_0(z)$, B is the static stability $1/\theta_0\,(\mathrm{d}\theta_0/\mathrm{d}z)$ and S is some unspecified diabatic heat source. Using the hydrostatic equation

$$\frac{\partial}{\partial z}\left(\frac{p'}{\rho_0}\right) = g\frac{\theta'}{\theta_0}$$

equation (3) may be written as

$$\frac{\mathrm{D}}{\mathrm{D}t_{\mathrm{H}}}\left\{\frac{\partial}{\partial z}\left(\frac{p'}{\rho_0}\right)\right\} + N^2 w = gS \qquad \ldots \ldots \ldots \ldots \ldots \quad (4)$$

where g is the acceleration due to gravity and $N = (gB)^{1/2}$ is the Brunt-Väisälä frequency. By eliminating w

from equations (1) and (4), and substituting for (u_g, v_g) and ζ_g using the expressions in equations (2a) and (2b), a single equation for p' can be obtained and written as

$$\frac{D}{Dt_H}\left[\nabla_H^2 p' + \frac{\partial}{\partial z}\left\{\frac{\rho_0 f_0^2}{N^2}\frac{\partial}{\partial z}\left(\frac{p'}{\rho_0}\right)\right\}\right] + \beta\frac{\partial p'}{\partial x} = f_0^2 g\frac{\partial}{\partial z}\left(\frac{\rho_0 S}{N^2}\right) \qquad \ldots \ldots (5)$$

with

$$\frac{D}{Dt_H} = \frac{\partial}{\partial t} + \frac{1}{f_0\rho_0}\left(\frac{\partial p'}{\partial x}\frac{\partial}{\partial y} - \frac{\partial p'}{\partial y}\frac{\partial}{\partial x}\right)$$

(cf. Gill (1982), page 530, equation (12.8.7) — the adiabatic case).

3. Free Rossby wave solutions

Consider now the special case of equation (5), where N^2 = constant and $S = 0$, and linearize the equation about an atmosphere with uniform zonal wind U. This involves the substitution of $p' = -\rho_0 f_0 Uy + \delta p$, where δp is the pressure perturbation associated with the Rossby wave, and the neglect of terms quadratic in δp so that

$$\left(\frac{\partial}{\partial t} + U\frac{\partial}{\partial x}\right)\left[\nabla_H^2 \delta p + \left(\frac{f_0}{N}\right)^2\frac{\partial}{\partial z}\left\{\rho_0\frac{\partial}{\partial z}\left(\frac{\delta p}{\rho_0}\right)\right\}\right] + \beta\frac{\partial}{\partial x}\delta p = 0. \qquad \ldots \ldots (6)$$

Wave solutions to equation (6) have the form

$$\delta p = \mathrm{Re}\,[F(z)\exp\{i(kx \pm \mu y - \sigma t)\}]$$

where $F(z)$ is a complex vertical structure function, k and μ are zonal and meridional wave numbers respectively, and σ is the angular frequency. Substituting this expression in equation (6) gives

$$(-\,i\sigma + Uik)\left[-\,K^2F + \left(\frac{f_0}{N}\right)^2\frac{d}{dz}\left\{\rho_0\frac{d}{dz}\left(\frac{F}{\rho_0}\right)\right\}\right] + \beta ikF = 0$$

where $K^2 = k^2 + \mu^2$. This further simplifies to

$$\frac{d^2F}{dz^2} + \frac{1}{H_0}\frac{dF}{dz} + \left\{\left(\frac{N}{f_0}\right)^2\frac{\beta}{U-c} - K^2\right\}F = 0 \qquad \ldots \ldots \ldots \ldots (7)$$

where $c = \sigma/k$ is the phase speed. It is easily verified that $F(z)$ has solutions of the form

$$F(z) = \exp\left(i\nu z - \frac{z}{2H_0}\right)$$

where ν is a vertical wave number given by the dispersion relation

$$\nu^2 + \frac{1}{4H_0^2} = \left(\frac{N}{f_0}\right)^2\left(\frac{\beta}{U-c} - K^2\right). \qquad \ldots \ldots \ldots \ldots \ldots (8)$$

A linear combination of solutions of the form

$$\delta p = \exp\left\{i(kx \pm \mu y \pm \nu z - \sigma t) - \frac{z}{2H_0}\right\}$$

will satisfy equation (6) (different combinations of + and − are used). Note that if ν^2 is positive, ν is a real quantity and the solutions will be wave-like in the vertical as well as the horizontal. Otherwise, ν would be a pure imaginary number and δp would be given by

$$\delta p = \exp\left\{ \mathrm{i}(kx \pm \mu y) \pm |\nu| z - \frac{z}{2H_0} \right\}.$$

It is instructive to calculate the kinetic energy per unit volume $\frac{1}{2}\,\rho_0\,(u_g^2 + v_g^2)$ averaged over a horizontal wavelength in the zonal and meridional directions. When $\nu^2 > 0$ this is easily shown to be a constant, otherwise

$$\tfrac{1}{2}\,\rho_0\,(u_g^2 + v_g^2) \propto \exp\,(\pm\, 2|\nu| z)$$

and the energy grows or decays exponentially with height. Therefore it is physically reasonable to reject the solution with $\nu = -\mathrm{i}|\nu|$ corresponding to $\nu^2 < 0$ since the energy source for the disturbance cannot originate at infinite height.

The condition $\nu^2 > 0$ may be re-expressed as

$$K^2 < \left(\frac{\beta}{U-c} - \frac{f_0^2}{4H_0^2N^2}\right) \qquad \ldots\;\ldots\;\ldots\;\ldots\;\ldots\;\ldots\; (9)$$

or

$$0 < U-c < \frac{\beta}{K^2 + \left(\frac{f_0}{N}\right)^2 \frac{1}{4H_0^2}} \qquad \ldots\;\ldots\;\ldots\;\ldots\;\ldots\; (10)$$

and was first put forward by Charney and Drazin (1961). The conditions given by equations (9) and (10) suggest that only the largest horizontal scales of wave motion will be capable of propagating vertically and that strong westerly winds may act as a barrier to Rossby wave energy. Note also that for stationary waves ($c = 0$) vertical energy propagation is impossible in easterly winds. Figs 1 and 2 show geopotential height and temperature maps of the 10 mb pressure surface for winter and summer in the northern hemisphere. The westerly zonal circulation in winter allows planetary wave energy (typically only wave numbers 1 and 2) to propagate from the troposphere up to the mesosphere so that the time-averaged stratospheric circulation exhibits persistent features such as the Aleutian High. In contrast, the easterly summer-time regime of the stratosphere is opaque to upward propagating stationary planetary waves and the flow is extremely zonal.

Setting $\mu = 0$ for convenience, it can be shown that wave solutions of the form

$$\delta p \propto \exp\left\{ \mathrm{i}(kx + \nu z - \sigma t) - \frac{z}{2H_0} \right\} \qquad \ldots\;\ldots\;\ldots\;\ldots\;\ldots\; (11)$$

transmit disturbance energy upwards and since their lines of constant phase are given by $kx + \nu z - \sigma t$ equal to a constant, they tilt upstream with height (Fig. 3). In fact it is this type of solution which is most relevant to the real atmosphere since the principal energy sources for these waves are found in the lower troposphere and their upward propagation is unimpeded — even by the sudden change in static stability at the tropopause.

The dispersion relation equation (8) can be re-expressed in terms of σ yielding

$$\sigma = Uk - \frac{\beta k}{K^2 + \left(\frac{f_0}{N}\right)^2 \left(\nu^2 + \frac{1}{4H_0^2}\right)}$$

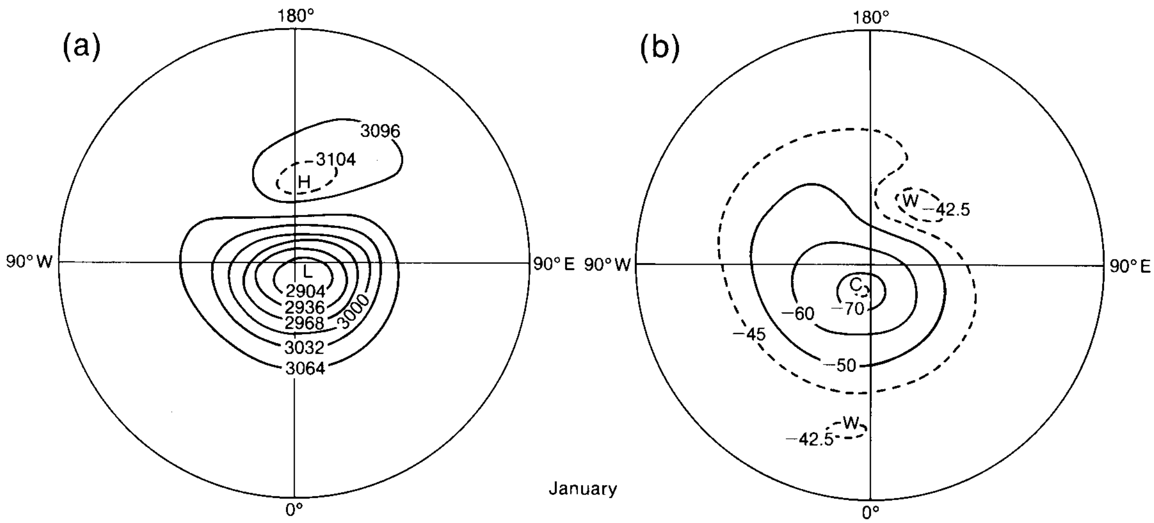

Figure 1. Synoptic charts at 10 mb for the northern hemisphere in January showing fields of (a) geopotential height (dam) and (b) temperature (°C) averaged over several years.

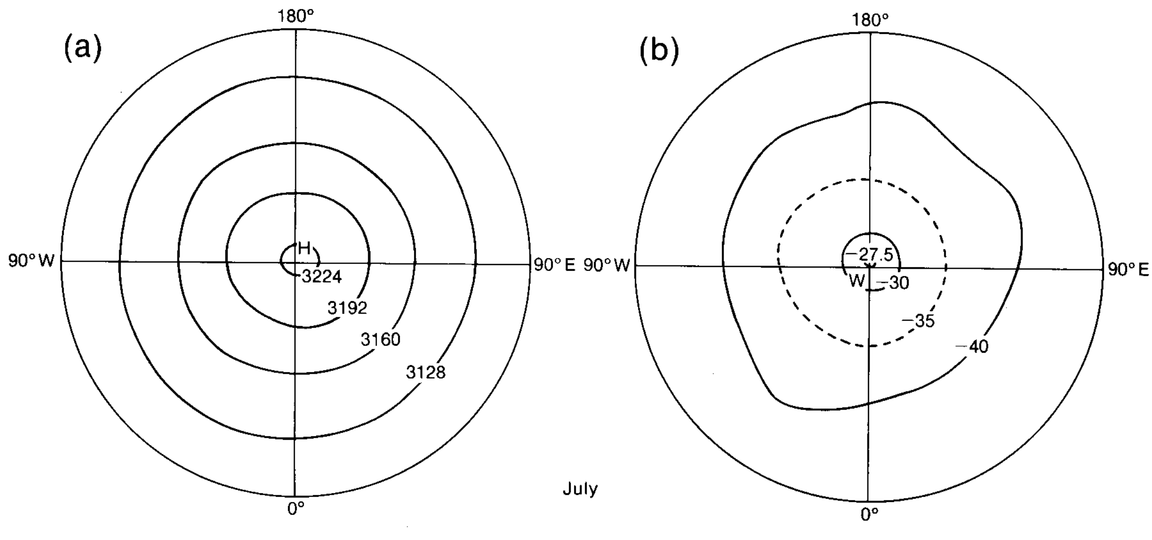

Figure 2. As Fig. 1 but for July.

and the vertical component of the group velocity (C_{gz}), which represents the speed and direction of energy propagation, can be obtained by differentiating with respect to ν giving

$$C_{gz} = \frac{\partial \sigma}{\partial \nu} = \frac{2\beta k \left(\dfrac{f_0}{N}\right)^2 \nu}{\left\{K^2 + \left(\dfrac{f_0}{N}\right)^2 \left(\nu^2 + \dfrac{1}{4H_0^{\,2}}\right)\right\}^2} \quad \ldots \quad (12)$$

Upward energy propagation ($C_{gz} > 0$) is then associated with $\nu > 0$ as selected for equation (11).

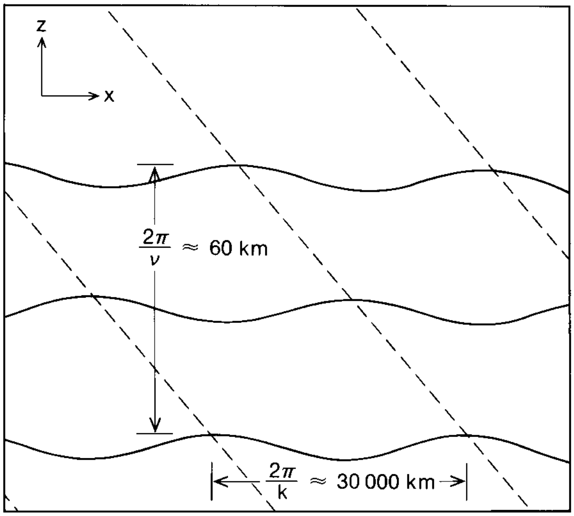

Figure 3. Phase lines of upward energy radiating planetary Rossby waves.

Alternatively, equation (12) can be written as

$$C_{gz} = \frac{2\beta k \left(\frac{f_0}{N}\right)^2 \nu}{\left(\frac{\beta}{U-c}\right)^2}$$

by making use of equation (8). If $K^2 << \beta/(U-c)$ and $1/(4H_0^2) << \nu^2$ then equation (8) gives

$$\nu^2 \approx \left(\frac{N}{f_0}\right)^2 \frac{\beta}{U-c}$$

and the expression for C_{gz} becomes

$$C_{gz} \approx \frac{2f_0k}{N\beta^{1/2}} (U-c)^{3/2} . \qquad \dots \dots \dots \dots \dots \dots (13)$$

Substituting typical values, e.g., $f = 10^{-4}\ \mathrm{s^{-1}}$, $k = 2\pi/(30\,000\ \mathrm{km})$, $N = 10^{-2}\ \mathrm{s^{-1}}$, $U-c = 10\ \mathrm{m\ s^{-1}}$ and $\beta = 1.6 \times 10^{-11}\ \mathrm{m^{-1}\ s^{-1}}$, gives $C_{gz} \approx 3$ km/day suggesting a time-scale of about 1 week for wave number 1 disturbances forced near the surface to reach the stratosphere. Note also that even stationary waves ($c = 0$) are capable of transmitting disturbance energy upwards.

The free Rossby waves discussed in this section are really just a convenient device for establishing the dispersive properties of purely sinusoidal inviscid, adiabatic motion and are not a specific model of an atmospheric phenomenon.

Following is a description of specific time-independent solutions to equation (5) which relate stationary Rossby wave structure to particular forcing mechanisms. The general characteristics of these stationary solutions may be compared to the observed time-mean long-wave pattern, though quantitative agreement only implies the plausibility of the model not its accuracy.

4. Orographic planetary waves

Linearizing equation (5) about an atmosphere of uniform static stability and zonal wind gives

$$U\frac{\partial}{\partial x}\left[\nabla_H^2\,\delta p + \frac{\partial}{\partial z}\left\{\rho_0\left(\frac{f_0}{N}\right)^2\frac{\partial}{\partial z}\left(\frac{\delta p}{\rho_0}\right)\right\}\right] + \beta\frac{\partial}{\partial x}\,\delta p = f_0^2\,g\frac{\partial}{\partial z}\left(\frac{\rho_0 S}{N^2}\right). \qquad \ldots\ldots\ldots (14)$$

Stationary solutions to equation (14) with $S=0$ are easily obtainable for flow over a sinusoidal 'mountain' whose height $h(x, y)$ is given by

$$h\,(x, y) = h_m \sin kx \cos \mu y$$

$$= h_m \,\mathrm{Re}\,[-\mathrm{i}\exp(\mathrm{i}kx)\cos\mu y] \qquad \ldots\ldots\ldots\ldots\ldots (15)$$

where h_m is the height of the peak.

Linearizing the interface condition $w = \mathrm{D}h/\mathrm{D}t$ at $z=h$ gives $w = U(\partial h/\partial x)$ at $z=0$, which may be substituted into the linearized form of the thermodynamic equation (4) yielding

$$U\frac{\partial^2}{\partial x\partial z}\left(\frac{\delta p}{\rho_0}\right) + N^2U\frac{\partial h}{\partial x} = 0$$

or

$$\frac{\partial}{\partial z}\left(\frac{\delta p}{\rho_0}\right) = -N^2h(x, y) \qquad \ldots\ldots\ldots\ldots\ldots\ldots (16)$$

at $z=0$.

The upward propagating stationary solutions are given by

$$\frac{\delta p}{\rho_0} = D\exp\left(\mathrm{i}\nu z + \frac{z}{2H_0} + \mathrm{i}kx\right)\cos\mu y$$

where D has to be determined from the lower boundary condition; equation (16) implies that

$$D\left(\mathrm{i}\nu + \frac{1}{2H_0}\right) = \mathrm{i}N^2h_m$$

or

$$D = \frac{N^2h_m\left(\nu + \frac{\mathrm{i}}{2H_0}\right)}{\nu^2 + \frac{1}{4H_0^2}}\quad .$$

Consequently $\delta p/\rho_0$ is given by

$$\frac{\delta p}{\rho_0} = \mathrm{Re}\left[\frac{N^2h_m}{\nu^2+\frac{1}{4H_0^2}}\left(\nu + \frac{\mathrm{i}}{2H_0}\right)\exp\left\{\mathrm{i}(\nu z + kx) + \frac{z}{2H_0}\right\}\right]\cos\mu y$$

or

$$\frac{\delta p}{\rho_0} = \frac{-h_mN^2}{\left(\nu^2+\frac{1}{4H_0^2}\right)^{1/2}}\sin(kx+\nu z-\delta)\exp\left(\frac{z}{2H_0}\right)\cos\mu y$$

where $\delta = \tan^{-1}(2H_0\nu)$. The phase difference between p'/ρ_0 and $h(x, y)$ at $z=0$ implies that the planetary wave is exerting a drag force on the orography. Taking $h_m = 200$ m, $B = 3 \times 10^{-5}$ m^{-1}, $U = 10$ m s^{-1}, $k = 2\pi/(30\,000$ km) and $\mu = 2\pi/(12\,000$ km) (corresponding to one middle-latitude maximum in the meridional structure of the wave) gives a pressure perturbation δp of about 4 mb.

Since most of the terrain height variation is due to mountain ranges which are smaller in extent than the continental scale relevant to planetary waves, the significance of these solutions is rather questionable. In view of this uncertainty we shall proceed to the case of diabatically-forced long waves and their comparison with observations.

5. Stationary thermally-forced wave solutions

Differences in thermal energy budgets over land and sea lead to large zonal asymmetries in the diabatic heating rate averaged over, say, 1 month. In the northern hemisphere winter slow radiative cooling (about 1 K/day) dominates over continental interiors (e.g. Siberia) in marked contrast to flow over the oceans which experiences rapid heating (about 3 K/day) due to the vigorous transfer of sensible and latent heat from the sea (Fig. 4). Linear theory can be used to get some idea of the large-scale stationary wave response to zonally-asymmetric, time-averaged heat sources.

Consider the response of δp in equation (14) to a sinusoidal distribution of heating which decays exponentially with height, i.e.

$$S = a \sin kx \cos \mu y \exp(-bz)$$

or

$$S = \mathrm{Re}[-\mathrm{i}a \exp(\mathrm{i}kx - bz) \cos \mu y] \qquad \ldots \ldots \ldots \ldots \ldots (17)$$

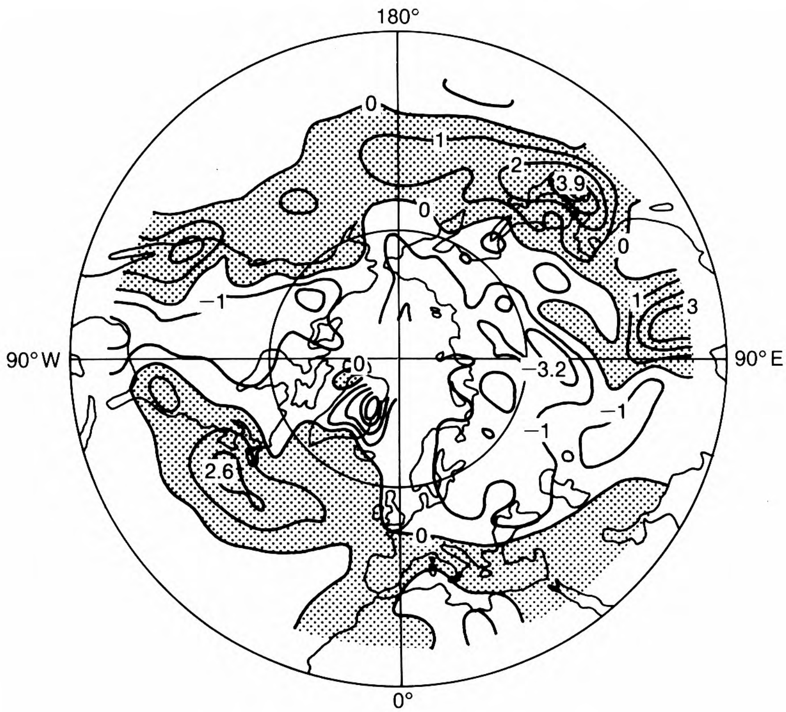

Figure 4. Diabatic heating computed for the 700 mb level in winter (contour interval 1 K/day) as estimated by Lau (1979). Shaded areas indicate regions of positive heating.

where a is a constant, k and μ are as defined previously and $1/b$ represents a depth scale for the diabatic source. The form of equation (17) suggests solutions of the kind

$$\delta p = \mathrm{Re}\,[F(z)\exp(\mathrm{i}kx)\cos\mu y] \qquad \ldots\ \ldots\ \ldots\ \ldots\ \ldots\ (18)$$

where we expect $F(z)$ to be a complex function of z.

Substituting equations (17) and (18) into equation (14) leads to an ordinary differential equation for $F(z)$ as follows

$$\frac{\mathrm{d}}{\mathrm{d}z}\left\{\rho_0\frac{\mathrm{d}}{\mathrm{d}z}\left(\frac{F}{\rho_0}\right)\right\} + \frac{N^2}{f_0^{\,2}}\left(\frac{\beta}{U} - K^2\right)F = \frac{\rho_s a g}{Uk}\gamma\exp(-\gamma z) \qquad \ldots\ \ldots\ \ldots\ (19)$$

where $\rho_s = \rho_0\,(z=0)$ and $\gamma = (b + 1/H_0)$. The general solution to this equation will involve a 'particular integral' which satisfies equation (19) on its own, together with a 'complementary function' which satisfies equation (19) when the right-hand side is zero (the homogeneous equation). The complementary function will in general involve two independent solutions to the homogeneous equation with multiplying factors to be determined by applying boundary conditions to the general solution.

Particular integrals of equation (19) will be of the form $C\exp(-\gamma z)$ and it can be shown that

$$C = \frac{\rho_s a g\gamma}{Uk\left\{bg + \left(\dfrac{N}{f_0}\right)^2\left(\dfrac{\beta}{U} - K^2\right)\right\}}\,.$$

The full solution will be of the form

$$\delta p = \mathrm{Re}\,[\{C\exp(-\gamma z) + \text{complementary function}\}\exp(\mathrm{i}kx)\cos\mu y] \qquad \ldots\ \ldots\ \ldots\ (20)$$

and must satisfy boundary conditions at $z = 0$ and ∞. As for the free solutions discussed earlier, the physically relevant complementary function is $A\exp(\mathrm{i}\nu z - z/2H_0)$ which is consistent with upward energy propagation; A remains to be determined by the lower boundary condition as shown below. We shall require that the vertical velocity vanishes at the plane horizontal surface at $z = 0$ (representing the ground). Again this condition can be enforced through the linearized form of the thermodynamic equation (4), i.e.

$$U\frac{\partial^2}{\partial x\partial z}\left(\frac{\delta p}{\rho_0}\right) + N^2 w = gS\,. \qquad \ldots\ \ldots\ \ldots\ \ldots\ \ldots\ \ldots\ (21)$$

The lower boundary condition is then

$$U\frac{\partial^2}{\partial x\partial z}\left(\frac{\delta p}{\rho_0}\right)\bigg|_{z=0} = -\,\mathrm{i}ag\exp(\mathrm{i}kx)\cos\mu y$$

which can be shown, using equation (20) and the expression for C, to imply that

$$A = \frac{\dfrac{\rho_s a g}{Uk}\left(\mathrm{i}\nu - \dfrac{1}{2H_0}\right)}{b\gamma + \nu^2 + \dfrac{1}{4H_0^{\,2}}}$$

In deriving this expression, the dispersion relation equation (8), with $c = 0$, has been used. The full solution is therefore given by

$$\delta p = \mathrm{Re}\left[\frac{\dfrac{\rho_s a g}{Uk} \cos \mu y}{b\gamma + \nu^2 + \dfrac{1}{4H_0^2}} \left[\gamma \exp(-\gamma z) + \left(\mathrm{i}\nu - \frac{1}{2H_0}\right) \exp\left\{\left(\mathrm{i}\nu - \frac{1}{2H_0}\right) z\right\} \exp(\mathrm{i}kx)\right]\right] \qquad (22)$$

where

$$\nu^2 = \left(\frac{N}{f_0}\right)^2 \left\{\frac{\beta}{U} - (k^2 + \mu^2)\right\} - \frac{1}{4H_0^2}$$

Notice that if the Charney/Drazin condition given by equation (9) is not satisfied, ν is imaginary and the disturbance energy decays with height. Equation (22) also implies that the response is inversely proportional to the basic state wind speed U. This is because air parcels spend a time proportional to $1/U$ in, say, the heating region of S and so the longer the time they spend there, the bigger the response. Fig. 5 shows some typical amplitude and phase plots of the geopotential height and temperature for wave numbers 1, 2 and 3 derived from equation (22) taking $a = 3$ K day^{-1}/260 K, $k = 2\pi m/30\,000$ km (where m is the wave number), $b = 1/(4 \text{ km})$, $U = 10 \text{ m s}^{-1}$, $B = 3 \times 10^{-5} \text{ m}^{-1}$, and μ chosen to correspond to a disturbance with one amplitude maximum in middle latitudes tending to zero at the pole and equator. Note that the geopotential height amplitude is given by $\delta p/\rho_0 g$. In Fig. 5 the phase of the wave ridge is plotted in trigonometrical degrees and not degrees longitude. However, for wave number 1 these coincide to within an arbitrary constant.

Characteristic features of these energy radiating solutions are:

(a) a strong surface pressure response (about 10 mb),
(b) mid-troposphere minimum amplitude (at about 3 or 4 km),
(c) wind amplitude increase at $\exp(z/2H_0)$ as $z \rightarrow \infty$ (specific kinetic energy, $\frac{1}{2} \rho_0 (u_g^2 + v_g^2) = \text{constant}$),
(d) strong westward tilt with height particularly in the heating region, and
(e) cold anticyclones on the eastern sides of continental land masses.

Characteristic (e) occurs because the surface pressure maximum occurs about 50° downstream of the diabatic cooling rate maximum. For evanescent waves with $\nu^2 < 0$, this phase difference is 90° and the same general conclusion holds. The diabatic cooling rate maximum is assumed to be central to the land mass and so the high pressure will occur to the east.

Waves which tilt to the west with height and which are geostrophically and hydrostatically balanced, transport heat polewards in the sense that $\overline{v_g\theta} > 0$ where the overbar denotes the zonal average. To show this, let the geopotential height perturbation associated with *any* wave field be given by

$$h = \frac{\delta p}{\rho_0 g} = H(z) \cos\{kx + \epsilon(z)\}$$

where $H(z)$ is the amplitude and $\epsilon(z)$ the phase. The hydrostatic equation can then be used to find θ' so that

$$\frac{\theta'}{\theta_0} = \frac{\partial h}{\partial z} = \frac{\mathrm{d}H}{\mathrm{d}z} \cos(kx + \epsilon) - H \sin(kx + \epsilon) \frac{\mathrm{d}\epsilon}{\mathrm{d}z}\ .$$

Also the geostrophic wind relation gives

$$v_g = \frac{g}{f} \frac{\partial h}{\partial x} = -\frac{g}{f} H(z)\, k \sin(kx + \epsilon)$$

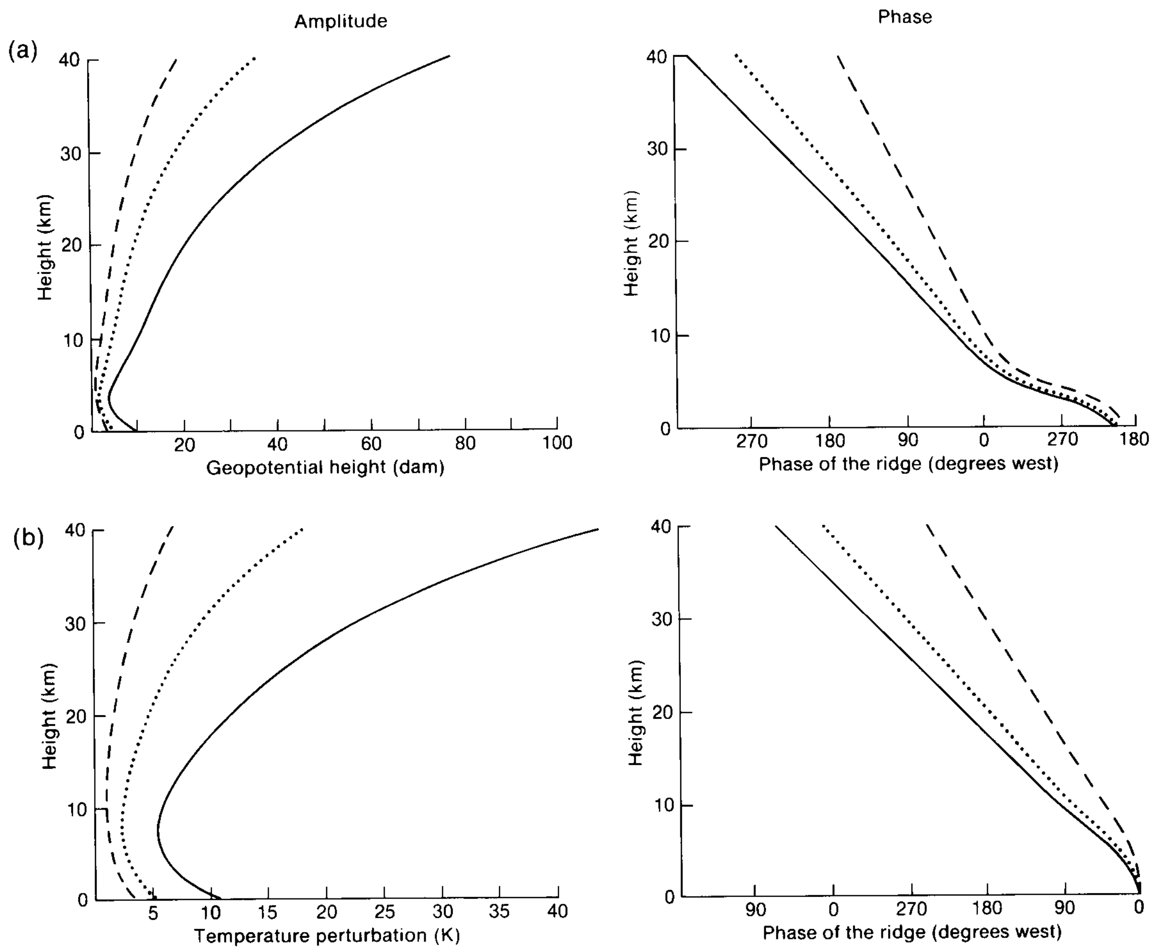

Figure 5. Amplitude and phase plots of (a) geopotential height and (b) temperature for wave numbers 1 (———), 2 (··········) and 3 (— — —) derived from equation (22).

so that

$$\overline{\theta' v_g} = \tfrac{1}{2}\, g\theta_0 \frac{k}{f} H^2 \frac{d\epsilon}{dz} \; .$$

Since westward phase tilt with height implies $d\epsilon/dz > 0$ then heat transport is poleward. Fig. 6 shows $\overline{v_g\theta}$ for wave number 1 derived from the analytic solution, equation (22). Above the heat source $\rho_0\overline{v_g\theta'}$ is independent of height. For reasons beyond the scope of this analysis one should be cautious before equating $\rho_0\overline{v_g\theta'}$ to any real tendency of stationary waves to transport heat. In the adiabatic regions of the model flow, parcels return from high latitudes with the same potential temperature as they set out with so that no real transport is achieved. This is not true of parcels in the lower tropospheric heating region which experience heating (on average) as they travel poleward and cooling as they travel equatorward, thereby achieving real heat transport.

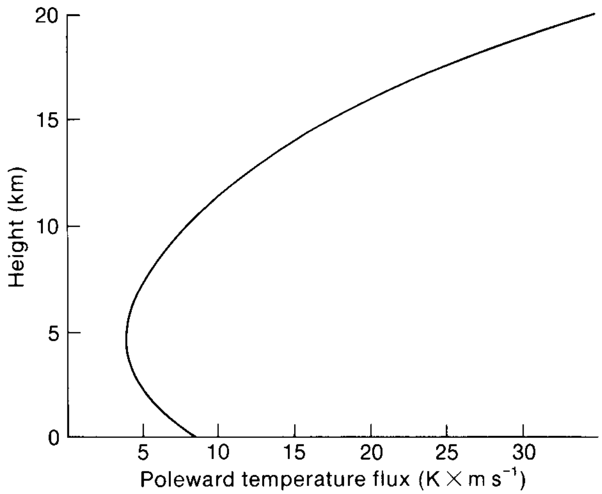

Figure 6. Height variation of poleward heat flux associated with the solution given by equation (20) for wave number 1.

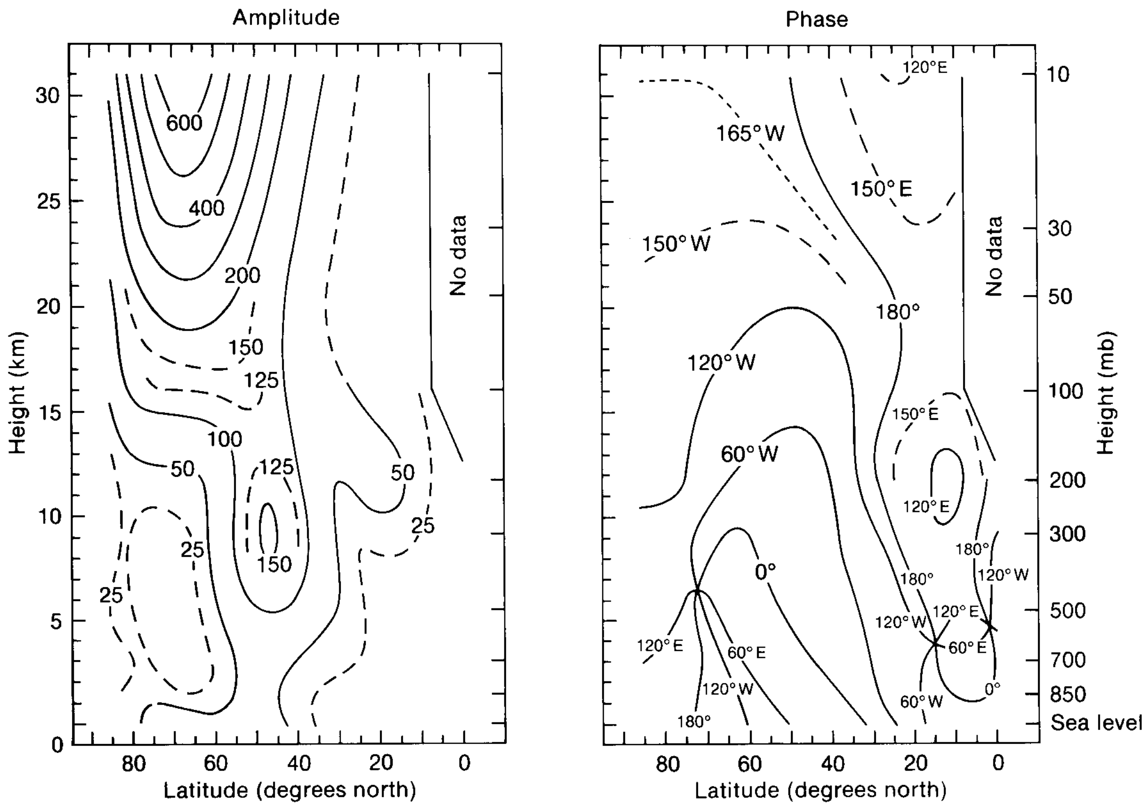

Figure 7. Long-term mean amplitude (m) and phase (degrees longitude) for the northern hemisphere in January for wave number 1, plotted as a function of height and latitude (van Loon *et al.* 1973).

6. Comparison with observations

Fig. 7 shows the observed, time-averaged winter-time amplitude and phase of wave number 1 as a function of height and latitude (from van Loon *et al.* 1973). There are many interesting points of agreement with the highly idealized solutions presented here including rapid phase tilt westward with height, amplification with height, and even the suggestion of an amplitude minimum near 3 km. Observations of the amplitude of wave numbers 1 and 2 up to a height of 100 km have been collated by Green (1972) and plotted on a logarithmic scale (Fig. 8(a)). The specific kinetic energy is found to be approximately constant with height up to 40 or 50 km, above which it falls off rapidly. The accompanying phase diagram (Fig. 8(b)) shows rapid phase tilt westward with height.

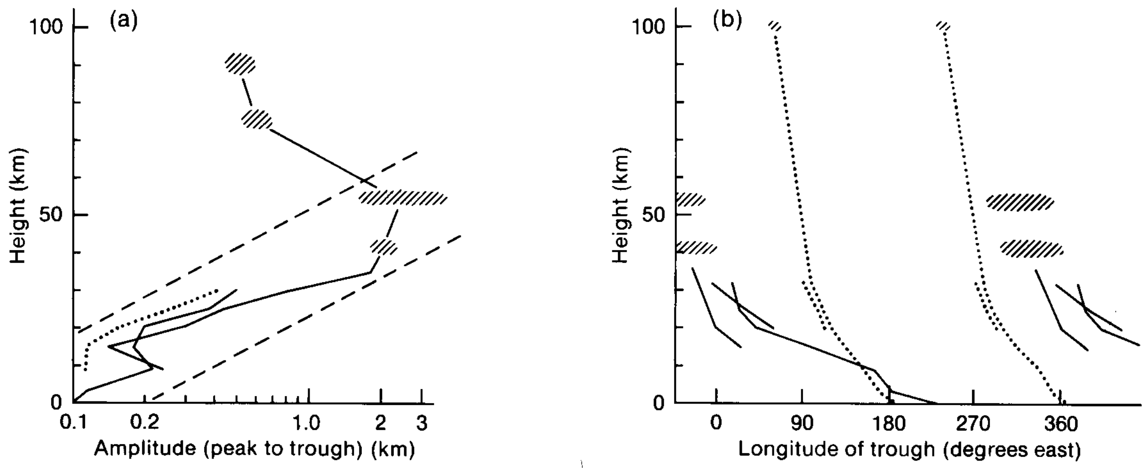

Figure 8. Observed variation with height of (a) geopotential height amplitude (plotted on a logarithmic scale) and (b) phase of the January mean eddy motion at 50° N for wave numbers 1 (———) and 2 (·········). Where the specific kinetic energy in (a) is constant with height the curve is parallel to the dashed lines. The shaded areas indicate the uncertainty inherent in the middle atmosphere data. For origin of data see Green (1972).

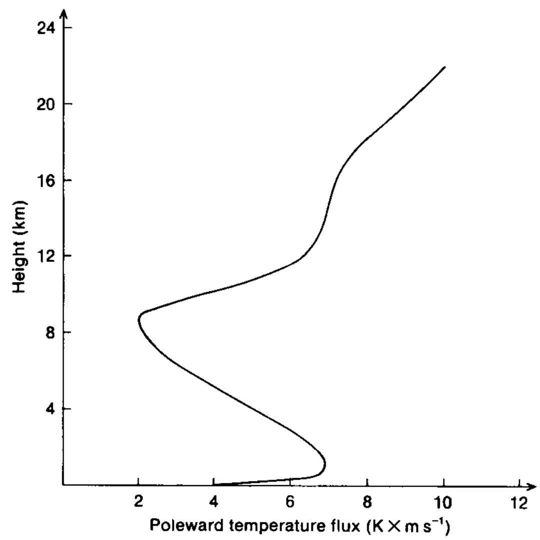

Figure 9. Vertical variation of the latitudinally-averaged poleward temperature flux caused by stationary waves for January 1963 (Shutts 1978).

The linear solution, equation (22), must break down at some height since the pressure perturbation amplitude falls off as exp $(-z/2H_0)$, compared to exp $(-z/H_0)$ for the basic state pressure, so that at some height the total pressure would become negative. In practice wave breakdown occurs long before this as a non-linear advection process. The absorption of disturbance energy in the stratosphere through the breakdown process is probably the dominant mechanism for the tail-off of the specific kinetic energy.

Fig. 9 shows the observed poleward heat transport due to stationary waves in January 1963. The low-level maximum and 'whip-lash' amplification effect in the stratosphere are both in agreement with the model heat flux portrayed in Fig. 6. Since the stationary wave heat transport (primarily wave numbers 1, 2 and 3) constitutes about 50% of the total atmospheric poleward heat transport in winter, vertically propagating ultra-long waves probably play an important role in the global heat budget. Further solutions for more realistic distributions of N^2 and U (with height) can be found in Shutts (1978).

References

Charney, J.G. and Drazin, P.G. 1961 Propagation of planetary-scale disturbances from the lower into the upper atmosphere. *J Geophys Res*, **66**, 83–109.

Gill, A.E. 1982 Atmosphere-ocean dynamics. London, Academic Press, International Geophysics Series, Vol. 30.

Green, J.S.A. 1972 Large-scale motion in the upper stratosphere and mesosphere: an evaluation of data and theories. *Philos Trans R Soc London*, A, **271**, 577–583.

Lau, N–C. 1979 The observed structure of tropospheric stationary waves and the local balances of vorticity and heat. *J Atmos Sci*, **36**, 996–1016.

Shutts, G.J. 1978 Quasi-geostrophic planetary wave forcing. *Q J R Meteorol Soc*, **104**, 331–350.

van Loon, H., Jenne, R.L. and Labitzke, K. 1973 Zonal harmonic standing waves. *J Geophys Res*, **78**, 4463–4471.

551.553.6(427)

An analysis of wind speed and direction at a high-altitude site in the southern Pennines

P.A. Smithson

University of Sheffield

Summary

An analysis is presented of hourly wind data from High Bradfield, a high-altitude (405 m) anemograph site in the southern Pennines, based on the period 1975–84. Comparison is made with other UK sites to assess the distinctive properties of airflow at this site. Mean values, extremes, return periods and gale frequencies are examined.

1. Introduction

The wind climatology of the British Isles, based on a scattered distribution of anemographs, has been described by Shellard (1976) and its application to building design has been surveyed by Lacy (1977). A number of locations have been examined in detail, e.g. Sheffield (Lee 1975) and Ballykelly (Glassey and Durbin 1971). Hardman *et al.* (1973) and Caton (1976) have also produced generalized maps of extreme wind speeds and hourly mean wind speeds respectively by interpolating between the rather sparse network of anemometer sites. However, few anemometers are located in upland areas, so the results over high ground may not be very reliable. Barry (1981) states that the most important characteristics of wind velocity over mountains are related to topography rather than altitude. It is unlikely, therefore, that the wind characteristics of an upland site could be predicted fully by extrapolating or modelling based on lowland data alone.

An anemometer has been operational at High Bradfield, South Yorkshire since November 1974. Its vane-level altitude is 405 m and it is the most southerly high-level anemograph site in the United Kingdom. The other three sites above 400 m published in the *Monthly Weather Report* are in Scotland (Lowther Hill, 754 m), the Isle of Man (Snaefell, 628 m) and the northern Pennines (Great Dun Fell, 857 m). No detailed analyses appear to have been published for any of these sites, though brief notes about Cairn Gorm automatic weather station (1245 m) have appeared (Curran *et al.* 1977 and Barton 1981). Wind observations were taken on Ben Nevis (1343 m) from 1883 to 1904 but were based on a relative, rather than an absolute, scale which makes their use difficult. With over 10 years' data being available, the High Bradfield record is now sufficiently long to draw some general conclusions about the nature of airflow at high levels in the southern Pennines.

2. Site details

The anemometer at High Bradfield is sited on the flat summit of a ridge extending in an approximately west to east direction on the eastern slopes of the Pennines, 7.5 km north-west of the University of Sheffield's anemometer (Fig. 1). To the south-west, the Loxley valley has incised deeply into the foothills of the Pennines, generating a tendency for funnelling in the valley with winds from

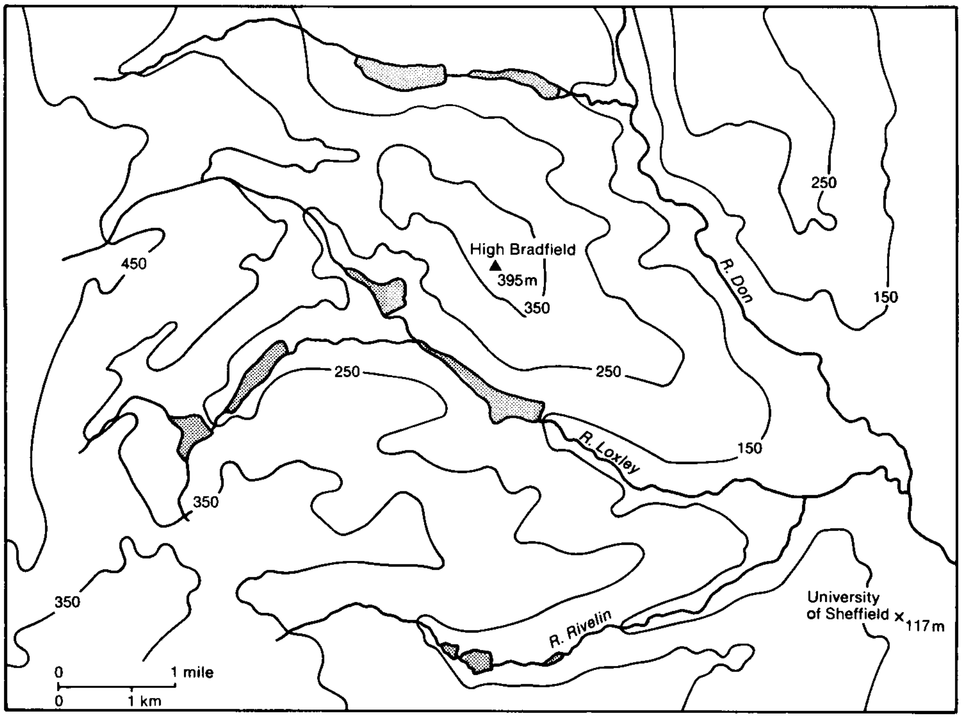

Figure 1. Map of the area around the High Bradfield site with heights shown in metres and reservoirs stippled.

between north-west and south-west. In general the site (with an effective anemometer height of 10 m) is fully exposed in all directions apart from minor turbulence produced by low buildings and walls in the vicinity. There has been no change of location during the period of operation. A number of minor interruptions to the record have occurred due to instrumental faults or severe weather when icing or rime has affected the operation of the cups or vane. No more than 4.7% of the total speed record was missing. The direction trace was a little more erratic with about 11% of the record missing; September had the highest incidence of non-operation. Although this figure may appear high compared with lowland sites, defective records are much more frequent at higher altitudes.

The data are in the form of hourly mean wind speeds and directions, speeds of the maximum gust for each hour and for the daily maximum gusts; directions of the gusts are also available. For the 10-year period 1975–84, a total of over 83 000 hourly values have been analysed. Manual extraction of data for the subsequent period was possible and used in sections 3.3, 4 and 5 to increase the sample size, but did not form part of the computer analysis in sections 3.1 and 3.2.

3. Mean speeds

3.1 *Monthly variation of mean speed*

Table I shows the monthly variations of hourly mean wind speeds at High Bradfield. A seasonal pattern is evident with the highest value in January and the lowest in August; there is also a secondary peak in March. An interesting feature is that the values for February and October are somewhat less than might be expected from adjacent monthly values; an identical result to that found by Smith (1984) at Elmdon (Birmingham Airport) for the period 1965–79. Smith argued that these anomalies were almost certainly caused by sampling inadequacies because a more regular change throughout the year was obtained when using pressure values as surrogate measures of wind speed for a 100-year period (Smith 1983). Nevertheless, it is surprising that a similar pattern to that at Elmdon was found despite the differences in altitude, physical separation and only a 5-year overlap in the time periods. Presumably Februarys and Octobers of the 1965–84 period have been less windy than formerly, perhaps associated with more frequent blocking in February and the warming which has taken place in October (Clarke 1966, Wright 1976).

Table I. *Means and standard deviations of hourly wind speeds (kn) at High Bradfield, 1975–84*

	Mean	Standard deviation	Sample size
Jan.	18.7	11.2	7 411
Feb.	13.4	8.4	6 439
Mar.	15.9	9.1	7 069
Apr.	13.1	7.6	7 000
May	11.4	6.1	7 135
June	11.9	6.4	6 966
July	11.2	6.0	6 963
Aug.	10.6	6.3	7 062
Sept.	14.8	8.1	6 506
Oct.	14.7	8.6	6 981
Nov.	17.0	9.7	6 945
Dec.	16.5	9.6	7 061
Year	14.1	8.6	83 538

Seasonal differences in mean speed at High Bradfield are large in contrast to more lowland sites. Using the average values of mean wind speed for 1961–70 at sites listed in Shellard (1976), the ratios of the windiest month to the least windy month range from 1.81 for the Isles of Scilly to 1.21 at Elmdon. High ratios tend to be at coastal sites and low ratios at inland sites. The seasonal ratios do suggest that high-altitude sites, as exemplified by High Bradfield, have a similar seasonal pattern of wind speeds to those of the most exposed coastal locations on the west and south coasts. However, the ratio does tend to vary depending upon the time period examined. At Great Dun Fell, the highest anemometer site for which long-period records are available, the ratio for the period 1974–84 is 1.67 which is similar to that of High Bradfield for a similar period, but for the period 1964–84 the ratio drops to 1.40. It would appear that a 10-year period may be too short to provide an adequate assessment of the ratio of winter to summer monthly mean wind speed. However, some sites, e.g. Heathrow and the Isles of Scilly, do show similar ratios from 1961–70 to 1971–80. Unfortunately there are insufficient long-period anemograph sites at high altitudes to test this similarity with exposed coastal locations in the south and west.

Instead of using the absolute values, it is possible to examine the seasonal variation in wind speed by calculating a standardized anomaly for each monthly mean speed, i.e. expressing each monthly value as the deviation from the annual mean divided by the standard deviation of the monthly speeds. Smith (1983) used this method to distinguish between lowland locations in the west and extreme north of the United Kingdom and all other lowland sites. The mean standardized anomalies for the two areas obtained by Smith are plotted in Fig. 2 together with the equivalent values for High Bradfield (1975–84) and Great Dun Fell (1964–84). A similar pattern is exhibited by all sites, but the two high-altitude sites emphasize the difference noted by Smith, i.e. for the western and extreme northern areas, the standardized anomalies tend to be weaker than for the area further south and east in the spring but stronger in autumn and early winter.

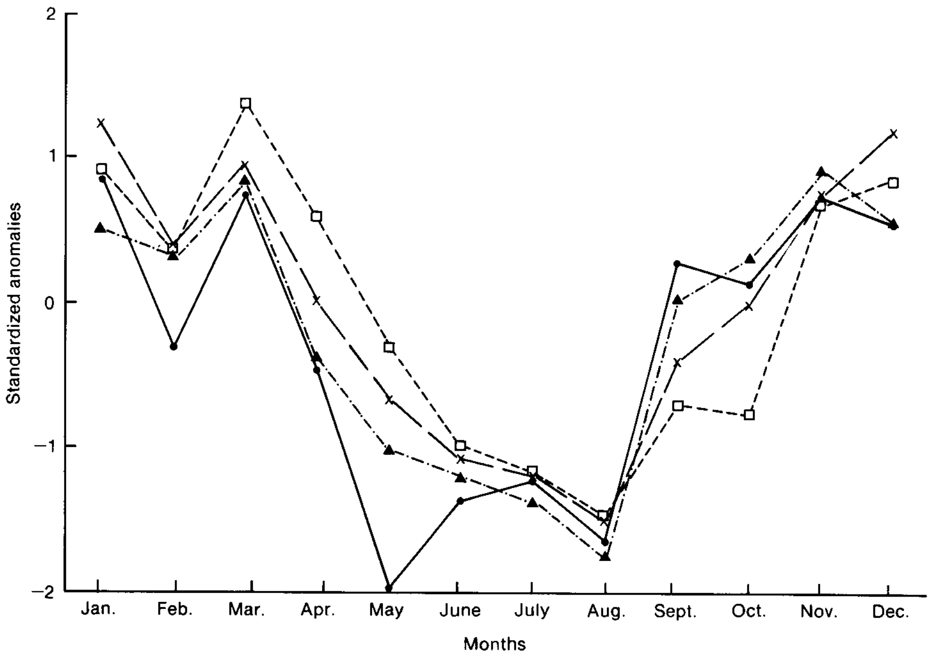

Figure 2. Mean standardized anomalies of monthly wind speeds for western and extreme northern sites of the United Kingdom (× — — ×) and all other lowland locations (□- - □) (after Smith 1983), High Bradfield (1975–84) (•——•) and Great Dun Fell (1964–84) (▲ ·— ·▲).

3.2 *Cumulative frequency*

The use of mean values of wind speed is not always justified because wind speed does not have a statistically normal distribution. Work on wind speed distribution in the United Kingdom indicates that, for speeds greater than about 10 knots, the Weibull distribution is a good approximation to the cumulative frequency pattern (Caton 1976). For each month of the 10-year period, frequencies of hourly mean wind speeds at High Bradfield were obtained for the standard speed classes listed in published work, viz. 1–3, 4–6, 7–10, 11–16, 17–21, 22–27, 28–33, 34–40, 41–47, 48–55, 56–63, and >63 knots. From the cumulative percentage frequencies the Weibull distribution parameters were derived and estimates made of the speed which would be exceeded for specified proportions of time (Tackle and Brown 1978). Table II lists the wind speeds in knots for each month of the year which would be exceeded for 75%, 50%, 25%, 10%, 5%, 1% and 0.1% of the time. For each category the ranking of monthly speeds is similar to that given by the monthly mean figures. Points worthy of note are that August, whilst having the lowest speeds for the majority of the time, is prone occasionally to much stronger winds; this is supported by the nature of 1985 (outside the period of the analysis) when 37 hours on 8 days had hourly mean wind speeds above 29 knots, the 1% value. July demonstrates the reverse pattern with fewer strong winds than would be expected from its mean speed. Although October appears anomalous by exhibiting a decline in mean wind speed relative to September, there is little difference between the two months on the basis of the Weibull distribution. January stands out as the windiest month in the period studied; it has a slightly higher frequency of low speeds than November but this is more than compensated for by its greater frequency of high speeds.

Table II. *Wind speeds (kn) likely to be exceeded by a given percentage of the time at High Bradfield, 1975–84, based on the Weibull distribution*

	Percentage of time						
	75	50	25	10	5	1	0.1
Jan.	8.7	16.1	24.1	32.8	38.4	48.9	62.1
Feb.	6.8	11.4	17.5	23.7	28.3	36.9	46.6
Mar.	8.3	13.6	20.2	27.4	31.6	40.7	50.8
Apr.	6.6	11.1	16.7	22.9	27.0	34.9	44.2
May	6.2	10.1	14.6	19.2	22.5	28.3	34.9
June	6.8	10.5	14.9	19.6	22.9	28.9	34.9
July	6.4	10.1	14.6	19.2	22.1	27.5	34.5
Aug.	5.6	9.3	14.2	19.0	22.9	29.3	37.2
Sept.	8.1	13.2	19.4	25.8	30.5	38.6	48.1
Oct.	7.8	12.8	19.0	26.0	30.5	38.8	48.9
Nov.	9.3	14.7	21.5	28.7	33.0	40.9	50.8
Dec.	8.9	14.6	21.7	29.1	34.3	43.1	54.3

Caton (1976), in his study of hourly mean wind speeds over the United Kingdom for the period 1965–73, mapped the speeds likely to be exceeded for various percentages of time for sites between mean sea level and an altitude of 70 m after local effects had been eliminated. Where a site exceeded 70 m in altitude, a correction factor to the mapped value was recommended. The 75 and 50 percentile values were to be increased by 7%, the 25, 10 and 5 percentile values by 8% and the 1 and 0.1 percentile values by 9% per 100 m of height above the plain or above the 70 m contour as appropriate. It was stressed that these corrections were very tentative, particularly above 400 m. Although based on a different time period, the High Bradfield data have been analysed in a similar manner to that used by Caton, so should provide an interesting check on Caton's correction factors. The lowland wind speed value at the location of High Bradfield was extracted from the maps, adjusted by the altitudinal correction factor suggested by Caton, and then converted to knots for comparison with the remaining data (Table III). As can be seen, the predicted hourly mean wind speeds are consistently less than those for High Bradfield by about 20%. To give a good estimate of the actual values, the lowland speeds should have a correction factor of about double that used by Caton, i.e. 14% for the 75 and 50 percentiles, 16% for the 25 and 10 percentiles and 18% per 100 m for the 5, 1 and 0.1 percentiles. It should not be forgotten that Caton's work was based on a different period from that at High Bradfield.

Confirmation of the validity of the higher correction factor for speeds at heights above 400 m is indicated by the Great Dun Fell data. Taking the 50% value for lowland speeds at the site of Great Dun Fell, and applying the 14% per 100 m above 70 m altitude correction factor, gives a mean speed only slightly below that for 1964–84.

Table III. *Comparison of observed wind speeds (kn) for High Bradfield, 1975–84 with values predicted by Caton's (1976) method, based on the Weibull distribution as in Table II.*

	Percentage of time						
	75	50	25	10	5	1	0.1
Observed (a)	7.2	12.0	18.4	25.0	29.3	38.0	48.1
Caton (lowland) (b)	4.9	8.0	11.6	15.5	17.8	23.5	31.2
Caton (for 405 m) (c)	6.1	9.9	14.7	19.7	22.6	30.6	40.6
(c)/(a) (per cent)	85	83	80	79	77	81	84

3.3 *Extreme values*

The series of annual maximum hourly speeds was analysed using standard statistical methods of extreme values (Gumbel 1958). The maximum value likely to be exceeded only once in T years can then be calculated. This approach was taken by Hardman *et al.* (1973) for 144 stations over the United Kingdom in order to map the isopleths of once in 50-year hourly mean wind speeds and gust speeds over open country. Attempts were also made to predict extreme winds on exposed hilltops on the basis of nearby (but lower) stations using a power law with exponent 0.17. For gust speeds, the power-law expression provided estimates which were lower than the value obtained from the original record but the application of a gust factor of 1.4 to the hourly mean wind speeds gave estimates which were comparable. Estimates of the maximum hourly mean wind speeds for given return periods are listed in Table IV. Inevitably the computed extremes should be treated with caution as the error terms in the prediction are high. However, they do provide a guide to the magnitude of extreme winds likely to be experienced at high-altitude sites in the United Kingdom.

Table IV. *Maximum hourly mean wind speeds and gusts (kn) for given return periods at High Bradfield, (1975–85)*

Hourly mean wind speeds						Gust speeds					
	Return period (years)						Return period (years)				
Mean	10	20	50	100	120	Mean	10	20	50	100	120
59	68	72	76	80	81	84	99	106	114	120	121

4. Maximum gusts

Hourly mean wind speed provides a good measure of wind strength at a site but of equal importance is the instantaneous strength of wind to which individuals or buildings may be exposed. It is these gusts of wind which are responsible for much of the damage which occurs during stormy weather and hence are of considerable practical importance. Table V lists the mean monthly maximum gust for the period December 1974 to June 1986 at High Bradfield together with the highest gust recorded. A similar pattern of ranking to that given by the mean speeds is obtained, with January as the month with the highest gusts and July with the lowest. As expected, the period from April to August has the lowest mean maximum gusts together with relatively low variability as indicated by the standard deviations. In winter, not only are the gusts stronger on average but also there is a greater inter-annual variability.

Table V. *Maximum gust data (kn) for High Bradfield based on monthly values from December 1974 to June 1986*

	Mean monthly maximum gust	Standard deviation	Maximum gust	Year of occurrence
Jan.	76.4	11.9	99	1984
Feb.	57.3	13.9	82	1983
Mar.	63.6	9.0	74	1978
Apr.	55.8	9.5	68	1985
May	50.0	8.1	64	1982
June	49.1	6.9	62	1983
July	45.8	4.6	52	1977
Aug.	48.4	9.6	63	1985
Sept.	64.5	11.5	84	1975
Oct.	62.0	7.4	72	1981, 83
Nov.	68.9	11.5	94	1980
Dec.	70.9	15.6	99	1974

In addition to considering only the highest gust for each month, the data enable the maximum gust for each hour to be analysed though its significance will be less than the monthly maxima referred to earlier. For more than half the year, between September and March inclusive, hourly maximum gusts are likely to exceed 20 knots for 50% of the time (Table VI). During the period studied, only February did not achieve this level. Earlier discussion about anomalies in the seasonal pattern caused by short-period sampling would indicate that the lower value for February is a sampling problem rather than a real feature of the climate. A value of 0.1% of the time represents seven occurrences in 10 years with hourly maximum gusts reaching or exceeding the given speed. Examination of the actual frequency of occurrence for the period 1975–84 indicates that the Weibull distribution slightly underestimates the frequency for the five months which had seven occurrences or less of the 0.1% speed. May and August recorded 23 occasions of hourly maximum gusts above the 0.1% value.

Estimates of the gust speeds for specified return periods are given in Table IV using the same method as Hardman *et al.* (1973); gusts of over 100 knots would be expected at least once in 10 years. The gust factor based on hourly values averages 1.64 with only slight variability throughout the year. This is in accordance with its exposed and relatively unobstructed situation and only slightly above the figure of 1.6 quoted by Shellard (1976) for the gust factor over more or less flat country with few obstructions. The effect of altitude on this wind property would appear to be of less importance than local factors.

Table VI. *Maximum hourly gust speeds (kn) likely to be exceeded by a given percentage of the time at High Bradfield from December 1974 to June 1986, based on the Weibull distribution*

	Percentage of time						
	75	50	25	10	5	1	0.1
Jan.	16.1	25.4	37.2	49.9	57.4	71.8	88.9
Feb.	10.9	17.8	27.0	35.9	42.3	53.9	67.9
Mar.	14.4	22.5	32.0	41.1	46.8	58.2	71.4
Apr.	11.8	18.6	27.2	35.5	40.7	50.8	62.0
May	10.9	16.5	23.1	29.3	33.4	40.7	49.3
June	11.6	17.7	24.8	31.6	36.1	44.4	53.5
July	10.7	16.5	23.3	29.9	34.1	42.1	50.8
Aug.	9.5	15.1	22.3	29.5	34.1	42.7	52.4
Sept.	14.0	21.5	30.5	38.8	44.6	54.3	65.6
Oct.	13.2	20.8	29.9	39.2	45.0	53.9	68.3
Nov.	15.3	23.9	33.6	43.1	49.5	60.5	73.7
Dec.	14.9	23.5	34.1	45.0	52.0	64.4	79.5
Year	11.3	18.6	28.9	39.4	46.0	58.6	73.9

5. Gales

Gale frequencies are often quoted as a measure of the windiness of a site. A day of gale is defined as a day on which the wind speed at the standard height of 10 metres attains a mean value of 34 knots or more over any period of ten consecutive minutes during the day (Meteorological Office 1972). The data at High Bradfield are not easily related to this definition as only hourly mean wind speeds and hourly maximum gusts are recorded. Two alternative definitions could be used. The more rigorous one would be for a day of gale to experience a speed of at least 34 knots for a period of one hour. A second definition could be, a day on which at least one gust reached 34 knots or more. As the latter definition is not normally applied, only data satisfying the former definition are analysed.

Breaks in the record make it impossible to give a precise total of the number of hours between December 1974 and June 1986 which experienced an hourly mean wind speed above 33 knots, though on occasion some interpolation was possible. For short interruptions, weather maps could be examined and comparison made with the nearby anemograph at Sheffield to check if any hours were likely to have reached the critical mean speed. For longer breaks no interpolation was possible. To reduce the impact of interruptions in the record, Table VII gives the proportion of the available record that hourly mean wind speeds were equal to or above the critical values rather than monthly average figures.

Year-to-year variability characterizes the record; some years are very windy whilst others are relatively calm. All months except January and December experienced at least one occurrence with no hourly mean wind speed above 33 knots. At the other extreme, more than 35% of all hours in December 1974 had a mean speed above gale force, a factor no doubt important in making it the second mildest December in the last hundred years over England and Wales. The ranking of the number of hours with gales does conform closely to the mean speed rank, though August contains more gales than its mean speed suggests whilst June and September have fewer gales. The value for September could be anomalous as only seven months had complete records and two with incomplete records had already received more than the average value. For severe gales with hourly mean wind speeds of at least 48 knots, January and December became the only months with a significant number of hours and even in these months some years did not attain this speed. From April to August inclusive, hourly mean wind speeds of at least 48 knots are very unlikely.

Table VII. *Frequency and percentage data of occasions when hourly mean wind speeds exceeded given values (kn) for High Bradfield from December 1974 to June 1986*

	No. of hours ⩾34	Range* in no. of hours	Percentage of record ⩾34	No. of hours ⩾48	Range* in no. of hours	Percentage of record ⩾48
Jan.	912	11–192	10.3	142	0–56	1.6
Feb.	172	0–60	2.1	11	0–7	0.2
Mar.	413	0–99	5.2	16	0–7	0.2
Apr.	140	0–66	1.7	2	0–1	0.02
May	63	0–11	0.7			
June	18	0–7	0.2			
July	10	0–8	0.1			
Aug.	37	0–14	0.5			
Sept.	144	0–30	2.0	12	0–4	0.1
Oct.	267	0–66	3.4	4	0–2	0.05
Nov.	482	0–115	6.3	13	0–4	0.2
Dec.	794	3–265	9.3	65	0–30	0.8

* Lower value of range for complete months only.

6. Diurnal variations

The diurnal variation of wind speed at inland locations is usually well marked with a maximum in the early afternoon and a minimum shortly before sunrise, the actual times and the amplitude of the average variation depending upon the time of year (Shellard 1976). The upland location of High Bradfield would suggest that diurnal heating and therefore the amplitude of the diurnal wind speed would be less than that at lowland sites. At Kew, the diurnal amplitude for June–August was 4.5 knots for the period 1959–68 compared with only 2.2 knots for December–February despite the higher mean speed. At High Bradfield, the mean diurnal variation for the same two periods was only 2.5 knots and 1.2 knots respectively; this supports the belief that the diurnal amplitude would be less at higher altitudes. For most months of the year, the highest mean speed occurs between 1100 and 1700 GMT. Only in February and November does it occur during night-time hours. With reduced solar heating at this time of year, the time of maximum mean speed is randomly distributed, especially in view of the limited diurnal range in these months. The difference between the highest and lowest hourly mean value was found to be non-significant at the 5% level using Student's *t*-test for the months from November to February whereas the difference was significant for the remaining months. For the year as a whole, the hours from 1200 to 1500 GMT have the highest mean speed at 15.1 knots and from 0400 to 0700 GMT have the lowest mean speed at 13.5 knots, a range of only 1.6 knots. Because of the large sample size, the difference in this instance was statistically significant at the 0.1% level.

7. Direction

Wind direction is less likely to be affected by altitude than wind speed. The reduced surface roughness and friction at hilltop sites should produce a slight veering of the wind relative to lower altitude sites so that the airflow more closely resembles the gradient wind. The annual pattern (Fig. 3) shows the prevailing direction to be from 230° to 250°, with a secondary and minor maximum from 020° to 040°. Winds between 080° and 160° are infrequent and calms and variable winds unusual. The annual figures mask monthly variations in wind direction which reflect the seasonal cycle of pressure patterns and depression tracks throughout the year (Perry 1976). The main features of the seasonal pattern (Fig. 4) are the dominance of westerly sector winds from September to January, and a higher frequency of

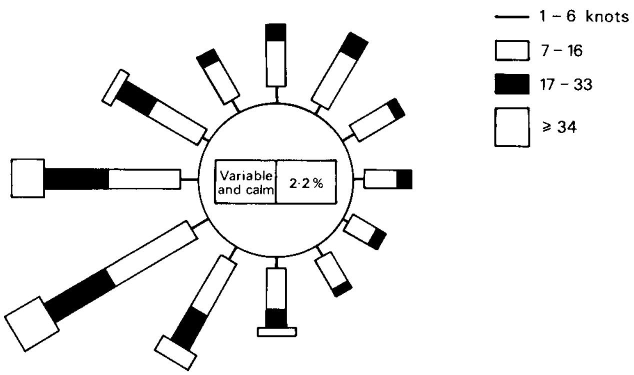

Figure 3. Annual wind rose of hourly means for High Bradfield.

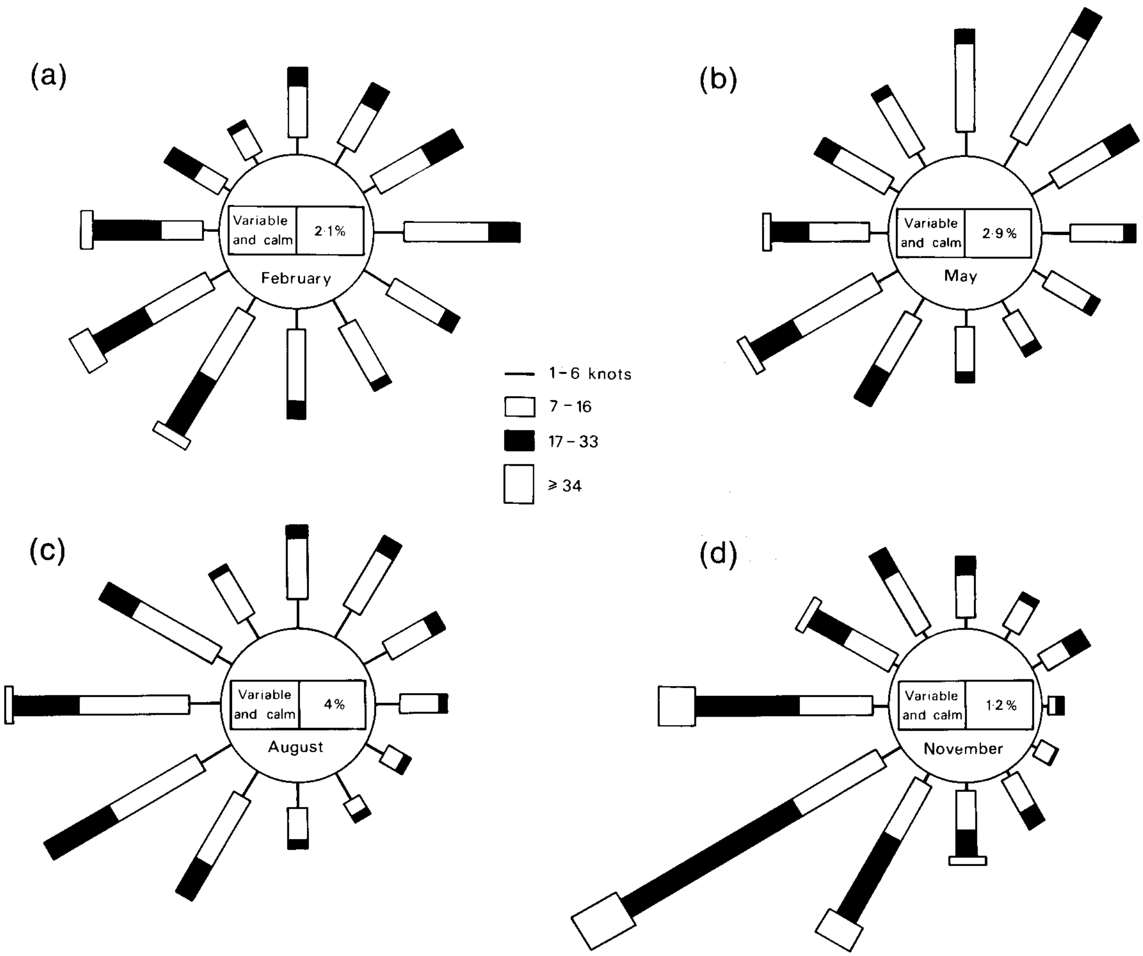

Figure 4. Wind roses of hourly means for (a) February, (b) May, (c) August and (d) November for High Bradfield.

easterly winds in February and northerly sector winds from March to May when westerlies reach their lowest proportion, a frequently noted aspect of our climate. The distribution for the summer months is similar to the annual pattern though there is a reduced dominance of westerlies in August. Winds between 170° and 220° are most common in autumn. In general the directional properties of airflow at High Bradfield do not differ markedly from those at lower altitudes. Local factors, such as sea-breezes or topography, which can be significant in affecting the wind rose on the coast or at low-altitude inland locations, do not appear to be important at this hilltop site.

The relationship between direction and speed reinforces the general dominance of westerly winds. Not only are winds most frequent from this direction but also the higher speeds are almost always between 200° and 280°. More than 75% of hourly mean winds greater than 33 knots blow from between 230° and 280° and more than 90% from between 200° and 280°. For the year as a whole, the 11–16 knot class represents the modal value for all directions. However, minor differences occur during the year, with a tendency for a lower modal value for northerlies and easterlies during the summer half-year and for a higher modal value for westerlies in the winter half-year.

8. Conclusions

The pattern of wind speeds over lowland United Kingdom has been well established (Hardman *et al.* 1973, Caton 1976, Shellard 1976) in terms of mean speeds and probabilities of extreme events. Few anemographs have operated above 150 m, so information about wind speed at higher altitudes has been limited. Short-period instrumentation or model predictions from lowland sites have been used to overcome the problem with some success but verification of the models from longer-period sites has been needed. The anemometer at High Bradfield has been in operation since 1974 and, although a proportion of records are missing, it provides an indication of the range of wind speeds which can be expected at only moderate altitudes in England. Gales are a frequent feature of its climate. Winter storms batter the area with westerly winds of severe-gale strength and even in summer, gales occur in most months although of more moderate intensity and duration than their winter counterparts. All sites possess an element of uniqueness derived from local factors of altitude, surface roughness and exposure. The open nature of the High Bradfield site should provide a satisfactory measure of hilltop airflow from which modifications at other sites could be generated by funnelling or shelter.

9. Acknowledgements

The author would like to thank the Meteorological Office for kindly providing the data on magnetic tape and R. Coleman of the Computer Services Unit, University of Sheffield for all her programming efforts.

References

Barry, R.G.	1981	Mountain weather and climate. London, Methuen.
Barton, J.S.	1981	Severe wind chill on Cairn Gorm. *Weather*, **36**, 313.
Caton, P.G.F.	1976	Maps of hourly mean wind speed over the United Kingdom 1965–73. *Climatol Mem, Meteorol Off*, No.79.
Clarke, P.C.	1966	Temperature and rainfall trends in October. *Weather*, **21**, 364–366.
Curran, J.C., Peckham, G.E., Smith, D., Thom, A.S., McCulloch, J.S.G. and Strangeways, I.C.	1977	Cairngorm summit automatic weather station. *Weather*, **32**, 61–63.
Glassey, S.D. and Durbin, W.G.	1971	Wind at Ballykelly. *Climatol Mem, Meteorol Off*, No. 68.
Gumbel, E.J.	1958	Statistics of extremes. New York, Columbia University Press.

Hardman, C.E., Helliwell, N.C. and Hopkins, J.S.	1973	Extreme wind speeds over the United Kingdom for periods ending 1971. *Climatol Mem, Meteorol Off*, No. 50A.
Lacy, R.E.	1977	Climate and building in Britain. Building Research Establishment report. London, HMSO.
Lee, B.E.	1975	The wind climate of Sheffield. Building Science Report No. 27, (Unpublished, copy available in the University of Sheffield.)
Meteorological Office	1972	Meteorological Glossary. London, HMSO.
Perry, A.H.	1976	Synoptic climatology. *In* Chandler, T.J. and Gregory, S. (eds); The Climate of the British Isles. London, Longman.
Shellard, H.C.	1976	Wind. *In* Chandler, T.J. and Gregory. S. (eds); The Climate of the British Isles. London, Longman.
Smith, S.G.	1983	Seasonal variation of wind speed in the United Kingdom. *Weather*, **38**, 98–103.
	1984	A stochastic model to generate sequences of hourly mean wind speeds for different sites in the United Kingdom. *J Climatol*, **4**, 133–148.
Tackle, E.S. and Brown, J.M.	1978	Note on the use of Weibull statistics to characterize wind-speed data. *J Appl Meteorol*, **17**, 556–559.
Wright, P.B.	1976	Recent climatic change. *In* Chandler, T.J. and Gregory, S. (eds); The Climate of the British Isles. London, Longman.

Correspondence

551.551.5

Comments on 'Prolonged clear air turbulence over the British Isles on 4 September 1985'

Dr Hisscott's article* on prolonged clear air turbulence over the British Isles has been read with interest, as it is not often that the same aircraft encounters turbulence over such a long period of time. Although he says that the turbulence covered a large area, was there any evidence to support the view that turbulence affected a large area vertically and laterally, other than longitudinally along the track?

The frontal zone shown on the Aberporth sounding for 0600 GMT on 4 September is at around 600 mb (14 000 ft approximately) which, with the surface warm front near south-west Ireland at 0600 GMT, gives an average frontal slope of 1:135. Moving this frontal slope at the speed of the surface warm front (north-east at about 27 kn) would put the frontal zone on the 0600 GMT sounding very near to the flight path both vertically and longitudinally at 0800–0900 GMT; indeed the pilot mentioned that they were flying just below the (pre-frontal) thick layer cloud. By 1000–1100 GMT (assuming no changes of frontal speed or slope) the frontal zone and thick cloud would have lowered some 4000 ft — to the new flight level of 10 000 ft!

On the 0600 GMT Aberporth sounding there is a vertical wind shear of 16 kn between 600 mb and 623 mb (a height difference of about 1000 ft) giving a shear of 16 kn/1000 ft (neglecting the small wind direction change with height). In aviation forecasting a vertical wind shear of over 6 kn/1000 ft is taken to be a condition suitable for moderate turbulence, and a vertical wind shear of over 10 kn/1000 ft to be a condition for severe turbulence. A vertical wind shear of over 15 kn/1000 ft is in my experience a rare event, which I have occasionally seen on ascents from Atlantic weather ships and Europe, usually underneath (i.e. below 18 000 ft) or above (i.e. above 40 000 ft) the polar front jet streams. Shears in

*Hisscott, L.A.; Prolonged clear air turbulence over the British Isles on 4 September 1985, *Meteorol Mag*, **115**, 1986, 329–331.

excess of 10 kn/1000 ft can often be followed over 06–24 hour intervals in the relatively dense upper-air network over Europe, together with reports of associated turbulence.

The two most potent mechanisms responsible for clear air turbulence are vertical and horizontal shears, and waves in the lee of a mountain barrier (see, for example, WMO Technical Note No 155, 1977). It is very likely that on this occasion there was sufficient vertical shear present to account for the turbulence, neglecting any effect of the less easily measured horizontal shear and the effect of a wind in excess of 20 kn blowing in a stable airstream over the Welsh mountains. The decision to fly lower on the return leg, presumably in order to stay in clear air under the frontal cloud sheet, may have put the aircraft in the same zone of strong vertical shear as on the outward leg.

Although it was stated in the article that the turbulence was associated with the diffluence and anticyclonic turning below the warm frontal zone, it is hard to visualize physically this effect producing turbulence of that intensity and duration, considering that the winds in the lower troposphere were not all that strong, that there was little change in pattern shape, and that there was comparatively little change in the degree of turning. The jet stream of about 135 kn at around 35 800 ft from central Ireland to Cumbria to Norfolk at 0600 GMT may well have produced some turbulence due to diffluence, anticyclonic turning and wind shears, accounting for the SIGMET issued, but I would suggest that the prolonged and moderate to occasionally severe turbulence on that occasion was primarily due to flying in a shallow zone of very strong vertical wind shear under the frontal zone as it moved north-east and lowered, perhaps complicated by the fact that there was a dry adiabatic lapse rate between 700 mb (10 000 ft) and 623 mb ($\approx$ 12 800 ft).

D.J. George

Regional Area Forecast Centre
Bracknell, Berkshire

551.551.5

Reply by L.A. Hisscott

As Mr George suggests, it is likely that the aircraft was flying in a similar position relative to the frontal zone on both sectors, and the strong vertical wind shear under the frontal zone is the probable cause of this phenomenon. Assuming that the conditions were not orographically induced, the warm front moving approximately perpendicular to the track at around 27 kn for the duration of the reported clear air turbulence would suggest a lateral extent of at least 80 n mile. The dry adiabatic lapse rate in the layer below the frontal zone may have pre-existed or been generated by the wind-shear induced turbulence, but in either case turbulent momentum transfer within the layer would probably distribute the disturbance vertically, perhaps so assisting the maintenance of the strong shear below the frontal zone for the observed duration.

L.A. Hisscott

Meteorological Department
Ronaldsway Airport, Ballasalla
Isle of Man

551.501.81:551.507.362.2:551.509.56

Meteosat and radar rainfall imagery interpretation on the night of 20/21 November 1986

A.J.Waters
Meteorological Office, Bracknell

Summary

Satellite and radar imagery often reveal striking patterns. Correct interpretation of the imagery can improve weather prediction, especially short-period forecasts. Examples of imagery available in near real time on 20/21 November 1986 are shown, and important signatures highlighted.

1. Introduction

Overnight on the 20/21 November 1986, severe weather, including thunderstorms and heavy rain, occurred in a band some 200 km wide extending from south-west Wales to the eastern English Channel (Fig. 1). A tornado at Swindon around 2330 GMT and a waterspout at Selsey around 0045 GMT caused extensive structural damage. These were examples of some of the mesoscale convective phenomena observed within the circulation of a deepening depression that moved eastwards across England and Wales (Fig. 2). Classically, this could be considered as a 'left exit' development in the diffluent trough ahead of a very strong north-westerly jet (maximum wind around 320° / 160 kn near 280 mb).

There now follows an examination of how the imagery from Meteosat and the UK weather radar network for 2200 GMT on 20 November and 0100 GMT on 21 November (Figs 3 and 4) displayed key signatures that could be interpreted and related to some of the mesoscale phenomena that occurred.

2. Key signatures

The four key signatures considered are line convection and deep convection on the radar imagery, and the dry tongue and comma-shaped cloud area on the Meteosat imagery.

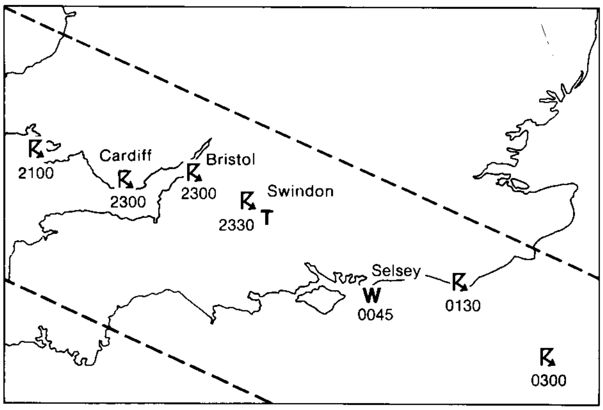

Figure 1. The zone, with approximate boundaries (— — —), in which severe weather was observed overnight on 20/21 November 1986, showing the approximate times of occurrence and positions of thunderstorms (K), waterspout (W) and tornado (T).

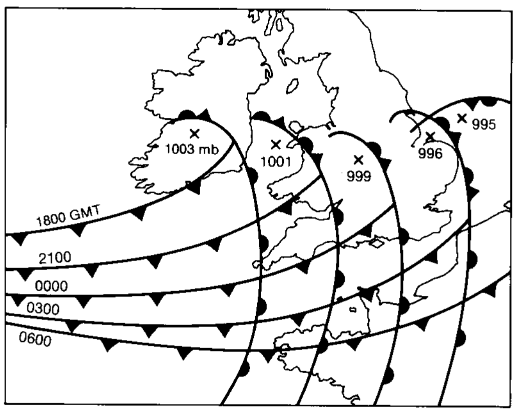

Figure 2. Continuity chart from 1800 GMT on 20 November to 0600 GMT on 21 November 1986, showing the position of the surface fronts and the low pressure centre at 3-hour intervals.

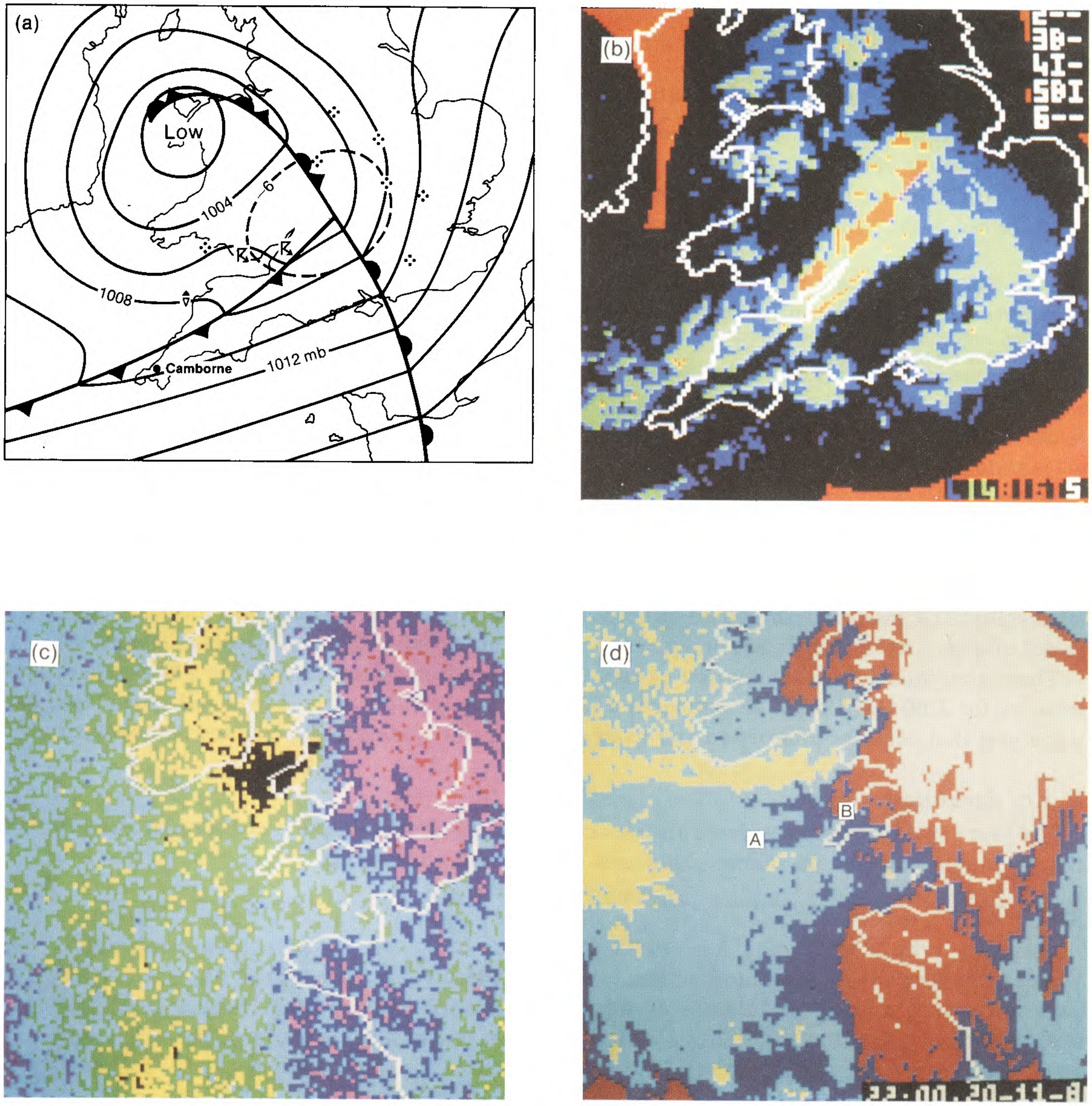

Figure 3. Surface analysis and imagery at 2200 GMT on 20 November 1986. (a) Surface analysis including the −6 mb/3 h isallobar (— — —) and surface observations of heavy precipitation, hail (▲) and thunderstorm (K). (b) Rainfall distribution from the UK weather radar network with intensities indicated by colours as follows: blue ≥ 0.1 mm h^{-1}, green ≥ 1 mm h^{-1} and orange ≥ 8 mm h^{-1}. The outer orange areas are spurious and the marks and letters in the top right hand corner refer to the radar sites, calibration adjustment type and bright-band height. For detail on these, and radar display systems in general, see Blackall (1983). (c) Meteosat false-colour water vapour image, black represents the driest and red the moistest air. (d) Meteosat false-colour infra-red image, approximate temperatures indicated by colours as follows: white ≤ −40 °C, red ≤ −20 °C, dark blue ≤ −10 °C, light blue ≤ 0 °C and green > 0 °C.

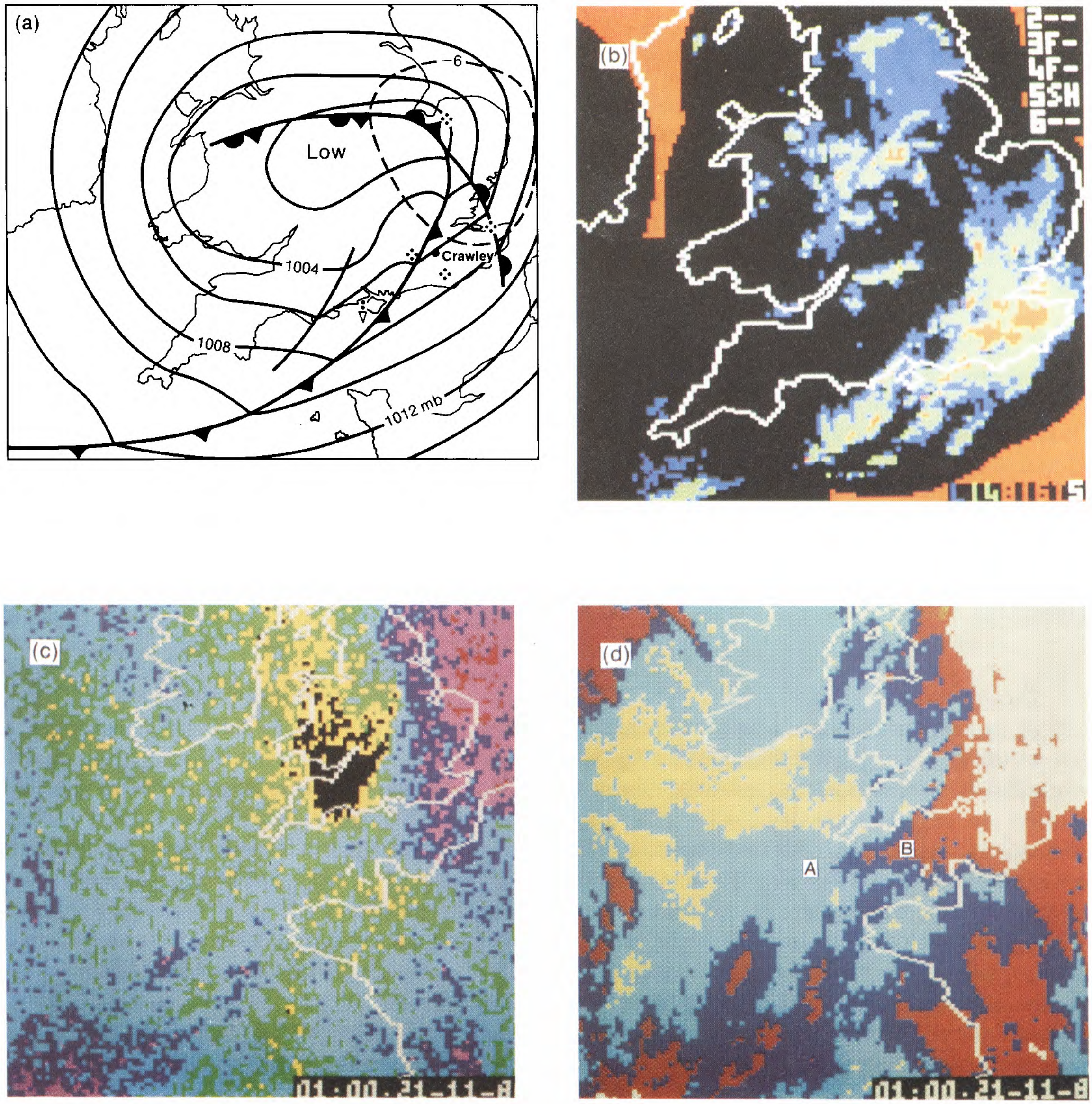

Figure 4. As Fig. 3 but for 0100 GMT on 21 November 1986.

2.1 *Line convection*

Line convection is a relatively shallow phenomenon caused by forced ascent of stable air at an active rearward-sloping cold front (Browning 1985). It can be identified on the 2200 GMT radar rainfall imagery by narrow elements of heavy rainfall ($\geqslant 8$ mm h^{-1}) in a line extending from south-west to north-east just to the east of Bristol (Fig. 3(b)). By recognizing line convection the forecaster can accurately locate the surface cold front. However, because of the shallow nature of the convection, it can only be detected by network radars when within approximately 120 km of individual radar sites. This means that on current network displays line convection may not be continuously observed. However, expansion of the network, with suitably sited radars, should help to reduce this problem.

2.2 *Deep convection*

Just to the rear of the line convection, more extensive areas of heavy rainfall ($\geqslant 8$ mm h^{-1}) present a more striking signature (Fig. 3(b)); note the associated thunderstorm at Cardiff in South Wales (Fig. 3(a)). The movement of these heavy rainfall areas and their decay, and the subsequent development of new areas of heavy rain could be followed on successive pictures. At 0100 GMT most of the heavy rainfall is located over south-east England and the English Channel (Fig. 4(b)).

The Selsey waterspout was probably associated with a small cell (approximately 25 km^2) which was first identified at 2300 GMT about 200 km to the west of Selsey (just east of Torquay). This cell was observable as a discrete entity until around 0100 GMT when it merged with a larger area of heavy rain. During this period of observation the cell had a mean velocity of 250° / 65 kn.

2.3 *The dry tongue*

Meteosat water vapour imagery indicates moisture content in the middle and upper troposphere (Eyre 1981). Imagery from 2200 GMT (Fig. 3(c)) reveals a tongue of very dry air extending south-eastwards from Northern Ireland to St. George's Channel. Maximum pressure falls at the surface are located just ahead of the dry tongue (Fig. 3(a)). A similar relationship between the largest surface pressure falls and the position of the dry tongue has been established in other cases such as Young *et al.* (1987). The origin of the dry air in these cases could be traced back to the stratosphere — this air being injected into the troposphere on the cold side of the upper tropospheric jet.

Most of the thunderstorms overnight on 20/21 November occurred over the sea or near exposed coasts. The upper-air sounding for Crawley (Fig. 5(a)) shows that deep convection could be generated by the relatively high prevailing sea surface temperatures (10–13 °C), even within the so-called 'warm sector'. Inland, however, different generating mechanisms would have been required. Triggers could have been supplied by:

(a) orographic lifting,

(b) the surface cold front (SCF) or

(c) the overrunning of low-level air with a relatively high wet-bulb potential temperature (θ_w) near the SCF by drier, lower θ_w air aloft and the subsequent release of potential instability.

The Camborne upper-air sounding (Fig. 5(b)), representative of air just to the rear of the SCF, does show dry air above 650 mb and potential instability between 750 and 600 mb. Note also the very strong winds above 600 mb.

The water vapour imagery for 2200 GMT (Fig. 3(c)) shows the leading edge of the dry air aloft to be just west of the Swindon area. Thunderstorms and the reported tornado occurred in the Swindon area during the following few hours. So, if overrunning is anticipated, the imagery can help identify areas most likely to be affected by deep convection.

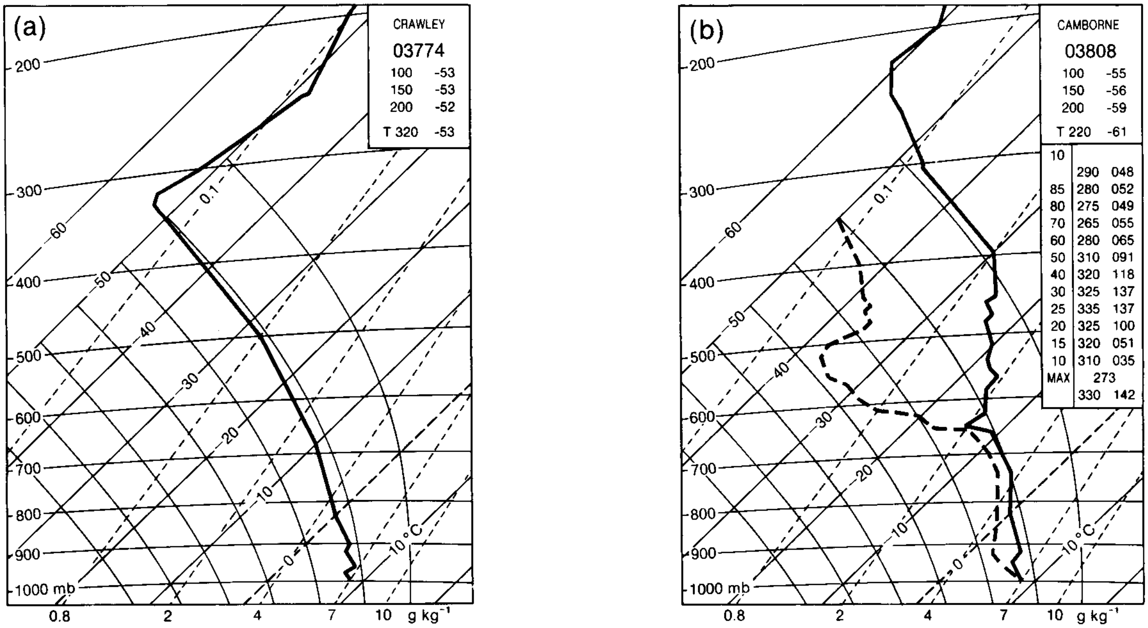

Figure 5. Radiosonde ascents at 0000 GMT on 21 November 1986 for (a) Crawley (humidity data were not available) and (b) Camborne.

2.4 *Comma-shaped cloud area*

A frontal wave that undergoes rapid cyclogenesis has an associated comma-shaped cloud pattern which can be easily identified on infra-red satellite imagery (Carlson 1980). This is one of the key signatures in this case since a large comma-shaped area of cold cloud-top temperature ($\leqslant -20$ °C) can be clearly identified (Fig. 3(d)).

Rapid lowering of cloud-top temperature along a frontal band is indicative of general ascent. This behaviour is apparent in the imagery for 2200 GMT (Fig. 3(d)) and 0100 GMT (Fig. 4(d)) following the path AB as indicated.

3. Conclusions

The forecaster not only has conventional ground-based observations and model products for guidance, but also increasingly has imagery from remote sounding techniques. Good interpretation of signatures revealed by the imagery, examples of which have been highlighted here, allied with some simple airflow models to help in interpretation, should put the forecaster in a better position to produce more accurate forecasts, especially in the short term.

References

Blackall, R.M. 1983 Weather radar systems displays (Jasmin users guide).(Unpublished, copy available in the National Meteorological Library, Bracknell.)

Browning, K.A. 1985 Conceptual models of precipitation systems. *Meteorol Mag*, **114**, 293–319.

Carlson, T.N. 1980 Airflow through mid latitude cyclones and the comma cloud pattern. *Mon Weather Rev*, **108**, 1498–1509.

Eyre, J.R. 1981 Meteosat water vapour imagery. *Meteorol Mag*, **110**, 345–351.

Young, M.V., Monk, G.A. and Browning, K.A. (1987) Interpretation of satellite imagery of a rapidly deepening cyclone. (Submitted to *Q J R Meteorol Soc.*)

Reviews

Chemistry of atmospheres: an introduction to the chemistry of the atmospheres of earth, the planets and their satellites, by Richard P. Wayne. 160 mm × 240 mm, pp. xii + 361, *illus*. Oxford, Clarendon Press, 1985. Price £30.00 (hardback), £14.50 (paperback).

In recent years there have been many textbooks addressing a wide variety of aspects in atmospheric science. This particular book concerns itself specifically with the chemistry of atmospheres — mainly the terrestrial atmosphere but not exclusively so. The author is a physical chemist and while the approach of the book reflects this, it seems designed not to be restricted to those with chemistry backgrounds. The chapters each give overviews of particular aspects of atmospheric chemistry and related areas, and each ends with a fairly extensive bibliography which provides a very useful introduction to those wishing to follow up particular topics. The contents of the chapters reflect the rapidly advancing state of atmospheric chemistry and generally appear up to date. One point of possible concern is that in order to encompass the admittedly wide scope of this book, some of the discussions have been abbreviated or simplified to the point where prior knowledge of the issue in question is desirable or necessary. One pleasing aspect, however, is that the author does (for example in Chapter 9 on the evolution of atmospheres) discuss wider issues than pure chemistry and readers are, for example, encouraged to consider the implications of books such as *Gaia. A new look at life on earth* (Lovelock 1979)*.

Chapter 1 introduces the terrestrial atmosphere to the reader, highlighting specific processes which play or have played significant roles in creating and maintaining the present atmosphere — even heterogeneous chemistry, a subject of some topical interest, is mentioned in passing.

Chapter 2 describes, using basic physical laws, how the temperature and pressure structure of the terrestrial atmosphere arises, with a quite lengthy discussion of the role of radiation in the earth's atmosphere. A minor blemish is that $\sec^2\theta$ on page 49 should in fact be $\sec\theta$. There then follow sections on transport and winds. In the former the rather superficial discussion ranges from vertical eddy diffusion coefficients to tropopause folding in less than a page — certainly an example of excessive compression! The chapter ends with sections on particle nucleation and scattering.

Chapter 3 outlines from first principles the basic photochemical processes using, usefully, examples from the terrestrial atmosphere. The discussions of chemical kinetics are extensive but the weakness of this chapter is the section (about 3 pages) on numerical modelling which is unhelpfully brief.

Chapters 4 and 5 deal with the chemistry of the lower and middle terrestrial atmosphere. Chapter 4 addresses the important subject of ozone in the earth's stratosphere; again a wide ranging but brief résumé. One concern is that between pages 116 and 120 'odd oxygen' becomes 'ozone' and perhaps in consequence the height dependence of the odd oxygen destruction reaction (page 118) is ignored. This is followed by an extensive discussion of catalytic ozone destruction, and the likelihood of man perturbing the ozone balance in the stratosphere is clearly presented. In keeping with the general tone of the book, it might have been pointed out in the section 'Comparison of experiment with theory' that even though 'the general pattern of stratospheric chemistry' is 'well understood' (page 139) there is a 30% discrepancy between modelled and observed ozone in the upper stratosphere — a region where the chemical time constants are much shorter than those for transport, and where the models might be expected to perform in some sense 'best'. Chapter 5 deals with chemistry in the troposphere. The format is much the same as Chapter 4. There are sections describing sulphur chemistry (important in so-called 'acid rain') and photochemical smog. In the latter it would have been worth emphasizing that much of the apparent

* Lovelock, J.E.; *Gaia. A new look at life on earth.* Oxford University Press, Oxford, 1979.

diurnal variations of ground-level ozone can be attributed to meteorological rather than chemical causes.

The upper atmosphere is considered in Chapters 6 and 7. Chapter 6 discusses the role of ions and ion chemistry in various atmospheric regions. It is interesting in the light of recent depletions in Antarctic ozone that the possible importance of ion catalysed reactions in the low stratosphere and troposphere is mentioned briefly. Chapter 7 is concerned with the airglow. There is a useful discussion of various excitation mechanisms, although it does not seem necessary to introduce the complications of Einstein 'A' coefficients (page 263).

Chapter 8 discusses extra-terrestrial atmospheres — in particular their chemical composition on Venus, Mars, the giant planets and the one satellite possessing a significant atmosphere, Titan. This chapter is interesting because it not only describes the composition of each in turn, but also attempts to assess, in the light of the photochemistry described earlier, what chemical reactions might be important in the different regimes.

Chapter 9 considers the evolution and possible future trends of planetary atmospheres, mainly the earth's. The complexity of the role that man can play in altering atmospheric composition and ultimately climate is well illustrated and, as far as is possible in five pages, the climatic consequences are assessed.

Overall, the book provides a useful introduction to atmospheric chemistry. The author has attempted to put atmospheric chemistry into a wider context and in this he has been largely successful. It is perhaps inevitable in a book of this scope that some topics, for example meteorology and dynamics, are treated rather sketchily. However, the fairly extensive bibliographies should enable this problem to be, to some extent, overcome. Overall the book is to be recommended.

R.L. Jones

Notes on numerical fluid mechanics, Volume 13: Proceedings of the sixth GAMM-Conference on numerical methods in fluid mechanics, edited by D. Rues and W. Kordulla. 155 mm × 230 mm, pp. x + 408, *illus*. Braunschweig/Wiesbaden, Friedr. Vieweg and Sohn, 1986. Price £31.00.

This volume contains the 51 papers which were presented at the sixth GAMM (Gesellschaft für Angewandte Mathematik und Mechanik) Conference on numerical methods in fluid mechanics held in Göttingen, Federal Republic of Germany, in September 1985. This conference is organized every two years at different places in Western Europe. The papers cover a broad range of topics, from the mathematical development and investigation of algorithms to their application to fluid mechanical problems in acoustics, aerodynamics, car aerodynamics, gas dynamics, hydrodynamics, meteorology, oceanography,turbo-machinery, etc. This volume also includes a brief report on the GAMM workshop 'The efficient use of vector computers with emphasis on computational fluid dynamics' which followed the conference.

There are only two papers specifically on meteorological problems, by Th.L. van Stijn and F.T.M. Nieuwstadt of the Royal Netherlands Meteorological Institute on 'Large eddy simulation of atmospheric turbulence' and by H. Volkert and U. Schumann of Deutsche Forschungs — und Versuchsanstalt für Luft — und Raumfahrt, Oberpfaffenhofen, on 'Development of an atmospheric mesoscale model'. The first of these papers presents a number of interesting computations as well as a brief description of the model used. The second paper is part of a series of contributions to these conferences and it is very uninformative read on its own.

The remainder of the volume can be roughly divided into papers on algorithms in general and papers on applications, mostly in aerodynamics. The same bias is clear in the papers on algorithms. Nearly all discuss finite difference or finite volume methods. The latter are finite difference schemes formulated to ensure satisfaction of integrated conservation requirements. A recurrent theme is the need to compute sharp discontinuities without generating spurious overshoots. Quite successful methods are now available for doing this in two dimensions in the presence of strong but steady shock waves. Interest in this area of atmospheric modelling is growing with the increasing attention given to very-high-resolution modelling. Many of the applications are to steady flows and there is a great deal of work on design of grids that most accurately represent the flow features. This approach is not common in atmospheric modelling since the use of an irregular grid to represent an unsteady flow often causes large errors.

Even though the papers in the volume are restricted to a maximum of approximately eight pages, a high proportion of them are understandable by anyone with a reasonable knowledge of numerical methods. There has always been a gap between numerical modelling in meteorology and the mainstream of computational fluid dynamics. Though this probably reflects genuinely large differences in the problems to be solved, there is much that meteorologists can learn from experiences in other fields. There is a considerable interchange of techniques used in modelling turbulent flows but the similarity between methods of modelling low speed flows, e.g. past motor cars, with those for modelling certain atmospheric structures has not been fully exploited.

M.J.P. Cullen

Prediction of solar radiation on inclined surfaces, edited by J.K. Page. 165 mm × 238 mm, pp. xii + 459, *illus.* Dordrecht, D. Reidel Publishing Company, 1986. Price £59.50, US $85.00, Dfl 180.00.

This book describes the results of several years of collaborative research, involving a number of groups within the European Community, aimed at providing a comprehensive set of techniques for calculating solar radiation on inclined surfaces. The declared objective is to help solar energy practitioners in all fields, with methods presented in a practical form that can be used by designers. These have been tested for many locations and are intended to be widely applicable.

Modellers of solar radiation fall mainly into two camps. Those concerned with radiation schemes within numerical climatological or synoptic models tend to subdivide the solar spectrum into narrower bandwidths which can be dealt with by approximations based on the full radiative transfer equations; those concerned with solar radiation as a source of energy, mainly for buildings and agriculture with both passive solar heating and active energy generation, usually require site-specific and climatological data. The latter group tend to deal with broad-band radiation components with complex pragmatic relations depending upon sunshine amount and other readily available observations. This book lies entirely within the second category and describes in detail both these pragmatic relations and the ideas behind them.

A brief theoretical background is provided in the text, with a major proportion of the volume being given up to tables and diagrams describing the comparison of observed data with various models' results. The early chapters describe the development of a technique for predicting solar radiation on a horizontal surface under cloudless skies. Here the major uncertainty lies in specifying the turbidity, i.e. the attenuation due to aerosol, which varies considerably both with location and from day to day. The next section displays recent observations of the angular distribution of the radiance of cloudless skies and indicates how these data may be applied to estimating clear sky radiation on inclined surfaces. A method of prediction for overcast days is then described, demonstrating the considerable statistical fluctuations due to the presence of clouds. The final chapters catalogue the synthesis of these results into techniques for predicting mean solar radiation on inclined surfaces.

This volume provides a wealth of information for the solar energy user interested in the detailed availability of solar radiation, using the most recent techniques tried and tested with modern data, for many European locations. In particular a useful guide is given to estimating the turbidity for areas where conventional data are absent. A series of look-up tables can be consulted which simplify the process of determining radiation values for arbitrary orientations of the surface. A number of appendices include useful supplementary data concerning the sun–earth geometry, day length and other radiation related factors.

The main drawback with this book lies in the sheer amount of information presented and in its organization, perhaps unavoidable in a subject which relies heavily on establishing numerous empirical dependences, with several authors contributing to the final product. It would have been useful to separate more clearly the verification of methods from their application in calculating solar radiation in practice. The casual user of solar radiation data should be directed towards the maps of radiation on horizontal and inclined surfaces already prepared by the methods described (*CEC European Solar Radiation Atlas, Vols I and II*). It is difficult to decide whether the complexity of the presented techniques is justified by the accuracy required by most users, particularly with the uncertainties in sunshine amount and turbidity. This is compounded by the complication that different criteria are needed for different averaging periods, as is common in climatological problems. It seems unlikely that the bulk of the detailed developmental results would be of interest to any but the most specialized worker. Summarizing, this book will serve as a useful reference work for those in the solar energy community who are interested in the details of simulating solar radiation climatology, but not as an easily accessible source for the uncommitted reader.

F. Rawlins

Books received

The listing of books under this heading does not preclude a review in the Meteorological Magazine at a later date.

Basic meteorology, a physical outline, by J.F.R. McIlveen (Wokingham, Van Nostrand Reinhold (UK) Co. Ltd, 1986. £15.95 (paperback only)) attempts to merge the two usual approaches to meteorology: describing the facts of atmospheric behaviour and explaining the physical mechanism involved. It is intended for students during the first two years of relevant degree courses, and the author is an experienced lecturer on the subject.

The uncertainty business, by W.J. Maunder (London, Methuen and Co. Ltd, 1986. £45.00) argues that weather information is a valuable commodity for decision-making in many key areas of human activity. A manifesto is issued for the development of new areas of research, requiring the skills from several disciplines.

Climate, weather and Irish agriculture, edited by T. Keane (Dublin, Mount Salus Press Ltd, 1986. Ir. £9.95 (paperback), Ir. £14.95 (hardback)) details the relationship between Irish weather and agriculture. There are four main strands: climate and weather, soil management, crop production and animal production. In each area the most recent research is included and many subjects which were only in scattered sources are drawn together.

Satellite photograph — 15 December 1986 at 0548 GMT

The NOAA-9 infra-red image received and displayed via the Meteorological Office HERMES system, shows a distinctive cloud whirl associated with an intense Atlantic depression of unusual depth. The Central Forecasting Office (CFO) surface analysis for 0600 GMT suggested the depth to be 920 mb with an observed pressure of 926.6 mb reported near the centre. The minimum central pressure of the low was 916 mb (6 hours earlier) following 36 hours of rapid cyclogenesis as two separate centres combined, accompanied by a pressure fall of 70–80 mb.

The occluded front, marked in the CFO analysis as terminating west of the depression centre, is seen in the image to spiral into the centre. South of the depression centre, the depth and scale of the convection (originating in the Labrador region) increases progressively, such that over the warm waters of the central Atlantic considerable cumulonimbus cloud is present, with anvils shearing off ahead and to the left of the track of the convection cells in the strong upper winds, within a region of cold air advection.

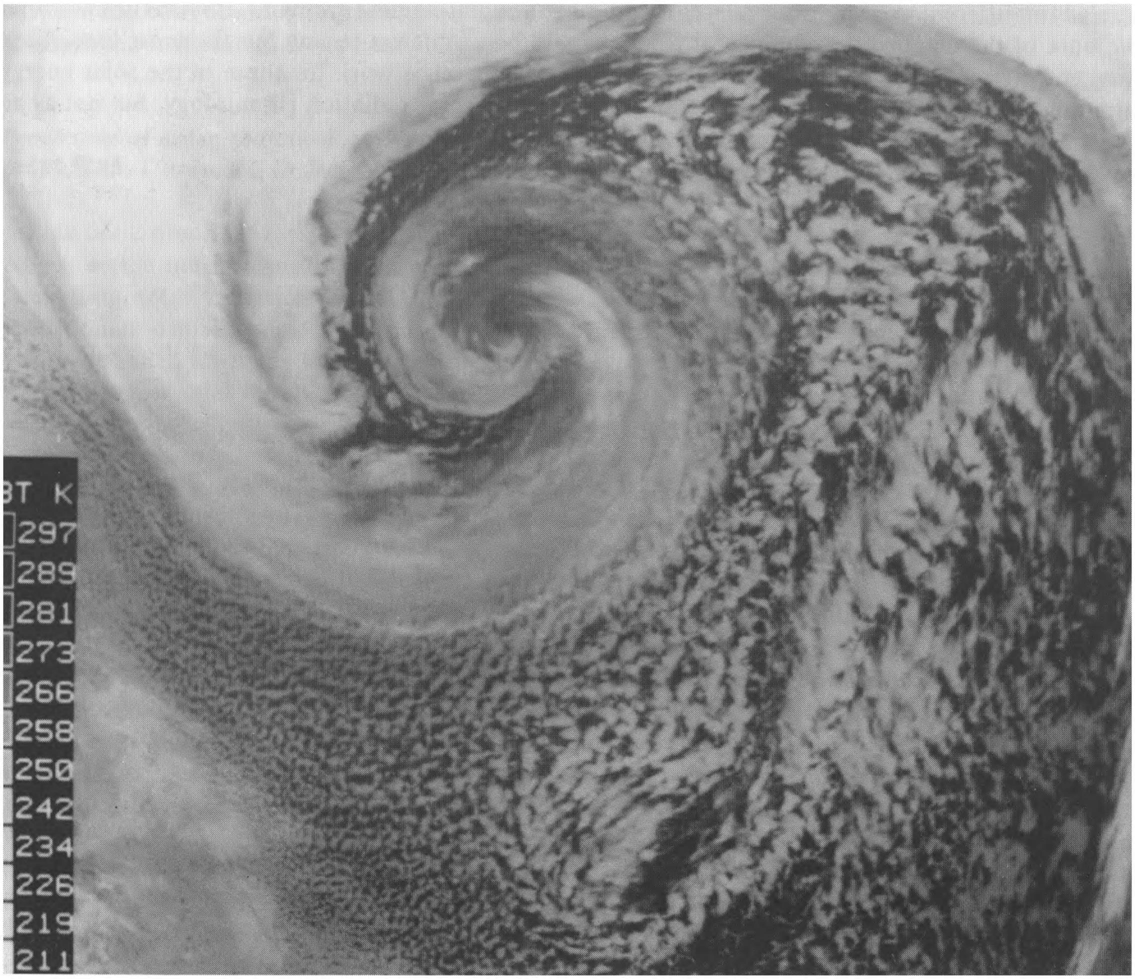

Meteorological Magazine

GUIDE TO AUTHORS

Content

Articles on all aspects of meteorology are welcomed, particularly those which describe the results of research in applied meteorology or the development of practical forecasting techniques.

Preparation and submission of articles

Articles for publication and all other communications for the Editor should be addressed to the Director-General, Meteorological Office, London Road, Bracknell, Berkshire RG12 2SZ and marked 'For *Meteorological Magazine*'.

Articles, which must be in English, should be typed, double-spaced with wide margins, on one side only of A4-size paper. Tables, references and figure captions should be typed separately.

Spelling should conform to the preferred spelling in the *Concise Oxford Dictionary*.

References should be made using the Harvard system (author, date) and full details should be given at the end of the text. If a document referred to is unpublished, details must be given of the library where it may be seen. Documents which are not available to enquirers must not be referred to.

Tables should be numbered using roman numerals and provided with headings. We consider vertical and horizontal rules to be unnecessary in a well-designed table; spaces should be used instead.

Mathematical notation should be written with extreme care. Particular care should be taken to differentiate between Greek letters and Roman letters for which they could be mistaken. Double subscripts and superscripts should be avoided, as they are difficult to typeset and difficult to read. Keep notation as simple as possible; this makes typesetting quicker and therefore cheaper, and reduces the possibility of error. Further guidance is given in BS1991: Part 1: 1976 and *Quantities, Units and Symbols* published by the Royal Society.

Illustrations

Diagrams must be supplied either drawn to professional standards or drawn clearly, preferably in ink. They should be about 1½ to 3 times the final printed size and should not contain any unnecessary or irrelevant details. Any symbols and lettering must be large enough to remain legible after reduction. Explanatory text should not appear on the diagram itself but in the caption. Captions should be typed on a separate sheet of paper and should, as far as possible, explain the meanings of the diagrams without the reader having to refer to the text.

Sharp monochrome photographs on glossy paper are preferred: colour prints are acceptable but the use of colour within the magazine is at the Editor's discretion. In either case contrast should be sufficient to ensure satisfactory reproduction.

Units

SI units, or units approved by WMO, should be used.

Copyright

Authors wishing to retain copyright for themselves or for their sponsors should inform the Editor when they submit contributions which will otherwise become UK Crown copyright by right of first publication.

It is the responsibility of authors to obtain clearance for any copyright material they wish to use before submitting it for publication.

Free copies

Three free copies of the magazine are provided for authors of articles published in it. Separate offprints for each article are not provided.

Meteorological Magazine

March 1987

Vol. 116
No. 1376

CONTENTS

Contributions: it is requested that all communications to the Editor and books for review be addressed to the Director-General, Meteorological Office, London Road, Bracknell, Berkshire RG12 2SZ, and marked 'For *Meteorological Magazine*'. Contributors are asked to comply with the guidelines given in the *Guide to authors* which appears on the inside back cover. The responsibility for facts and opinions expressed in the signed articles and letters published in *Meteorological Magazine* rests with their respective authors. Authors wishing to retain copyright for themselves or for their sponsors should inform the Editor when submitting contributions which will otherwise become UK Crown copyright by right of first publication.

Subscriptions: Annual subscription £27.00 including postage; individual copies £2.30 including postage. Applications for postal subscriptions should be made to HMSO, PO Box 276, London SW8 5DT; subscription enquiries 01–211 8667.

Back numbers: Full-size reprints of Vols 1–75 (1866–1940) are available from Johnson Reprint Co. Ltd, 24–28 Oval Road, London NW1 7DX. Complete volumes of *Meteorological Magazine* commencing with volume 54 are available on microfilm from University Microfilms International, 18 Bedford Row, London WC1R 4EJ. Information on microfiche issues is available from Kraus Microfiche, Rte 100, Milwood, NY 10546, USA.

ISBN 0 11 727967 6 ISSN 0026–1149

Printed for HER MAJESTY'S STATIONERY OFFICE
by Delco Printing Co.Ltd. 3/87 Dd. 739131 C1400

THE METEOROLOGICAL MAGAZINE

HER MAJESTY'S STATIONERY OFFICE

April 1987

Met.O.978 No. 1377 Vol. 116

METEOROLOGICAL OFFICE Met.O.978

THE METEOROLOGICAL MAGAZINE

No. 1377, April 1987, Vol. 116

551.5:06:33

The Meteorological Office — a ten-year perspective

J.T. Houghton
Director-General, Meteorological Office, Bracknell

Summary

The Meteorological Office's main responsibility is to provide meteorological services (including weather forecasts and advice regarding weather and climate) to defence, civil aviation, shipping, other government departments, public bodies, the media, industry and commerce and the general public. It is widely perceived as one of the leading national meteorological services in the world, a position which results from the integrated nature of the Office's activity and remit (especially the integration between defence and civil activities), from the way in which the Office has concentrated its effort into key areas and from the quality of personnel the Office has been able to attract. This is an appropriate time to review the activities of the Office and to present the major components of its programme over the next ten years.

In the international sphere, close co-operation between national meteorological services must be maintained, as must the principle of the free exchange of data and products between them.

Future developments in observations will be governed by the need to improve data quality and coverage, and the need to improve the cost effectiveness of data acquisition through a programme of automation. Of particular importance will be the improvement of space observing techniques both in improved hardware in space and also in better methods of data retrieval and interpretation.

A major equipment replacement programme is planned. Replacement of the central computer, the Cyber 205, will also be required before the end of the decade.

Expansion of the Office's repayment services is an important task during the next few years. Much of this expansion will occur through co-operative arrangements with other bodies, especially in industry and commerce.

The Office's programme of research and development will be strongly geared to the improvement of its operational products. Developments can also be expected in the way in which the human forecaster uses computer aids, the man–machine mix, in producing his products. Other important areas where the Office needs to pursue research to maintain expertise are those concerned with climate and atmospheric chemistry. Steps are being taken to enhance the co-operation between the Office and research groups elsewhere, particularly in the universities.

1. Introduction

During my first two years in office as Director-General, I have become familiar with the wide-ranging work of the Office both in operations and research, and with the variety of associations the Office has with the outside world both nationally and internationally. I believe, therefore, it is a good time to review the activities of the Meteorological Office and to present the primary goals of the Office and the major components of its programme over the next ten years. I shall first deal with the general matters of objectives, philosophy and organization, and then turn to more particular scientific and technical matters. Finally, I shall address the question of resources. Relevant background details regarding the activities of the Meteorological Office can be found in its Annual Report.

2. Objectives and philosophy

2.1 *Functions of the Meteorological Office*

The functions of the Meteorological Office as laid out in recent Annual Reports provide a broad statement of the Office's responsibilities. Its main responsibility is to provide meteorological services to defence, civil aviation, shipping, other government departments, public bodies, the media, industry and commerce, and the general public. The provision of meteorological services includes the provision of weather forecasts for the surface and the upper air, and the provision of information or advice concerning all aspects of weather or climate, especially as they affect human activity. The Office's remit is therefore a very broad one. In recent years, as forecasts have become considerably more accurate, as the amount of relevant information has increased and as the means for its dissemination have become more readily available, the demand on the Office for more and better information of all kinds has increased manyfold, an increase which is likely to continue unabated for some years into the future. Some of the problems this poses, together with some of the opportunities created, are now considered.

Regulation. Because of the broad nature of the Office's responsibilities and because the Office is not governed by any statute or charter, questions are often asked regarding how the Office's activities are regulated. Regulation occurs in four ways.

(a) There is the normal continual internal review of activities within the Office itself in response to scientific and technical possibilities on the one hand and to customer pressure and perceived demand on the other, limited always by the resources available and the need to be cost effective.

(b) There is the annual process in the Ministry of Defence in which the Office's assumptions, and requirements stemming from these, are rigorously examined.

(c) There are the results of a number of reviews and investigations of the Office's activities. Of these the most important (and the most thorough) is the Rayner Resource Control Review* (RCR). Its recommendations as modified and approved by ministers form, in most regards, a firm basis for the way forward for the Office.

(d) There is the regular scrutiny of the Office's programme by the Meteorological Committee with its broad scientific and customer representation.

These four mechanisms together form quite a tight regulation of the Office's activities while leaving room for appropriate initiative and evolution.

Provision of services. In taking any view of the Meteorological Office it is important to understand the basic means by which the services are provided. The source of most of the information provided to customers and users comes from the generation of weather forecasts that cover the whole globe and which extend to a few days ahead; these are made twice every day. The tools required to generate them are world-wide observations, global communications and large computer models of the atmospheric circulation. This central operation (including the UK's share of the collection of world-wide observations) takes up nearly two thirds of the total resources of the Office. Without it, none of the Office's major customers could be provided with the services they require. This fact is recognized by the inclusion in the listed functions of the Meteorological Office of the organization of meteorological observations and the collection and dissemination of meteorological information (both in concert with other national meteorological services), the provision of meteorological training and the carrying out of research in meteorology and geophysics, all of which are required if the main responsibility of the provision of a wide range of services is to be properly discharged.

* Ministry of Defence; Report of the resource control review of the Meteorological Office, 1983, London, HMSO.

2.2 *A leading national meteorological service*

The Meteorological Office is widely perceived both nationally and internationally as a leading national meteorological service in the world in the quality of its forecasting products. The performance of the Office's forecasting models and the skill of its forecasters bear very favourable comparison with any other service. Yet, as has been pointed out by the RCR, this excellence is achieved at modest cost, in fact a lower cost per caput than for comparable countries in the developed world. It is worth at the start of this review asking what are the reasons for this pre-eminence and cost-effectiveness. I put forward three main reasons: integrated nature of the Office's work, concentration of effort and quality of personnel.

Integrated nature of the Office's work. Operational meteorology in the United Kingdom is concentrated in the Meteorological Office. This is not the case in many countries where operational meteorology for defence is separated from that for the civil sector, or where services for commerce and industry are separated from services to the public. The integrated nature of the work of the Meteorological Office not only avoids unnecessary duplication but also provides the opportunity for the staff to acquire experience over a broader range than would otherwise be possible, and broad experience translates significantly into forecasting skill.

Concentration of effort. Over the years, the Office has concentrated its effort into key areas, and ensured that its work in research and development (R and D) has been followed through into operational products. Good integration (achieved largely through regular interchange of staff) between the services side and the R and D side of the Office has ensured that there has been a continuous flow of information from the service side about the requirements and a similar flow from the R and D side regarding what is feasible. This concentration of effort and close integration of activity has been particularly true of the Office's numerical modelling. Scientists in the Office were some of the first to recognize the potential of numerical modelling for forecasting and were able, single-mindedly, to develop appropriate models and to acquire the computing capacity to run them effectively for operational purposes. The small proportion of the Office's resources devoted to R and D has, therefore, been effectively used. I say small — it is small (currently less than 12%) in proportion to the whole of the Office's resources and very small in comparison to what has been devoted to similar activity elsewhere, for instance in the USA (see section 6).

Quality of personnel. The Office has been fortunate in achieving over the years a high level of attractiveness to some of the best graduates in physics and mathematics. This situation is in no small part due to the enthusiasm with which my predecessor, Sir John Mason, publicized the exciting science going on in the Office, not least through the high quality lectures he gave in academic institutions throughout the United Kingdom. The high profile given to the quality of science being carried out in the Office has attracted some of the best intellects to the research side of the Office, many of whom, after a significant research career, have turned their abilities and energies to furthering the services and applications side of the Office's work. I consider it high priority to continue to recruit and retain the highest quality graduates — a task which has become more difficult as the Civil Service has become less attractive compared with industry or research abroad.

Cost-effectiveness. Meteorological Office customers continue to demand high quality information. Defence certainly requires the best information possible not only because war remains a highly weather-dependent activity but also because the best use of flying training time must be made whilst maintaining aircraft safety. The public at large also welcome a good forecast — the improvement in accuracy of public forecasts over recent years has been noticed and appreciated. Further, in the area of repayment services, the commercial edge possessed by the Office is highly dependent on the quality of its products. If these were not perceived as the best available, the demand for Meteorological Office services and the amount which customers would be prepared to pay would be much reduced. For instance, the fact that a significant proportion of the world's airlines demand our global wind products (and pay additional handling and communication costs for direct computer access to them) because they are perhaps 10% more accurate than other available products, demonstrates the value that they put on quality.

However, one cannot talk of excellence without considering its cost — value for money is also important. I have already pointed out that the quality of the Office's products has not been bought at a high price but is due to the quality of its personnel and to selectivity in its programme. The cost of providing excellence as opposed to mediocrity is not high; it is of the order of a few per cent (probably less than 10%) of the whole budget of the Office. I believe, that so far as global modelling and forecasting skill is concerned, we will be able to maintain a leading position without an undue increase in cost providing that:

(a) we maintain our quality of personnel,

(b) we continue to maintain our integrated service, and

(c) we continue to capitalize on our ability to exploit profitably the full capacities of the most advanced computers.

An implication of the integrated operation is that the Meteorological Office should remain an integral part of the Ministry of Defence — the Office's largest single customer. It is unfortunate that the simple arrangement with an integrated Meteorological Office as part of the Ministry of Defence has commonly been seen in recent years as untidy or illogical. Numerous reports have been commissioned to look into the situation. Of these the RCR is by far the most thorough. While considering a number of alternatives, it supported unequivocally, in the interest of efficiency and cost effectiveness, the present arrangement. I am convinced that any other arrangement would tend to lead to a break-up of the service (see section 5.1) and would certainly lead to inefficiency and increased cost because of the multiplication of technical, financial and administrative support.

3. The international context

3.1 *International arrangements*

World Meteorological Organization. Operational meteorology is a highly international activity. National meteorological services co-operate through the World Meteorological Organization (WMO), an inter-governmental organization which is often regarded as one of the most efficient of the international agencies. It has a clear organizational and technical remit, and is flexible and pragmatic in the way it pursues its objectives.

The WMO does not itself make observations or produce forecasts, all that is done by national meteorological services. What the WMO does is:

(a) to organize through the Global Telecommunication System (GTS) and the Global Observing System (GOS) the exchange of data, forecasts, analyses and products between national services, and

(b) to stimulate and co-ordinate research, education and technology transfer.

A keystone of the WMO arrangements and agreements is that the exchange of data and products takes place completely freely, an arrangement which has many advantages. Countries, by and large, play their part in the provision of basic observations from their territory or regions of interest. In return, they have free access to the data and products of other services. There is concern in WMO that increasing commercial pressures might begin to erode these very open arrangements. Along with all other heads of national services, I am keen to see that the close co-operation between services and the free exchange of data and products are maintained. If these were to break down, world meteorology would lose a great deal.

World Area Forecast Centre. A particularly important area of international collaboration in the application of meteorology is the field of civil aviation. The two meteorological services with the most advanced global forecasting models, namely the USA and the United Kingdom, share the responsibility for providing global meteorological information (upper-air winds and significant weather) to the world's airlines for operational and route-planning purposes. This role as a World Area Forecast Centre will become increasingly important as the demand from airlines for more accurate and more timely information increases.

Assistance to small and developing countries. A concern often expressed by small countries and developing countries is that they want to see the benefits of meteorological activity shared equitably between the nations. Such countries, especially those in Africa, have received and are receiving a great deal of help for their meteorological services. For our part, we are using the modest resources available to us to provide appropriate assistance and training especially to countries in the Commonwealth with whom we have close links. For instance, a Conference of Directors of Commonwealth Meteorological Services which is held every 4 years, the most recent in 1985, clearly still serves a useful purpose. We are also taking a lead within WMO in considering new ways in which assistance programmes in meteorology can be financed. Further, we are currently taking steps to make our forecast products more widely available to other national services. Our reasons for these efforts are not just to provide assistance to the developing world; we ourselves require high quality data from these countries. I consider it important, both from the point of view of improvement in the quality of meteorological data and from the point of view of the health of the world meteorological community, that the Meteorological Office, which is widely perceived as a world leader, should also be seen to continue, through the mechanisms provided by WMO, to use its competence and influence for the benefit of the meteorological community at large.

3.2 *Regional co-operation*

A trend of recent years in international meteorology is co-operation between national services on a regional basis. An example of such co-operation is the European Centre for Medium Range Forecasts (ECMWF) whose base is at Shinfield Park, Reading and within which 17 nations are co-operating in the development of forecasts 4–10 days in advance. The achievement of useful accuracy in deterministic forecasting that far ahead will require a great deal of research into the mathematics and technology of computer modelling, into the physics of relevant atmospheric processes and into the requirements for data. The ECMWF is widely recognized as being the leading centre in this field and it is also providing a great deal of stimulation for European meteorology. Over a ten-year period, a substantial increase in the accuracy of medium-range forecasts from the Centre can be anticipated which, from the point of view of the Meteorological Office, should lead to an increase in demand for those commercial services of the Office which are geared to this range.

There are many further examples of European co-operation in meteorology. For instance the geostationary meteorological satellite, Meteosat (through the European Meteorological Satellite (EUMETSAT) organization) and various co-operative programmes in science and technology (COST). The most notable of the COST projects is the linked operational weather radar network and a number of research projects (e.g. those on mesoscale frontal dynamics and on wave modelling) in which, through the concentration of resources from several nations, a concerted attack on important problems is possible.

A particularly important area where further European collaboration will develop is that of satellite observations. Over the past 25 years the USA have been generous in the way that they had made data available from their satellites, but they now frequently express the view that they are bearing too great a share of the cost. There is a constant threat that the polar orbiting satellite system run by the National Oceanic and Atmospheric Administration (NOAA) might be reduced to a single operational satellite — a reduction which would be particularly disadvantageous to Europe because satellite observations would be lost at a critical time for European services. Various solutions have been proposed to this problem, all of which inevitably mean that nations other than the USA, especially advanced nations, will have to make a larger contribution to the system. A possible way for Europe to assist will come through the Polar Platform which is being proposed as a European contribution to the US Space Station. Operational meteorological instruments could be part of the payload of this platform. The UK contribution to satellite observations is considered more fully in section 4.1.

4. The core operational activity

In section 2.1, I mentioned the core operational activity of the Meteorological Office in the making and the collection of observations, in global communications and in global computer modelling of the atmosphere leading to forecasts with world-wide coverage. The various components of this core activity will be addressed in this section.

4.1 *Observations and instrumentation*

Global data are required not only for global models but also to set the boundary conditions for more limited-area forecasting models (e.g. those giving detailed coverage of the United Kingdom). The world system of data collection and communication is therefore vital to the success of any forecast. It is sensible to ask, therefore, what part the United Kingdom plays in the world system (organized by the WMO and known as World Weather Watch (WWW)) and whether that part is seen as a fair share of the whole. The annual cost of observations to the United Kingdom is about £20 million, about £12 million for conventional observations and £8 million for satellite observations — amounting in total to over 25% of the Office's budget. Conventional observations are concentrated in the land and continental shelf areas of the United Kingdom and the eastern Atlantic Ocean where observations are particularly important in the context of UK weather. We also provide such observations where we have military bases (Federal Republic of Germany, Cyprus, Gibraltar, Ascension Island and the Falkland Islands). In the USA, a similar proportion of the total spent on operational meteorology (approaching $2000 million per annum) goes towards observations including satellites. In absolute terms, however, it is much larger than that of the United Kingdom — about twenty times as large — or over twice as large in proportion to the Gross National Product (GNP). Some other countries, for instance Australia, Canada and Japan, contribute in proportion to GNP somewhat more than the United Kingdom, although many smaller countries contribute considerably less. Therefore, to play our part properly we need, if anything, to increase our contribution to the world acquisition of data.

Guidance for future work on observations and instrumentation arises from two requirements, that of improving data quality and coverage (see section 4.3) and that of improving the cost effectiveness of data acquisition largely through a programme of automation.

Land surface observing network. The next few years will see a significant increase in the deployment of Automatic Weather Stations (AWS). These are important but currently provide only a limited amount of information. There is an expectation that useful automated measurement of cloud base and visibility will be achieved at such stations in the near future but reliable automated measurement of general weather conditions and cloud amount and type has yet to be demonstrated. These latter measurements are an essential input to the forecaster and are mandatory at key observing stations.

Over the next few years, trials of a Semi-Automatic Meteorological Observing System (SAMOS) will take place at military and, hopefully, civil airfields. This system automates as much as possible of the processes of gathering, displaying and communicating meteorological observations whilst requiring the human observer to key only those data which he or she must provide. Thereby some saving in observer time is possible. However, substantial savings in the number of observers required will only be possible when accurate, reliable automatic measurement of all parameters has been achieved. The development and testing of suitable instrumentation for this will take place during the next ten years. Adequate performance will, however, not be easy to achieve and it is unlikely that operational deployment of such instrumentation will begin to occur until the end of the ten-year period covered by this review.

Upper-air observations. Plans are currently underway, in response to the recommendations of the RCR, to deploy a more cost-effective and a more automated system of upper-air observations. It is planned that this will be in place at all upper-air stations before 1990.

Because of the high cost of dedicated weather-ships, the deployment of more cost-effective observing systems over the oceans is under consideration. Upper-air soundings from merchant ships are becoming possible through ASAP (Automated Ship Aerological Programme); free floating buoys again deployed from merchant ships can provide basic surface observations, and automated observations from commercial aircraft are being generated through the ASDAR (Aircraft to Satellite Data Relay) programme. For all of these systems, data are relayed from the observing device in the ship, buoy or aircraft via a satellite link to an appropriate connection to the meteorological network. In setting up all of these programmes, the United Kingdom has played a leading role and is planning to contribute to them as resources become available through the winding down of the weather-ship operation.

Radar and microwave techniques. Relatively new methods of observation which are of increasing importance are those employing radar and microwave techniques from the surface. Radar data are of vital importance for local and short-term forecasting. The recent establishment of an operational weather radar network covering England, Wales and Northern Ireland is a big step forward; the operational value of this data as exploited by the Office, the Water Authorities and other commercial users is apparent. It has also provided essential data for analysis and assessment of the movement of radioactivity in the atmosphere following the accident at the Chernobyl nuclear power station. It can be expected that sufficient support will be forthcoming from other interested bodies and that the radar network can be extended to cover Scotland during the next few years.

Techniques for making observations of wind and temperature above a surface location by vertical radar coupled with passive microwave radiometry have recently been pioneered in the USA and promise to be a valuable addition to the observing system, particularly because of the potential they offer for a dense network of observations important for local and short-range forecasting. A programme of assessment of these techniques has begun in the Office, the expectation being that in a few years' time several 'Profilers' as they are called will be in operational use.

Satellite observations. Plans for the deployment of operational satellite systems during the next ten years are largely in place (satellite plans need to be made a long time ahead). So far as the United Kingdom is concerned the plans assume a continued contribution to operational Meteosat through the European consortium EUMETSAT, and the continued provision of instrumentation for the TIROS-N polar-orbiting series of the USA. The new TIROS-N instrumentation which the Office is developing in co-operation with industry, the universities and the Rutherford Appleton Laboratory (RAL) is part of the Advanced Microwave Sounding Unit (AMSU) which will be incorporated into the TIROS-N payload around 1990. Significant improvement in the accuracy of satellite soundings of atmospheric temperature will result from this instrument.

Important priorities for the future in satellite meteorology are:

(a) the better exploitation of data from existing satellite systems, and

(b) an involvement in the design and planning of future satellite systems to ensure that the plans are soundly based so far as operational meteorology is concerned.

There is a need for the acquisition of satellite data with high horizontal resolution to provide adequately detailed input into the finer-mesh models and to assist in short-term forecasting. The combination of satellite soundings from polar-orbiting satellites (and later hopefully from geostationary satellites, see below) with radar data is potentially very powerful in this regard.

Because of the influence of cloudiness below the satellite on the measurements, there is a problem in maintaining an adequate quality of satellite observations of atmospheric temperature. Work on the improvement of the quality of satellite soundings is being pursued by the Meteorological Office Unit at the Hooke Institute at Oxford. Improved techniques for the assimilation of satellite data into operational models also need to be developed; because of their difference in character from such conventional data there is a long way to go before their full potential is realized.

Regarding satellite instrumentation, because of the growing importance of satellite observations and because of the large potential for carrying instruments into space offered by developments in the space field such as the Space Station and Polar Platform (already mentioned in section 3.2), the Office is working with other groups in the United Kingdom and abroad on investigations into new methods of measuring quantities of meteorological and geophysical interest. For the European Remote Sensing Satellite ERS-1, the Office is assisting in small ways with the Along Track Scanning Radiometer (ATSR) — an instrument for accurate measurement of sea surface temperature being built by RAL — and is also planning to assist with data analysis and interpretation from the wind scatterometer on ERS-1. Data from both instruments will be useful for routine operational purposes. For the future, the Office is helping to define the payload for the Second Generation Meteosat due for launch around 1995 and with others is suggesting suitable instrumentation to be included on the European Space Agency's (ESA) Eureka platform should that be made available for earth observation, and for the polar and other free flying platforms which it is proposed should be associated with the Space Station.

The new arrangements for the management of space activities in the United Kingdom through the British National Space Centre (BNSC) are of considerable importance to the Office. Following on from ERS-1, other government departments are showing a lot of interest in the pursuit, through ESA, of a programme in remote sensing probably associated with the Polar Platform which is expected to be a component of the US Space Station. The Office possesses substantial expertise in the relevant technologies for this programme. The global computer models possessed by the Office will also be an important vehicle for the assimilation of meteorological and oceanographic data acquired in the programme, and for ensuring that the user community receive the maximum benefit from the data. The formation of the Space Centre should provide a mechanism for the United Kingdom to develop a space programme scientifically and technically sound, working for the benefit of the United Kingdom as a whole (including of course, UK industry) — it should also enable the United Kingdom to play its part in Europe more effectively.

Use of satellite and conventional observations. Constantly in view is the question as to how far satellite observations can replace conventional ones. So far, observations from space have largely complemented conventional data by enabling better coverage in both space and time to be realized, although they lack the detail required particularly in the lower atmosphere for some purposes. Further, so far it has also been necessary to employ conventional observations to calibrate those made from space. As forecasting models become more sophisticated and more detailed, the requirements for data at a higher spatial and temporal density, with better coverage and higher accuracy, will continue to become more severe. It will continue, therefore, to be necessary to exploit to the full both conventional and satellite techniques. Although in small ways there can be a trade-off between satellite and conventional observations (for instance, because satellite observations of atmospheric temperature are now regularly available, most aerological soundings do not need to reach such a high altitude, with some small saving in equipment and in time) it is not likely that during the next decade this trade-off will be very large.

Evaluation of observing systems. A significant effort over the next few years will go into the evaluation of observing systems. This is being planned in co-operation with other nations. However, since few nations possess a global operational numerical model of high quality, it is inevitable that much of the burden of this work will fall on the United Kingdom. The aim is to assess the value of different combinations of observations so far as forecast performance is concerned. It is a difficult task because of the varied character and accuracy of the observations, because of the influences which may be introduced by assimilation procedures and because of the wide variety of forecasts for which the Office is responsible from global upper-air forecasts for airlines on the one hand, to highly specific forecasts for a local area on the other.

4.2 *Telecommunications and data processing*

Forecasters require timely access to observations and products from the numerical models. The data rates from new observational tools such as satellites and radars are many times greater than from conventional observations; there is therefore a requirement for faster methods of data distribution. The amount of data available for distribution continues to increase, particularly from satellites and higher-resolution global forecasting models. Over the past few years the Office has made substantial investment in automated data handling and message-switching systems in its Telecommunication Centre at Bracknell to keep pace with the growth in international exchanges of data and products whilst permitting reductions in manpower. Mini-computer based systems have been successfully introduced at the three Principal Forecasting Offices, with links to Bracknell providing speedy access to data and products. However, communication networks serving outstation forecasting offices are overloaded. Many of these offices do not have access to important products, such as radar and satellite data, and their means for handling and displaying data have not changed significantly for several decades. Also their equipment is obsolete and the efficiency of outstation personnel is seriously hampered through their lack of access to essential data. The potential value of these offices to the public and to the customers they are attempting to serve is not being fully realized.

Weather Information System. A high priority for the Office is to carry through a major equipment replacement programme at outstations serving both civil and military customers. Computer-based facilities with a local data base, together with a new higher capacity digital communications network, will provide the forecaster with a wider range of timely information and the ability to manipulate it efficiently to generate and issue products which will meet more effectively the needs of his various customers. A prototype of the outstation display system has been developed. Systems will be installed by April 1987 at eight important offices serving the RAF. Design of the communications system is underway. It is proposed that these new facilities, known as the Weather Information System (WIS), will be extended to all outstations over the period 1987–91. A new central processing facility will be developed for handling high resolution digital satellite imagery and generating products suitable for distribution to forecasting offices. A high-speed local network will be provided to improve the efficiency and flexibility of exchange of data and products between various computer systems and communication facilities at Bracknell.

Cyber 205. Current operational numerical forecasting models are run on the Cyber 205 'super-computer' which was installed in 1981. This machine is already fully occupied with forecasting and research tasks. Realization of the potential improvements in forecasting models, including the operational use of a numerical model for very-short-period forecasting, research into long-range forecasting and ocean modelling (including realistic ocean–atmosphere coupling for climate research and to meet Royal Navy requirements) will all require more powerful computing capacity. Current projections are that a computer at least 50 times faster and having appreciably greater capacity than the Cyber 205 will be required in the early 1990s. The Office will be making proposals to meet these expanding requirements in the light of super-computers which may be available. The most cost-effective solution may involve replacement of the Cyber 205 with a next generation machine around 1987, upgrading that to its full capacity in the early 1990s. Software compatability with the Cyber 205 will be a major consideration. It is anticipated that the two IBM 3081Ds (the second procured in 1985) which act as front ends for the Cyber 205 will, with some upgrading of processing power and peripherals, meet the general purpose computing needs of the Office until around 1993.

4.3 *Forecasting*

Forecasting skill has shown a steady improvement over the last 25 years. During the last 5 years or so the accuracy of forecasts up to 5 days ahead has been such that the public and the specialized Meteorological Office customers put much greater reliance than hitherto on the forecasts as a guide to their activities.

This gain in performance has been achieved by progressive improvements in:

(a) the quality and coverage of weather observations, and the ways in which observations are incorporated into the numerical models,

(b) the numerical methods employed in the models and the computing power available, and

(c) the parametrization of physical processes included in the forecasting models.

No improvement on its own can be singled out as the main reason for greater forecasting skill. Many relatively small improvements have all played their part. From the point of view of meteorology as an applied science, it is most encouraging that the consistent inclusion of better physics and mathematics is leading to better forecasts. Although, because of the basically unpredictable nature of some atmospheric processes, there clearly are limits to what will eventually be attainable in forecast skill and forecast range, we are a long way yet from reaching those limits. For these reasons, continued improvements in the three areas mentioned above will form a significant part of the R and D effort of the Office over the next ten years.

Very short-range forecasting. The highest priority in forecasting R and D is being given to the very short range — the first 12 hours — partially because the demand for detailed information, high accuracy and precise timing in the short term is apparent from many of our customers, not least from Defence, and partially also because research on medium-range forecasting techniques is being carried out elsewhere, notably at the ECMWF (see section 3.2).

The improvement of forecasting in this very short range is being attacked from two sides — through the provision of better observations which has already been addressed in section 4.1, and through the development of a mesoscale model which has a much higher horizontal resolution (about 15 km instead of 75 km for what is called the fine-mesh model). The mesoscale model is currently quasi-operational and is already proving of value. It is, however, still at an early stage of development and its full potential will not be realized for perhaps 5 years. During the development period, not only will it be necessary to put a lot of effort into understanding the behaviour of the model but also it will be necessary to learn the optimum way in which the variety of relevant observations can be assimilated into it.

Extended-range forecasting. Some R and D will also continue into forecasting for the extended range (10 days up to about 1 month) beyond the limit at which deterministic forecasting is possible, but still at a range where there is good hope that general circulation models have some predictive capability regarding the general character of weather patterns. Should significant predictability be possible at this range, demand for extended range forecasts would be high. Research in this area is also closely connected with the Office's investigations into climate and the causes of climate change (see section 6).

Man–computer interaction. An area currently receiving a lot of attention and which will see substantial changes over the next decade, is that of the man–computer interaction involved in forecasting. The practice of forecasting provides excellent examples of many of the techniques in information technology which are currently receiving a large amount of emphasis. A number of the activities connected with model input or output currently carried out by human operators will be taken over by appropriate computer routines, leaving the forecaster free to exploit his expertise and experience more fully in other ways. Careful consideration will be given to the computer aids which can be provided to enable the best use to be made of the skill and experience of the human forecaster both in coming up with the best possible forecast and interpreting that forecast in terms of the needs of the wide variety of users.

5. Meteorological Office services

In this section I review likely developments in the four main areas of Meteorological Office services, namely; defence, civil aviation, the free public service and repayment services.

5.1 *Defence services*

The Meteorological Office serves the RAF, the Army Air Corps and other Defence establishments through its forecasting offices at airfields and other locations. These offices are staffed by civilian personnel who, by taking a full part in operational activities and exercises, demonstrate their capability to provide a fully effective service under peacetime conditions, periods of tension and of transition to war. An important reason for the Meteorological Office remaining as an integral part of the Ministry of Defence is the effectiveness of these arrangements which are advantageous both to the Armed Services (in that they provide forecasting personnel of high competence and with wide experience) and to the Meteorological Office (in that they provide a wide remit and excellent training).

Defence outstations urgently require better access to the range of forecasting products, data and aids now available at Bracknell. As was mentioned in section 4.2, this is planned; Defence outstations will be the first to be supplied with display units of WIS. A lot of the emphasis at Defence outstations is on low-level local, short-range forecasting, the improvement of which is the aim of many of the developments mentioned in section 4.

The requirement for meteorological services laid down by the Air Staff clearly includes the requirement for a forecasting presence at operational RAF stations and for face-to-face briefing. With the increased sophistication of aircraft and weapon systems the requirement for the local on-the-spot expert is likely to be strengthened. However, in addition to the deployment of WIS into RAF stations there is an urgent need for better ways of disseminating data between the various locations within an airfield, especially at sites where there is hardened accommodation.

Army ground operations are becoming even more weather sensitive and senior Army personnel are increasingly realizing the tactical value of accurate and timely weather information over and above that already required for the Army Air Corps. A statement of the Army's requirements is currently being prepared which will form the basis of the Office providing a modest but effective service.

The Office will continue to work closely with the Royal Navy. Plans are under way to connect their establishments more effectively to the Office's data and products through the use of WIS. The Office is also co-operating with the Royal Navy in ocean-modelling research. Modelling the ocean has much in common with modelling the atmosphere, although the computing demands for ocean modelling tend to be greater (a smaller grid length is required to cover comparable dynamical systems in the ocean which are of smaller scale than those in the atmosphere). Through the enhanced ocean-modelling capability which is being developed for the climate research programme, the Office is beginning to assist in developing models appropriate to the interest of the Royal Navy. Because of the close link between the atmosphere and the ocean (atmospheric forcing drives the ocean circulation) it is appropriate that the research on coupled ocean–atmosphere forecast models be carried out on the Meteorological Office computer.

Further, in the Defence Services area, the Office will continue to become involved in providing support and advice to a variety of organizations and projects, for example to NATO, Civil Defence and USAF establishments in the United Kingdom.

5.2 *Services for civil aviation*

During the last few years, substantial changes have taken place within the organization of world-wide meteorological services for civil aviation. These are now centred on the new World Area Forecast System (WAFS), for which Bracknell is one of the two world centres (see section 3.1), and the arrangements are beginning to work well. The improved upper-wind information now available to airlines by direct link from the Bracknell computer is proving very valuable indeed to airlines — savings of the order of 1 to 2% of the total airline fuel bill (i.e. £60 million out of £4000 million for the airlines employing Bracknell data) have been quoted to us as resulting from the use of Bracknell information for route planning, rather than information available from other sources*. During the next 5–10 years, more comprehensive flight and route planning will be introduced by world airlines with an accompanying requirement for higher accuracy in upper-air wind forecasts and more reliable predictions about weather situations likely to affect landing schedules at airfields. Research and development directed towards these requirements will continue, as will research relevant to other

* In 1986 a team from the Meteorological Office were awarded the Royal Society Esso Energy Award for their work for aviation forecasting, see *Meteorol Mag*, **116**, 1987, 29–31.

particular aviation problems such as icing and fog formation. The Meteorological Office will be looking at ways of improving the means of communication of this information to airlines as well as ways of improving the forecasts.

During the next few years substantial changes will occur in the way forecast information is disseminated at airfields, especially the smaller airfields where the introduction of automation will improve the service considerably. Streamlining of the service to general aviation will occur as more automated means of communication with pilots are introduced by the Civil Aviation Authority.

5.3 *The free public service*

A basic dilemma is the requirement on the one hand to provide the best possible service to the general public through the media and other information channels, and on the other hand to meet a significant part of the Office's costs through selling services on repayment. The better the Office does the former, the harder it is to do the latter. A balance therefore has to be drawn. The RCR suggested how the 'free' service might be defined, a definition subsequently modified after discussion by Ministers. Because of the continuously changing nature of the content and quality of the Office's products and of the requirements of customers, a continual appraisal of this balance needs to be made. Being aware of what services are possible, the Office needs to be sensitive to the needs and desires of the public at large while also having an eye for commercial areas where substantial returns to the Office (and therefore to the taxpayer) might be achieved.

Apart from special requirements in emergency situations, the policy is to continue to restrict the provision of individual forecasts but to concentrate efforts on the dissemination of forecast information through the press, radio, television, videotext, recorded telephone services and the like. For these outlets there is a varying degree of recovery of the cost of communication or presentation.

Some of these services are provided centrally, some regionally. Concentrations of the provision of the regional services is now in the Weather Centres and the Main Meteorological Offices (MMOs); virtually no public services are now provided from RAF airfields and Defence outstations except in emergency.

During the past few years a review of the work of the Weather Centres in different areas has been carried out and some rationalization had been carried through or is planned. Work in south-west Scotland has recently been reorganized and concentrated in one Weather Centre in Glasgow. A similar operation has been carried out for the Manchester area and plans for south-west, central southern and south-east England are currently being formulated. Relocation and reorganization of the Aberdeen and Birmingham Offices are also being looked into. The development of the Weather Centres is discussed further in section 5.4 covering repayment services.

Although, as I have said, the situation needs to be kept continually under review, I do not expect the scale of material provided for the free public service or the extent of services for which a subsidy is provided to change significantly during the next few years. However, the efficiency of dissemination of forecast information will expand considerably to the benefit of both the 'free service' and repayment services.

5.4 *Other repayment services*

A priority of the Office in recent years has been the expansion of its repayment services — a priority which was endorsed by the RCR. A marketing branch has been set up and over the last 2 years receipts from customers outside civil aviation have increased by over £1 million. The possibilities for further expansion are good.

A fundamental question which needs to be raised is whether it is appropriate for the Office to engage in these repayment services. Why not, as in the USA, pass the information over to the private sector and allow them free rein? There are various arguments why the present mixed arrangement is sensible and effective.

(a) There is a significant return to the taxpayer.

(b) The value of the integrated service — the quality of the product is improved by having those responsible for the products also engaged in selling them to customers. Forecasters and advisers are kept more in touch with the customer.

(c) Weather Centres established in major centres to service the general public and civil aviation can utilize their staff for part of the time for repayment services, many of them essential to the well-being of commerce and industry, thereby making better use of their time and resources.

(d) The quality of the service can be maintained — the private sector has a quality product by which to judge its service.

(e) The private sector (even in the USA) is unable or unwilling to invest in the infrastructure required to maintain a quality service over the whole range.

Given that the market for repayment services can be expanded, how should that expansion be pursued. There are three possible options: to sell relevant data to companies in the private sector, to set up joint commercial arrangements with appropriate companies or to expand the Office's commercial activities to meet the demand.

Selling relevant data. The opportunities for selling data as such are very limited largely because much of the data is available elsewhere. The WMO's Global Telecommunication System network, on which flows a large proportion of meteorological data and products, is becoming increasingly accessible at no charge or very small charge to private companies primarily through access points in the USA where a policy of free access to all data exists.

Joint commercial arrangements. The setting up of joint commercial arrangements fits the Office's position very well and was strongly recommended both by the RCR and by the Sharp/Hansford* report. A number of arrangements can be envisaged in which the Office co-operates with firms having particular commercial expertise or skill, in marketing or in information technology. Combining skills and 'know-how' in this way under arrangements where both parties have a stable and long-term commitment, should enable much greater returns to be forthcoming and should ensure that the returns are shared out in an equitable way.

Expansion of commercial activities. The final option is that the Office should expand its commercial infrastructure so that it can provide for itself outlets for its products. Although there are clearly opportunities here it is neither desirable or politically acceptable for there to be large growth in the Office in the area of commercial infrastructure. The Office needs to strike the right balance and pursue selectively those areas of commercial activity which fit in well with its other activities and responsibilities.

An important area of activity which is ripe for exploitation is that of cable and direct broadcast television and viewdata services. Here facilities need to be set up not just for providing data and products but to provide packaged forecasts via text or through live presenters in forms which are attractive to the variety of needs of the companies involved.

So far in this section I have addressed new possibilities for commercial activity. Significant room also exists for the development of existing repayment services especially through the Weather Centres. As a first means of improving their efficiency, up-to-date technology is required, a need which has already

* Sharp, K.J. and Hansford, J.; The Meteorological Office financial management, 1985, London, HMSO.

been mentioned in sections 4.2 and 5.1. The Public Services Branch and the Marketing Branch are also looking carefully at activities in the Weather Centres with a view to increasing their effectiveness, for instance more attention is being given to those areas where our specialized and expert services can provide the greatest financial return. It is planned to increase the commercial awareness of the Weather Centres and their marketing skill by providing them with financial targets which will make them more cost conscious. Similar considerations apply to the future of the Meteorological Office Advisory Services, both as part of the free public service and as a component of the repayment services.

6. Research and development

One of the listed functions of the Meteorological Office is to carry out research in meteorology and geophysics. Without any qualification, this is an enormous remit and could absorb any amount of resource. In the USA, for instance, nearly $400 million per annum is spent on research in meteorology and atmospheric physics. On the civil side, $70 million is spent through NOAA, $60 million through the National Aeronautics and Space Administration (NASA), and $110 million through the National Science Foundation (NSF). Equivalent figures in this country are £8 million by the Meteorological Office, £3.5 million by the Natural Environment Research Council (NERC) and about £2 million by the Science and Engineering Research Council (SERC). It should be pointed out that care should be taken in interpreting these figures; some (such as the figure quoted for the Meteorological Office) include a substantial amount of development — others refer almost entirely to fundamental research. Nevertheless, the figures clearly show the degree to which there are overwhelmingly more resources available for research in the USA.

What, therefore, is the Meteorological Office's role in research and how does it fit in with the rest of the national and international scene? What should be the size of the research programme and what are its priorities for the next ten years?

6.1 *Research programme*

The reasons for the Meteorological Office's research programme are:

(a) to provide support for, and the basis for improvement of, the operational services provided by the Office, and

(b) to provide a basis for continuing expertise in the areas of the field where the Office is required to provide expert advice.

About three quarters of the total Research and Development effort and resources are directed towards improvements in forecasting and operational services. They have, however, already been discussed in section 4. Therefore I turn to those areas where the Office needs to maintain special expertise. Climate is the most important of these. Expertise is required on the climate of the past, especially the most recent (i.e. the last 100 years or so during which a reasonable coverage of accurate observations has been available), and on the future trends in climate from a month or two ahead to tens or perhaps hundreds of years ahead. Of particular interest and importance are the possible effects of man's activities on climate. The tools for this climate research are firstly the large climate data base which the Office maintains for a variety of reasons and secondly global numerical models of the atmosphere and ocean circulation.

Because knowledge of the state of the ocean is probably as important as knowledge of the atmosphere for climate beyond a few months ahead, a high priority over the next decade will be the development of ocean models coupled to the atmospheric models. The topic of ocean modelling is in its infancy and is likely to develop rapidly. The Office has taken the initiative in setting up a small ocean modelling unit, which NERC is also supporting, in the Hooke Institute for Atmospheric Research at Oxford. Although only small in size it is amongst the foremost groups in the subject in the world at the present time.

Another significant area where advice is required from the Office is in atmospheric chemistry, especially as related to pollution (e.g. acid rain) — an area which demands expertise not only in atmospheric chemistry but in atmospheric physics and dynamics (including that related to the boundary layer). Although the Office's contribution here cannot be large, enough work has to be carried out within the Office to maintain adequate expertise. Because of the integrated nature of the Office's programme and the wide range of data, knowledge and experience possessed by the Office, the maintenance of a small team working in a topic such as atmospheric chemistry is mutually beneficial so far as the rest of the Office is concerned and can be carried out very cost-effectively.

A major facility available to the Office is the Meteorological Research Flight Hercules aircraft. It contributes to many of the areas we have already mentioned, in particular to the development of adequate parametrizations of physical processes (e.g. the boundary layer, cloud–radiation interaction, turbulence, etc.) for mesoscale dynamics and cloud physics investigations, and to atmospheric chemistry and pollution research. The potential of the array of instruments now fitted to the aircraft, together with the sophisticated data recovery system recently installed, is considerable and a decade of exploitation can be looked forward to. During this period, to ensure the best use of the facility, the generation of well-focused projects carried out jointly with other laboratories in the United Kingdom and overseas will be important. Because the Hercules is so well instrumented — possibly better than any other meteorological research aircraft in the world — there is no difficulty in developing co-operation, but this co-operation clearly has to be of the right kind. Collaboration by university scientists in the aircraft projects and in the analyses of data will be particularly welcomed.

A central theme underlying much of the Office's research programme is that of the development of numerical models which are required on a wide variety of scales ranging from a particular part of the boundary layer, perhaps a few kilometres across, to global circulation models covering the whole extent of the atmosphere. Despite the large range and the varied purposes for which models are developed, all employ the same basic physics and fluid mechanics, and a great deal of commonality exists between them. This is an illustration of an important feature of the Office's research programme — namely its integrated nature. Work in almost any part of the programme has influence on a number of other programme areas. In any review of the programme, therefore, it must be seen as a whole. In this regard the Research Sub-Committee of the Meteorological Committee performs a valuable function.

6.2 *Co-operation*

The main part of the Office's research programme is of necessity rather well defined and directed. It is therefore of importance that there is a lively research community outside the Office, especially in the universities with whom the Office can interact. Those of us working in the subject also feel that meteorology and geophysics are excellent academic disciplines possessing a great deal of intellectual challenge, demanding a lot of technical ingenuity and having the advantage of being thoroughly anchored in the real world. I am keen, therefore, to see the Office use its influence to encourage the development of viable, effective research teams in the universities. I shall be working along with the NERC and the University Grants Committee (UGC) to this end. A particularly useful means of co-operation between the Office and universities are the CASE (Co-operative Award in Science and Engineering) studentships. These can be valuable in any subject — perhaps the most valuable is in areas of rather fundamental science where joint supervision by an academic scientist and an Office expert can be especially rewarding to all the parties involved. It is important for the Office, by such means or otherwise, to keep abreast of fundamental developments and important also that a few of the Office's scientists should achieve individual merit status when they can spend some of their time pursuing fundamental problems and ideas.

As an example of joint activity with a university, the arrangements at the Hooke Institute at Oxford which have already been mentioned are worth describing in more detail. Within the Meteorological Office Unit at the Institute there are research groups in satellite meteorology, ocean modelling and stratospheric dynamics — each of which is tied very closely to the work in its parent Meteorological Office Branch. Although their work is formally under Meteorological Office management, their broad programme of work is also agreed with the other members of the Institute (i.e. the University and NERC) through the Institute Steering Committee, the intention being that there should be very close collaboration between those working within the Institute to whatever parent body they belong. By this means it is hoped to avoid the problems which have been associated with NOAA — University Joint Research Institutes in the USA where the work of the Institutes has tended to become almost entirely divorced from the operational work of NOAA, to their and NOAA's detriment. The Hooke Institute has got off to a good start; clear benefit is accruing to the Office in that students and others within the Institute are becoming involved in Meteorological Office programmes. The Institute is already recognized as one of the world's leading centres in meteorological and oceanographic research.

Co-operation in research internationally is vital if the Office is to remain in a leading position. It is also necessary because many problems are too large to be solved by a single nation alone. Of the current international research programmes relevant to the Office, the most important is the World Climate Research Programme (WCRP) in which members of the Office are thoroughly involved.

6.3 *Size of the research programme*

The final question to ask regarding the Office's R and D programme is whether it is of the right size. In terms of resources compared with similar programmes in the USA it appears to be very poorly supported indeed. On the other hand, compared with the total budget of the Office, the proportion of resources devoted to R and D (about 12% — compared with 16% for the USA) is not so grossly out of line.

The Office's R and D programme must continue to be highly selective regarding those areas which it tackles and must be consistent with the requirements I have outlined. Within these areas the teams must be viable in order to be effective. Savings in staff and resources in recent years — the research budget has fallen from about 16% in 1979 to just under 12% at present during a period when activity in the subject elsewhere has increased dramatically — have resulted in some activities being marginally viable. The decline in resources for R and D has now been halted. I believe, in order for the standard to be maintained and to pre-empt a drift of research scientists abroad, over the next five years it should be allowed to revert back to the 1979 figure.

7. Resources

7.1 *Cost benefit*

Before looking at resources, it is appropriate to consider the question of cost-benefit. Questions are often asked regarding the cost-benefit of the services provided by the Meteorological Office. For the Office's work related to Defence it is difficult to be quantitative; it might be noted however that military activity is, and is likely to remain, highly weather sensitive — as are many of the weapons systems employed by all the Services. A comparison between the annual cost of the Meteorological Office services to Defence with the possible losses due to ignorance of weather elements — for instance it is only slightly more than the value of one Tornado aircraft — shows that it is potentially a very cost-effective service. Regarding other areas of the economy served by the Office, again it is not easy to be precise. A study of the value of meteorological services was carried out by Mason (1966)*. Crude but plausible estimates were made of benefit in different areas of activity. His conclusion that the overall cost-benefit ratio lies between about 10 and 20 is probably conservative; to my knowledge it has not been seriously disputed. The benefit, although real, is in many areas spread so broadly that only a small proportion of it is realizable in terms of revenue.

7.2 *Resources required*

I now turn to consider what resources will be required in the light of the priorities I have stated, i.e. that the Meteorological Office should maintain its leading position, improve and expand its services, and increase its commercial activity and return.

Personnel. The Meteorological Office complement fell from about 3650 in 1974 to 3200 in 1979 and was further reduced to 2700 in 1984 — a drop of 26% during the ten-year period. The introduction of automation in communications and data handling, together with contracting out, has made most of this reduction possible during a period when the range and quantity of services provided by the Office has shown a substantial increase as has its income from repayment services. A further 7% reduction to about 2400 net of loans and secondments is planned by 1988.

By 1988 most of the savings possible from the current programme of automation and from the contracting out of services will have been made. Some small growth in the numbers of personnel involved in the repayment services will be necessary during the next few years if the potential growth in that area is to be realized. There should, therefore, be a levelling off in the complement at about the 1988 figure — small savings due to further automation being fed into increased customer activity.

A trend in the personnel structure which will continue is that the proportion of senior staff will increase. Increases in efficiency due to automation or otherwise, or savings of staff due to contracting out of services, imply the loss of junior not senior staff. A leaner more professional and cost-effective complement of staff eventually means more staff at senior grades relative to junior ones.

There is currently a significant secondment of Meteorological Office staff to industry — numbers should increase if appropriate contractual arrangements for joint activities with commercial concerns are introduced (see section 5.4). I believe a great deal more exchange between the Office, universities and industry would be healthy and beneficial. Such statements have frequently been made about the Civil Service as a whole but implementation has so far been disappointing due, I believe, to over rigid but long-standing Parliamentary rules surrounding Civil Service appointments and unrealistic Treasury attitudes to allowances and secondary remuneration. The status and effectiveness of Government service, and of the other sectors involved, could be improved enormously if such exchange were commonplace.

A continuing important activity concerning personnel is that of training. Already, through the College at Shinfield Park, Reading and otherwise, the Office is very involved with training. I anticipate that during the next decade there will be increasing emphasis here, including more frequent scientific and technical 'updating' courses for forecasters and a broader range of training, e.g. in marketing skills.

Accommodation. The central accommodation occupied by the Meteorological Office, the London Road building at Bracknell will continue to serve as the Office's headquarters site because of the large investment already made in specialized operational facilities. Increased automation is expected to lead to further centralization on Bracknell and some transfer of staff from shift-working operation tasks to

* Mason, B.J.; The role of meteorology in the national economy, *Weather*, 21, 1966, 382–393.

day work. The London Road building is already overcrowded and conference room facilities are below standard. Additional accommodation is urgently needed at or very near to the London Road site. An assessment of the long-term requirements is being carried out jointly with Property Services Agency (PSA). This is likely to lead to proposals to reduce the number of sites in the Bracknell area used for supporting activities, although at the cost of re-building some specialized facilities, e.g. the technical archives.

The other main site where development is likely to occur is at Shinield Park where the Meteorological Office College and the ECMWF are accommodated. At that site, those parts of the domestic facilities and residential accommodation currently provided by temporary buildings are in urgent need of replacement.

Resources as a whole. It is interesting to note that despite the increased commitments of the Office and the improved forecasting products, the gross Meteorological Budget has not changed much in real terms in recent years. Since 1979, during a period when the MOD budget as a whole has risen by nearly 20%, apart from the cost of Meteosat (the development and early operations of Meteosat were paid for by the Department of Trade and Industry and the Meteorological Office assumed responsibility for new satellites and their continued operation in 1983) the gross cost of the Office has fallen by about 4% in real terms, the charges to CAA have fallen by 2% in real terms and the income from repayment services (other than CAA) has risen by 100% in real terms.

During this period of a reduction in resources, the Office has concentrated on ensuring that adequate resources have been available to maintain its central forecasting capability at a high level. Very little resource has, however, gone into improving the technical capability of the outstations; there is, therefore, considerable catching up to be done so far as the outstations are concerned (see section 4).

Concerning provision for equipment and facilities, priority must be given during the decade to:

(a) ensure that meteorological personnel serving Defence, aviation, the public service and repayment customers have efficient access to, and the ability to manipulate and utilize easily, the data and products that are available from the central facility, so that their time and expertise is most effectively employed,

(b) ensure that adequate computing resources continue to be available within the central facility, and

(c) ensure that improvement in observational capability continues and that the United Kingdom continues to play its proper role in meteorological observation especially in satellite-based observations.

During the next ten years a progressive increase in the receipts from repayment services (other than from other government departments) is planned. Current receipts amount to about £5 million per annum. A target increase of 10% per annum has been set which would lead to receipts of £12 million per annum by 1995. During the first few years the increased revenue from repayment services will be required to provide resources for the developments I have listed above. The net cost of the Office in real terms would remain roughly constant, therefore, over the first few years but would fall by the end of the period by about 5%. At that time approximately half of the increased revenue from repayment services would go towards increased facilities and equipment for the Office, the other half into reducing the Office's net cost. That there should be a sharing of increased revenue of this kind was, in fact, suggested by the RCR.

Finally, I turn to the methods for allocation and control of resources. I consider it a high priority to achieve a more rational arrangement for the allocation of resources from MOD to the Office. Although I have responsibility for the formulation and execution of the Meteorological Office programme, I do not have any formal responsibility for resources. It is generally agreed that the Meteorological Office should have responsibility for resources delegated to it; strong recommendations to this effect have been made by both the RCR and the Sharp-Hansford report. The next few years will see substantial progress in this direction.

8. Concluding remarks

I believe that the next ten years will be both exciting and rewarding for the Meteorological Office as developments in both science and technology enable us to improve the quality, the effectiveness and the range of the services we are able to offer to our varied customers.

551.513.2:551.509.334

Persistent anomalous circulation and blocking*

G.J. Shutts
Meteorological Office, Bracknell

Summary

The most extreme weather conditions over the United Kingdom often arise when the normal progression of Atlantic weather systems is halted by blocking patterns characterized by the splitting of the jet stream into two branches; one passing to the north of the country and the other passing to the south. In summer these may give persistent spells of fine weather (e.g. 1976) or in winter are usually accompanied by severe cold (e.g. February 1986). The predictability of the atmosphere on the monthly time-scale is likely to be strongly dependent on those physical mechanisms responsible for the maintenance and stability of blocking patterns. For this reason, substantial effort has been invested recently in the study of blocking dynamics, with the proposal of several new theories. In this paper some of these new developments are examined.

1. Introduction

The study of blocking underwent a resurgence of interest in the late 1970s with the appearance of some new(?) theoretical ideas and with the greater availability of high quality global data sets. Since then many of the properties of blocking known to forecasters have found expression in highly simplified models of the atmosphere and are better quantified in terms of new diagnostics. Nevertheless it is probably also true to say that our ability to forecast blocking in the extended range sense (e.g. 7 days–1 month) has not benefitted noticeably from these studies.

There are two particular types of anomalous circulation that need emphasizing. The first and most important type is the familiar regional blocking for which the anomalous circulation is predominantly confined to a certain longitude sector and occurs in geographically preferred regions. It typically has a time-scale of the order of 2 weeks and tends to be most frequent at certain times of the year (e.g. western Europe in spring). The second type is what can be referred to as the 'severe winter' pattern. It is epitomized by the northern hemispheric circulation patterns of winters such as 1947 and 1962/63 when the axes of the major jet streams were much further south than normal and low wave number planetary waves were of very large amplitude. These anomaly patterns are even more persistent than blocking and, as in the 1962/63 winter, last longer than 2 months.

The main characteristics of blocking patterns are sketched briefly in section 2 and the concept of potential vorticity is introduced. Steady-state solutions of certain approximated equations of motion are discussed in section 3 in order to clarify how an isolated block dipole can remain stationary when

* Lecture note from a series of lectures entitled 'Dynamical Processes in Meteorology' given as part of the 1986 Advanced Lectures (Meteorological Office, 15 September–3 October 1986).

embedded in westerly flow. In section 4, the old idea that blocking is some sort of resonance phenomenon is examined with a beta-plane model of barotropic flow. Green (1977) drew attention to the possible role of momentum transfer induced by travelling weather systems in the maintenance of blocking anticyclones against surface friction. This transient eddy theory has developed and gained much acceptance since then and is outlined in section 5. Finally in section 6, a hemispheric scale circulation anomaly pattern, which sometimes accompanies blocking, is identified and is defined as the 'severe winter' pattern. In such winters, the surface wind is anomalously easterly throughout much of the mid-latitude belt.

2. The blocked flow type

Blocking 'highs' are characterized by a region of warm air with higher than ambient pressure which extends upwards from the surface to the lower stratosphere. Within them the winds are generally light and the tropopause is higher than average. They are usually accompanied by a somewhat smaller region of low pressure with the opposite properties. This combined 'dipole' is embedded in a diffluent flow field and tends to fluctuate in amplitude and phase (longitude) with the passage of travelling weather systems (Fig. 1). There is often a tendency for high pressure cells to collapse only to rebuild further to the west causing an overall westward translation of the pattern.

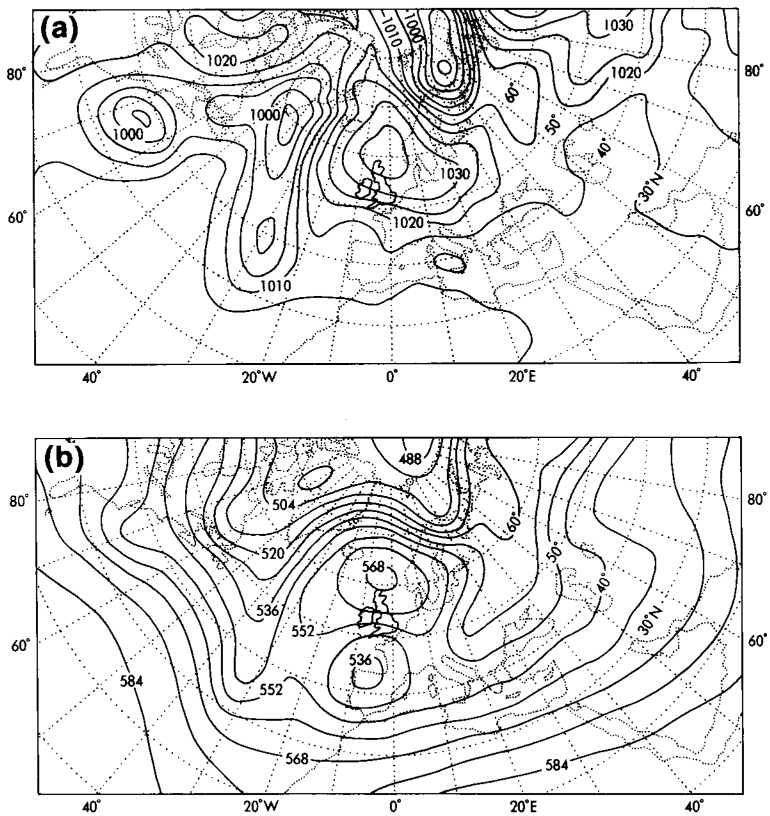

Figure 1. Surface pressure (mb) field (a) and geopotential height contours (dam) of the 500 mb surface (b) for 12 GMT on 15 February 1983.

Much of our theoretical understanding of large scale atmospheric dynamics is derived from approximate forms of the equations of motion which involve the conservation of some quantity following the motion of an air parcel, e.g. absolute vorticity conservation in barotropic flow. In three-dimensional stratified flows, the vorticity vector of an air parcel may be changed by a number of different mechanisms though, at large scales, principally by vortex stretching. Nevertheless, the scalar product of the vorticity and vector gradient of potential temperature (all divided by the density) is conserved without approximation for adiabatic frictionless flow. This quantity, known as the potential vorticity, provides a valuable link between simplified theoretical models involving analogues of this conservation principle and analyses of real atmospheric motion which may be carried out using the unapproximated quantity. For instance, many phenomena described by the two-dimensional, barotropic equations with latitudinal variation of the Coriolis parameter can be related to real upper tropospheric flow dynamics by interpreting absolute vorticity as potential vorticity, though only when the latter is computed on isentropic surfaces (Hoskins *et al.* 1985). Since potential temperature and potential vorticity are conserved for adiabatic, frictionless flow, the evolution of the field of potential vorticity on an isentropic surface gives a visual indication of air-mass transport; in other words it is a tracer and provides a valuable means of studying the interaction of 'blocking pattern' flows with transient weather systems.

A dynamically significant aspect of the blocked flow field is the reversed potential vorticity gradient (from the normal poleward gradient) as is clearly portrayed by isentropic analyses of Ertel potential vorticity (Shutts 1986). Potential vorticity within the blocking anticyclone is low relative to the ambient flow but high in the accompanying cut-off low further south (Fig. 2). As the following section demonstrates, this dipole arrangement enables the pattern to remain stationary in the presence of a background westerly flow.

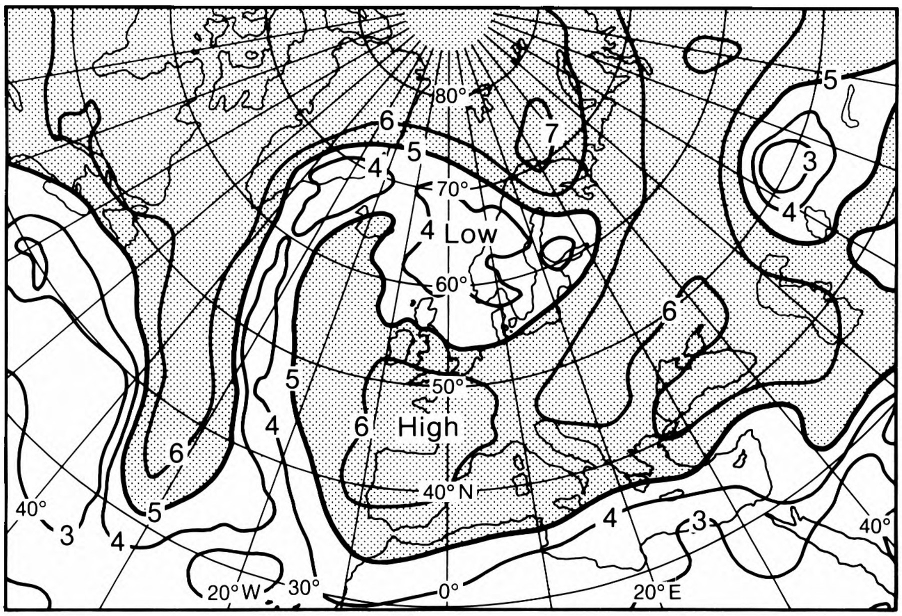

Figure 2. Contours of the Ertel potential vorticity (arbitrary units) calculated on the 320 K isentropic surface for 12 GMT on 15 February 1983. The contour interval is variable so as to enhance the detail in the potential vorticity field where gradients are small. The shaded regions are of high potential vorticity and represent stratospheric air.

3. Free-mode model

Studying sequences of synoptic charts frequently gives the impression that changes in weather type are often accompanied by an abrupt change in the configuration of the planetary-scale flow and a new quasi-equilibrium pattern set up. Such behaviour is characteristic of some idealized non-linear systems containing quasi-equilibrium or 'attractor' points. The free-mode approach to representing blocking flow patterns involves finding time-independent solutions to approximated forms of the equations of motion and examining their sensitivity to governing parameters.

Perhaps the simplest free-mode model with any relevance to blocking is the vortex doublet of classical hydrodynamics embedded in a uniform flow. For a purely barotropic, incompressible and two-dimensional fluid on an f-plane (the 'dishpan' case) fluid parcels conserve their vorticity. The vorticity associated with a point vortex at a position $\mathbf{r}_0$ in the (x, y) plane is zero everywhere except at $\mathbf{r}_0$ where it is effectively infinite. The tangential velocity associated with such a vortex is inversely proportional to the distance from the vortex core. Two point vortices of opposite sign (though equal circulation strength) self-induce a translational movement of the vortex pair in a direction at right angles to their dipole axis and with a speed inversely proportional to their separation. The doublet can be rendered stationary by adding to this solution a uniform opposing current (Fig. 3).

This solution is restricted to systems with no spatial variation in background rotation, i.e. no planetary beta effect. Stern (1975) showed how dipole solutions (named Modons) could be constructed for the beta-plane case and McWilliams (1980) used the equivalent barotropic equations to obtain a stationary Modon solution which serves as a model of blocking (Fig. 4). In contrast to the vortex dipole whose pressure is infinite at the vortex points, the Modon has a physically reasonable pressure distribution everywhere. Various extensions of these barotropic models to the baroclinic case have been made though, as yet, no primitive equation solutions have been found. Of course, real atmospheric blocking is never time-independent and these solutions should at best be regarded as a zero-order description (in the language of perturbation theory) of the phenomenon.

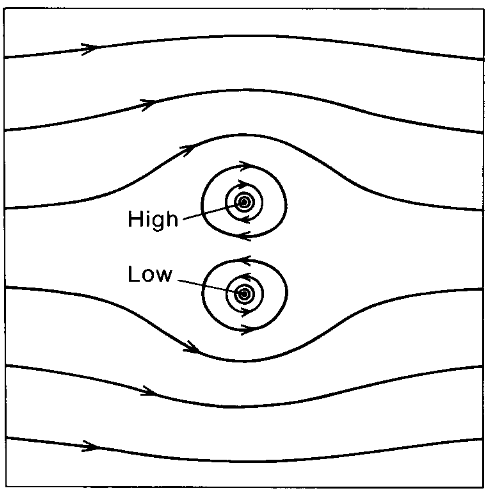

Figure 3. Streamlines of a stationary vortex doublet embedded in uniform flow.

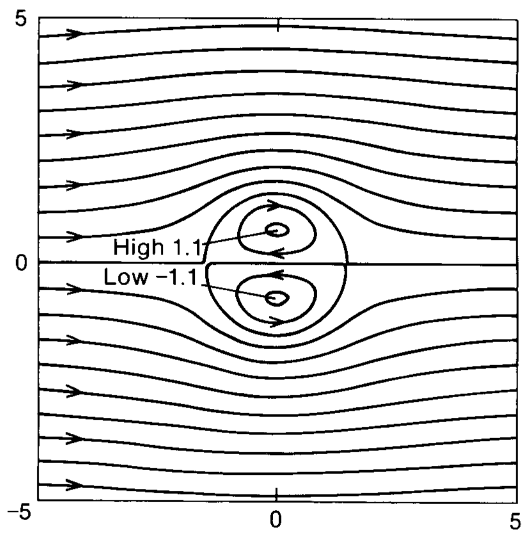

Figure 4. Streamlines of a stationary equivalent barotropic 'Modon' taken from McWilliams (1980).

4. Resonance theories

The idea that blocking may be a manifestation of some kind of internal resonance is old and difficult to trace back to the originator. As a simple example of the principle, consider the barotropic absolute vorticity equation

$$\frac{\mathrm{D}}{\mathrm{D}t}(\zeta + f) = F \qquad \ldots \ldots \ldots \ldots \ldots \ldots \ldots (1)$$

where ζ is the vorticity, f is the Coriolis parameter and F is some unspecified source of vorticity due, for instance, to vortex compression associated with flow over mountains. In terms of the non-divergent stream function ψ defined such that $u = -\partial\psi/\partial y$ and $v = \partial\psi/\partial x$, equation (1) becomes

$$\left(\frac{\partial}{\partial t} + \frac{\partial\psi}{\partial x}\frac{\partial}{\partial y} - \frac{\partial\psi}{\partial y}\frac{\partial}{\partial x}\right)\left(\frac{\partial^2\psi}{\partial x^2} + \frac{\partial^2\psi}{\partial y^2}\right) + \beta\frac{\partial\psi}{\partial x} = F \qquad \ldots \ldots \ldots (2)$$

where $\beta = \mathrm{d}f/\mathrm{d}y$ is assumed constant. Consider a purely sinusoidal forcing function F such that

$$F = F_0 \sin kx \cos \mu y$$

where k and μ are wave number vector components. Now look for stationary solutions for ψ involving a constant zonal flow component U such that

$$\psi = -Uy + A \cos kx \cos \mu y$$

and where A is constant. It can be shown that the non-linear terms (terms in A^2) cancel and that

$$A = \frac{F_0}{k[U(k^2 + \mu^2) - \beta]} \cdot \qquad \ldots \ldots \ldots \ldots \ldots \ldots (3)$$

From equation (3) it can be seen that waves satisfying Rossby's stationary wave formula

$$k^2 + \mu^2 = \beta/U$$

will be resonant in the sense that this inviscid theory predicts an infinite amplitude response.

Accepting the assumptions of this model, it is difficult to see why the atmosphere is not perpetually resonant since the Fourier spectrum of F will always contain some contribution near to the stationary wave number. The analysis is complicated in general by the non-uniform spatial variation of the background wind with height as well as horizontally. The existence of resonant modes then hinges crucially on whether or not Rossby wave energy can be dynamically 'contained' by, for instance, strong westerly winds in the stratosphere. Lateral containment is more difficult to realize since stationary Rossby waves have 'critical lines' (where $U = 0$) in the sub-tropics which tend to absorb wave energy.

When the flow is not precisely uniform, the non-linear terms do not cancel and a perturbation analysis is required to establish the relationship between A and U, given k and μ. It turns out that the equation to be solved for this non-linear case is analogous to that of the anharmonic oscillator (Trevisan and Buzzi 1980). The resonance curve (A against U) now folds over and no finite value of k gives an unbounded response (Fig. 5). Instead, for a range of values of U, high and low amplitude responses are possible. There is an interesting analogy here between the dynamics of the finite amplitude pendulum and these weakly non-linear flows when Uk is interpreted as an angular frequency of oscillation, i.e. $2\pi/$(oscillation period experienced by a parcel).

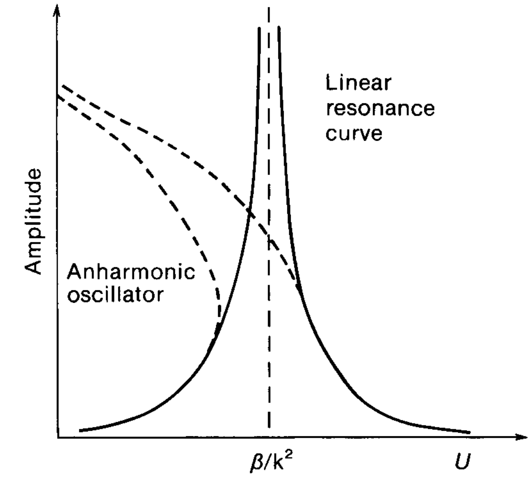

Figure 5. The steady state amplitude of a disturbance forced by barotropic flow over orography plotted against the uniform speed (U) of the current. The solid curve indicates the linear response when the orography is sinusoidal and the basic flow has uniform speed. The dashed curve is the modified response when certain non-linear terms are included.

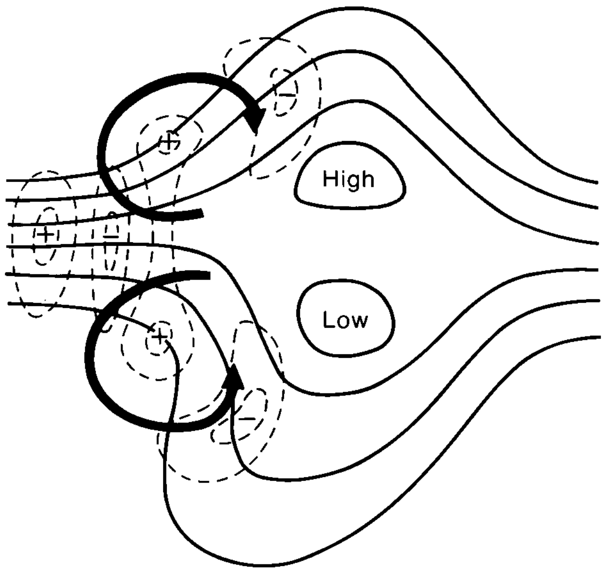

Figure 6. A schematic picture of the deformation of meridionally elongated eddies as they propagate into a split jet-stream region upstream of a blocking dipole. The associated sense of time-mean eddy vorticity forcing is indicated by the black arrows.

5. Transient eddy-forced models

The characteristic diffluence and jet-stream splitting associated with blocking causes transient baroclinic waves to become deformed immediately upstream of the block. The resulting anomalous local fluxes of vorticity and heat (Fig. 6) lead to a time-mean dipole vorticity source orientated so as to reinforce the block dipole pressure pattern (Shutts 1983). Although this conceptual model is incomplete in the sense that it only describes the nature of the time-averaged forcing function of, for instance, equation (2), it can be studied in the context of a time-dependent barotropic model. There is a growing consensus of opinion that the resonant forcing of local non-linear free-mode patterns by their interaction with transient eddies is the essential mechanism at work in blocking. The geographical distribution of blocking is then controlled by the long quasi-stationary wave pattern forced by orographic and land–sea thermal influences.

A particular problem with the conceptual eddy forcing model is that no clear distinction between eddy and block can be defined in practice. During the lifetime of a single blocking episode only two or three eddy 'events' may contribute to the forcing of the block. The definition of eddy as the deviation from a time–mean value is barely useful and is frustrated by the movement of the blocking pattern during the period. An alternative is to dispense with the block–eddy decomposition of the fields of motion and take a Lagrangian view, for which trajectories of air parcels are the main interest. On the time-scale of a few days, the adiabatic assumption is not grossly in error for upper tropospheric flow and isentropic analysis provides a useful tool for studying air movement. Two conserved quantities (for adiabatic, inviscid flow) are useful to plot on isentropic surfaces: Ertel potential vorticity and mixing ratio. By looking at sequences of potential vorticity maps plotted on a chosen isentropic surface, the injection of high or low potential vorticity air into the block by transient eddies can be seen. Ideally, the block would be characterized by an inner region where air is trapped as a pair of counter-rotating cells of high and low potential vorticity as in the Modon. The slow spin-down of this dipole by surface friction coupled with radiative cooling would be offset by the intermittent injection of 'fresh' high and low potential vorticity brought about by transient eddies. This can be seen to happen in the sequence shown in Fig. 7. For a full account and diagnostic analysis of this blocking episode see Shutts (1986).

6. The 'severe winter' pattern

In contrast to the usual concept of blocking, the 'severe winter' pattern is a hemispheric circulation anomaly with a strong zonally-averaged component. Fig. 8 shows the sea-level pressure and 500 mb height anomalies over the northern hemisphere for February 1947, and highlights the characteristic dominance of anomalous high pressure in latitudes north of 50° N with a ridge into the mid-west of the United States and with anomalously low pressure extending across the north Pacific and Atlantic. The implied geostrophic wind anomaly is easterly almost everywhere between 50° and 60° N, and Siberian air extends well into Europe. A brief perusal of monthly mean sea-level pressure anomaly charts, such as those stored in the Synoptic Climatology Branch of the Meteorological Office, shows that this hemispheric pattern tends to occur quite frequently, though it is not necessarily associated with severe winter conditions in the British Isles, due to minor local differences. Furthermore, empirical orthogonal analyses of real data and a 15-year general circulation model integration have both revealed that this pattern dominates the interannual variation at sea-level and 500 mb (Lau 1981).

Since this type of anomaly is hemispheric, fairly zonal and of long time-scale (1–2 months) it should be regarded as a change in the *modus operandi* of the general circulation rather than an anomalous Rossby wave pattern. As for normal circulation types, transient eddies probably play an important role in maintaining this type of anomalous flow. Changes in the distribution and intensity of the major atmospheric heat sources (Palmer and Owen 1986) could also play an important part in supporting an anomalous pattern such as this, though it would be difficult to distinguish cause and effect.

7. Concluding remarks

There is a growing consensus of opinion that blocking and circulation anomalies are primarily nearly free-mode flow structures excited by their interaction with travelling weather systems. Even so, their geographic location, seasonal dependence and interannual variability are probably controlled

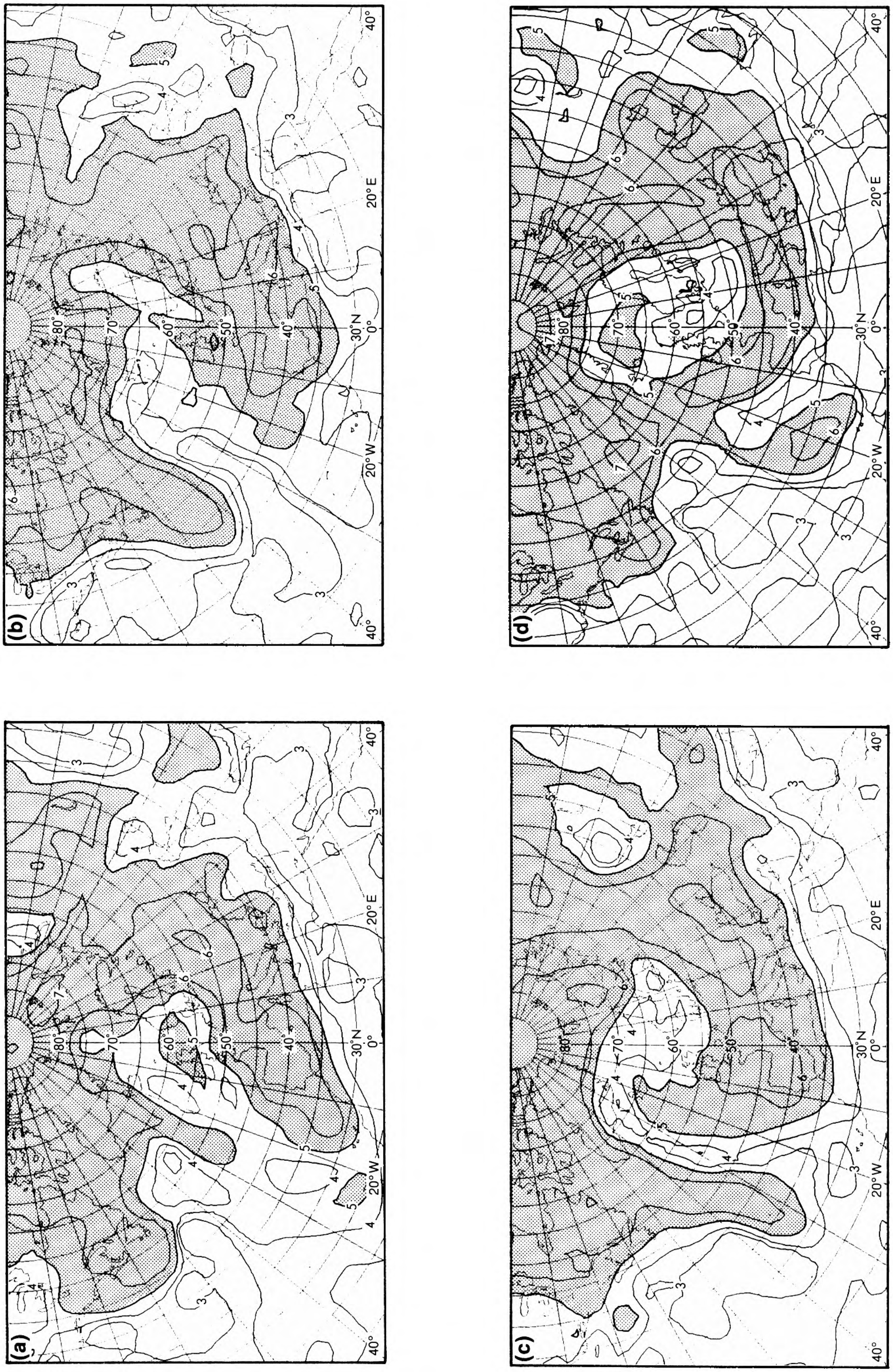

Figure 7. Ertel potential vorticity (arbitrary units) maps for 12 GMT on (a) 13 February, (b) 14 February, (c) 15 February and (d) 16 February 1983 for part of the northern hemisphere, plotted on the 320 K isentropic surface. The areas with values greater than 5 have been stippled.

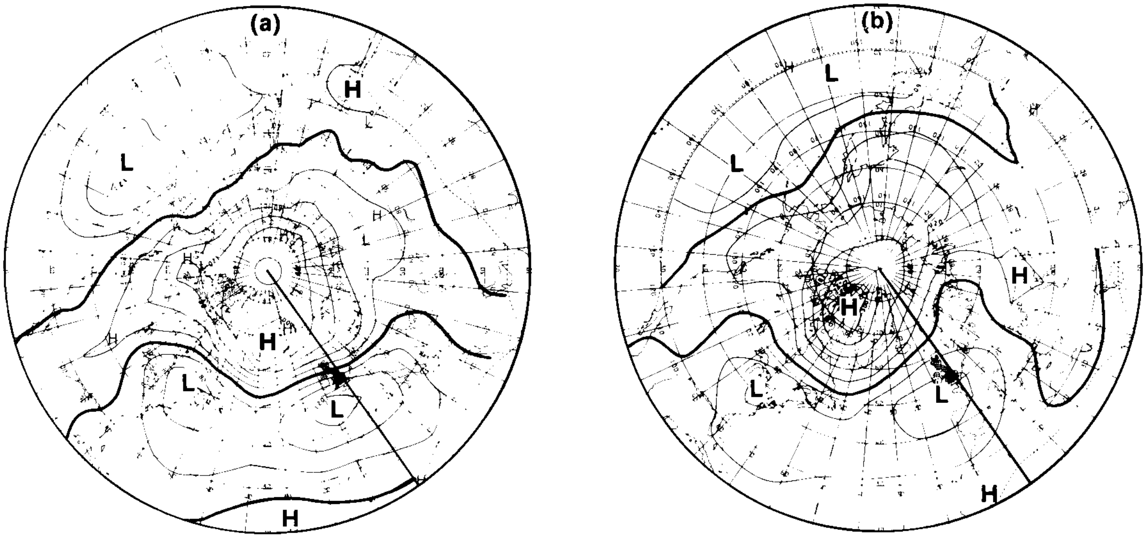

Figure 8. Anomalies of (a) surface pressure (tenths of mb) and (b) 500 mb geopotential height (m) for the northern hemisphere (north of 20° N) during February 1947. Isopleths are drawn at 4 mb and 60 m intervals respectively.

indirectly, through the planetary-scale circulation pattern, by the prevailing distribution of diabatic heat sources and sinks. These, in turn, may be determined to a large extent by the distribution of sea surface temperature, surface ice and snow, soil moisture,etc. Given the slow time-scale of change associated with the above surface properties, there is a hope that blocking episodes may be forecast a month or so ahead if a sufficiently strong causal link exists between heat sources and planetary scale circulation.

References

Green, J.S.A. 1977 The weather during July 1976: Some dynamical considerations of the drought. *Weather*, **32**, 120–126.

Hoskins, B.J., McIntyre, M.E. and Robertson, A.W. 1985 On the use and significance of isentropic potential vorticity maps. *Q J R Meteorol Soc*, **111**, 877–946.

Lau, N–C. 1981 A diagnostic study of recurrent meteorological anomalies appearing in a 15-year simulation with a GFDL general circulation model. *Mon Weather Rev*, **109**, 2287–2311.

McWilliams, J.C. 1980 An application of equivalent Modons to atmospheric blocking. *Dyn of Atmos and Ocean*, **5**, 43–46.

Palmer, T.N. and Owen, J.A. 1986 A possible relationship between some 'severe' winters in North America and enhanced convective activity over the tropical west Pacific. *Mon Weather Rev*, **114**, 648–651.

Shutts, G.J. 1983 The propagation of eddies in diffluent jetstreams: eddy vorticity forcing of 'blocking' flow fields. *Q J R Meteorol Soc*, **109**, 737–761.

1986 A case study of eddy forcing during an Atlantic blocking episode. *Adv in Geophys*, **29**, 135–162.

Stern, M.E. 1975 Minimal properties of planetary eddies. *J Mar Res*, **33**, 1–13.

Trevisan, A. and Buzzi, A. 1980 Stationary response of barotropic weakly non-linear Rossby waves to quasi-resonant orographic forcing. *J Atmos Sci*, **37**, 947–957.

551.509.0:92

A forecaster's life in the fifties

D.S. Gill
Meteorological Office, Bracknell

Summary

Some experiences of a junior forecaster at various outstations in the United Kingdom and Hong Kong during the period 1951–63.

I joined the Office in 1951 as a direct entrant Assistant Experimental Officer on the magnificent salary of £360 per annum. It wasn't bad pay in those days when lodgings, even in London, could be had for £2 per week including all meals at weekends. After a few weeks at Finningley, I went on one of the first forecasting courses to be held at the new Training School at Stanmore.

After surviving the great smog of 1951, I went back to Finningley as a trainee forecaster. Not for long though as I had 18 postings in my first 3 years. That first posting ruined the best short-term fog forecasting technique I ever developed. Finningley always fogged out 1½ hours after Lindholme. Where did I get posted to from Finningley? Yes, Lindholme!

I spent 3 years on the 'north-east circuit' of RAF stations: Finningley, Lindholme, Leconfield, Driffield, Full Sutton, Cranwell and Acklington to name but a few. Communications consisted solely of teleprinters in those days, no FAX and no satellite pictures. We did have a routine reconnaisance flight out into the Atlantic — code-named Bismuth — done by Shackleton aircraft of Coastal Command. If the teleprinter broke down there were two possible back-ups; if you were very lucky an RAF wireless operator could be found to take down the short wave Morse broadcast, otherwise it was a case of ringing round other offices and collecting bulletins by phone. I remember one assistant who could actually plot the observations on to the chart while they were being read over the phone, but he was an exceptionally fast plotter. All charts were hand plotted at every station and every forecaster had the pleasure of drawing up his own chart plotted in red and black ink on decent paper. The charts I remember most vividly were on a winter evening in early 1953. I was struggling to fit the isobars in the Scottish area of the chart when an off duty pilot came in to see 'how things were'. I had to admit I was out of my depth but felt something dreadful was going to happen. It was the night of the east coast floods which eventually led to the setting up of the storm-tide warning service.

Upper-air charts were drawn by hand and the 1000–500 mb thickness analysis was produced by 'back-gridding' from a 1000 mb and 500 mb chart on a light table. Forecasts were duplicated by the incredibly crude process of jellygraph. The forecast was written or typed with a special backing carbon. It was then placed on a tray of gelatine and the carbon image was absorbed by the gelatine. Blank forecast forms were then pressed on the gelatine face down and peeled off with a copy of the forecast on them.

In 1955 I was posted to Hong Kong. The RAF had an airfield there with an army co-operation squadron of Vampires. Being such an outpost we did not have any modern communications like teleprinters; just our own observation and anything we could persuade the local civil airfield (Kai Tak) to dictate over the telephone. It didn't matter all that much because the Vampires, even at take off, hadn't enough fuel to reach the nearest diversion anyway. Thus the main object was to make sure that no aircraft were airborne when local conditions deteriorated below landing limits. Sudden deteriorations were almost always due to showers and fortunately I had access to an ex-army radar known affectionately as 'Zippy' from its acronym MZPI (Microwave Zone Position Indicator?). Zippy was powerful enough to pick up the leading and trailing edges of showers out to a range of 40 miles. We gained quite a reputation with Kai Tak because of the ability to produce short-range forecasts of the onset and cessation of showers.

The main event of the day was the afternoon pilot-balloon ascent. In autumn, given clear skies, low-level westerlies and high-level easterlies we always tried for a minimum of 30 000 feet. With daily practice one soon became adept at working out the wind and coding up the PILOT at the same time as following the balloon, so the PILOT was ready for transmission as soon as the ascent was finished. As an extra handicap we used to try our hand out with a tail balloon (a large sheet of coloured paper hanging from the balloon by a measured length of thread). The angle subtended by the tail could be used to calculate the height of the balloon.

The meteorological unit also provided support for the Royal Artillery in Hong Kong; calibration shoots once a year and Meteors for practice shoots as required. Meteors were pilot-balloon ascents coded as mean winds over layers of the atmosphere, rather than at standard levels, through which artillery shells would pass during their flight. Calibration shoots required double theodolite ascents every 30 minutes; no chance of calculating the winds at the same time as the ascent, and after a days shooting it was well into the night before we had all the results available.

While on temporary duty at Kai Tak I had the privilege (?) of a forecasting duty which covered the passage of a typhoon directly over the airfield. There were winds to well over 100 knots (the anemometer broke under the strain so we never knew what the strongest gust was), then about 20 minutes of eerily calm conditions followed by howling winds which were now 180° different from the original direction. Meteorologically not an experience to be missed, but on almost any other grounds to be avoided if at all possible.

Forecasting typhoons was not easy in those days since there was no satellite information. As soon as a typhoon warning was issued, any of the few observing ships within hundreds of miles of the forecast track started steaming away at full speed. If a typhoon reached the Phillipines it created so much damage we lost communications at the critical time. The only accurate information came from a group of dedicated American airmen in a weather squadron based, I think, on Guam. They used to fly into the centre of a typhoon at least once a day to provide an accurate fix. By the time I was involved it was a high-level penetration with a dropsonde in the centre. Prior to dropsondes, I was told they had made low-level penetrations with an ascent in the centre; a very dangerous and at times fatal procedure, although they had the satisfaction of knowing that many lives were saved as a result of accurate information on the movement of typhoons.

Kai Tak duties involved a lot of route forecasts which meant drawing pictorial cross-sections and giving a personal briefing for each individual flight (no significant weather charts or spot winds in those days). We used to do half-route ROFORs (coded route forecasts rather similar to TAFORs but with changes specified by position rather than time) for each route, the destination airfields doing the other half. Making the two ROFORs match in the middle was sometimes more of an artistic problem than a meteorological one. Kai Tak in those days had much too dangerous an approach for night landings so a lot of aircraft used to land just before dusk, stay overnight then take off at dawn. On a night duty it took about six hours to draw the forecasts, so the duty forecaster used to take a last look at this charts around midnight and then drew steadily throughout the rest of the night to be ready for briefings starting around 0600 local time.

For most of my time in Hong Kong the charts looked rather bare because they had no Chinese observations plotted on them. This was a political problem because China was still officially represented in the United Nations (and therefore WMO) by Taiwan. Officially, therefore, the two observations from Taiwan were the Chinese observations. It meant nearly half the chart was blank until my last few months there.

After three years it was back to the United Kingdom and civil aviation, Preston first then Liverpool. As an Experimental Officer pay was rising to the dizzy heights of around £600 per year. On the early morning shift at Preston Air Traffic Control Centre it was certainly earned. In at 0600 local time, draw up the 700, 500, 300, 200 and 100 mb charts, convert the senior forecaster's surface chart to a 1000 mb chart, grid a 1000–500 mb thickness, produce 12-hour forecast thickness, 500, 700 and 300 mb charts and write out the forecast winds for the Preston Flight Information Region all before 0700. Then there was time for a cup of tea.

Liverpool was less hectic, except on Saturdays in summer (package holidays had started) and at any time when Manchester was closed by fog and Liverpool wasn't. Then we had the little game of guessing where the next aircrew to walk in through the door wanted to go. We were still working on individual route forecasts and personal briefings. Foggy days produced another problem. Smoke control was only just starting and we were still getting the real old pea-soup fogs. In addition there was no Weatherline service and all requests had to be handled personally. We used to decide on the forecast then confine incoming public calls to one line and sit one person by the telephone with the forecast. As fast as the telephone was replaced it would ring again; all through the day if the fog persisted.

Another duty was dealing with the Worcester THUM (Temperature and HUMidity) flight. This was an aircraft ascent done every morning around 0800. The aircraft was a Mosquito equipped with temperature and humidity measuring instruments. It took off from Woodvale, flew to Worcester and then climbed to 300 mb taking readings all the way up. Then it returned to Liverpool with the raw data and we converted them into corrected temperatures and dew-points at standard heights and coded them as a TEMP. Of course there were times when landing at Liverpool was not possible but the THUM pilots always took off anyway and landed where they could (anywhere between Kinloss and St Mawgan or Belfast and the near continent) and telephoned the data to us. They rarely missed a day.

The most difficult forecasts were for flights to Norway. We had quite a lot of these, exchanging ships crews. There were no oil rigs then, so only a few observations were available over the North Sea. If the aircraft had come from Norway the pilot had a much better picture of conditions over the North Sea than we had, but by dint of supplying them with good tea we made sure they always came in for a debriefing. Some of the Norwegian crews threatened to submit my forecasts to the museum of modern art in Oslo on the grounds that they were great examples of imaginative art, even if they were not very good forecasts.

By 1961 things were starting to change. We got a FAX machine and said farewell to our hand-plotted charts and HB pencils. We started to hear about experimental forecast charts produced by one of these new-fangled computer things and I decided that some of the fun was going out of the work. So, when the chance came to move to Bracknell in 1963 with perhaps some computer work, I took the 'if you can't beat them, join them' approach and left forecasting; for ever as it turned out.

Books received

The listing of books under this heading does not preclude a review in the Meteorological Magazine at a later date.

The greenhouse effect, climatic change and ecosystems, edited by B. Bolin, B.R. Döös, J. Jäger and R.A. Warwick (Chichester, New York, Brisbane, Toronto and Singapore, John Wiley and sons, 1986. £56.00) addresses a number of questions which have been of concern in recent years. These include the projection of energy use, increased emission of carbon dioxide and modifications to its cycle, expected increases in other gases in the atmosphere, possible climate change and the overall response of terrestrial ecosystems. Scientists drawn from a number of disciplines contribute to this analysis of these problems.

Satellite photograph — 13 January 1987 at 0359 GMT

This NOAA-9 infra-red image was taken during a period of extreme cold over western and central Europe. Although part of the mainland of Europe is cloud free, convective cloud forms rapidly in the strong east to north-east airflow over the warm waters of the North Sea and the Atlantic Ocean. Over part of the North Sea and the Bay of Biscay, the convection is obscured by upper cloud. A well-defined cyclonic circulation is present off Iberia. The low centre was moving eastwards, and the vigorous convection that can be seen immediately ahead of the vortex lay within an area of positive vorticity advection.

Of particular interest is the pattern of convection to the west of the British Isles, where cloud forms rapidly downwind of significant bays and river estuaries, whilst cloud apparently forms less readily downwind of peninsulas. It is probable that these effects are largely due to land-breezes, although the band downwind of the Strait of Dover (between France and England) is probably at least partly due to coastal convergence, and is very similar in structure to cloud bands observed downwind of the North Channel (between Scotland and Ireland) in cold north-north-westerly outbreaks (Browning *et al.*, *Meteorol Mag*, **114**, 1985, 325–331).

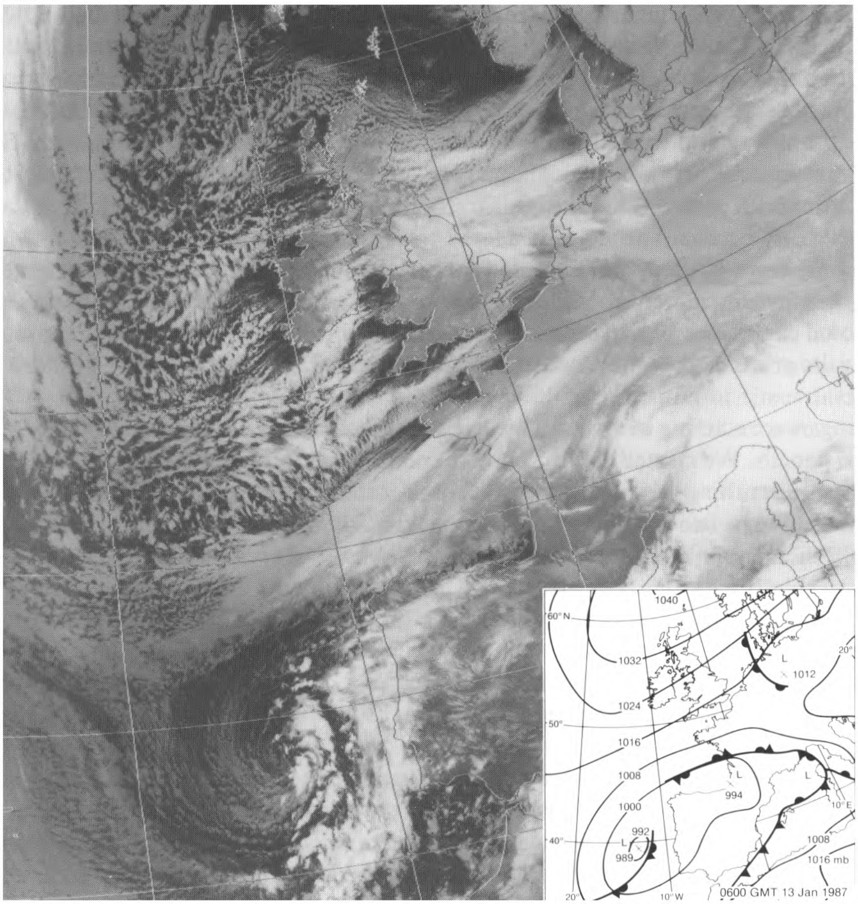

Photograph by courtesy of University of Dundee

Meteorological Magazine

GUIDE TO AUTHORS

Content

Articles on all aspects of meteorology are welcomed, particularly those which describe the results of research in applied meteorology or the development of practical forecasting techniques.

Preparation and submission of articles

Articles for publication and all other communications for the Editor should be addressed to the Director-General, Meteorological Office, London Road, Bracknell, Berkshire RG12 2SZ and marked 'For *Meteorological Magazine*'.

Articles, which must be in English, should be typed, double-spaced with wide margins, on one side only of A4-size paper. Tables, references and figure captions should be typed separately.

Spelling should conform to the preferred spelling in the *Concise Oxford Dictionary*.

References should be made using the Harvard system (author, date) and full details should be given at the end of the text. If a document referred to is unpublished, details must be given of the library where it may be seen. Documents which are not available to enquirers must not be referred to.

Tables should be numbered using roman numerals and provided with headings. We consider vertical and horizontal rules to be unnecessary in a well-designed table; spaces should be used instead.

Mathematical notation should be written with extreme care. Particular care should be taken to differentiate between Greek letters and Roman letters for which they could be mistaken. Double subscripts and superscripts should be avoided, as they are difficult to typeset and difficult to read. Keep notation as simple as possible; this makes typesetting quicker and therefore cheaper, and reduces the possibility of error. Further guidance is given in BS1991: Part 1: 1976 and *Quantities, Units and Symbols* published by the Royal Society.

Illustrations

Diagrams must be supplied either drawn to professional standards or drawn clearly, preferably in ink. They should be about 1½ to 3 times the final printed size and should not contain any unnecessary or irrelevant details. Any symbols and lettering must be large enough to remain legible after reduction. Explanatory text should not appear on the diagram itself but in the caption. Captions should be typed on a separate sheet of paper and should, as far as possible, explain the meanings of the diagrams without the reader having to refer to the text.

Sharp monochrome photographs on glossy paper are preferred: colour prints are acceptable but the use of colour within the magazine is at the Editor's discretion. In either case contrast should be sufficient to ensure satisfactory reproduction.

Units

SI units, or units approved by WMO, should be used.

Copyright

Authors wishing to retain copyright for themselves or for their sponsors should inform the Editor when they submit contributions which will otherwise become UK Crown copyright by right of first publication.

It is the responsibility of authors to obtain clearance for any copyright material they wish to use before submitting it for publication.

Free copies

Three free copies of the magazine are provided for authors of articles published in it. Separate offprints for each article are not provided.

Meteorological Magazine

April 1987

Vol. 116
No. 1377

CONTENTS

Contributions: it is requested that all communications to the Editor and books for review be addressed to the Director-General, Meteorological Office, London Road, Bracknell, Berkshire RG12 2SZ, and marked 'For *Meteorological Magazine*'. Contributors are asked to comply with the guidelines given in the *Guide to authors* which appears on the inside back cover. The responsibility for facts and opinions expressed in the signed articles and letters published in *Meteorological Magazine* rests with their respective authors. Authors wishing to retain copyright for themselves or for their sponsors should inform the Editor when submitting contributions which will otherwise become UK Crown copyright by right of first publication.

Subscriptions: Annual subscription £27.00 including postage; individual copies £2.30 including postage. Applications for postal subscriptions should be made to HMSO, PO Box 276, London SW8 5DT; subscription enquiries 01–211 8667.

Back numbers: Full-size reprints of Vols 1–75 (1866–1940) are available from Johnson Reprint Co. Ltd, 24–28 Oval Road, London NW1 7DX. Complete volumes of *Meteorological Magazine* commencing with volume 54 are available on microfilm from University Microfilms International, 18 Bedford Row, London WC1R 4EJ. Information on microfiche issues is available from Kraus Microfiche, Rte 100, Milwood, NY 10546, USA.

ISBN 0 11 727968 4 ISSN 0026–1149

Printed for HER MAJESTY'S STATIONERY OFFICE
by Delco Printing Co Ltd 4/87 Dd. 739131 C14

THE METEOROLOGICAL MAGAZINE

HER MAJESTY'S STATIONERY OFFICE

May 1987

Met.O.978 No. 1378 Vol. 116

METEOROLOGICAL OFFICE Met.O.978

THE METEOROLOGICAL MAGAZINE

No. 1378, May 1987, Vol. 116

551.515.3:551.515.9(53)

Tornadic waterspout at the Jebel Ali Sailing Club

B.J. Davey*

International Aeradio plc, Minhad, United Arab Emirates

Summary

At approximately 2215 GMT on 15 March 1986, a tornadic waterspout tracked through the boat park of the Jebel Ali Sailing Club, situated 25 km south-west of the city of Dubai in the United Arab Emirates. This article describes the synoptic situation leading up to the development of the storm and its devastating effects, and aims to provide some useful indicators for local meteorologists to help them in the difficult task of forecasting these severe storms, and any associated tornadoes and tornadic waterspouts.

1. Introduction

The Emirate of Dubai (see Fig. 1) is situated just to the north of the Tropic of Cancer on the south-eastern shore of the Arabian Gulf (formally better known as the Persian Gulf), and is one of the seven emirates in a federation established in 1971 called the United Arab Emirates (UAE). Here the weather is dominated for much of the year by the subtropical high pressure belt, producing subsiding air, clear skies and generally weak pressure gradients which, in turn, produce regular land and sea breezes shunting large amounts of evaporated Gulf moisture back and forth across the flat coastal plains. Summers are very hot and humid with daily maximum temperatures frequently exceeding 45 °C, making life in summer without the assistance of air conditioners rather unpleasant, if not unbearable, for most Europeans. Blue skies persist throughout the summer with the moisture confined to the lower levels of the atmosphere beneath the subsiding drier air aloft. By contrast, winter weather in the UAE is very pleasant, comparing favourably with the best British summers. Rainfall is scanty and very variable from year to year with means of around 100 mm along the coast and somewhat higher values near the Hajar Mountains which run northwards along the east coast of the UAE up into the Omani Musandam Peninsula. Much of this rainfall is produced ahead of eastward moving shemal troughs or pseudo cold fronts driven by long-wave upper troughs which sweep these latitudes in winter with the annual southward migration of the subtropical jet stream.

Quite often these winter troughs produce little in the way of much needed rainfall or even cloud. However, in the case described here, there was not only a substantial amount of rainfall but also the relatively rare occurrence of a tornadic waterspout which fortunately led to no loss of life, though it did cause a considerable amount of damage to the Jebel Ali Sailing Club.

* Now at Meteorological Office, Aberdeen.

2. Synoptic situation

Fig. 2 shows that at 0900 GMT (1300 local time) on 15 March 1986, a surface trough was lying from the Yemen Arab Republic through central Saudi Arabia to Kuwait. Ahead of this trough, pressure was falling steadily. Pressure falls during the previous 24 hours were 5.0 mb at Dubai and Abu Dhabi, 6.3 mb at Doha and 7.7 mb at Ras Tannūrah (24-hour tendencies are used because of the large diurnal pressure variations in the tropics). The air mass in the lower Gulf region was very dry ahead of this trough, e.g. temperature 30 °C and dew-point 3 °C at Dubai. However, at 0900 GMT on 15 March 1986, along the Omani coast, Salalah was reporting a moderate south-east wind with temperature 30 °C and dew-point 23 °C, and Masirah was reporting a temperature of 27 °C and a dew-point of 21 °C.

At 1200 GMT, around mid-afternoon local time, freshening south-easterly winds ahead of the trough were already causing deteriorating visibilities due to dust haze or rising sand (see Fig. 3). Although the air mass was still relatively dry at Dubai and Abu Dhabi, higher dew-points were evident in the lower Gulf region at Bu Hasa, Asab and Jebel Dhanna, and also in the state of Qatar at Umm Said and Doha. The pressure gradient was strong enough to prevent the formation of the usual afternoon sea-breeze, a rare event for Dubai. As a result the maximum temperature was 32.6 °C at Dubai and 34.5 °C at Minhad, which was 4 °C above the mean maximum temperature for March, and the highest recorded temperature up to this date for 1986. Apart from small amounts of altocumulus, surface observations and satellite images in the afternoon showed little cloud development ahead of the trough.

At 0001 GMT on 16 March 1986, which is shortly after the storm, thunderstorms and rain were still occurring at Dubai and Ras Al Khaimah. To the west of the shemal trough, fresh to strong shemal (Arabic for northerly) winds were advecting a cooler air mass into the southern Gulf region (see Fig. 4), the temperature at Kuwait of 14 °C being 13 °C lower than the temperature at Abu Dhabi.

3. Upper-air flow

Analysis of the upper-air flow in the Middle East is handicapped by communication problems and by a dearth of radiosonde reports from underdeveloped and sparsely populated areas in north Africa and the Arabian peninsula. In addition to this, the continuing war between Iraq and Iran has resulted in a complete black-out of all meteorological observations from both these countries since the beginning of the war in September 1980. However, in the UAE there is a radiosonde station at Abu Dhabi which is only 90 km from the location of the tornadic waterspout.

The Abu Dhabi tephigrams for 1200 GMT on 15 March and 0001 GMT on 16 March 1986 (see Fig. 5) show an increase in moisture with time at lower levels but the air mass had remained quite dry above 550 mb. However, both ascents show potential instability, with wet-bulb potential temperatures decreasing with height above about 900 mb.

Analysis of the upper-air charts at 0001 GMT on 15 March 1986 showed a marked trough at 850 and 700 mb lying from north-central Saudi Arabia to Sudan with the 850 mb winds well backed to 180° / 15 kn at Jeddah on the Red Sea coast of Saudi Arabia. The trough at 850 mb appeared much sharper than at 700 mb and higher levels, and favourable for the entrainment of moister low-level air from the Red Sea, Gulf of Aden and the Arabian Sea. At 500 mb the upper trough was less pronounced and orientated through the northern Red Sea and central Egypt. No upper trough was evident at 300 mb; there was a zonal flow over the Arabian peninsula with the sub-tropical jet core maximum of approximately 140 kn situated over northern Saudi Arabia.

Fig. 6(a) shows that by 0001 GMT on 16 March 1986, the 850 mb trough had advanced eastwards to be orientated through the southern Arabian Gulf to the People's Democratic Republic of Yemen just about 60 n miles west of the surface position of the shemal trough, while the 700 mb trough (see Fig. 6(b)) was lying approximately 550 n miles further to the west, through central Saudi Arabia and the

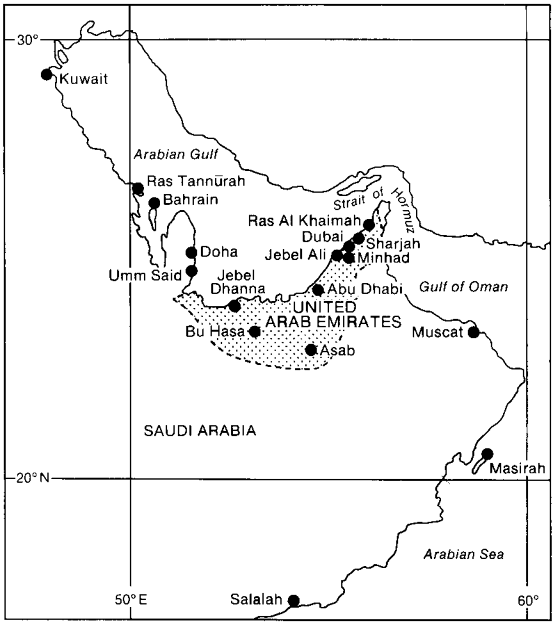

Figure 1. Map showing the relative positions of places mentioned in the text. The stippled area shows the extent of the United Arab Emirates.

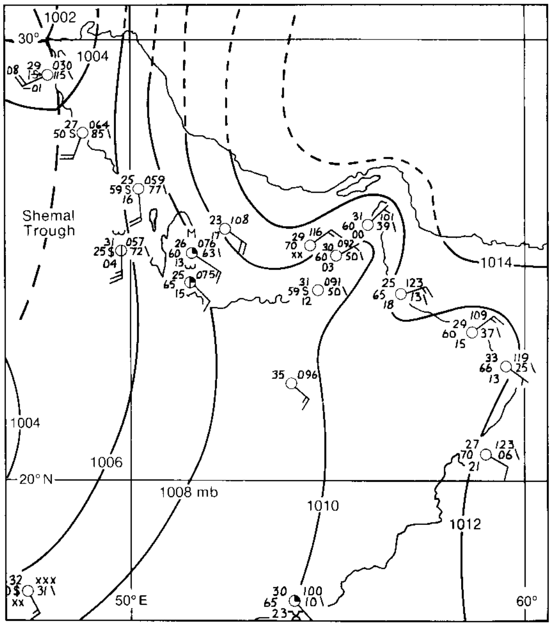

Figure 2. Surface analysis at 0900 GMT on 15 March 1986, with observations plotted (pressure tendencies are for the previous 24 hours).

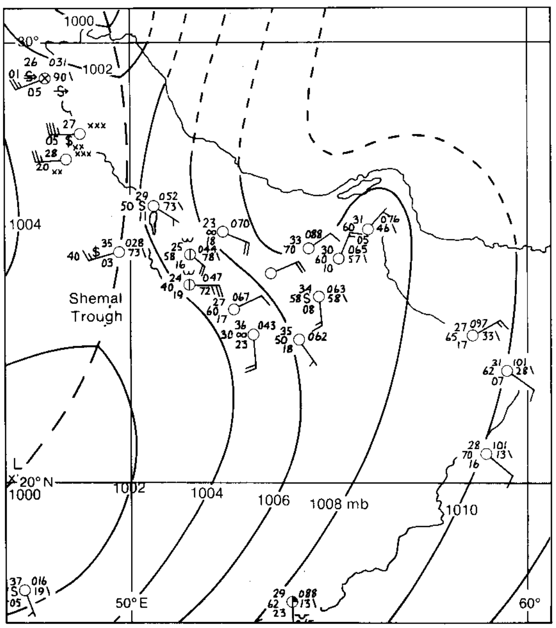

Figure 3. As Fig. 2 but for 1200 GMT on 15 March 1986.

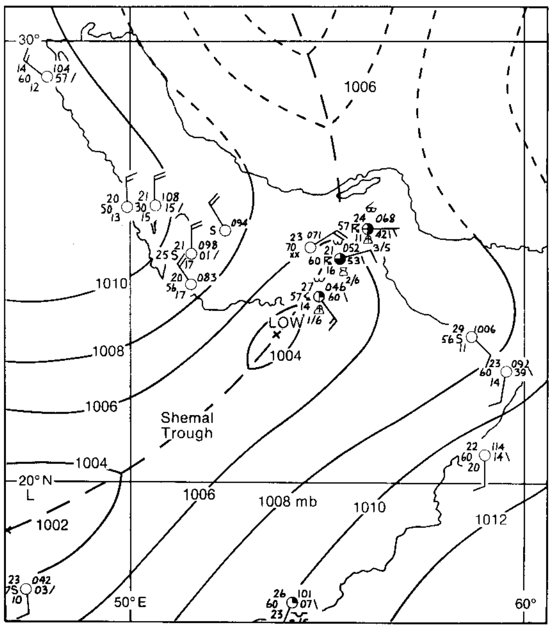

Figure 4. As Fig. 2 but for 0000 GMT on 16 March 1986.

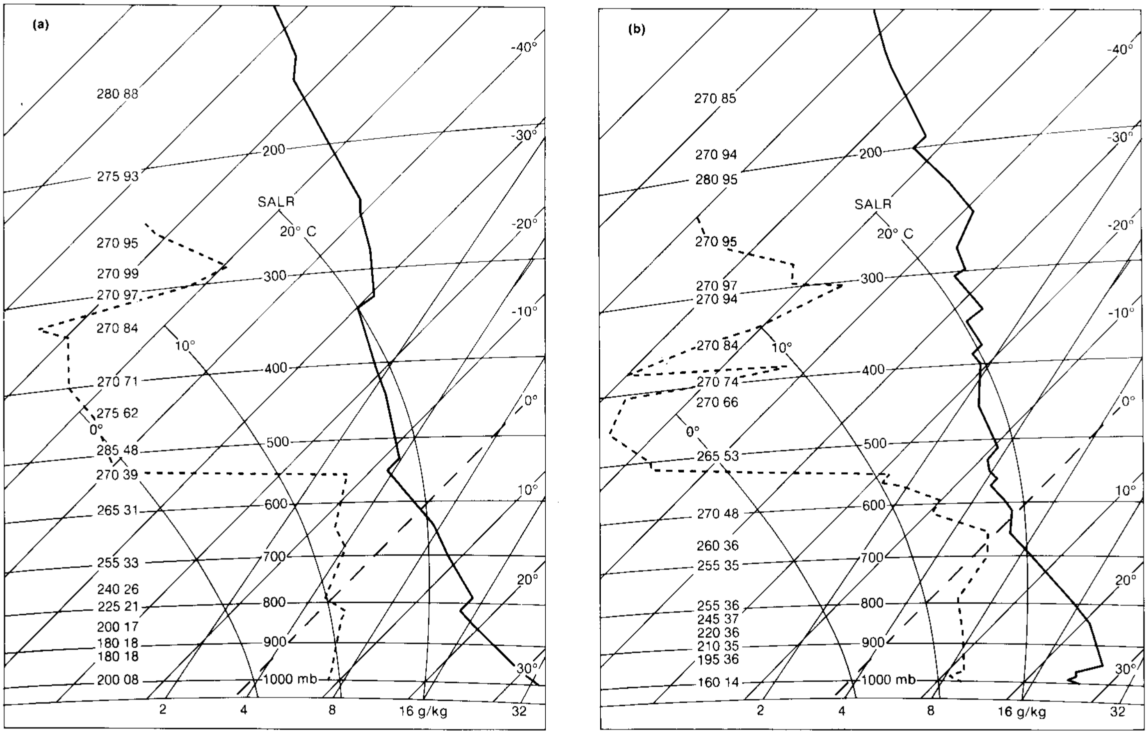

Figure 5. Radiosonde ascents for Abu Dhabi for (a) 1200 GMT on 15 March 1986 and (b) 0000 GMT on 16 March 1986.

Yemen Arab Republic. This indicates a steep leading edge to the cold air, not untypical of a fast-moving cold front of more temperate climes. A less-marked trough at 500 mb (see Fig. 6(c)) was lying through central Saudi Arabia, while at 300 mb a strong zonal flow was maintained (see Fig. 6(d)) with a westerly wind of around 100 kn over the Jebel Ali area.

4. The storm

At 2213 GMT on 15 March 1986, the first flash of lightning heralded the beginning of the storm over the Jebel Ali area. In the village on the periphery of the thunderstorm, lightning was observed mainly from altocumulus castellanus cloud but no precipitation was experienced, and the wind speed was estimated at less than 15 kn. However, at the 'one hundred beach villas', situated 5 km from the village and just to the south of the Jebel Ali Sailing Club, thunder, lightning and heavy rain were observed. Winds in excess of 45 kn were measured on a roof-mounted anemometer before readings went off the instrument scale. At about the same time, hurricane-force winds were estimated to be 100–120 kn at the Sailing Club according to reports in the Khaleej Times on 17 March 1986. However, this may have been an overestimate. A better estimate is given by the damage caused; this suggests that the winds may have been in the range 63–97 kn, on the Fujita Scale F1 for Damaging Wind or TORRO force T2–T3 on the Elsom and Meaden Tornado Intensity Scale — a moderate to strong tornado. Heavy sailing dinghys and catamarans, which would normally take up to six people to lift, were picked up along with their launching trailers and scattered around the beach and boat park. In the harbour two cruisers were overturned and sunk, and a small cruiser parked on a road trailer was turned upside-down. Heavy

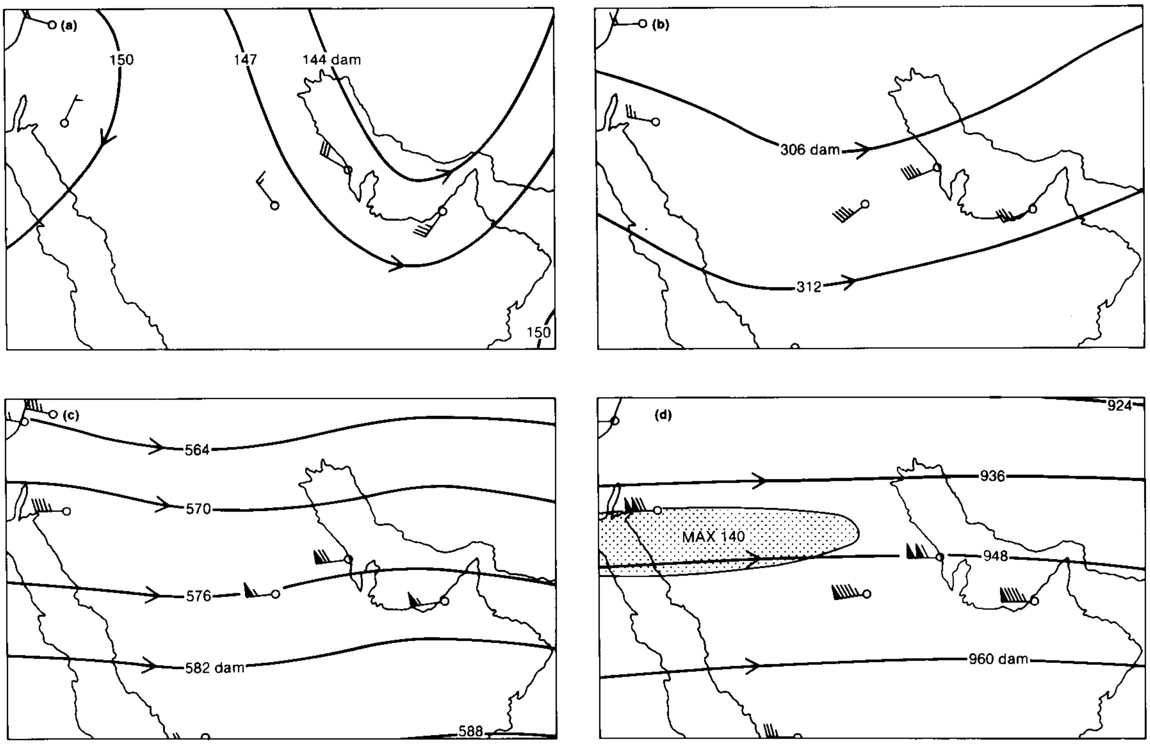

Figure 6. Upper-air analyses for 0000 GMT on 16 March 1986 for (a) 850 mb, (b) 700 mb, (c) 500 mb and (d) 300 mb (stippled region indicates speeds above 120 kn).

cable-drum tables, which were embedded in the sand in front of the club house, were hurled through the air and the gate-house was turned upside down and carried about 10 metres (see Fig. 7).

The final resting positions of the Wayfarer dinghy fleet and other debris after the storm gives some clue to the probable track of the tornadic waterspout funnel. These heavy sailing dinghys were all parked together at the top of the slipway before the storm. After the storm they were found in the positions shown in Fig. 8, to the east and north of the Wayfarer park. This implies that the tornadic waterspout funnel tracked in from the sea over the slipway in an east to east-north-east direction.

It is interesting to note that ahead of the upper trough, at 0001 GMT on 16 March 1986, the upper winds at Abu Dhabi were 220° / 36 kn at 850 mb and 255° / 35 kn at 700 mb.

NOAA-9 infra-red satellite images at 2327 GMT on 15 March 1986 (see Fig. 9) show numerous cumulonimbus cells over Dubai and the northern Emirates, and across the Gulf of Oman to southern Iran. Of particular interest is the Spembly density slice (Fig. 9(b)), which is a computerized video technique that enhances the NOAA-9 infra-red image shown in Fig. 9(a) and highlights the coldest cumulonimbus tops and the large multi-cell thunderstorms in the Jebel Ali area of the Dubai Emirate.

Around 0240 GMT on 16 March 1986, other cumulonimbus cells produced peanut-size hail in Bur Dubai, according to reports in a local newspaper, the Gulf News. At Dubai International Airport 15.8 mm of rainfall was measured overnight, while at Minhad only a trace of rainfall was recorded. By 0700 GMT the thunderstorms had cleared most of the northern Emirates and were followed by moderate to fresh north-westerly shemal winds and very hazy conditions. This sand and dust haze was

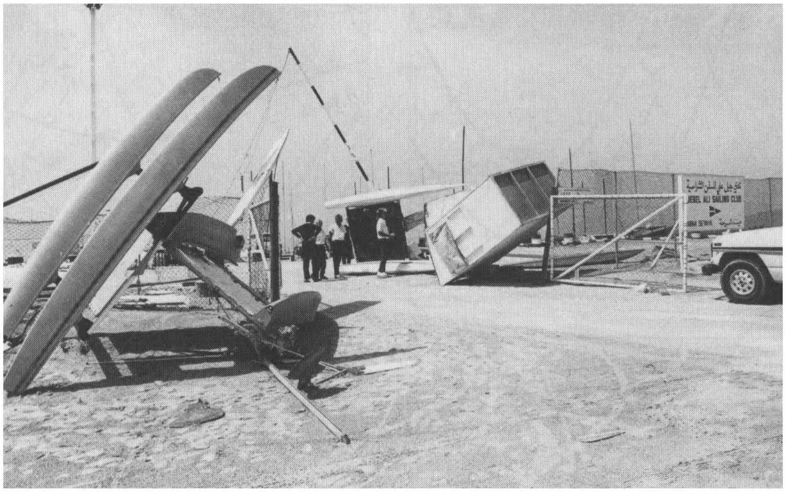

Figure 7. Photograph from the Khaleej Times showing the aftermath of the storm at Jebel Ali Sailing Club.

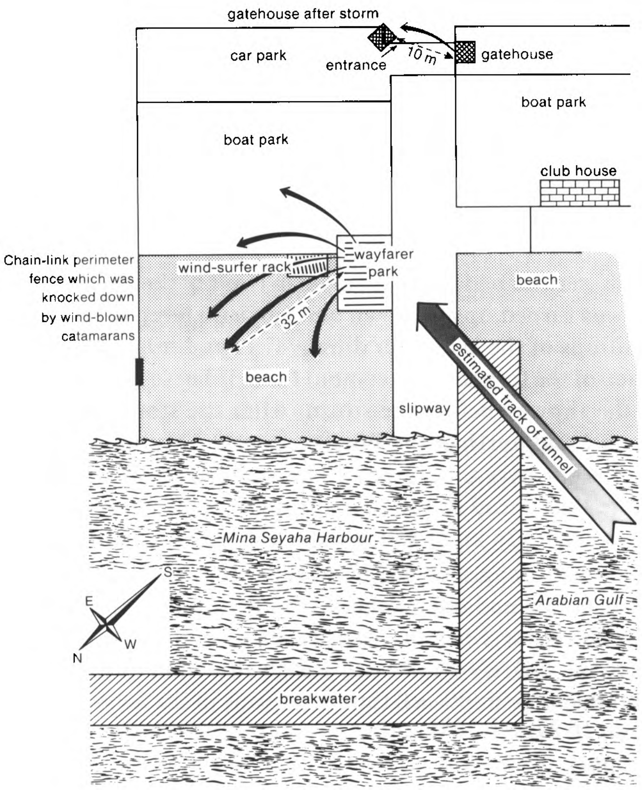

Figure 8. Plan of the Jebel Ali Sailing Club (not drawn to scale) showing movement of boats and gatehouse caused by the tornadic waterspout. Its estimated track is shown by the arrow.

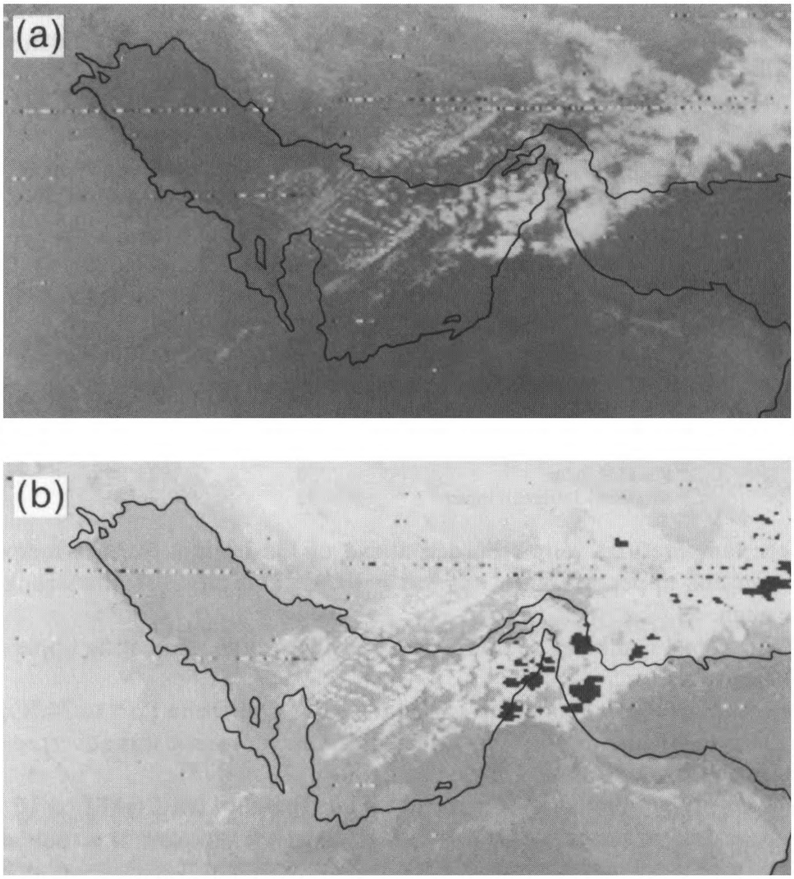

Figure 9. (a) NOAA-9 infra-red satellite image at 2327 GMT on 15 March 1986 and (b) Spembly density-slice image of the satellite picture.

raised by the strong winds 24 hours previously over the Lower Mesopotamian Plain and northern Saudi Arabia. It was then advected by the shemal winds 800–1000 km down the Arabian Gulf and reduced the visibility to 1000 metres or less in places in the UAE.

5. Discussion

The development of this tornadic waterspout was brought about by a combination of favourable circumstances. Some of the more important atmospheric conditions observed in this development were as follows:

(a) A mobile trough over the Arabian Peninsula at the surface, 850, 700 and 500 mb produced dynamical ascent ahead of the surface trough.

(b) The air mass was initially dry at the surface layers and moist at medium levels. Advection of moist surface air from the Arabian Sea and the Omani coast to the Asab, Bu Hasa, Jebel Dhanna area occurred only 6–9 hours before the storm development. This provided the necessary moisture to produce the cloud and precipitation often absent in the southern Arabian Gulf with approaching troughs.

(c) Winds were of jet-stream strength (60 kn or more) above 450 mb. The maximum wind in the vicinity of the storm was approximately 270° / 100 kn and occurred around 300 mb. At this level the jet stream removes air so quickly that air from below is drawn up to replace it thereby enhancing convection. However, from Fig. 6(d) it is not apparent that the Jebel Ali area is in a strongly diffluent region such as a left exit or right entrance with respect to the 300 mb jet.
(d) Vigorous warm advection was evident ahead of the trough. Wind speeds below 500 mb increased with time. At lower levels winds were southerly, while above 650 mb the winds were westerly. Vertical wind speed shear was about 3 kn per 1000 ft between 700 and 300 mb. Although these particular values do not appear to be excessive, increasing wind speed with height and vertical wind direction shear are necessary requirements for the updraught inside the storm to rotate cyclonically.
(e) The air mass was potentially unstable ahead of the trough. Instability indices devised for use in the United Kingdom are also useful indicators for instability in winter in the Middle East.

	Index	Threshold
Boyden instability index	99	94/95
Rackliff index	30	29/30
Modified Jefferson index	32	26/28

(f) High surface temperatures were recorded ahead of the trough. Surface temperature contrast between the lower and upper Arabian Gulf was 6–10 °C. This established a strong baroclinic zone ahead of the trough.
(g) Pressure falls were 4–7 mb per 24 hours ahead of the trough, indicating upper-level divergence and ascent of the surface air.
(h) Sea temperatures in the Arabian Gulf varied from 21 °C at Doha Port to 24 °C at Sharjah Port. This may have also contributed to the instability of the air mass as it was advected over the slightly warmer waters of the south Arabian Gulf.
(i) The 850 mb wet-bulb potential temperature at Abu Dhabi for 0001 GMT on 16 March 1986 was 18.5 °C. It is interesting to note that David (1976)* observed that one of a number of parameters associated with severe storms which produced tornadoes in North America was an 850 mb wet-bulb potential temperature of 18 °C.
(j) To say that orography played no part in the development of the storm would be a bold statement, given the shape and natural features of the lower Gulf basin. It is surrounded by the Zagros Mountains of Iran to the north, the Hajar Mountains to the east and the gradual upslope across the Rub Al Khali or Empty Quarter, leading to the Hadhramaut Mountains of the People's Democratic Republic of Yemen and the Tihamah Mountains of Saudi Arabia and the Yemen Arab Republic. Indeed the only low-level outlet for any airstream from the Arabian Gulf is through that politically sensitive bottle-neck, the Strait of Hormuz and this in itself can often produce orographic troughs in the south Gulf region. However, on this particular occasion it would be imprudent to attribute too much influence to the orography, given the flat low-lying terrain of the coastal plain in the Jebel Ali area.

6. Conclusion

This article has attempted to summarize the main features of the synoptic situation concerning the development of this particular tornadic waterspout. Given the limited data and observations available to the bench forecaster working in the Arabian Gulf region, we can speculate that the parent

* David, C.L.; A study of upper air parameters at the time of tornadoes, *Mon Weather Rev*, **104**, 1976, 546–551.

thunderstorm which spawned this waterspout was triggered by displacement of the warm air ahead of the trough. This air mass had been supplied with sufficient moisture by low-level advection from the Arabian Sea. The warm, moist air was then pushed aloft by the colder, denser air to the rear of the trough. Although it remains impossible to forecast the exact locations of these severe local storms and associated tornadoes and tornadic waterspouts, it is hoped that recognition of the features noted above will help Gulf forecasters to become more aware of the rapid and violent changes that can occur, given cloudless conditions over and to the west of this area only 6–9 hours before storm development.

Acknowledgements

Discussions with the following members of staff of International Aeradio plc during the preparation of this article are gratefully acknowledged: H. Rodda (Senior Met. Officer, Central Air Base Minhad), W.H. Owen (Senior Met. Officer, Dubai International Airport) and C.C.E. Jackson (Senior Met. Officer, Sharjah International Airport). Grateful thanks are also extended to the Commanding Officer, Central Air Base Minhad for permission to publish this article and to the Khaleej Times for the photograph showing the aftermath of the storm.

551.513.1:551.58

Dynamics of the monthly-mean climate*

G.J. Shutts

Meteorological Office, Bracknell

Summary

The lay person might quite reasonably ask, 'Why are the winds in temperate latitudes predominantly westerly?' or 'Why do the major arid regions occur near 30 ° N (and S)?' When faced with such questioning how should the climatologist respond, or is causal explanation hopeless? In this article, the dominant physical processes and constraints are identified and, with some judicious simplification, a 'back-of-the-envelope' theory of the zonally-averaged general circulation is sought. It is argued that poleward momentum transport by large-scale weather systems plays a crucial role in driving the observed surface wind pattern and organizing the release of latent heat energy.

1. Introduction

One month is considered to be the smallest averaging time-interval that can be used for a local (in space) definition of climate to make sense. Implicit in this choice is the need to average over many baroclinic wave life cycles (life cycle time-scale $\approx$ 7 days). Ideally, one would like to explain all of the major time-averaged synoptic features, such as the Icelandic low and Siberian anticyclone in winter and the Azores anticyclone and Indian monsoon in summer, together with the positions of the major storm tracks. A physical understanding of the principal dynamical factors involved in determining the strength and position of these phenomena might then allow their inter-annual variability to be forecast. Whilst this is a rather ambitious goal, the idealized theoretical models developed along the way provide a dynamical framework with respect to which diagnostics can be developed and interpreted, e.g. **Q**-vectors (Hoskins *et al.* 1978). The classical approach has been to try to understand features of the zonally-averaged climate (e.g. three-cell mean meridional circulation) and relate them to heat and

* Lecture note from a series of lectures entitled 'Dynamical Processes in Meteorology' given as part of the 1986 Advanced Lectures (Meteorological Office, 15 September–3 October 1986).

momentum budget requirements. Since the zonally-averaged climatic fields represent much of the observed variation across the globe, it is important to have a dynamically-consistent picture of the underlying mechanics which determine them.

A few salient features of the global heat energy budget are examined in section 2 and various hypotheses concerning the magnitude of poleward heat transport and the observed meridional temperature gradient are reviewed. The role of poleward momentum transport is emphasized in section 3 and related to the zonal-mean distribution of surface pressure, wind and precipitation: a summary of how these eddy transfer processes determine the zonally-averaged state of the troposphere is then given in section 4.

2. Heat transfer

The latitudinal imbalance of net heating in vertical columns (extending into the ground/sea and throughout the atmosphere) is determined primarily by the geometrically-controlled variation of insolation and the weak latitudinal dependence of outgoing infra-red radiation. The latter is at least partly due to the dominance of water vapour amongst the other infra-red radiating tri-atomic molecules and the fact that the uppermost optically black layer of water vapour occurs at a temperature fixed by freezing and precipitation (≈ -18 °C). Much of the heat energy surplus in the tropics is not immediately available since solar radiation over large regions is absorbed into the upper few metres of the oceans. It is subsequently released to the atmosphere mainly through evaporation into the trade winds and ultimately converted to sensible heat and gravitational potential energy through condensation on ascent in deep tropical convection. The warming influence of this latent heat release is transmitted to tropical regions distant from the convection by forced subsidence in association with the radiation of inertia-gravity waves — particularly Kelvin and Rossby-gravity modes (Gill 1982).

Heat energy is removed from the subtropics in the familiar organized baroclinic weather systems of synoptic charts and quasi-stationary planetary wave systems (Shutts 1987). This type of large-scale 'sloping' convection (Green 1979) transfers heat polewards and upwards so as to balance the radiative sink in higher latitudes. During autumn and winter, the middle latitude oceans give up much heat energy stored in them during the summer, providing depressions with considerable latent heat energy which can be organized and released in 'explosive cyclogenesis'.

A simple zonally-averaged climate model much loved by the climatologist requires the tropospheric, depth-averaged temperature to be determined, given fixed or parametrized heat sources and sinks. From this temperature distribution, the thermal wind equation can be invoked to find a consistent wind field provided that some assumption is made about the surface wind, e.g. no flow. In these models, poleward heat transport is usually represented by a non-linear diffusion law where the eddy diffusion or transfer coefficient (Green 1970) is a function of the poleward temperature gradient. In fact, Green gives theoretical and observational support for the existence of a heat transfer law of the form:

$$\overline{v\phi} = 5.5 \times 10^{-3} \left(\frac{g}{B}\right)^{1/2} \Delta\phi^2 \ \mathrm{m\ s^{-1}}$$

where the overbar refers to a zonal, height, and time average, v is the meridional wind speed, g is the acceleration due to gravity, B is the mean static stability, ϕ is the logarithm of potential temperature and $\Delta\phi$ is the pole-equator difference in ϕ. In spite of being cast in the form of a diffusion law, Green's transfer theory is independent of mixing ideas.

Stone (1978) takes a very different viewpoint and suggests that baroclinic instability is super-efficient at transporting heat for temperature gradients in excess of a certain critical gradient, defined in accordance with two-level quasi-geostrophic theory on a beta-plane. He argues that the observed poleward temperature gradients will never be far from this critical value since smaller gradients lead to very weak baroclinic instability which is unable to satisfy the global heat budget requirement and a slightly larger temperature gradient causes too much heat to be transported. This critical temperature gradient turns out to be proportional to the cotangent of latitude and to the static stability. Observational evidence is given in Stone's paper to support this 'baroclinic adjustment' hypothesis in middle latitudes.

Another interesting hypothesis concerning the zonal-mean temperature is that of maximum available potential energy generation (Lorenz 1960, Paltridge 1978 and Shutts 1981). Given heat sources and sinks which are themselves some function of temperature, it is hypothesized that the time- and zonal-mean temperature is such that the Available Potential Energy (APE) generation rate is a maximum. If, for instance, the time-mean diabatic heating rate $Q(y)$ can be written as:

$$Q(y) = -\gamma(\delta T(y) - \delta T_*(y))$$

where y is latitude, γ^{-1} is a time constant, δT is the temperature perturbation about some mean and δT_* is some known equilibrium temperature perturbation such that the mean of Q is zero, then the APE generation rate is proportional to:

$$\int Q\delta T\,\mathrm{d}y = -\gamma\int(\delta T - \delta T_*)\delta T\,\mathrm{d}y$$

which is a maximum if $\delta T = \frac{1}{2}\,\delta T_*(y)$. Of course in practice Q is not merely a function of δT and the detailed physics, e.g. cloud albedo, cannot be ignored.

3. Momentum transfer

A theory which predicts the latitudinal distribution of temperature is of very limited use since it fails to tell us anything about the sense of the winds at the surface and, by inference, the frictionally-induced mean meridional circulation. What is required is a dynamical model which can account for the time-mean surface westerlies of middle latitudes and easterlies in the subtropics. Since there are no internal atmospheric sources or sinks of momentum in the zonally-averaged sense, frictional stress and wave drag at the surface can only be balanced by the height-integrated flux convergence of momentum. Of course, the surface wind pattern exists because of the momentum transport, though observations alone do not show this. The poleward momentum transport required to maintain the mid-latitude surface westerlies is brought about almost entirely by large-scale eddies (quasi-stationary forced planetary waves and baroclinic instabilities) and only in the tropics is the mean meridional circulation important. Even then the very existence of the observed 'Hadley circulation' relies on the presence of large-scale eddy momentum transport and it is incorrect to think of it as an independent agency for transporting heat and momentum. The often quoted notion of the Hadley circulation as the 'flywheel of the general circulation' is misleading. It is simply an ageostrophic response resulting from the destruction of the zonally-averaged thermal wind balance by:

(a) diabatic heating in equatorial cumulonimbus,
(b) frictional deceleration of the trade winds,
(c) a net upper tropospheric sink of westerly momentum due to the poleward transport by large-scale eddies — this causes the trade winds and therefore (b), and
(d) radiational cooling in non-precipitating regions throughout the tropics.

The principal reason that eddy transport of momentum dominates the total height-integrated poleward momentum transport is that the net Coriolis torque

$$\int_{\mathrm{D}} \rho f v \, \mathrm{d}x \, \mathrm{d}z$$

vanishes at any latitude since there must be no long-term mass flux polewards. (D refers to the region of the longitude–height plane above the surface.) The term

$$\int_{\mathrm{D}} \rho v \frac{\partial \bar{U}}{\partial y} \mathrm{d}z$$

which represents the poleward flux of relative momentum due to the mean meridional circulation is small except in the tropics (where ρ is the density and U is the zonal wind — the overbar denotes the zonal average). Fig. 1 shows latitude–height cross-sections of the poleward momentum transport split into (a) transient and (b) stationary wave contributions for January 1979 based on FGGE (First GARP Global Experiment) data. Note that the transient eddies transport momentum polewards (except north of 60° N) whereas the stationary waves have a pronounced equatorward component near 60° N. In general, eddy momentum transfer is vertically coherent with a strong peak near the tropopause. The height-integrated momentum flux convergence from these pictures implies a westerly momentum sink at the surface between 30° and 60° N (in the time-mean) and an easterly sink between the Equator and 30° N. The pattern of zonal winds observed in that month (Fig. 2) was consistent with this required surface momentum exchange — representing as they do the normal climatological picture.

The zonally-averaged pressure field consistent with this distribution of zonal winds (through geostrophy) implies a low pressure belt at 60° N and a subtropical anticyclone belt at 30° N. Frictionally-induced ageostrophic motion at the surface then suggests that the former regions will be cloudy and wet and the latter clear and dry.

The transport of momentum by large-scale eddies is therefore crucial to the determination of the mean state of the atmosphere. The question that dynamical meteorologists have tried to address for at least 40 years is, 'What dynamical principles govern the sense of the momentum transport?' Many different ways of interpreting the tendency of baroclinic waves to transport momentum polewards have been proposed — all of which seem perfectly plausible. Most depend upon the existence of a 'beta-effect', i.e. variation of the Coriolis parameter with latitude. It can be shown that disturbances forced in mid-latitudes will tend to propagate as Rossby waves towards the Equator and in the process exhibit a marked north-east to south-west orientation — the signature of poleward momentum transfer (Hoskins *et al.* 1977). Baroclinic instability can, to some extent, be regarded as an initial disturbance energy-growth phase associated with the conversion of zonal to eddy-available potential energy followed in the mature phase by upward and equatorward Rossby wave radiation (Edmon *et al.* 1980).

The polar easterlies north of 60° N are not a very important aspect of the general circulation since they only occupy a small area of the earth's surface and are highly variable from month to month. Even so, they appear to be consistent with the observed equatorward flux of momentum in high latitudes, particularly by the stationary waves.

4. Summary

The zonally-averaged mean state of the troposphere can be thought of as being governed by two eddy transport properties:

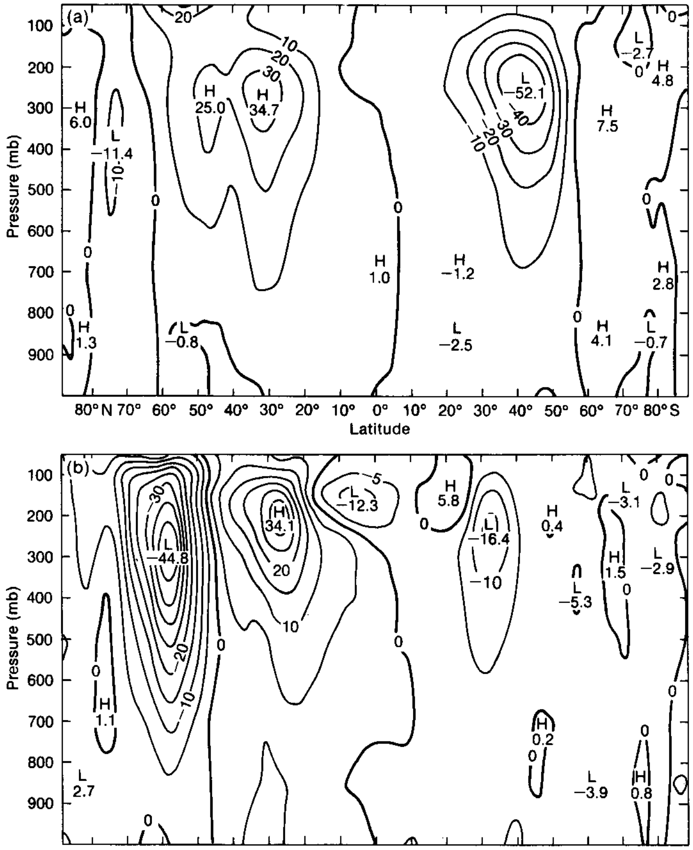

Figure 1. Latitude–height cross-section (zonally-averaged) of (a) transient and (b) stationary eddy momentum flux $(\mathrm{m\,s^{-1}})^2$ for January 1979, based on FGGE data and derived through the ECMWF analysis system.

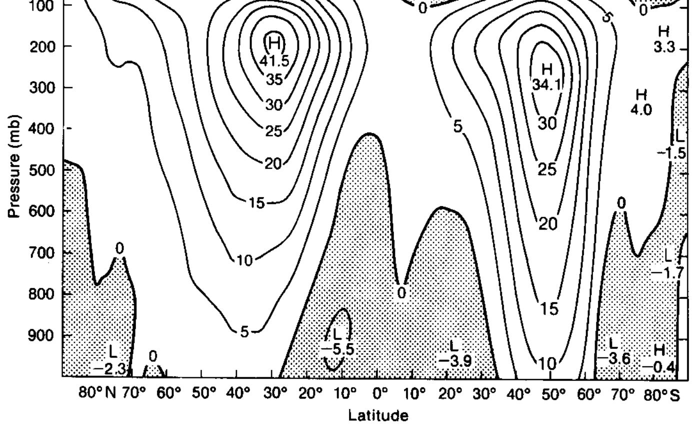

Figure 2. The zonally-averaged zonal component $(\mathrm{m\,s^{-1}})$ of the wind vector corresponding to Fig. 1. Stippling indicates zonal-mean easterlies.

(a) The height-integrated poleward momentum flux which determines the surface winds.
(b) The height-integrated poleward heat flux which gives, through the thermal wind relation, the mean vertical wind shear — though parametrized relations between the surface stress and wind, and the temperature and heat source are required to complete the description.

Longitudinal variations of eddy heat and momentum transport are currently thought to contribute strongly to the zonal asymmetry of the mean circulation in addition to the topographical forcing functions discussed by Shutts (1987).

References

Edmon, H.J., jun, Hoskins, B.J. and McIntyre, M.E. 1980 Eliassen-Palm cross-sections for the troposphere. *J Atmos Sci*, **37**, 2600–2616.
Gill, A.E. 1982 Atmosphere–Ocean Dynamics. International Geophysics Series, Vol. 30, London. Academic Press.
Green, J.S.A. 1970 Transfer properties of the large-scale eddies and the general circulation of the atmosphere. *Q J R Meteorol Soc*, **96**, 157–185.
1979 Topics in dynamical meteorology: 8. Trough-ridge systems as slantwise convection (1). *Weather*, **34**, 2–10.
Hoskins, B.J., Draghici, I. and Davies, H.C. 1978 A new look at the ω-equation. *Q J R Meteorol Soc*, **104**, 31–38.
Hoskins, B.J., Simmons, A.J. and Andrews, D.G. 1977 Energy dispersion in a barotropic atmosphere. *Q J R Meteorol Soc*, **103**, 553–567.
Lorenz, E.N. 1960 Generation of available potential energy and the intensity of the general circulation. *In* Pfeffer, R.L. (ed.); Dynamics of Climate, Oxford, London, New York, Paris, Pergamon Press.
Paltridge, G.W. 1978 The steady-state format of global climate. *Q J R Meteorol Soc*, **104**, 927–945.
Shutts, G.J. 1981 Maximum entropy production states in quasi-geostrophic dynamical models. *Q J R Meteorol Soc*, **107**, 503–520.
1987 Linear models of stationary planetary waves forced by orography and thermal contrast. *Meteorol Mag*, **116**, 61–74.
Stone, P.H. 1978 Baroclinic adjustment. *J Atmos Sci*, **35**, 561–571.

551.511.61:551.551.8

Random walk models of atmospheric dispersion

D.J. Thomson
Meteorological Office, Bracknell

Summary

Random walk models are being increasingly exploited as a means of simulating the dispersion of material in the atmosphere. In this paper a description of the random walk approach is given and its advantages and limitations discussed. To illustrate the approach, three examples of applications of random walk models are presented.

1. Background

There is a wide range of man's activities which either involve the release of substances into the atmosphere or have the potential for such releases; an understanding of atmospheric dispersion is important both in planning such activities and in responding to accidental discharges. The range of dispersion problems is large. For example, one might be interested in dispersion over a few hundred metres in the event of a tanker accident or over several thousand kilometres in the case of acid rain. To understand these different problems requires an understanding of the atmospheric eddies over a wide range of scales, from the turbulence of micrometeorology to synoptic-scale depressions and anticyclones. Further complications are the chemical properties of the dispersing substances (which affect, for example, the rate at which the substance is absorbed by the ground) and the density of the release (as typified by the difference between hot buoyant plumes from chimneys and releases of dense gases such as chlorine).

So-called 'random walk' models constitute a promising approach to some of these problems; however, the range of problems to which such models are applicable is rather modest compared with the full range of dispersion problems. These models assume that the dispersing material is passive (i.e. it moves with, and does not affect, the flow) and that the eddies have at least some of the properties of randomness characteristic of three-dimensional turbulence. Thus they are not directly applicable to buoyant or heavy plumes, or to long-range problems where the eddies responsible for the dispersion are predominantly two dimensional. The main area of application of random walk models is to the dispersion of a passive substance in the turbulent boundary layer of the atmosphere.

Before discussing random walk models, it is appropriate to review the alternative methods which have been applied to the dispersion problem. Perhaps the most widely used method from a practical viewpoint is the Gaussian plume model, in which the shape of the concentration distribution across the plume is assumed to be Gaussian, i.e. a normal distribution. The width of the plume in the lateral and vertical directions is determined from tables or nomograms based on experimental observations of plume behaviour. Although it will be a while before this method is superseded from a practical point of view, such models are essentially empirical and do not explain the dispersion in terms of the flow properties. A second approach which has been extensively applied is the use of the diffusion equation. In this approach, it is assumed that the turbulent flux of material is proportional to the concentration gradient, the constant of proportionality being the diffusivity K. There are various ways in which K and its spatial and temporal variation can be estimated in terms of the flow properties. However, the fundamental assumption underlying the diffusion equation, namely that the length- and time-scales of the motions responsible for the dispersion are small compared with the scales on which the concentration and flow properties vary, is not true in general. This leads to a number of qualitative errors in the results. For example, a plume from an elevated source grows linearly for small times after release (because fluid elements travel in straight lines over short distances) whereas the diffusion equation predicts parabolic growth as in Fig. 1. Also, in a convective boundary layer, a large part of the turbulent energy is contained in eddies whose sizes are comparable to the boundary-layer depth; as a result the diffusion equation fails to represent the most important qualitative features of the dispersion (see section 3). High-order closure models constitute a promising technique which overcomes some of the problems associated with eddy-diffusivity models. However, these models cannot represent the initial stages of the dispersion in a natural way and cannot easily represent the dispersion from complex source distributions (Deardorff 1978). There are a number of other techniques available such as similarity theory and Taylor's statistical theory, but these are of limited applicability. All these methods are discussed in more detail by Pasquill and Smith (1983). Random walk techniques provide a method of overcoming the most serious problems in the other approaches.

One does not have to watch a turbulent flow for long to realize that there is little hope of being able to predict the evolution of the flow in detail over a period of time much in excess of the time-scale of a single eddy. The usual response to this problem (which is adopted in random walk models and which is also implicit in the Gaussian plume and diffusion equation models) is to abandon any attempt to calculate the evolution of a particular flow and to concentrate instead on statistical quantities. More specifically the flow is considered to be one realization of an ensemble of flows in which the external conditions (e.g. geostrophic wind, lapse rate and surface conditions) are identical but in which the details of the turbulence differ. Attempts are then made to predict ensemble-average quantities such as the ensemble-mean concentration of the dispersing material at a particular point P (this will be denoted by C(P)) or the standard deviation of the concentration at P (denoted by σ_c(P)). It is important to realize that C(P) is not necessarily equal to the concentration in any particular realization (Fig. 2); this is why an estimate of the variability in the concentration between the realizations, such as σ_c(P), is of some importance. In spite of this, most of the effort which has been devoted to understanding dispersion, including the study of

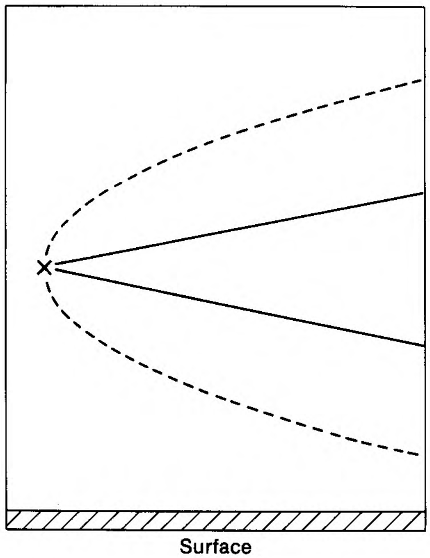

Figure 1. Plume growth downwind of an elevated source in the atmospheric boundary layer. The solid line indicates the true behaviour and the dashed line the result of using the diffusion equation. X marks the source position.

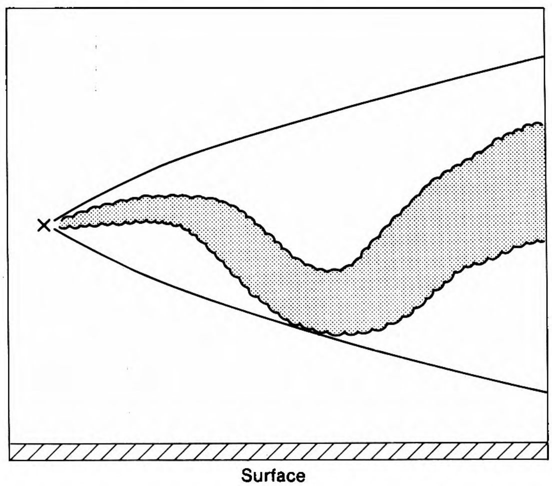

Figure 2. An illustration of the relation between the instantaneous plume in a particular realization and the ensemble-average plume. The shaded area indicates the instantaneous plume and the solid line denotes the boundary of the ensemble-average plume. X marks the source position. The ensemble-average plume width is generally larger than the instantaneous width because of the tendency of the plume to meander.

random walk models, has been directed towards predicting C(P), and this emphasis on C(P) is reflected in the current article. The more difficult problem of estimating σ_c(P) using random walk methods is discussed briefly in section 4.

2. What is a 'random walk' model?

The basic idea behind random walk models is to simulate the motion of many particles of the dispersing substance. Fig. 3 shows some simulated trajectories for the case of an elevated source in a neutral boundary layer. The particles are assumed to be drawn at random from among all the particles of the dispersing material in the ensemble of flows; hence they move independently. To calculate the ensemble mean concentration at point P, a small box is constructed (metaphorically speaking) around the point and the number of trajectories passing through the box is counted. In order to obtain statistically reliable values for the concentration it is necessary to ensure that many particles pass through the box. This means that it is impossible to make the box infinitesimal and hence the resulting concentrations are not point values but always averaged over some region. In order to be able to make these regions small, a large number of trajectories, typically ten thousand, are calculated.

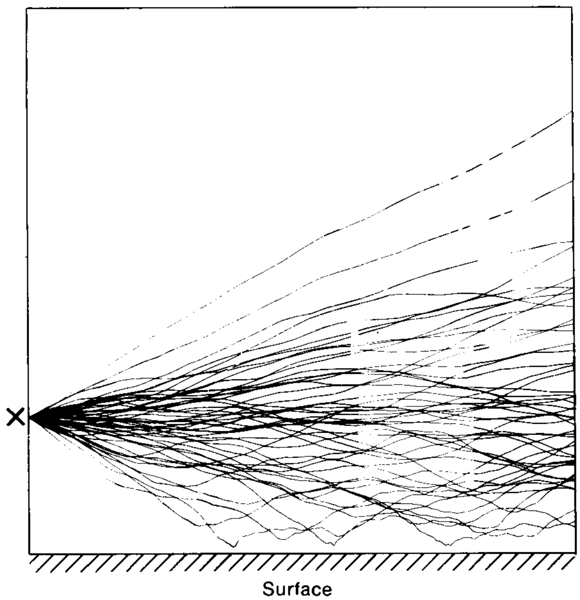

Figure 3. 50 trajectories from a random walk simulation of dispersion downwind of an elevated source, marked X, in a neutral boundary layer.

To implement the above scheme it is necessary to have a model of the way the particles move. One of the simplest schemes is that suggested by Langevin (1908) in connection with the study, not of turbulent dispersion, but of Brownian motion. In finite difference form, Langevin's equation for the vertical velocity of a particle (for simplicity only the vertical velocity is considered here) takes the form

$$w(t+\Delta t) = (1 - \Delta t/\tau)w(t) + r \quad \dots \dots \dots \dots \dots \dots \quad (1)$$

where $w(t)$ is the vertical velocity of the particle at time t, Δt is the time step, τ is a time-scale characteristic of the particle motions and r is a normally distributed random number with mean zero and prescribed variance. The height of the particle at time t can then be calculated from

$$z(t+\Delta t) = z(t) + w(t)\Delta t.$$

The physical interpretation of equation (1) is that over a period Δt the particle loses a small fraction $\Delta t/\tau$ of its momentum to the surrounding air and in return receives a random impulse r. By choosing the variance of r appropriately, it is possible to ensure that the variance of the vertical velocity of the particles has the correct value. Of course a random walk model cannot predict properties of the mean flow and turbulence (such as the velocity variance or the time-scale τ); however, given this information, the random walk model can predict the dispersion.

Although this is not an appropriate place to discuss in detail the formulation of more general models, it is worth pointing out that the simple model given by equation (1) is not adequate in many situations. Consider, for example, a horizontally homogeneous situation where there is a gradient in the vertical velocity variance. Under these conditions the particles passing through a given point have, in reality, a non-zero mean vertical acceleration even though the mean vertical velocity at every fixed point is zero. To obtain realistic results it is necessary to include this non-zero mean acceleration in the model; failure to do so results in a model where a tracer which is initially well-mixed becomes 'un-mixed' and non-uniform in space at later times. The way in which a random walk model should be designed to take account of this and other similar effects is now well understood (Thomson 1984, van Dop *et al.* 1985, Thomson 1987). In essence, the model must be designed so that it does not lead to paradoxes if it is assumed that all 'particles' of air, and not just particles of the dispersing material, move according to the model. Models which are designed in this way agree with many of the exact results known in dispersion theory; this gives us some confidence that the models are capturing the essential physics of the dispersion process.

Random walk models have a long history. The idea that it is possible to explain the evolution of the concentration field by studying the statistics of the motions of fluid elements is due to Taylor (1921), who also discussed what is essentially the simple model described above. The idea is a natural one, since it is, of course, the motion of the individual elements of the dispersing substance which determines the dispersion. However, it is only comparatively recently that the computational resources have become available to allow widespread application of the technique.

Random walk models are very simple in concept, but might perhaps be thought to be a little simplistic. However, as indicated above, random walk models are an improvement in some respects over sophisticated high-order closure models, as well as over the simpler Gaussian plume and diffusion equation approaches. This is because, in the terminology of high-order closure models, the advection terms (which are always approximated in high-order closure models) are represented exactly. A consequence of this is that random walk models can represent the near-source behaviour of a plume easily and realistically. It may seem a little inelegant to calculate the motion of several thousand particles explicitly, but it is not clear how this can be circumvented without losing some of the good properties of random walk models. In some simple situations, e.g. homogeneous stationary turbulence, C(P) can be calculated analytically from the model equations but this is not so in most cases of practical interest.

3. Applications

Random walk models have now been tested in a wide range of situations. Three examples are described below, two involving dispersion over flat ground (in the surface layer and throughout the depth of a convective boundary layer) and one example over more complex terrain.

3.1 *Vertical dispersion in the surface layer*

In the surface layer of the atmosphere, which occupies typically the lowest few tens of metres of the atmosphere, the properties of the flow are well understood and are determined by three quantities: the roughness length, the surface heat flux and the surface stress. This knowledge of the flow can be used to construct a random walk model along the lines indicated in section 2 (Ley and Thomson 1983). Fig. 4 shows comparisons between the modelled vertical dispersion and that observed during the Project Prairie Grass experiment (Barad 1958) at 100 m downwind of the source. The three graphs show the dispersion under different stability conditions, with the Monin–Obukhov length, a standard measure of stability which is infinite in neutral conditions, taking values of 8 m (very stable), −87 m (slightly unstable) and −7.7 m (very unstable). Although there are some small differences, the model results show encouraging agreement and vary correctly with stability (note the different vertical scales — the variation of the dispersion with stability is quite substantial).

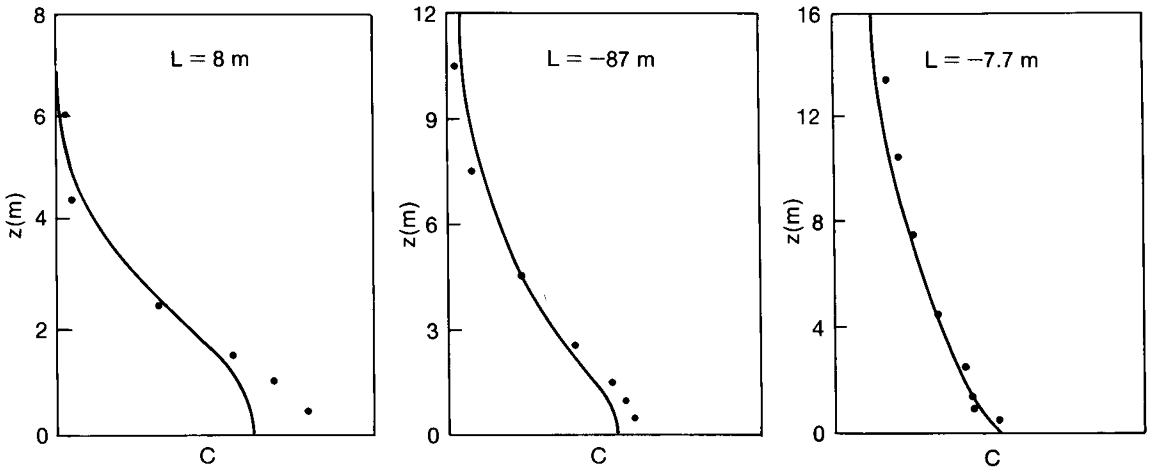

Figure 4. Comparison between the modelled vertical dispersion and that observed during the Project Prairie Grass experiment (taken from Ley and Thomson 1983). The concentration C is in arbitrary units, L is the Monin–Obukhov length and z is the height above the ground. The solid line indicates the model's behaviour and the dots the observations.

3.2 *Vertical dispersion in a convective boundary layer*

In a convective boundary layer the turbulence structure is dominated by large eddies comparable in size to the boundary-layer depth. These take the form of narrow vigorous updraughts surrounded by regions of slowly descending air. This flow structure results in a strong increase in the vertical velocity variance with height in the lower part of the boundary layer and a positive skewness in the vertical velocity distribution at all heights. The dispersion in such circumstances is quite complex.

Recently de Baas *et al.* (1986) have applied a model of the type outlined in section 2 to this problem. The results are shown in Fig. 5 for sources at two different heights. The results agree well with the experimental data of Willis and Deardorff (1976, 1981). Two features of the dispersion deserve comment. When the source is near the ground the plume centre-line lifts off the ground while, for an elevated source, the height of the maximum concentration descends to near ground level. This means that at a downwind distance of $z_i U / w_*$ (where z_i is the inversion height, U the mean boundary layer wind and w_* the convective velocity scale which is typically 1 m s^{-1} in a moderately convective boundary layer) the ground-level concentration is greater for an elevated source than for a source at ground level. These features are good examples of aspects of dispersion which are not represented at all in simpler models such as Gaussian plume and diffusion equation models.

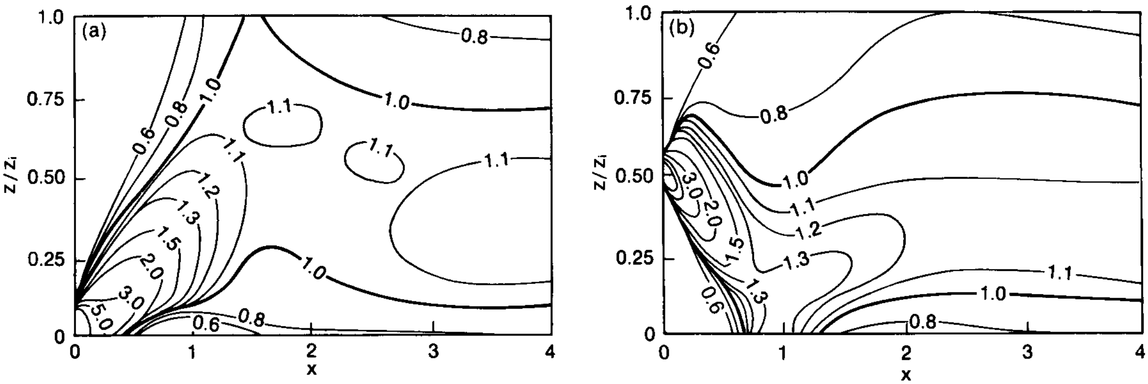

Figure 5. Model contours of concentration downwind of a source in a convective boundary layer for two source heights (a) $z/z_i = 0.067$ and (b) $z/z_i = 0.49$ (taken from de Baas *et al.* 1986). z is the height above ground and x is the downwind distance, non-dimensionalized by $z_i U/w_*$ where z_i is the inversion height, U is the mean boundary-layer wind and w_* is the convective velocity scale.

3.3 *Dispersion in a valley*

The third example presented here is that of dispersion in a valley. Between 1980 and 1983 an experimental study of the flow properties and dispersion characteristics in the Sirhowy Valley , South Wales, was undertaken by the Boundary Layer Branch of the Meteorological Office (Mason and King 1984, Callander 1986). The flow in the valley is complex. When the wind blows across the valley the flow separates, with a recirculating eddy occurring in the lee of the high ground. Also the turbulence intensity in the valley is much larger than is found over flat terrain.

A random walk model of dispersion in the valley was constructed (Thomson 1986a) utilizing the knowledge of the flow which had been obtained from the field experiment and from the modelling studies of Mason and King (1984). Fig. 6 shows the variation of concentration with distance downstream, as obtained from the model and from the experimental data. Also shown are the concentration levels which would be expected over flat ground, as taken from Turner's (1969) Gaussian plume model. Two situations are considered, namely the release of material from the summit upwind of the valley (Fig. 6(a)) and from the valley floor (Fig. 6(b)), with the wind blowing across the valley and the static stability close to neutral. For the summit release, the model shows a substantial reduction in concentration compared to what would be expected over flat ground. Although the scatter in the experimental data is too great to make a detailed quantitative comparison, the data shows the same trend. For the valley release, the model predicts concentrations which are larger than those observed by a factor of about three. However, this error is small compared with that which would be obtained by using a Gaussian plume model designed for flat terrain. Such a model would overestimate the concentration by a factor of 25 if the summit wind speed was chosen as the appropriate wind speed for use in the model, and by a factor of 80 if the wind speed at the source was used.

4. Fluctuations in concentration

Fluctuations in concentration are often comparable with, or larger than, the mean concentration. This can be of great importance in situations where the dispersing substance is explosive or toxic. Consider, for example, a steady source of an explosive gas. The risk of an explosion will be related more to the peak values of the concentration than to the ensemble- or time-average value. Random walk models can predict a measure of the size of the fluctuations, namely σ_c, if the motions of pairs of particles, instead of single particles, are simulated. The idea that σ_c can be expressed in terms of the

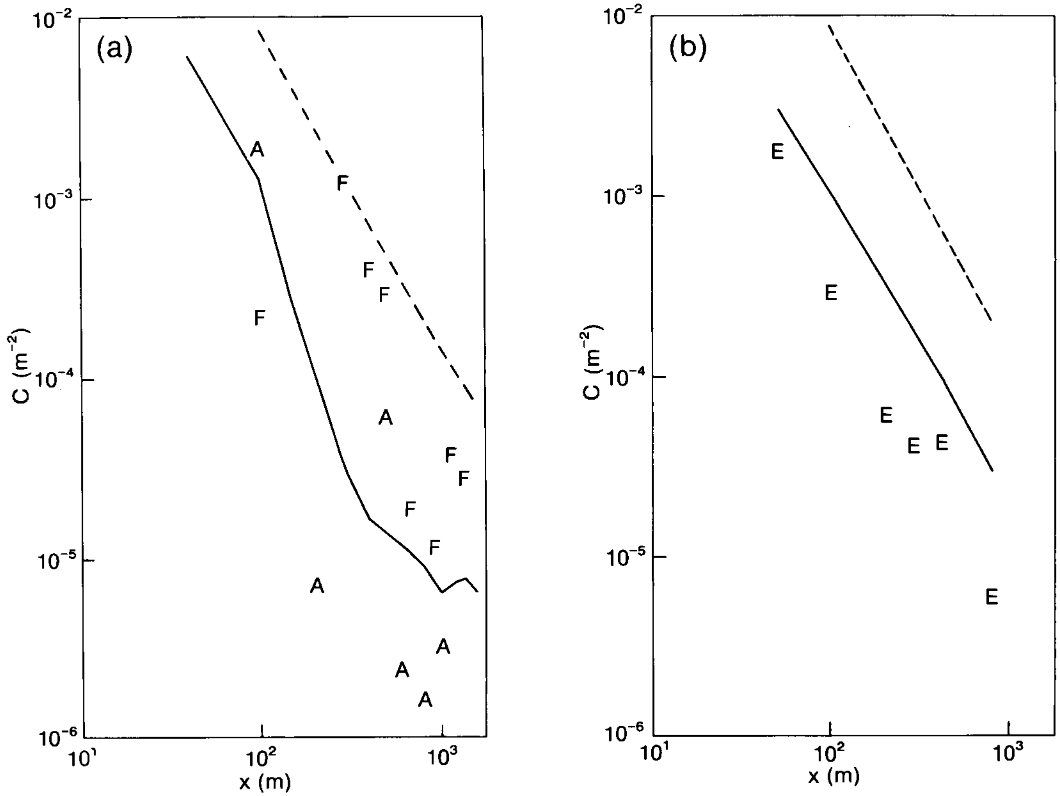

Figure 6. Variation of concentration with distance downwind for a source on (a) the summit upwind of the valley and (b) the floor of the valley (taken from Thomson 1986a). x is the downwind distance and C is the concentration normalized by Q/U, Q being the source strength and U the 8 m summit wind speed. The solid line is the random walk prediction, the dashed line is a prediction from Turner's (1969) Gaussian plume model using the summit wind speed, and A, E and F denote observed concentrations from different experiments.

motion of pairs of particles is due to Batchelor (1952), but it is only comparatively recently (Durbin 1980) that this has been exploited by simulating the motion of particle pairs numerically. Such models have had some success in predicting concentration fluctuations in simple situations (see for example Durbin (1982) who considered concentration fluctuations in homogeneous wind tunnel turbulence). However, there is no consensus about how such models should be formulated (see for example Egbert and Baker (1984), Sawford (1984) and Thomson (1986b)). Their application to the problem of obtaining quantitative predictions of σ_c in atmospheric flows is a matter for the future.

5. Conclusion

Random walk models are a promising approach to the problem of the dispersion of a passive substance in the atmospheric boundary layer. Although simple in concept, they avoid many of the problems inherent in other techniques. They are particularly suited to situations where the flow properties are inhomogeneous (e.g. the convective boundary layer); many other techniques fail in these situations. Although they involve a number of assumptions and cannot be justified in any fundamental way, so far they show good agreement with experimental data. It seems likely that such models will be increasingly exploited in the future.

Acknowledgement

The author would like to thank the Royal Meteorological Society for permission to reproduce Fig. 5.

References

Barad, M.L. 1958 Project Prairie Grass, a field program in diffusion, Vol. I. Geophysics Research Paper 59, Air Force Cambridge Research Centre. AFCRC-TR-58-235(I).

Batchelor, G.K. 1952 Diffusion in a field of homogeneous turbulence. II. The relative motion of particles. *Proc Cambridge Philos Soc*, **48**, 345–362.

Callander, B.A. 1986 Short range dispersion within a system of regular valleys. *In* Proceedings of the Fifteenth NATO/CCMS International Technical Meeting on Air Pollution Modelling and its Application. London, New York, Plenum Press.

de Baas, A.F., van Dop, H. and Nieuwstadt, F.T.M. 1986 An application of the Langevin equation for inhomogeneous conditions to dispersion in a convective boundary layer. *Q J R Meteorol Soc*, **112**, 165–180.

Deardorff, J.W. 1978 Closure of the second- and third-moment rate equations for diffusion in homogeneous turbulence. *Phys Fluids*, **21**, 525–530.

Durbin, P.A. 1980 A stochastic model of two-particle dispersion and concentration fluctuations in homogeneous turbulence. *J Fluid Mech*, **100**, 279–302.

1982 Analysis of the decay of temperature fluctuations in isotropic turbulence. *Phys Fluids*, **25**, 1328–1332.

Egbert, G.D. and Baker, M.B. 1984 Comments on paper 'The effect of Gaussian particle-pair distribution functions in the statistical theory of concentration fluctuations in homogeneous turbulence' by B.L. Sawford (*Q J R Meteorol Soc*, **109**, 339–353). *Q J R Meteorol Soc*, **110**, 1195–1199.

Langevin, P. 1908 Sur la théorie du mouvement brownien. *Comptes Rendus Hebdomadaires des Séances*, Paris, **146**, 530–533.

Ley, A.J. and Thomson, D.J. 1983 A random walk model of dispersion in the diabatic surface layer. *Q J R Meteorol Soc*, **109**, 867–880.

Mason, P.J. and King, J.C. 1984 Atmospheric flow over a succession of nearly two-dimensional ridges and valleys. *Q J R Meteorol Soc*, **110**, 821–845.

Pasquill, F. and Smith, F.B. 1983 Atmospheric diffusion, 3rd edition. Chichester, Ellis Horwood Ltd.

Sawford, B.L. 1984 Reply to comments by Egbert and Baker. *Q J R Meteorol Soc*, **110**, 1199–1200.

Taylor, G.I. 1921 Diffusion by continuous movements. *Proc London Math Soc*, Ser 2, **20**, 196–211.

Thomson, D.J. 1984 Random walk modelling of diffusion in inhomogeneous turbulence. *Q J R Meteorol Soc*, **110**, 1107–1120.

1986a A random walk model of dispersion in turbulent flows, and its application to dispersion in a valley. *Q J R Meteorol Soc*, **112**, 511–530.

1986b On the relative dispersion of two particles in homogeneous stationary turbulence and the implications for the size of concentration fluctuations at large times. *Q J R Meteorol Soc*, **112**, 890–894.

(1987) Criteria for the selection of stochastic models of particle trajectories in turbulent flows. (Submitted to *J Fluid Mech*).

Turner, D.B. 1969 Workbook of atmospheric dispersion estimates. US Department of Health, Education and Welfare, Public Health Service Publication No. 999-AP-26.

van Dop, H., Nieuwstadt, F.T.M. and Hunt, J.C.R. 1985 Random walk models for particle displacements in inhomogeneous unsteady turbulent flows. *Phys Fluids*, **28**, 1639–1653.

Willis, G.E. and Deardorff, J.W. 1976 A laboratory model of diffusion into the convective planetary boundary layer. *Q J R Meteorol Soc*, **102**, 427–445.

1981 A laboratory study of dispersion from a source in the middle of the convectively mixed layer. *Atmos Environ*, **15**, 109–117.

551.509.5:551.509.333:551.513.1:551.526.6

The skill of dynamical long-range forecasts*

D.A. Mansfield
Meteorological Office, Bracknell

Summary

The Meteorological Office 5-level general circulation model has been used to investigate the skill of winter-time long-range forecasts. Even with climatological sea surface temperatures, the large-scale features of the flow are found, on average, to have a small but significant correlation with the real atmospheric evolution out to about 20 days. The use of observed tropical sea surface temperatures improved the forecast in four out of five years.

1. Introduction

It is well established that the prediction of instantaneous weather patterns is impossible beyond about 10–15 days. The upper limit of deterministic predictability has been estimated by calculating how quickly small differences in the initial state (representing the uncertainty in our knowledge of the true state of the atmosphere) grow to reach saturation value. The lower limit is found by comparing the model evolution directly with the real atmosphere. Beyond 10–15 days some large-scale features of the circulation may remain predictable, but on average the degree of skill is likely to be small.

It appears that the degree of skill obtainable may depend rather heavily on the initial conditions. If this is the case, then a large number of integrations from independent initial conditions are required before the true potential of the forecasts can be assessed. Furthermore, the limitations of even the most up-to-date models are such that, over a period of 30–50 days, the model drifts towards an average state which differs from the real climatology by an amount comparable with typical departures from that climatology. This means that a model is useful for long-range forecasting experiments only if it has a realistic climatology.

In 1978 the Meteorological Office began systematically to produce 50-day experimental forecasts with a hemispheric version of the 5-layer general circulation model described by Corby *et al.* (1977). (Routine global analyses were not available at the time.) These forecasts were carried out once or twice a month from January 1978 to January 1982. In addition, ten forecasts from the winters of 1974/75 to 1977/78 were available.

In spite of the low vertical resolution of the model and the relatively simple parametrization of physical processes (by present-day standards), the winter climatology of the model is realistic in terms of the time-mean flow and the behaviour of transients. Therefore the set of winter forecasts provides a basis for testing the skill of dynamical forecasts from a wide range of initial conditions.

A correct prediction of, say, 500 mb height anomaly over the United Kingdom would be a useful forecast, even if the magnitude was much less than that observed. Therefore it is preferable to use an anomaly correlation as a measure of skill rather than the root-mean-square difference since emphasis needs to be placed on the phase of the anomalies rather than their magnitude. The anomaly correlation is defined as the correlation between the forecast anomaly (i.e. the difference between the forecast and the model's climatology) and the corresponding observed anomaly. This means that a perfect forecast has a correlation of 1.0, whereas if the correlation is zero the forecast has no skill. The model climatology has been constructed by averaging seventeen 50-day integrations from initial conditions separated by at least 5 days and spanning 8 winters.

* An abridged version of a paper by Mansfield (1986) which appeared in the Quarterly Journal of the Royal Meteorological Society.

The forecast results from integrations with climatological Sea Surface Temperatures (SSTs) are discussed in section 2, while in section 3 an attempt is made at assessing the impact of observed SSTs.

2. Forecast skill with climatological sea surface temperatures

Fig. 1(a) shows the daily anomaly correlation averaged over the 18 forecasts which used climatological SSTs. The correlation is significantly greater than zero at the 5% level up to and including day 16. Therefore, for this model, there is a small degree of skill observable in daily forecasts up to about 2 weeks.

There is evidence that by considering time-meaned fields instead of daily forecasts, the signal to noise ratio is increased because the unpredictable (i.e. synoptic scale) part of the flow is filtered out — thus allowing an extension of the period over which skill can be detected. This is illustrated by Fig. 1(b) which shows the correlation of 15-day mean forecasts, averaged over the 18 forecasts (the correlation has been calculated for overlapping 15-day means, centred 5 days apart, commencing with days 1–15). Note that the skill remains significantly different from zero for only about 4 days longer than for the daily forecasts. This is a disappointing result, as it might have been expected that the small degree of skill shown in the daily forecasts would have been amplified to a greater extent. One reason for this is that the small degree of skill remaining after the first 10 days or so is not uniformily distributed. Three of the forecasts showed some skill throughout the 50 days, whereas in five cases the anomaly correlation fell to zero within 10 days. Any subsequent negative correlations in the poor forecasts will be amplified by the averaging, as well as the positive correlations in the successful forecasts. The large dispersion in the skill of the forecasts at the extended range is not just due to sampling fluctuations but is a result of genuine differences in predictability between different atmospheric states.

In order to concentrate on those forecasts which exhibit most skill, those eight forecasts which had positive correlations up to or beyond the 16–30 day mean were chosen for further analysis. Since the mean-sea-level pressure (MSLP) is perhaps more easily interpreted in terms of weather, this has been chosen as the field to be used to illustrate the maximum skill obtainable with the model. Results for the limited area surrounding the United Kingdom used for statistical long-range forecasts at the Meteorological Office (30–87.5° N, 45° W–25° E) were computed to facilitate interpretation in terms of synoptic patterns. Since the skill is due to the largest scales of motion, values are similar to those of the hemisphere as a whole.

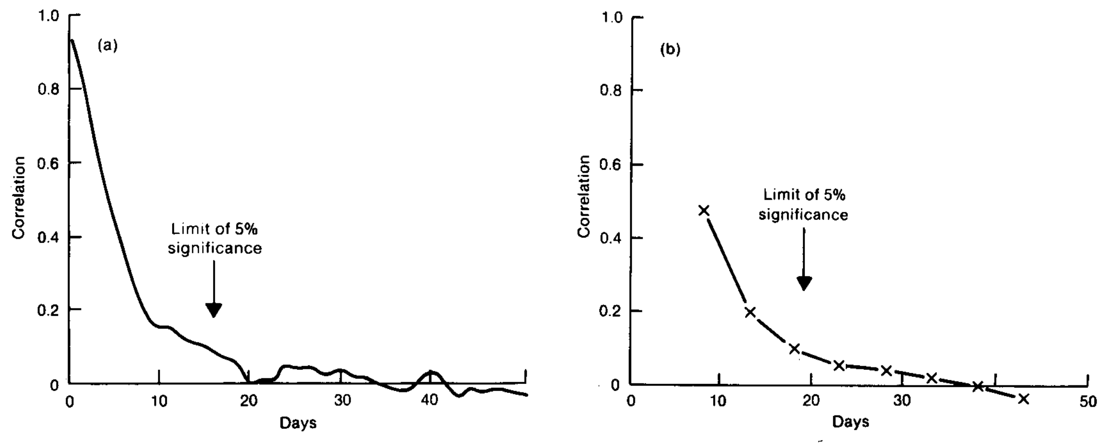

Figure 1. (a) Daily and (b) 15-day-mean anomaly correlations, averaged over 18 winter forecasts for the 500 mb height in the region 30–85° N.

Fig. 2 shows the anomaly correlation of 15-day-mean MSLP for the eight most skilful forecasts and all eighteen forecasts for the region. Also included is the average skill of persistence forecasts based on the mean observed anomaly for the 15 days up to and including day zero of each of the 18 forecasts. Overall, the 15-day-mean model forecasts are better than persistence only for the first 15-day mean. However, the best eight model forecasts display skill above that of persistence to beyond day 30. These more skilful forecasts tend to be associated with greater than average persistence in the real data, but the difference in persistence anomaly correlation between these runs and all 18 runs is not significant at the 5% level. Thus persistence alone cannot explain the extended predictability.

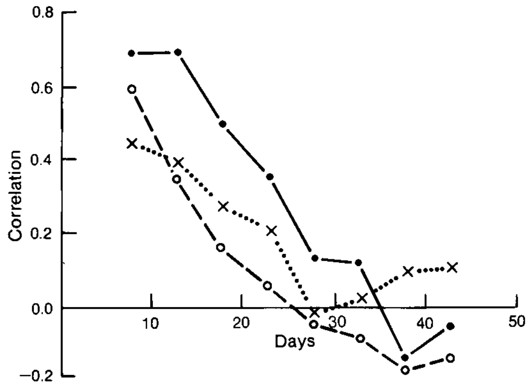

Figure 2. Anomaly correlations of 15-day-means of mean-sea-level pressure for the area 30–87.5°N, 45°W–25°E for all 18 forecasts (dashed line), the best 8 forecasts (solid line), and the persistence forecasts averaged over all 18 cases (dotted line).

An illustration of what the degree of skill of one of the better forecasts represents in synoptic terms is given in Fig. 3 which shows the real and model mean MSLP anomalies for 1–15 and 16–30 January 1978 (corresponding to days 1–15 and 16–30 of the model forecasts). The anomaly correlations in this particular case, 0.43 and 0.66 for the first and second periods, are equalled or surpassed by four other forecasts. At first sight the forecasts do not look very good, particularly during the first period. However, the forecast pressure anomaly would produce a generally westerly anomaly in the wind over much of the region and this would suggest a predominantly mobile situation with probably above normal temperatures at least in the south of the British Isles. In the second period, the anomaly was more cyclonic and more north-westerly in both the model and reality. Thus the forecast correctly indicated a colder and wetter second half-month, especially in the north of the United Kingdom. The increased westerly gradient in the second period would have implied a stronger-than-average temperature contrast between north and south and, coupled with the above average precipitation, would have suggested more snow than usual in the north. In fact, some unusually heavy snowfall did occur in northern Britain in the second half of the month.

To be able to utilize the higher degree of skill in some forecasts it is necessary to know, a priori, which forecasts are likely to be successful. One possibility is that these forecasts would display above average short-range skill, but this turned out not to be the case. There is no indication of above average daily skill in the first 6 days, even in the largest scales, in those forecasts with skill at extended range.

3. The effect on skill of including observed sea surface temperatures

There is ample evidence that SSTs affect the atmospheric circulation, though experience suggests that the atmosphere is more responsive to tropical SST anomalies than it is to those in mid-latitudes. For

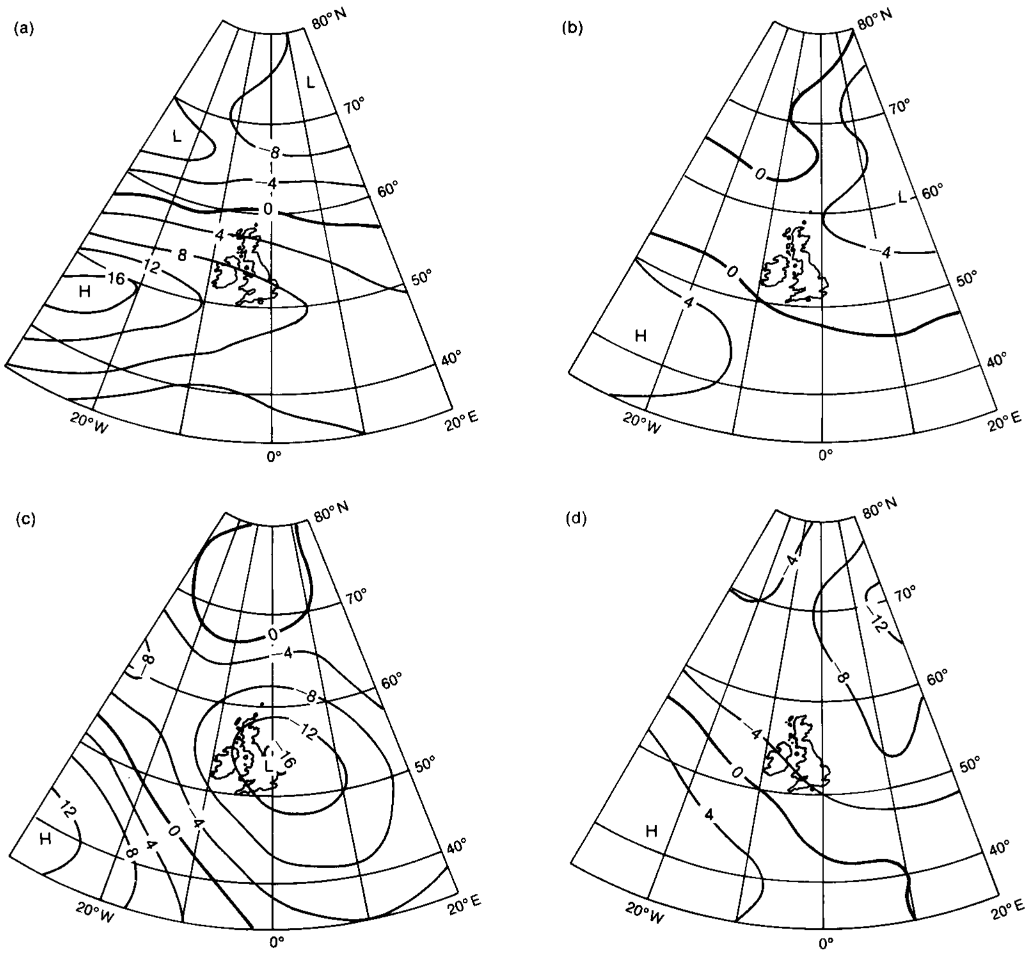

Figure 3. (a) Observed and (b) forecast mean-sea-level pressure anomalies (mb) for 1–15 January 1978. (c) and (d) are as (a) and (b) respectively, but for 16–30 January 1978.

example, it has been found that, in terms of the surface pressure field, the mid-latitude response of the model used in this investigation is likely to be 3–4 times greater for tropical than mid-latitude forcing. Certainly, sensitivity experiments have shown that mid-latitude SST anomalies have little consistent beneficial effect on forecast skill, but the large response to tropical SSTs suggests that the use of observed SSTs rather than the climatological values would lead to an improvement in forecast skill.

Nine of the forecasts were rerun with the observed SST anomalies south of 30° N. The values used were the average for January of each year involved, and were held fixed throughout the forecast. Where more than one forecast was performed for a given winter, the same SSTs were used in each.

The results in terms of 15-day-mean anomaly correlations of the 500 mb height show that using realistic SSTs improved the correlations averaged over the whole forecast by more than 0.1 in four experiments, in three they were marginally improved, one was made slightly worse, and in one it was made very much worse. Averaged over all forecasts, the improvement in correlation of only 0.06 is clearly not statistically significant. However, the worst three results all occurred in the same winter, i.e. with the same SST anomaly. Fig. 4 shows that, if the 15-day-mean anomaly correlations are averaged

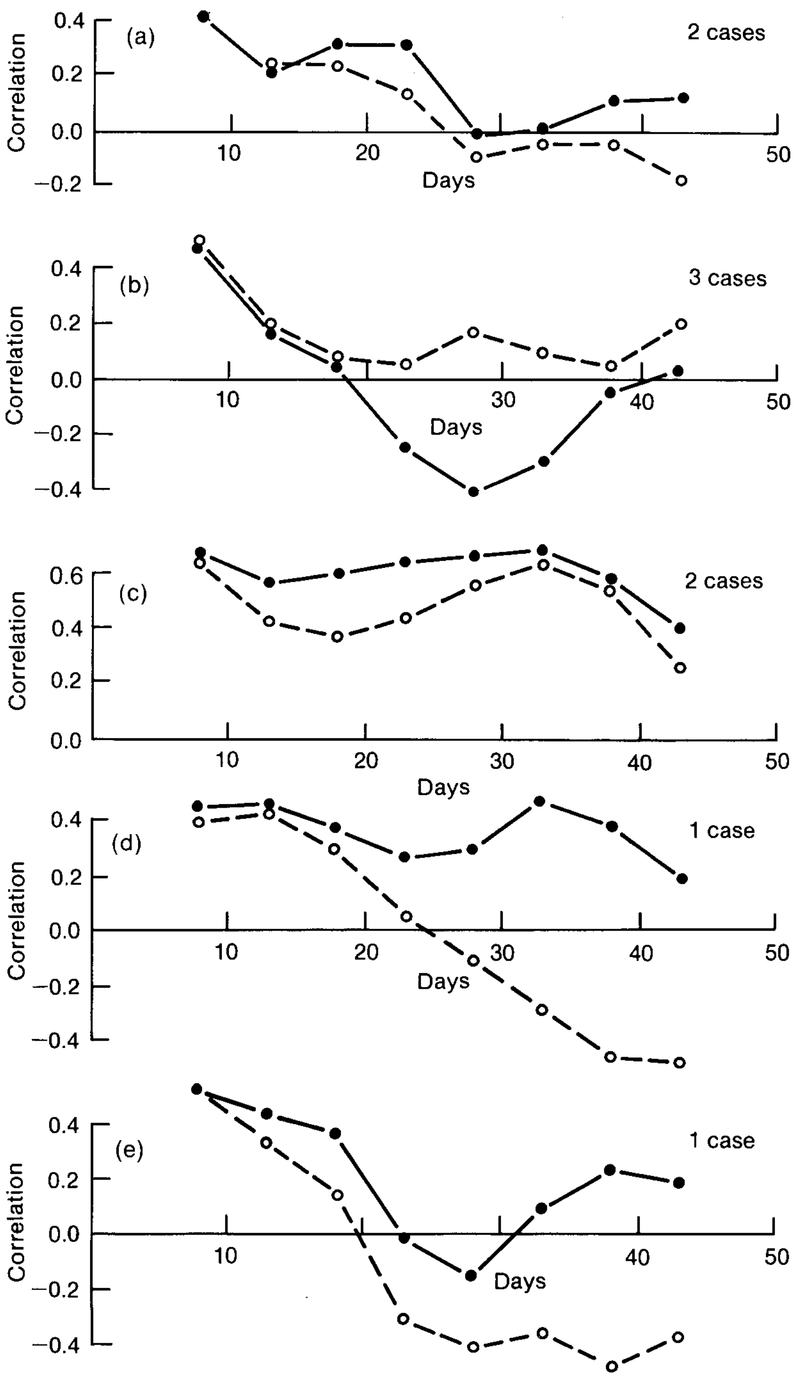

Figure 4. Anomaly correlation of 15-day-mean forecasts of 500 mb height for 30–85° N for runs with observed (solid line) and climatological (pecked line) SSTs. Results averaged over runs with the same SSTs for (a) 1975, (b) 1976, (c) 1977, (d) 1978 and (e) 1981.

for each SST pattern used, there is a clear improvement in skill in four out of five years. As might be expected, if the improvement in skill is real, there is a tendency for the improvement to increase with time. The exceptions are 1976 when there was no improvement and in 1977 where the forecasts with climatological SSTs already showed a large degree of skill.

These results suggest that the use of observed tropical SSTs will, in general, increase the skill of 50-day forecasts. There will, of course, be occasions when the reverse is true. This can occur for several reasons:

(a) The SST observations may not be representative enough, though this problem should decrease with increased reliability of satellite measurements.

(b) The effect of SSTs may be misrepresented due to inadequate parametrization of the surface exchanges or of deep convection, or due to an error in the large-scale flow field.

(c) If the forcing is weak, chance variations in the mid-latitude flow may overwhelm the effect of the SST anomaly.

4. Concluding remarks

The results presented here suggest that, on average, model forecasts of the large-scale features of the flow have a small but significant correlation with the real atmospheric evolution out to about 20 days.

The degree of extended-range skill is not uniformly spread between forecasts; five forecasts were more skilful than persistence to beyond three weeks, whereas seven were better than persistence for less than 10 days. Although it is difficult to prove, it is believed that the apparent extended skill in some forecasts is genuine and not the result of chance sampling fluctuations. An important aspect of future work will be to search for a way of detecting, a priori, forecasts which are likely to prove more skilful. To this end, experiments are being carried out in the Synoptic Climatology Branch of the Meteorological Office with ensembles of forecasts from similar initial conditions, and relationships are being sought between the degree of dispersion of the forecasts and their skill.

In the absence of other than climatological mean boundary forcing, even the largest scales must eventually become unpredictable. If, however, anomalous forcings such as those due to SST anomalies are included, this restriction may be removed and some forecast skill may be available as long as the anomalous forcing is correctly modelled. The experiments described here do show some increase in skill when observed (as opposed to climatological) SSTs are included, and in spite of the hemispheric domain this increase in skill is, on occasion, quite substantial.

Other experiments, described in Mansfield (1986), suggest that the atmosphere may be particularly sensitive to SSTs in certain areas, such as the western part of the tropical oceans. In these regions anomalies as small as 1 K or less have a significant effect on the forecast. This is close to the limit of accuracy of SST measurements in these areas and indicates that great care is needed in ensuring that the best possible SST analyses are used. It also indicates the degree of accuracy needed in ocean models before a coupled ocean–atmosphere model can be used to attempt seasonal forecasts.

These results have been achieved with a model of limited short-range skill and known deficiencies, such as a hemispheric domain and simplified physics. Outside the winter season, the model has a climatology too poor to be used for long-range forecasts. It remains to be seen what degree of skill can be obtained using global models (based on the operational and climate models) and how this skill varies with season.

References

Corby, G.A., Gilchrist, A. and Rowntree, P.R. 1977 The United Kingdom Meteorological Office five-level general circulation model. *Methods Comput Phys*, **17**, 67–110.

Mansfield, D.A. 1986 The skill of dynamical long-range forecasts, including the effect of sea surface temperature anomalies. *Q J R Meteorol Soc*, **112**, 1145–1176.

Awards

L.G. Groves Memorial Prizes and Awards

The presentation of the L.G. Groves Memorial Prizes and Awards for 1985 was made on 8 January 1987 by Major J. Groves who is the great-nephew of the founders of the memorial fund established in memory of Louis Grimble Groves. Air Vice-Marshal J.R. Walker, CBE, AFC, FBIM presided and Air Commodore P. King, CBE, FBIM (Inspector of Flight Safety) read the citations. The ceremony was also attended by members of the Groves family and representatives of the RAF and the Meteorological Office. This was the first time that the presentation had taken place in the Meteorological Office at Bracknell.

Mr J. Findlater, who has recently retired from the Meteorological Office, was awarded the Meteorology Prize for his work on fog, particularly sea fog which affects airfields in the Moray Firth area. He devised and directed 'Project Haar', an experimental study of sea and coastal fog around north-east Scotland involving a variety of new measuring techniques as well as the use of the Hercules aircraft of the Meteorological Research Flight (MRF). The results are already proving of value to local forecasters. His deep interest in aviation has been reflected by the many hours he has flown as Mission Scientist during his investigations, and by his dedication to aviation safety in much of his own work; typical of this is his membership of the UK Flight Safety Committee as representative of the Royal Meteorological Society.

The Meteorological Observer's Award was presented to Mr P. Joy of the Meteorological Office for his invaluable work as an observer on the MRF Hercules aircraft. He has flown over 1750 hours on scientific missions and there are few experiments of recent years that have not benefited from his reliability and dedication.

Mr J. Findlater, winner of the Meteorology Prize, receives his prize from Major J. Groves.

Mr P. Joy, winner of the Meteorological Observer's Award, receives his award from Major J. Groves.

Major J. Groves with Wing Commander M.W. Ball, who received the Air Safety Prize on behalf of the Tornado Operational Evaluation Unit, and Flight Lieutenant G.B. Jones, winner of the Ground Safety Award.

The Air Safety Prize was awarded to the Tornado Operational Evaluation Unit at Boscombe Down for their Head-Up Autopilot and Flight Director System. The Unit was tasked to move the indicators and selectors for the autopilot and flight director system in the Tornado to a position where they were in the pilot's field of view. The modification was designed, tested and approved, and it was so successful that it was installed in the aircraft which competed so successfully in the 1985 Strategic Air Command Bombing Competition. In developing the modification the Unit demonstrated thoroughness, both in research and engineering, in providing a solution which exceeded the criteria specified.

Flight Lieutenant G.B. Jones, also from Boscombe Down, received the Ground Safety Award for his computer produced safety trace for air weapons ranges. He devoted over 1000 hours, much of it in his own time, to developing the computer program which has now been authorized for unrestricted use in the work of the Armament Division at Boscombe Down. The Ordnance Board are examining the wider application of the program to other ranges.

Review

Intrinsic geodesy, by A. Marussi, translated from the Italian by W.I. Reilly. 160 mm × 240 mm, pp. xvii + 219, *illus*. Berlin, Heidelberg, New York, Tokyo, Springer-Verlag, 1985. Price DM 160.00.

Modern geodesy owes much to two papers, published after the Second World War, which introduced the global and local treatments of the earth's gravity field, namely M.S. Molodensky's *Investigations of the fundamental problems of geodetic gravimetry* and Antonio Marussi's *Fondementes de géométrie différentielle absolue du champ potential terrestre*. The difficult task of determining the form of the earth's surface from gravimetric data was treated by Molodensky as a boundary-value problem of potential theory. Marussi formulated the problem as one to which modern differential geometry could be applied, thus employing a vector calculus which has been termed 'intrinsic', 'absolute' or 'autonomous' by various writers.

Intrinsic geodesy reproduces 21 of Marussi's papers grouped under the headings 'Fundamentals of intrinsic geodesy' (6 papers), 'Structure of the gravity field and Laplace's equation' (2 papers), 'Principles of intrinsic geodesy applied to the normal reference field' (3 papers), 'Propagation of light in continuous isotropic refracting media' (2 papers) and 'Posthumous work' (1 paper with C. Chiaruttini). The book starts with a short appreciation of the life and work of Marussi by Professor A. H. Cook, introductory remarks by the author, who died in 1984 before the book was completed, and a preface by Dr W.I. Reilly, who translated many of the original papers from Italian into English. The book ends with an appendix on the vertical homographies of Burali-Forti and Marcolongo by Dr W.I. Reilly, a list of Marussi's scientific papers, and an obituary of Marussi by Professor H. Moritz.

Intrinsic geodesy is not a book for the mathematically faint-hearted, and its links with meteorology are less direct than they are with branches of the earth sciences that deal with gravitational tides and the structure of the solid earth. But theoretical geodesists will find much of interest in *Intrinsic geodesy*, and other mathematically-qualified scientists who read the book will have their appreciation of the subject greatly enhanced.

R.Hide

Radar photograph — 18 March 1987 at 0800 GMT

The display shows radar information from the United Kingdom, Republic of Ireland, France and Switzerland superimposed on a background field showing regions of 'cold' cloud as indicated by Meteosat. The data from the mainland of Europe have recently become available at the Meteorological Office, Bracknell following considerable software development within their Operational Instrumentation Branch.

The European Weather Radar Project, COST 73 (Co-operation in Science and Technology), is a joint project involving most countries in Europe. One of the aims is to study how a radar network might be set up across Europe. The addition of data from Northern Ireland and the Netherlands (De Bilt) is imminent, and data from the first two radars in a German network, as well as additional radars within the United Kingdom, should be available in 1988.

The picture below was taken as a cold front moved steadily southwards across western Europe ahead of a very cold polar north-westerly airstream. The rainfall, in two main bands, corresponds well with the associated region of cold cloud. Over the British Isles, showers are observed over Wales and western Ireland, whilst over the north Midlands there is a trough line present which later, following daytime heating, produced thunderstorms and hail over southern England.

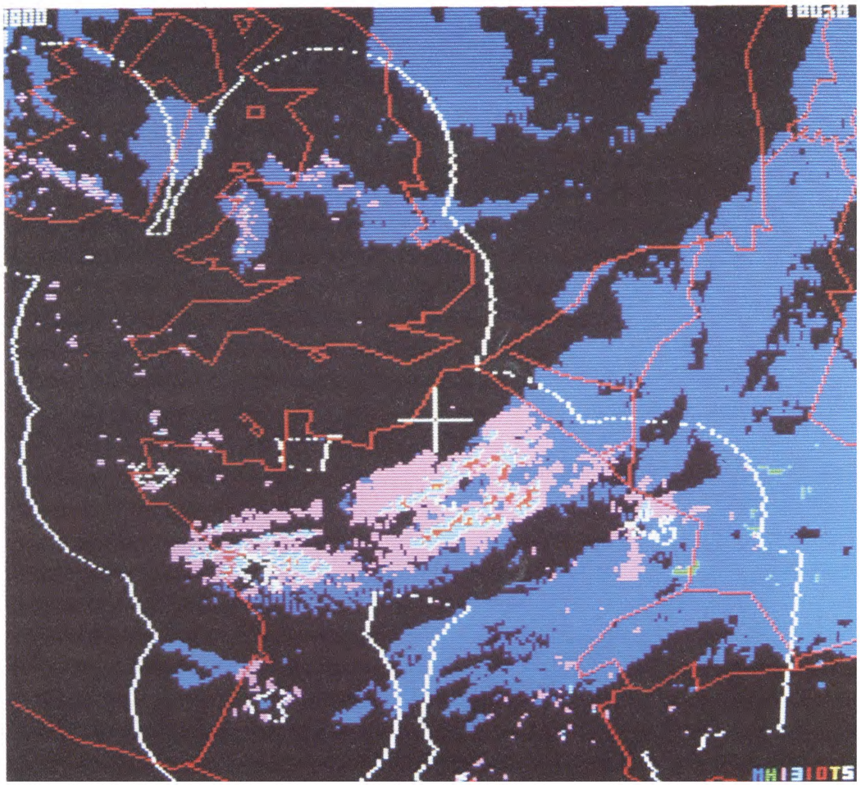

Key. Cloud: blue <-15 °C to -40 °C, green <-40 °C. Rainfall intensity: magenta 0.3 to 1 mm h^{-1}, cyan 1 to 3 mm h^{-1}, red 3 to 10 mm h^{-1}, yellow 10 to 30 mm h^{-1} and white >30 mm h^{-1}. Data resolution 5 km. Radar boundaries are shown white. (Note that permanent clutter close to the French radar sites is removed, but other clutter is not cancelled as is done in the United Kingdom).

Meteorological Magazine

GUIDE TO AUTHORS

Content

Articles on all aspects of meteorology are welcomed, particularly those which describe the results of research in applied meteorology or the development of practical forecasting techniques.

Preparation and submission of articles

Articles for publication and all other communications for the Editor should be addressed to the Director-General, Meteorological Office, London Road, Bracknell, Berkshire RG12 2SZ and marked 'For *Meteorological Magazine*'.

Articles, which must be in English, should be typed, double-spaced with wide margins, on one side only of A4-size paper. Tables, references and figure captions should be typed separately.

Spelling should conform to the preferred spelling in the *Concise Oxford Dictionary*.

References should be made using the Harvard system (author, date) and full details should be given at the end of the text. If a document referred to is unpublished, details must be given of the library where it may be seen. Documents which are not available to enquirers must not be referred to.

Tables should be numbered using roman numerals and provided with headings. We consider vertical and horizontal rules to be unnecessary in a well-designed table; spaces should be used instead.

Mathematical notation should be written with extreme care. Particular care should be taken to differentiate between Greek letters and Roman letters for which they could be mistaken. Double subscripts and superscripts should be avoided, as they are difficult to typeset and difficult to read. Keep notation as simple as possible; this makes typesetting quicker and therefore cheaper, and reduces the possibility of error. Further guidance is given in BS1991: Part 1: 1976 and *Quantities, Units and Symbols* published by the Royal Society.

Illustrations

Diagrams must be supplied either drawn to professional standards or drawn clearly, preferably in ink. They should be about 1½ to 3 times the final printed size and should not contain any unnecessary or irrelevant details. Any symbols and lettering must be large enough to remain legible after reduction. Explanatory text should not appear on the diagram itself but in the caption. Captions should be typed on a separate sheet of paper and should, as far as possible, explain the meanings of the diagrams without the reader having to refer to the text.

Sharp monochrome photographs on glossy paper are preferred: colour prints are acceptable but the use of colour within the magazine is at the Editor's discretion. In either case contrast should be sufficient to ensure satisfactory reproduction.

Units

SI units, or units approved by WMO, should be used.

Copyright

Authors wishing to retain copyright for themselves or for their sponsors should inform the Editor when they submit contributions which will otherwise become UK Crown copyright by right of first publication.

It is the responsibility of authors to obtain clearance for any copyright material they wish to use before submitting it for publication.

Free copies

Three free copies of the magazine are provided for authors of articles published in it. Separate offprints for each article are not provided.

Meteorological Magazine

May 1987

Vol. 116
No. 1378

CONTENTS

Contributions: it is requested that all communications to the Editor and books for review be addressed to the Director-General, Meteorological Office, London Road, Bracknell, Berkshire RG12 2SZ, and marked 'For *Meteorological Magazine*'. Contributors are asked to comply with the guidelines given in the *Guide to authors* which appears on the inside back cover. The responsibility for facts and opinions expressed in the signed articles and letters published in *Meteorological Magazine* rests with their respective authors. Authors wishing to retain copyright for themselves or for their sponsors should inform the Editor when submitting contributions which will otherwise become UK Crown copyright by right of first publication.

Subscriptions: Annual subscription £27.00 including postage; individual copies £2.30 including postage. Applications for postal subscriptions should be made to HMSO, PO Box 276, London SW8 5DT; subscription enquiries 01–211 8667.

Back numbers: Full-size reprints of Vols 1–75 (1866–1940) are available from Johnson Reprint Co. Ltd, 24–28 Oval Road, London NW1 7DX. Complete volumes of *Meteorological Magazine* commencing with volume 54 are available on microfilm from University Microfilms International, 18 Bedford Row, London WC1R 4EJ. Information on microfiche issues is available from Kraus Microfiche, Rte 100, Milwood, NY 10546, USA.

ISBN 0 11 727969 2 ISSN 0026–1149

Printed for HER MAJESTY'S STATIONERY OFFICE
by Delco Printing Co Ltd 5/87 Dd. 739131 C13

THE METEOROLOGICAL MAGAZINE

HER MAJESTY'S
STATIONERY
OFFICE

June 1987

Met.O.978 No. 1379 Vol. 116

METEOROLOGICAL OFFICE Met.O.978

THE METEOROLOGICAL MAGAZINE

No. 1379, June 1987, Vol. 116

551.507.362.2:551.509.58:551.515(41-4)

Application of satellite imagery in nowcasting and very short range forecasting

K.A. Browning
Deputy Director (Physical Research), Meteorological Office, Bracknell

M.J. Bader, A.J. Waters, M.V. Young and G.A. Monk
Meteorological Office, Bracknell

Summary

Meteosat imagery from the visible, infra-red and water vapour channels is used for identifying weather systems and describing their evolution and structure. The features on the imagery are related to the distribution of rainfall and other variables of concern to the forecaster. These aspects are discussed using recent case studies of cold fronts, cyclogenesis and topographically induced convection over the British Isles.

1. Introduction

Weather systems on the synoptic scale and mesoscale can be monitored using frequent Meteosat imagery; such imagery is particularly useful for describing systems over the sea and other data-sparse areas.

Meteosat imagery can be applied in several ways, some are listed below:

(a) Areas of cloud can be identified and their properties — extent, height, type and motion — determined. Very short range forecasts can be made by extrapolating these cloudy areas.

(b) Precipitation areas can be inferred from imagery by computing a calibration factor between radar-derived rainfall and co-located imagery, then applying this factor to areas outside radar coverage (Lovejoy and Austin 1979, Brown 1987).

(c) Synoptic-scale and mesoscale phenomena (depressions, fronts, convective cloud clusters and bands, etc.) can be identified from their characteristic cloud signatures in one or more spectral channels. Given an understanding of these phenomena in the form of conceptual models, cloud, precipitation and other related quantities can be inferred, enabling analyses to be enhanced.

(d) Very short range forecasts of these parameters can be made using extrapolation. Beyond the period of valid extrapolation (which is longer for systems that move at steady speeds and maintain their structure), forecasts can be produced using conceptual life-cycle models.

In this paper, some examples are given of how Meteosat imagery can identify phenomena that are forced dynamically and topographically, and how features on the imagery can be related to precipitation and other parameters.

2. Cold fronts

2.1 *The archetypes*

Meteosat imagery is helpful for interpreting the mesoscale structure and characteristics of the commonly observed cold-frontal cloud bands in mid-latitudes. Such bands, seen on the infra-red imagery as cold cloud tops thousands of kilometres long and up to hundreds of kilometres wide, fall into two main archetypes that may be distinguished by careful examination of the imagery.

These archetypes have been described in terms of conceptual models showing the principal airflows (Browning 1985) and are reproduced in Figs 1 and 2. In the first archetype (Fig. 1), the main flow of warm air — the 'warm conveyor belt' (WCB) with high wet-bulb potential temperature (θ_w) — rises rearwards relative to the advancing frontal system over dry descending air; it corresponds to the classical cold-frontal model of the Norwegian school. The cloud and rain lie on and to the rear of the surface cold front (SCF). At the front itself, the air may ascend rapidly through a layer 2–3 km deep, giving a narrow line of heavy precipitation — line convection. Behind the front, where the ascent is slower, the precipitation is lighter.

In the second archetype (Fig. 2), the WCB is overrun aloft by dry air as the warm air ascends ahead of the SCF with a component forward relative to the frontal system. The cloud and rain are therefore ahead of the SCF. Aloft, the leading edge of the dry air is called the upper cold front (UCF).

For obvious reasons, the first archetypal case is referred to as a cold front with 'rearward-sloping' ascent and the second as a cold front with 'forward-sloping' ascent. Because the second type is characterized by clearly separated upper and surface fronts, it is also referred to as a 'split' front. Examination of Meteosat imagery can help the analyst to distinguish between the two archetypes which give quite different sequences of weather relative to the surface front. An example of each is described in sections 2.2 and 2.3.

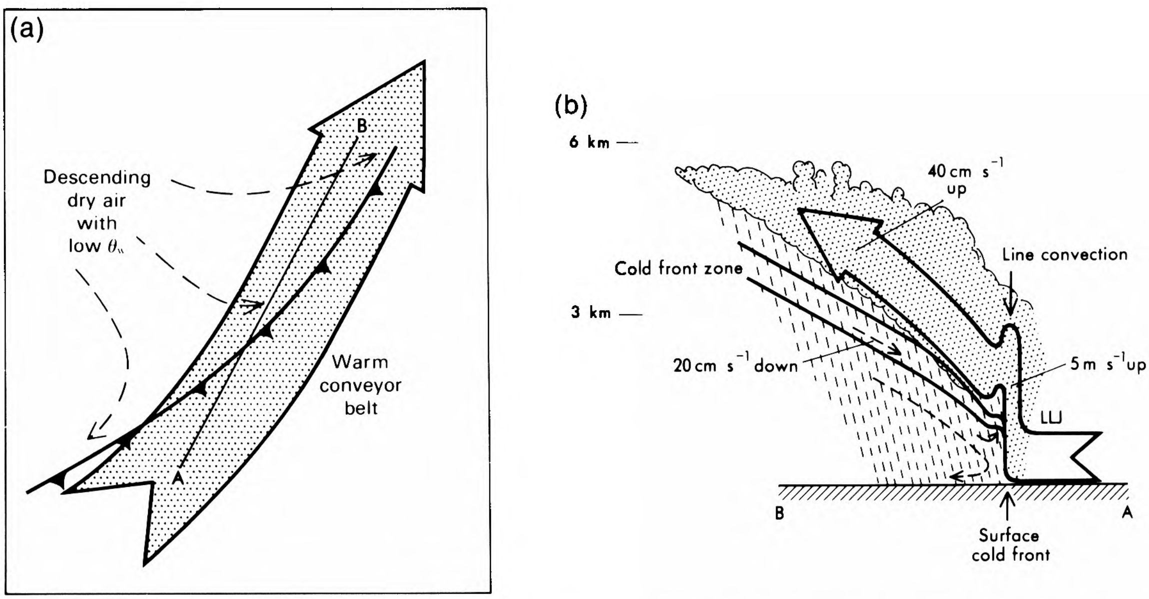

Figure 1. Schematic portrayal of the airflow in a classical ana cold front showing the warm conveyor belt (stippled arrow) undergoing rearward-sloping ascent above the cold-frontal zone. (a) Plan view. (b) Vertical section along AB in (a); flows are shown relative to the moving frontal system and LLJ marks the axis of a low-level jet (from Browning 1985).

2.2 *Example of a cold front with rearward-sloping ascent*

The main features of a rearward-sloping cold front were present on 3 September 1986 (Fig. 3). The infra-red and water vapour imagery show conspicuous coincident areas of cold cloud tops and high moisture content, both with a sharp western boundary over England and Wales (Figs 3(a) and 3(b)). (The water vapour imagery represents the moisture content of the air, typically in the middle and upper troposphere.) In this case, the SCF lies ahead of the western boundary of the upper cloud and most of the rain falls on and/or behind the SCF (Figs 3(c) and 3(d)).

According to a sequence of hourly observations from Boscombe Down (Fig. 4), rain fell for an hour or two after the south-eastward passage of the SCF, the latter being clearly shown by the customary wind veer, pressure rise, and fall in dew-point. On 3 September, there was more fine-scale structure to the rainfall than the observations in Fig. 4 suggest. According to the information from the UK weather radar network (Fig. 3(d)) there was a broken narrow band of heavy rain exceeding 8 mm h^{-1} in places along the SCF. Indeed, an autographic rain-gauge trace close to London measured a short burst of very heavy rain — 17 mm h^{-1} over 5 minutes — at about the time of the radar picture, followed by 1–2 hours of lighter rain. This heavy rain was related to cloud that, according to the infra-red picture, was not particularly cold (tops about −20 °C), so satellite imagery is insufficient by itself for pinpointing the heavy rain. All these observations are consistent with the conceptual model (Fig. 1) depicting vigorous convection of limited depth in the form of line elements at the SCF and gentler slantwise ascent behind.

The vertical structure of 3 September is depicted in Fig. 5. The radiosonde sounding ahead of the SCF at Camborne (south-west England) at 0000 GMT shows that the air is stable and moist — especially up to 600 mb. Relative to the moving front there is a wind component perpendicular to and blowing to the rear of the front, especially above 800 mb and around 900 mb. According to the 0000 GMT numerical fine-mesh model analysis (Fig. 6), the air with highest θ_w lies just ahead of the SCF. The isopleths of θ_w slope rearwards and the dry air aloft is well behind the SCF as depicted by the water vapour imagery. Although not shown, the region of strongest ascent is over the SCF. These characteristics are consistent with those presented in the conceptual model.

If the high-cloud canopy is not extensive, as in a weaker front, bright areas within the frontal-cloud band seen on the visible imagery (if available) may be useful for identifying the main areas of rain. An

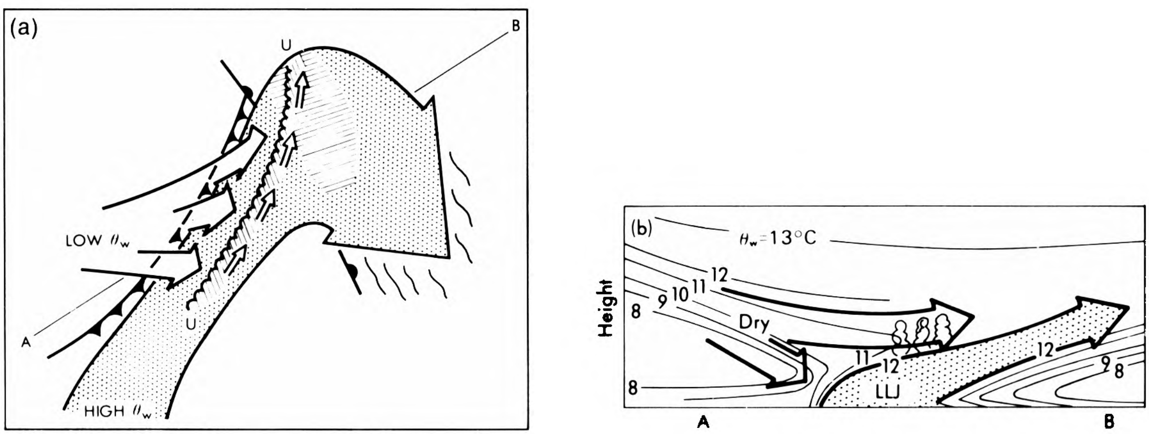

Figure 2. Schematic portrayal of the airflow in a cold front in which the warm conveyor belt (stippled arrow) undergoes forward-sloping ascent. (a) Plan view showing the separate upper cold front UU and the surface cold front producing the split front; hatched shading denotes precipitation. (b) Vertical section along AB in (a); LLJ denotes a low-level jet (from Browning 1985).

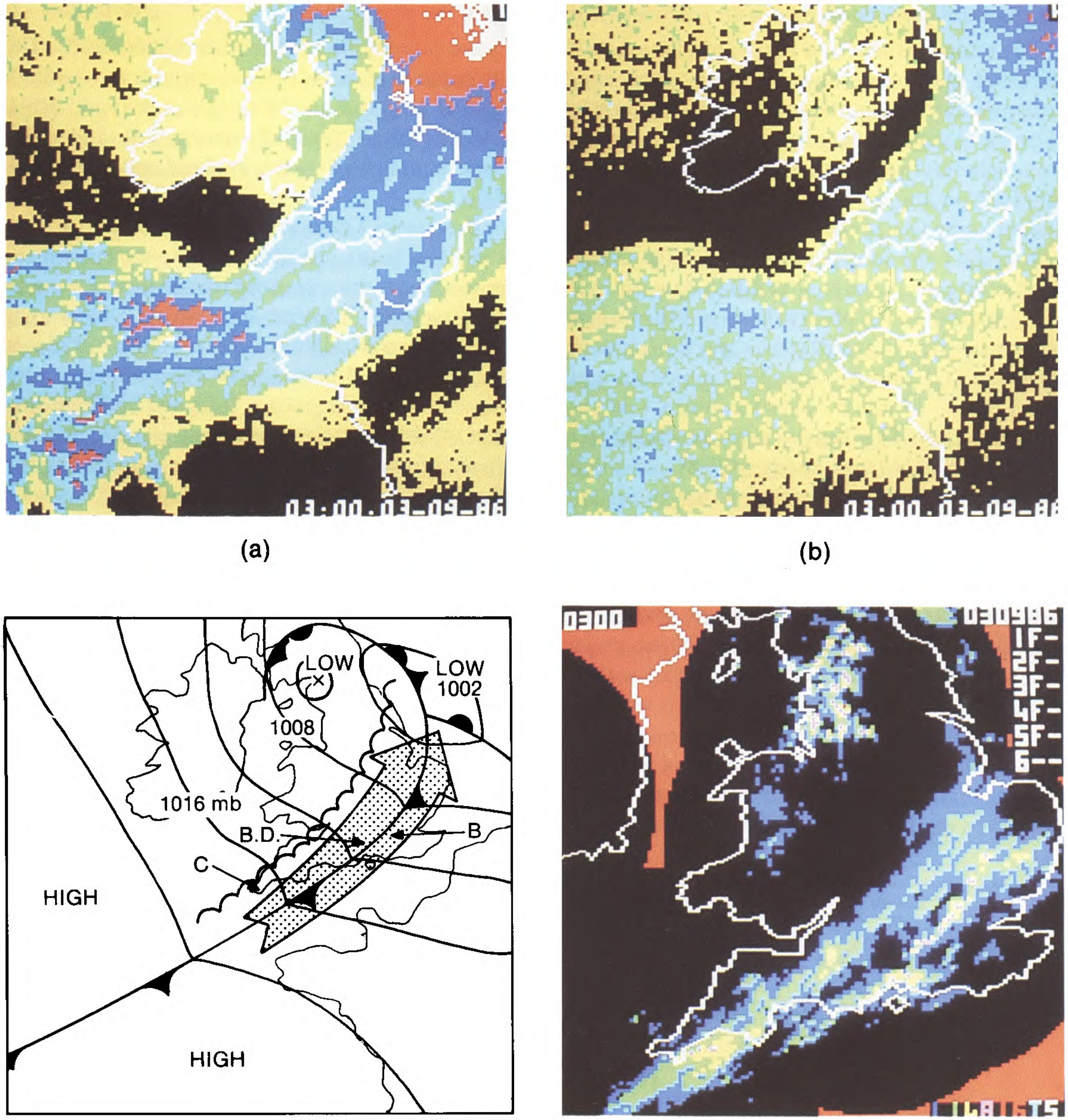

Figure 3. False-colour Meteosat imagery, surface analysis and weather radar imagery for 0300 GMT on 3 September 1986 showing a cold front with rearward-sloping ascent. (a) Infra-red image indicating cloud-top temperatures as follows: white $\leqslant -40$ °C, red $\leqslant -30$ °C, dark blue $\leqslant -20$ °C, light blue $\leqslant -10$ °C, green $\leqslant 0$ °C, yellow $\leqslant 10$ °C and black > 10 °C. (b) Water vapour image; black indicates dry air and red the moistest air. (c) Surface analysis with the warm conveyor belt shown by the stippled arrow and the upper cold front by the cusped line; B indicates Bracknell, B.D. Boscombe Down and C Camborne. (d) Rainfall distribution from the UK weather radar network with intensities shown as follows: red $\geqslant 16$ mm h^{-1}, pink $\geqslant 8$ mm h^{-1}, yellow $\geqslant 4$ mm h^{-1}, green $\geqslant 1$ mm h^{-1} and blue < 1 mm h^{-1}. The red areas near the corners are outside radar coverage and do not indicate rain. The numbers and letters in the top right-hand corner refer to radar sites, real-time calibration and bright-band height. For further information see Blackall (1985).

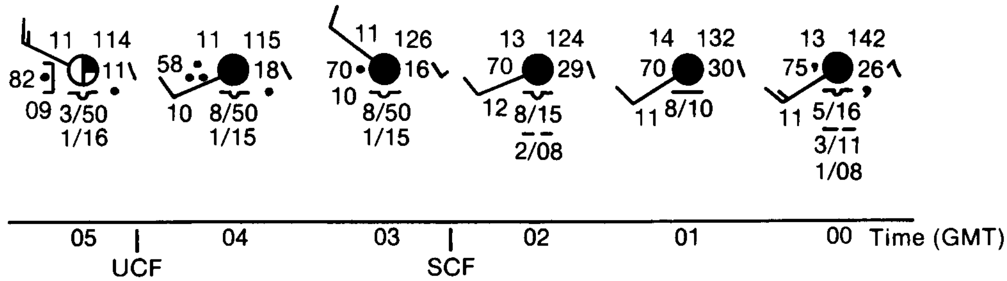

Figure 4. Synoptic observations at Boscombe Down (B.D. in Fig. 3(c)) between 0000 and 0500 GMT on 3 September 1986. Passage of the surface cold front and the upper cold front are marked as SCF and UCF.

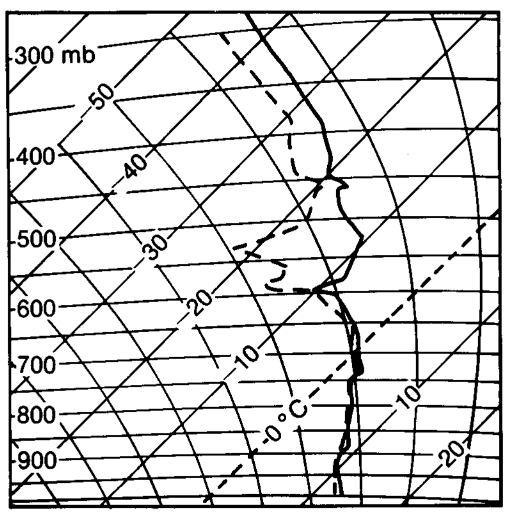

Measured wind	Rearward perpendicular wind component
255/72	2
255/63	6
255/63	6
255/53	12
260/43	13
270/39	7
285/40	1
280/32	9

Figure 5. Tephigram and winds (kn) for Camborne (C in Fig. 3(c)) at 0000 GMT on 3 September 1986, ahead of the surface cold front.

example is shown in Fig. 7(a) along with the associated infra-red and weather radar imagery and the surface analysis (Figs 7(b), 7(c) and 7(d)). As in the previous case, the rain falls at and behind the SCF (Figs 7(c) and 7(d)). However, since there is little cold cloud ahead of the front, the SCF is close to the forward edge of the band, clearly seen on the infra-red imagery (Fig. 7(b)).

2.3 *Example of a cold front with forward-sloping ascent (split cold front)*

Meteosat imagery for a forward-sloping case is shown in Fig. 8. At 1200 GMT on 1 August 1986 well-defined cloud-top temperature and moisture gradients are present just west of the United Kingdom and France (Figs 8(b) and 8(c)) and correspond to the UCF (see analysis in Fig. 8(d)). A second but less steep temperature boundary is located some tens of kilometres behind. This second boundary coincides with a very well-defined edge on the visible imagery (Fig. 8(a)) and corresponds to the surface cold front (see Fig. 8(d)).

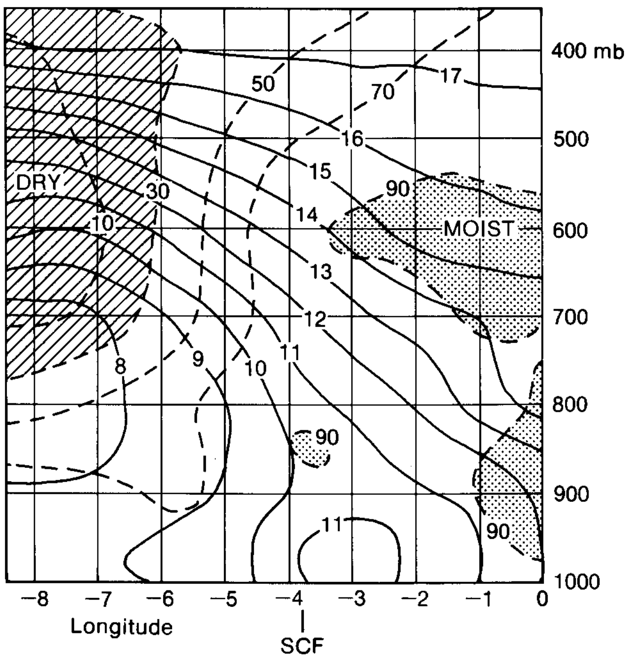

Figure 6. Vertical section through the cold front at 0000 GMT on 3 September 1986 (taken from west to east from southern Ireland, through central Wales to near London from the numerical fine-mesh model) showing wet-bulb potential temperature (°C) as solid lines, and relative humidity (%) as dashed lines. The stippling shows areas of relative humidity ⩾ 90% and the hatching ⩽ 30%.

Successive imagery showed these basic patterns being preserved and by 1800 GMT (Fig. 9), as the frontal system moved eastwards over the United Kingdom, the radar rainfall imagery could be used to relate the rainfall to the cloud structure.

The visible imagery (Fig. 9(a)) shows brighter cloud along and ahead of the UCF being highlighted by the low sun angle. According to the radar imagery (Fig. 9(c)) most of the precipitation falls near and ahead of the UCF. Between the UCF and the SCF, in a zone with high moisture content at low levels but with relatively warm cloud-top temperatures (Fig. 9(b)), there was little radar-detectable rain, but surface observations showed extensive drizzle, especially over hills where there was orographic uplift and perhaps the release of potential instability at the top of this 'shallow moist zone' (SMZ). In this case the precipitation ceased at the surface cold front with cloud rapidly breaking to a more convective type. The sequence of hourly observations at St. Mawgan (Fig. 10) shows clearly the passage of the 'split' front. The important features are:

Ahead of the UCF	:	Moderate or heavy rain.
In the SMZ	:	Rain and drizzle, low cloud, maximum dew-point.
Behind the SCF	:	Cessation of rain and drizzle, lifting and breaking of low cloud, decrease of dew-point.

The radiosonde ascent at Crawley (south-east England) for 0000 GMT on 2 August 1986 was just ahead of the SCF and is typical of the structure of the air in the SMZ between the UCF and SCF (Fig. 11). In this case, the top of the SMZ was at 740 mb (approximately 3 km) where the air temperature was about 5 °C. This corresponds well with the cloud-top temperature behind the UCF on the infra-red imagery. The dry air above the SMZ is well shown. The component of wind perpendicular and relative

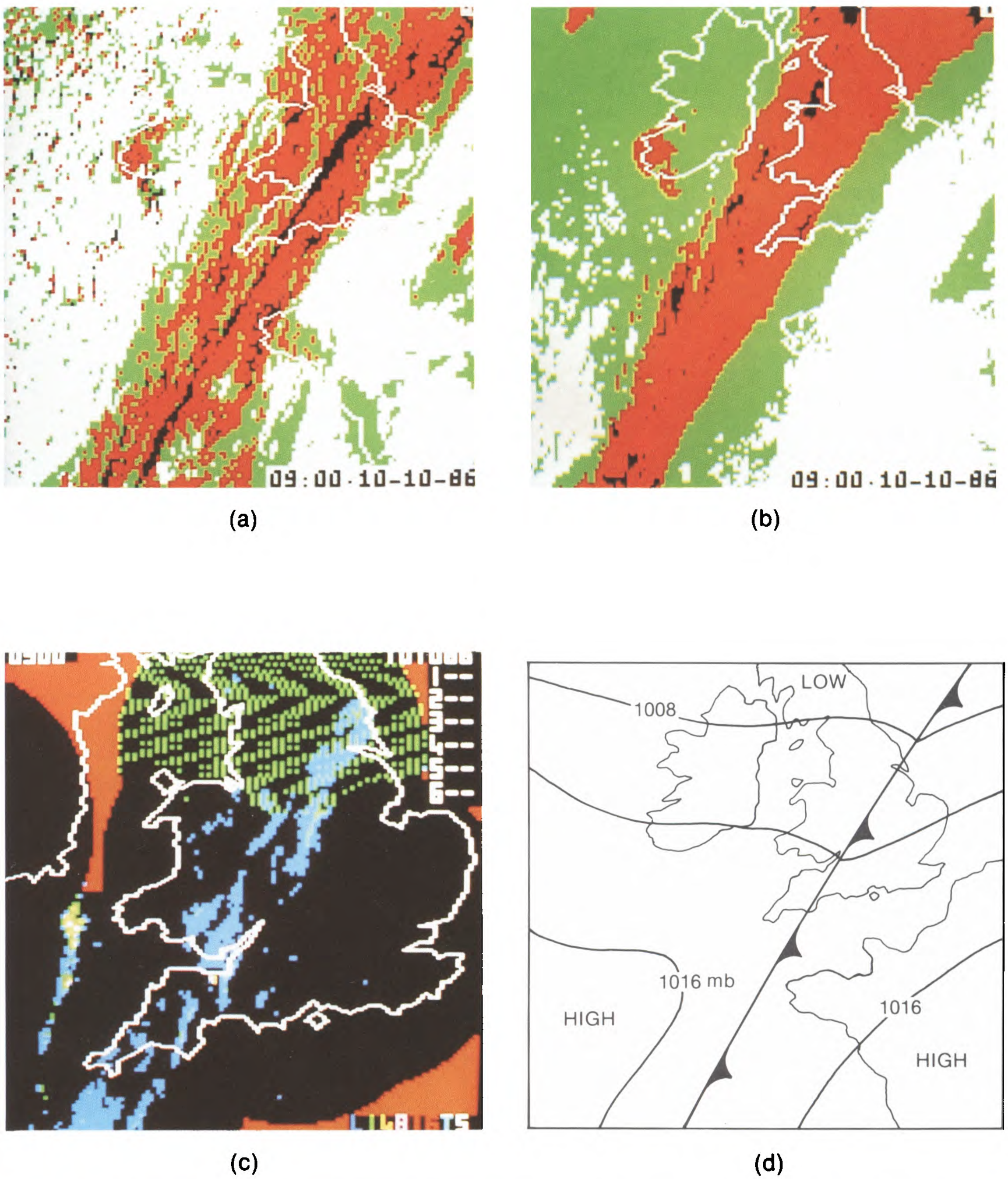

Figure 7. False-colour Meteosat imagery, weather radar imagery and surface analysis for 0900 GMT on 10 October 1986 showing a cold front with rearward-sloping ascent. (a) Visible image; black represents the thickest cloud and green the thinnest cloud. (b) Infra-red image indicating cloud-top temperatures as follows: black $\leqslant -30$ °C, red $\leqslant -10$ °C, green -10 to $\leqslant 10$ °C and white > 10 °C. (c) Rainfall distribution from the UK weather radar network; legend as Fig. 3(d). The areas of green over northern England are interference and should be ignored. (d) Surface analysis.

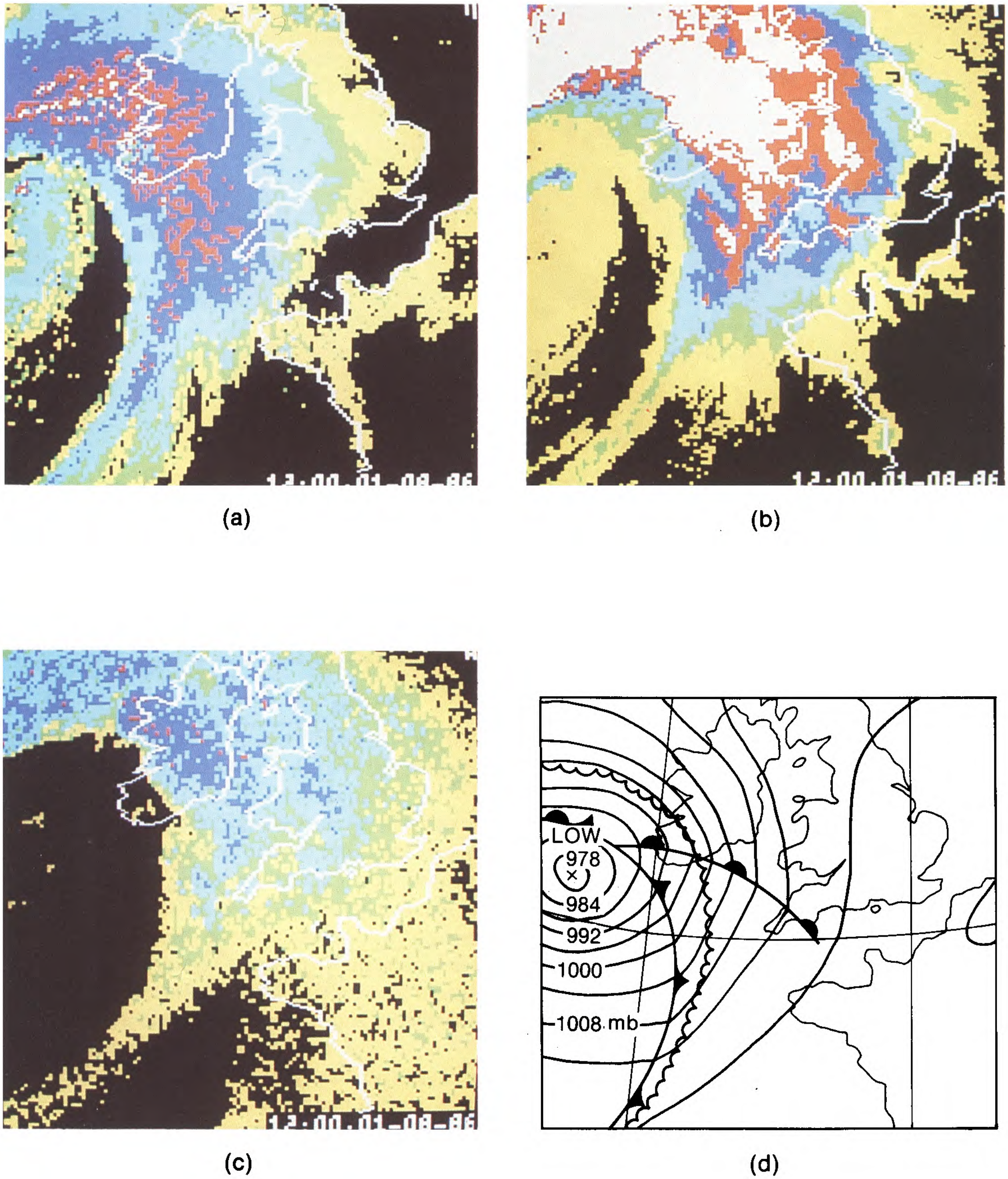

Figure 8. False-colour Meteosat imagery and surface analysis for 1200 GMT on 1 August 1986 showing a cold front with forward-sloping ascent. (a) Visible image; red represents the thickest cloud and yellow the thinnest cloud. (b) Infra-red image; legend as Fig. 3(a). (c) Water vapour image; legend as Fig. 3(b). (d) Surface analysis; the cusped line is the upper cold front.

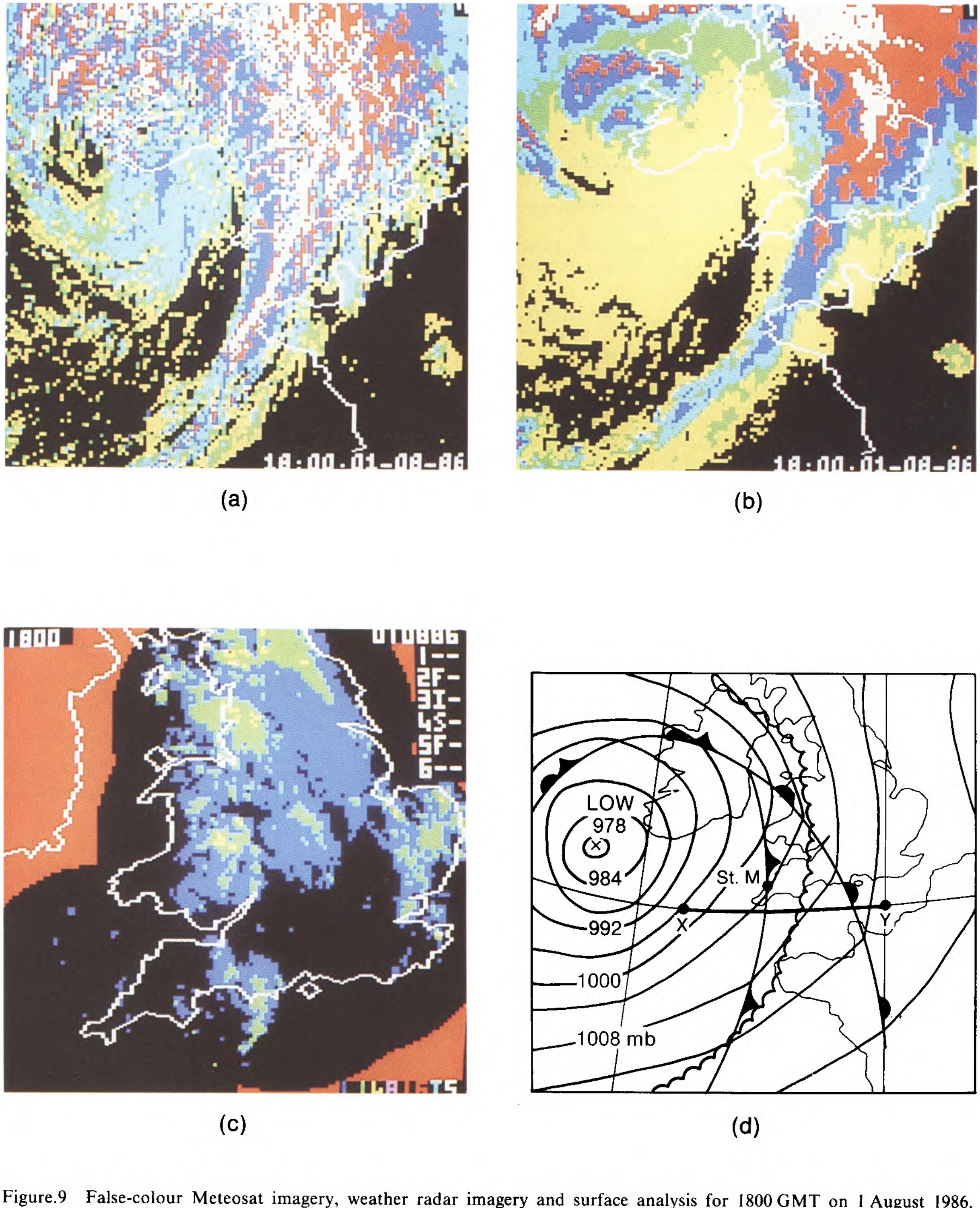

Figure.9 False-colour Meteosat imagery, weather radar imagery and surface analysis for 1800 GMT on 1 August 1986. (a) Visible image; legend as Fig. 8(a). (b) Infra-red image; legend as Fig. 3(a). (c) Rainfall distribution from the UK weather radar network; legend as Fig. 3(d). (d) Surface analysis; XY marks the cross-section shown in Fig. 12 and the cusped line the upper cold front. St. M. indicates St. Mawgan.

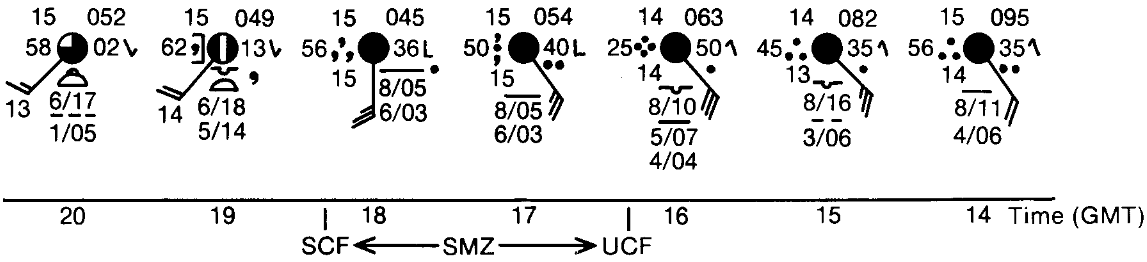

Figure 10. Synoptic observations at St. Mawgan (St. M. in Fig. 9(d)), between 1400 and 2000 GMT on 1 August 1986. Passage of the upper cold front, shallow moist zones and surface cold front are marked as UCF, SMZ and SCF.

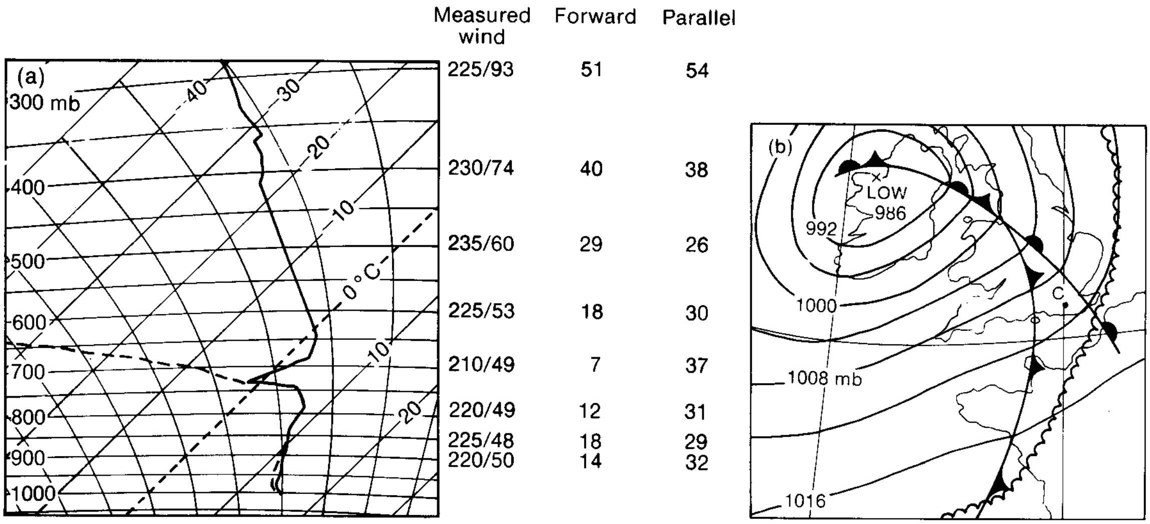

Measured wind	Forward	Parallel
225/93	51	54
230/74	40	38
235/60	29	26
225/53	18	30
210/49	7	37
220/49	12	31
225/48	18	29
220/50	14	32

Figure 11. (a) Tephigram, winds and wind components (kn) relative to the moving SCF for Crawley at 0000 GMT on 2 August 1986, representative of the air in the shallow moist zone. (b) Surface analysis for 0000 GMT on 2 August 1986; the cusped line is the upper cold front and C indicates Crawley.

to the moving SCF is forward at all levels. The component parallel to the SCF shows a maximum of 32 kn at 900 mb (near 1 km), consistent with the idea of a low-level jet shown in the conceptual model (Fig. 2).

Output from the operational fine-mesh model (Fig. 12) confirms many of the features described above. It shows the forward-sloping zone of air with high θ_w and the leading edge of dry, low θ_w air at 700 mb (approximately 3 km) at the position of the UCF, with the highest θ_w at the surface occurring some distance behind, between the position of the UCF and the SCF.

3. Example of cyclogenesis

3.1 *Large-scale evolution*

The Meteosat infra-red picture in Fig. 13 shows an example of an incipient frontal wave. At 0000 GMT on 10 June 1986 a band of frontal cloud with coldest tops stretching south-westwards from the United Kingdom to the Bay of Biscay exhibited a convex rear edge, indicating the presence of a wave. To the west was a cluster of lumpy (convective) cloud, a feature accompanying a well-marked upper-air trough, often seen close to frontal waves.

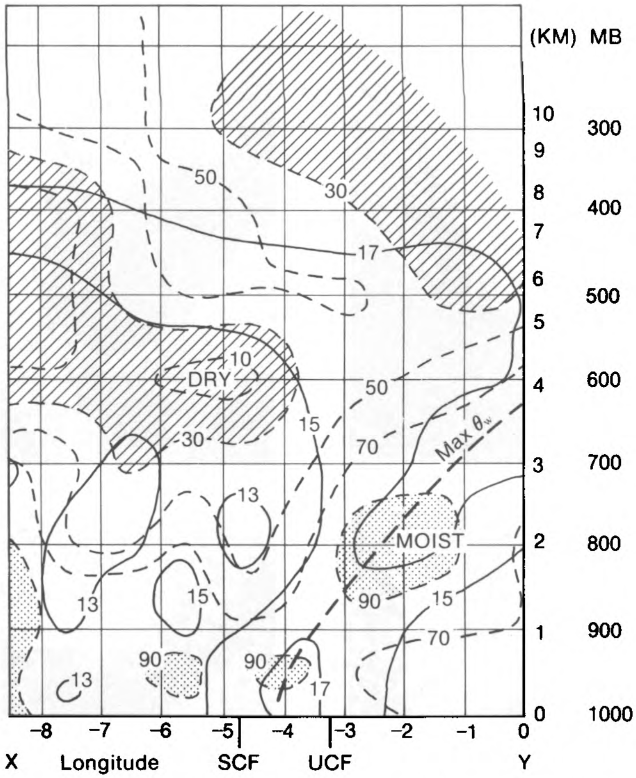

Figure 12. Vertical section through the front at 1800 GMT on 1 August 1986 along the line XY in Fig. 9(d) from the numerical fine-mesh model. Legend as Fig. 6.

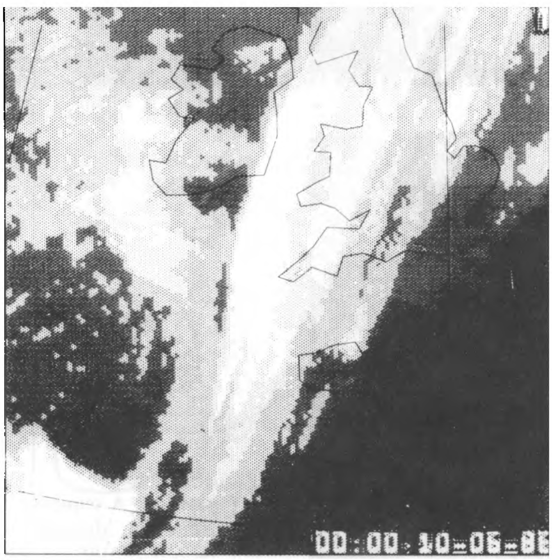

Figure 13. Meteosat infra-red image for 0000 GMT on 10 June 1986. White areas represent cloud tops colder than −30 °C. Successively darker areas represent warmer temperatures in steps of 10 °C.

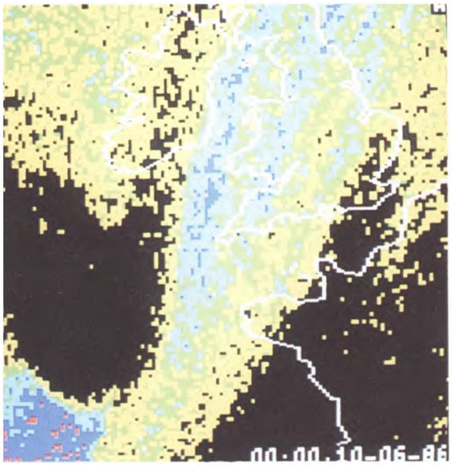

(a)

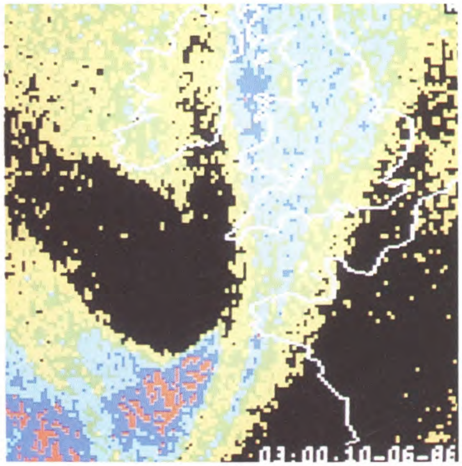

(b)

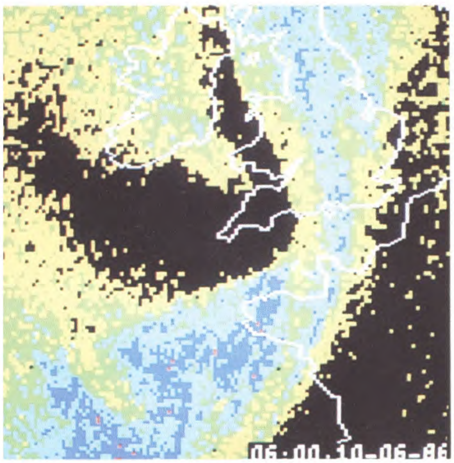

(c)

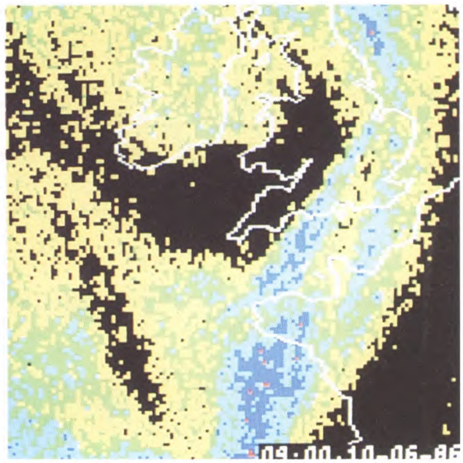

(d)

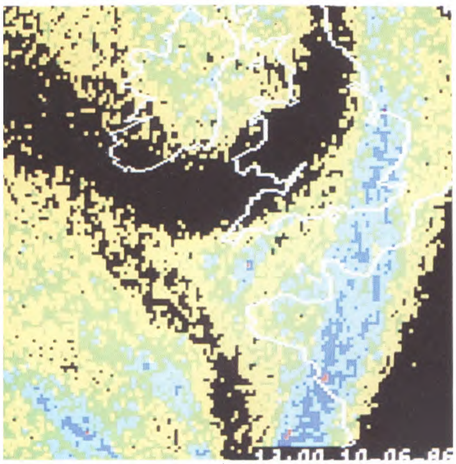

(e)

Figure 14. A sequence of images on 10 June 1986 from the Meteosat water vapour channel for (a) 0000, (b) 0300, (c) 0600, (d) 0900 and (e) 1200 GMT. Legend as Fig. 3(b).

3.2 *Evolution and mesoscale characteristics*

The evolution of the developing wave is shown in the sequence of five water vapour pictures from Meteosat taken 3 hours apart (Fig. 14). Between 0000 and 0600 GMT the convex western edge of the wave increased its curvature, and the associated medium- and upper-level cloud over the British Isles broadened and rotated cyclonically. Meanwhile, moistening of the air within the bulge indicates that ascent was taking place.

On the mesoscale the most notable feature in Fig. 14 is the north-eastward surge of dry upper-tropospheric air into the developing wave. The location of the initial surge of dry air off south-west England becomes apparent between 0000 and 0300 GMT. By 0600 GMT a nose of dry air begins to intrude into the north–south band of frontal moisture; this intrusion pushes on to the east coast of England by 0900 GMT and out over the North Sea by 1200 GMT, and forms a narrow cloud-free slot within the, by now, comma-shaped cloud mass. Fig. 15 shows that the largest pressure falls occur at the leading edge of this dry tongue, and is similar to the case described by Young *et al.* (1987). The surge of dry air aloft overtakes the SCF and in doing so the front evolves from a classical ana cold front with rearward-sloping ascent before 0000 GMT, to a split front, with the upper-level moisture boundary advancing ahead of the SCF.

Identification of such patterns on imagery can, given correct interpretation, provide some useful early information on the weather characteristics when the system is in a data-sparse area, and especially before it reaches the weather radars and synoptic network of north-west Europe.

A closer look at the infra-red and visible imagery identifies sub-synoptic-scale features that help to determine detail about the precipitation patterns not supplied by conventional analysis. At 0000 GMT the SCF and rainfall were located close to the forward side of the coldest tops seen in Fig. 13. However, as the dry air aloft began to push eastward (Fig. 14) and overrun the western edge of the frontal cloud, the cloud-top temperature in the southern part of the wave develops a step function structure as the cold

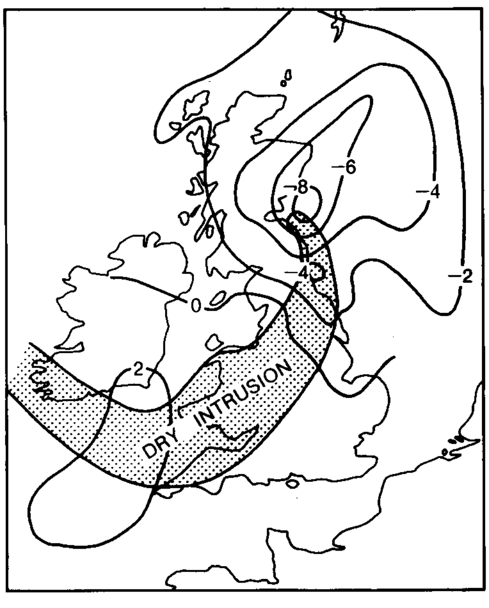

Figure 15. Dry air intrusion (stippled) from the Meteosat water vapour channel, and pressure tendencies (mb) from 0900 to 1200 GMT on 10 June 1986.

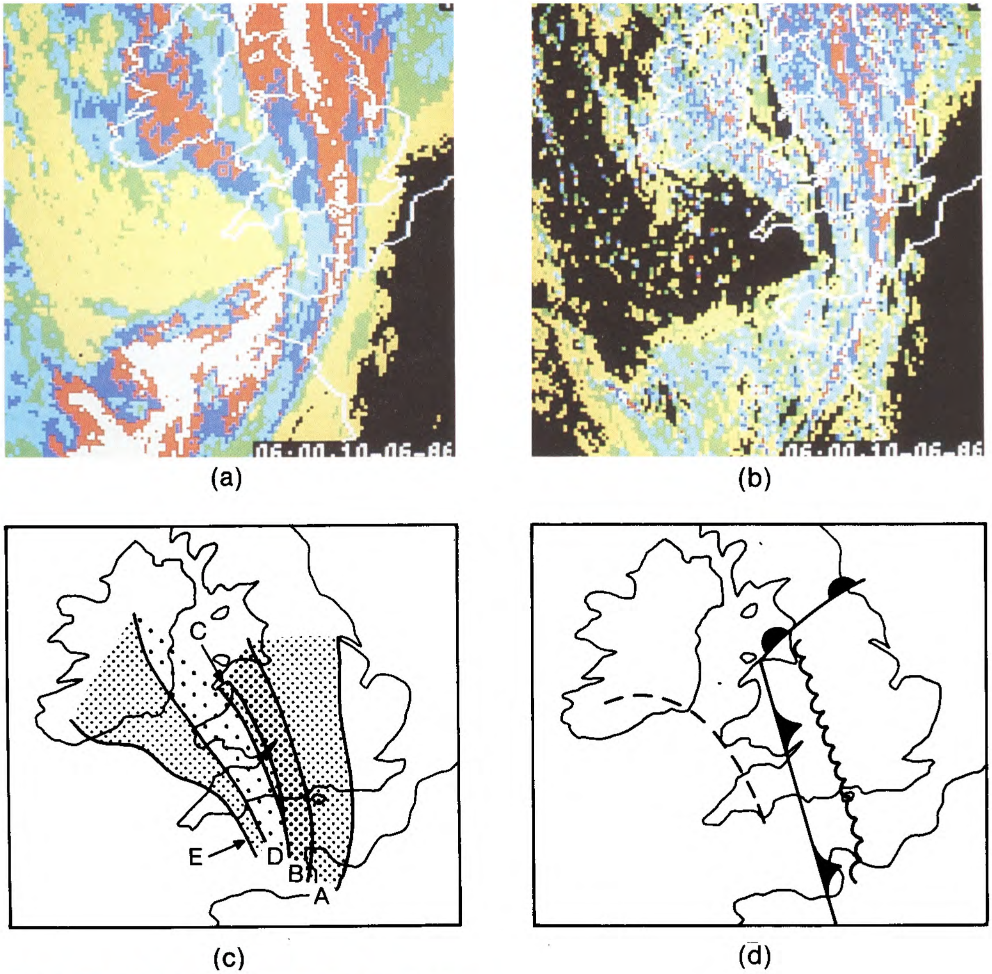

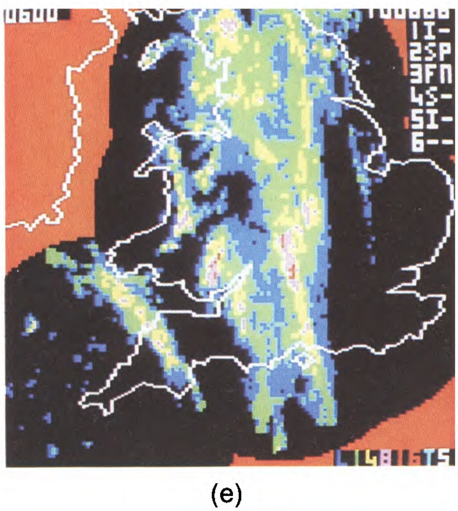

'igure 16. False-colour Meteosat imagery, surface analyses and weather radar imagery for 0600 GMT on 10 June 1986. (a) Infra-red image; legend as Fig. 3(a). (b) Visible image; legend as Fig. 8(a). (c) Schematic diagram from (a) and (b) showing the main cloud zones (dense stippling) south of the depression centre. (d) Analysis of the main features; the cusped line is the upper cold front and the dashed line the post-frontal trough. (e) Rainfall distribution from the UK weather radar network; legend as Fig. 3(d).

front acquired split frontal characteristics of the kind described in section 2.3. Now consider the Meteosat imagery, surface analysis and weather radar imagery at 0600 GMT (Fig. 16). The infra-red imagery (Fig. 16(a)) shows the following five distinct zones (Fig. 16(c)):

Zone A : A band of cold cloud tops lying north-north-west to south-south-east across central England; the western edge marks the UCF. Ahead of the UCF (Fig. 16(d)) lies a band of moderate and occasionally heavy rain (Fig. 16(e)).

Zone B : A band of warmer cloud tops lying north-north-west to south-south-east to the west of Zone A with less-heavy rain (Fig. 16(e)) — the SMZ. The visible imagery (Fig. 16(b)) shows the cloud in the SMZ to be of limited depth.

Zone C : A narrow band of colder tops and thicker cloud along the rear edge of Zone B — the SCF (easily located from the wind and pressure observations). Rainfall intensity is enhanced along a line from North Wales to the Severn estuary.

Zone D : A zone with no cold cloud.

Zone E : A band of cold cloud tops from Ireland to south-west England — a post cold-frontal trough.

The post cold-frontal trough was responsible for a very well-defined line of showery rain extending into south-west England seen from both radar (Fig. 16(e)) and surface observations. In this case the line of cloud remained separate from the main frontal-cloud canopy. In other cases such a cloud line may combine with a frontal wave tip, forming a so-called instant occlusion.

3.3 *Features on the imagery related to the release of potential instability beneath the dry intrusion*

The overrunning of dry air shown in Fig. 14 has been well simulated in the analysis of the fine-mesh numerical forecast model (Fig. 17(a)), especially over England and Wales. It is therefore possible to use the model products for interpreting features on the imagery. One seemingly anomalous feature which the model helps us to understand is the abundance of rain between the UCF and the SCF. Normally in this zone the cloud tops are no higher than 2 or 3 km, as in the example in section 2.3, producing rain and drizzle. In this case, however, the tops were about 5 km. There were no soundings that show the vertical structure of the air in this zone, but ascents from the numerical forecast model show that potential instability was present up to 770 mb and the air moist up to about 600 mb (4 km), approximately in agreement with the observations of cloud top. General lifting of this air as indicated by the model was probably responsible for the moderate and heavy rain on, and ahead of, the SCF.

Fig. 18 shows that another feature of this case was the development of abundant convective showers behind the SCF. Thus by 1100 GMT (Fig. 18(b)) an area of heavy convective showers had developed over north-west England. The tops had temperatures less than −30 °C (Fig. 18(a)) and were high enough to be revealed in the water vapour imagery (Fig. 14). Evidence from the numerical model suggests that these convective showers were caused by the release of potential instability within a region of ascent (Fig. 17(b)) where the belt of high θ_w air ahead of the SCF was being overrun by the low θ_w air in the dry intrusion. Heavy rain has also been observed in other cyclogenesis cases within the forward portion of the dry intrusion, due to the lifting of potentially unstable air from within the SMZ.

Although the showers were heaviest in the Lake District where they were sustained by high θ_w air, showers also occurred extensively throughout much of the region overrun by the dry intrusion. The cloud-top temperatures for these showers were about −10 °C, corresponding to a height of about 3 km; too low to be seen on the water vapour imagery but deep enough to give rainfall rates of several millimetres per hour. The showers were situated within an area of ascending air as shown by the model (Fig. 17(b)).

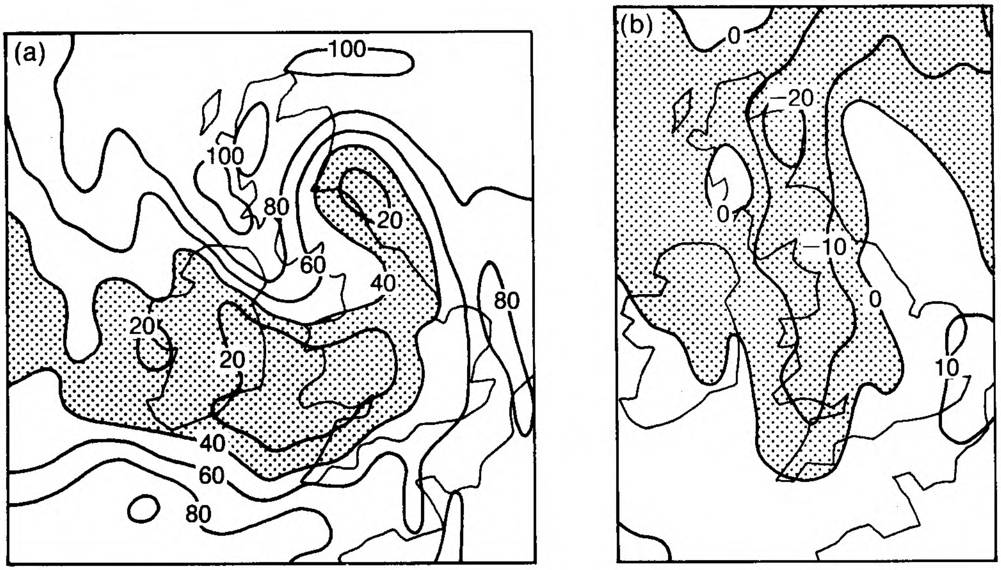

Figure 17. Numerical fine-mesh forecast model analysis for 1200 GMT on 10 June 1986. (a) 400 mb relative humidity (%); the stippled areas denote values $\leqslant 40\%$. (b) 800 mb vertical velocity (mb h^{-1}); the stippled areas denote ascending air.

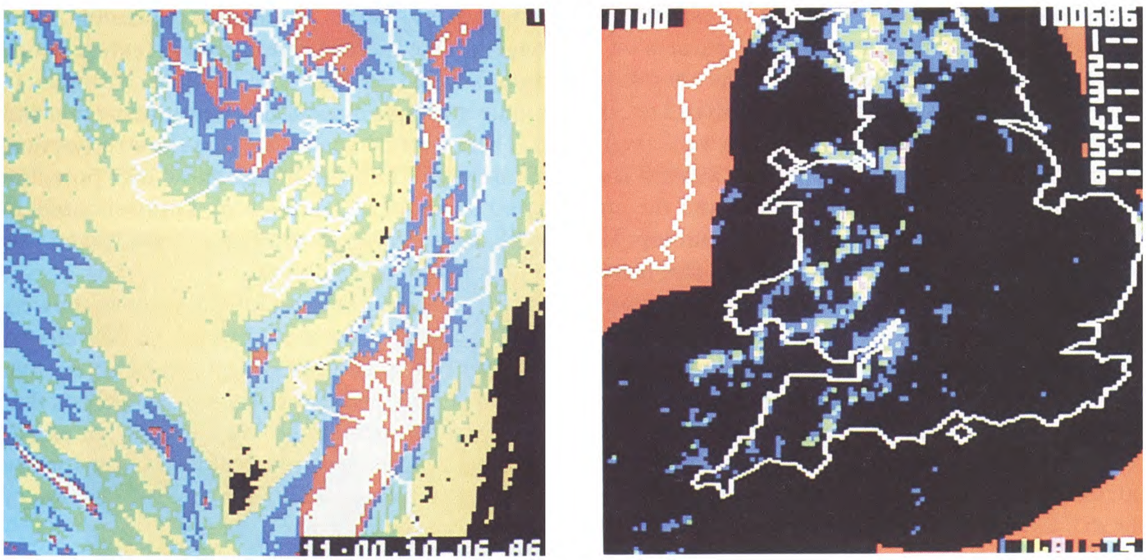

(a) (b)

Figure 18. False-colour Meteosat and weather radar imagery for 1100 GMT on 10 June 1986. (a) Infra-red image; legend as Fig. 3(a). (b) Rainfall distribution from the UK weather radar network; legend as Fig. 3(d): The important feature in (a) is the area of cold cloud tops over north-west England, correlated with the area of heavy rain in (b). The line of cold cloud tops from south-east England to north-west France is mostly non-precipitating high cloud.

4. Topographically induced systems

So far, systems produced by synoptic forcing have been discussed. However, because of its complex topography, the United Kingdom is very prone to persistent bands of convective cloud that develop in unstable airstreams during periods of weak synoptic forcing. The cloud bands are preferred areas of moist convection only a few tens of kilometres wide, but sometimes extending to many hundreds of kilometres in length. They may occur as the only cloud within an otherwise cloudless region, or as an organized band of vigorous convection within a larger region of weaker convection. Meteosat imagery clearly identifies such bands and their evolution, and indicates that their formation is related to topography. In addition to identifying such bands over the sea, the imagery can add considerably to the information from the routine synoptic network over land, where even a relatively dense network may not resolve the existence of such narrow bands.

Cloud bands with different locations and orientations, depending on wind direction, are frequently observed within unstable polar air masses over and around the United Kingdom. During the winter half of the year when the sea is warmer than the land, bands are initiated over the sea and little diurnal variation in their intensity may be apparent. A common location for such bands over the British Isles is downwind of the North Channel, between Scotland and Ireland, when the wind direction is between west-north-west and north. A number of cases were described in Browning *et al.* (1985).

In the summer half of the year, during the afternoons when the land becomes warmer than the sea, bands are seen to form over the land. In south-westerly polar maritime air masses, sea-breeze circulations frequently produce zones of convergence along the length of the peninsulas in south-west England and Wales, as described in Satellite and Radar Studies Group (1986).

In north-westerly airstreams, a band of cloud sometimes develops along a 350 km stretch of the east coast of England during the afternoon in spring and summer. Occasionally it may develop into a line of deep cumulonimbus cells that forms initially at about midday and persists throughout the afternoon. A typical example of the latter is shown in Fig. 19; isolated cumulonimbus close to the east coast of England and over the North Sea prior to 1200 GMT quickly develop into an organized line along a zone of low-level convergence adjacent to the east coast. The line is thought to form because in an unstable north-westerly air mass (Fig. 20(a)) winds are parallel to the coast and differential friction between land and sea, possibly aided by orographic deflection over south-east Scotland, combines with a sea-breeze circulation to give a zone of low-level convergence (Fig. 20(b)). Under these conditions, successive cells follow the same track and remain within the zone of convergence for perhaps several hours. However, cells appear to decay only slowly on emerging from the convergence zone, leading to progressive extension of the band south-eastwards across the southern North Sea towards the Low Countries.

Vigorous showers were associated with the band, and reports of thunder were widespread. Over eastern England at 1500 GMT, the time of peak intensity, there was a continuous line of radar echoes (Fig. 19(d)) along the western edge of the coldest cloud tops. Places lying beneath the band received a succession of showers giving total rainfall accumulation of greater than 10 mm, whilst places a few kilometres to the west had a dry afternoon.

5. Conclusion

The examples discussed have demonstrated that the mesoscale characteristics of weather systems can be identified from Meteosat imagery and that the observed structure and evolution of these systems can be explained in terms of simple concepts that convey the important dynamical and physical processes at work. These concepts, illustrated in the form of schematic diagrams showing principal airflows, can be used for relating features on imagery to 'weather' for different phenomena. This improved interpretation should provide a valuable aid for very short range forecasting.

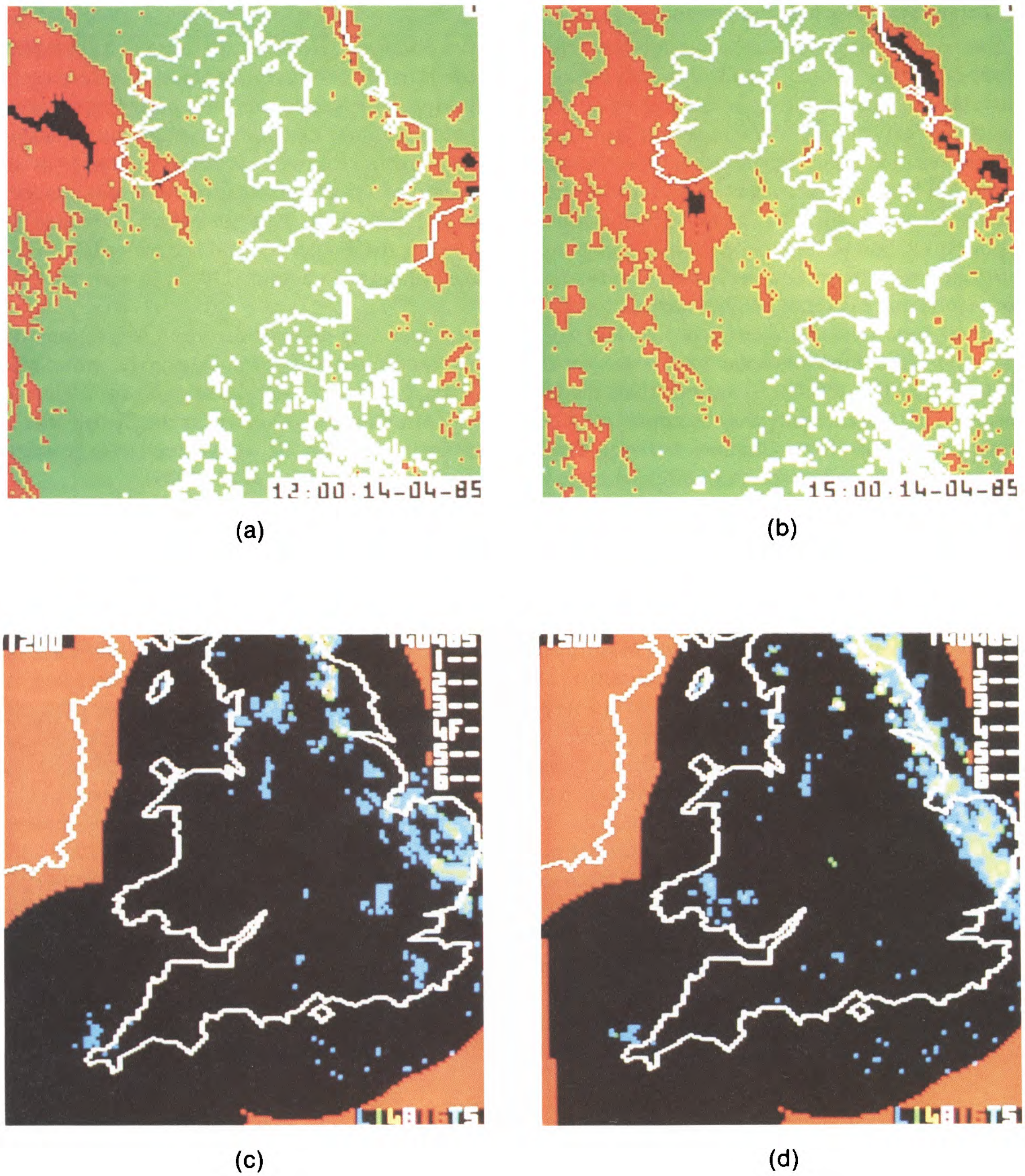

Figure 19. False-colour Meteosat and weather radar imagery on 14 April 1985. (a) and (b) imagery for 1200 and 1500 GMT showing cloud growth along the east coast of England; legend as Fig. 7(b). (c) and (d) rainfall distribution from the UK weather radar network for 1200 and 1500 GMT; legend as Fig. 3(d).

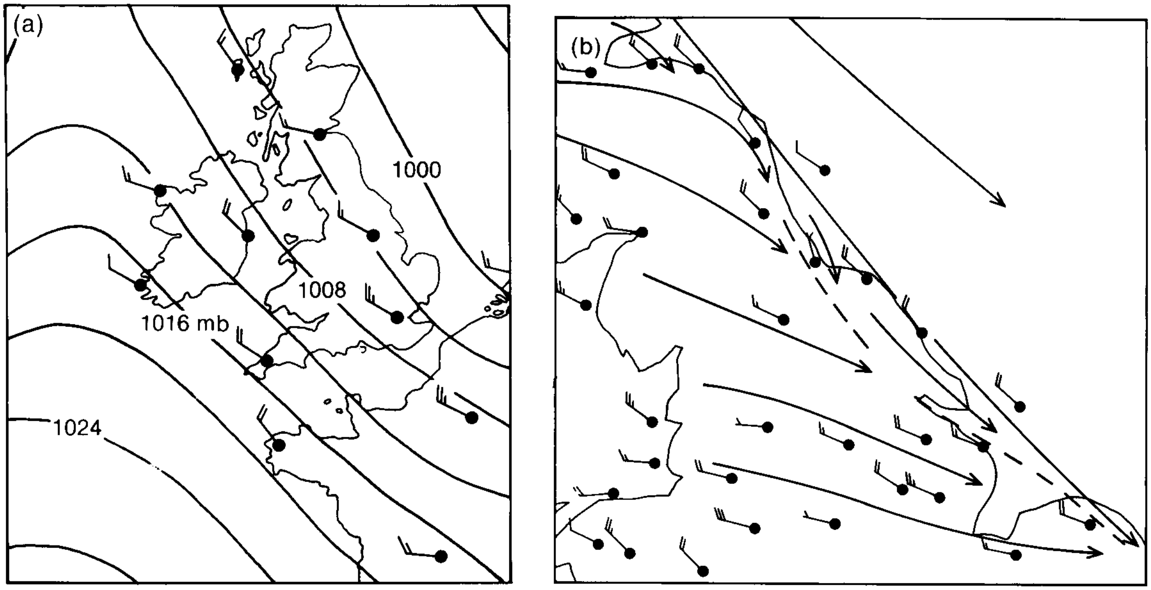

Figure 20. Surface analyses for 1200 GMT on 14 April 1985 showing (a) isobaric analysis and (b) wind observations and streamlines over eastern England; the convergence zone is shown by a dashed line.

References

Blackall, R.M. 1985 Weather radar systems (displays) formerly the 'Jasmin users guide'. (Unpublished, copy available in the National Meteorological Library, Bracknell.)

Brown, R. (1987) The use of METEOSAT data in the FRONTIERS nowcasting system. The proceedings from the 6th METEOSAT scientific users meeting in Amsterdam, November 1986. (To be published.)

Browning, K.A. 1985 Conceptual models of precipitation systems. *Meteorol Mag*, **114**, 293–319.

Browning, K.A., Eccleston, A.J. and Monk, G.A. 1985 The use of satellite and radar imagery to identify persistent shower bands downwind of the North Channel. *Meteorol Mag*, **114**, 325–331.

Lovejoy, S. and Austin, G.L. 1979 The delineation of rain areas from visible and IR satellite data for GATE and mid-latitudes. *Atmos-Ocean*, **17**, 77–92.

Satellite and Radar Studies Group 1986 Daytime peninsula convection — 13 May 1986. *Meteorol Mag*, **115**, 282–284.

Young, M.V., Monk, G.A. and Browning, K.A. (1987) Interpretation of satellite imagery of a rapidly deepening cyclone (Submitted to *Q J R Meteorol Soc*.)

551.509.329:551.525.2:625.7

The Meteorological Office forecast road surface temperature model

P.J. Rayer
Meteorological Office, Bracknell

Summary
The structure and development of a numerical model for predicting road surface temperatures is described. During the winter of 1986/87, many local authorities across the United Kingdom used products from this model in order to forecast road icing.

1. Introduction

The formation of ice on a road surface represents a potential hazard to all road users. Local authorities are responsible for salting and gritting highways in an attempt to alleviate this problem, but it is an expensive exercise in labour, materials, fuel, and machinery. In order to deploy resources efficiently, highway engineers should, at any time, be able to supplement their own local knowledge, not only with actual data from the roads, but also with an indication of how road temperatures and surface moisture are likely to change in the coming hours.

In recent years, many local authorities have been installing road sensors and associated roadside equipment at selected sites. The aim is to keep engineers informed of the present situation at each of these sites by the automatic transmission of sensor readings over public telephone lines. In the summer of 1986 the Department of Transport (DTp), co-ordinating a nation-wide winter road scheme, issued a specification for what it calls a National Ice Prediction Network (see Fig. 1) with which any local scheme will be encouraged to conform. As its name suggests, this specification concerns itself, not only with the routeing and accessibility of the raw sensor data, but also with a predictive element — a possibility which had been prompted by the development of a numerical model for this purpose by Dr J. Thornes (Parmenter and Thornes 1986) at the University of Birmingham while under contract with the DTp's Transport and Road Research Laboratory.

During 1985, when the specification was being drafted, the advice of the Meteorological Office was sought and it was brought to the attention of the DTp that the Office itself could offer a model of this type (Roach 1987). This model, initially developed to investigate the thermal response under 'high sun' of smooth surfaces, had been modified by the inclusion of physical schemes to cope with clouds, rain and the changing solar declination, and the results of experimental runs for a site in the United Kingdom (Lyneham) aroused the DTp's interest in an extended trial during the winter of 1985/86.

2. The model

The model is constructed as shown in Fig. 2. It is designed to provide a forecast of the road surface temperature at a site whose location and thermal properties are known and for which initial values of the road temperature at the site can be estimated or sensed. It is assumed that the surface, the road bed, and the underlying soil are horizontally homogeneous so that a given vertical core is always in thermal equilibrium with its neighbours. The model considers such a core (see Fig. 3) extending from the road surface to a depth of just over 1 metre; its base lies deep enough to be unaffected by changes on the diurnal time-scale while its top surface exchanges energy with the atmosphere. The flux of energy through the surface is determined by a set of physical schemes in which energy transfers from radiative and turbulent processes are calculated from values of air temperature, dew-point, wind speed and cloud — these being supplied for the forecast period along with the time of any precipitation.

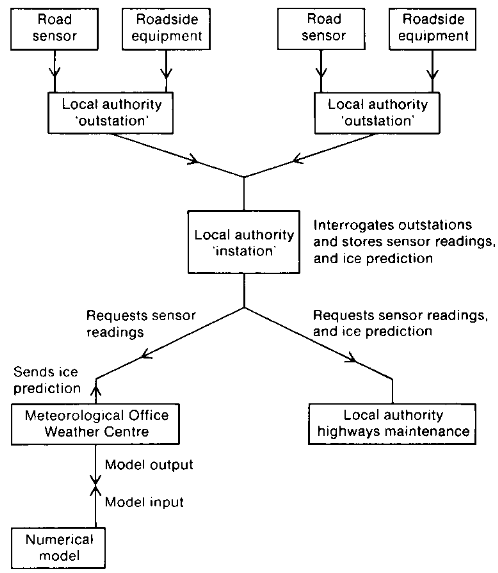

Figure 1. The National Ice Prediction Network according to the specification drawn up by the Department of Transport.

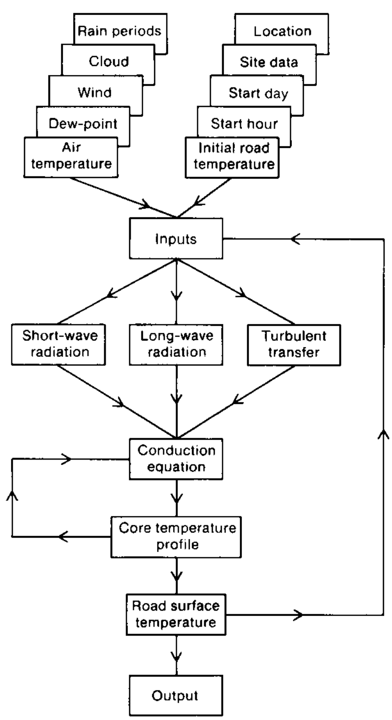

Figure 2. The road surface temperature model.

2.1 *Radiation*

The atmospheric attenuation of the extra-terrestrial radiative flux, S', from the sun will depend upon the length of the solar beam through the atmosphere. Therefore, the solar zenith angle, η, must be calculated by spherical trigonometry from the latitude, date, and time. Allowance for atmospheric extinction is then made as follows:

(a) Water vapour — Roach (1961) suggested that, where observations of specific humidity, q, are available only near the surface, the atmospheric profile of q can be taken to vary directly as the fourth power of the pressure p; after integration over the atmospheric column above the site and elimination of the constant term using the surface values q_0 (g kg^{-1}) and p_0 (mb) the precipitable water, w (g cm^{-2}), in the column is determined approximately by

$$w = \frac{q_0 p_0}{500\,g}$$

where g (m s^{-2}) is the acceleration due to gravity, q_0 is derived from the forecast dew-point while, for operational convenience, p_0 is usually taken as 1000 mb. The transmissivity of the atmosphere after allowing for absorption by water vapour is taken as

$$\tau_w = 0.896 - 0.0636 \log_{10}(w \sec\eta)$$

using the absorptivity curve given in Slingo and Schrecker (1982) for the Thekaekara/Drummond spectrum assuming that $w > 1$ g cm^{-2}.

(b) Aerosol — the transmissivity of the atmosphere after attenuation by aerosol follows a relation verified by Unsworth and Monteith (1972)

$$\tau_p = \exp(-\mu \sec\eta)$$

where μ is a measure of the particulate matter in the column above the site for which, at present, a fixed value of 0.1 is taken.

The short-wave flux, S, absorbed at the site by the top of the core is then determined according to the formula

$$S = S' \tau_w \tau_p \cos\eta\,(1-c)\,(1-\alpha)$$

where c is a function of the sky fraction of cloud and α is the surface albedo at the site.

Radiation from clouds and from the atmosphere produces a downward long-wave flux, L, at the site. The flux due to cloud, B, is calculated by assigning a nominal height to each cloud type and using a lapse rate of 6.5 °C km^{-1} with the assumption that the cloud emits black body radiation at the cloud-base temperature; this is added to the sky radiation (Monteith 1973) to yield

$$L = (208 + 6T_A) + B$$

where T_A is the screen temperature in °C. The road surface itself is asumed to radiate an upward long-wave flux, R, as a black body at the temperature last calculated for the surface.

2.2 *Turbulent transfer*

The model assumes horizontal homogeneity in the atmosphere above the site — advective effects enter only from the weather forecast; however, vertical gradients will exist. At the surface there is a thin zone of molecular conduction of heat and, should the surface be moist, of molecular diffusion of water vapour. Above this layer atmospheric instability and the wind will induce turbulent mixing, a transfer mechanism which is usually of great importance in the surface energy budget. The rate of diffusion of properties such as heat and moisture due to turbulence will depend very much on local conditions; in the treatment followed here, the turbulent flux of a property across a given air layer is related to its vertical gradient by a resistance term which is representative of the layer and derived at any given time from the local atmospheric conditions. The resistance, r_M, to the downward transfer of momentum between the surface and anemometer height (10 m) is given by

$$r_M = \frac{\rho u}{\tau} = \frac{u}{u_*^2}$$

where ρ is the surface air density, u is the wind speed at a height of 10 m, and τ is the vertical flux of momentum. The friction velocity, u_*, is derived from

$$u_* = \sqrt{\frac{\tau}{\rho}} = \frac{ku}{\ln(10/z_0 - \psi_M)}$$

where k is Kármán's constant, and z_0 is the roughness length for momentum exchange — here taken to be 3 mm. The logarithmic wind profile has been modified by the term ψ_M, a correction to allow for non-neutral stability. In earlier versions of the model, the value of ψ_M was fixed at the outset with the proviso that, in very stable conditions, turbulent transfer would be eliminated; the resistance, r_H, to the upward vertical turbulent transfer of sensible heat in the layer between the surface and screen height (1.22 m) was taken to vary directly with the calculated value of r_M. Current developments include the estimation of ψ_M by a Richardson number calculation for the layer below 10 m. The resistance, r_H, is then directly calculated using

$$r_H = \frac{\Delta T}{u_* T_*}$$

where ΔT is the difference between the temperature last calculated for the surface and that at screen height. The temperature, T_*, is calculated from the relation

$$T_* = \frac{k\Delta T}{\ln(1.22/z_T - \psi_T)}$$

where z_T, the roughness length for sensible heat exchange, is taken to be one fifth of z_0. In this case the stability correction term ψ_T is estimated from a Richardson number calculation for the layer below 1.22 m.

The flux of sensible heat from the surface is then given by

$$H = \frac{C_A \Delta T}{r_H}$$

where C_A is the volumetric heat capacity of the air. The model assumes that the latent heat due to water vapour exchange at the surface is transported by the same mechanism and so r_H is also taken to be the resistance to the upward vertical turbulent transfer of latent heat in the layer below screen height. For a moist surface, the flux of latent heat is given by

$$V = \frac{C_A \Delta e}{\gamma(r_H + r_S)}$$

where γ is the psychrometric constant, Δe is the difference between the vapour pressure (saturated) at the surface and that of the air at screen height, and r_S is a term expressing the resistance of the surface itself to evaporation. The road surface is assumed to be wet ($r_S = 0$) during precipitation and also until the calculated cumulative upward water vapour flux is sufficient to evaporate a thin film of water of a specified depth — here taken to be 0.2 mm. Thereafter, r_S is made to increase rapidly from zero as the surface dries.

2.3 *Ground conduction*

The downward vertical flux of energy at the surface at any time, t, is given by

$$G(0, t) = S + L - R - H - V. \qquad \ldots \quad (1)$$

Within the core the vertical flux is

$$G(z, t) = -k(z)\frac{\partial T(z, t)}{\partial z}$$

where $k(z)$ is the thermal conductivity and $T(z, t)$ is the temperature at depth z; at the surface the local temperature gradient is controlled by $G(0, t)$. The evolution of the temperature with time is given by

$$\frac{\partial T(z, t)}{\partial t} = \frac{-1}{C(z)}\frac{\partial G(z, t)}{\partial z}$$

where $C(z)$ is the volumetric heat capacity. The process of sub-surface heat transfer is therefore expressed in the Fourier equation of thermal conduction

$$\frac{\partial T(z, t)}{\partial t} = \frac{1}{C(z)}\frac{\partial}{\partial z}\left\{k(z)\frac{\partial T(z, t)}{\partial z}\right\} \qquad \ldots \quad (2)$$

in which the rate of change in temperature is governed, at any time, by local thermal properties and the local variation with depth of the vertical temperature gradient. Integration of this equation with the above constraint at the surface and a fixed temperature at the base of the core will yield the vertical temperature profile, $T(z, t)$, and with it the surface temperature, $T(0, t)$, at any time t.

2.4 *Solution of equations*

In most cases equation (2) cannot be solved analytically and so it is rewritten in a finite difference form using a vertical grid which divides the road core at the site into successive layers whose thickness expands with depth (Figs 3 and 4), and for which the heat capacity and thermal conductivity are specified over each layer. The scheme is explicit in the sense that, for each level, z_i, it can be solved for $T(z_i, t_j)$ in terms of quantities calculated at time t_{j-1}. The temperature profile is forced by the energy balance at the surface (equation (1)) and must change continually to maintain equality between this energy balance and the surface heat flux from below.

3. Results of the Lyneham study and Birmingham trial

3.1 *The Lyneham study*

Experimental model runs were made using data obtained at Lyneham, where resistance thermometers installed 5 mm below the surface of a tarmac slab allowed hourly readings — taken to represent the surface temperature — to be recorded along with the routine meteorological observations. A comparison was made between the surface temperatures generated by the model from several days of meteorological data and the sensed tarmac temperatures for the same period. In three runs of 15 days each, verification graphs (see Fig. 5) confirmed that the physical schemes used in the model were

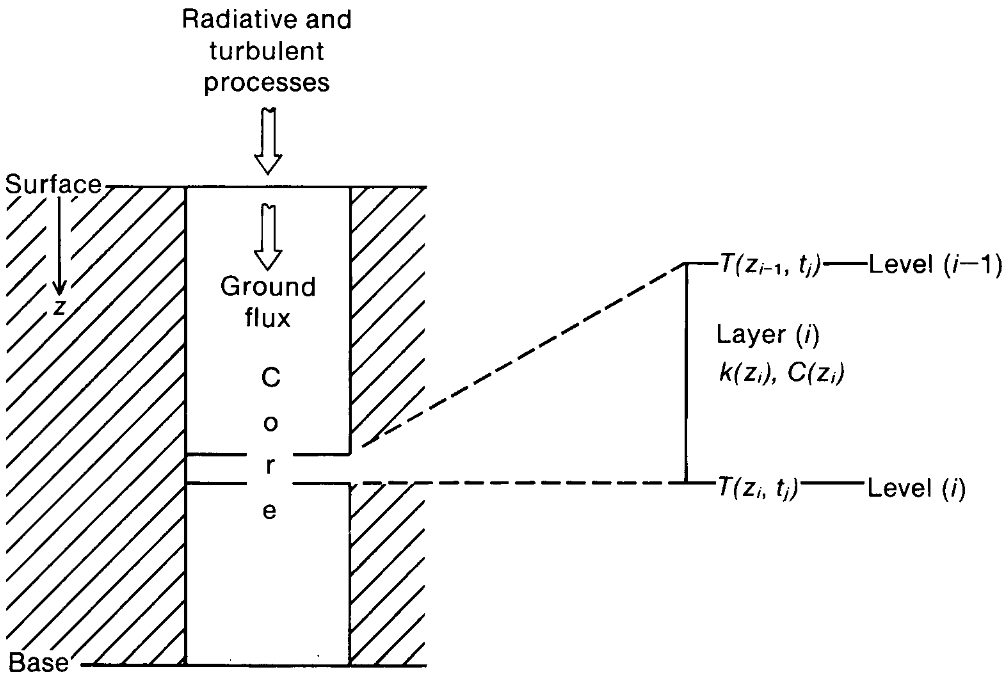

Figure 3. Vertical section taken at the site. The detail shows, for a given time t_j, a single layer from the grid used in the difference scheme. For explanation of symbols see text.

	Depth (cm)		Thickness (cm)	
Level 0	0.0			←Surface
		Layer 1	1.0	
Level 1	1.0			
		Layer 2	1.5	
Level 2	2.5			
		Layer 3	2.0	
Level 3	4.5			
		Layer 4	2.5	
Level 4	7.0			
		Layer 5	3.0	
Level 5	10.0			
•	•	•	•	
•	•	•	•	
•	•	•	•	
Level 17	85.0			
		Layer 18	9.5	
Level 18	94.5			
		Layer 19	10.0	
Level 19	104.5			
		Layer 20	10.5	
Level 20	115.0			←Base

Figure 4. Vertical grid for the conduction scheme used to solve equation (2); temperatures are assigned to the levels whereas the thermal properties are specified for the layers.

adequate and consistent enough to cope with widely different weather regimes. Since a summer road-temperature service would assist local authorities in the organization of surface dressing operations, the runs were based on data from summer as well as winter periods and the response of the model to very warm weather, dry or showery, clearly indicated the possibility of such a summer service. Initially, however, attention was focused more strongly on running the model for ice prediction in winter.

3.2 *The Birmingham trial*

Towards the end of 1985, plans were in progress for the Meteorological Office at Birmingham Airport to provide a commercial winter road icing service based upon the model developed by Thornes. Using a microcomputer, the forecasters were able to begin operations for six sensor sites from January 1986. The results of the Lyneham study had interested the DTp in a trial of the Meteorological Office model over the same period and, to this end, batches of data were sent from Birmingham to the Office's Headquarters in Bracknell for testing and verification. The data included sensor readings for road temperature, air temperature, and dew-point, together with 3-hourly observations of wind speed, total cloud, low cloud, cloud type, and precipitation made routinely at the airport itself. These were additional to the operational input for each site which comprised a set of 3-hourly forecast values of the same meteorological variables from midday.

The Chapmans Hill site, which is on the M5 motorway just south of Birmingham, was chosen for special study and eventually provided 77 days of usable data over the first quarter of 1986. For each of these days 24-hour model runs were made, firstly using the forecast inputs and then using the corresponding actual observations (see Fig. 6) — the latter constituting the case of 'perfect prognosis' where errors in the output should be due to the model alone.

For each daily run, the sequence of differences, δT_i, between the n ¼-hourly model output temperatures and the corresponding linearly interpolated readings from the sensor were used to produce daily figures for

$$\text{bias} = \frac{1}{n}\sum_{i=1}^{n} \delta T_i \text{ and root-mean-square (r.m.s.) error} = \sqrt{\frac{1}{n}\sum_{i=1}^{n} \delta T_i^2}.$$

For the winter period these daily statistics, together with the daily difference between calculated and sensed minimum temperatures, are summarized in Table I. According to these results, the perfect prognosis case at Chapmans Hill showed:

(a) A cool bias of 0.5 °C or less for daily runs in January and February which became a warm bias in March, and also a cool bias for the daily minimum temperatures which also seem to follow a similar monthly trend.

(b) A r.m.s. error of less than 1.5 °C for daily runs in January and February, and a comparable r.m.s. error for the daily minimum temperatures; however, in March, while errors in the minimum temperature remained low, those for daily runs increased significantly.

It must be remembered that the criterion for a night's road-salting operation does not depend only on a sub-zero minimum in the road temperature. Indeed, where ice prediction is concerned, the surface moisture is just as important. After precipitation the road is considered wet for as long as the calculations of turbulent transfer leave the surface resistance to evaporation at zero; in addition, the condensation of moisture from the surface air is predicted whenever the same calculations produce a downward flux of latent heat, though trace deposition can usually be ignored. Thus the local authority engineer receives a forecast of both road temperature and road wetness and should also consult any recent sensor data and his own salting log for information on salinity which might affect the formation of ice.

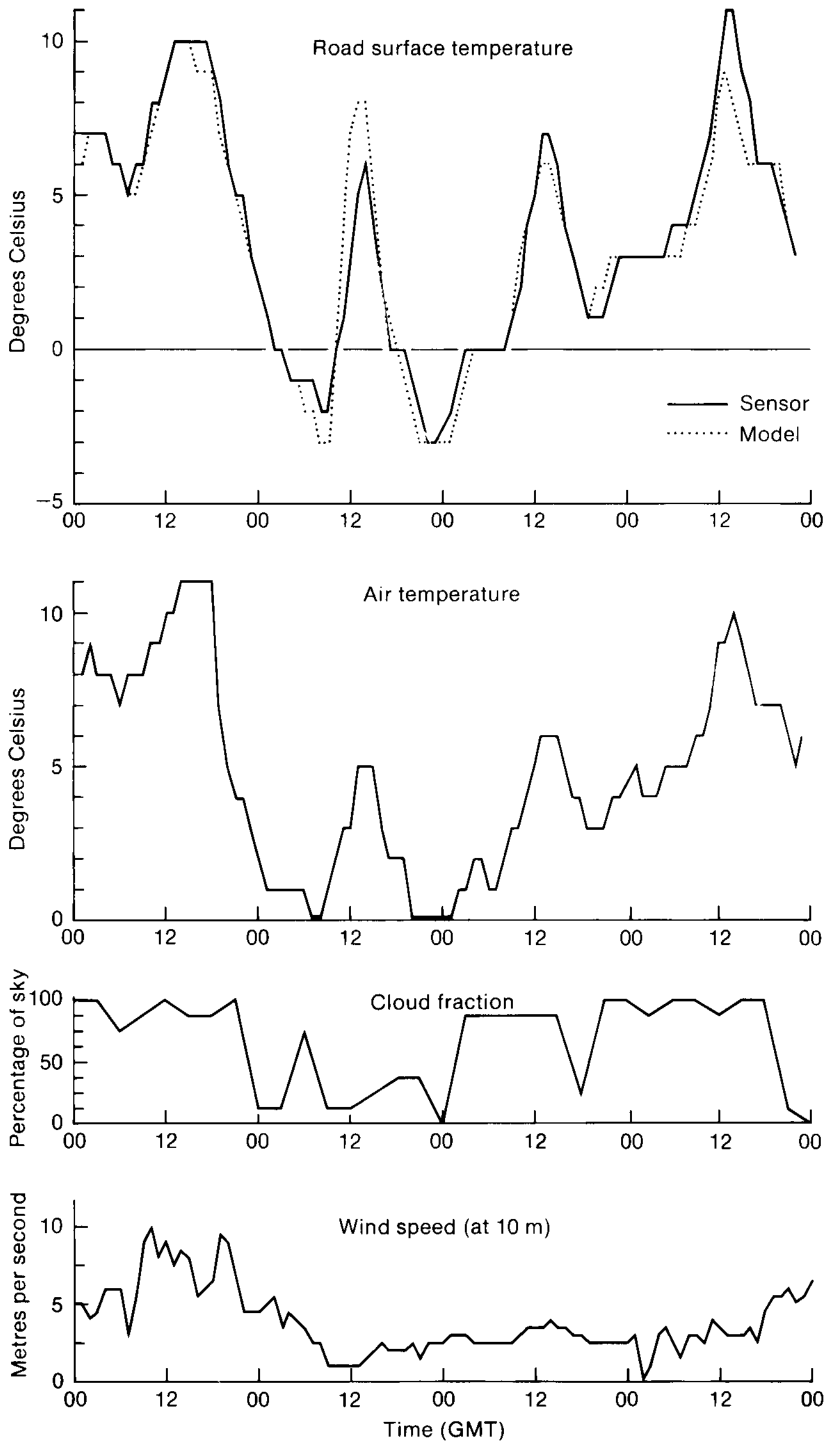

Figure 5. Verification graphs for 4 days from 30 November 1981 — the model was run on actual observations from Lyneham.

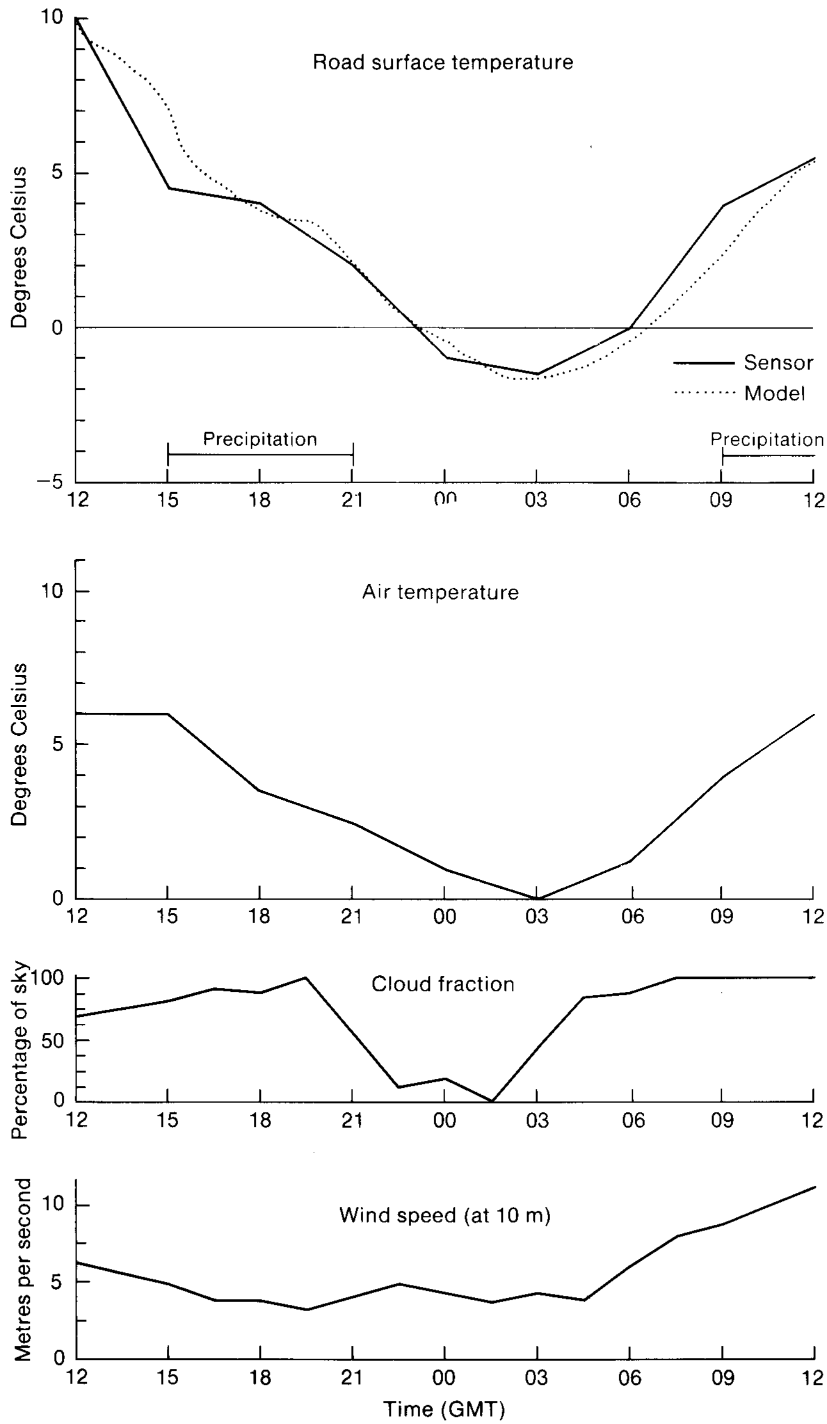

Figure 6. Verification graphs for a 24-hour run of the model for 21 January 1986 — the model was run on actual observations from the Chapmans Hill site.

Table I. *Verification statistics for the 1985/86 winter trial of the model at the Chapmans Hill site*

	On perfect prognosis (°C)	On forecast input (°C)
Mean daily bias		
Jan.	−0.5	0.1
Feb.	−0.1	0.7
Mar.	0.3	1.3
Quarter	−0.1	0.7
Bias of the daily minimum temperatures		
Jan.	−0.7	−0.2
Feb.	−0.3	0.3
Mar.	−0.0	0.8
Quarter	−0.4	0.3
Mean daily r.m.s. error		
Jan.	1.0	1.5
Feb.	1.1	1.7
Mar.	1.7	2.9
Quarter	1.3	2.0
r.m.s. error of the daily minimum temperatures		
Jan.	1.3	1.8
Feb.	1.0	1.7
Mar.	0.9	2.5
Quarter	1.1	2.0

4. Operational service

Besides setting out a local communication network (see Fig. 1), the DTp specification also establishes a protocol for data transmission through the network. To satisfy this protocol, the model has been furnished with additional routines for decoding sensor readings and encoding model output. In 1986, although many local authorities had already installed road sensors and the means with which to interrogate them, few in fact were fully equipped for the DTp scheme. This calls for the provision, via a central processor, of auto-dial modem links between the sensors, the local Weather Centre, and the highways engineer — who also requires the means for reconstructing the data streams into a usable format. Indeed the Birmingham operations in the winter of 1985/86 showed that, to run a model for a routine road icing service, the local Weather Centre itself requires considerable software support.

Nevertheless, it was realized that graphical model output (see Fig. 7) could be transmitted by other means using existing equipment and the Meteorological Office decided to go ahead on this basis, and adopted a flexible approach which would allow developments to be easily assimilated. In 1986 microcomputers were procured for the Weather Centres and part of the required software package was written; software suitable for this purpose had, however, already been developed by Thermal Mapping International Ltd (TMI), a company set up by the University of Birmingham in the wake of Thornes' original studies of the road icing problem, and an agreement was reached under which this software could be used by Weather Centres to run the Meteorological Office model. In return, the fullest

```
        + 9 +-----+-----+----  MARDEN  ---+-----+-----+-----+
  R     + 8 +     +     +     +     +     +     +     +     R
  O     + 7 +     +     +     +     +     +     +     +     +
  A     + 6 +-----+-----+-----+-----+-----+-----+-----+-----+
  D     + 5 + R R +     +     +     +     +     +     +   R + AREA CODE X
        + 4 +     R     +     +     +     +     +     +     + SITE   3
  S .   + 3 R-----+-----+-----+-----+-----+-----+-----+ R---+
  U D   + 2 +     + R   +     +     +     +     +     +     + 17/02/87
  R E   + 1 +     +   R +     +     +     +     +     +     + 1200HRS
  F G     0-+-+-+-+-+-+ R-+-+-+-+-+-+-+-+-+-+-+-+-+-+ R-+-+-+
  A     - 1 +     +       R R +     +     +     +     +     +
  C C   - 2 +     +     +     R R   +     +     +     +     +
  E .   - 3 +-----+-----+-------- R R R R R-----+-- R-+-----+
        - 4 +     +     +     +     +     + R R +     +     +
  T     - 5 +     +     +     +     +     +     R R   +     + MIN TEMP
  E     - 6 +-----+-----+-----+-----+-----+-----+-----+-----+  R  -4.5
  M     - 7 +     +     +     +     +     +     +     +     +
  P     - 8 +     +     +     +     +     +     +     +     +
        - 9 +-----+-----+-----+-----+-----+-----+-----+-----+
TIME (HRS) 12    15    18    21    00    03    06    09    12
STATE       ...PPPPPWWWWWWWWWWWWWWWWWWWWWWWWWWWWWWWWWWWWW....

NO MESSAGE
NO MESSAGE
ORIGINATED 12:19 HRS - NO UPDATE LIKELY.
```

Figure 7. Example of the operational graphical output from a model run made by Bristol Weather Centre. A plot of the forecast road surface temperature (R) is shown, with precipitation (P) and subsequent road wetness (W) indicated below the graph.

co-operation was given to TMI's plan to provide a comprehensive ice prediction package for Cheshire County Council.

From November 1986 numerical ice prediction products were introduced to many local authorities across the country as a major item in the Meteorological Office's new 'Open Road' service. At each Weather Centre a data base has been installed carrying the site data and run specifications for all its customer authorities. To users in the Weather Centre, the menu-driven software presents a panel for entering the input weather forecast and the initial sensed or estimated road temperature. The model establishes a 'first guess' vertical temperature profile and, within a few tens of seconds, displays its prediction and allows messages to be added; then, depending on the wishes of the local authority, this output is either directly transmitted by modem, plotted as a graph for distribution by facsimile, or disseminated via viewdata. The initial run of the day for any site is always from noon but, should sensor readings or a later weather forecast indicate the need for modification, the facility exists for additional 'update' runs to be made from any subsequent hour — in such a case, the above procedure is still applied but the initial vertical temperature profile for that hour is automatically picked up from the previous run and, if necessary, a smooth correction applied at each level.

The role of the model is advisory and decisions on when and where to salt remain firmly with local authorities. It is hoped to extend this advice into summer where road temperatures will be useful for authorities engaged in road dressing operations. Such an all-season service promises substantial financial benefit for the local authorities and advantage to the road user.

Acknowledgements

The author is indebted to Dr W.T. Roach (Meteorological Research Flight, Farnborough) who wrote the original version of the model and guided its initial development. Thanks are also due to Mr A. Dawe (Meteorological Office, Birmingham) for his co-operation during trials of the model, and to Mr D.W.G. Dancey (Meteorological Office, Bracknell) for his assistance in developing the operational software.

References

Monteith, J.L.	1973	Principals of environmental physics. London, Edward Arnold.
Parmenter, B. and Thornes, J.E.	1986	The use of a computer model to predict the formation of ice on road surfaces. TRRL Research Report RR71. (Unpublished, copy available from Transport and Road Research Laboratory, Crowthorne.)
Roach, W.T.	1961	The absorption of solar radiation by water vapour and carbon dioxide in a cloudless atmosphere. *Q J R Meteorol Soc*, **87**, 364–373.
	(1987)	The role of surface temperature in the surface energy budget (Submitted to *Q J R Meteorol Soc.*)
Slingo, A. and Schrecker, H.M.	1982	On the shortwave radiative properties of stratiform water clouds. *Q J R Meteorol Soc*, **108**, 407–426.
Unsworth, M.H. and Monteith, J.L.	1972	Aerosol and solar radiation in Britain. *Q J R Meteorol Soc*, **98**, 778–797.

551.513.1:551.588.5:551.467

Sea-ice and the Antarctic winter circulation*

J.F.B. Mitchell and T.S. Hills

Meteorological Office, Bracknell

Summary

A numerical experiment has been conducted to test the sensitivity of a global general circulation model to changes in sea-ice extent in the Antarctic during winter. Three 112-day integrations have been made in which all the sea-ice equatorward of 66° S was removed (the anomaly simulations) and these were compared with the corresponding control simulations. There was a large increase in sensible heat flux over the anomaly, a warming over the Antarctic confined to the lower atmosphere and a reduction in the westerlies around the periphery of the (new) sea-ice. The increased heating over the anomaly was accompanied by a decrease in surface pressure.

1. Introduction

The presence of sea-ice has two profound effects on the transfer of energy between the atmosphere and the underlying surface:

(a) the fluxes of sensible and latent heat into the atmosphere over sea-ice are substantially smaller than over the ocean and

(b) sea-ice has a much higher reflectivity than open water, so the absorption over ice is considerably reduced.

The first of these processes influences the atmosphere directly whilst the second has an indirect effect by altering the solar energy absorbed by the surface and hence the subsequent development of surface type (sea or ice). If the main concern is with the response of the atmosphere to given surface conditions, the second process need not be considered.

There is evidence that the heat flux into the atmosphere increases by at least an order of magnitude between the central Antarctic and the neighbouring oceans. This suggests that, given the tendency for anomalies of sea-ice cover to persist for several months, it is likely that the surface heat flux associated with anomalous sea-ice will influence the atmospheric circulation. Observations and experiments with atmospheric circulation models indicate that this does indeed happen in the Arctic. However, the evidence about the influence of the Antarctic sea-ice is contradictory.

* This is an abridged version of an article by Mitchell and Hills (1986) published in the Quarterly Journal of the Royal Meteorological Society.

2. A numerical experiment

In view of the lack of observational data in southern latitudes and the inconclusive nature of numerical studies, a winter Antarctic sea-ice anomaly experiment has been carried out with the global 5-layer model which has been developed in the Meteorological Office. The general approach is to compare control simulations with those in which the anomaly has been introduced. In the case considered here, the anomaly simulations had all the sea-ice equatorward of 66° S replaced by water at 0 °C (Fig. 1). Three 112-day anomaly simulations were made, commencing from data for 10 June in the second, third and fourth years of the 3½-year control simulation. The changes over the final 92 days (July, August and September) have been analysed. Further details about the model and experimental procedure can be found in the original article by Mitchell and Hills (1986).

One of the objectives of the investigation was to reassess the work of Simmonds (1981) who carried out a September simulation using a hemispheric general circulation model with reduced Antarctic sea-ice extents. Those experiments showed that the reduced sea-ice caused surface pressure to increase in high and middle latitudes, though the simulated depression track did not shift south with the ice edge as might have been expected.

The experiments with the 5-layer model showed that the immediate thermal response of replacing sea-ice by open water is to raise the surface temperature near where the sea-ice was removed (Fig. 2(a)). At the same time, the maximum in the flux of sensible heat into the atmosphere near 52.5° S in the control run shifts poleward to the vicinity of the new ice edge. Consequently the change in sea-ice produces a large decrease in the flux near 52.5° S and a massive increase where the maximum temperature increase takes place (Fig. 2(b)). Although there is a sharp increase in the sensible heat flux, the atmospheric warming is distributed more evenly with latitude due to lateral mixing by atmospheric

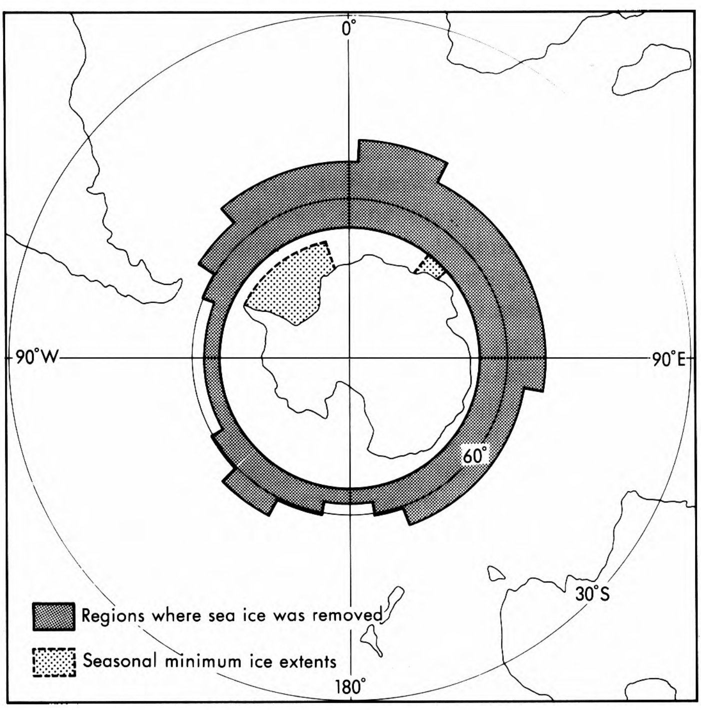

Figure 1. Model sea-ice extents and changes in sea-ice (heavy stippling) for mid-August. Observed minimum ice extents are indicated by light stippling.

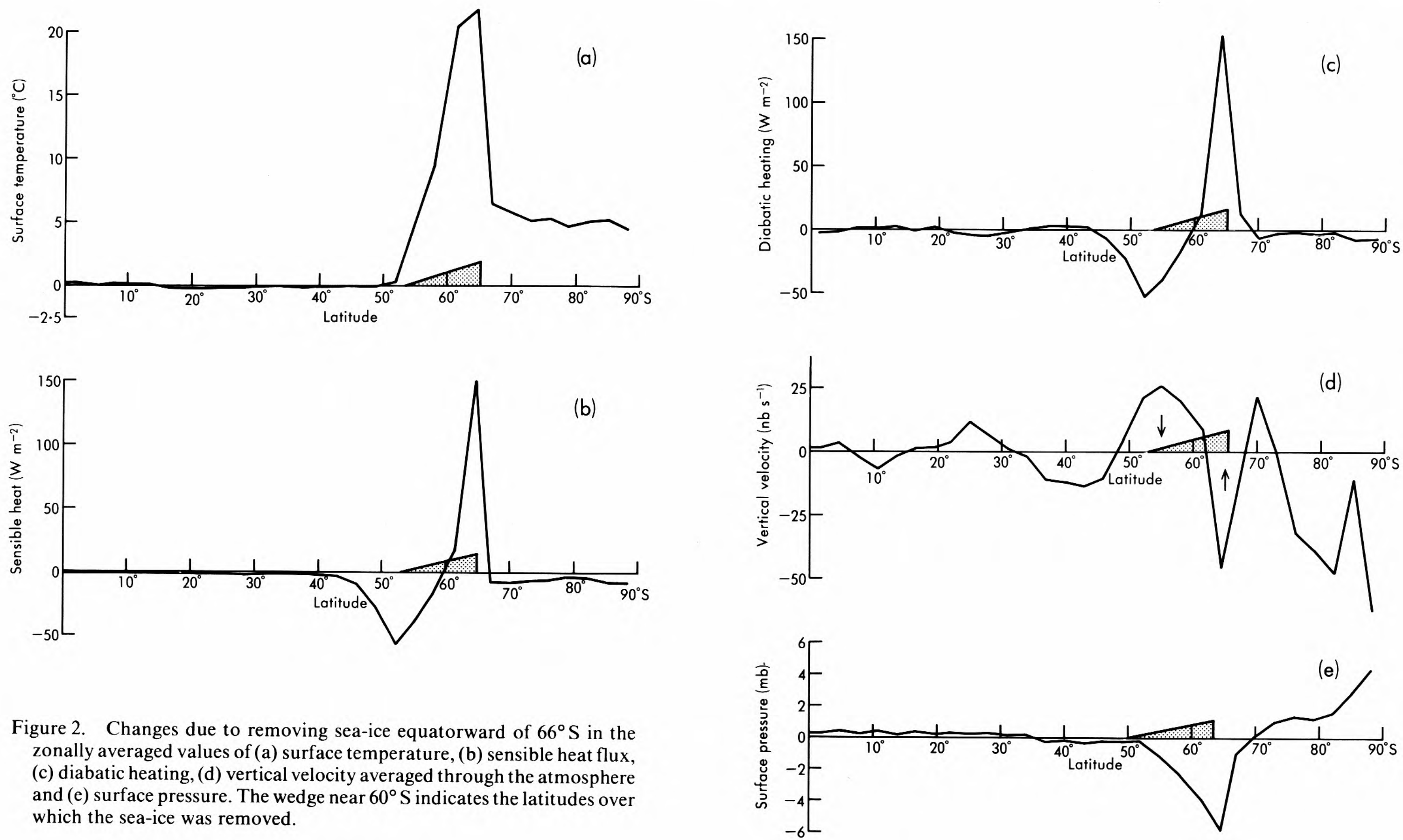

Figure 2. Changes due to removing sea-ice equatorward of 66°S in the zonally averaged values of (a) surface temperature, (b) sensible heat flux, (c) diabatic heating, (d) vertical velocity averaged through the atmosphere and (e) surface pressure. The wedge near 60°S indicates the latitudes over which the sea-ice was removed.

systems. Also the warming is confined to the lowest layers of the atmosphere because the vertical profile of temperature is extremely stable in these regions.

The changes in the diabatic heating of the atmosphere (Fig. 2(c)) are dominated by the transfer of sensible heat from the surface. Corresponding intensification of the mean upward motion near the ice edge is compensated in the neighbouring regions by relative descent (Fig. 2(d)) and accompanied by a reduction in zonally averaged surface pressure (Fig. 2(e)) with increases further poleward over the Antarctic continent. The changes in surface pressure alone would produce and enhance easterly flow over the Antarctic continent and strengthen the westerly flow equatorwards of the new ice edge. However, the warming of the lower atmosphere and consequent raising of the height of isobaric surfaces over Antarctica weakens the westerly flow around the continent in all but the lowest model layer.

The decrease in the surface pressure along the new ice edge (corresponding to a shift in the depression tracks) was not found by Simmonds (1981) although other features, including a general increase in surface pressure over Antarctica, were found in both experiments. Explanations of the differences between the simulations have been discussed in the original paper by Mitchell and Hills (1986). In the same paper a full account of the results is given along with a discussion of the attempts which have been made to do the following:

(a) quantify the sensitivity of the model to the insulation of the atmosphere from the ocean by sea-ice,
(b) assess the impact of prescribed changes in sea-ice on the results of studies of the effects of CO_2 on climate and
(c) estimate the likely effect on the atmosphere of errors in the simulation of sea-ice extents in coupled ocean–atmosphere models.

3. Closing remarks

The results indicate the importance of taking into account observed anomalies in sea-ice extent for forecasting in high latitudes, and the need for an accurate representation of the growth and decay of sea-ice when modelling climate change. To these ends, a coupled ocean–atmosphere model incorporating a thermodynamic model of sea-ice has been developed for use in climate studies by the Dynamical Climatology Branch of the Meteorological Office. There are also plans to develop a more realistic dynamical model of sea-ice in which internal forces within the ice and movement due to wind stress will be taken into account.

References

Mitchell, J.F.B. and Hills, T.S. 1986 Sea-ice and the Antarctic winter circulation: a numerical experiment. *Q J R Meteorol Soc*, **112**, 953–969.

Simmonds, I. 1981 The effect of sea ice on a general circulation model of the Southern Hemisphere. *In* Sea level, ice and climate change. Allison, I. (ed), IAHS Pub. No. 131, 193–206.

Review

Physical fundamentals of remote sensing, by E. Schanda. 153 mm × 232 mm, pp. ix + 187, *illus.* Berlin, Heidelberg, New York, Tokyo, Springer-Verlag, 1986. Price DM 48.00.

This book is based on a lecture course given to graduate students and, as is evident when reading the book, is divided up into 15 well-defined sections, each one being an individual lecture. It is aimed at the person who is interested in, or working in, the field of remote sensing and wants to know more about the physical mechanisms which enable us to infer surface and atmospheric variables from satellite or aircraft measurements. The author assumes a good knowledge of undergraduate physics since some of the physical concepts described become quite complex. A comprehensive list of references is given at the back which allows the interested reader to delve more deeply into particular areas of the subject. The author's background appears to be in remote sensing at microwave frequencies; this becomes obvious from one or two examples which the author gives to illustrate various concepts.

The first chapter gives a basic introduction to the subject, including a revision of electromagnetic wave theory. There then follows a very useful chapter on the absorption and emission of radiation by atmospheric gases. This is the best description of this particular subject that I have come across, since the author goes into some detail, but at the same time does not get too involved with complex mathematics. My only criticism is that, although line absorption is described well, there is no mention of the continuum absorption exhibited by some atmospheric gases. I found this rather surprising as at infra-red window wavelengths ($\approx$10 μm), where much remote sensing is carried out, one of the primary absorption mechanisms is the water-vapour continuum.

The first section of the third chapter on the interaction of radiation with condensed matter is rather heavy going, unless you are familiar with quantum mechanics. In the following section there are some interesting examples of the spectral properties of plants at visible wavelengths. The fourth chapter deals with scattering of radiation by molecules, aerosols and surfaces. Again the subject is comprehensively but clearly covered and would be useful reading for any atmospheric physicist. The final chapter is perhaps the most useful, with sections on radiative transfer theory, radiometry, and the theory of atmospheric temperature profile and constituent retrieval. I felt there could have been a longer section here on the theory of the retrieval of other surface–atmospheric variables from radiometric measurements, for instance a discussion of radiation budget measurements and the retrieval of sea surface temperature would have been interesting.

The text and figures are well presented throughout the book, although anyone expecting to see any satellite pictures will be disappointed. It could be argued that a few satellite pictures to illustrate various aspects of the 'physics' being described would have improved the text further, but this is only a minor criticism. Overall, I felt the book achieved its purpose of giving the reader an understanding of the basic physical processes which are relevant to remote sensing. I would recommend this book to anyone who has an interest in remote sensing and wants to understand in more detail the physical mechanisms involved.

R.W. Saunders

Satellite photographs — 7 April 1987 at 1537 GMT

The satellite photographs in Fig. 1 were both taken from NOAA-9 at 1537 GMT on 7 April 1987. They demonstrate the misleading impression of cloud structure that can sometimes be gained from infra-red imagery which, in this case (Fig. 1(a)), shows a cloud mass south of Ireland suggestive of a frontal wave. This cloud had originally been linked to the band which can be seen over Orkney and had wrapped itself around the leading edge of a slow-moving cold pool to the west of Ireland. The cloud area expanded in the region of ascent ahead of the upper trough and extended eastwards as it engaged the stronger flow on the northern side of a minor jet across the Bay of Biscay. Inspection of the visible picture (Fig. 1(b)) reveals that the feature consisted mainly of thin high cloud, through which a band of lower cloud can be seen oriented at right angles to the upper flow. The lower cloud was associated with a cold-air trough which phased in with a wave on the polar front over Spain; it has a rather lumpy appearance and gave outbreaks of rain over England and Wales during the following night, with amounts of rain being very variable from place to place.

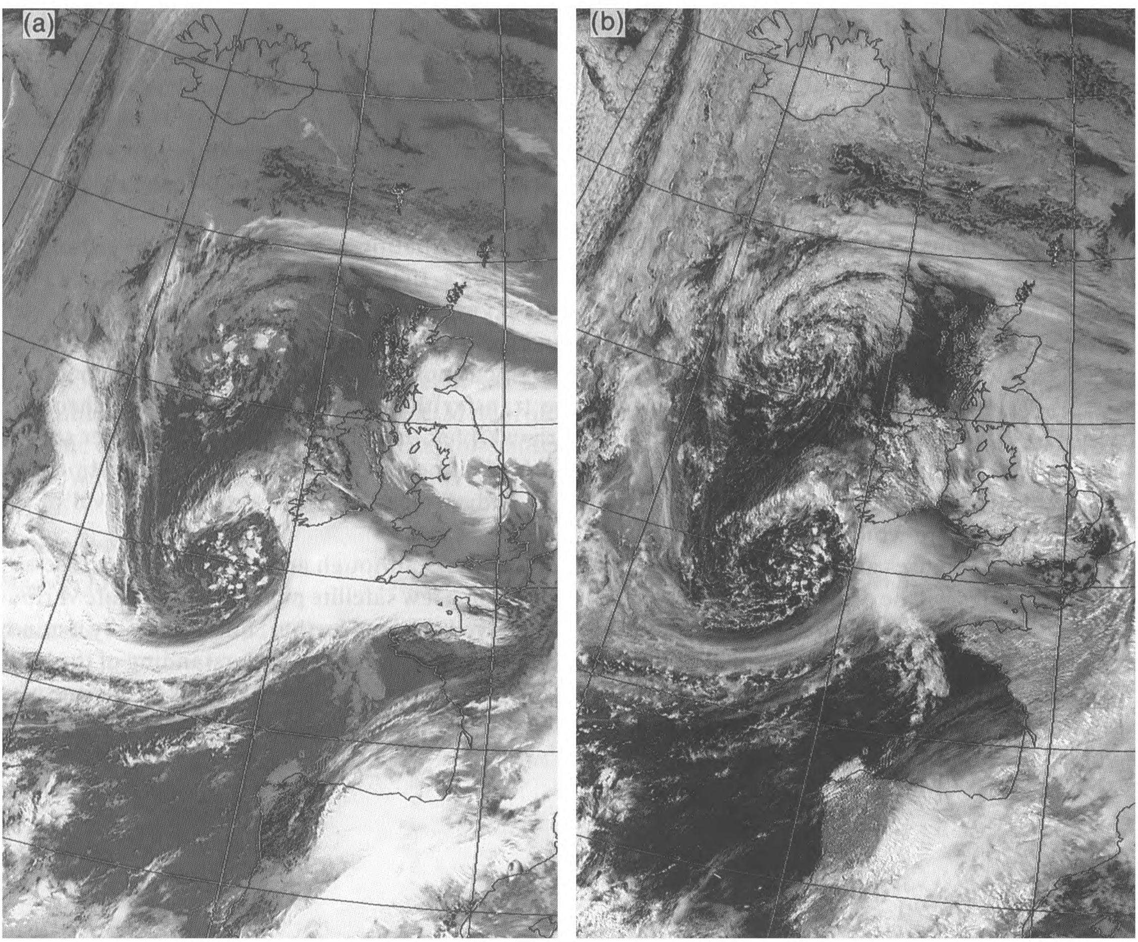

Photograph by courtesy of University of Dundee *Photograph by courtesy of University of Dundee*

Figure 1. (a) Infra-red image and (b) visible image.

Meteorological Magazine

GUIDE TO AUTHORS

Content

Articles on all aspects of meteorology are welcomed, particularly those which describe the results of research in applied meteorology or the development of practical forecasting techniques.

Preparation and submission of articles

Articles for publication and all other communications for the Editor should be addressed to the Director-General, Meteorological Office, London Road, Bracknell, Berkshire RG12 2SZ and marked 'For *Meteorological Magazine*'.

Articles, which must be in English, should be typed, double-spaced with wide margins, on one side only of A4-size paper. Tables, references and figure captions should be typed separately.

Spelling should conform to the preferred spelling in the *Concise Oxford Dictionary*.

References should be made using the Harvard system (author, date) and full details should be given at the end of the text. If a document referred to is unpublished, details must be given of the library where it may be seen. Documents which are not available to enquirers must not be referred to.

Tables should be numbered using roman numerals and provided with headings. We consider vertical and horizontal rules to be unnecessary in a well-designed table; spaces should be used instead.

Mathematical notation should be written with extreme care. Particular care should be taken to differentiate between Greek letters and Roman letters for which they could be mistaken. Double subscripts and superscripts should be avoided, as they are difficult to typeset and difficult to read. Keep notation as simple as possible; this makes typesetting quicker and therefore cheaper, and reduces the possibility of error. Further guidance is given in BS1991: Part 1: 1976 and *Quantities, Units and Symbols* published by the Royal Society.

Illustrations

Diagrams must be supplied either drawn to professional standards or drawn clearly, preferably in ink. They should be about 1½ to 3 times the final printed size and should not contain any unnecessary or irrelevant details. Any symbols and lettering must be large enough to remain legible after reduction. Explanatory text should not appear on the diagram itself but in the caption. Captions should be typed on a separate sheet of paper and should, as far as possible, explain the meanings of the diagrams without the reader having to refer to the text.

Sharp monochrome photographs on glossy paper are preferred: colour prints are acceptable but the use of colour within the magazine is at the Editor's discretion. In either case contrast should be sufficient to ensure satisfactory reproduction.

Units

SI units, or units approved by WMO, should be used.

Copyright

Authors wishing to retain copyright for themselves or for their sponsors should inform the Editor when they submit contributions which will otherwise become UK Crown copyright by right of first publication.

It is the responsibility of authors to obtain clearance for any copyright material they wish to use before submitting it for publication.

Free copies

Three free copies of the magazine are provided for authors of articles published in it. Separate offprints for each article are not provided.

Meteorological Magazine

June 1987

Vol. 116
No. 1379

CONTENTS

Contributions: it is requested that all communications to the Editor and books for review be addressed to the Director-General, Meteorological Office, London Road, Bracknell, Berkshire RG12 2SZ, and marked 'For *Meteorological Magazine*'. Contributors are asked to comply with the guidelines given in the *Guide to authors* which appears on the inside back cover. The responsibility for facts and opinions expressed in the signed articles and letters published in *Meteorological Magazine* rests with their respective authors. Authors wishing to retain copyright for themselves or for their sponsors should inform the Editor when submitting contributions which will otherwise become UK Crown copyright by right of first publication.

Subscriptions: Annual subscription £27.00 including postage; individual copies £2.30 including postage. Applications for postal subscriptions should be made to HMSO, PO Box 276, London SW8 5DT; subscription enquiries 01–211 8667.

Back numbers: Full-size reprints of Vols 1–75 (1866–1940) are available from Johnson Reprint Co. Ltd, 24–28 Oval Road, London NW1 7DX. Complete volumes of *Meteorological Magazine* commencing with volume 54 are available on microfilm from University Microfilms International, 18 Bedford Row, London WC1R 4EJ. Information on microfiche issues is available from Kraus Microfiche, Rte 100, Milwood, NY 10546, USA.

ISBN 0 11 727970 6

ISSN 0026–1149

Printed for HER MAJESTY'S STATIONERY OFFICE
by Linneys Colour Print, Dd. 739131 C13 6/87 52821

THE METEOROLOGICAL MAGAZINE

HER MAJESTY'S STATIONERY OFFICE

July 1987

Met.O.978 No. 1380 Vol. 116

METEOROLOGICAL OFFICE Met.O.978

THE METEOROLOGICAL MAGAZINE

No. 1380, July 1987, Vol. 116

551.515.1:551.553.8:359:93/99

The Trafalgar storm 22–29 October 1805

D.A. Wheeler
Geography Department, Sunderland Polytechnic

Summary

The Battle of Trafalgar is one of the best-known events in British history. Yet in that heyday of the sailing ship weather often had a critical role to play in the outcome of naval engagements. This observation is no less true of Trafalgar, and this paper takes as its subject the storm that followed the battle and examines its character and possible origins. Its historical importance is matched by its unusual ferocity and duration, making it in every sense a notable occurrence.

1. Introduction

The author (Wheeler 1985) has recently offered some tentative suggestions concerning the weather of the Trafalgar campaign, which can be thought of as embracing the Royal Navy's blockade of Cadiz, the battle itself and the week-long storm that followed the engagement. All these events fell into the single month of October 1805. Of particular interest, to both historians and meteorologists, is the storm; an event of unusual ferocity visited upon an already weary fleet whose very survival is a signal testimony to the qualitities of its leadership and manning.

Here an attempt is made to draw comparisons between what is known of the weather of that tempestuous week and present-day examples of what may be similar synoptic conditions, and to analyse the nature of the storm. Such an undertaking is fraught with inevitable hazards and the interpretations offered here can never be wholly proven on the basis of the relatively scant evidence currently available. They are, nevertheless, offered with a reasonable degree of confidence.

2. Data sources

Recent analogous events may be sought in the published daily charts of the Meteorological Office (covering the period before 1981) or the Deutscher Wetterdienst. Information for the events of October 1805 is inevitably more sketchy, geographically inconsistent and, however accurate the data may be, subject to a variety of interpretations. But, setting aside these reservations, there exists a surprising fund of information on the Trafalgar storm. Data exist for a number of sites in Britain. The Goodwood House Observatory, Sussex, was active in recording wind direction, air pressure, temperature, and weather features thrice daily. In Newcastle upon Tyne, James Losh maintained a valuable sequence of observations covering those same aspects, again thrice daily, as did Samuel Robertson at Ednam in the

Tweed valley between Kelso and Coldstream. Information from further north is found in the diary of James Ramsey, who lived not far from Perth. He maintained a daily record of wind and weather for a number of years about this time. Data from mainland Europe in these troubled times are less forthcoming. The forces of revolution had swept away the potentially fruitful sources of the Société Royale de Médecine of France (Kington 1970) and no Iberian material is available.

The most valuable sources have been the logs of ships engaged at Trafalgar or blockading the French Atlantic ports further north. Oliver and Kington (1970) have examined the utility of such documents as meteorological source material and confirmed their value. In addition to general observations on the running and progress of the vessel, the logs pay close attention to the prevailing weather during the day's watches. The essential meteorological data consist of wind-speed estimates that are all but identical to the descriptions used in the Beaufort scale. Thus, for example, terms such as 'fresh' or 'strong' breezes are commonplace and can be confidently interpreted as force 5 and 6 respectively. Associated wind direction is recorded using a 32-point compass, and further useful information appears in the form of comments made on the incidence of thunder, lightning, squalls, rain, fog, etc., which despite their qualitative presentation help to create an impression of conditions at the time. Such descriptive observations were, to a greater or lesser degree, discretionary and not all ship's masters, for it was their responsibility to maintain the logs, were as assiduous as others and the quality and usefulness of account varies from vessel to vessel. Unfortunately no shipboard barometric data exist for this period. The simultaneous existence of the captain's or junior officer's logs gives a misleading impression of a wealth of data. In reality the latter were only a copy, often abridged, of the master's log which should always be the preferred reference. To this brief account of the sources little need be added other than to confirm the author's faith in their general reliability. Indeed an event such as the blockade of Cadiz gathered many ships together in the same waters and allows their logs to act as mutual checks on consistency and accuracy; in the present case no serious discrepancies were encountered in the 12 closely studied logs. But, although such clusterings have their uses, the general geographical spread of data is poor, with gaps between the areas of principal naval activity. Furthermore, the observations are inevitably limited to those aspects important to mariners; rainfall amounts and temperature are notable absences.

Supplementary information can also be drawn from the private letters and reports, both English and Franco-Spanish, written after the battle. But these lack the close attention to meteorological detail found in the official logs and are best used in a supporting role.

3. The Trafalgar storm 22–29 October 1805

The storm which seized upon friend and foe alike after the battle of Trafalgar figures prominently in the private and official correspondence. Of its severity there can be little doubt. The logs record almost continuous 'hard gales' reaching a peak on the 26th. Frederick Ruckert, master of the fleet's senior frigate *Euryalus*, noted on the morning of the 23rd '...strong gales and rain with heavy squalls. The topmast staysail split and blown away by a heavy squall from the westward.' The small cutter *Entrepenante* was even less fortunate. Her log records '...hard gales with heavy seas. Split the mainsail...shipped several heavy seas. Made several signals of distress.' Whether these signals were answered is not recorded; the larger vessels were fully occupied with their own survival. But survive the *Entrepenante* did, to reach Gibraltar on the 26th. Thomas Watson, master of the *Achille*, wrote in his entry for the 23rd '...strong gales with showers of rain, at 9 the hawser broke from the Spanish prize which we had in tow. At 11 strong gales and heavy squalls, with rain. Split the main staysail.' And so it goes on around the fleet, varying only in detailed timing and estimate of intensity, all vessels relating the same story of battle against this unrelenting and tireless foe.

The letters from the seamen are no less eloquent. The seasoned Captain Henry Blackwood, again of the *Euryalus*, wrote to his wife on the 23rd '...it has blown like a hurricane.' Henry Walker, midshipman on the *Bellerophon*, wrote to his mother on 22 November; his letter contains the following description of the battle and its aftermath '...but in the ensuing night (of 21st) a storm came on, such as I have never witnessed, and for the four following days we had a much severer struggle against the elements than the enemy.' The day of the battle had, however, been tranquil. The two fleets, some 10 miles distant at dawn, were not able to engage at close quarters until after midday. The English fleet was in two columns vaguely line-ahead, with a following wind, such as it was, and even with full spreads of canvas made little more than 2 knots as it bore down on the enemy line. But even as the events of the day unfolded the growing westerly swell forced Nelson to turn his thoughts to the hours after battle and even in his dying moments, aware of the impending storm portended in the sea conditions, urged Captain Hardy to anchor the fleet at close of action to prevent the weary crews from being driven onto the rocky lee shore of Cape Trafalgar.

The ominous westerly swell (Fig. 1) was also noted as early as the evening of 20 October by Captain Jean Jacques Lucas of the French ship *Redoutable* (from whose tops Nelson was shot). Most English logs make their first entry of the swell a little later. Such disagreements on precise timing are not uncommon and make it difficult, for example, to be confident concerning the arrival time of the storm, but a most probable point would be about midday on the 22nd. The storm then raged, albeit with fluctuations, until 29 October. Throughout this time the winds were largely from between west and south-south-west. Again, however, precise uniformity should not be expected as the log of the *Royal Sovereign*, for example, notes a west-north-west wind. Meanwhile the squadron then blockading the port of Brest was battling against east to south-east gales; an important observation as this suggests that the storm's circulation embraced also these northern latitudes. A storm centre somewhere approximately midway between the two may be postulated, perhaps off the Spanish Cape Finisterre. Shipboard barometers were in use at that time and Nelson was known to have used one, but the records, if any were kept, appear not to have survived and their absence is to be regretted.

Photograph by courtesy of the National Maritime Museum, London

Figure 1. 'Evening at Trafalgar'. This oil on canvas painting by William Huggins (1781–1845) depicts the scene at dusk on 21 October 1805. Although Huggins was not present at the battle he may well have drawn upon contemporary sources for his picture and the impression he creates of vessels wallowing in a heavy swell certainly echoes the evidence of the contemporary documents. This heavy westerly swell was the herald of the storm that was to break the following day.

4. Interpretation and hypothesis

Certain points concerning the Trafalgar storm, even on the basis of the meagre evidence to hand, can be agreed upon; its cyclonic nature, its duration, its seeming lack of mobility over the final week and, most notably, its intensity and geographical extent. Is it possible from these conclusions to hypothesize its nature? The brief answer is yes.

One may first be tempted to be persuaded by Captain Blackwood's vivid account and view it as a hurricane, but there are good grounds for declining this opinion. Firstly, Blackwood's use of the term 'hurricane' was indiscriminate, the word did not enjoy the currency it possesses today and was applied to any severe storm, tropical or otherwise. Indeed, one of the Trafalgar logs demonstrates just such an inconsistent application, but with respect to the term 'gale'. Captain Henry Digby of the *Africa* prepared a log in which the term 'gale' appears on days when no other log records anything above strong breezes. But Digby may not have been consistently miscalculating the strength of the wind, merely following the old convention of describing any stiffish breeze as a gale. A second reason for rejecting the hurricane hypothesis is found in the study by Neumann *et al.* (1981) of hurricane tracks of the North Atlantic between 1871 and 1980 which fails to yield a single example of such a feature even entering the Trafalgar sea area (as currently defined), let alone lingering actively for 7 days. The majority of hurricanes recurving across the Atlantic do so along routes followed by mid-latitude systems, leaving Iberia undisturbed to their south. There is a tendency, though no more, for late-season storms to follow slightly more southerly routes, but not to the degree required here.

There is, interestingly, evidence for at least one 'hurricane' in the North Atlantic during that historic month. The New England cleric James Bentley describes a storm to strike the coast of Maine on 3 October '...in the morning it began to rain at north east, wind increasing till noon and then blew violently. Houses, barns, trees and fences were in devastation...it is called a tornado, hurricane and storm. It appears to have been a violent north-east rain storm.' The confused terminology is significant, warning against unquestioning reliance on qualitative description. However, this storm can hardly have been that which struck the English fleet 19 days later off Cadiz. In fact the nearest-ever mapped approach by a designated hurricane to the region came as recently as November 1966 when hurricane Louis, though at that stage moribund, reached a point about 500 miles west of Cape Finisterre, where it finally dispersed on the 14th. The position is best summarized thus '...very few depressions enter the region (Azores to Britain) as well-developed hurricanes.' (Meteorological Office 1978).

Yet storms and gales were a well-known hazard in these waters. The archives at Lloyds of London contain an interesting memorandum in an unknown hand concerning navigation in a storm off Cape Trafalgar. It begins 'People who are ignorant of the navigation of the coast between Cape Trafalgar and Cape St. Maries (*sic*) are much alarmed with the idea of a south-west gale, and for want of a proper knowledge how these gales come on frequently get into difficulties. The gale is always far southerly on its outset for six or eight hours, but at the same time the sea will make from the westward.' The document goes on to describe how winds will veer to the south-west as the storm rises. Indeed, so distinguishable are these south-westerly gales that they enjoy the distinction of the local name *los vendavales*. But, more importantly, the pattern here described in such general terms bears a strong resemblance to the sequence of events already related. On leaving Cadiz, the combined French and Spanish fleets were prevented from making a rapid passage to the Strait of Gibraltar by a southerly wind, while the subsequent westerly swell and veering winds are well documented.

These waters are too far south to be influenced by normal mid-latitude cyclones but fall well within the latitude of those features generally described as cut-off lows. Here lies the most likely explanation of the Trafalgar storm and the most fruitful source of comparison with more recent and well-studied events.

With regard to these cut-off features the Meteorological Office (1978) has amply demonstrated that October and November are the very months when they occur most frequently. In a study period of

10 years, 75 were recorded of which 20 arrived during those 2 months. Most persisted for only a few days but, significantly, almost 20% lasted for a week or more.

Capel Molina (1980) has shown that the development of meridional upper-air streams leads to cut-off lows and pools of cold air at the latitude of Iberia. Of the routes the consequent lows follow, 36% track south-eastwards to approach the Gulf of Cadiz but only half of those fail to pass through the Strait of Gibraltar, and founder against the abrupt relief of the Iberian massif. In this position they bring some of southern Spain's heaviest rainfalls and strongest winds. Another route, but followed by only 11% of cut-off lows and generally in the summer months, is to approach Iberia from the west. Such depressions bring occasional heavy showers to interior Spain but have generally dissipated their energies before reaching the east coast.

The general characteristics of the Trafalgar storm, its timing, location and behaviour, conform to those of a cut-off low. Such an interpretation gains further support from the contemporary British conditions. Pressure data for three sites, Goodwood House, Newcastle upon Tyne and Ednam, all indicate a rise of pressure on the 18th, the anticyclonic conditions lasting until the 24th. Correction to appropriate sea-level figures is a hazardous process but there is a clear impression of a northward increase in pressure which at Newcastle was above 1030 mb, approximately 5 mb higher than at Goodwood House. In addition Newcastle recorded air frosts on the 20th and 21st and Ednam on the 19th, 20th and 21st. Both locations variously described the weather as fine, dry and calm. Further north, James Ramsey's diary records calms from the 19th to 22nd with frost every night, snow having already fallen on the nearby hills. Winds were variable and light in the north throughout this period. This evidence of anticylconic conditions supports, though obviously cannot prove, the cut-off hypothesis.

Southern England appears to have been peripheral to both the storm and the anticyclone. The Goodwood House records reveal 'brisk' easterlies and north-easterlies with temperatures possibly 9 °F above those in Newcastle. *Foudroyant*'s log makes reference to south-easterly gales on the 22nd, 23rd and 24th, at which time this former command of Nelson's was weathering the conditions some 70 km off Ushant. Fig. 2 depicts the general pressure patterns as they may have appeared on 22 October 1805 and is based on the contemporary evidence discussed in the foregoing paragraphs.

The most probable date for the birth of the storm is 19 October. The arrival of a cold pool of air over Iberian waters at this season would have found the seas at their warmest, between 17 and 20 °C, giving ample scope for instability and intensified activity. Indeed such southward eruptions of cold air are a feature of the Spanish climate, often bringing the summer to an abrupt close. The following quotation is of more than passing interest 'In terms of pressure patterns the most striking feature is the autumn break which shows up prominently about 20 October on all pressure curves from Perpignan and Gibraltar to Malta...' (Meteorological Office 1962).

However, the duration of the anticyclone does not match that of the storm. The anticyclone dispersed, or retreated, on 24 October to be replaced in all areas by much milder, wetter conditions. The winds became moderate to fresh north-east and east until the 28th over the whole of Britain. The weather was occasionally sunny, but with rain showers in the north developing into more persistent and frequent rain in the south. Numerical data from the records of the Reverend James Cowe at Sunbury (Middlesex) show 0.86 inches of rainfall on the 24th, nil on the 25th, 0.48 on the 26th and 0.1 on the 27th. Such a pattern of wet easterlies argues in favour of a depression passing to the south of England and, in view of *Foudroyant*'s records, possibly along the English Channel; 'variable with rain' appears as an entry on the 25th.

This disruption to the anticylcone may have invigorated the storm to the south. There is a suggestion from the logs that by the 25th it was on the decline, many vessels noting strong breezes to replace gales. All this changed on the 26th which, if the logs are to be believed, must have had the most serious day's weather of the week, most ships recording gales which were frequently strong in nature and severe enough to cause Admiral Cuthbert Collingwood to order his fleet to cast off and scuttle the few valuable prize ships left at this stage. This important resurgence of activity may have been brought about by the further introduction of cold northerly air following in the wake of the northerly located depression. But, whatever the cause, the storm was vigorous enough to sustain itself until 29 October when it finally yielded to more settled conditions.

5. Analogues

The behaviour of cut-off systems is sufficiently consistent to have enabled Boyden (1963) to identify some useful criteria for their prediction. Nevertheless, a search of the past 25 years of weather charts has failed to produce a sequence of events to match those of that fateful October week in 1805. Given the inherent variability of weather systems this failure is not unexpected and need not refute the arguments offered above. It may also be added that Colman's (1986) research has shown the first two decades of the nineteenth century to be the northern hemisphere's coldest for over 200 years, suggesting that the general conditions then and now may not be perfectly comparable. Nevertheless, some situations were found that echoed, in part, those of 1805 in general character though not in degree or persistence.

Tolerably close analogues for the first phase of the storm between 20 and 24 October are not hard to find and of the several encountered that of January 1963 came as close as any. The situation was again one of severe weather, but with respect to the anticyclone and not the cut-off depression itself, for January 1963; indeed the whole of that winter was a time of exceptionally cold weather. This aspect may not be without further importance, for Birkeland's (1949) study of the Norwegian temperature records from 1761 showed October 1805 to have been a month of unusually low temperatures, departing from

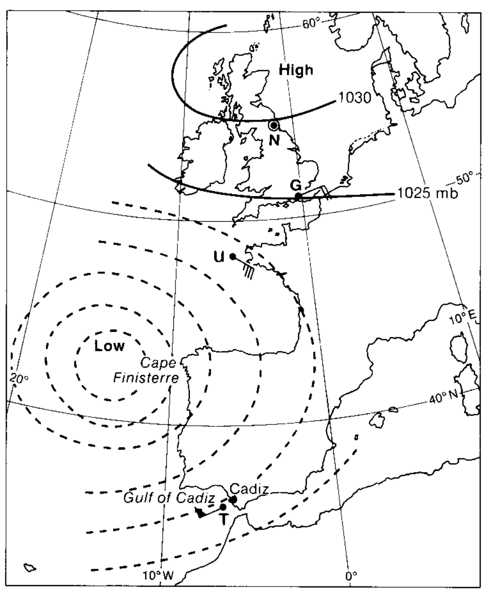

Figure 2. Reconstructed synoptic situation for 22 October 1805. It was on this day that the storm struck the vessels which survived the battle. It seems probable that the strong south-easterlies recorded off Ushant (U) would have been part of the same circulation that generated the gales at Trafalgar (T). Contemporary data for the British Isles indicate east-north-east winds at Goodwood House (G) and calms over much of northern Britain, as for example at Newcastle upon Tyne (N). The barometric data for the latter two locations allow an approximate quantification of the local isobars, but elsewhere on the map such evidence is lacking and the isobars are used merely to indicate the interpreted general trend of pressure over the Atlantic seaboard.

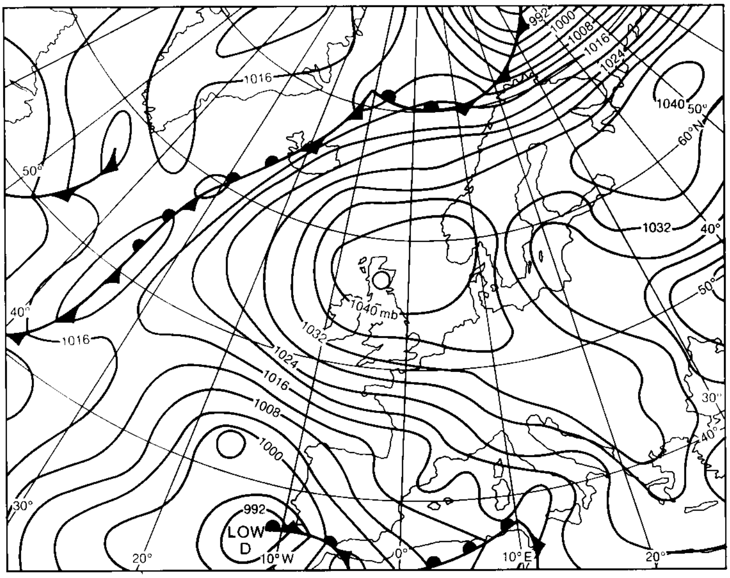

Figure 3. Surface analysis at 1200 GMT on 17 January 1963. In terms of at least the disposition of pressure systems the situation resembles that of 22 October 1805. Only the strength of the south-west winds over the Gulf of Cadiz fall short of the requirements. The generally easterly air flow over southern England and the English Channel, together with a calmer atmosphere in the north corresponds well with what is known of weather over Britain around the time of the battle.

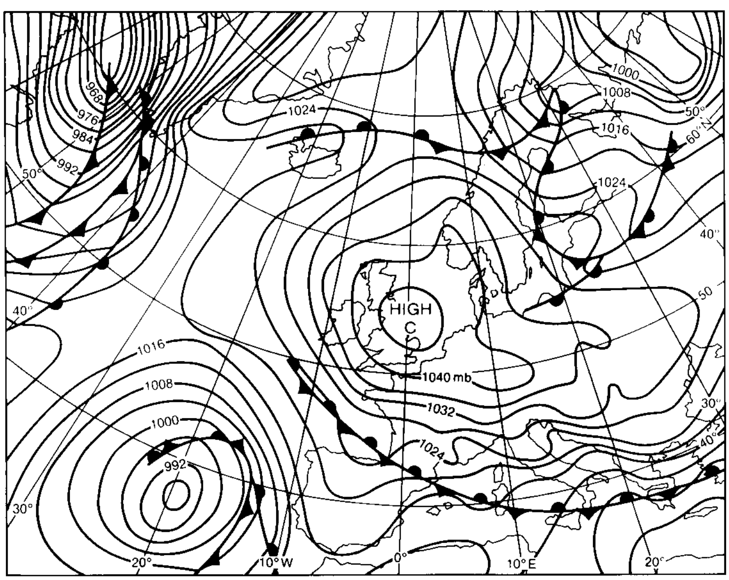

Figure 4. Surface analysis at 1200 GMT on 22 January 1963. The large and well-developed cut-off low, then approaching Iberia, had formed on the 19th and travelled east-south-east to its location. The situation, with the advancing depression and light winds over the Gulf of Cadiz (and a probable westerly swell), echoes that of the day of battle (21 October 1805). The high pressure over Britain conforms to the impression given by contemporary observations, with easterlies in southern districts but calmer, more anticyclonic, conditions to the north.

the mean by as much as 2.9 °C. Indeed the 1762–1946 records used by Birkeland show only six colder Octobers. Manley's (1974) central England temperature record also shows the month to have been cool, nearly 2 °C below average. January 1963 was the coldest month on record at many sites; the England and Wales deficit was 5.3 °C while at Kew it was the coldest month since January 1838.

Against this significant background the events of 17–29 January 1963 may be reviewed. In fact this 2-week period produced two cut-off situations off Iberia, both with possible similarities to the first phase of the Trafalgar storm. On 17 January (Fig. 3) the well-established anticyclone over Britain, together with the depression centred west of the Gulf of Cadiz, represented a situation not unlike that of 22 October 1805. The 'high' is seemingly more intense and the 'low' less well developed but the wind directions conform perfectly with the evidence already reviewed: south-west off Cadiz, east to south-east over the English Channel and southern Britain and calm over northern Britain. However, low 'D' then pursued an unusual northerly track along the Iberian coast before filling on 20 January off Cape Finisterre. The system was, then, neither so long-lived nor stationary as its 1805 predecessor. In addition the anticyclone remained active for much longer and was associated with the second analogous event of 21 January.

High 'C' (Fig. 4) was born out of the merging of the northward-moving anticyclone discussed above with another system over Greenland on the 19th. This new feature drifted south-south-east then south to lie off the coast of north-east England on the 22nd. The large and active 'low' nearing the Gulf of Cadiz formed at 43° N, 38° W on the 19th and then moved east-south-east. The situation depicted in Fig. 4 is similar to that on the day of battle (21 October) when light winds prevailed over the Gulf of Cadiz but were about to give way before the advancing depression. Although the 1963 system remained identifiable until the 29th, and thus matched the original in its duration, it failed to continue its progress and remained too far to the west to influence inshore waters. The anticyclone over Britain persisted unabated throughout this time to deny any further southward movement of cold air at this longitude.

6. Conclusion

It is the nature of weather events that no two will ever be perfectly alike. But patterns and similarities in cause and consequence do exist. This paper has attempted to reconstruct the synoptic situation for a momentous historical event in which weather exercised a major influence. The storm threatened to destroy the English fleet but had it arrived only 48 hours sooner would have saved the Franco-Spanish vessels, for it would have dispersed Nelson's fleet and enabled the enemy to slip through the Strait of Gibraltar and make good their flight into the Mediterranean, and the battle of Trafalgar might never have been fought.

The study has called upon instrumental and qualitative information, both of which have yielded an encouragingly consistent view of conditions. The analogue of January 1963, the closest to be found for recent times, was interesting in that it was also a month of exceptionally cold conditions in northern latitudes although this feature is more likely to be a consequence than a cause of the synoptic situation. But more informative is the failure to find a close analogue in terms of the combined intensity and duration of the Trafalgar storm; a fact that emphasizes its exceptional meteorological character.

Acknowledgements

The author would like to express his gratitude to David Ludlum (Princeton, New Jersey) for kindly providing information from the diary of James Bentley, and Marjorie Roy (Edinburgh Meteorological Office) for making data available from the Meteorological Office archives at Edinburgh. Financial support for this study was given by Sunderland Polytechnic.

References

Birkeland, B.J.	1949	Old meteorological observations at Trondheim. Geofysiske Publikasjoner, Vol. XV. Norsk Videnskaps-Academi i Oslo.
Boyden, C.J.	1963	Development of the jet stream and cut-off circulations. *Meteorol Mag*, **92**, 287–299.
Capel Molina, J.J.	1980	Los Climas de Espãna. Barcelona, Oikas-Tau.
Colman, A.R.	1986	Northern hemisphere temperature fluctuations within the instrumental period. *J Meteorol*, **11**, 306–312.
Kington, J.A.	1970	A late eighteenth century source of meteorological data. *Weather*, **25**, 169–175.
Manley, G.	1974	Central England temperatures: monthly means 1659 to 1973. *Q J R Meteorol Soc*, **100**, 389–405.
Meteorological Office	1962	Weather in the Mediterranean, Vol. I (second ed.). London, HMSO.
	1978	Weather in home waters, Vol III; The waters around the Azores and off south-west Europe and off north-west Africa. London, HMSO.
Neumann, C.J., Cry, G.W., Caso, E.L. and Jarvinen, B.R.	1981	Tropical cyclones of the North Atlantic Ocean 1871–1980. Ashville NC, NOAA.
Oliver, J. and Kington, J.A.	1970	The usefulness of ships' logs in the synoptic analysis of past climates. *Weather*, **25**, 520–528.
Wheeler, D.A.	1985	The weather at the battle of Trafalgar. *Weather*, **40**, 338–346.

551.579:551.506.3:551.582.2(410):556.1

The MORECS climatological data set — a history of water-balance variables over Great Britain since 1961

M.S. Shawyer and P. Wescott

Meteorological Office, Bracknell

Summary

Hydrometeorological and water-balance variables are calculated weekly from meteorological observations over Great Britain by the Advisory Services Branch of the Meteorological Office using the Meteorological Office Rainfall and Evaporation Calculation System (MORECS). To allow current values to be placed in perspective, meteorological data from 1961 onwards have been used retrospectively in MORECS to produce a climatological data set of these variables.

1. Introduction

Although the hydrological cycle is well known for its contrasting properties of being conceptually simple yet difficult to quantify, calculations of the values of its constituent parameters are increasingly required for cost-effective and efficient water management over areas ranging from fields to river catchments. For example, a reliable assessment of irrigation requirements benefits farmers, whereas the evaluation of catchment water balance and river flow assists water authorities in managing water supplies and handling flood situations.

The relevant variables are precipitation amount, evaporation, and soil moisture deficit (SMD). All are capable of being measured, and the first is sampled extensively, but the other two are hardly measured at all, their values being derived from pertinent meteorological information. Rainfall values have been measured and collected in an organized and consistent manner since the formation of the British Rainfall Organization in 1860. However, the absolute accuracy of surface point rainfall measurements has not increased appreciably since that time, mainly due to the cost and logistics of improving the simple rain-gauge. Although there are inaccuracies in point rainfall totals and, more importantly, inaccuracies in areal rainfall totals derived for use in water-balance calculations, there is considerably more uncertainty associated with measurements of evaporation and SMD.

Evaporation has been measured using tanks of water placed in the ground and noting the difference in the levels of water over a period of time with allowance being made for any precipitation during that period. This technique was established on a regular basis more than 100 years ago when it was discussed, together with other evaporimeters, in the 1869 edition of *British Rainfall.* Tanks of a similar design were still in use recently and the results from these should indicate potential evapotranspiration (PE), i.e. the quantity of water vapour added to the atmosphere from a surface covered by green vegetation with no lack of available water; however, there is evidence that the exposure of these tanks was less than ideal. Data from a few lysimeters are available, but these instruments need careful maintenance and are, therefore, usually sited only at research establishments. They consist of pans on a weighing mechanism within a cavity created by removing a section of land, that section being placed in the pan with as little alteration to its structure as possible. The lysimeters are capable of measuring PE or actual evaporation (AE) depending upon whether or not they are irrigated.

The SMD can be determined using a device called a neutron probe. Fast neutrons, emitted by a portable source inserted in the ground, lose energy at a rate dependent upon the soil moisture. The slow neutrons can be detected and an estimate derived of ground moisture. This is a comparatively recent invention and again, very few measurements are available, and none routinely to the Meteorological Office.

United Kingdom observations of evaporation and SMD are thus insufficient in quantity or quality for any operational or climatological purpose. However, estimates of these parameters can be derived from meteorological observations. The near real-time requirement for water balance information is satisfied by the Advisory Services Branch of the Meteorological Office using the operational system called MORECS (Meteorological Office Rainfall and Evaporation Calculation System) which uses observations provided by the synoptic meteorological observing stations (Thompson *et al.* 1981)*. MORECS is the successor to the ESMD (Estimated Soil Moisture Deficit) bulletins and, as such, uses a more sophisticated theoretical model together with realistic information on vegetative cover and land use. MORECS has been used to produce historical values of water-balance variables, using carefully monitored data going back to 1961, to give a 26-year climatological data set over Great Britain†. Although the detection of climatic change in water-balance variables would need observations over many years, a useful description of their variation from year to year can be obtained over such a period.

2. MORECS

The input data to MORECS are rainfall, sunshine duration, temperature, vapour pressure and wind speed. Because of the need for a timely dissemination of MORECS products, data can be used only from those stations reporting daily in near real time, approximately 200 for rainfall and sunshine and 50 for vapour pressure, temperature and wind speed. Rainfall and sunshine are reported as daily totals, the

---

* Thompson, N., Barrie, I.A. and Ayles, M.; *The Meteorological Office Rainfall and Evaporation Calculation System MORECS (July 1981).* Meteorological Office, 1981.

---

† Further information about the climatological data set may be obtained from the Advisory Services Branch, Meteorological Office, London Road, Bracknell, Berkshire RG12 2SZ.

remaining variables are usually sampled more than once per day and a daily-mean value calculated. The data are then normalized as follows:

(a) Rainfall is expressed as a percentage of the annual station average.

(b) Sunshine is converted to a percentage of the average daily duration for the month.

(c) Temperature and vapour pressure are corrected to mean sea level using standard factors.

(d) The 10-metre wind speed is converted to a value appropriate to a standard site using an empirical factor related to the general terrain roughness around the station.

The weekly values for these normalized data at a network of irregularly spaced stations are then used in an interpolation procedure to produce estimates for an array of 190 grid points with a 40 × 40 km spacing covering Great Britain. In general, the interpolation is more realistic if the field upon which it is operating has only a small range, and this is a justification for normalizing the raw data prior to using the procedure. The grid-square (areal) values are then obtained from the grid-point values; for example, for rainfall, the product of interpolated grid-point percentage and average annual rainfall (1941–70) for the square yields the grid-square rainfall.

The daily PE is computed for each grid square for a range of surface vegetation by using the appropriate grid-square values as input to the Penman–Monteith equation. This equation takes into account aerodynamic mass transfer and energy-budget considerations together with the inclusion of physiological factors via atmosphere–plant–soil resistance terms. Estimates of AE are then formed for soils with high, medium and low available water capacity. The daily water balance is calculated for various types of cropped surfaces and also for the average land use for each square. The final step is the construction of computer-drawn maps for grass and real land use, showing the grid-square weekly averages of temperature, vapour pressure and wind speed, the weekly totals of rainfall and sunshine, together with weekly totals of PE, AE and hydrologically effective rainfall (the rainfall remaining after SMD and evaporation loss is removed) and end of week SMD. An example of the type of map produced by MORECS is given in Fig. 1.

Each week, the MORECS suite of programs is run operationally using data from the previous seven days and the output is disseminated to customers by post, telex, facsimile or Prestel. The MORECS climatological data set exists in machinable form and can be browsed, or used as input to statistical routines to provide, for example, 26-year averages of the hydrometeorological and water-balance variables, their standard deviations and maxima and minima for one or more squares. The climatological data set is continually updated from the operational MORECS products.

3. Some results from the MORECS climatological data set

The 25-year monthly averages of SMD, AE, PE and rainfall for two contrasting MORECS squares are shown in Fig. 2, and Table I lists the corresponding variability and ranges for rainfall. Fig. 2(a) contains information for square 83 which covers the Lake District, the major land use being permanent grass and rough grazing, whilst Fig. 2(b) refers to square 141 which covers Suffolk (and includes the much drier and flatter countryside around Bury St. Edmunds) where the land use is mainly permanent grass, cereals and main-crop potatoes. The location of these squares is shown in Fig. 1.

The most noticeable features about the soil moisture budget of the Lake District are:

(a) the very large rainfall totals (100 mm or more, on average, every month),

(b) the comparatively small SMDs, and

(c) the similarity between AE and PE.

As the ground, on average, is not far from being at field capacity (i.e. the ground is nearly saturated), it would be expected that evaporation occurs at very nearly the potential rate and, indeed, the two curves are almost coincident.

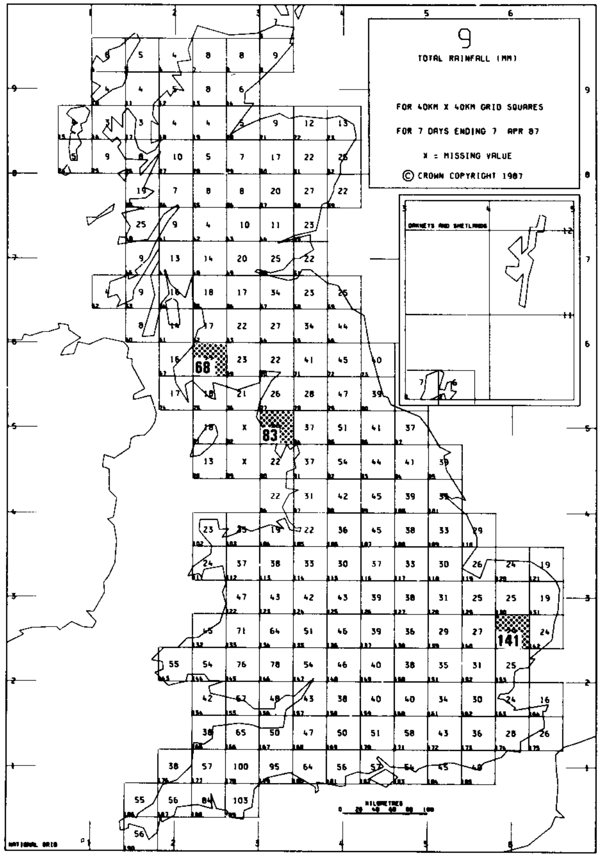

Figure 1. A computer-drawn map showing rainfall values produced by MORECS. The shaded squares are those referred to in the text.

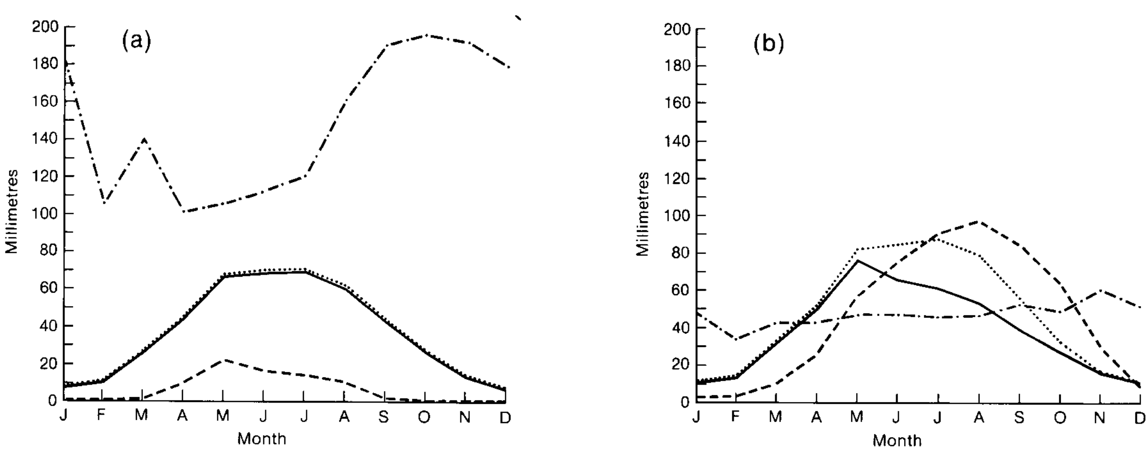

Figure 2. Mean monthly soil moisture budget for (a) MORECS square 83 (Lake District) and (b) MORECS square 141 (Suffolk), showing soil moisture deficit (dashed line), actual evaporation (solid line), potential evapotranspiration (dotted line) and rainfall (dot-dash line).

Table I. *Variability of rainfall and its range, for two MORECS squares (25-year monthly averages)*

Square number	Month	Coefficient of variation	Maximum rainfall (mm)	Minimum rainfall (mm)
83 (Lake District)	Jan.	0.42	414.0	34.9
	Feb.	0.54	231.3	16.4
	Mar.	0.45	284.2	58.0
	Apr.	0.51	184.2	7.0
	May	0.52	244.8	21.1
	June	0.36	187.4	51.1
	July	0.41	248.7	48.6
	Aug.	0.46	334.6	14.4
	Sept.	0.35	306.5	28.4
	Oct.	0.48	427.0	78.0
	Nov.	0.33	322.2	90.8
	Dec.	0.42	294.4	56.3
	Mean	0.44		
141 (Suffolk)	Jan.	0.40	88.2	14.6
	Feb.	0.49	68.2	9.9
	Mar.	0.51	96.4	7.3
	Apr.	0.51	92.3	8.7
	May	0.43	78.6	9.8
	June	0.58	117.6	5.6
	July	0.51	94.5	5.9
	Aug.	0.54	110.7	12.9
	Sept.	0.66	124.1	1.3
	Oct.	0.70	121.9	2.8
	Nov.	0.46	154.2	19.8
	Dec.	0.42	101.4	15.4
	Mean	0.52		

By contrast, the data for Suffolk show that:

(a) the average monthly rainfall totals are more variable and much less than those in the Lake District,

(b) the maximum SMD is approximately five times greater than the maximum in the Lake District, and

(c) the difference between PE and AE is now significant because of the dryness of the ground, and this is an indication that irrigation of some crops may prove beneficial.

In Table I it can be seen that the variability of monthly rainfall totals over Suffolk is larger than that in the Lake District, and substantially so in summer; a consequence of the increased susceptibility of the former to showery activity.

Fig. 3 shows the end of July SMD over grass for both squares varying from year to year. Notable features include the rainfall deficiency of 1976, shown by the relatively high SMD. In addition to graphical output, tabular output is available detailing monthly values of a wide range of variables for the 25-year period.

4. Some uses of the climatological data set

An important application for such a data set will be to place specific, especially notable, meteorological events in perspective. The rainfall deficiency of 1984 which affected mainly northern and western districts of the United Kingdom between February and the end of August provides a comparatively recent example. Several places experienced a 5-month (April to August) rainfall total of

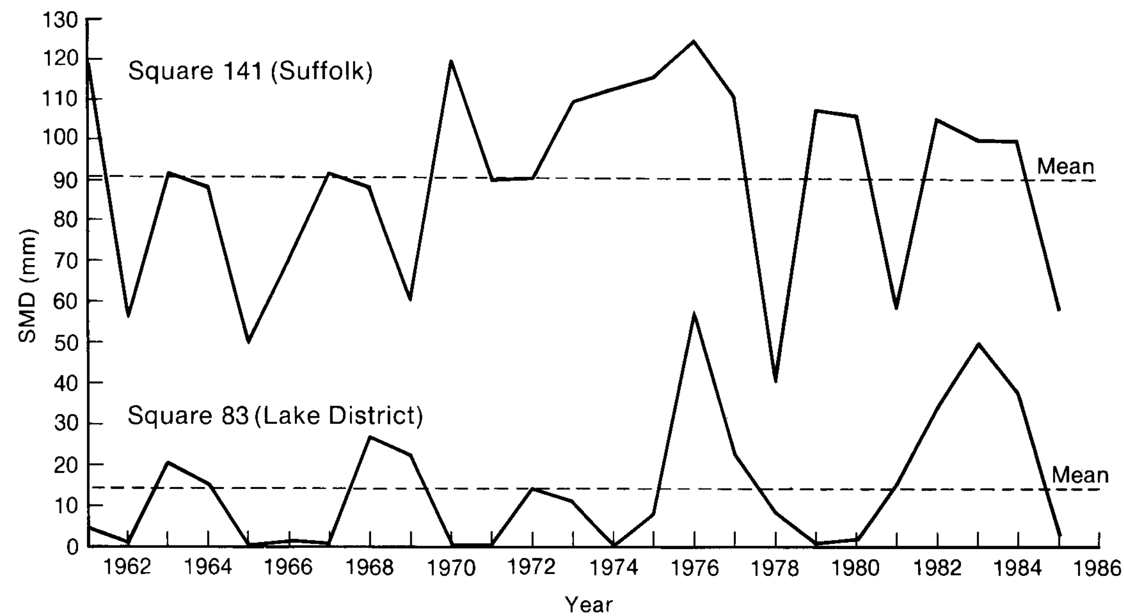

Figure 3. End of July soil moisture deficits (grass) for MORECS squares 141 and 83 for the period 1961–85.

less than 30% of the 1941–70 average, whilst over the area administered by the Welsh Water Authority only 44% of the long-term average rainfall was recorded for these same months, an event with an estimated return period of at least 200 years. The values of SMD and rainfall for February–September 1984 for square 68 (Dumfries and Galloway, Scotland) are listed in Table II, together with values for the same months of 1976. Although well remembered as a period of below-average rainfall, 1976 is seen to have been less severe than the event of 1984. Similar results have been obtained for other squares in Scotland.

Table II. *Values of rainfall (R) and soil moisture deficit (SMD) for the period February–September in 1976 and 1984 for MORECS square 68 (Dumfries and Galloway, Scotland). Values in millimetres*

	Feb.		Mar.		Apr.		May		June		July		Aug.		Sept.	
	R	SMD	R	SMD	R	SMD	R	SMD	R	SMD	R	SMD	R	SMD	R	SMD
1976	133.7	0.0	130.8	0.0	69.5	25.3	192.2	0.0	70.6	26.3	53.3	57.4	35.5	81.9	171.5	0.0
1984	138.1	0.2	56.4	2.1	40.3	26.5	21.8	74.9	76.0	69.6	42.7	85.0	75.9	77.4	180.4	0.0

Another obvious use of the climatological data set will be to allow current (operational) MORECS values to be categorized, thereby enabling customers to make informed commercial decisions in the light of their own previous experiences. The agricultural community would be potential users, for example in irrigation planning, although such information could be of considerable value to commodity brokers in assessing the probabilities of bumper or meagre harvests.

5. Conclusions

A consistent and comprehensive climatological data set of the main hydrometeorological and water-balance variables has been produced for the period 1961–85. It is intended that the operational

MORECS values will be added to the climatological data set, thereby improving the usefulness of the results.

The network of stations contributing data to the model has remained fairly static over the past 25 years, but the implementation of automatic weather stations should result in an increase in the number of stations reporting in near real time, particularly rainfall stations. This is important because the current 200 or so are insufficient to represent reliably the spatial characteristics of this very variable meteorological parameter. It is possible that radar measurements of rainfall can also be used to supplement the rain-gauge observations. If the climatology is to be of benefit in the years to come, then the effects of an increasing amount of input data on the computed water balance must be investigated to enable relevant comparisons to be made.

551.576.11:551.521.14:551.521.325(265.2)

Meteorological Office catches FIRE!

S. Nicholls
Meteorological Office, Bracknell

Summary

During June and July 1987, a field experiment designed to study in detail the processes active in extensive low-level cloud sheets is being held off the coast of California. This is one part of a larger programme called FIRE which aims to investigate the properties of those cloud fields which play an important role in determining the earth's climate through cloud–radiation feedback mechanisms. This article briefly describes the major objectives of the programme and the observations which will be made during the field experiment.

1. Introduction

Although it has long been recognized that clouds are one of the most important factors influencing the global climate, the representation of large-scale cloud systems in numerical climate models remains one of their weakest points. Since it has been estimated that a change in the global cloud cover of only a few per cent could offset the anticipated global warming due to a doubling in carbon dioxide levels, this clearly constitutes a major source of uncertainty in such forecasts. One of the main factors contributing to this uncertainty is undoubtedly the limited understanding of the processes which control the formation and dispersal of various cloud types, and therefore the cloud amount. It is also not clear how this balance varies in different areas of the world or how radiation and cloud fields interact. A better understanding of these issues is a prerequisite for better representations of clouds in numerical models. Indeed, the World Climate Research Programme has placed the highest priority for climate research on two areas: ocean–atmosphere interaction and cloud–radiation feedbacks, and clouds are a central element in both problems.

Of course, it is not only through their effect on climate that clouds exert an important influence, since virtually all areas of meteorological interest are either closely associated with cloudy processes or are affected by their presence. Weather forecasters and the public are, therefore, likely to be eventual beneficiaries from increased understanding in this area.

Until quite recently there have been very few comprehensive, quantitative measurements of clouds, largely because of the observational difficulties, and most of the measurements have been taken during specialized research projects of limited duration. Routine operational data have traditionally relied on reports from ground-based observers with little benefit from quantitative instrumentation. Cloud climatologies have, therefore, been based on limited information and are essentially local, not global, in scope. In an attempt to improve this situation, the International Satellite Cloud Climatology Project (ISCCP) is currently gathering satellite observations to provide better information about the distribution of cloudiness around the globe (Schiffer and Rossow 1983). Furthermore, analyses of geostationary satellite data have already revealed features in cloud fields which were hitherto undetected. One example is the coherent diurnal and seasonal variation of subtropical stratus cloud which is clearly important and which requires explanation (e.g. Minnis and Harrison 1984). At the same time, the treatment of clouds in numerical models has also been quite rudimentary, partly reflecting the lack of observational data. It is therefore highly desirable to improve cloud models and methods of parametrizing their effects to include representations of the important physical processes and to compare the predictions of these models with the new observations.

With all these points in mind, a broadly based research programme, called the First ISCCP Regional Experiment (FIRE), was set up in the United States to carry out a comprehensive study into some of these issues, within the context of the ISCCP.

FIRE consists of a set of self-contained experiments, designed to address specific parts of the cloud–radiation feedback problem, containing both observational and modelling programmes.

Two types of cloud system have been identified for special attention:

(a) marine stratocumulus which occupies extensive areas especially over the eastern ocean-basins where it is associated with the regions of highest-average global cloud cover, and

(b) cirrus whose global distribution is still very uncertain.

Marine stratocumulus exerts a strong influence on the energy transfers between the atmosphere and the ocean and on the structure of the boundary layer, while cirrus has a major effect on the flux of infra-red radiation lost to space.

Because an independent Meteorological Office research programme with many similar aims was already under way (Nicholls 1984, Nicholls and Leighton 1986, Turton and Nicholls 1987, Nicholls 1987), the Office was invited to participate in FIRE. As a result, three Meteorological Office research groups from the Cloud Physics Branch, Boundary Layer Research Branch and the Meteorological Research Flight (MRF) will make a sizeable contribution to the FIRE marine stratocumulus investigation.

The objectives and experimental strategy discussed in the next two sections refer to the situation as it existed in May 1987.

2. The objectives of the FIRE marine stratocumulus investigation

The goal of the FIRE marine stratocumulus studies is to seek a better understanding of the interaction of the physical processes which determine the evolution of these cloud systems, especially their radiative properties. Observations will be made on a wide variety of time and spatial scales to enable current ideas and models to be tested and refined (Randall *et al.* 1984). It is hoped that this will ultimately lead to better representations in global climate studies and provide a data base suitable for testing a wide variety of models, including detailed radiative transfer and microphysical calculations, and different types of boundary layer model.

This broad strategy may be further broken down into a number of more specific aims. Although not a complete list, attempts will be made to:

(a) investigate the relationship between the cloud structure, its microphysical properties and its radiative properties by making simultaneous measurements at different levels,

(b) study the droplet distributions within the clouds, the processes influencing them and the growth of precipitation,

(c) measure and investigate the factors controlling the entrainment rate at cloud top,

(d) determine how radiation affects mixing within the boundary layer, especially the response of the clouds to the diurnal cycle,
(e) characterize the structure of cloud fields on various time and spatial scales using satellite observations,
(f) test satellite cloud retrieval algorithms, e.g. for cloud amount and cloud-top height,
(g) determine the factors that affect fractional cloud cover and cloud morphology,
(h) study the formation and break-up of cloud sheets and provide data to enable models of these processes to be constructed and tested, and
(i) assess the role of mesoscale processes and their effects on these cloud fields.

3. Implementation — experimental strategy

Achieving the aims of the investigation requires a diverse set of observational and modelling techniques — this demands a collaborative approach. The logistics are being co-ordinated through a FIRE project office set up by the National Aeronautics and Space Administration (NASA), while the scientific aspects are managed by the 40-strong FIRE science team which comprises most of the principal investigators. The FIRE participants have agreed to pool their data in a common format for use by any of the others.

The area chosen for the marine stratocumulus experiment lies off the coast of California (see Fig. 1). Stratocumulus covers extensive areas of the eastern Pacific, including this region, for much of the summer. The cloud lies beneath a strong temperature inversion associated with the subtropical anticyclone and over a relatively cool ocean surface. Similar conditions exist in other eastern ocean-basins at similar latitudes. Climatological records show that offshore cloud cover at San Nicolas Island (see Fig. 1) exceeds 6 oktas for 40% of the time during June and July.

There are basically two types of observational strategy:

(a) Extended Time Observations (ETO) based largely on routine satellite products with a minimum of local ground-based measurements, and
(b) Intensive Field Observations (IFO) where an intensive local measurement campaign is organized for a relatively short period.

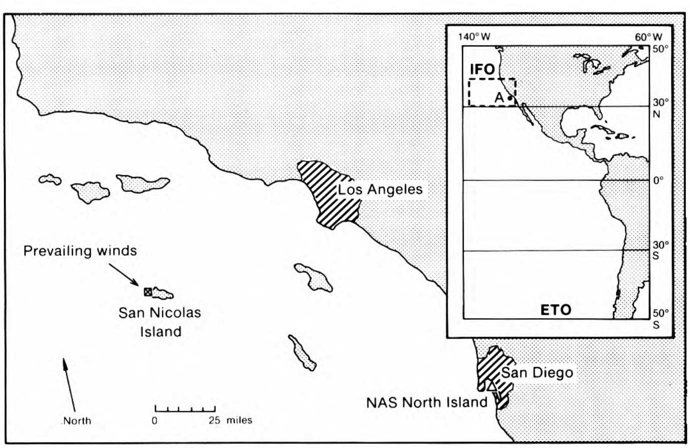

Figure 1. The location of the experimental areas for the FIRE marine stratocumulus Extended Time Observations (ETO) and the Intensive Field Observations (IFO). The more detailed map shows the locations of the aircraft base and IFO Operations Center at Naval Air Station North Island and the offshore San Nicolas Island site.

The two are designed to be complementary. The ETO provide data on large spatial and long time-scales, while the IFO provide the high-resolution, detailed, small-scale data with the ETO as a background.

The ETO began in April 1986. The first IFO will take place during a three-week period in June and July 1987, with a second follow-up IFO period in the same area planned for summer 1989. There will be three groups of measurements during the IFO: high-resolution satellite observations, and aircraft data and surface-based data, as listed in Table I. The instrumentation will comprise the largest, most diverse set ever assembled to investigate these conditions.

The MRF C-130 Hercules will be based, with most of the other aircraft and the IFO Operations Center, at the Naval Air Station, North Island, San Diego. It will fly in conjunction with the other aircraft making *in situ* measurements of turbulence, cloud and aerosol microphysics, and radiation (both broad-band irradiance and narrow-band multi-angle measurements). These multi-aircraft combinations will be a particularly exciting part of FIRE since they offer an opportunity to overcome many of the restrictions imposed by the limited resources available to individual groups, which limit the scope of the investigations that can be undertaken by single investigators. Thus, extended-trajectory

Table I. *Summary of the main FIRE marine stratocumulus observing systems*

Satellite observations	
GOES	VISSR data — 1 km resolution visible, 8 km resolution infra-red, every 30 minutes VAS sounder data
NOAA polar orbiters	AVHRR HRPT data — 1 km resolution, 5 spectral bands TOVS radiance data — 20 spectral bands
LANDSAT	Thematic mapper data — 30 m and 120 m resolution, 7 spectral bands
ERBS	All available archived ERBE and relevant SAGE II data
DMSP	1 km resolution visible and infra-red data
SPOT	10 m or 20 m resolution, visible and near infra-red data
Aircraft observations	
NASA ER-2	Downward-looking lidar mapping cloud top, multi-channel scanning radiometer, thematic mapper simulator, other radiometers
NCAR Electra	Turbulence, cloud microphysics, broad-band radiometers, downward-looking lidar, atmospheric chemistry, constant-level balloon tracker
UW C-131	Cloud microphysics, aerosols, cloud-absorption radiometer
MRF C-130	Turbulence, cloud microphysics, aerosols, multi-channel scanning radiometer, broad-band radiometers
NOSC Navajo	Cloud microphysics, aerosols
All aircraft	Standard meteorological data: winds, temperatures, etc.
Surface observations on San Nicolas Island	
19 m tower	Turbulence, standard meteorological data, aerosols
Surface instruments	Broad- and narrow-band radiometers, cloud-base recorder
NASA tethered balloon	MRU Cardington multiple turbulence probes, single CSU radiation and cloud microphysics package
NRL/NOSC tethered balloon	Single package with standard meteorological data, liquid water
Rawinsonde	2 to 8 soundings per day
UHF profiler	404 MHz Doppler wind-profiling radar
Acoustic sounders	Doppler trimonostatic — wind and turbulence profiles Doppler bistatic — inversion interface structure
Microwave radiometer	Dual 21 and 32 GHz channels giving column-integrated liquid and water vapour
Other surface-based observations	
Ship Point Sur	Radiation, aerosols, microphysics, standard meteorological data, release of constant-level balloons
Coastal rawinsondes	Standard network with extra stations

flights, day–night flights, co-ordinated flights with simultaneous sampling above and within the cloud layer and multi-aircraft runs in broken-cloud conditions will be feasible, all of which are needed to achieve the aims outlined in section 2. Flights will be carried out over the open ocean, away from possible continental influence, and in conjunction with the surface-based instrumentation around San Nicolas Island. Flights will be planned to coincide with satellite passes (especially LANDSAT) and will also be co-ordinated with high-flying aircraft carrying satellite-derived instrumentation to view the clouds at many different scales, angles and frequencies.

Instruments from the Meteorological Research Unit (MRU), Cardington will be flown by the NASA tethered-balloon facility which will be located with the other surface-based equipment on San Nicolas Island. Several of the new turbulence probes designed and built at the MRU will be deployed at intervals along the balloon's tether cable to make simultaneous, multi-level measurements with fine height-resolution. The balloon itself is expected to fly at heights which comfortably exceed the cloud top (which is typically near 1 km). Another instrument package primarily measuring cloud microphysics and radiation data is being developed at Colorado State University (CSU) and this will also be flown from the balloon. The other instrumentation which is expected to be deployed is listed briefly in Table I, and represents a very wide range of observations.

4. Concluding remarks

The marine stratocumulus component of FIRE will probably be the most comprehensive study of these clouds undertaken during the next decade. It offers new opportunities to improve our understanding of the processes controlling layer clouds, especially their interaction with radiation, and will stimulate and focus future research effort in this area. The collaborative nature of the project is an exciting and efficient use of the diverse resources committed to it. Moreover, the wide range of observational methods should result in a number of simultaneous, independent interpretations of the same situation, although each will have a slightly different perspective. It is hoped that this combination will increase our understanding of these types of cloud sufficiently to enable improved representations to be developed in numerical models.

Acknowledgements

Much of the information on which this article is based has been drawn from the FIRE research, implementation and operations plans produced by various members of the FIRE science team.

References

Minnis, P. and Harrison, E.F. 1984 Diurnal variability of regional cloud and clear-sky radiative parameters derived from GOES data. Part II: November 1978 cloud distributions. *J Clim Appl Meteorol*, **23**, 1012–1031.

Nicholls, S. 1984 The dynamics of stratocumulus: aircraft observations and comparisons with a mixed layer model. *Q J R Meteorol Soc*, **110**, 783–820.

(1987) A model of drizzle growth in warm, turbulent, stratiform clouds. (Submitted to *Q J R Meteorol Soc.*)

Nicholls, S. and Leighton, J. 1986 An observational study of the structure of stratiform cloud sheets. Part I. Structure. *Q J R Meteorol Soc*, **112**, 431–460.

Randall, D.A., Coakley, J.A., jun., Fairall, C.W., Kropfli, R.A. and Lenschow, D.H. 1984 Outlook for research on subtropical marine stratiform clouds. *Bull Am Meteorol Soc*, **65**, 1290–1301.

Schiffer, R.A. and Rossow, W.B. 1983 The International Satellite and Cloud Climatology Project (ISCCP). The first project of the World Climate Research Programme. *Bull Am Meteorol Soc*, **64**, 779–784.

Turton, J. and Nicholls, S. (1987) A study of the diurnal variation of stratocumulus using a multiple mixed layer model. (Submitted to *Q J R Meteorol Soc.*)

551.509.57(26)

Verification of global model forecasts of tropical cyclones during 1986

C.D. Hall

Meteorological Office, Bracknell

Summary

Forecasts of tropical cyclones from the Meteorological Office operational global model have been verified. Two examples of model forecasts are shown and verification statistics are given for mean and median errors of the forecast position of all major tropical cyclones in the North Atlantic and North Pacific during 1986.

1. Introduction

Since the introduction of the Meteorological Office operational global model in 1982, its accuracy in middle and high latitudes has been closely monitored. Numerical products covering much of the globe are now distributed to a great many users world-wide and there has been increasing interest in the quality of tropical forecasts, in particular the accuracy of forecasts of tropical cyclones. During 1986, forecasts of all major cyclones in the North Atlantic and North Pacific have been verified and the results are presented below.

The movement of tropical cyclones is difficult to predict by subjective forecasting methods; persistence and climatology offer useful guidance on occasions, but sudden variations in direction and speed of movement are common, especially when systems interact with troughs in the middle-latitude flow. A great many statistical methods have been developed for the prediction of cyclone tracks. Most use multiple regression techniques based on past movement, present fields, and, perhaps also, on forecast fields from a coarse-resolution numerical model. Verification of these methods shows that useful accuracy can be achieved (e.g. Ramage 1980, Allen 1984). Models have also been developed which represent cyclone structure at relatively high resolution (40–60 km perhaps) within a limited area. Boundary conditions to these models are supplied by a coarser-resolution global or hemispheric model so that they can be used for operational forecasting (Harrison and Fiorino 1984, Marks 1985).

The successful forecasting of tropical cyclone movement almost certainly requires not only an accurate representation of the physical processes close to the cyclone centre but also an accurate representation of the large-scale dynamics of the tropics and of the troughs in the middle-latitude flow which frequently extend towards the equatorial regions. These last two large-scale aspects are handled relatively well by global models and, in spite of their low resolution, it is reasonable to expect them to offer some help in the problem of tropical cyclone forecasting. The Meteorological Office global model, having a resolution of around 200 km near the equator, is unable to resolve any of the small-scale structure occurring in tropical cyclones, and indeed the resolution of the model is too coarse to define some of the smaller tropical systems. However, mature typhoons and hurricanes may have horizontal dimensions of 1000–1500 km, and it is these that the model should be able to represent quite well.

2. Verification method

Model forecasts have been verified against reports received regularly on the global telecommunication system from the major tropical forecasting centres. The reports give position and intensity at least every six hours and are based on satellite imagery and observational data, some of which may not be widely available (e.g. from reconnaissance flights). Since reports of cyclones in the Indian Ocean and southern hemisphere are received irregularly at the Meteorological Office, only the North Atlantic and North Pacific areas have been considered in this study.

The forecasts verified have been restricted to those for which the reported maximum wind speed of the cyclone was in excess of 50 kn at the time of verification. No attempt has been made to verify forecasts of weaker systems which are often beyond the model resolution. The verification of the cyclone positions has been performed manually and is presented as the distance between the lowest pressure on the forecast mean-sea-level pressure chart and the reported position. Only forecasts valid for T+24, T+48 and T+72 hours from 00 GMT analyses have been evaluated.

3. Results

There were 169 occasions when the reported maximum wind of cyclones in the North Atlantic and North Pacific was in excess of 50 kn at 00 GMT. Many of the cyclones were large systems having a horizontal scale of, typically, 1000 km; an example of a model analysis and 72-hour forecast for one of them (typhoon Ben) is shown in Figs 1(a) and 1(b). The forecast in this case was particularly good and demonstrates what can be achieved by a numerical model having a resolution of just 200 km. The observed and forecast tracks of this typhoon are shown in Fig. 2. Between 20 and 24 September the typhoon moved fairly steadily north-west becoming gradually more intense, and by 0600 GMT on the 25th maximum winds of 100 kn were estimated. For the next two days it became almost stationary before accelerating north-east on the 28th as it engaged the flow on the forward side of an amplifying upper trough over Japan. In general, both the slowing down and the final accelerating phase of the typhoon movement were well forecast by the model even at T+72 hours. This was a large tropical system, which the model was well able to resolve, and clearly in the final stages the accurate handling of the middle-latitude upper trough was crucial for successful forecasts.

A second example of forecast tracks is given in Fig. 3 for hurricane Charley which passed close to the east coast of North America. The hurricane was almost stationary during 16 and 17 August, and maximum winds of 65 kn were reported. By the 18th it was accelerating north-east and on the 20th it became extra-tropical and moved east in the middle-latitude flow across the Atlantic. As in the first case the accelerating phase of the hurricane movement was handled well by the model, though the forecast from 00 GMT on the 18th failed to predict the subsequent north-easterly track.

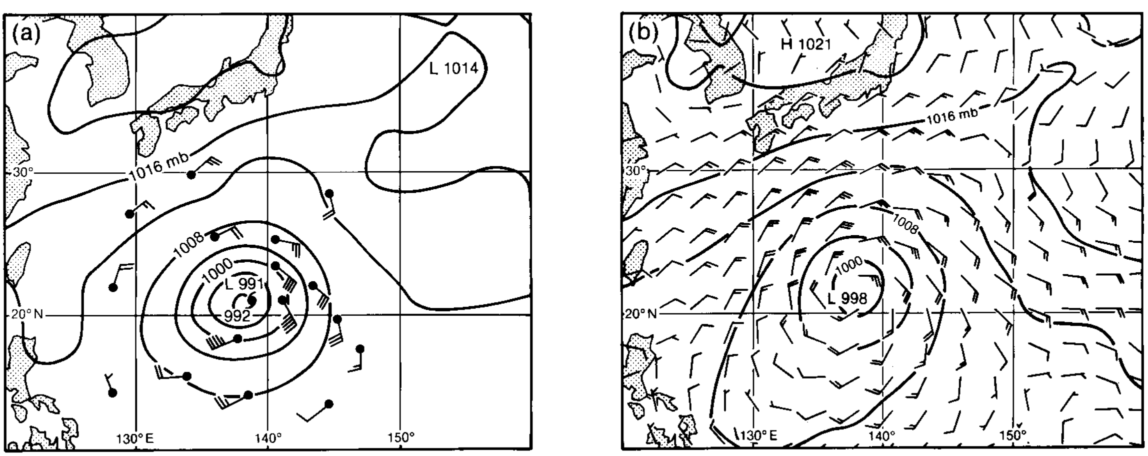

Figure 1. (a) Model mean-sea-level pressure analysis and observed surface winds for 00 GMT on 26 September 1986; the hurricane symbol (🌀) marks the reported centre of typhoon Ben. (b) The T+72 hours forecast mean-sea-level pressure and surface winds for 00 GMT on 26 September 1986.

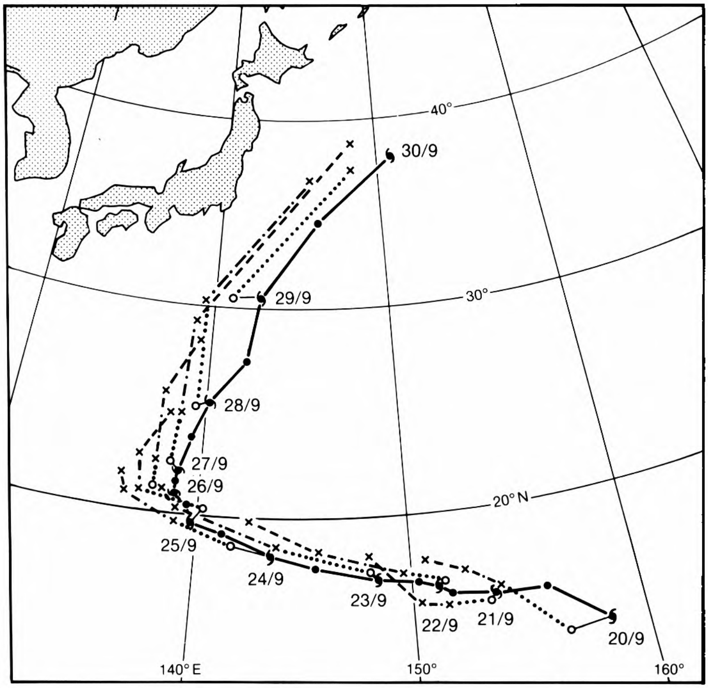

Figure 2. Observed and forecast tracks of typhoon Ben, 20–30 September 1986. The observed track is shown by a solid line with the hurricane symbol marking the 00 GMT positions used for verification, with the date shown alongside. The position of the cyclone centre analysed by the model is shown by an open circle connected by a thin line to the corresponding observed position. The forecast positions at 24-hour intervals are shown by crosses connected by a dotted line for the T+0 to T+24 hours forecast, a dot-dash line for the T+24 to T+48 hours forecast and a dashed line for the T+48 to T+72 hours forecast.

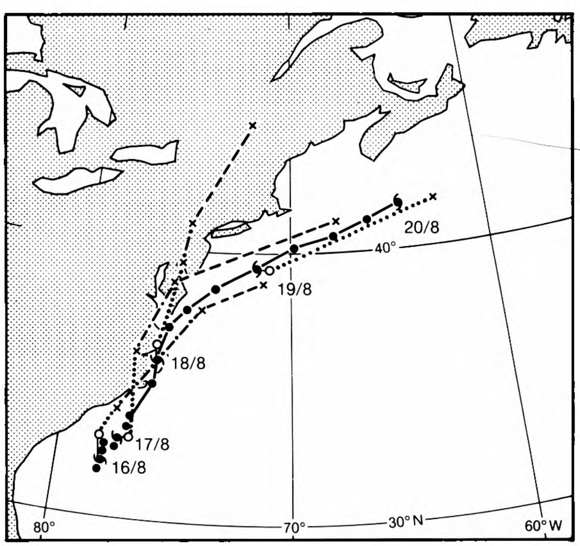

Figure 3. Observed and forecast tracks of hurricane Charley, 16–20 August 1986; legend as Fig. 2.

The tracks of all the cyclones in 1986 have been verified and the mean and median forecast errors are given in Table I. The number of cases where no low centre corresponding to the cyclone was identifiable on the analyses and in the forecasts are also given. Care must be taken when comparing these forecast errors with other published figures since their magnitude is very dependent on which cyclones are chosen for verification. Some tropical systems are poorly defined by the model analyses and have a weak circulation or are totally missing in the forecasts. The criteria used to define which cyclones are identifiable, and therefore used for verification, can have a large impact on the magnitude of the forecast errors obtained.

In general, there seems to be useful skill in the forecasts of cyclone position, especially at T+48 and T+72 hours when persistence and climatology can lead to large errors. The tracks of some of the systems were particularly irregular and model guidance in these cases often has a great deal to offer. On several occasions it seems likely that poor analyses led to poor forecasts. Data are sparse over much of the tropical oceans and there are large areas with no radiosonde observations. Cloud-track winds are an aid to the analysis of the tropical wind field and occasionally they are available within the circulation of a cyclone. Ship reports provide a relatively good coverage in parts of the west Pacific, but over much of the tropical Atlantic and especially in the east Pacific they are received very infrequently.

Global model analyses are regularly monitored in the Meteorological Office and there is a facility to introduce data generated by the human analyst (bogus data) when the model analyses are believed to be in error. On several occasions in 1986 bogus data were used to adjust the analysed cyclone position to the reported position. Due to time constraints this was seldom achieved before the operational forecast run. However, this action affected the update analysis and consequently the first-guess fields for the next analysis cycle were improved.

Table I. *Verification of the analysed/forecast positions of tropical cyclones by the Meteorological Office global operational model in 1986; 00 GMT runs only. Reported maximum winds ⩾50 kn.*

		T+0 hours			T+24 hours			T+48 hours			T+72 hours		
Area	N	NA	MNE	MDE	NF	MNE	MDE	NF	MNE	MDE	NF	MNE	MDE
Atlantic	14	1	84	90	2	135	85	3	202	130	5	241	220
East Pacific	34	7	111	118	15	180	140	10	198	165	14	249	220
West Pacific	121	1	80	68	13	143	120	17	214	175	31	270	215
All	169	9	86	77	30	148	122	30	210	164	50	264	217

N = number of cases
NA = number of cases where cyclone not analysed by model
NF = number of cases where cyclone not forecast by model
MNE = mean error in the analysed/forecast position of the cyclone in n miles
MDE = median error in the analysed/forecast position of the cyclone in n miles

4. Conclusions

The Meteorological Office operational global model has shown considerable skill in predicting the movement of tropical cyclones during 1986, especially when they engage upper troughs in the middle-latitude flow. On some occasions there was a poor representation of the cyclone position in the model's initial state, largely as a result of the poor data coverage over the tropical oceans. Clearly there is a role for the human analyst to improve the model analysis in such cases. Further investigations need to be made into the most effective methods of using bogus data, and the impact they have on the forecasts has yet to be fully assessed.

Acknowledgements

Thanks are due to Captains Phillips, Hall and Borthwick of the Ship Routeing Section of the Meteorological Office, Bracknell for doing much of the manual plotting of cyclone positions and forecasts.

References

Allen, R.L., jun. 1984 COSMOS: CYCLOPS objective steering model output statistics. Proceedings of 15th Conference on hurricanes and tropical Boston, American Meteorological Society.

Harrison, E.J., jun. and Fiorino, M. 1984 Worldwide use of the US Navy nested tropical cyclone model. Proceedings of 15th Conference on hurricanes and tropical meteorology. Boston, American Meteorological Society.

Marks, D.G. 1985 Hurricane track forecasting models at NMC. Extended abstracts from proceedings of 16th Conference on hurricanes and tropical meteorology. Boston, American Meteorological Society.

Ramage, C.S. 1980 Forecasting tropical cyclone movement — retrospect and prospect. Proceedings of 13th Technical conference on hurricanes and tropical meteorology. Boston, American Meteorological Society.

551.5(09):551.501.9(829)

The historical background to the collection of meteorological observations from South Georgia

S.D. Merrick*

Meteorological Office, Royal Air Force, Mount Pleasant

Summary

A brief history of meteorological observations from South Georgia is given; this is based on evidence from original letters which describes these observations.

South Georgia is a barren, rocky and mountainous island (Fig. 1) situated about 1400 km to the east-south-east of the Falkland Islands (Fig. 2). Much of the island is covered in snow and ice throughout the year, but despite its unfavourable climate it has several good deep harbours on the northern side of the island, and it was there that settlements developed. Whaling was the major industry in the period up to about 1930, but after that time a long period of decline set in.

The early meteorological observations at South Georgia were made by the naturalist Johan Reinhold Forster who in 1775 accompanied Captain James Cook in the ship HMS *Resolution* on his second epic voyage of exploration. One of the objects of this voyage was to investigate the little known 'Southern Continent' of Antarctica. Cook landed at Possession Bay in South Georgia, and Forster must have found much to delight a naturalist. Whilst there Forster noted temperatures daily and recorded an average of 2.4 °C on deck and 5.5 °C in his cabin!

The next important meteorological event was the arrival in 1882 of the German International Polar Year expedition. One of their primary tasks was to observe the transit of Venus on 6 December 1882, but hourly meteorological observations were also made. The expedition left the island in September 1883.

* Now at Royal Air Force, Brize Norton.

Photograph by courtesy of J. Elliott

Figure 1. Grytviken and the surrounding mountains.

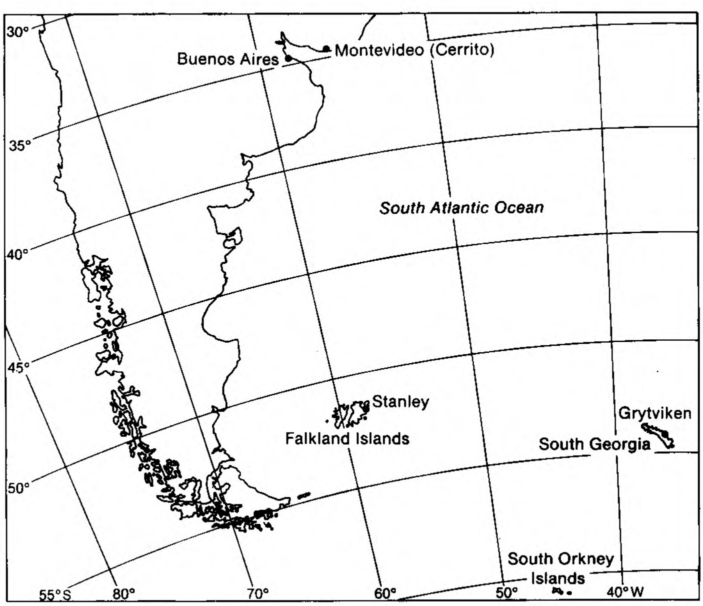

Figure 2. Positions of places mentioned in the text.

The growth of the whaling industry by the early 1890s led to the establishment of the 'Compania Argentina de Pesca', a Buenos Aires based whaling company led by a colourful Norwegian whaling captain named Carl Anton Larsen. Under the terms of its lease, the company was obliged to make regular meteorological observations. These were initiated at Grytviken on 17 January 1905 and use was made of instruments provided by Walter Davis, formerly of the Ben Nevis Observatory in Scotland, who had become the head of the newly established Argentine Meteorological Office in Buenos Aires*. At about the same time the Argentinians had taken over the running of the meteorological station at Laurie Island (in the South Orkney Islands) from the Scottish National Antarctic Expedition.

This was the state of affairs up to the year 1923 when, at the Meteorological Conference held in Utrecht in September of that year, Resolution 34 proposed that increased attention should be paid to the collection of observations from the South Atlantic.

Subsequently a letter dated 17 November 1925 from the Brazilian Embassy in London to the Right Honourable Austen Chamberlain MP, His Majesty's Secretary of State for Foreign Affairs, proposed that:

> Every effort should be made by the meteorological services interested with a view to prepare daily synoptical charts for the South Atlantic Ocean.

The same letter also stated that:

> The main obstacle for the realisation of a complete service is the equipment and maintenance of radiotelegraphic posts in all these islands, and the Brazilian Department of Meteorology suggest, as the only means of a satisfactory solution, that the Governments interested in the matter should divide the expenses thereby incurred.

The matter was duly considered and, in a letter dated 18 March 1926 from the Air Ministry to the Under Secretary of State at the Colonial Office, the Air Council instructed that the Brazilian Ambassador be informed that it was in favour of the proposal and that:

> The Council consider that every encouragement should be given to Colonies and Dominions concerned to take their part in the proposed organisation.
>
> The ever increasing practical applications of meteorology depend upon the rapid collection of data from as large an area as possible. This has largely been achieved in the Northern Hemisphere by the various governments concerned collecting observations within their own territories and transmitting them broadcast from high power telegraph stations. It frequently happens that most important observations are required from distant islands or sparsely inhabited regions and the duty of the government concerned to provide such information is generally recognised.

The letter continued:

> If this system is to be extended to the Southern Hemisphere, it will be necessary for the British Empire to take a large part, for the outlying islands from which observations of great importance are required, are generally British territory.
>
> South Africa and Australia are also very much interested in this question and the Council understand that the meteorological services of Brazil, South Africa and Australia are in communication with the object of organising the exchange of information necessary to the preparation of daily meteorological charts for the whole of the Southern Hemisphere. Thus any help given in response to the request from Brazil will help a scheme in which the British Empire has a preponderating interest.

Finally, the letter suggested what action should be taken:

> The Air Council consider that the Government of the Falkland Islands should be asked to co-operate with the meteorological services of South America and South Africa, and to undertake the issue from the wireless stations the meteorological information required.
>
> With regard to the reply which should be given to the Brazilian Ambassador, the Air Council suggest that the above information might be given to him with a promise to use our good offices with the British Administrations concerned to obtain the meteorological information required. The Council do not consider that at this stage the particulars to be included in the daily transmissions need be considered. These details should be left to be arranged by the meteorological services concerned who would no doubt draw up a suitable scheme in collaboration.

---

* Headland, R.K.; *The island of South Georgia*, Cambridge University Press, 1984.

The problem was then referred to the Governor of the Falkland Islands, Sir John Middleton, KBE, CMG, for action. This resulted in a letter dated 20 September 1926 from the Governor's Office to the Magistrate in South Georgia which requested that:

> You will furnish your observations on the proposal that the meteorological station at Grytviken should co-operate in the arrangement.

The reply from the Magistrate on 21 October 1926 indicated that there were no difficulties foreseen and asked what particulars should be included in the message. A further letter from the Colonial Secretary dated 15 February 1928 said:

> With reference to the proposed arrangements for radio telegraphic transmission of meteorological observations taken at Grytviken in accordance with the scheme outlined by the Brazilian Government for the development of synoptic meteorology in the Southern Hemisphere, I am directed by the Governor to inform you that it has now been decided that daily midday Greenwich observations should be telegraphed to Cerrito from which station they will be broadcast.
>
> I am accordingly to request that you will arrange with the observer at Grytviken that messages in the form and code set out in the accompanying pamphlet should be telegraphed daily to Stanley for retransmission to Cerrito.

The outcome was indicated in a letter dated 21 September 1928. This letter originated in the Ministry of Foreign Affairs in Rio de Janeiro and was addressed to His Excellency Sir Beilby Alston, KCMG, BE, His Brittanic Majesty's Ambassador to Brazil, stating:

> The telegrams sent daily from Cumberland Bay, South Georgia through the intermediary of the radiotelegraphic station at Cerrito, Montevideo, have been amply sufficient for the requirements of our weather service.

These arrangements continued until 1950 when the Falkland Islands Dependencies Meteorological Service assumed responsibility for the meteorological station at Grytviken. In 1950 responsibility was transferred to the British Antarctic Survey, and there was no further change until April 1982. This long tradition of meteorological observations continues to the present day with the army detachment at Grytviken making six-hourly observations. The South Georgia observations continue to be invaluable to modern day meteorologists based at the newly constructed airport at Mount Pleasant, Falkland Islands, and presumably are of equal value to the Brazilian meteorologists, at whose instigation the observations were first broadcast.

The letters on which this article is based are dated from around 1926 and were recently discovered when the Meteorological Office at RAF Stanley, Falkland Islands moved to the new site at Mount Pleasant Airport. They are the property of the Falkland Islands Government, and the originals have now been returned to the Attorney-General's Office in Stanley.

Reviews

Wind as a geological process on Earth, Mars, Venus and Titan, by R. Greeley and J.D. Iversen. 155 mm × 235 mm, pp. xii + 333, *illus.* Cambridge University Press, 1985. Price £35.00, US $59.50.

It is crucial to an appreciation of the author's aims, and indeed in the prospective reader's interest, that proper regard be paid to the planetary references in the full title of this book. The stated intention is that the book be used 'as reference and text for . . . graduate courses in comparative planetology', a discipline which, apparently, 'has as its goal the definition of the fundamental processes that have shaped and modified the planets, satellites and other "solid surface" bodies in the solar system'. Indeed, it is claimed to be the first book to deal with aeolian (i.e. wind-related) processes in a truly planetary context. The preface rightly opens with due reference to the universally acknowledged classic, *The physics of blown sand and desert dunes*, by R.A. Bagnold (published in 1941 by Methuen, London), while the authors are at pains to emphasize that it is not their intent to 'replace' Bagnold's book or the research it represents. Rather, they claim to have built upon its solid foundation and, as is manifest from their title, to have extrapolated some of Bagnold's results to other planetary environments.

Those who do not adhere to the 'because-it-is-there' school of justification for any study may be more persuaded by the authors' claim that some processes which are difficult to assess on the Earth are easier to understand on the other planets. The argument being that although the Earth is the primary data base for interpreting aeolian processes, its surface processes are much more complicated than those of other planets mainly because of the presence of liquid water and vegetation. The specific list of Earth, Mars, Venus and Titan (the last named being the largest of the Saturnian satellites) in the title has been compiled by surveying the solar system and acknowledging that any body with a dynamic atmosphere and a solid surface might be subject to surface-based aeolian processes. In spite of a clear exposition of the authors' purpose, this intriguingly selective, yet comprehensive, title still seems somewhat contrived to this reviewer who, admittedly, lays no claim to being well versed in comparative planetology.

Aeolian processes have shaped, and continue to shape, the character of the Earth's surface and are known to be active also on Mars. Varying degrees of faith and/or speculation are needed, however, in order to stretch the list to include Venus and Titan. Venus is completely enveloped in a perpetual shroud of cloud that hides the surface from view and is the least understood of the terrestrial planets. However, Russia has landed several spacecraft which have survived long enough to return pictures and sufficient wind and surface-composition data to encourage some 'experts' to infer, somewhat speculatively, the likelihood of past and present aeolian activity. In contrast, so little is known about Titan's atmosphere and surface that the authors are reduced to statements such as 'Dunes composed of methane ice particles and ice grains being blown in the dense, extremely cold nitrogen atmosphere border on the realm of science fiction but remain a possibility'. The specific inclusion of Titan in the title is thus based effectively on pure speculation about the existence and importance of aeolian processes at its surface. In the same vein, one might be tempted to recommend (tongue-in-cheek) the science fiction classic, '*The Sirens of Titan*' by Kurt Vonnegut — but I digress. If the authors genuinely seek data bases other than the Earth for the study of surface aeolian processes, it would seem that the only conceivably practical alternative at present is Mars. Hence my contention that the title is somewhat contrived.

It is mooted that 'perhaps more than in any other field, planetology requires a multi-disciplinary approach'. This, it is acknowledged, leads in turn to the severe difficulty of communication among the various disciplines involved. Greeley and Iversen bring their combined talents as geologist and engineer, respectively, to their discourse which deals mainly with the geological aspects of windblown material. They do not claim (nor do they display) any particular meteorological expertise. Likewise, this reviewer is neither geologist nor engineer. The risk of being too critical of the sections where the authors may be least familiar with the underlying basic meteorology is compounded by my inability to provide adequate critical appraisal of the areas in which the authors have been presumed expert. However, any inadvertent bias resulting from this dichotomy may not prove too amiss in a review written for practising meteorologists.

The structure and scope of the seven main chapters are displayed clearly and in detail in the contents. Chapter 1, *Wind as a geological process*, introduces the reader to aeolian processes and provides a general overview of such activity on other planets. It also serves to remind us of the significance of aeolian processes on Earth, from the effects of local-scale dust storms to the global-scale problem of desertification with its consequent implications for climate change. The recent, seemingly continuous, exposure of the problems of Africa goes only part way to preparing us for an appreciation of the full enormity of the extent of desertification. 'Although more than one third of the Earth's land is arid or semi-arid, somewhat less than half of this area is so dry that it cannot support human life. Over 600 million people live in dry areas, and about 80 million of these live in lands that are nearly useless because of soil erosion and encroachment of sand dunes or other effects of desertification. Desertification of arid lands . . . is evident on all inhabited continents of Earth'.

Chapter 2, *The aeolian environment*, is the most meteorological section of the book; however, considering the stated goal of comparative planetology and the emphasis on a knowledge of atmospheres, it is particularly disappointing. In spite of the authors' earlier claims of the need for a multi-disciplinary approach, this chapter does not appear to lay a foundation of basic meteorological theory, whose understanding is invoked in later sections of the book. On the contrary, it seems more a token acknowledgement that some basic meteorology needs to be included for appearance's sake. Section 2.4, which deals with the atmospheric boundary layer, was the easiest for this reviewer to examine critically. Even allowing that meteorology may not be the authors' strong point, it would be remiss of me not to comment on the several significant errors that occur in the basic equations and figures. Some of the 'explanations' of the most fundamental concepts I found, at best, confusing. The whole tenor of this section cast a cloud over my enjoyment of the book which I found difficult to dispel when viewing it in its entirety. I doubt whether the students for whom it is intended will find this particular section informative or easy to comprehend fully. I was left with perhaps the rather jaundiced opinion that the authors are clearly more confident when speculating about aeolian features on the unseen surface of Titan than they are when trying to explain the rudiments of the Earth's atmospheric boundary layer. Fortunately, but perhaps sadly, a proper understanding of the fundamentals of this chapter does not appear to be crucial to an appreciation of the rest of the book.

Chapter 3, *Physics of particle motion*, is the most mathematical and quantitative of the chapters. I only hope that its 41 'engineering' equations are more free of errors than those of the preceding chapter — I did not check. It is tempting to suggest that chapters 2 and 3 could be glossed over by the general reader who does not need, nor wish, to know the mathematical detail. Chapter 4, *Aeolian abrasion and erosion*, returns to a more descriptive and qualitative style and introduces ventifacts (wind-modified objects) and yardangs (aerodynamically shaped, elongated hills oriented parallel to the wind). There are several intriguing and striking pictures, in particular those depicting such surface features on Mars. Chapter 5, *Aeolian sand deposits and bedforms*, is the largest single chapter and is devoted effectively to sand dunes. Dune classification is bewildering on first acquaintance and, in that sense, is very reminiscent of cloud classification. One can contend readily with the three primary types, viz. longitudinal, transverse and parabolic, and that they may be simple, compound or complex; but then comes falling, climbing, echo, reversing, dome, star, and a host of other terms. Examples of many of the special dune structures discussed are illustrated in a most dramatic series of pictures. Chapter 6 considers the interaction of wind and topography and finally chapter 7, *Windblown dust*, discusses problems concerning fine-grained material carried aloft in suspension.

The book itself is very stylishly produced as one expects from an issue in the Cambridge Planetary Science Series (editors: W.I. Axford, G.E. Hunt, R. Greeley). Its clear, comprehensive appendices include very helpful nomenclature, glossary and reference sections. The nature and considerable number of the errors in the meteorological sections rather dulled my appetite for the book and prevent me from recommending it unreservedly. I would be interested to see a review written by someone more knowledgeable than me in the planetary and geological aspects of the book. Arguably, the book's most striking, instructive and successful feature is its remarkable and generous gallery of pictures.

D.J. Carson

Atmospheric chemistry and physics of air pollution, by J.H. Seinfeld. 155 mm × 230 mm, pp. xxiii + 738, *illus*. New York, Chichester, Brisbane, Toronto, Singapore, John Wiley and Sons Ltd, 1986. Price £61.35.

In his introduction Professor Seinfeld gives an all-embracing definition of air pollution as 'any atmospheric condition in which substances are present at concentrations high enough above their normal ambient levels to produce a measurable effect on man, animals, vegetation, or materials'. It is clear that no book could hope to address all the topics implicit in such a catch-all definition, and indeed the author only makes brief excursions into areas that might not normally be considered mainstream air-pollution chemistry and physics, e.g. radiative effects of carbon dioxide and the influence of halocarbons in the stratosphere. However, within the areas where Seinfeld concentrates, he does for the most part produce a good effort.

The book's 18 chapters are divided into 6 parts. Chapters 1, 2 and 3 which form Part 1 deal with *Air pollutants, their sources and effects*. Setting the scene for the book, they indicate what sort of substances air pollutants are, the concentrations they can be expected at, the effects that they can induce and where such pollutants originate. This part of the book, which could stand alone, is full of data from a wide variety of sources, which one might not normally come across. Did you know, for instance, that nasal breathing removes almost all particles with diameters greater than 10 μm while oral breathing only removes particles with diameters greater than 15 μm? Well now you do! There is also quite an interesting description and analysis of the internal combustion process and the effects of 'lean burn' on carbon monoxide and nitrogren oxide output. This sets the trend in the rest of the book for quite detailed and specific mathematical analysis of the processes involved.

Part 2 deals with *Air pollution chemistry*. This covers gas-phase reaction, aqueous-phase reactions, and chemical aspects of the transfer of chemical species from atmosphere to droplet. Chapter 4 on gas-phase chemistry is, for me, one of the highlights of the book. It contains a great deal of information on many important chemical species and sets out in a very clear way the complex pathways by which hydrocarbons are oxidized to carbon dioxide, producing several ozone molecules on the way. The introduction of complexity in a hierarchical fashion, when it is required to bring out a new feature of such chemical systems, works very well. As with elsewhere in the book, the important processes are put on a quantitative footing with the working of a few examples. There is also a small section on the destructive effects of nitrogen oxides and halocarbons on stratospheric ozone. The next two chapters on solution chemistry and transfer processes (which describes how different species get into water droplets) could have usefully been reversed, so that one has an idea of the physical processes which control how gas molecules enter the droplet, before discussing the chemical equilibria which control the uptake within the droplet. However, within the chapters the various processes are handled in a consistent and logical manner.

Part 3 deals with *Aerosols*, in four chapters starting with size distributions, processes relevant to single aerosols, nucleation processes, i.e. how individual aerosol particles form, and finishing with the processes which govern how aerosol populations evolve. Much of this could be considered as a generalization of cloud microphysics. Some interesting facts come out of these chapters, for instance, sulphuric acid vapour can promote rapid nucleation of water droplets at 50% relative humidity with only a few parts per billion of sulphuric acid, suggesting why pollution episodes produce a very hazy atmosphere as various photochemical processes convert sulphur dioxide molecules into sulphuric acid molecules. Incidentally, sulphuric acid is 10^9 times more effective in these processes than another common atmospheric acid, nitric acid.

Part 4 entitled *Air pollution meteorology* is really about meteorology relevant to air pollution problems, since both chapters in this section make almost no mention of air pollution. Seinfeld begins with a brief look at radiation, parcel theory and air motions, continuing in chapter 12 with micrometeorology which relies heavily (but not completely) on *The structure of atmospheric turbulence* by Lumley and Panofsky (1964) (also published by Wiley) for much of its mathematical development, but has nevertheless been well presented. Seinfeld redeems himself in Part 5, *Atmospheric diffusion*, by weaving into material from Lumley and Panofsky an extension to include chemical species, which exacerbate the closure problem and is a specific instance of a general problem in atmospheric chemistry, i.e. that of describing rate equations containing products such as $[A] \cdot [B]$ since if, as is usual, we represent the concentration of a species A, $[A]$ as a mean term $\overline{[A]}$ and a fluctuating term $[A]'$, we have no real basis to speculate on the magnitude and sign of the terms $\overline{[A]' \cdot [B]'}$.

Finally, Part 6 on *Special topics* discusses air pollution statistics, i.e. probability of exceeding threshold values, and goes into some detail on the atmospheric aspects of acid rain.

Each chapter of the book has a few pages of questions, many of a numerical nature, which if worked through (I did not) would give the student a feel for the size of numbers he is dealing with, and a fairly comprehensive list of references. The quality of the printing is good, as is the quality of the diagrams. There are few errors (I found only five or six minor typographical errors) and most of the mathematics is clear. However, there are two or three points which I would make. In chapter 4 on gas-phase chemistry, the symbols $[A^*]$ are used to denote the concentration of species A in an activated state; an asterisk is also used to reference a footnote, thus $[A]^*$. While this combination of symbols has no specific meaning it could very well cause confusion to the uninitiated. In chapter 11, Fig. 11.4 has been copied inaccurately from the original source. It has the absorptivity of ozone in the 9.6 μm band in excess of one, and other spectral features in the wrong place. Lastly, throughout the book, Seinfeld takes us through the derivation of most of the important equations. However, there can be too much of a good thing, and multiple derivations are one of them; for example, I do not really need three derivations of equation 13.60 for the slender plume approximation, especially when there is little new physical insight in subsequent derivations.

At £61.35 I would not recommend that students buy a copy, but should persuade their library to obtain one, as the book contains many clear expositions. The book has a reasonable index and is a handy reference text as I have discovered through usage.

D.S. McKenna

Books received

The listing of books under this heading does not preclude a review in the Meteorological Magazine at a later date.

Arctic air pollution, edited by B. Stonehouse (Cambridge University Press, 1987. £30.00, US $49.50) presents an up-to-date review of this increasingly important subject for both scientists and administrators concerned with world-wide, as well as polar, pollution problems. It consists of an edited collection of papers first presented at a conference held at the Scott Polar Research Institute in Cambridge in 1985.

The Irish Meteorological Service: the first 50 years, 1936–86, edited by L. Shields (Dublin, The Stationery Office, 1987. Ir. £6.00) contains an historical perspective followed by a group of articles about the meteorological services available today. The second half contains many more articles on various facets of Irish meteorology. The book is fully illustrated, many in colour.

Satellite photograph — 13 May 1987 at 1410 GMT; visible image

The pattern of convection covering much of Britain and the near Continent typifies that which occurs in cool north-westerly airstreams during spring and summer, daytime convection being restricted to inland areas, well away from onshore coasts. The exception to this can be seen over narrow peninsulas, in particular, north-west Wales and the Cherbourg peninsula, where convection and resulting shower activity is concentrated into bands parallel to the flow.

Thicker cloud is approaching north-west Britain. It is associated with a frontal system (see inset) which is 'forward sloping', with the cold front lying along the rear (western) edge of the cloud mass. Behind the front, extensive shallow convection cells can be seen.

Peninsular convection and forward-sloping cold fronts are common over the British Isles, and are discussed in more detail in Browning *et al.* 1987*.

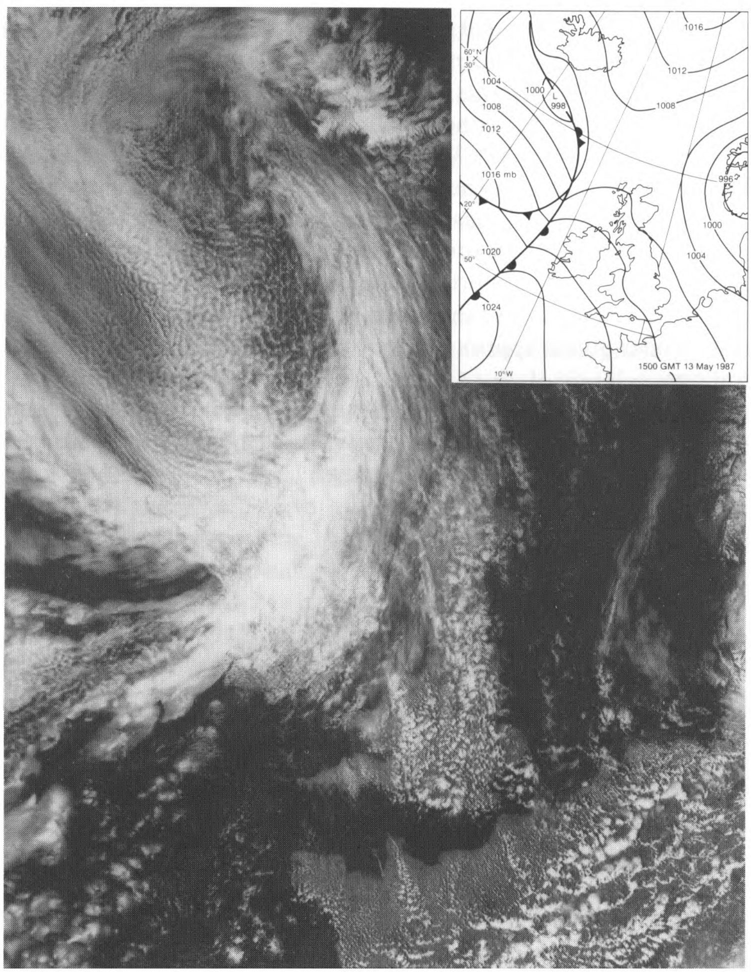

Photograph by courtesy of University of Dundee

* Browning, K.A., Bader, M.J., Waters, A.J., Young, M.V., and Monk, G.A.; Application of satellite imagery in nowcasting and very short range forecasting, *Meteorol Mag*, **116**, 1987, 161–179.

Meteorological Magazine

GUIDE TO AUTHORS

Content

Articles on all aspects of meteorology are welcomed, particularly those which describe the results of research in applied meteorology or the development of practical forecasting techniques.

Preparation and submission of articles

Articles for publication and all other communications for the Editor should be addressed to the Director-General, Meteorological Office, London Road, Bracknell, Berkshire RG12 2SZ and marked 'For *Meteorological Magazine*'.

Articles, which must be in English, should be typed, double-spaced with wide margins, on one side only of A4-size paper. Tables, references and figure captions should be typed separately.

Spelling should conform to the preferred spelling in the *Concise Oxford Dictionary*.

References should be made using the Harvard system (author, date) and full details should be given at the end of the text. If a document referred to is unpublished, details must be given of the library where it may be seen. Documents which are not available to enquirers must not be referred to.

Tables should be numbered using roman numerals and provided with headings. We consider vertical and horizontal rules to be unnecessary in a well-designed table; spaces should be used instead.

Mathematical notation should be written with extreme care. Particular care should be taken to differentiate between Greek letters and Roman letters for which they could be mistaken. Double subscripts and superscripts should be avoided, as they are difficult to typeset and difficult to read. Keep notation as simple as possible; this makes typesetting quicker and therefore cheaper, and reduces the possibility of error. Further guidance is given in BS1991: Part 1: 1976 and *Quantities, Units and Symbols* published by the Royal Society.

Illustrations

Diagrams must be supplied either drawn to professional standards or drawn clearly, preferably in ink. They should be about 1½ to 3 times the final printed size and should not contain any unnecessary or irrelevant details. Any symbols and lettering must be large enough to remain legible after reduction. Explanatory text should not appear on the diagram itself but in the caption. Captions should be typed on a separate sheet of paper and should, as far as possible, explain the meanings of the diagrams without the reader having to refer to the text.

Sharp monochrome photographs on glossy paper are preferred: colour prints are acceptable but the use of colour within the magazine is at the Editor's discretion. In either case contrast should be sufficient to ensure satisfactory reproduction.

Units

SI units, or units approved by WMO, should be used.

Copyright

Authors wishing to retain copyright for themselves or for their sponsors should inform the Editor when they submit contributions which will otherwise become UK Crown copyright by right of first publication.

It is the responsibility of authors to obtain clearance for any copyright material they wish to use before submitting it for publication.

Free copies

Three free copies of the magazine are provided for authors of articles published in it. Separate offprints for each article are not provided.

Meteorological Magazine

July 1987

Vol. 116
No. 1380

CONTENTS

Contributions: it is requested that all communications to the Editor and books for review be addressed to the Director-General, Meteorological Office, London Road, Bracknell, Berkshire RG12 2SZ, and marked 'For *Meteorological Magazine*'. Contributors are asked to comply with the guidelines given in the *Guide to authors* which appears on the inside back cover. The responsibility for facts and opinions expressed in the signed articles and letters published in *Meteorological Magazine* rests with their respective authors. Authors wishing to retain copyright for themselves or for their sponsors should inform the Editor when submitting contributions which will otherwise become UK Crown copyright by right of first publication.

Subscriptions: Annual subscription £27.00 including postage; individual copies £2.30 including postage. Applications for postal subscriptions should be made to HMSO, PO Box 276, London SW8 5DT; subscription enquiries 01–211 8667.

Back numbers: Full-size reprints of Vols 1–75 (1866–1940) are available from Johnson Reprint Co. Ltd, 24–28 Oval Road, London NW1 7DX. Complete volumes of *Meteorological Magazine* commencing with volume 54 are available on microfilm from University Microfilms International, 18 Bedford Row, London WC1R 4EJ. Information on microfiche issues is available from Kraus Microfiche, Rte 100, Milwood, NY 10546, USA.

ISBN 0 11 727971 4

ISSN 0026–1149

Printed for HER MAJESTY'S STATIONERY OFFICE
by Delco Printing Co Ltd 7/87 Dd. 739131 C13

THE METEOROLOGICAL MAGAZINE

HER MAJESTY'S STATIONERY OFFICE

August 1987

Met.O.978 No. 1381 Vol. 116

METEOROLOGICAL OFFICE Met.O.978

THE METEOROLOGICAL MAGAZINE

No. 1381, August 1987, Vol. 116

551.509.313:551.521.14:551.551.8:551.588.3

An introduction to the parametrization of land-surface processes Part I. Radiation and turbulence*

D.J. Carson†

Assistant Director (Dynamical Climatology), Meteorological Office, Bracknell

Summary

An introduction is given to the subgrid-scale land-surface processes which, it is generally acknowledged, need to be included by parametrization in three-dimensional numerical models for studying climate and climate change, and for numerical weather prediction. The discussion is restricted in the main to the relatively simple case of non-vegetated land surfaces.

Part I describes the general boundary conditions for momentum transfer and the balance equations for energy and mass (moisture) transfer at a bare-soil surface. Also the surface radiative properties and fluxes, and the physical character and the parametrization of the surface turbulent exchanges, are considered.

Part II (Carson 1987) will concentrate upon soil heat conduction and the land-surface temperature, and surface hydrology and the soil water budget.

1. Introduction

The atmospheric boundary layer is the lowest layer of the atmosphere characterized by significant vertical flux divergences of momentum, heat and moisture, which result directly or indirectly from interactions between the atmosphere and the underlying surface. The turbulent nature of boundary-layer flows is a vital factor in the efficient exchange of momentum, heat and moisture between the earth's surface below and the 'free' atmosphere above. In general, until fairly recently, designers and users of global atmospheric general circulation models (AGCMs) and operational numerical weather prediction models (NWPMs) have not been concerned with the details of boundary-layer and surface properties and processes in their own right but mainly with the influence they exert on weather systems and circulation characteristics on the much larger, synoptic or even global scales. However, the recent upsurge in the simultaneous developments of three-dimensional AGCMs for the study of climate and climate change, and of increasingly sophisticated and more highly resolved operational NWPMs, has resulted in more effort now being directed towards delineating details in boundary-layer structure and in

* Abridged version of lecture notes prepared for the Centre National d'Études Spatiales (CNES) Summer School of Space Physics, 'Climatology and Space Observations', Roscoff, France, July 1986.

† Now at Natural Environment Research Council, Swindon.

determining the characteristics of surface climatologies. Studies with AGCMs have indicated considerable sensitivity of their simulations to changes in surface properties such as albedo, soil moisture and surface roughness. Also, some NWPMs now in operational service are expected to forecast the near-surface meteorological variables, and even changes in surface properties. The importance then of 'land-surface processes' and the need to understand and represent them better in AGCMs and NWPMs are now well established.

Following the Joint Scientific Committee Scientific Steering Group on Land-Surface Processes of the World Climate Research Programme (World Climate Programme 1985), I shall adopt the pragmatical definition of land-surface processes as those phenomena which control the fluxes of heat, moisture and momentum between the surface and the atmosphere over the continents. These processes influence both the circulation of the atmosphere, often remotely, and the climate of the surface.

Many important dynamical and physical processes are governed by spatial (and temporal) scales very much smaller than the typical limits of resolution of either a numerical model or an observing system. Such subgrid-scale processes cannot be dealt with explicitly in the models; however, their statistical effects at the resolved scales must be included and are determined in terms of the explicitly resolved variables. This technique is called parametrization and usually introduces empirical terms (parameters) into a model's prescription of the processes. For a fuller discussion of parametrization in numerical models see, for example, Smagorinsky (1982).

My aim here is to introduce the range of subgrid-scale land-surface processes which, it is generally recognized, need to be represented by parametrizations in climate and numerical weather prediction models. Discussion is restricted in the main to non-vegetated land surfaces and focuses in particular on the surface-energy and mass (moisture) fluxes. A more general and fairly comprehensive review of the then current practices in AGCMs was provided by Carson (1982), with an update for Meteorological Office models only in Carson (1986a). As implied above, the parametrization of land-surface processes is a very active field of research and model development, and methods labelled 'current' may quickly become susperseded. New approaches ('schemes') are being developed and tested continuously. A single paper cannot do justice to the range and complexity of tried schemes and unresolved problems even in the apparently restricted topic of land-surface processes. The special characteristics and problems of vegetated land surfaces, ice-covered surfaces and ocean surfaces are not dealt with here. It should be assumed throughout that discussions refer only to non-vegetated, snow-free land surfaces, unless explicitly stated otherwise. Some of the particular problems associated with snow-covered, non-vegetated land surfaces will be described briefly in Part II (Carson 1987).

It should also be stressed that there are many factors in a typical AGCM or NWPM which will have a direct or indirect bearing on the character and performance of the land-surface processes but which are not themselves governed directly by, nor specified explicitly in terms of, surface properties. Obvious examples amongst the other physical parametrizations include components of the radiation scheme, the cloud scheme, the representation of rainfall and snowfall, the delineation of the atmospheric boundary layer and the parametrization of turbulent mixing within it away from the surface, deep convection, etc. A numerical model's general structure with respect to, for example, horizontal domain, spatial and temporal resolutions, distribution and number of surface types, specification of orography, etc. will also determine to some extent the quality of its simulations or predictions of the surface and near-surface climatologies. Such considerations of the general problem of representing the effects of land-surface processes in AGCMs and NWPMs are beyond the scope of this introductory paper.

For convenience, this paper has been divided into two parts. Part I will deal with the general boundary conditions for momentum transfer and the balance equations for energy and mass (moisture) transfer at a bare-soil surface. Also the surface radiative properties and fluxes, and the physical character and parametrization of the surface turbulent exchanges, are considered. Part II (Carson 1987) will concentrate upon soil heat conduction and the land-surface temperature, and surface hydrology and the soil water budget. A brief description of some of the special features of snow-covered surfaces will also be given.

2. The boundary conditions for momentum, energy and mass (moisture) transfer at a bare-soil surface

A natural and instructive way to delineate and introduce the various land-surface processes of interest is through the boundary conditions for momentum transfer and the balance equations for the energy and mass (moisture) transfer that apply at the surface. Most of the current generation of AGCMs and NWPMs involve such boundary conditions, but with varying degrees of complexity and sophistication in their use, and in the parametrizations chosen to represent individual components of the system. For the moment consider in turn the boundary constraints on and relations between the momentum, energy and mass fluxes.

2.1 *Surface momentum flux*

In an aerodynamic sense the atmospheric boundary layer is simply the lowest layer of the atmosphere under the direct influence of the underlying surface from which momentum is extracted and transferred downwards to overcome surface friction. Thus the aerodynamically rough land surface provides a sink for atmospheric momentum, the removal of which is represented by the viscous drag (i.e. horizontal shearing stress), $\underline{\tau}$, which, by convention, is a vectorial measure of the downward flux of horizontal momentum.

The surface boundary conditions for momentum transfer are the no-slip condition (i.e. the mean horizontal wind is zero at the surface) and the constraint that $\underline{\tau}$ is parallel to the limiting wind as the surface is approached.

2.2 *Surface energy flux balance*

The energy flux balance at a bare-soil surface may be expressed as

$$G_0 = R_N - H - Q \qquad \ldots \ldots \ldots \ldots \ldots \ldots \quad (1)$$

where R_N is the net radiative flux, H is the turbulent sensible-heat flux, Q is the latent-heat flux due to surface evaporation and G_0 is the flux of heat into the soil. All these terms (units W m^{-2}) are positive when the fluxes are in the directions indicated by the arrows in Fig. 1.

2.3 *Mass flux at the surface*

For our purposes the mass flux at the surface will be taken to be simply the moisture flux expressed as

$$M_0 = P_r - E - Y_0 \qquad \ldots \ldots \ldots \ldots \ldots \ldots \quad (2)$$

where P_r is the intensity of surface rainfall, E is the surface evaporation rate (turbulent flux of water vapour), Y_0 denotes intensity of surface run-off and M_0 represents the net mass flux of water into the soil layer. As defined, the flux terms in equation (2) strictly have SI units of kg m^{-2} s^{-1}, but it is common to refer to the rates involved in terms of a representative depth (of water) per unit time. The fluxes are positive when they have the directions indicated in Fig. 2.

Since $Q = L_e E$ where L_e is the latent heat of evaporation, the evaporative flux appears explicitly in equations (1) and (2), and thus provides a direct and important coupling between the heat and moisture budgets at the surface.

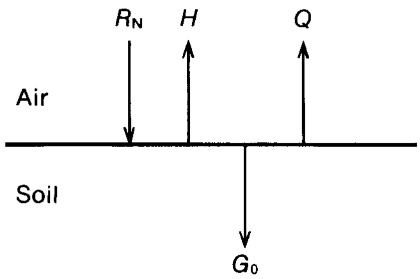

Figure 1. Schematic representation of the energy flux balance at a bare-soil surface (see text for definitions of symbols).

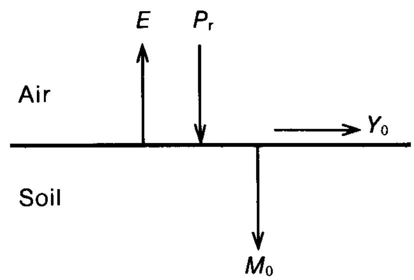

Figure 2. Schematic representation of the mass (moisture) flux balance at a bare-soil surface (see text for definitions of symbols).

2.4 *The parametrization problem*

A knowledge of heat conduction and water transport in the soil is needed to parametrize the terms G_0 and M_0 respectively. In AGCMs and NWPMs this usually leads to the reformulation of equation (1) as a prognostic equation for the surface temperature, and of equation (2) as a prognostic equation for the mass of water stored in a specified depth of surface-soil layer, i.e. the soil moisture content.

The boundary conditions and surface balance equations described above involve a wide range of subgrid-scale physical and dynamical processes in both the atmosphere and the soil. Therefore it is convenient to consider the nature and parametrization of the various individual components separately:

(a) surface radiative properties and fluxes,
(b) surface turbulent exchanges,
(c) soil heat conduction and the land-surface temperature, and
(d) surface hydrology and the soil water budget.

3. Surface radiative properties and fluxes

Since solar radiation provides most of the energy needed to maintain the general circulation of the atmosphere and since the major input of this energy to the earth–atmosphere system occurs at the surface, it seems natural to start a discussion of land-surface processes by considering the surface radiative properties and fluxes. The term R_N in equation (1) acknowledges the importance of, and the need to determine, the net imbalance of radiative fluxes to and from the land surface, expressed here simply as the sum of the net short-wave radiative flux, R_{SN}, and the net long-wave radiative flux, R_{LN}. Therefore, R_N is given by

$$R_N = R_{SN} + R_{LN} . \qquad \ldots \ldots \ldots \ldots \ldots \ldots \quad (3)$$

The components of R_{SN} and R_{LN} are shown schematically in Fig. 3.

3.1 *Surface short-wave radiation balance*

Short-wave radiation is reflected at the earth's surface. Therefore if $R_{S\downarrow}$ is the downward short-wave radiative flux (including both the direct solar flux and diffuse radiation from the sky), the upward short-wave radiative flux is given by $R_{S\uparrow} = \alpha R_{S\downarrow}$ where α is the surface short-wave reflectivity, which is usually called the albedo. The net short-wave radiation, R_{SN}, is the difference between the downward and upward fluxes.

$$R_{SN} = R_{S\downarrow} - R_{S\uparrow} = (1 - \alpha) R_{S\downarrow} . \qquad \ldots \ldots \ldots \ldots \ldots \quad (4)$$

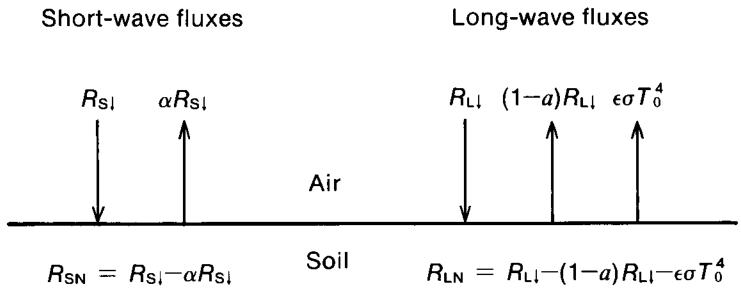

Figure 3. Schematic representation of the short-wave and long-wave radiative fluxes at a bare-soil surface (see text for definitions of symbols).

The albedo depends on the solar zenith angle, the spectral distribution of solar radiation incident on the surface and whether the radiation is direct or diffuse, as well as on the character of the surface as determined by the vegetation (type, density and state), soil type, soil moisture, and whether the surface is snow- or ice-covered. Although generally a long way removed from representing the full complexity of its functional dependence on all such quantities, nevertheless α in AGCMs and NWPMs is usually accorded some variation with the broad character of the surface. In AGCMs it has a specific geographical dependence (see, for example, Carson 1982) and in many models it is still the only land-surface or soil parameter which is given such a geographical variation (see, for example, Carson 1986a).

A good illustration of the current status of the global specification of α suitable for use in large-scale atmospheric models is the recent work of Wilson and Henderson-Sellers (1985) on which is based the distribution of grid-box, snow-free, land-surface albedos used in the Meteorological Office weather forecasting and climate models (see, for example, Carson 1986a). The values range from about 0.12, typical of, for example, the northernmost fringes of land and also tropical forests, to 0.35 used for the most arid, light-coloured desert regions; 0.18 is thought appropriate to the United Kingdom.

3.2 *Surface long-wave radiation balance*

If $R_{L\downarrow}$ is the downward long-wave radiation and a is the surface absorptivity to long-wave radiation, then the net incoming flux from the atmosphere is $aR_{L\downarrow}$. From Stefan's law, the upward flux due to thermal emission at the earth's surface is $\epsilon\sigma T_0^4$, where T_0 is the surface temperature, ϵ is the long-wave emissivity at the surface and σ is the Stefan–Boltzmann constant. Therefore the net long-wave radiative flux, R_{LN}, is given by

$$R_{LN} = aR_{L\downarrow} - \epsilon\sigma T_0^4 . \qquad \ldots \ldots \ldots \ldots \ldots \ldots (5)$$

It is common practice to simplify equation (5) by combining the definition of ϵ with Kirchhoff's law to give $a = \epsilon$. Equation (5) then reduces to

$$R_{LN} = \epsilon(R_{L\downarrow} - \sigma T_0^4) . \qquad \ldots \ldots \ldots \ldots \ldots \ldots (6)$$

It is known that ϵ has a wavelength dependence and that it varies according to the character of the surface as discussed, for example, by Buettner and Kern (1965), Kondratyev (1972), Paltridge and Platt (1976) and Kondratyev *et al.* (1982). Values quoted for ϵ range from 0.997 for wet snow to 0.71 for quartz. Kondratyev *et al.* (1982) comment that, on average, ϵ for natural surfaces lies within the range

0.90–0.99 and they cite several authors who have inferred that 0.95 may be assumed as the mean relative emissivity of the earth's surface. They do caution, however, that the problem of measuring the emissivity of natural surfaces is far from solved.

Although there are exceptions, the most common practice in AGCMs and NWPMs is to assume explicitly or implicitly that all surfaces act like perfect black bodies for long-wave radiation with $\epsilon = 1$. To a large extent this simply reflects the preoccupation of numerical modellers with other apparently more important and immediate problems with their physical parametrizations. It is likely that the increasing complexity and sophistication of land-surface descriptions in models will also generate more critical and discriminatory approaches to the specification of ϵ.

3.3 *Evaluation of* R_N

The net radiation, R_N, is found by substituting equations (4) and (6) into (3) to give

$$R_N = (1-\alpha)R_{S\downarrow} + \epsilon(R_{L\downarrow} - \sigma T_0^4)\,. \qquad (7)$$

The parametrization of $R_{S\downarrow}$ and $R_{L\downarrow}$ is beyond the scope of this paper; they are not formally classed as land-surface processes and may be regarded here as externally given forcing factors. It should be stressed though that a correct evaluation of $R_{S\downarrow}$ and $R_{L\downarrow}$ is a crucial element in establishing sensible energy and moisture balances at the surface.

From equation (7) it is clear that once T_0 and the downward fluxes of short-wave and long-wave radiation are known, the net radiation can be determined if ϵ and α are specified.

4. Surface turbulent exchanges

4.1 *Definition of the surface turbulent fluxes*

The atmospheric boundary layer (sometimes called the planetary boundary layer or mixing layer) is the lowest layer of the atmosphere under the direct influence of the underlying surface. The flow in this layer is turbulent except possibly in very stable conditions (e.g. at night in the presence of strong surface-based temperature inversions). The velocity, temperature, humidity and other properties in a turbulent flow can be considered as random functions in space and time, and it is usually necessary to resort to a statistical approach for the calculation of many boundary-layer properties. In particular this introduces the concepts of mean values, fluctuations and variances into the description of the turbulent properties of the flow. For example, if ξ is some conservative quantity which fluctuates because of the turbulent motion, then it is usually written as

$$\xi = \bar{\xi} + \xi' \qquad (8)$$

where $\bar{\xi}$ is some suitably defined mean value of ξ, and ξ' is called the turbulent or eddy fluctuation (see schematic illustration in Fig. 4).

In the notation of equation (8), the term $\overline{w'\xi'}$ represents the eddy covariance of ξ and the vertical component of the flow, w, and denotes the vertical turbulent flux of ξ at a given height in the atmospheric boundary layer. Let

$$F_\xi = (\overline{w'\xi'})_0 \qquad (9)$$

denote the surface value of this flux.

In the context of this discussion about land-surface processes, it is the turbulent fluxes of momentum, $\underline{\tau}$, sensible heat, H, and water vapour, E, that are of particular interest and are given by

$$\underline{\tau} = \rho\{-(\overline{w'u'})_0, -(\overline{w'v'})_0\} \qquad \ldots (10)$$

$$H = \rho c_p(\overline{w'\theta'})_0 \qquad \ldots (11)$$

$$E = \rho(\overline{w'q'})_0 \qquad \ldots (12)$$

where u and v are the components of the horizontal wind, θ is the potential temperature, q is the specific humidity, ρ is a representative mean air density near the surface and c_p is the specific heat of air at constant pressure. The direction of $\underline{\tau}$ is determined by the limiting wind direction as the surface is approached.

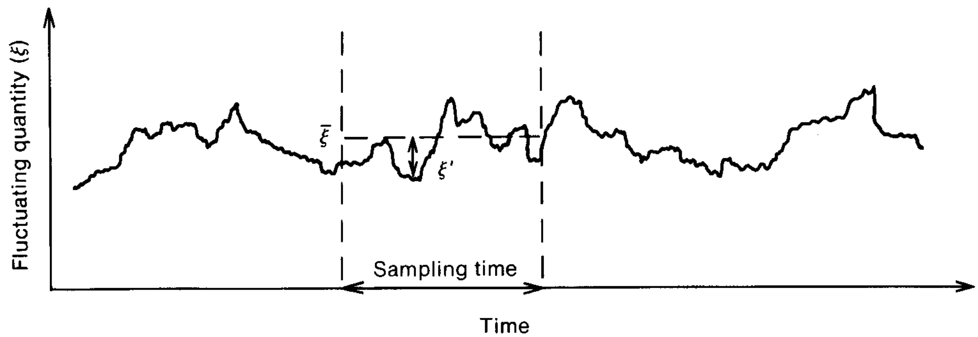

Figure 4. Schematic representation of the mean value, $\bar{\xi}$, and the eddy fluctuation, ξ', determined for a particular sampling time from a time trace of the fluctuating quantity, ξ.

4.2 *The bulk-aerodynamic formulae*

It is standard practice, particularly in AGCMs and NWPMs, to represent the mean vertical turbulent flux, F_ξ, by

$$F_\xi = -C_\xi V(z_l)\Delta\xi(z_l) \qquad \ldots (13)$$

where $\Delta\xi(z_l) = \xi(z_l) - \xi_0$, z_l is some specified height above the surface but within the boundary layer, $\xi(z_l)$ and $V(z_l)$ are the mean values of ξ and the horizontal wind speed at z_l, and ξ_0 is the surface value of ξ. (Note that the bar notation to denote mean values has been omitted to simplify the symbolism.) The bulk transfer coefficient, C_ξ, defined in a strictly mathematical sense by equation (13), is a complicated function of height, atmospheric stability, surface roughness and, for a vegetated surface, of other physical and physiological characteristics of the vegetation.

Without loss of generality, z_l may be taken as the notional height of a particular numerical model's first level above the underlying surface.

In bulk-aerodynamic form, the surface turbulent fluxes of equations (10) to (12) are

$$\underline{\tau} = \rho C_D V(z_l)\underline{V}(z_l) \qquad \ldots (14)$$

$$H = -\rho c_p C_H V(z_l)\{\theta(z_l) - \theta_0\} \qquad \ldots (15)$$

$$E = -\rho C_E V(z_l)\{q(z_l) - q_0\} \qquad \ldots (16)$$

where C_D, C_H and C_E are the bulk transfer coefficients for momentum transfer, heat transfer and water vapour transfer (note that C_D is the traditional drag coefficient), and θ_0 and q_0 are the surface values of the potential temperature and specific humidity.

To determine the fluxes from equations (14) to (16) C_ξ must be prescribed or expressed in terms of modelled variables and parameters and, in addition to the variables modelled explicitly at z_l, θ_0 (simply related to the surface temperature T_0) and q_0 need to be known. The prediction of T_0 is usually based on knowledge of heat transfer through the soil, but the prediction of q_0 is not so easy since its implied value is inextricably linked to the parametrization of surface hydrology.

A related approach to equation (13) for the representation of the turbulent fluxes at natural surfaces is the so-called resistance approach. Turbulent transfer in the atmospheric boundary layer is seen as a process analogous to the flow of electric current and, in the spirit of Ohm's law, F_ξ is written as

$$F_\xi = -\frac{\Delta\xi}{r_\xi} \qquad \ldots \ldots \ldots \ldots \ldots \ldots (17)$$

where, in a similar manner to C_ξ in equation (13), equation (17) can be regarded as defining r_ξ, the aerodynamic resistance to the 'flow' of F_ξ. Comparison of equations (13) and (17) yields $r_\xi = \{C_\xi V(z_l)\}^{-1}$. The resistance approach has particular appeal when dealing with the complicated and multiple routes for sensible heat transfer and evaporation from vegetated surface (see, for example, Monteith 1965, Perrier 1982 and Rosenberg *et al.* 1983).

For a discussion of the large variety of specifications of C_ξ then in current use in AGCMs see, for example, Carson (1982). However, discussion here is limited to the approach most acceptable to boundary-layer experts and increasingly more prevalent in the current generation of AGCMs and NWPMs — the use of the Monin–Obukhov similarity theory.

4.3 *Use of the Monin–Obukhov theory of the surface-flux layer to determine the bulk transfer coefficients*

Adjacent to the surface is a shallow layer in which the turning of the wind with height may be ignored and the vertical fluxes of momentum, heat, and water vapour may be approximated closely by their surface values (i.e. for many practical purposes the turbulent fluxes in this layer may be assumed to be virtually constant with height). This layer is often referred to as the constant-flux layer, but this terminology can mislead the unwary (e.g. the fluxes generally have their largest vertical gradients at the surface) and so it is better to use the more appropriate term of surface-flux layer.

The Monin–Obukhov similarity hypothesis for the surface-flux layer is the most widely accepted approach for describing the properties of the surface layer. Brought down to the very simplest terms, similarity methods depend on the possibility of being able to express the unknown variables in non-dimensional form, there being suitable arguments for saying that there exist a length scale, velocity scale (or time-scale) and temperature (and humidity) scale relevant in doing this. The non-dimensional forms are then postulated to be universal in character and this will hold for as long as the scales remain the relevant ones.

From the Monin–Obukhov theory of the surface-flux layer (see Appendix for details) it can be shown that

$$C_\xi = C_\xi(z_l/z_0, Ri_B)$$

where z_0 is the surface roughness length and Ri_B is a bulk Richardson number for the surface layer.

Over bare soil z_0 is a characteristic of the surface and is usually independent of the flow. There are also corresponding characteristic 'surface roughness lengths' for heat and water vapour transfer. The problems of evaluating effective areal roughness lengths and of discriminating between them for the different properties are complex, and it remains common practice to use the same estimate of z_0 when computing all three bulk transfer coefficients.

The bulk Richardson number, Ri_B, is a measure of the stability of the surface layer. In stable conditions $Ri_B > 0$, whereas $Ri_B < 0$ in unstable conditions; $Ri_B = 0$ when the surface layer is neutral. The Ri_B can be computed easily from the model variables using

$$Ri_B = \frac{gz_l}{T} \frac{\{\Delta\theta(z_l) + 0.61\, T\Delta q(z_l)\}}{V^2(z_l)}$$

where g is the acceleration due to gravity and T is a representative air temperature in the surface layer. To illustrate the behaviour of bulk transfer coefficients derived from the Monin–Obukhov theory, Fig. 5 shows how C_D, C_H and C_E used in the Meteorological Office 11-layer AGCM vary with Ri_B. In that particular model $z_l = 100$ m, over land $z_0 = 0.1$ m and over the sea $z_0 = 10^{-4}$ m.

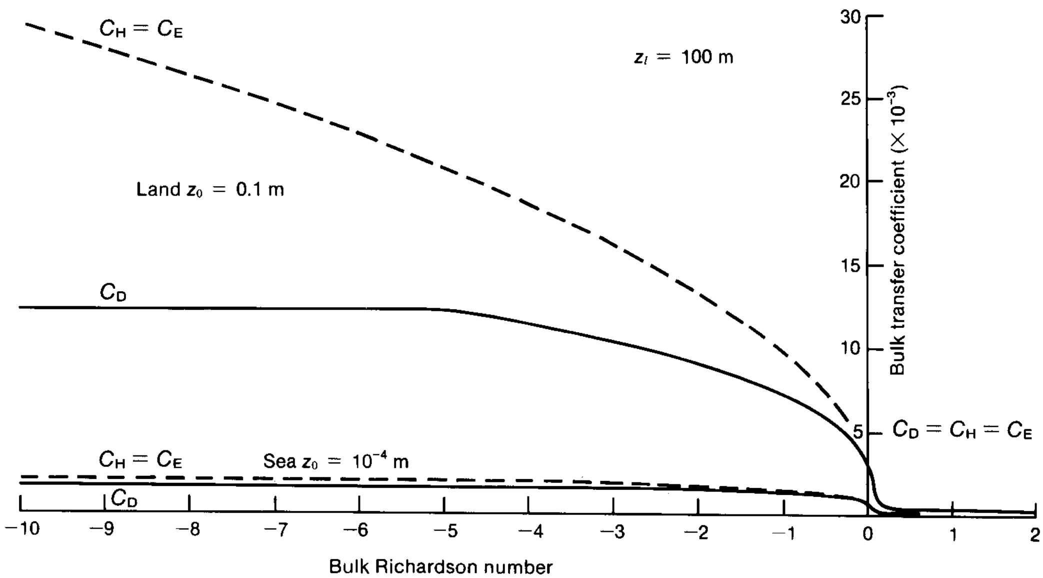

Figure 5. Surface-layer bulk transfer coefficients derived from the Monin–Obukhov similarity theory and used in the Meteorological Office 11-layer AGCM.

4.4 *Surface roughness length*

The surface roughness length, like the surface albedo, is a land-surface characteristic which has a marked geographical variation. In most of the current generation of AGCMs and NWPMs, z_0 has direct and indirect effects on the surface turbulent exchanges of sensible heat and moisture, as well as on the surface shearing stress. However, the evaluation of an effective areal surface roughness length for heterogeneous terrain is an important practical issue that poses a variety of, as yet unsatisfactorily resolved, problems.

The effective areal z_0 for natural surfaces is rarely estimated from the wind profile and/or surface-shear stress measurements. Instead, it is most likely to be determined indirectly from a knowledge of, for example, terrain relief (elevation, slope, etc.), land use, and type and distribution of the surface roughness elements. Algorithms, however qualitative, are needed to perform this function sensibly, at least in a fairly local (1 km × 1 km) sense. The pros and cons of alternative approaches to the question of how to average over larger areas have been discussed by Carson (1986b).

Most standard boundary-layer textbooks provide a table of values of z_0 as a function of terrain type described qualitatively in terms of relief and vegetation characteristics. Such traditional relationships may well be adequate on the very local scale for the smoother, quasi-homogeneous types of terrain, but can be expected to be less well founded for areal averages over rough, heterogeneous terrain typical of, say, a European semi-rural landscape with small hills, woods, fields, crops, hedges, towns, lakes, etc. Wieringa (1986) has addressed this problem and produced a table giving effective areal z_0 in terms of a terrain classification when there are no significant orographic features (see Table I).

Table I. *Effective mesoscale surface roughness length, z_0, expressed as a function of land use and proposed by Wieringa (1986); h is the height of the major surface obstacles.*

Land use category	z_0 *metres*
Sea (minimal fetch 5 km)	0.0002
Small lake, mud flats	0.006
Morass	0.03
Pasture	0.07
Dunes, heath	0.10
Agriculture	0.17
Road, canal (in Dutch landscape, tree lined)	0.24
Orchards, bushland	0.35
Forest	0.75
Residential built-up area ($h \leqslant 10$ m)	1.12
City centre (high-rise building)	1.6

For a fuller discussion of issues concerning the evaluation of effective z_0 see recent papers by Smith and Carson (1977), Mason (1986), Carson (1986b), Wieringa (1986) and André and Blondin (1986).

References

André, J-C. and Blondin, C. 1986 On the effective roughness length for use in numerical three-dimensional models. *Boundary Layer Meteorol*, **35**, 231–245.

Buettner, K.J.K. and Kern, C.D. 1965 The determination of infrared emissivities of terrestrial surfaces. *J Geophys Res*, **70**, 1329–1337.

Carson, D.J. 1982 Current parametrizations of land-surface processes in atmospheric general circulation models. *In* Eagleson, P.S. (ed); Land surface processes in atmospheric general circulation models. Cambridge University Press.

1986a Parametrizations of land-surface processes in Meteorological Office numerical weather prediction and climate models. (Unpublished, copy available in the National Meteorological Library, Bracknell.)

1986b Issues concerning the evaluation of effective surface roughness of heterogeneous terrain. *In* Proceedings of the ISLSCP conference on parametrization of land-surface characteristics, use of satellite data in climate studies, and first results of ISLSCP, Rome, 2–6 December, 1985. Paris, ESA No. SP-248.

(1987) An introduction to the parametrization of land-surface processes. Part II. Soil heat conduction and surface hydrology. (To appear in *Meteorol Mag.*)

Carson, D.J. and Richards, P.J.R. 1978 Modelling surface turbulent fluxes in stable conditions. *Boundary Layer Meteorol*, **14**, 67–81.

Dyer, A.J. and Hicks, B.B. 1970 Flux-gradient relationships in the constant flux layer. *Q J R Meteorol Soc*, **96**, 715–721.

Kondratyev, K.Ya. 1972 Radiation processes in the atmosphere. Geneva, WMO No. 309.

Kondratyev, K.Ya., Korzov, V.I., Mukhenberg, V.V. and Dyachenko, L.N. 1982 The shortwave albedo and the surface emissivity. *In* Eagleson, P.S. (ed); Land surface processes in atmospheric general circulation models. Cambridge University Press.

McBean, G.A., Bernhardt, K., Bodin, S., Litynska, Z., van Ulden, A.P. and Wyngaard, J.C. 1979 The planetary boundary layer. Geneva, WMO No. 530.

Mason, P.J. 1986 On the parametrization of orographic drag. *In* ECMWF seminar on physical parametrization for numerical models of the atmosphere, Vol. 2.

Monteith, J.L. 1965 Evaporation and environment. *Symp Soc Exp Biol*, **19**, 205–234.

Paltridge, G.W. and Platt, C.M.R. 1976 Radiative processes in meteorology and climatology. Developments in atmospheric science, **5**. Amsterdam, Elsevier.

Panofsky, H.A. and Dutton, J.A. 1984 Atmospheric turbulence. Models and methods for engineering applications. New York, Wiley.

Perrier, A. 1982 Land surface processes: vegetation. *In* Eagleson, P.S. (ed); Land surface processes in atmospheric general circulation models. Cambridge University Press.

Rosenberg, N.J., Blad, B.L. and Verma, S.B. 1983 Microclimate. The biological environment. Second edition. New York, Wiley.

Smagorinsky, J. 1982 Large-scale climate modelling and small-scale physical processes. *In* Eagleson P.S. (ed); Land surface processes in atmospheric general circulation models. Cambridge University Press.

Smith, F.B. and Carson, D.J. 1977 Some thoughts on the specification of the boundary layer relevant to numerical modelling. *Boundary Layer Meteorol*, **12**, 307–330.

Webb, E.K. 1970 Profile relationships: the log-linear range, and extension to strong stability. *Q J R Meteorol Soc*, **96**, 67–90.

Wieringa, J. 1986 Roughness-dependent geographical interpolation of surface wind speed averages. *Q J R Meteorol Soc*, **112**, 867–889.

Wilson, M.F. and Henderson-Sellers, A. 1985 A global archive of land cover and soils data for use in general circulation climate models. *J Climatol*, **5**, 119–143.

World Climate Programme 1985 Report of the first session of the JSC scientific steering group on land surface processes and climate. Geneva, WCP No. WCP-96.

Appendix — Use of the Monin–Obukhov similarity theory

A.1 *The Monin–Obukhov similarity theory*

The Monin–Obukhov similarity hypothesis for the fully turbulent surface-flux layer (where the Coriolis force is neglected) states that for any transferable property, the distribution of which is homogeneous in space and stationary in time, the vertical flux–profile relation is determined by the parameters

$$\frac{g}{T}, \frac{|\underline{\tau}|}{\rho}, \frac{H}{\rho c_p}, \frac{E}{\rho}$$

where g/T is the Archimedean buoyancy parameter, g is the acceleration due to gravity and T is a representative air temperature in the surface layer.

It is convenient to introduce scaling parameters u_*, θ_* and q_* which are defined in terms of $\underline{\tau}$, H and E by $|\underline{\tau}| = \rho u_*^2$, $H = -\rho c_p u_* \theta_*$ and $E = -\rho u_* q_*$ (in general, the surface turbulent flux of ξ is given by

$F_\xi = -u_*\xi_*$). Using these three equations means that the above set of four parameters is equivalent to the set

$$\frac{g}{T},\ u_*,\ \theta_*,\ q_*$$

where θ_* and q_* can be combined to give

$$\psi_* = \theta_* + 0.61\,Tq_*$$

which is akin to a virtual potential temperature scaling value.

Instead of using the buoyancy parameter g/T it is convenient to use the length scale L, called the Monin–Obukhov length, defined uniquely by g/T, q_* and ψ_*.

$$L = \frac{Tu_*^2}{kg\psi_*} = \frac{-\rho c_p T u_*^3}{kg(H + 0.61 c_p TE)}\ .$$

By convention Kármán's constant ($k \approx 0.4$) is introduced solely as a matter of convenience. In the surface-flux layer, L is effectively constant. The turbulent flow is classed as unstable when $L<0$ (i.e. when the net surface-buoyancy flux is positive), stable when $L>0$ (i.e. when the net surface-buoyancy flux is negative), and neutral when $|L| \rightarrow \infty$ (i.e. when the net surface-buoyancy flux is zero).

Now L, u_*, θ_* and q_* may be taken as the set of basic parameters which uniquely determine the relationships between the surface-layer vertical gradients of wind, potential temperature and specific humidity to the corresponding surface turbulent fluxes. Dimensional analysis leads to the vertical flux–gradient relationship expressed in the general form

$$\frac{\partial \xi}{\partial z} = \frac{\xi_*}{kz}\,\phi_\xi(z/L) \qquad \ldots\ \ldots\ \ldots\ \ldots\ \ldots\ \ldots\text{(A1)}$$

where z is height above the surface. It is then hypothesized that $\phi_\xi(z/L)$ is a universal function of z/L only, which may be of different form for each mean transferable property, ξ. The form of the functions has to be determined empirically from analysis of surface-layer data; the overall observational evidence is that they decrease with unstable stratification ($L<0$) and increase with stable stratification ($L>0$).

For specified functions for ϕ_ξ, equation (A1) can be integrated to provide flux–profile relationships for the surface layer:

$$\frac{k\{\xi(z) - \xi(z_r)\}}{\xi_*} = \int_{\zeta_r}^{\zeta} \frac{\phi_\xi(\eta)\,\mathrm{d}\eta}{\eta} = \Phi_\xi(\zeta, \zeta_r). \qquad \ldots\ \ldots\ \ldots\text{(A2)}$$

where $\zeta = z/L$ and $\zeta_r = z_r/L$, and z_r is some reference height at which ξ is known. In practice, equation (A2) used in conjunction with the basic equations relating surface fluxes to the scaling parameters can be used to estimate the surface turbulent fluxes of momentum, heat and moisture from a knowledge of the corresponding surface-layer profiles of wind, potential temperature and humidity.

A.2 *The similarity functions*

The general character of the similarity functions is fairly well established over a limited range of stability conditions centred on neutral, but their specification for extreme stability conditions (both stable and unstable) is much more debatable and uncertain. The general behaviour of the functions is that ϕ_ξ increases with increasing stability — decreasing turbulence decreases the mixing and hence increases the normalized gradient of ξ. Fig. A1 illustrates schematically the changing character of the surface-layer wind profile throughout a clear day and clear night. For details see, for example, chapter 6 of Panofsky and Dutton (1984).

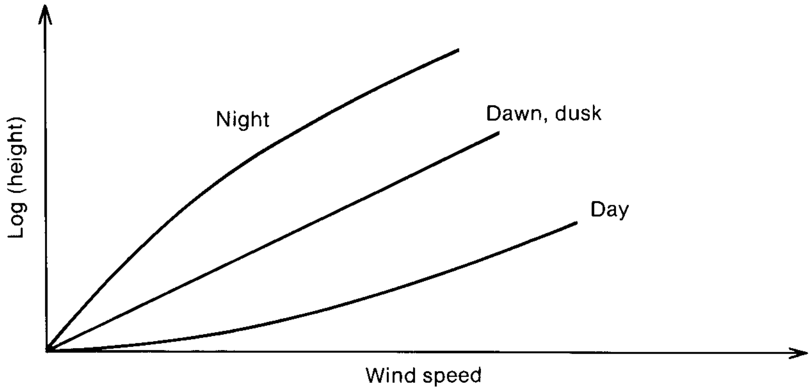

Figure A1. Schematic representation of the diurnal variation of the surface-layer wind profile.

There is a variety of postulated, empirical forms of ϕ_ξ (see, for example, chapter 6 of McBean *et al.* 1979). The following examples have been selected subjectively, but are typical of the type of formulae commonly adopted as the basis of parametrizations for the turbulent fluxes in numerical models.

(a) *Unstable and neutral conditions* ($z/L \leqslant 0$). The Dyer and Hicks (1970) formulae are

$$\phi_H = \phi_E = \phi_M^2 = (1-16z/L)^{-1/2} \qquad 0 \geqslant z/L \geqslant -1$$

where ϕ_M, ϕ_H and ϕ_E are the respective ϕ_ξ for the turbulent transfers of momentum, sensible heat and water vapour. Since these formulae are limited to when $|z/L| \leqslant 1$, other empirical approaches may need to be invoked for more unstable conditions. For a particular choice of extrapolation beyond the Dyer and Hicks limit towards the free-convection limit see Carson (1982, 1986a).

(b) *Stable conditions* ($z/L > 0$). The formulae proposed by Webb (1970) are

$$\phi_H = \phi_E = \phi_M = \begin{cases} 1+5z/L & 0 < z/L \leqslant 1 \\ 6 & 1 < z/L < 6 \end{cases}$$

The problem of extending the functional form of ϕ_ξ to highly stable conditions was discussed by Carson and Richards (1978).

A.3 *C_ξ from the Monin–Obukhov similarity theory*

The bulk transfer coefficients introduced in section 4.2 can be derived from the Monin–Obukhov similarity theory. The surface flux, F_ξ, can be written in terms of u_* and ξ_*, and also in terms of C_ξ, namely

$$F_\xi = -u_*\xi_* = -C_\xi V(z_l)\Delta\xi(z_l)$$

which yields

$$C_\xi = \left(\frac{u_*}{V(z_l)}\right)\left(\frac{\xi_*}{\Delta\xi(z_l)}\right). \qquad \text{... ... ...(A3)}$$

For the Monin–Obukhov theory to be appropriate z_l must be fully within the surface layer so that equation (A2) can be invoked in the particular form

$$\frac{k\Delta\xi(z_l)}{\xi_*} = \int_{\zeta_\xi}^{\zeta_l} \frac{\phi_\xi(\eta)\,\mathrm{d}\eta}{\eta} = \Phi_\xi(\zeta_l, \zeta_\xi) \qquad \ldots\ \ldots\ \ldots\ \ldots\ \ldots\text{(A4)}$$

where $\zeta_l = z_l/L$, and $\zeta_\xi = z_\xi/L$ is defined such that $\xi(z_\xi) = \xi_0$.

The nature of the similarity formulation implies a logarithmic singularity in Φ_ξ as $z \to 0$. This is avoided by defining the level z_ξ as the virtual height at which the ξ-profile, defined by equation (A2) and extrapolated towards the surface, attains the actual surface value ξ_0. For momentum transfer this level, denoted by z_0 and called the surface roughness length, is defined as the virtual height at which $V = 0$ on the postulated wind profile.

From equations (A3) and (A4), C_ξ can be specified in terms of finite integrals of the Monin–Obukhov similarity functions, thus

$$C_\xi = k^2\, \Phi_M^{-1}(\zeta_l, \zeta_0)\, \Phi_\xi^{-1}(\zeta_l, \zeta_\xi) \qquad \ldots\ \ldots\ \ldots\ \ldots\ \ldots\text{(A5)}$$

where

$$\Phi_M(\zeta_l, \zeta_0) = \int_{\zeta_0}^{\zeta} \frac{\phi_M(\eta)\,\mathrm{d}\eta}{\eta} = \frac{kV(z)}{u_*}$$

and $\zeta_0 = z_0/L$. In general, with ϕ_ξ specified as discussed earlier, equation (A5) gives C_ξ as a function of ζ_l, ζ_0 and ζ_ξ.

It is generally more convenient for modelling purposes to express C_ξ directly as a function of the explicitly modelled variables $V(z_l)$ and $\Delta\xi(z_l)$. This can be achieved by using a bulk Richardson number for the surface layer, Ri_B, instead of ζ_l as the stability indicator. In terms of model variables Ri_B is given by

$$Ri_B = \frac{gz_l}{T}\,\frac{\{\Delta\theta(z_l) + 0.61\,T\Delta q(z_l)\}}{V^2(z_l)}$$

which can be related to ζ_l through

$$Ri_B = \frac{\zeta_l C_D{}^{3/2}}{kC_H}$$

For a full description of the method and assumptions made see, for example, Carson and Richards (1978).

551.552:551.501.75:551.507.23:551.506.3(26)

A comparison of numbers of visually estimated and instrumentally measured wind observations from merchant ships

D.S. Ive

Meteorological Office, Bracknell

Summary

A comparison is made of the numbers of reports of visually estimated and instrumentally measured winds stored in the Meteorological Office main marine data bank. The geographical distribution of the two types of observation is analysed and the effects are discussed.

1. Introduction

The Meteorological Office has a marine data bank (Shearman 1983) containing 55 million observations collected from 1854 to 1984. This is the main source of information for climatological analyses and therefore it is important to be aware of any limitations or inconsistencies in the contents of the data bank.

Observations of wind speed are used more frequently than those of any other variable. There are two types of wind speed observation in the marine data bank, namely those that are visually estimated and those that are instrumentally measured. Visually estimated wind speeds are derived by assessing the state of sea, a particular Beaufort force corresponding to a particular sea state. Before 1960 the majority of wind speeds reported by ships were visually estimated, but in recent years anemometers of various types have become more widely used and the bank now contains a mixture of the two types of observation. The majority of the more recent reports specify the method of observation by the inclusion of a coded indicator.

Instrumental observations may be made using hand-held or permanently mounted anemometers and give the wind speed in knots or metres per second. Although instrumental observations may be thought to have a greater accuracy than visual estimates, such wind speeds should be treated with caution because there is always the possibility that the anemometer was not properly exposed. The wind speed is nearly always affected by the air flow over the ship, particularly in the case of hand-held anemometers where the observer may be sheltered from a wind from a certain direction by the superstructure of the vessel. The speed of the ship and the height of the wind sensor above sea level are additional complications which may or may not have been taken into consideration before the reports were despatched.

Some Voluntary Observing Fleets (VOFs) appear to be changing to instrumentally measured wind speeds as a matter of policy. It is inevitable that the data bank will contain a mixture of visual and instrumental wind speeds. In this paper the proportions of each type of data are described, together with any underlying national trends, and an assessment is made of the consequences of the data mix when carrying out a standard climatological analysis such as the derivation of extremes.

2. The data base

Marine meteorological observations are available in the Meteorological Office marine data bank from 1854 to 1984; most of the observations have been made by deck officers during the course of their duties aboard merchant vessels of the VOF. Data are also received from ocean weather ships, light-vessels, gas and oil rigs, and buoys.

In the early 1960s nine countries were nominated by the World Meteorological Organization to act as collecting centres for meteorological observations from specified ocean areas of the world and to be responsible for archiving the data from their nominated areas of responsibility. Each of the eight countries actively remaining in the scheme (see Fig. 1) has a complete archive of data for its own area and, to some extent, an incomplete archive for the rest of the world based upon observations from ships of its own VOF.

Additionally the United Kingdom has acquired further data, by exchange or purchase, from each of the other data centres with the exception of the USSR and India, although the data from India will become available when they have been processed. The marine data bank is complete up to the end of 1981 for all observations, except those from these two centres, and for some centres until the end of 1984. However, there is a known shortfall of data for the US area of responsibility from 1965 to 1972 which will be remedied in the near future.

Since 1960 an indicator should have been added to the coded observations to distinguish between instrumental and visual data. However, it is possible that an error occurred in coding the indicator for data from the US VOF because there are apparently no instrumentally measured wind speeds reported from 1975 to 1981, although prior to 1975 and since 1981 a large number were reported.

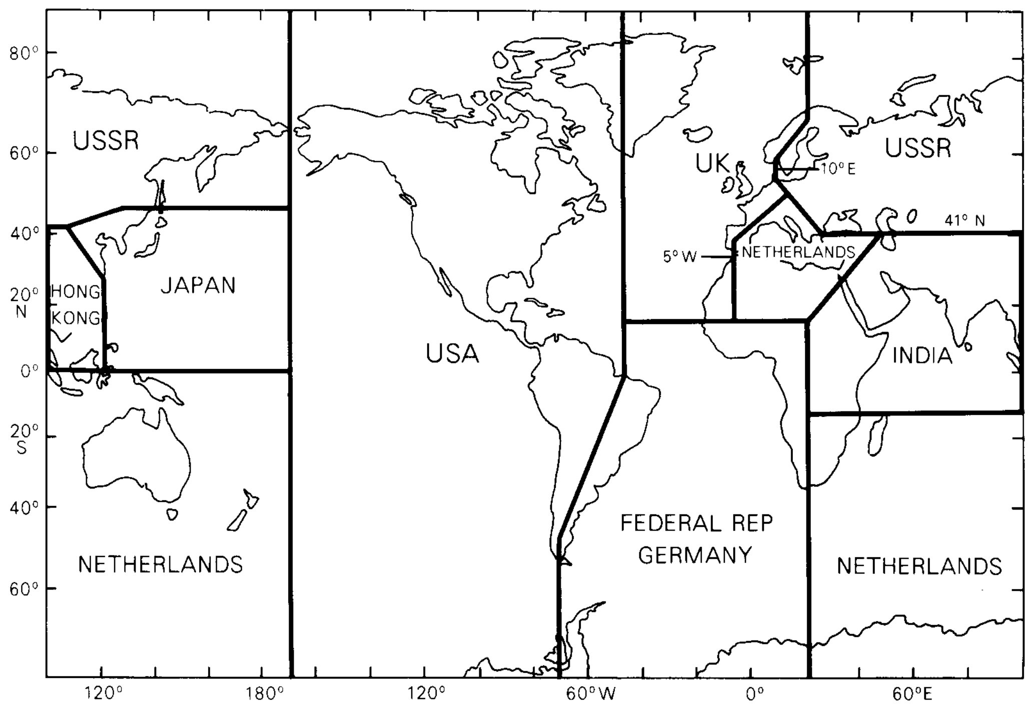

Figure 1. Areas of responsibility of the eight countries acting as collecting centres for meteorological observations.

3. Analysis and results

The two different types of wind data were compared for areas which lay on major shipping routes so that a significantly large sample of observations could be analysed. Reports were examined from vessels recruited by 16 countries which possessed large VOFs, for the period 1854–1984. The numbers of visually estimated and instrumentally measured wind speeds were calculated for 5-year periods, starting from 1960, for the eight countries of origin shown in Table I.

It can be seen that ships recruited by India have only reported visually estimated wind speeds. The number of measured wind speed reports made little contribution to the overall total of reports for vessels registered in the Federal Republic of Germany, the Netherlands and Yugoslavia. During the late 1960s around a quarter of wind observations from ships of the UK VOF were reported as measured, but since then the total has decreased to between 5 and 10%. Figures for American-recruited vessels indicate that up to a quarter of their observations are measured but since the coding error was corrected in 1982 around a half of the observations received have been measured. The proportion of measured wind speeds reported by France and, in particular, Japan increased markedly during the period since 1960, and Japan now reports 90–100% instrumental wind speeds. The decrease in the total number of observations is due in part to a slight decline in the size of the VOF.

Table I. *Numbers of instrumental (I) and visual (V) wind speeds, by country of origin and year (expressed in units of 100 observations)*

	1960–64		1965–69		1970–74		1975–79		1980–84	
	I	*V*	*I*	*V*	*I*	*V*	*I*	*V*	*I*	*V*
USA	53	859	416	1163	414	1097	—	2500	177	820
France	—	210	56	291	220	176	189	92	98	31
Federal Republic of Germany	1	406	84	780	7	770	22	638	49	1209
India	—	59	—	86	—	68	—	—	—	—
Japan	27	2789	511	1274	993	138	883	31	375	5
The Netherlands	0	530	3	672	—	567	8	419	14	436
United Kingdom	9	430	28	98	97	701	84	1081	118	1030
Yugoslavia	—	31	—	141	—	90	—	41	1	11

To illustrate the geographical effect of individual countries' practices in the use of anemometers, maps have been produced showing the percentage of instrumentally measured winds, covering the area 50° S to 60° N and 180° W to 180° E, for four consecutive 5-year periods between 1960 and 1979, using data from all operating countries. The map for 1960–64 is shown in Fig. 2. Values are plotted at the centre of each 10-degree square; squares containing less than 100 observations have been left blank.

On examining this map it is clear that only 1–2% of the wind speeds reported in the North Atlantic during the period 1960–64 were measured. Similar maps for 1965–69, 1970–74, and 1975–79 are shown in Figs 3, 4 and 5 respectively; it can be seen that in the period 1965–69 the percentage rose to approximately 10% and thereafter remained fairly steady. Data from the Indian Ocean followed a similar pattern, but the percentage rose slightly during the period 1975–79 to about 15%.

In the Mediterranean area approximately 6–7% of reported wind speeds between 1960 and 1964 were measured, rising to about 20% and 35% for the following two periods respectively and decreasing to about 15% in 1975–79.

The number of measured wind speeds reported from the South Atlantic increased steadily from 5% of the total in the period 1960–64 to 20% in the period 1975–79. Along the coast of South America the percentage of measured wind speeds appeared generally higher than in the open seas. This may be due to a ship with an anemometer working continuously in the area.

The Southern Ocean (off the coast of Antarctica) had a consistently higher percentage of measured wind speeds over the 20-year period, although the number of observations was small. This almost

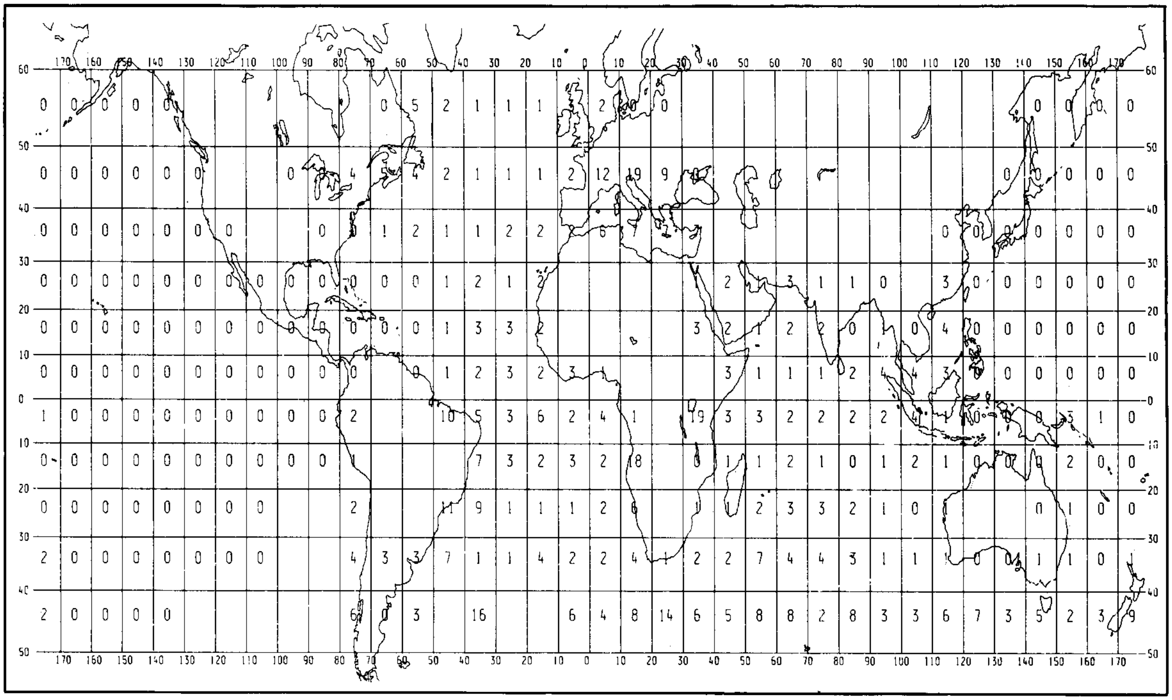

Figure 2. Percentage of instrumentally measured wind observations for the period 1960–64.

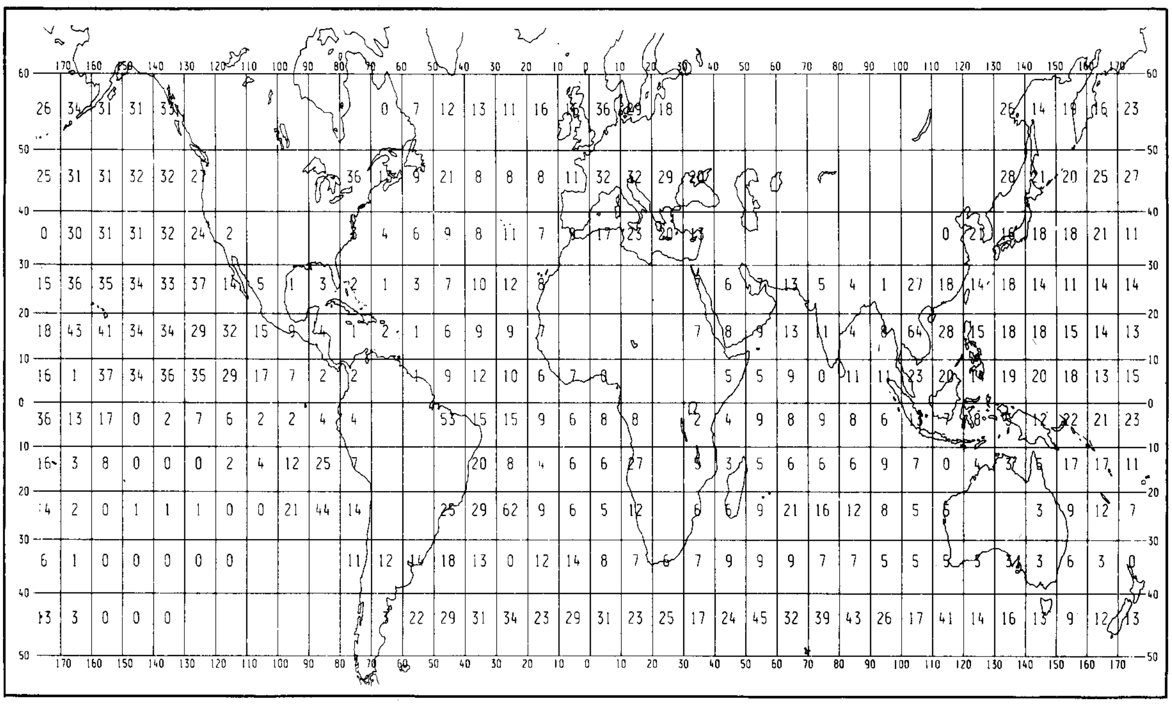

Figure 3. Percentage of instrumentally measured wind observations for the period 1965–69.

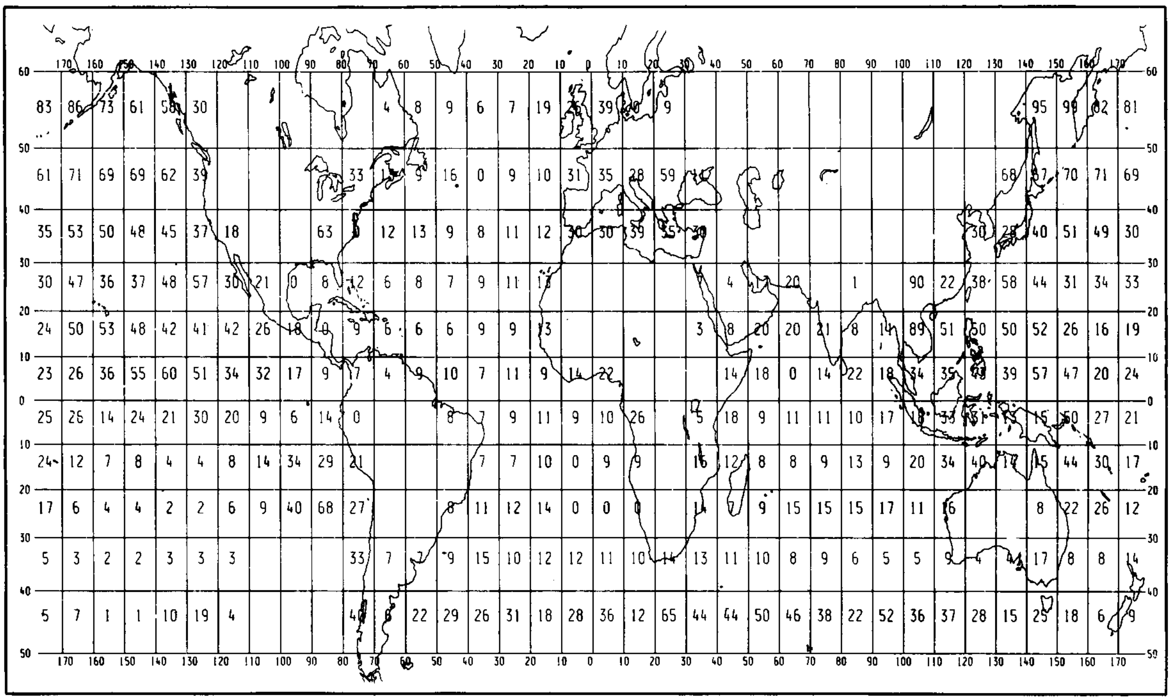

Figure 4. Percentage of instrumentally measured wind observations for the period 1970–74.

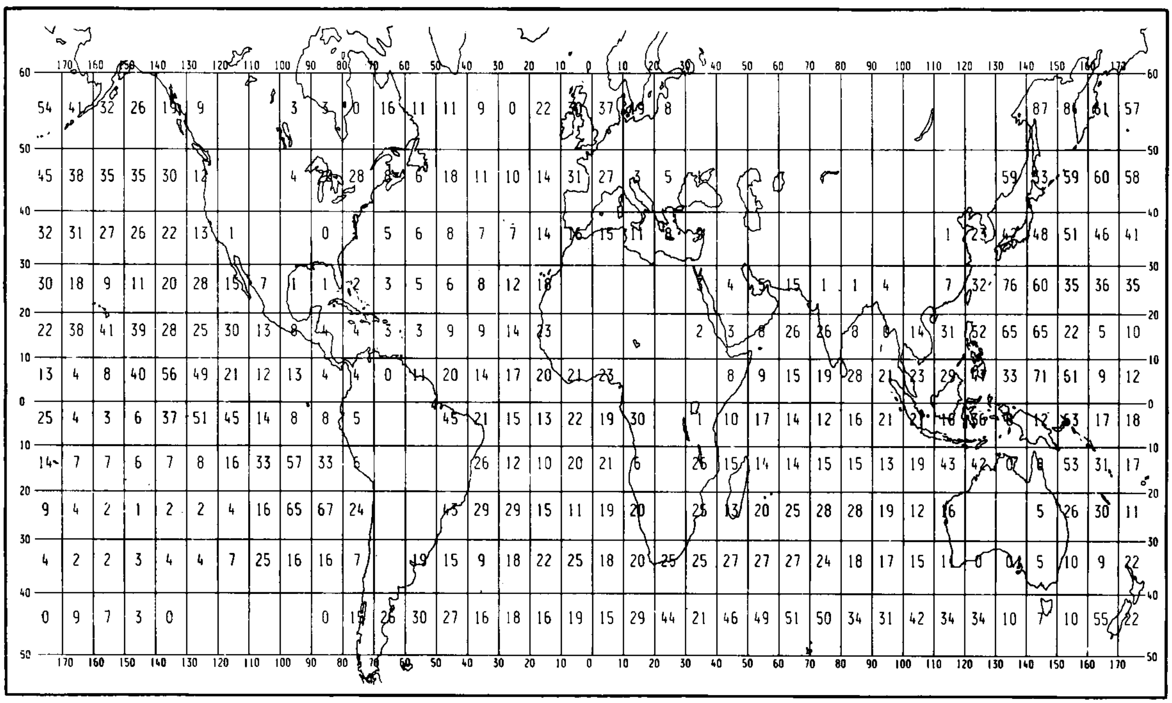

Figure 5. Percentage of instrumentally measured wind observations for the period 1975–79.

certainly reflects the anomalously high contribution from research vessels which are usually equipped with anemometers.

In the period 1960–64 there were virtually no measured wind speeds reported from the whole of the Pacific Ocean. In the second period, from 1965 to 1969, the percentage of measured wind speed observations in the western Pacific rose to 15–20% and in the eastern Pacific to 30–40% of the total. Thereafter, in the eastern Pacific the percentage rose to 40–50% reducing to about 40% in 1975–79. In the western Pacific approximately half the wind speed observations were reported as measured for the period 1970–74, and this figure rose to 60% in 1975–79.

4. Analysis of mixed data

The marine data bank is extensively used to provide data for climatological analyses; therefore it is important to consider the effect on climatological analyses of using a mixture of visual and instrumental data. The area chosen for such an assessment extends from 10 to 20° N and from 130 to 140° E, and since 1970 has contained approximately 50% measured and 50% estimated wind speeds. The frequency of occurrence of instrumentally measured and visually estimated wind speeds for each 'scientific Beaufort scale' point, for the period 1970–74, was calculated and is shown in Table II.

Table II. *Numbers of measured and visual wind speeds, by scientific Beaufort force, for the area 10–20°N, 130–140°E, for the period 1970–74*

Scientific Beaufort force	Number of observations		
	Measured	Visual	Total
0	563	182	745
1	654	622	1 276
2	2 425	1 960	4 385
3	4 596	4 196	8 792
4	5 936	6 292	12 228
5	3 340	4 032	7 372
6	1 474	2 379	3 853
7	619	700	1 319
8	210	192	402
9	35	26	61
10	9	12	21
11	3	3	6
12	1	0	1
Total	19 865	20 596	40 461

For wind speeds of force 3 and below there were more measured than visually estimated wind speeds; for force 4–7 this relationship was reversed; and for force 8 and above the difference was minimal. This confirms that instrumental measurements and visual estimates are providing differing climatologies.

The overall effect of this difference can be best illustrated by deriving extreme values from the two sources of data. This was done by fitting a Weibull function (Weibull 1951) to the distributions of both the measured and visually estimated wind speeds. Extreme values were estimated for return periods, of 1, 2, 5, 10, 20, 50, 100 and 200 years and are presented in Table III. Extremes derived from the measured wind speeds are 3–5 knots lower than those from the visually estimated wind speed distribution. The so-called scientific Beaufort scale (World Meteorological Organization 1970) was used in the calculation. A Weibull analysis of the mixed distribution gave extreme values which were 1–2 knots lower than the values obtained using only visually estimated wind speeds.

Table III. *Extreme values, calculated by fitting a Weibull function to the distributions of the measured and visual wind speeds, using the scientific Beaufort scale*

Return period	Measured wind speed	Visual wind speed	Combined wind speed
years	*knots*	*knots*	*knots*
1	45.4	48.3	47.6
2	46.8	49.9	49.2
5	48.5	52.1	51.1
10	49.8	53.6	52.6
20	51.0	55.1	54.0
50	52.6	57.0	55.8
100	53.7	58.3	57.0
200	54.8	59.7	58.3

5. Conclusion

It appears from the results shown that a few countries are reporting a very large percentage of their wind speed observations as instrumentally measured and it therefore follows that the areas in which the VOF of these countries predominantly operate will also have a higher percentage of measured wind speeds than other areas. For example, the percentages of measured wind speeds reported by Japan and the USA are amongst the highest. Both these countries operate vessels predominantly in the Pacific and the South China Sea and it is these areas which contain the largest percentages of measured wind speeds. Therefore, geographical location should be taken into account when considering the strengths and weaknesses of the data bank in application to marine climatology.

The differences in extreme wind speeds, estimated by fitting a Weibull function to distributions of visual and measured wind speeds, are very significant. They are large enough to lead to inadvertant 'under-designing' if measured wind speeds are used without due care. For example, whereas visual estimates indicate that the return period of a 50-knot wind is about 2 years for an area in the South China Sea, instrumental measurements produce a return period of greater than 10 years. Any adverse effect could also be magnified when wind data are combined with wave or other data to establish the design criteria for structures such as oil rigs, since high waves which add to the structural loading normally occur in association with high winds.

References

Shearman, R.J. 1983 The Meteorological Office main marine data bank. *Meteorol Mag*, **112**, 1–10.

Weibull, W. 1951 A statistical distribution function of wide applicability. *J Appl Mech*, **18**, 293–297.

World Meteorological Organization 1970 The Beaufort Scale of wind force (Technical and operational aspects). Reports on marine science affairs, Report No. 3, Geneva, WMO.

551.526.6:551.506.3:551.509.331

The Meteorological Office Historical Sea Surface Temperature Data Set*

D.E. Parker
Meteorological Office,,Bracknell

Summary

The Meteorological Office Historical Sea Surface Temperature Data Set was created from the main marine data bank (Shearman 1983) to fulfil diverse needs in research into practical long-range forecasting and into climatic fluctuations observed since the mid-nineteenth century. This short paper provides an account of the origins, quality control, and applications of the data set.

1. Introduction

Ships' observations have been recorded since the mid-nineteenth century following the plan of Maury and Glaisher (British Meteorological Society 1852) to cover the whole world with observing stations. Many of these records were stored in archives of ships' logbooks until the 1960s when they were keyed into computerized data sets such as the 'TDF-11' data set created at the National Climatic Data Center, Asheville (North Carolina).

These data sets were supplemented by records for more recent years which have been exchanged internationally under the World Meteorological Organization's 'Resolution 35' carried in 1963. The main marine data bank of the Meteorological Office (Shearman 1983) was formed by combining these data sources, careful checks being made to remove any duplicate observations. The Meteorological Office Historical Sea Surface Temperature Data Set (MOHSST) has been created by extracting the sea surface temperature (SST) observations from the main marine data bank. Similar historical data sets have also been created for night-time and daytime marine air temperature. All these data sets contain monthly values for 5° latitude × 5° longitude areas, beginning at January 1854 and ending at December 1981.

2. Quality control

Observations of SST are beset by systematic biases, individual inaccuracies, and irregular distribution in space and time.

Systematic biases occur because of changes in instrumentation, siting, or procedures. The most notable example is the change from uninsulated bucket measurements (which were taken until the Second World War) to a mixture of engine-intake, hull-sensor, or insulated bucket readings. Bottomley *et al.* (n.d.) describe and incorporate compensation factors designed to take account of these changes. However, research into the effects of the systematic changes is not yet complete, and the data in MOHSST have not had any instrumental corrections made to them.

Individual inaccuracies were treated in the following way. First, no SSTs were included in the main marine data bank if they were outside the range −5 °C to 35 °C. Second, a provisional climatology with 1° latitude × 1° longitude and 5-day resolution was formed during the creation of MOHSST, and all SSTs deviating from this climatology by more than 6 °C were excluded. Third, after averaging over 1° latitude × 1° longitude areas for 5-day periods, the SSTs were converted into deviations from the provisional climatology and then subjected to a modified averaging process known as 'Winsorization'

* For greater details the reader is referred to the new Global Ocean Surface Temperature Atlas (Bottomley *et al.* n.d.) which is currently being produced jointly with the Massachusetts Institute of Technology.

(Afifi and Azen 1979). In this computation, which was made for each 5° latitude × 5° longitude area and month, values exceeding the top quartile were replaced by that quartile, and values below the bottom quartile were replaced by the bottom quartile. The adjusted set of values was then averaged. The resulting average is less influenced by outlying values than a straightforward average would be.

The problems of patchy distribution on the global scale have not entirely been overcome, and the geographical completeness of the climatology to be published by Bottomley *et al.* (n.d.) results only from the merging of a climatology based on MOHSST with an earlier climatology published by Alexander and Mobley (1976). This earlier climatology was complete only because the authors interpolated in the Southern Ocean between the southern limit of observed data and an assumed ice-edge temperature of −1.8 °C. Also, an earlier version of MOHSST was found to have major gaps in the data for the Pacific between 1961 and 1972; when creating the present version of MOHSST, these gaps were filled with values obtained from the US Navy Consolidated Data Set via the Massachusetts Institute of Technology (MIT).

The effects of irregular distribution of data within smaller areas were, however, allowed for in the quality control, firstly by comprehensive non-linear interpolation and smoothing of the provisional climatology within 10° latitude × 10° longitude areas, and secondly by working with 'anomalies' (deviations from climatology) on a geographical resolution of 1° latitude × 1° longitude and a time resolution of 5 days. The latter process avoids considerable biases; if an observation at 41° N, 18° W on 31 May 1856 was the only one in May 1856 in the area 40–45° N, 15–20° W, it would almost certainly be warmer than the average for that area and month even if it were colder than the local average for 31 May. The Winsorization described above, being applied to anomalies with respect to 1° latitude × 1° longitude areas and 5-day periods, produces a representative anomaly for the 5° latitude × 5° longitude area and month.

MOHSST is available as monthly 5° latitude × 5° longitude values computed by adding the quality-controlled anomalies to the smoothed climatology averaged over the area and month. Quality-control flags indicate where values failed extreme-value and scatter tests carried out during Winsorization and also where blank areas were supplemented with the data received from MIT.

3. Applications

MOHSST was created with the realization that it would find many uses. The major applications at present are:

(a) Input to statistical methods of long-range forecasting (Ratcliffe and Murray 1970, Palmer and Sun 1985, Folland and Woodcock 1986).

(b) Provision of boundary conditions for integrations of atmospheric general circulation models for

(i) dynamical long-range forecasting (Mansfield 1986),

(ii) assessment of the mechanisms underlying particular events, e.g. drought in sub-Saharan Africa, or hot summers in the United Kingdom (Folland *et al.* 1986), and

(iii) investigation of the role of SST in climatic change.

(c) Formulation of relationships between SST and particular events, in order to gain understanding of the physical processes involved (Folland *et al.* 1986).

(d) Monitoring of climatic change, particularly with a view to assessing the effects of increasing concentrations of carbon dioxide in the atmosphere (Parker *et al.* 1986).

A dramatic recent application was to the study of drought in sub-Saharan Africa. The Meteorological Office Synoptic Climatology Branch's 11-layer global atmospheric general circulation model was integrated for 6 months of simulated time, firstly with SSTs corresponding to those observed from May to October 1950, and secondly with SSTs representing those observed in the same period of 1984. Fig. 1

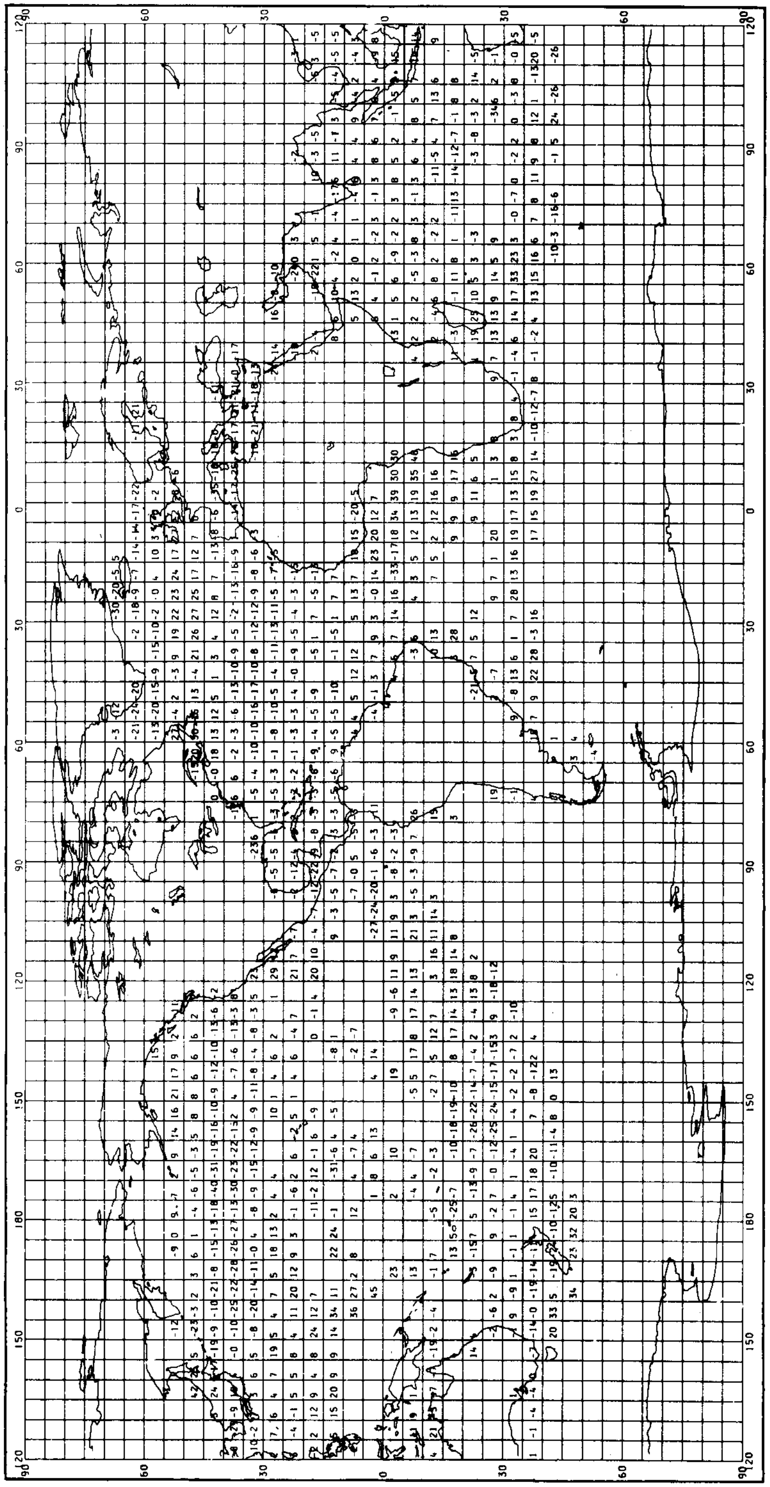

Figure 1. Sea surface temperature (tenths °C) August 1984 minus August 1950.

illustrates the SST differences between these years at the peak of the Sahel rainy season (August). The wettest year this century in the Sahel was 1950 and one of the driest was 1984. The model successfully reproduced the marked contrast of rainfall between the 2 years (Fig. 2). This study also served to elucidate some of the links in the chain of events between SST and Sahel rainfall, such as large-scale changes in atmospheric circulation and moisture convergence, and changes in soil moisture in the Sahel itself.

4. Future plans

The present version of MOHSST was created in 1983. Since then the main marine data bank has been improved by the addition of several data sources, which *inter alia* have covered the gap in Pacific Ocean data in 1961–72. The data bank has also been updated. Plans are being made, therefore, to produce a new version of MOHSST from the main marine data bank. The quality-control procedures will be similar, but separate daytime and night-time data sets will be created so that time-of-observation biases can be estimated. These are important for assessing the SSTs obtained from polar-orbiting satellites which sometimes have nearly fixed transit times. New daytime and night-time data sets of marine air temperature will also be created.

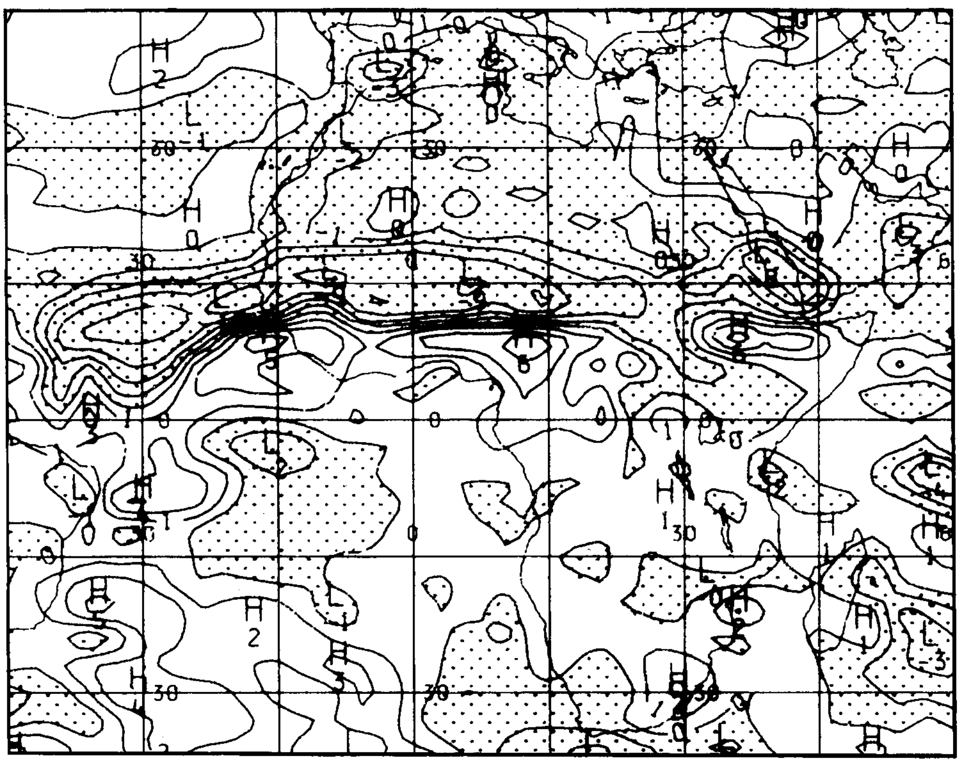

Figure 2. Model rainfall (mm d^{-1}) August 1984 minus August 1950. Stippled areas are negative (1984 drier).

References

Afifi, A.A. and Azen, S.P. 1979 Statistical analysis: A computer oriented approach. Second edition, New York, Academic Press.

Alexander, R.C. and Mobley, R.L. 1976 Monthly average sea-surface temperatures and ice-pack limits on a 1° global grid. *Mon Weather Rev*, **104**, 143–148.

Bottomley, M., Folland, C.K., Hsiung, J., Newell, R.E. and Parker, D.E.	n.d.	Global Ocean Surface Temperature Atlas (GOSTA). (To be published.)
British Meteorological Society	1852	Correspondence between J. Glaisher and M.F. Maury. Report of the Council of the British Meteorological Society, May 25, 1852, 6–10.
Folland, C.K., Palmer, T.N. and Parker, D.E.	1986	Sahel rainfall and worldwide sea temperatures, 1901–85. *Nature*, **320**, 602–607.
Folland, C.K. and Woodcock, A.	1986	Experimental monthly long-range forecasts for the United Kingdom. Part I. Description of the forecasting system. *Meteorol Mag*, **115**, 301–318.
Mansfield, D.A.	1986	The skill of dynamical long-range forecasts, including the effect of sea surface temperature anomalies. *Q J R Meteorol Soc*, **112**, 1145–1176.
Palmer, T.N. and Sun, Z.	1985	A modelling and observational study of the relationship between sea surface temperature in the north-west Atlantic and the atmospheric general circulation. *Q J R Meteorol Soc*, **111**, 947–975.
Parker, D.E., Folland, C.K. and Carson, D.J.	1986	The climate of the world. VI — Carbon dioxide and climate (with appendix on simple climate models). (Unpublished, copy available in the National Meteorological Library, Bracknell.)
Ratcliffe, R.A.S. and Murray, R.	1970	New lag associations between North Atlantic sea temperature and European pressure applied to long-range weather forecasting. *Q J R Meteorol Soc*, **96**, 226–246.
Shearman, R.J.	1983	The Meteorological Office main marine data bank. *Meteorol Mag*, **112**, 1–10.

551.509.58(41):656:33

Dealing with winter chaos*

R.D. Hunt

London Weather Centre

Summary

Transport chaos in winter is costly for industry and the country. Features of the British weather are briefly discussed together with some of the developments taking place in the Meteorological Office and elsewhere to deal with the problem.

1. Introduction

There are a number of features of winter weather in the United Kingdom which create special problems. Two of the more significant are:

(a) The weather is rarely severe for very long; the number of days with severe weather is a very small percentage of the total number of winter days. This makes the allocation of financial resources to deal with the problem very difficult.

(b) The weather situations which bring chaos to the country are notoriously difficult to forecast in detail because they are often very marginal. While forecasting technology has increased to such an extent nowadays that the onset of a cold spell can be predicted several days in advance (and indeed much publicity was given to the correct forecast of the massive change to severe weather in January 1987), trying to pinpoint where snow is going to be heaviest, just how much will fall, whether or not it will lie, etc. is very difficult.

* A lecture presented to the Institution of Civil Engineers' Conference, 'Winter chaos — can we buy our way out of it?', London, 31 March 1987.

In countries with a more continental type of climate, temperatures stay below freezing for long periods of time, frost is often a near certainty and any precipitation which falls can be expected to be snow, usually of the dry, powdery kind. In the British Isles there is often doubt as to whether the temperature will fall below freezing point at night because of difficulties in assessing cloud amount or wind speed, both of which have an affect on temperature, while the situations which lead to widespread heavy snow usually involve the coming together of cold and mild air; there is, therefore, uncertainty about whether to expect snow or rain. What snow does fall is often wet and sticky.

Snow usually occurs in the United Kingdom when the temperature is close to freezing point. Even when snowfall can be predicted with a high degree of confidence, there is still the problem of deciding whether it will lie at all levels, or just on higher ground. A drop in temperature of just 1 °C can make all the difference between a wet day and a day of winter travel chaos.

There is no question that accurate forecasts in winter are of great financial benefit to whole sections of industry as well as to the authorities responsible for road and rail transport. The developments outlined below indicate how the Meteorological Office is trying to improve its forecasts of ice and snow and also the liaison with the transport authorities in order to reduce the effects, and costs, of winter chaos.

2. Computer forecast models

The Meteorological Office has developed sophisticated computer models for forecasting weather around the world for a week ahead. One model is used for producing detailed weather forecasts in the British Isles for the following 36 hours. It has a resolution of about 75 km in the vicinity of the United Kingdom and is capable of predicting not only the pressure patterns and fronts, familiar from television and newspapers, but also where and how much rain is likely to fall. By calculating temperatures through the atmosphere, it is also able to indicate probabilities of precipitation falling as snow rather than rain.

The results from these models have been very impressive and are probably the main reason why the general public's perception of weather forecast accuracy has risen so much in the last few years. Nevertheless, the computer is unable to produce all the answers; there is still a great deal of human input necessary both in interpreting the information and in assessing up-to-date observations.

Although the resolution of 75 km is good for many purposes, the weather can change over much smaller distances than that. Hills and coasts affect the weather over small areas, while bands of rain and showers often get organized on a small scale. Because of this, a new model has been developed with a resolution of only 15 km to cover the whole British Isles. This should become fully operational soon and will lead to more accuracy in forecasts a day ahead, including forecasts of snowfall and frost. Initial results from the development phase have been encouraging.

3. Weather radar

Weather radar is now used by forecasters to see not only where rain or snow is falling but also how much. By looking at a time sequence of displays over the most recent few hours, judgements can be made about which areas are most likely to receive snow in the next few hours.

The radars are quite expensive and their range is fairly limited. Nevertheless, it has been possible for the Meteorological Office, in conjunction with the Water Authorities and other interested parties, to cover large areas of England, Wales and Northern Ireland with a radar network. Information from this network has already been an invaluable aid. During the severe weather in January 1987, for instance, forecasters were able to see just how far snow showers coming across the coast were penetrating inland and to assess what track they were taking. It was, therefore, possible to indicate which areas were likely to be most affected. (Unfortunately Kent is on the edge of the radar picture and so the data there were of less use, particularly as the snow was coming in from the North Sea.) Similarly, in conditions of more

Photograph by courtesy of A.J. Byrne

general precipitation it was possible to assess the speed of the spread of snow and to indicate where it was heaviest. Plans are already well advanced to expand the network further, in eastern England, in the south-west and into Scotland.

4. Road surface temperature forecasting

For many years the Meteorological Office has been able to give warnings of night frost in a general sense. But the increasing cost of salting roads has led to the development of more sophisticated techniques for forecasting temperatures actually on road surfaces. Models have been developed, both in the Meteorological Office* and at the University of Birmingham, which can forecast road temperatures for the overnight period thereby not only showing whether sub-freezing temperatures are expected but also giving the time at which the temperature is expected to fall below freezing and the minimum temperature.

In order for the models to produce results, detailed forecasts of cloud amounts, air temperature and wind speed are required, so improvements in general forecasting mentioned earlier are important. The output from this, or any other model, is only as good as the data put into it.

Also, for the model forecasts to be of maximum benefit, they should be for specific locations at which there are road sensors installed. If road temperature information is available in real time, the forecaster can update his forecast as necessary — he can also verify the output. This increases the confidence in the

* For details see P.J. Rayer; The Meteorological Office forecast road surface temperature model, *Meteorol Mag*, **116**, 1987, 180–191.

forecasts and assists with further development of the model. Road sensors can be placed at locations of most benefit to the local authorities, making use of thermal mapping techniques to select cold spots and to relate temperatures at one site to a much wider area.

5. Practical assistance to transport maintenance and planning

The winter of 1986/87 has seen the biggest growth ever in the amount and quality of services provided by the Meteorological Office to assist maintenance of the road and rail network. A new service, called Open Road, was launched in the autumn of 1986 and many local authorities have taken advantage of it.

Open Road has combined many of the features described above to produce a forecast service as accurate as possible within the current state of the science. Road temperature forecasts are provided routinely to the authorities, together with detailed forecasts in pictorial and text form and copies of the weather radar output with comments added by forecasters. Apart from forecasts for the coming night, planning outlooks to 5 days are provided as well as a summary of the previous night's weather. Similar services have been arranged with many of the British Rail regions and also the London Underground.

One of the attractions of Open Road is that it has led to an increase in the liaison between the local authorities and the forecasters. The improved contact, as well as the better product, has given rise to a much higher level of confidence in the forecasts. It should also be stressed that far more information is coming back from the authorities as well. Latest reports about conditions around the counties are vital to the forecaster who, even with satellite pictures, radar, and computer products, still needs more knowledge about what is actually happening on the ground.

Apart from giving information on expected weather conditions, the Meteorological Office has been able to give considerable advice on the positioning of new roads and motorways in order to minimize the occurrence of fog and high winds and to maximize the use of warning signs. This is very much a growth area and one which should lead to more efficient use of financial resources.

6. Concluding remarks

Severe weather is nearly always going to occur at some stage in a British winter. Sometimes conditions may be so severe that transport chaos would occur even if forecasts were perfect; indeed January 1987 may well have seen extreme conditions, in parts of Kent especially, when this would have applied. But, generally speaking, an accurate forecast a few days ahead of the possibility of wintry weather combined with detailed forecasts out to about 1 day ahead can be of great practical assistance.

Because of the developments described above, and others not mentioned here, forecasts are now far more accurate than they used to be. This enables a much more comprehensive service to be provided. Obviously the amount of work and technology involved is much larger than hitherto and this is reflected in the cost. Nevertheless, costs are very low compared to the total winter maintenance budget.

As in so many other areas, it is necessary to spend some money in order to save considerably more. Winter chaos can be alleviated by taking advantage of improved weather services, but not eliminated.

Review

Contemporary climatology, by A. Henderson-Sellers and P.J. Robinson. 157 mm × 234 mm, pp. xvi + 439, *illus.* Harlow, Longman, 1986. Price £12.95.

For most subjects, there are now many books to which one can refer for up-to-date information. Amongst the meteorological titles, *Contemporary climatology* is worthy of consideration. This joint offering by A. Henderson-Sellers and P.J. Robinson, of the Geography Departments at the University of Liverpool and North Carolina respectively, was written in 1984 and is aimed at undergraduates without a strong mathematical background. It generally succeeds, although the level of complexity varies greatly, thus making sections of it potentially useful to the interested layman. Equations are few and far between, but the text carries the reader lucidly through a variety of concepts, supplemented by many clear illustrations and black and white photographs together with a useful glossary of climatological and meteorological terms, an appendix of SI units and a comprehensive index.

The book can be effectively divided into two parts. Part 1 (chapters 1–3) deals with the science of climatology from its early beginnings through its unhappy recent past ('...climatologists were the halt and the lame...') to its current place as a subject with important contributions to make. Basic ideas that govern the behaviour of the climatic system are introduced and these include a discussion of the radiation budget of the earth and the importance of the latitudinal imbalance in absorbed and emitted radiation, the hydrological cycle and the effects of water vapour in the atmosphere, cloud formation, evaporation and global precipitation distribution. The difficulties encountered in obtaining accurate measurements of precipitation and evaporation are brought to the reader's attention but a consideration of soil moisture deficit and its seasonal variation, a parameter that can affect precipitation amounts, is missing.

This discussion of physical climatology then gives way to a study of dynamical aspects in Part 2 (chapters 4–7). The general circulation and global climate are introduced and ideas on the causes of the circulation, Coriolis force, barotropic and baroclinic conditions, Rossby waves, etc. are stated in a simple but effective fashion. A change of scale leads to a consideration of regional climates and the methods used to classify them. The Köppen system is widely used and this is clearly explained. Tropical, mid-latitude and polar climates are examined and results from a simulation model, used to quantify precipitation changes resulting from deforestation of the Amazon basin and its conversion to savannah grassland, are included. Our attention is then turned to local climates, where we are introduced to the influence of topography as a modifying force, pollution, the human response to climate and the effect of human activities on climate. Very scant attention has been given to what is perhaps one of the more important effects of increasing urbanization, namely its tendency to increase local precipitation totals, a finding that arose out of the METROMEX program. A particularly interesting diagram is included of the locally named winds of the Mediterranean basin, approximately 50 of them. In rounding off the book, the authors look to the future and ponder the issue of climatic change. The possible causes of such a change are discussed, the models that simulate climates and the problems associated with these models are considered, and the evidence to suggest that climatic change has taken place in the past is presented. Finally, the carbon dioxide problem is given considerable space.

Both authors are well known and have collaborated to produce a comprehensive and comparatively error-free book, which will no doubt find its way on to many bookshelves. Two points of criticism; firstly, the narrative, although clear, fails in my opinion to convey the great excitement which can characterize a study of the earth's climatic systems, and secondly, why was the book produced at all? Much of what is between the covers of this work has appeared in other books — do we really need this degree of repetition?

Nevertheless, a great deal of care has been taken by the authors in its preparation and for that reason, it deserves to be a success.

M.S. Shawyer

Books received

The listing of books under this heading does not preclude a review in the Meteorological Magazine at a later date.

Landolt-Börnstein: numerical data and functional relationships in science and technology, V/4a, edited by G. Fischer (Berlin, Heidelberg, New York, London, Paris, Tokyo, Springer-Verlag, 1987. DM 1220.00) contains meteorological data, mainly in tabular and diagrammatic form, on the physics of the atmosphere. This subvolume covers the thermodynamic structure and dynamics of the global atmosphere.

Remote sensing digital image analysis, by J.A. Richards (Berlin, Heidelberg, New York, London, Paris, Tokyo, Springer-Verlag, 1986. DM 138.00) includes an overview of remote-sensing data sources and characteristics. It seeks to draw together the range of digital image-processing procedures into a single treatment.

A glossary of computing terms, edited by the British Computer Society Schools Committee Glossary Working Party (Cambridge University Press, 1987. £1.95, US $3.95) contains an explanation of over 800 computing terms divided into 15 sections, but with a complete index also. All aspects of computing are included.

Monsoons, edited by J.S. Fein and P.L. Stephens (New York, Chichester, Brisbane, Toronto, Singapore, John Wiley and Sons, 1987. £71.75) consists of 19 chapters on many aspects of the subject and takes a broad multi-disciplinary look at these variable natural phenomena.

Antarctic science, edited by D.W.H. Walton (Cambridge University Press, 1987. £25.00, US $39.50) reviews the major international developments in Antarctic science from its earliest beginnings, and attempts to forecast future developments in the area. Biology, the earth sciences and atmospheric science are examined, with emphasis on the achievements of the past 25 years.

Atmospheres and ionospheres of the outer planets and their satellites, by S.K. Atreya (Berlin, Heidelberg, New York, London, Paris, Tokyo, Springer-Verlag, 1986. DM 148.00) presents a theoretical discussion of the subject's relevant physical and chemical processes. Observational data, methods of their retrieval and the shortcomings of theoretical models are discussed with a view to further research.

Climate and plant distribution, by F.I. Woodward (Cambridge University Press, 1987. £8.95 (paperback), £22.50 (hardback)) examines the thesis that climate exerts the dominant control on the distribution of vegetation types. Firstly the distribution of species in relation to climate over different scales of time and place world-wide is considered, and secondly the approaches to explaining observed correlations between plant distribution and climate, and the mechanisms of physiological and biochemical control, are investigated.

Satellite photographs — 7 June 1987 at 1442 GMT

The infra-red (left) and visible (right) images show cloud over France and the Bay of Biscay associated with an eastward-moving low, and cold front. Considerable dense 'lumpy' cloud in both images indicates deep convection, especially along the cold front where an organized band of anvils is seen. Within the warm sector of the low, widespread layered cloud is present which over the mountains of northern Spain is broken into lee waves.

Detailed re-analysis of all the available surface observations near the cold front as it crossed western France indicated that: the front lay close to the forward edge of the cloud band (possibly along the narrow band of bright cloud in the south-east corner of the Bay of Biscay, as seen on the visible image); it was accompanied by a squall line some 300 km in length where winds suddenly changed from 5–10 kn southerly to 25–35 kn westerly, with 50–60 kn gusts; the front moved eastwards at 36 kn; surface pressure rose by about 3 mb; and surface temperatures fell by as much as 12 °C (from 26 °C to 14 °C at Bordeaux). The suddenness of the arrival of the squall line led to the deaths of at least eight people, mostly through drowning.

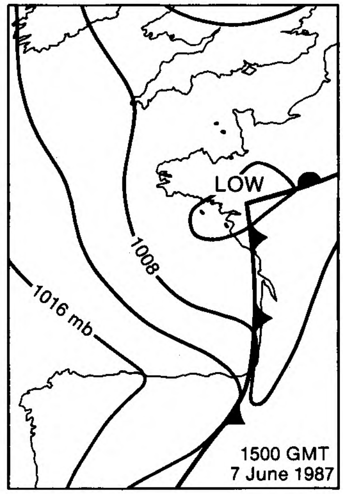

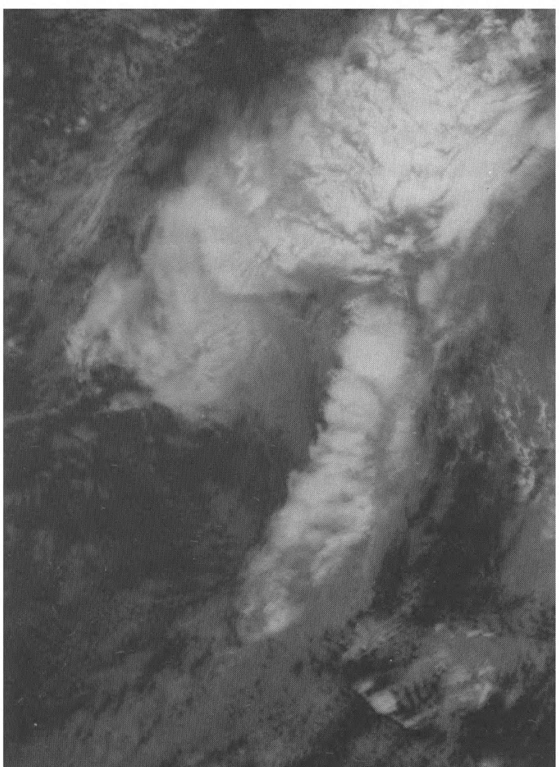

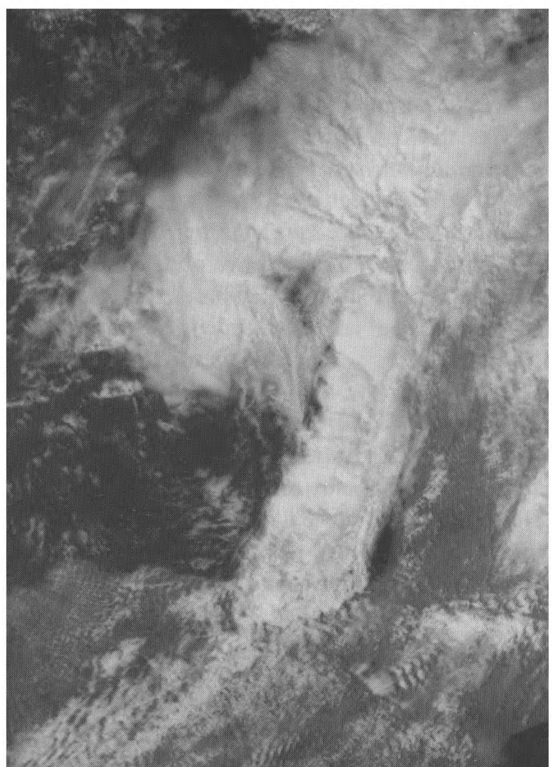

Photographs by courtesy of University of Dundee

Meteorological Magazine

GUIDE TO AUTHORS

Content

Articles on all aspects of meteorology are welcomed, particularly those which describe the results of research in applied meteorology or the development of practical forecasting techniques.

Preparation and submission of articles

Articles for publication and all other communications for the Editor should be addressed to the Director-General, Meteorological Office, London Road, Bracknell, Berkshire RG12 2SZ and marked 'For *Meteorological Magazine*'.

Articles, which must be in English, should be typed, double-spaced with wide margins, on one side only of A4-size paper. Tables, references and figure captions should be typed separately.

Spelling should conform to the preferred spelling in the *Concise Oxford Dictionary*.

References should be made using the Harvard system (author, date) and full details should be given at the end of the text. If a document referred to is unpublished, details must be given of the library where it may be seen. Documents which are not available to enquirers must not be referred to.

Tables should be numbered using roman numerals and provided with headings. We consider vertical and horizontal rules to be unnecessary in a well-designed table; spaces should be used instead.

Mathematical notation should be written with extreme care. Particular care should be taken to differentiate between Greek letters and Roman letters for which they could be mistaken. Double subscripts and superscripts should be avoided, as they are difficult to typeset and difficult to read. Keep notation as simple as possible; this makes typesetting quicker and therefore cheaper, and reduces the possibility of error. Further guidance is given in BS1991: Part 1: 1976 and *Quantities, Units and Symbols* published by the Royal Society.

Illustrations

Diagrams must be supplied either drawn to professional standards or drawn clearly, preferably in ink. They should be about 1½ to 3 times the final printed size and should not contain any unnecessary or irrelevant details. Any symbols and lettering must be large enough to remain legible after reduction. Explanatory text should not appear on the diagram itself but in the caption. Captions should be typed on a separate sheet of paper and should, as far as possible, explain the meanings of the diagrams without the reader having to refer to the text.

Sharp monochrome photographs on glossy paper are preferred: colour prints are acceptable but the use of colour within the magazine is at the Editor's discretion. In either case contrast should be sufficient to ensure satisfactory reproduction.

Units

SI units, or units approved by WMO, should be used.

Copyright

Authors wishing to retain copyright for themselves or for their sponsors should inform the Editor when they submit contributions which will otherwise become UK Crown copyright by right of first publication.

It is the responsibility of authors to obtain clearance for any copyright material they wish to use before submitting it for publication.

Free copies

Three free copies of the magazine are provided for authors of articles published in it. Separate offprints for each article are not provided.

Meteorological Magazine

August 1987

Vol. 116
No. 1381

CONTENTS

Contributions: it is requested that all communications to the Editor and books for review be addressed to the Director-General, Meteorological Office, London Road, Bracknell, Berkshire RG12 2SZ, and marked 'For *Meteorological Magazine*'. Contributors are asked to comply with the guidelines given in the *Guide to authors* which appears on the inside back cover. The responsibility for facts and opinions expressed in the signed articles and letters published in *Meteorological Magazine* rests with their respective authors. Authors wishing to retain copyright for themselves or for their sponsors should inform the Editor when submitting contributions which will otherwise become UK Crown copyright by right of first publication.

Subscriptions: Annual subscription £27.00 including postage; individual copies £2.30 including postage. Applications for postal subscriptions should be made to HMSO, PO Box 276, London SW8 5DT; subscription enquiries 01–211 8667.

Back numbers: Full-size reprints of Vols 1–75 (1866–1940) are available from Johnson Reprint Co. Ltd, 24–28 Oval Road, London NW1 7DX. Complete volumes of *Meteorological Magazine* commencing with volume 54 are available on microfilm from University Microfilms International, 18 Bedford Row, London WC1R 4EJ. Information on microfiche issues is available from Kraus Microfiche, Rte 100, Milwood, NY 10546, USA.

ISBN 0 11 727972 2 ISSN 0026–1149

Printed for HER MAJESTY'S STATIONERY OFFICE
by Delco Printing Co Ltd 8/87 Dd. 739131 C13

THE METEOROLOGICAL MAGAZINE

HER MAJESTY'S STATIONERY OFFICE

September 1987

Met.O.978 No. 1382 Vol. 116

METEOROLOGICAL OFFICE Met.O.978

THE METEOROLOGICAL MAGAZINE

No. 1382, September 1987, Vol. 116

Retirement of Mr D.E. Miller

Mr Derek Miller, Deputy Director (Communications and Computing), took retirement from the Meteorological Office at the early age of fifty years on 31 July 1987 after a career of twenty-nine years in the Office, most of which were spent in the area of high atmospheric research and in the development and use of rockets and satellite instrumentation to make measurements of the atmosphere.

Mr Miller was educated at Magdalen College School, Brackley (Northants) and at Wadham College Oxford, where he graduated with a first class Honours (BA) in Natural Sciences and won the Scott Prize for Physics in 1958. He joined the Office directly from Oxford, and took the usual Scientific Officer course at Stanmore where he was immediately recognized as one of those rare people who combine a first-class academic ability with a very practical approach to the problems of applied meteorology. Thus, after a short spell of forecasting experience at Wyton and London (Heathrow) Airport in 1959, he was posted into research with the High Atmosphere Research Unit which, at that time, was located at Kew Observatory under Dr K.H. Stewart.

Thus began a direct relationship with high-altitude and satellite meteorology which lasted up until 1985. At Kew he became deeply involved in the design and development of the instrumentation required to make observations of stratospheric ozone from Skylark rockets and from the Anglo-American satellite Ariel 2.

In October 1962 he was promoted to Senior Scientific Officer and continued to work in the same unit, which was now part of the Satellite Meteorology Branch (Met O 19), under Dr Stewart and Dr R. Frith. As the UK representative at the National Aeronautics and Space Administration in Washington, during tests of the equipment for the Ariel 2 satellite, his ability and personality earned great respect in the USA.

By 1965 the team had moved to Bracknell, and the Ariel 2 satellite ozone experiment involved him in programming with the KDF 9 computer, and a joint project between the Office and Dr J.T. Houghton's group at Oxford University on the measurement of molecular oxygen airglow in the infra-red was started.

Mr Miller was promoted to Principal Scientific Officer in 1967, staying in Met O 19, and that year was notable for his paper in the *Proceedings of the Royal Society* on measurements of stratospheric attenuation in the near ultraviolet. His work then expanded to cover the preliminary design for the instruments to measure molecular oxygen and ozone on the Nimbus F spacecraft, and further rocket work in Europe with the European Space Research Organization (ESRO), and in Canada and the USA.

From 1967 to 1976 he continued to be deeply involved in the development of new methods of observation, sensors and instruments on meteorological satellites and rockets. Papers were produced on the results of Skua rocket flights, and on an analysis of the correlation between air density and magnetic disturbances deduced from the change in the Ariel 2 satellite spin rate. He became a member (later the Chairman) of the ESRO Working Group on the Ground Facilities required for the new Meteosat Project, Chairman on the Working Group for the Meteorological Information Extraction Centre (MIEC) Software Development, and also was closely involved in the scientific development and contract monitoring of the Stratospheric Temperature Sounder Unit for the TIROS-N satellite. He became well known in European circles and was much sought after for his knowledge and experience.

In 1976 Derek Miller was promoted to Senior Principal Scientific Officer and became the Assistant Director of the Satellite Meteorology Branch. In this post he was able to use his administrative abilities and powers of scientific leadership. Much of his time was also devoted to national and international committee work and to consultancies with the European Space Agency (ESA) concerning the geostationary satellite Meteosat. He was a member of the Science Research Council Solar System Working Group and continued as Chairman of the *ad hoc* Group on Satellite Data Reception for Meteosat/ESA.

In 1982 he was again promoted, to Deputy Chief Scientific Officer (now Grade 5) as Deputy Director of Physical Research. In this post, looking after the administration and management of a number of branches ranging from Boundary Layer Research to the Meteorological Office Radar Research Laboratory at Malvern, his abilities made him a tower of strength, and he continued his interests in space meteorology as Chairman of an inter-departmental team charged with defining a costed national remote-sensing programme in support of the Earth Resources Satellite, ERS-1, and through working on the Natural Environment Research Council, the Science and Engineering Research Council and Royal Society committees on meteorological research in the universities and in industry.

In 1985 Mr Miller moved to the new area of Deputy Director (Communications and Computing) where he was able to exercise his administrative and organizational talents in a new field. He continued to set himself the highest standards, and his insight and judgement have been very evident, in particular in a recent study on the future of the Man–machine Interface in Forecasting. He has worked particularly hard on the new plans for the replacement of the Cyber 205 supercomputer, the Weather Information

System and the new satellite processing system AUTOSAT-2. All of these are going well despite the fact that he found the frustrations and delays inherent in the projects difficult to balance with his self-set standards of excellence.

Mr Miller is a man of energy and drive, and I cannot imagine that he will be idle for very long in his retired state. I shall miss his sound judgement and attention to detail in matters both large and small, and not least for his wise advice as Chairman of the Accommodation Committee over the past two years. I am sure that all his friends and colleagues will join me in wishing Derek a long and happy retirement, and I have no doubt we shall be meeting him again in matters of meteorological significance in the future.

D.N. Axford

551.509.313:551.525.2:551.578.46:551.579.5:551.588

An introduction to the parametrization of land-surface processes Part II. Soil heat conduction and surface hydrology*

D.J. Carson†

Assistant Director (Dynamical Climatology), Meteorological Office, Bracknell

Summary

This paper concludes an introduction to the subgrid-scale land-surface processes which, it is generally acknowledged, need to be included by parametrization in three-dimensional numerical models for studying climate and climate change, and for numerical weather prediction. The discussion is restricted in the main to the relatively simple case of non-vegetated land surfaces.

Part I (Carson 1987) described the general boundary conditions for momentum transfer and the balance equations for energy and mass (moisture) transfer at a bare-soil surface. The surface radiative properties and fluxes, and the physical character and the parametrization of the surface turbulent exchanges, were considered.

Part II concentrates mainly on soil heat conduction and the land-surface temperature, and surface hydrology and the soil water budget. It concludes with a brief discussion of some of the particular problems associated with snow-covered, non-vegetated, land surfaces.

1. Introduction

In Part I of this introduction to land-surface processes (Carson 1987) the balance equations for energy and mass (moisture) transfer at a bare-soil surface were described. Also the surface radiative properties and fluxes were considered along with the physical character and parametrization of the surface turbulent exchanges. Here emphasis will be placed on two topics:

(a) soil heat conduction and the prediction of the land-surface temperature using the surface energy balance (section 2);

(b) surface hydrology and the prediction of the soil moisture content using the moisture balance equation (section 3).

The way in which snow-covered surfaces are taken into account will also be considered (section 4).

---

* Abridged version of lecture notes prepared for the Centre National d'Études Spatiales (CNES) Summer School of Space Physics, 'Climatology and Space Observations', Roscoff, France, July 1986.

† Now at Natural Environment Research Council, Swindon.

There is a need to study heat conduction in the soil to provide a sound physical basis for evaluating the surface temperature. In the same way it is necessary to understand the dynamics which govern the movement of water in the soil so that changes in soil moisture content can be modelled. Although the concepts of surface temperature and soil moisture content are discussed separately, it is worth emphasizing the strong interactive coupling between the thermal and hydrological properties and processes in the soil. Not only does the evaporation rate appear explicitly in both the balance equations for energy and mass but also most of the other surface fluxes (including the momentum flux) depend, to varying degrees, on the surface temperature and soil moisture content. Indeed, in a model with both interactive surface hydrology and interactive land-surface temperature, the value of the soil moisture content has an important bearing on the surface temperature and vice versa.

2. Soil heat conduction and the land-surface temperature

The energy flux balance at a bare-soil surface may be expressed as

$$G_0 = R_N - H - Q \qquad \ldots \ldots \ldots \ldots \ldots \ldots \quad (1)$$

where R_N is the net radiative flux, H is the turbulent sensible-heat flux, $Q = L_e E$ is the latent-heat flux due to surface evaporation (E is the surface evaporation rate and L_e is the latent heat of evaporation) and G_0 is the flux of heat into the soil.

If the aim was solely to evaluate G_0, then use of the surface energy balance as given by equation (1) would be a legitimate method of obtaining such an estimate. Indeed, in principle, the energy balance method can be invoked to estimate any one of the terms in equation (1) if all the other terms are known by some other means.

The more direct, microphysical approach to understanding the soil heat flux term, G_0, is through the study of heat transfer in the soil itself, a process which is predominantly that of heat conduction. In general, G_0 will depend in a complicated way on the soil's thermal properties which in turn depend on, for example, the type of surface, the type of soil and whether it is wet, dry, frozen or snow-covered, and whether it is bare soil or vegetation. In simple, general terms a thin surface layer of the soil stores heat during the day (strictly, from equation (1), when $R_N > H + Q$, i.e. G_0 is positive) and acts as a source of heat energy to the surface at night (strictly, when $R_N - H - Q < 0$, i.e. G_0 is negative). On longer, seasonal and annual time-scales deeper soil layers act as a reservoir of heat which may be replenished during warm seasons and depleted during cold seasons.

Good estimates of the detailed behaviour of G_0 throughout the day and throughout the year are now recognized as important for inclusion in numerical weather prediction models (NWPMs), which attempt to forecast the characteristic diurnal cycle of land-surface temperatures, and also in climate models which need to simulate realistically and interactively the heat-storage properties of the soil over periods ranging from less than a day to at least several years.

Implicit in a knowledge of heat transfer through the soil is a knowledge of the soil temperature profile with depth. In particular, the land-surface temperature, T_0, features in each of the terms in equation (1) and it is now the common practice in atmospheric general circulation models (AGCMs) and NWPMs to invoke the surface energy balance as a diagnostic relation or prognostic equation for evaluating T_0. The variety of techniques commonly used in such models for representing G_0 in the surface energy balance has already been reviewed fairly comprehensively by, for example, Bhumralkar (1975), Deardorff (1978) and Carson (1982, 1986). In order to illustrate the relationships between soil heat flux, soil temperature profile and the thermal properties of the soil, I shall restrict my discussion to those methods which rely on a knowledge of heat conduction in the soil and invoke either simple, one-dimensional, analytical models or attempt to model explicitly the soil heat transfer in a multi-layer soil model.

2.1 *Heat transfer in a semi-infinite homogeneous soil*

Most parametrizations of G_0 are now based on considerations of heat conduction and conservation in the soil. The problem is usually simplified by assuming a semi-infinite, spatially homogeneous soil layer with no horizontal heat transfer and no melting or freezing within it. This restricted and idealized one-dimensional problem is governed by the following two equations:

(a) *The soil heat conservation equation*

$$\frac{\partial T_g}{\partial t} = -\frac{1}{C}\frac{\partial G}{\partial z_g} \qquad \dots \dots \dots \dots \dots \quad (2)$$

where T_g is the soil (ground) temperature, G is the soil heat flux, C is the volumetric heat capacity of the soil (units J m^{-3} K^{-1}), $z_g = -z$ is the vertical coordinate in the soil layer and t is time.

(b) *The flux–gradient relation for heat conduction*

$$G = -\lambda \frac{\partial T_g}{\partial z_g} \qquad \dots \dots \dots \dots \dots \quad (3)$$

where λ is the thermal conductivity of the soil (units W m^{-1} K^{-1}).

Substitution of equation (3) into equation (2), with the assumption of homogeneity, yields the one-dimensional equation for the conduction of heat in the soil

$$\frac{\partial T_g}{\partial t} = \kappa \frac{\partial^2 T_g}{\partial z_g^2} \qquad \dots \dots \dots \dots \dots \quad (4)$$

where κ is the thermal diffusivity of the soil (units m^2 s^{-1}). The thermal diffusivity is related to the other soil parameters by $\kappa = \lambda / C = \lambda / \rho_g c_g$ where ρ_g is the uniform soil density and c_g is the specific heat capacity (units J kg^{-1} K^{-1}).

The definitions and characteristics of the soil thermal properties C, λ, κ and c_g can be found in standard textbooks such as Geiger (1966), Sellers (1965), Oke (1978) and Rosenberg *et al.* (1983). The values in Table I come from Oke (1978) and illustrate the typical magnitudes of these terms for a few simple soil types (and for snow); an indication is also given of the sensitivity of the parameters to how wet or dry the soil is.

It is standard practice to use equations (1), (2) and (3) to produce a prognostic equation for T_0 (usually assumed equivalent to the soil surface temperature T_{g0}). The simplest approaches of this kind introduce the concept of an effective depth of soil, D, and an effective surface thermal capacity $C_{eff} = CD = \rho_g c_g D$ defined such that

$$G_0 = C_{eff}\frac{\partial T_{g0}}{\partial t} = CD\frac{\partial T_0}{\partial t}\ . \qquad \dots \dots \dots \dots \dots \quad (5)$$

Note that expressing G_0 in this way does not imply a priori that T_0 has been replaced by and equated to the mean temperature throughout the shallow surface soil layer of depth D, with neglect of conduction of heat to or from lower soil layers. Rather it is an attempt, if D can be determined sensibly, to parametrize the changing heat content of the whole soil layer by using the analogue of a single shallow layer of known thermal capacity, C_{eff}, which is fully insulated at its lower boundary and whose uniform temperature, T_0, increases or decreases uniformly in response to G_0.

Substituting equation (5) into equation (1) and remembering the assumption that $T_0 = T_{g0}$ gives

$$C_{eff}\frac{\partial T_0}{\partial t} = R_N - H - Q \qquad \dots \dots \dots \dots \dots \quad (6)$$

Table I. *Thermal properties of natural materials (from Oke 1978). For explanation of symbols see text.*

Material	Remarks	ρ_g kg m^{-3} × 10^3	c_g J kg^{-1} K^{-1} × 10^3	C J m^{-3} K^{-1} × 10^6	λ W m^{-1} K^{-1}	κ m^2 s^{-1} × 10^{-6}
Sandy soil (40% pore space)	Dry	1.60	0.80	1.28	0.30	0.24
	Saturated	2.00	1.48	2.96	2.20	0.74
Clay soil (40% pore space)	Dry	1.60	0.89	1.42	0.25	0.18
	Saturated	2.00	1.55	3.10	1.58	0.51
Peat soil (80% pore space)	Dry	0.30	1.92	0.58	0.06	0.10
	Saturated	1.10	3.65	4.02	0.50	0.12
Snow	Fresh	0.10	2.09	0.21	0.08	0.10
	Old	0.48	2.09	0.84	0.42	0.40

which can be solved for T_0 provided the radiative and turbulent fluxes at the surface are known along with C_{eff}. Many AGCMs and NWPMs contain rather arbitrary and empirical selections of C_{eff} (see, for example, Carson 1982).

The effective depth can be defined more formally by considering the soil heat conservation equation. If $G \rightarrow 0$ as $z_g \rightarrow \infty$ then equation (2) can be integrated to give

$$G_0 = C\int_0^\infty \frac{\partial T_g}{\partial t}\, \mathrm{d}z_g . \qquad \ldots \ldots \ldots \ldots \ldots \ldots \text{(7)}$$

Substituting equation (7) into equation (5) allows D to be defined in a strictly mathematical sense as

$$D = \left(\int_0^\infty \frac{\partial T_g}{\partial t}\, \mathrm{d}z_g\right) \Big/ \frac{\partial T_0}{\partial t} . \qquad \ldots \ldots \ldots \ldots \ldots \text{(8)}$$

2.2 *An analytical approach*

The problem of determining D can be overcome by appealing to the theory of heat transfer in a semi-infinite homogeneous medium when the surface is heated in a simple periodic manner (as discussed, for example, by Sellers 1965).

Assume that the surface temperature is given by

$$T_0 = T_g(0, t) = \hat{T}_g + a_0 \sin \omega t \qquad \ldots \ldots \ldots \ldots \text{(9)}$$

where ω is the angular frequency of oscillation, $\hat{T}_g$ is the mean soil temperature (over the period $P = 2\pi/\omega$) which is assumed to be the same at all depths, and a_0 is the amplitude of the surface wave. It can then be shown that the solution of equation (4) is

$$T_g(z_g, t) = \hat{T}_g + a_0 \exp(-z_g/\delta)\sin(\omega t - z_g/\delta) \qquad \ldots \ldots \ldots \text{(10)}$$

where $\delta = (\kappa P/\pi)^{1/2}$ is the e-folding depth of the temperature wave of period P, i.e. it is the depth where the amplitude of the oscillation is reduced to $1/e \approx 0.37$ times its surface value.

The effective depth, D, corresponding to this soil temperature profile can be found by using equations (9) and (10) in equation (8) to give

$$D = \frac{\delta}{\surd 2} \frac{\sin(\omega t + \pi/4)}{\cos \omega t} . \qquad \ldots \ldots \ldots \ldots \ldots (11)$$

Clearly D is not only a function of the thermal diffusivity of the soil and the period of the temperature forcing at the surface but also varies with time. Substituting for D from equation (11) into equation (5) gives a prognostic equation for T_0 which may be written as

$$\frac{\partial T_0}{\partial t} = \frac{2G_0}{C\delta} - \frac{2\pi}{P}(T_0 - \hat{T}_g) . \qquad \ldots \ldots \ldots \ldots \ldots (12)$$

This expression was first proposed, by a different argument, by Bhumralkar (1975) and has come to be referred to as the 'force-restore method', a term introduced by Deardorff (1978).

The period of the diurnal temperature oscillation is normally used in equation (12) as that appropriate for determining the thermal capacity of the effective surface layer. It is also necessary to specify $\hat{T}_g$. For short periods of a few days $\hat{T}_g$ may be fixed or diagnosed, but for longer periods of integration (e.g. in climate modelling) it needs to be determined prognostically. Deardorff (1978) has suggested a second prognostic equation for $\hat{T}_g$ analogous to equation (12) but with the appropriate effective depth determined by the e-folding depth of the annual temperature wave. However, extensions of this analytically based method (e.g. Deardorff 1978 and Carson 1982) soon become analogous to the more elaborate parametrization schemes which explicitly model the temperature profile through several soil layers.

2.3 *Multi-layer soil models*

The somewhat idealized analytical assumptions underlying the force-restore method and other simpler parametrization schemes can be avoided in principle by explicit modelling of the soil temperature profile and soil heat conduction with a multi-layer soil model of specified depth and with appropriate vertical resolution and boundary conditions. One approach would be to invoke equation (3) to evaluate G_0 explicitly from the modelled soil temperature profile such that

$$G_0 = \left(-\lambda \frac{\partial T_g}{\partial z_g}\right)_{z_g = 0} .$$

With this representaton of G_0, equation (1) could be solved diagnostically for T_0.

An alternative multi-layer approach is represented schematically in Fig. 1 for a three-layer soil temperature model. T_0 is represented by the mean temperature of a very thin surface layer of depth δ_0. Therefore, using simple finite differences, equation (2) becomes

$$\frac{\partial T_0}{\partial t} = \frac{G_0 - G_1}{C\delta_0} . \qquad \ldots \ldots \ldots \ldots \ldots \ldots (13)$$

Here G_0 is the net imbalance of the radiative and turbulent fluxes at the surface as given by equation (1) and G_1 is the soil heat flux into the next layer down, which is determined from the flux–gradient relationship by writing equation (3) in finite difference form

$$G_1 = \frac{\lambda(T_0 - T_{g1})}{\frac{1}{2}(\delta_0 + \delta_1)} . \qquad \ldots \ldots \ldots \ldots \ldots \ldots (14)$$

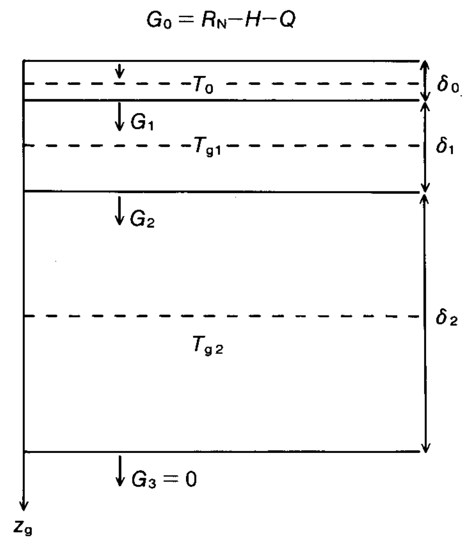

Figure 1. Schematic representation of a three-layer soil temperature finite difference model. For explanation of symbols see text.

Therefore equations (13) and (14) give

$$\frac{\partial T_0}{\partial t} = \frac{G_0}{C\delta_0} + \frac{2\kappa(T_{g1} + T_0)}{\delta_0(\delta_0 + \delta_1)} \qquad \ldots \ldots \ldots \ldots \ldots (15)$$

where $\kappa = \lambda / C$. The same general technique is used to provide the corresponding predictive equations for the temperatures of the other soil layers.

In the three-layer soil model illustrated in Fig. 1, all three soil temperatures are treated as prognostic variables during the integration of the model, with the condition that the soil heat flux is zero at the lower boundary ($G_3 = 0$). An alternative popular lower-boundary condition is to hold the temperature of the bottom layer at its initialized value. This approach is used, for example, in the four-layer model in the current Meteorological Office fine-mesh model (Carson 1986) and also in the three-layer soil model used at the European Centre for Medium Range Weather Forecasts (ECMWF) (Blondin 1986).

The selection of 'representative' soil thermal characteristics (C and λ, and hence κ) and suitable soil-layer depths ($\delta_0, \delta_1 \ldots \delta_{n-1}$ where n is the number of explicitly resolved layers in the soil) remains difficult, empirical and highly subjective. On the basis of a comprehensive study of the amplitude and phase responses of multi-layer soil schemes to periodic surface temperature forcing, Warrilow *et al.* (1986) have recommended a four-layer soil temperature scheme. Their paper gives full details of how the appropriate soil parameters were selected. The values which have been chosen for the fourth-annual cycle version of the Meteorological Office 11-layer AGCM are:

$$C = 2.34 \times 10^6 \text{ J m}^{-3} \text{ K}^{-1},\ \lambda = 0.56 \text{ W m}^{-1} \text{ K}^{-1},\ \kappa = \lambda / C = 2.39 \times 10^{-7} \text{ m}^2 \text{ s}^{-1},$$

$$\delta_0 = 0.037 \text{ m},\ \delta_1 = 0.143 \text{ m},\ \delta_2 = 0.516 \text{ m},\ \delta_3 = 1.639 \text{ m}$$

where $\delta_0 = (\kappa P / \pi)^{1/2}$ with $P = 0.2048$ days (4.8 hours).

Further information about values used in specific models can be found in, for example, Blondin (1986) and Carson (1982, 1986).

2.4 *The land-surface temperature*

It is usually assumed that the land-surface temperature is a well-defined and unique property of any natural land surface, and that the same T_0 is appropriate as:

(a) the radiative surface temperature used to compute the thermal emission from the earth's surface (see section 3.2 of Part I);

(b) the surface temperature as used in the extrapolated atmospheric boundary-layer profiles and surface-flux formulae (see section 4.2 of Part I);

(c) the surface soil temperature which is involved in the computation of the soil heat flux (see previous sections of this article).

The 'surface temperatures' implied by these different physical processes at the surface must be closely related but they are not necessarily the same. The ambiguity and difficulty in defining surface temperature become even greater when the surface has a vegetative canopy. Suffice it to state that at present the problem is very poorly understood and that many observational and theoretical studies are needed before any significant differences between the 'T_0' can be clearly delineated and incorporated sensibly in AGCMs and NWPMs.

3. Surface hydrology and the soil water budget

Most of the current generation of AGCMs and NWPMs now include some form of 'interactive' surface hydrology, usually of a very rudimentary nature. Such parametrizations are termed 'interactive' in the sense that the soil has some recognized hydrological property that is allowed to vary in response to the model's continuously evolving atmospheric state and surface boundary conditions and which in turn exerts both direct and indirect influences on the surface fluxes themselves. The most common practice is to define a variable 'soil moisture content' for some notional depth of surface soil layer which is constrained at all times to satisfy the surface moisture flux balance expressed as

$$M_0 = P_r - E - Y_0 \qquad \ldots \ldots \ldots \ldots \ldots \ldots (16)$$

where P_r is the intensity of surface rainfall, E is the surface evaporation rate (turbulent flux of water vapour), Y_0 denotes intensity of surface run-off and M_0 represents the net mass flux of water into the soil layer.

As in the case of the surface radiative fluxes, $R_S\downarrow$ and $R_L\downarrow$, in the context of the surface energy balance (discussed in section 3 of Part I), P_r is regarded here as an externally determined component of the surface moisture balance (equation (16)). Accurate evaluation of P_r is, of course, of crucial importance in establishing a realistic surface moisture balance and also, through the coupling discussed above, a realistic surface energy balance. The other processes involved in the hydrology of a bare soil, including evaporation, surface run-off, and transport and storage of water in the soil, are generally very complex and not so well understood nor as simple to parametrize sensibly as the individual terms in the surface energy balance. The very-small-scale spatial inhomogeneities within a typical soil layer appear to be more important in the determination of soil moisture movement than for the heat flow, and this presents formidable difficulties when trying to formulate a parametrization based soundly on underlying physical and dynamical hydrological principles. This is particularly so when one-dimensional hydrological models are applied to catchment-sized or typical AGCM/NWPM grid-box areas. Hence the importance of the HAPEX–MOBILHY project (André *et al.* 1986) aimed at studying the hydrological budget and evaporation flux at the scale of an AGCM grid square, i.e. $10^4\ km^2$. A 2½-month special observing period should provide detailed measurements of the relevant atmospheric fluxes and intensive remote sensing of surface properties. The main objective of the programme is to provide a data base against which parametrizations of the land-surface water budget can be developed and tested.

A proper discussion of the surface and subsurface hydrology of natural soils is beyond the scope of this paper. For this the reader is referred to the recent fuller expositions by, for example, Brutsaert (1982a, b), Dooge (1982), Eagleson (1982) and Dickinson (1984) in which the problems of areal representation of hydrological processes are specifically discussed. The remainder of this section is restricted to an introduction to the most simple form of the basic equations which govern the movement of water in the soil, and brief descriptions of some specific formulations for soil water transport, evaporation, and surface run-off. These examples, although chosen quite subjectively, should nevertheless give an indication of the general tenor and level of many of the current attempts to parametrize subgrid-scale hydrological processes.

3.1 *Water transport in a homogeneous soil*

There are various interrelated measures of soil moisture content, two of which are:

(a) the soil moisture concentration, χ, defined as the mass of water per unit volume of soil (units kg m^{-3}), and

(b) the volumetric soil moisture concentration, χ_v, defined as the volume of water per unit volume of soil (a dimensionless quantity).

Therefore $\chi = \rho_W \chi_v$ where ρ_W is the density of water. These are very appropriate measures in parametrizations based on simulating changes in the water mass of a specified layer of soil.

In an analogous fashion to the treatment of soil heat conduction discussed earlier, it is convenient to consider a grossly simplified hydrology of a spatially homogeneous soil layer with no horizontal water movement and no melting or freezing within it. This restricted and idealized one-dimensional problem is governed by the equation of continuity and the flux–gradient relation (Darcy's law). Combining these two equations yields Richards's equation for the vertical movement of water in an unsaturated soil. Solving the full Richards's equation for reasonable boundary conditions is by no means easy. However, proposals do exist which simplify the problem in a highly empirical way which is difficult to justify in all but the most idealized circumstances. In such cases Richards's equation takes the form of a diffusion equation for soil water

$$\frac{\partial \chi_v}{\partial t} = \frac{\partial}{\partial z_g}\left(\kappa_W \frac{\partial \chi_v}{\partial z_g}\right) - \frac{\partial K}{\partial z_g}$$

where K is the hydraulic conductivity of soil (units m s^{-1}) and κ_W is a moisture diffusivity of soil (units m^2 s^{-1}).

Prognostic equations for soil moisture content based on an idealized hydrology are beginning to appear in AGCMs and NWPMs (e.g. Dickinson 1984 and Warrilow *et al.* 1986). One particular multi-layer soil hydrology scheme which has attracted considerable support from numerical modellers is the force-restore treatment of Deardorff (1978) in which he postulates equations for soil moisture transport of a form directly analagous to the corresponding force-restore equations for soil temperature (see equation (12)). An effective three-layer version of Deardorff's approach is used, for example, in the ECMWF model (Blondin 1986). However, the most common current approach to modelling soil moisture content is probably still that based on a single surface-soil layer and a more detailed discussion of that example will suffice here.

3.2 *Single-layer soil hydrology models*

A common rudimentary approach to the parametrization of the hydrological processes at a bare-soil surface is to monitor the change of soil moisture content in a single shallow surface-soil layer of notional depth δ_W as depicted schematically in Fig. 2.

Let m_W denote the mass of liquid water per unit lateral area in the soil layer of depth δ_W, that is

$$m_W = \int_0^{\delta_W} \chi \mathrm{d}z_g = \hat{\chi}\delta_W = \rho_W \hat{\chi}_v \delta_W = \rho_W d_W \qquad \ldots\ \ldots\ \ldots\ (17)$$

where this equation also defines a layer-mean soil moisture concentration, $\hat{\chi}$, a layer-mean volumetric soil moisture concentration, $\hat{\chi}_v$, and a representative depth of water in the layer, d_W.

The continuity equation for χ is

$$\frac{\partial \chi}{\partial t} = -\frac{\partial M}{\partial z_g}$$

where M is the vertical mass flux of water. Integrating over the depth δ_W gives the water mass balance equation for the surface layer

$$\frac{\partial m_W}{\partial t} = M_0 - M_1$$

where M_0 is the net mass flux of water into the soil layer and M_1 is the vertical mass flux of water at the base of the surface layer. Substituting for M_0 from equation (16) yields

$$\frac{\partial m_W}{\partial t} = P_r - E - Y_0 - M_1 \qquad \ldots\ \ldots\ \ldots\ \ldots\ \ldots\ (18)$$

It should be noted that, in deriving equation (18), all horizontal fluxes of soil water have been neglected apart from the surface run-off, Y_0 .

With the terms E, Y_0 and M_1 evaluated according to a particular model's approach selected from the wide range of methods available, and P_r determined by some other parametrization in the model, equation (18) can be solved either in a simple explicit fashion or by more subtle implicit methods to determine the change in m_W (and hence $\hat{\chi}_v$, $\hat{\chi}$, d_W, etc.).

With P_r regarded in the present context as determined externally, then it remains here to illustrate, with the aid of specific examples, some of the problems of formulating parametrizations for E, Y_0 and M_1.

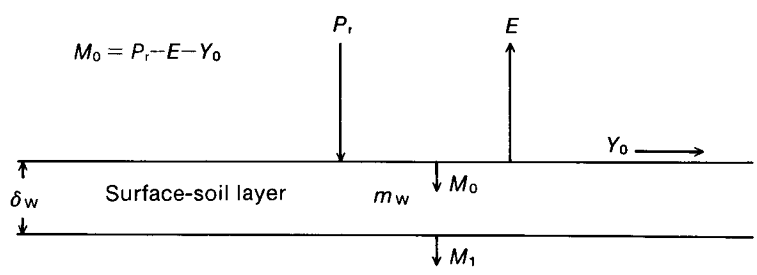

Figure 2. Schematic representation of moisture balance in a single shallow surface-soil layer. For explanation of symbols see text.

3.3 *Evaporation at a bare-soil surface, E*

In principle, E can be obtained as the residual flux from either the surface energy balance (equation (1)) or the surface moisture balance (equation (16)) and there are many empirical formulae for estimating E based on such approaches. A very useful introduction to the large variety of methods available can be found, for example, in Rosenberg *et al.* (1983); for more detailed discussions see, for example, Eagleson (1982) and Brutsaert (1982a, b). However, in this introduction to interactive soil temperature and soil moisture content parametrizations in AGCMs and NWPMs, I have selected the soil flux terms G_0 and M_0 as the residual components in the surface balance equations (1) and (16), and assumed implicitly that E can be evaluated in some independent manner.

Indeed, the method of estimating E has already been considered in Part I where E was ultimately parametrized in the bulk-aerodynamic form of

$$E = -\rho C_E V(z_l)\{q(z_l) - q_0\} \qquad \ldots \ldots \ldots \ldots (19)$$

with the recommendation that the bulk transfer coefficient, C_E, be evaluated from the Monin–Obukhov similarity theory (see section 4.2 of Part I). It was, however, also noted that the surface value of the specific humidity, q_0, required explicitly in equation (19) (and also, for example, in determining the bulk Richardson number and hence C_E) is not easy to determine. To overcome this problem it is standard practice to imply a value of q_0 through relations with $q_{sat}(T_0)$, the saturation specific humidity at the surface.

Two common methods are:

(a) to specify a surface relative humidity, r_0, such that $q_0 = r_0\, q_{sat}(T_0)$;

(b) to evaluate a potential evaporation rate $E_p = -\rho C_E V(z_l)\{q(z_l) - q_{sat}(T_0)\}$ and to specify an empirical 'moisture availability function', β, (usually ranging from 0 for an arid surface to 1 for a saturated surface) such that the actual evaporation rate is given by $E = \beta E_p$.

The second method is by far the more commonly adopted. For a discussion and comparison of the two approaches see, for example, Nappo (1975) and for examples of their use in specific AGCMs see Carson (1982). It is worth noting in passing that an alternative relation in the spirit of method (b) is used for computational convenience in some models and that is $\Delta q(z_l) = q(z_l) - q_0 = \beta\{q(z_l) - q_{sat}(T_0)\}$ which implies that $q_0 = \beta q_{sat}(T_0) + (1-\beta)q(z_l)$. The reasons for preferring this formulation are discussed in Carson (1982) (and more fully in Carson and Roberts 1977).

The most common method now employed is to express β as a simple linear function of the soil moisture content in the surface layer, $\hat{\chi}_v$, with $\beta = 1$ once $\hat{\chi}_v$ reaches a critical value, $\hat{\chi}_{v,c}$ (see Fig. 3(a)). However, Warrilow *et al.* (1986) have suggested an alternative formulation which involves the notion of a wilting point, $\hat{\chi}_{v,w}$ (see Fig. 3(b)). This represents a level of soil moisture concentration below which further water cannot be removed from the soil by the normal processes.

The critical value $\hat{\chi}_{v,c}$ is not well defined but for simplicity, and in line with previous practice (e.g. Carson 1982), it is given by

$$\hat{\chi}_{v,c} = \hat{\chi}_{v,w} + \tfrac{1}{3}(\hat{\chi}_{v,f} - \hat{\chi}_{v,w})$$

where $\hat{\chi}_{v,f}$ is a nominal field capacity used to define $\hat{\chi}_{v,c}$. The particular values of $\hat{\chi}_{v,w}$, $\hat{\chi}_{v,c}$ and $\hat{\chi}_{v,f}$ being used globally in the Meteorological Office AGCM, which assumes, for hydrological purposes only, a single surface layer of soil and nominal depth $\delta_W = 1$ m, are:

$$\hat{\chi}_{v,w} = 0.08, \qquad \hat{\chi}_{v,c} = 0.13, \qquad \hat{\chi}_{v,f} = 0.23.$$

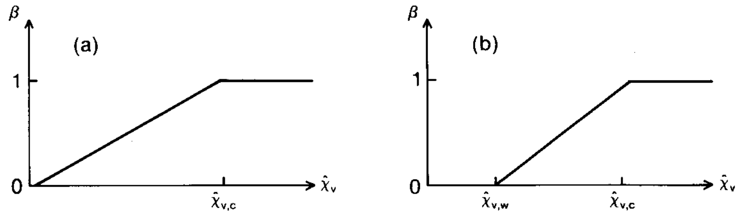

Figure 3. Variation of moisture availability function, β, with soil moisture content, $\hat{\chi}_v$, for (a) the most common scheme and (b) the scheme used in the Meteorological Office 11-layer model (see Warrilow *et al.* 1986). For explanation of other symbols see text.

Although β has been expressed in terms of $\hat{\chi}_v$, there is no reason why it should not be simply reformulated in terms of any of the other measures of soil moisture content, the most common of which is d_W.

It should be borne in mind that the more complex and real practical issue to be addressed is that of determining the actual evapotranspiration from partially vegetated surfaces and not simply the evaporation from a bare-soil surface.

3.4 *Surface run-off, Y_0*

Surface run-off is yet another of the complex surface hydrological processes which is treated very simplistically in current AGCMs and NWPMs. In models employing the single-layer water mass balance (equation (18)), the simplest approach is the so-called 'bucket method' for run-off in which rainfall (modified by evaporation loss) is allowed to increase the soil moisture content until $\hat{\chi}_{v,f}$ is reached. Any further attempt to increase $\hat{\chi}_v$ beyond the field capacity is implicitly assumed to be run-off water (a combination of Y_0 and M_1) which plays no further part in the model's hydrological cycle. This identifies the original role played in these simple hydrological parametrizations by the field-capacity term, in addition to its use to define $\hat{\chi}_{v,c}$. For a selection of the crude and highly empirical formulations used in specific AGCMs see Carson (1982).

A novel, but still relatively simple, parametrization has been developed by Warrilow *et al.* (1986) for use in the Meteorological Office AGCM. It is based, with considerable simplification, on a scheme proposed by Milly and Eagleson (1982). An attempt has been made to allow for the spatial variability of rainfall, since use of grid-box averages would give a marked underestimation of the surface run-off. It is assumed that rain only falls on a proportion, μ, of the grid area, where μ is chosen arbitrarily as 1 for the model's 'large-scale dynamic rain' and 0.3 for its 'convective rain'. The local rainfall rate, P_{rl}, throughout the grid-area is treated statistically by assuming that it has a probability density function given by

$$\mathrm{f}(P_{rl}) = \frac{\mu}{P_r} \exp\left(-\frac{\mu P_{rl}}{P_r}\right)$$

where P_r is the model's grid-point rainfall rate which is taken to represent the average grid-area rainfall. Whenever P_{rl} is greater than the surface infiltration rate, F, the local surface run-off is $Y_{0l} = P_{rl} - F$. Integration of Y_{0l} over all values of P_{rl} yields an expression for the total run-off rate for a grid area $Y_0 = P_r \exp(-\mu F / P_r)$ where Warrilow *et al.* (1986) have taken F to have a global value such that $F/\rho_W = 13.0\ \mathrm{mm\,h^{-1}}$.

3.5 *The vertical mass flux of water at the base of the surface layer, M_1*

The simplest single-layer approaches typically assume explicitly that in equation (18) M_1 is negligible, or implicitly that it is combined with Y_0 to give a total run-off. In the scheme of Warrilow *et al.* (1986), adapted from Milly and Eagleson (1982), M_l, referred to as the gravitational drainage from the base of the surface layer, is acknowledged as a separate hydrological component in equation (18) that has to be parametrized.

Warrilow *et al.* (1986) have argued, somewhat speculatively, that for horizontal averaging over a typical AGCM grid area M_l can be represented simply by $M_l = \rho_W\{K(\chi_v)\}_{Z_g = \delta_W}$ with the further assumption that χ_v is effectively spatially homogeneous in the surface-soil layer so that $M_l = \rho_W K(\hat{\chi}_v)$. Their particular prescription of the hydraulic conductivity as a function of $\hat{\chi}_v$, attributed to Eagleson (1978), is

$$K(\hat{\chi}_v) = K_{sat}\left(\frac{\hat{\chi}_v - \hat{\chi}_{v,w}}{\hat{\chi}_{v,sat} - \hat{\chi}_{v,w}}\right)^c$$

where $\hat{\chi}_{v,sat}$ is termed the saturation value of $\hat{\chi}_v$, K_{sat} is the saturation conductivity (i.e. $K(\hat{\chi}_{v,sat})$) and c is an empirically derived constant. The particular values adopted globally by Warrilow *et al.* (1986) are:

$$\hat{\chi}_{v,sat} = 0.445, \qquad K_{sat} = 13.0\ \mathrm{mm\ h^{-1}}, \qquad c = 6.6.$$

4. Snow-covered surfaces

A particular class of non-vegetated land surfaces which have their own very special characteristics and exercise significant influence on the climate system over a wide range of time-scales is that comprising snow-covered (and ice-covered) surfaces. As in the case of land-surface hydrology, it is generally true that little attention has yet been given to the representation in AGCMs and NWPMs of the special physical processes associated with such surfaces. However, I am confident that this particular area of the wider problem will receive increasing attention in the near future.

According to Kuhn (1982), in the course of the year about 50% of the earth's land surface is covered by snow or ice. He also comments that, although the polar ice sheets contain about 99% of the earth's freshwater ice by mass, nevertheless the seasonal snow cover with its large areal extent and its high spatial and temporal variability may have an equal or even greater impact on the atmospheric circulation. Undoubtedly then, a key issue will be how to deal sensibly with partial and rapidly changing snow cover, particularly in complex terrain, over the area of a typical grid box in a large-scale numerical model. The proper treatment of the processes associated with snow-covered surfaces is a major topic in its own right. The brief comments here are no more than a postscript to the main discussion of bare-soil surfaces. For fuller expositions of the varied and complex characteristics and the effects of snow and its associated physical processes see, for example, Martinelli (1979), Male (1980), Gray and Male (1981) and International Glaciological Society (1985). For discussions of snow-covered surfaces aimed specifically at the AGCM parametrization problem see, in particular, Kuhn (1982) and Kotliakov and Krenke (1982).

4.1 *Special conditions at snow- and ice-covered surfaces*

Kuhn (1982) has listed the special conditions for snow and ice layers as:

(a) the surface temperature cannot exceed the melting temperature of ice;
(b) evaporation and sublimation take place at the potential rate;
(c) the short-wave albedo is generally high;
(d) the medium is permeable to air and water and transparent to visible radiation;
(e) the snow pack is a good thermal insulator;
(f) the layer has a high storage capacity for heat and water;

(g) the roughness of the surface is extremely low;
(h) generally, the atmospheric surface layer over snow or ice is stably stratified.

Note that conditions (a)–(h) impinge on every aspect of the parametrization problem already discussed. The remainder of this section retraces the previous route and indicates briefly where modifications to the parametrizations are typically introduced into AGCMs and NWPMs in recognition of snow (or ice) covering the surface. In general, the thermal and hydrological properties of the snow pack are represented very simply and crudely in such models.

4.2 *The physical properties of snow- and ice-covered surfaces*

(a) *Short-wave albedo, α.* It is firmly established that the physical coupling between snow and ice cover, albedo, and the surface temperature is one of the most important feedback mechanisms to include in an AGCM. An important characteristic of snow- and ice-covered surfaces is their high reflectivity compared with other natural surfaces such that even a thin covering of fresh snow can alter significantly the albedo of a landscape. The local albedo of a snow-covered surface is very variable and is a complicated function of many factors including the age of the snow pack (α decreases markedly as the snow becomes compacted and soiled), the wavelength and angle of the incident radiation, and even diurnal cycles in the state of the snow surface, particularly when conditions are right for surface melting. The albedo may lie anywhere in the range from 0.95 for freshly fallen snow to about 0.35 for old, slushy snow (see, for example, Kondratyev *et al.* 1982).

At present the coupling between snow and ice and the surface albedo is generally prescribed very simply. Three types of snow- or ice-covered surfaces are generally acknowledged: surfaces with instantaneously variable depth of snow either predicted or implied, permanent or seasonally prescribed snow- and ice-covered land surfaces, and permanent or seasonally prescribed areas of sea-ice. The last category is not the concern of this paper. For models that 'carry' a snow depth a common approach is that of Holloway and Manabe (1971) who, following Kung *et al.* (1964), used:

$$\alpha = \begin{cases} \alpha_L + (\alpha_S - \alpha_L)\, d_{SW}^{1/2} & d_{SW} < 1 \text{ cm} \\ \alpha_S & d_{SW} \geq 1 \text{ cm} \end{cases}$$

where α_L is the snow-free land-surface albedo, α_S is the albedo (assumed in this case to be 0.60) of a deep-snow surface and d_{SW} is the water equivalent depth of snow (here expressed in centimetres). No allowance is usually made for the varying density of a snow pack, and d_{SW} is assumed typically to be about 1/10 of the actual snow depth.

In some models which predict and monitor snowfall, a single albedo value is used for any non-zero depth of snow (see Carson 1982, 1986). The first snowfall on a previously snow-free surface results in an immediate increase in surface albedo which will tend, at least initially, to accelerate the positive feedback of a further lowering of the surface temperature with an enhanced probability of further snow accumulation. Typical model values for land- and sea-ice are in the range 0.5–0.8 (see Carson 1982, 1986).

(b) *Long-wave emissivity, ϵ.* Kuhn (1982) states that this can be assumed to be unity for all practical purposes.

(c) *Surface roughness length, z_0.* The effective z_0 for extensive, uniformly covered snow and ice fields and the 'local' value of z_0 for snow-covered, simple heterogeneous terrain may indeed be very small (of the order of 10^{-3} m or less). However, in general, the effective areal z_0 of natural, heterogeneous and complex terrain with varied relief and vegetation is very difficult to determine and may be affected greatly or insignificantly by different degrees of snow cover. There is little scope for useful discussion of this problem in a global, large-scale modelling context except to note that, in principle, snow and ice cover can alter z_0.

(d) *Thermal properties of snow.* As noted above, a snow pack is generally a good thermal insulator for the soil below, but to capture this effect in a climate model implies a delineation and explicit modelling of the heat conduction (and the hydrology) in and between the two media. In general, the thermal and hydrological properties of snow and ice layers are treated very simply, if at all, in AGCMs and NWPMs. The thermal properties of a snow pack will, like its density and albedo, depend in a complicated fashion on many factors. Values thought to be appropriate for snow are given in Table I for comparison with the range of soil values also included there.

4.3 *Surface energy and mass flux balances at a snow-covered surface*

The surface energy flux balance (equation (1)) is modified for complete snow cover such that

$$G_0 = R_N - H - Q_s - Q_f \qquad \ldots\ldots\ldots\ldots\ldots (20)$$

where $Q_f = L_f S$ represents the latent-heat flux required to affect phase changes associated with melting or freezing at the surface (where S is the rate of snow melt or ice melt and L_f is the latent heat of fusion), $Q_s = L_s E_s$ represents the latent-heat flux due to surface sublimation by turbulent transfer (where E_s is the latent heat of sublimation ($L_s = L_e + L_f$)), and G_0 is now strictly the flux of heat into the snow layer at its upper surface.

A simple budget equation, corresponding to that used for soil moisture content in a single-soil layer (equation (18)), is also used for snow on the 'surface', viz.

$$\frac{\partial m_S}{\partial t} = P_S - E_s - S \qquad \ldots\ldots\ldots\ldots\ldots (21)$$

where P_S is the intensity of snowfall at the surface and m_S is the mass of snow lying per unit area of the surface. Therefore m_S is treated like m_W as a surface prognostic variable and is often represented as a snow depth, d_S, or more commonly as an equivalent depth of water, d_{SW}, such that $m_S = \rho_S d_S = \rho_W d_{SW}$ where ρ_S is the density of snow. Although it is recognized that the density of a snow pack varies, this again is a complicated issue in its own right and it is quite common practice in large-scale numerical models to assume simply that $\rho_S \simeq 0.1\ \rho_W$.

Equation (21) is usually complemented by the surface-layer balance equation for the soil moisture content (equation (18)) modified to include the snow-melt term, i.e.

$$\frac{\partial m_W}{\partial t} = P_r - E + S - Y_0 - M_1 . \qquad \ldots\ldots\ldots\ldots (22)$$

Each model has its own system of checks and algorithms for deciding which of the terms in equations (21) and (22) are in force simultaneously. One popular approach is as follows. When snow is lying, T_0 is not allowed to rise above 273 K and the snow depth accumulates without limit or decreases according to the net value of $(P_S - E_s)$. If, however, snow is lying and the solution of the heat balance equation, equation (20), excluding the term Q_f, produces an interim surface temperature value $T_0' > 273$ K then sufficient snow (if available) is allowed to melt to maintain $T_0 = 273$ K. The heat required to melt the snow and reduce T_0 to 273 K can be evaluated by specifying an effective surface thermal capacity of the snow pack (cf. equation (5)) such that

$$Q_f = L_f S = C_{\mathrm{eff,\,s}} \left(\frac{T_0' - 273}{\Delta t} \right) \qquad \ldots\ldots\ldots\ldots (23)$$

where Δt is the appropriate model time step. The change in the water equivalent snow depth, Δd_{SW}, resulting from the melting is determined from equations (22) and (23) such that

$$\Delta m_S = \rho_W \Delta d_{SW} = -S\,\Delta t$$

$$= -\frac{C_{\mathrm{eff,\,S}}}{L_f}(T_0' - 273).$$

It is usually assumed that the snow pack has no moisture-holding capacity; all melted snow is added directly to the soil moisture content (through equation (22)) following the corresponding reduction, Δd_{SW}, in the snow depth. In all cases it is only when the snow disappears through melting or sublimation that evaporation of moisture is allowed to resume at the surface.

5. Concluding remarks

It should be evident that, in many respects, the representations of land-surface processes in AGCMs and NWPMs are still rather crude and simple. The demands for improvements will come from both climate modelling studies and numerical weather forecasting. Indeed, the steadily increasing number of studies with AGCMs has already amply demonstrated the sensitivity of such models to surface properties and processes (see, for example, recent reviews by Mintz (1984), Rowntree (1983, 1984) and Rowntree *et al.* (1985)). Parametrizations thought adequate at present will undoubtedly be seen to be deficient in models which couple interactively further components of the climate system. This is already apparent with respect to sea–air interactions in coupled ocean–atmosphere models. Although the major developments in the longer term are more likely to come from climate modelling studies, nevertheless valuable feedback is being obtained from the continuous close scrutiny of the various models' performances in the acutely critical arena of operational weather forecasting — especially of local, near-surface variables such as wind and temperature.

A schematic résumé of the processes, variables and parameters introduced in this discussion of the specification of parametrizations for simple, non-vegetated land surfaces is given in Table II.

Table II. *Schematic résumé of the processes, variables and parameters involved in the specification of parametrizations at simple, non-vegetated land surfaces. For explanation of symbols see text.*

	Radiative	Thermal	Hydrological	Dynamical
'External forcing'	$R_{S\downarrow}$, $R_{L\downarrow}$		P_r, P_S	
Atmospheric variables		$\theta(T)$	q	$\underline{V}$
Surface variables	T_0	T_0	q_0, d_S	
Surface parameters	α, ϵ	z_0	z_0, β	z_0
Surface fluxes	R_N	H $Q = L_eE$ $Q_f = L_fS$ $Q_s = L_sE_s$ G_0	 E, E_S S M_0, Y_0	$\underline{\tau}$
Subsurface fluxes		G	M	
Subsurface parameters		λ, C	δ K Significant values of χ_v	
Subsurface variables		T_g	χ_v	

Acknowledgement

I am grateful to Dr R.W. Riddaway (Editor) for his considerable help in moulding the original lecture notes into an abridged form suitable for publication in the *Meteorological Magazine*.

References

André, J-C., Goutorbe, J-P. and Perrier, A. 1986 HAPEX–MOBILHY: A hydrologic atmospheric experiment for the study of water budget and evaporation flux at the climatic scale. *Bull Am Meteorol Soc*, **67**, 138–144.

Bhumralkar, C.M. 1975 Numerical experiments on the computation of ground surface temperature in an atmospheric general circulation model. *J Appl Meteorol*, **14**, 1246–1258.

Blondin, C.A. 1986 Treatment of land-surface properties in the ECMWF model. *In* Proceedings of the ISLSCP conference on parametrization of land-surface characteristics, use of satellite data in climate studies, and first results of ISLSCP, Rome, 2–6 December, 1985. Paris, ESA No. SP-248.

Brutsaert, W.H. 1982a Vertical flux of moisture and heat at a bare soil surface. *In* Eagleson, P.S. (ed); Land surface processes in atmospheric general circulation models. Cambridge University Press.

1982b Evaporation into the atmosphere. Theory, history and applications. Dordrecht, Reidel.

Carson, D.J. 1982 Current parametrizations of land-surface processes in atmospheric general circulation models. *In* Eagleson, P.S. (ed); Land surface processes in atmospheric general circulation models. Cambridge University Press.

1986 Parametrizations of land-surface processes in Meteorological Office numerical weather prediction and climate models. (Unpublished, copy available in the National Meteorological Library, Bracknell.)

1987 An introduction to the parametrization of land-surface processes. Part I. Radiation and turbulence. *Meteorol Mag*, **116**, 229–242.

Carson, D.J. and Roberts, S. 1977 Concerning the evaluation of the turbulent fluxes at unsaturated surfaces. (Unpublished, copy available in the National Meteorological Library, Bracknell.)

Deardorff, J.W. 1978 Efficient prediction of ground surface temperature and moisture, with inclusion of a layer of vegetation. *J Geophys Res*, **83**, 1889–1903.

Dickinson, R.E. 1984 Modeling evapotranspiration for three-dimensional global climate models, climate processes and climate sensitivity. *Geophys Monogr*, **29**, Maurice Ewing Vol. 5, 58–72.

Dooge, J.C.I. 1982 Parametrization of hydrologic processes. *In* Eagleson, P.S. (ed); Land surface processes in atmospheric general circulation models. Cambridge University Press.

Eagleson, P.S. 1978 Climate, soil and vegetation: 1. Introduction to water balance dynamics. *Water Resour Res*, **14**, 705–776.

1982 Dynamic hydro-thermal balances at macroscale. *In* Eagleson, P.S.(ed); Land surface processes in atmospheric general circulation models. Cambridge University Press

Geiger, R. 1966 The climate near the ground, Cambridge, Mass., Harvard University Press.

Gray, D.M. and Male, D.H. 1981 Handbook of snow. Principles, processes, management & use. Toronto, Pergamon.

Holloway, J.L. jun. and Manabe, S. 1971 Simulation of climate by a global general circulation model. I. Hydrological cycle and heat balance. *Mon Weather Rev*, **99**, 335–370

International Glaciological Society 1985 Proceedings of the symposium on snow and ice processes at the earth's surface, Sapporo, Japan, 2–7 September, 1984. Annals of glaciology, **6**. Cambridge, International Glaciological Society.

Kondratyev, K.Ya., Korzov, V.I., Mukhenberg, V.V. and Dyachenko, L.N. 1982 The shortwave albedo and the surface emissivity. *In* Eagleson, P.S. (ed); Land surface processes in atmospheric general circulation models. Cambridge University Press.

Kotliakov, V.M. and Krenke, A.N. 1982 Data on snow cover and glaciers for the global climatic models. *In* Eagleson, P.S. (ed); Land surface processes in atmospheric general circulation models. Cambridge University Press.

Kuhn, M. 1982 Vertical flux of heat and moisture in snow and ice. *In* Eagleson, P.S. (ed); Land surface processes in atmospheric general circualtion models. Cambridge University Press.

Kung, E.C., Bryson, R.A. and Lenschow, D.H. 1964 Study of a continental surface albedo on the basis of flight measurements and structure of the earth's surface cover over North America. *Mon Weather Rev*, **92**, 543–564.

Male, D.H. 1980 The seasonal snowcover. *In* Colbeck, S.C. (ed); Dynamics of snow and ice masses. New York, Academic Press.

Martinelli, M. jun. 1979 Research on snow and ice. Snow. *Rev Geophys and Space Phys*, **17**, 1253–1256, 1266–1271.

Milly, P.C.D. and Eagleson, P.S. 1982 Parametrization of moisture and heat fluxes across the land surface for use in atmospheric general circulation models. MIT Report No. 279, Cambridge, Mass.

Mintz, Y. 1984 The sensitivity of numerically simulated climates to land-surface boundary conditions. *In* Houghton, J.T. (ed); The global climate. Cambridge University Press.

Nappo, C.J. jun. 1975 Parametrization of surface moisture and evaporation rate in a planetary boundary layer model. *J Appl Meteorol*, **14**, 289–296.

Oke, T.R. 1978 Boundary layer climates. London, Methuen.

Rosenberg, N.J., Blad, B.L. and Verma, S.B. 1983 Microclimate. The biological environment. Second edition. New York, Wiley.

Rowntree, P.R. 1983 Land surface processes in climate models — parameterization and model sensitivity. Report of the fourth session of the Joint Scientific Council, Venice, 1–8 March. 1983, Appendix B, 57-75, World Climate Research Programme, International Council of Scientific Unions / World Meteorological Organization.

1984 Review of general circulation models as a basis for predicting the effects of vegetation change on climate. (Unpublished, copy available in the National Meteorological Library, Bracknell.)

Rowntree, P.R., Wilson, M.F. and Sangster, A.B. 1985 Impact of land surface variations on African rainfall in general circulation models. (Unpublished, copy available in the National Meteorological Library, Bracknell.)

Sellers, W.D. 1965 Physical climatology, Chicago, University of Chicago Press.

Warrilow, D.A., Sangster, A.B. and Slingo, A. 1986 Modelling of land surface processes and their influence on European climate. (Unpublished, copy available in the National Meteorological Library, Bracknell.)

551.501.75:551.501.795:551.507.362.2

Wind measurements from the Earth Resources Satellite (ERS-1)

D. Offiler

Meteorological Office, Bracknell

Summary

Within 3 years, a new form of satellite data will become accessible to operational meteorology; near-surface wind vectors. ERS-1 will have a complement of microwave instruments which will provide all-weather coverage of the world's oceans. The Meteorological Office has been involved in the design of this experiment and is currently assisting the European Space Agency with the development of data-processing algorithms. After launch the data will be available, within a few hours of measurement, to be incorporated into numerical models.

1. Introduction

The European Space Agency (ESA) is planning to launch its first remote sensing satellite, the Earth Resources Satellite (ERS-1), early in 1990. Its main complement of instruments are various types of radar, operating at microwave frequencies (5–15 GHz), plus a passive infra-red instrument, the Along

Track Scanning Radiometer (ATSR), which is being built by the Rutherford Appleton Laboratory with Meteorological Office assistance. Table I summarizes the instruments to be carried, their main purpose and expected accuracies. Primarily, the satellite's mission is to sense several oceanographic parameters, both for experimental purposes and as a demonstration that such instruments could have a role to play in operational meteorology and oceanography on the global scale.

Of these instruments, the one most applicable to meteorology is the Advanced Microwave Instrument (AMI) package in its wind mode of operation. This is designed to sense the near-surface (equivalent 10 m) wind vector over the oceans. This article will describe the principles of operation of this type of sensor, and the processing necessary to interpret its raw measurements into familiar geophysical units. Any form of instrument needs calibrating, and the AMI is no exception, so the plans to achieve this will also be outlined. Finally, the use to be made of the resulting data within the Meteorological Office will be mentioned.

Table I. *ERS-1 main geophysical measurement objectives*

Main geophysical parameter	Range	Accuracy	Main instrument
Wind field			
Velocity	4–24 m s^{-1}	± 2 m s^{-1} or 10% whichever is greater	AMI wind scatterometer and altimeter
Direction	0–360°	± 20°	AMI wind scatterometer
Wave field			
Significant wave height	1–20 m	± 0.5 m or 10% whichever is greater	Altimeter
Wave direction	0–360°	± 15°	AMI wave mode
Wavelength	50–1000 m	20%	AMI wave mode
Earth surface imaging			
Land/ice/coastal zones, etc.	80 km (minimum swath width)	Geometric/radiometric resolutions 30 m/2.5 dB	AMI Synthetic Aperture Radar (AMI-SAR)
Altitude over ocean	745–825 km	2 m absolute ± 10 cm relative	Altimeter
Satellite range		± 10 cm	Precise Range and Range-Rate Experiment (PRARE)
Sea surface temperature	500 km swath	± 0.5 K	Along Track Scanning Radiometer (Infra-Red) (ATSR/IR)
Water vapour	25 km spot	10%	Microwave sounder (part of ATSR experiment) (ATSR/M)

2. Theoretical and experimental background

As soon as microwave radar became widely used in the 1940s, it was found that at low elevation angles surrounding terrain (or at sea, waves) caused large, unwanted echoes. Ever since, designers and users of radar equipment have sought to reduce this noise (Harrold 1974). Researchers investigating the effect found that the back-scattered echo became larger with increasing wind speed, so opening the possibility of remotely measuring the wind (Krishen 1971, Jones and Schroeder 1978). Radars designed to measure this type of echo are known as 'scatterometers'.

The back-scattering is due principally to in-phase reflections from a rough surface; at microwave frequencies this arises from the small ripples (cat's paws) generated by the instantaneous surface wind stress. The level of back-scatter from an extended target, such as the sea surface, is generally termed the Normalized Radar Cross-Section (NRCS), or σ°. For a given geometry and transmitted power, σ° is proportional to the power received back at the radar. Experimental evidence from scatterometers operating over the ocean shows that σ° increases with surface wind speed (as measured by ships or buoys), decreases with incidence angle, and is also dependent on the radar beam angle relative to wind direction. Fig. 1 is a plot of σ° aircraft data against wind direction for various wind speeds. Direction 0° corresponds to looking upwind, 90° to crosswind and 180° to downwind.

Over the past three winters, ESA has co-ordinated a number of experiments to confirm these types of curves at 5.3 GHz, the AMI operating frequency. Several aircraft scatterometers have been flown close to instrumented ships and buoys, in the North Sea, the Atlantic and the Mediterranean. The σ° data are then correlated with the surface winds, which have been adjusted to a common anemometer height of 10 m (assuming neutral stability). An empirical model function has been fitted to these data (Long 1986) of the form

$$\sigma^\circ = a_0 U^{\gamma} (1 + a_1 \cos\phi + a_2 \cos 2\phi) \quad \ldots \ldots \ldots \ldots \ldots \quad (1)$$

where the coefficients a_0, a_1, a_2 and γ are dependent on the incidence angle. This model relates the neutral stability wind speed at 10 m, U, and the wind direction relative to the radar, ϕ, to the NRCS.

It may also be the case that σ° is a function of sea surface temperature, sea state and surface slicks (natural or man-made), but these parameters have yet to be demonstrated as having any significant effect on the accuracy of wind vector retrieval.

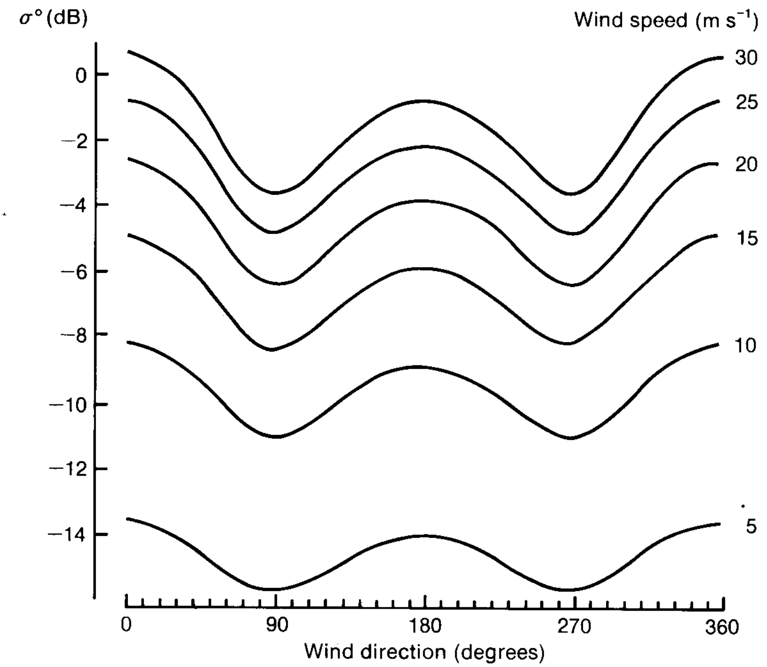

Figure 1. Measured aircraft back-scatter, σ°, against relative wind direction for different wind speeds. Data for 13 GHz, vertical polarization.

3. The AMI wind scatterometer

Since σ° shows a clear relationship with wind speed and direction, in principle, measuring σ° at two or more different azimuth angles allows both wind speed and direction to be retrieved. The first wind scatterometer to be flown on a satellite — SEASAT — was in 1978 and ably demonstrated the accuracy of this new form of measurement (Offiler 1984). The SEASAT-A Satellite Scatterometer (SASS) instrument used two beams either side of the spacecraft; the ERS-1 AMI scatterometer uses a third, central beam to improve wind direction discrimination, but is only a single-sided instrument, so its coverage is less. Fig. 2 shows the geometry of the ERS-1 scatterometer.

The three antennae each produce a narrow beam of radar energy in the horizontal, but wide in the vertical, resulting in a narrow band of illumination of the sea surface across the 500 km width of the swath. As the satellite travels forward, the mid beam, then the aft beam will measure from the same part of the ocean as the forward beam. Hence each part of the swath, divided into 50 km squares, will have three σ° measurements taken at different relative directions to the local surface-wind vector.

Fig. 3 shows the coverage to be expected of the scatterometer for the North Atlantic over 24 hours. These swaths are not static, but 'move' westwards to fill in the large gaps on subsequent days. Even so, the coverage will not be complete, owing to the relatively small swath width in relation to, say, the Advanced Very High Resolution Radiometer (AVHRR) imager on the NOAA satellites. However, there will potentially be a wind available every 50 km within the coverage area, globally, and ESA is committed to delivering this to operational users within three hours of measurement time. The raw instrument data are to be recorded on board and replayed to ESA ground stations each orbit, the principal station being at Kiruna in northern Sweden where the wind vectors will be derived.

4. Wind vector retrieval

As already mentioned, the AMI scatterometer principally measures the level of back-scatter at a given location at different azimuth angles. Since we know the geometry, such as range and incidence angles, it ought to be possible to use the model function (equation (1)) to extract the two pieces of information required — wind speed and direction — using appropriate simultaneous equations. However, in practice this is not feasible; the three values of σ° will have a finite-measurement error, and the function itself is highly non-linear. Indeed the model, initially based on aircraft data, may not be applicable to all circumstances.

The wind speed and direction must be extracted numerically, usually by comparing the measured values of σ° to those from the model function, using an initial estimate of wind speed and direction, then refining the estimate so as to minimize the σ° differences. Starting at different first-guess wind directions, the numerical 'solution' can converge on up to four distinct, or ambiguous, wind vectors, although often there are only two obviously different ones — usually about 180° apart. One of these is the 'correct' solution, in that it is the closest to the true wind direction and within the required root-mean-square accuracies of 2 m s^{-1} and 20°.

Selecting which of the ambiguous set of solutions is the correct one, when the true wind is unknown (as is the case for an operational system), is termed ambiguity removal. This is merely assigning a probability of correctness to each solution and choosing the one with the highest probability. This may sound easy, but to do this with a consistent high skill (ideally one would want to choose correctly on 100% of cases) is a difficult task. A first stage is to see which extracted vector best fitted the model function, ranking them in order of probability, and choosing the first rank. Simulations (Offiler 1985) have indicated that this technique might be expected to have a skill rating of not more than 70%. (Compare this with SASS which, with only two beams, could only manage a random 25% skill.)

Further processing may be done by objectively seeking areas of the swath where the first rank shows some consistency in direction, and selecting a different rank for nearby cells which do not at first agree with this general trend. This may yield a skill score of 90% or so in most cases, but areas which have been consistently ranked wrongly to start with will only be reinforced, so drastically reducing the skill in picking the right solution.

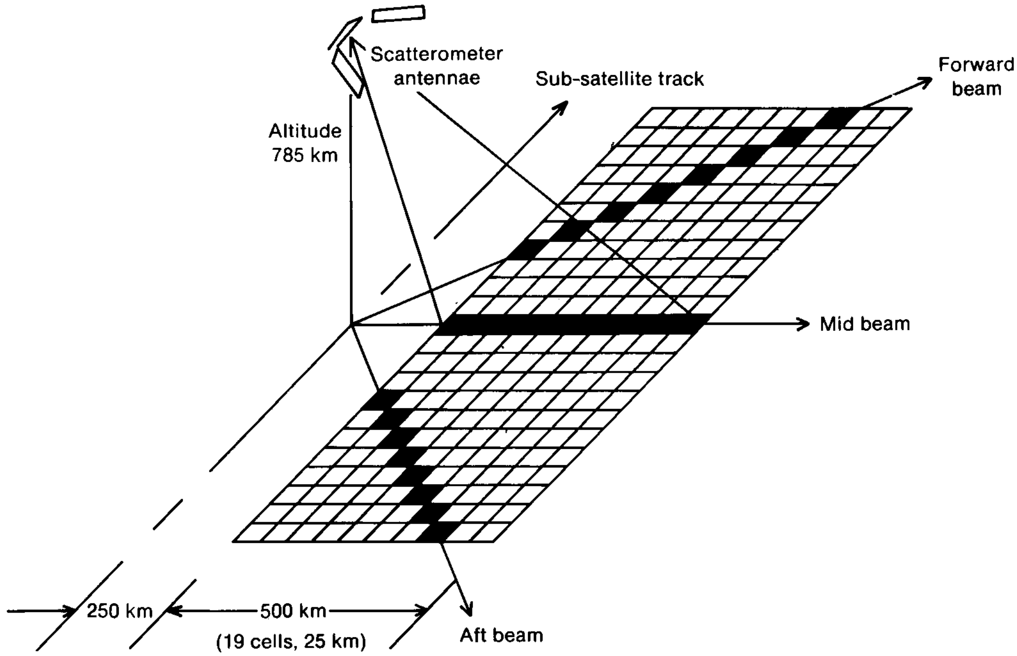

Figure 2. ERS-1 wind scatterometer geometry. For clarity the 500 km wide swath is shown as 10 non-overlapping cells. In reality there are 19 cells across the swath, on a 25 km grid, each one being 50 km × 50 km in size.

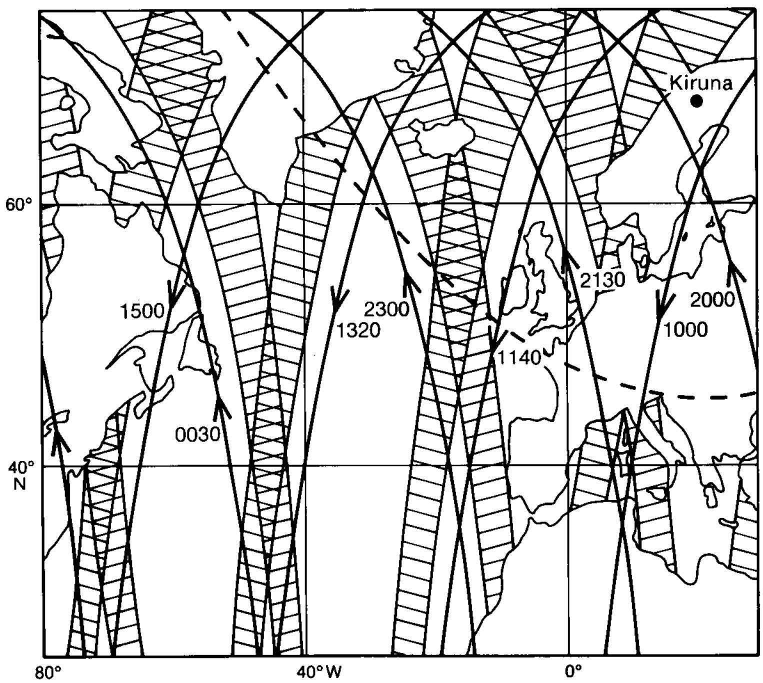

Figure 3. ERS-1 sub-satellite tracks (arrowed lines, with approximate times) and wind scatterometer coverage (hatched areas) of the North Atlantic region over 1 day. The large gaps are partially filled on subsequent days; nominally this occurs on a 3-day cycle. The dashed line shows the limit of reception for the Kiruna ground station.

Ideally, we would like some indication of the 'true' direction, such as from ships or buoys, or, even better, because of greater spatial coverage, the wind analysis from a numerical model. Unfortunately, while these may be available after a few hours, at the time the satellite winds are required these independent data will not be ready. The best that we could have is a forecast field of say 6 or 12 hours ahead for the verification time of the satellite data. Winds from a forecast grid can be interpolated to each scatterometer data point and the solution with the nearest direction chosen. While this can result in high skill scores (over 95%), there is a major drawback; if a forecast is wrong in the positioning of a circulatory feature by 100–200 km (a common occurrence), then there is an area of winds between the forecast centre and true centre which is 180° in error. Here, we will select exactly the wrong scatterometer solution. Worse, if fed back into the next analysis, these winds could reinforce the incorrect forecast which is also being used as the assimilation background. Whilst there are probably enough conventional surface data to prevent this in the North Atlantic region, there could be a problem in the southern oceans and the Pacific where other data are sparse.

5. Current involvement and future use of ERS-1 data

The problems of extracting accurate wind data within the time constraints of an operational system, and the problems of ambiguity removal are the continuing subject of study within the Satellite Meteorology Branch of the Meteorological Office, on behalf of ESA. As part of the ERS-1 project, the United Kingdom is setting up a dedicated off-line ERS-1 data centre, to be constructed at the Royal Aircraft Establishment, Farnborough. This will act as an archive and product-generation facility both for ESA and for the direct needs of the United Kingdom. Here too, the Meteorological Office is involved in developing the algorithms to produce the best possible satellite winds for users not requiring them in real time.

In order to utilize fully the data from ERS-1, ESA has issued an Announcement of Opportunity (AO) for scientists to use the data in operational meteorology, oceanography and for fundamental research. The Meteorological Office has responded positively to this AO, and expects to be a lead agency in assisting ESA to calibrate initially the wind and wave data after launch, and then validate and assimilate the information into its atmospheric and wave forecast models.

The calibration period is expected to be the first 3 months after launch, and will check the correct operation of the hardware and the wind retrieval algorithms. After this period, the model function (the coefficients in equation (1)) may need to be updated. Thereafter, validation — the process of keeping an objective eye on the quality of the satellite-derived data — will be continuous, using a three-way comparison of conventional ship and buoy data, the model analyses (which can be used in data-sparse areas) and the ERS-1 winds and waves. Simulated assimilation using SEASAT winds, currently being undertaken in the Dynamical Climatology Branch of the Meteorological Office, suggests that such satellite data could have most impact when fully utilized as a global data set.

6. Conclusion

The wind and wave data from ERS-1 will not be unique; by the mid 1990s there are expected to be two or three other satellites, operated by the USA, Canada and Japan which could have similar instruments. Indeed, the decision is to be taken soon on whether a follow-on satellite, ERS-2, can be funded within Europe. Further into the decade, the Polar Platform, part of the US Space Station project, is likely to carry similar microwave instruments as part of its fully operational payload. Although ERS-1 is strictly non-operational, ESA intends that it can demonstrate this capability during its 2- to 3-year life. The Meteorological Office, together with other agencies, has taken that challenge and intends to investigate the utility (or otherwise) of this new source of data, exploiting it fully in numerical models and for storm warning and ship routeing services.

References

Harrold, T.W. 1974 Ground clutter observed in the Dee weather radar project. *Meteorol Mag*, **103**, 140–141.

Jones, W.L. and Schroeder, L.C. 1978 Radar backscatter from the ocean: dependence on surface friction velocity. *Boundary Layer Meteorol*, **13**, 133–149.

Krishen, K. 1971 Correlation of radar backscattering cross sections with ocean wave height and wind velocity. *J Geophys Res*, **76**, 6528–6539.

Long, A.E. 1986 Towards a C-band radar sea echo model for the ERS-1 scatterometer. *In* Proceedings of the conference on spectral signatures of objects in remote sensing, Les Arcs, 16–20 December 1985. Paris, ESA No. SP-247.

Offiler, D. 1984 A comparison of SEASAT scatterometer-derived winds with JASIN surface winds. *Int J Remote Sensing*, **5**, 365–378.

1985 ERS-1 surface wind ambiguity removal by means of objective processing and subjective human intervention. Final report. ESA Contract No. 6154/85/NL/BI. London, Meteorological Office.

551.524.36:551.588(41-4)

The estimation of extreme minimum temperature in the United Kingdom

R.C. Tabony

Meteorological Office, Edinburgh

Summary

Current Meteorological Office procedures for the estimation of the lowest temperature to be expected once in 50 years are based on a map produced by Hopkins and Whyte (*Meteorol Mag*, **104**, 1975) in which topographic effects have been removed. More recently Tabony (*J Climatol*, 5, 1985) quantified some of the effects of topography on minimum temperature, and this paper develops a pragmatic scheme which enables some of his findings to be implemented.

1. Introduction

Hopkins and Whyte (1975) devised a procedure for estimating the maximum and minimum temperatures associated with given return periods by subjecting records from over 200 stations to extreme-value analysis. They produced sea-level maps of the maximum and minimum temperatures to be expected once in 50 years and to which altitudinal lapse rates of 10 °C km^{-1} (for maxima) and 5 °C km^{-1} (for minima) should be applied. The map values are clearly intended to apply to 'standard sites' to which topographical corrections should be freely applied; the authors quote an example of a frost hollow whose recorded extremes are 8 °C below the map value for minima. More recently Tabony (1985) attempted to quantify the effect of topography, and the aim of the present paper is to incorporate his results into an improved scheme for the estimation of minimum temperature. Although the 1985 investigation was limited to inland and rural locations and offered no new information on the effects of water or buildings, the implementation of the findings relating to the lie of the land is still very useful. Many of the requests for estimates of minimum temperature, including, for instance, those concerned with the erection of masts on hills, relate to locations where the effect of topography is dominant.

2. Departures from the Hopkins and Whyte values

The lowest temperature recorded in the United Kingdom, namely −27 °C at Braemar (for location of places in Scotland mentioned in text see Fig. 1), has been observed twice in the last 100 years or so and hence may be accorded a return period not very different from 1 in 50 years. The Hopkins and Whyte map is reproduced in Fig. 2 and it can be seen that the observed temperature is 5 °C below the map value, but as the station is not in the valley bottom it is quite likely that temperatures 8 °C below the map values could be observed in that area. In England the −25 °C reported from Shawbury is 7 °C below the map value and so, with the addition of the Hopkins and Whyte example, there is firm evidence that in the coldest frost hollows, temperatures 8 °C below the map values may be reached.

The lowest temperatures recorded on summits or high slopes, however, are well above the Hopkins and Whyte values, especially when the 5 °C km^{-1} altitude correction is applied. The examples from Scotland shown in Table I illustrate the point. The observed minima have been used to obtain the once in 50-year values by reference to the graph published by Hopkins and Whyte which indicates, for example, that the '20-year' and '50-year' minimum temperatures differ by only 2 °C. It can be seen that the Hopkins and Whyte estimates of minimum temperature on summits are up to 10 °C too low, although the maximum difference is reduced to 7 °C if the altitudinal correction is not applied.

Large lakes which do not freeze over also have a very large warming effect, as witnessed by the lowest recorded temperatures of −12 °C at Sloy on Loch Lomond (1965–78) and −13 °C at Ardtalnaig on Loch Tay (1958 onward). The largest effects are local, as demonstrated by the −17 °C observed at Fort Augustus (1914 onward) and −20 °C at Dall (1961 onward) where the stations are located further from the water's edge (of Lochs Ness and Rannoch respectively). The minima reported from these stations are close to the map values, but it has to be remembered that without the lakes temperatures in these valleys

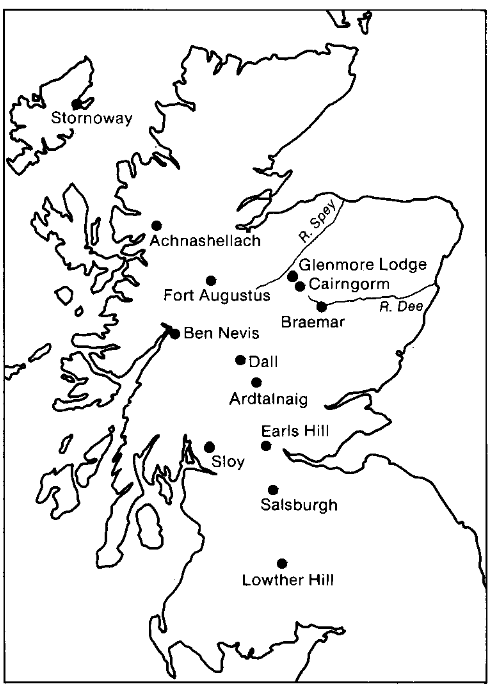

Figure 1. Map showing Scottish stations referred to in the text.

would be several degrees below map values. Valleys which drain directly to the coast are also much milder than those which do not, as exemplified by the modest minimum of −15 °C recorded at Achnashellach (1922–83).

Note that the likelihood of a lake remaining unfrozen in periods of severe weather is related to its depth rather than its area. The cooling of a lake will be related to the ratio of its surface area to its volume, and this will be least for deep, narrow lakes. Thus, large, shallow lakes such as Loch Leven (Kinross) and the southern end of Loch Lomond freeze over, while deep, narrow lakes such as the northern portion of Loch Lomond do not.

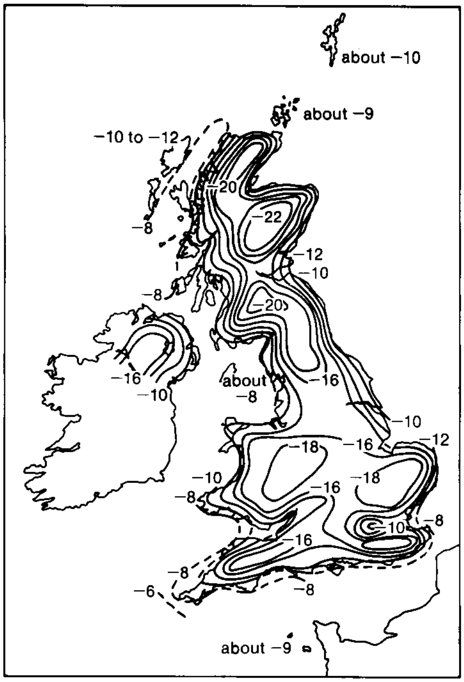

Figure 2. Hopkins and Whyte's map of the annual minimum temperature (°C) to be expected once in 50 years at mean sea level.

Table I. *Comparison of minimum temperatures observed on hills with those estimated by Hopkins and Whyte*

Station	Altitude	Period of record	Station analysis: Observed minima	Station analysis: 1-in-50-year minima	Hopkins and Whyte: Map value	Hopkins and Whyte: Altitude corrected
	m		°C	°C	°C	°C
Ben Nevis	1343	1884–1903	−17	−18	−14	−21
Cairngorm Chairlift	1090	1963–1971	−16	−18	−22	−27
Cairngorm Coire Cas	762	1964–1973	−15	−17	−22	−26
Cairngorm Car Park	663	1980 onward	−12	−15	−22	−25
Lowther Hill, Lanarkshire	754	1960–1968	−12	−14	−20	−24
Earls Hill, Stirlingshire	335	1962–1980	−12	−13	−17	−19
Salsburgh (summit of M8 motorway)	275	1965–1974	−11	−13	−17	−18

In the west of Scotland many of the valleys contain lochs, or drain direct to the sea, and this is reflected in the siting of the majority of observing stations. In the east, however, large lochs are rare and hence observations from them are in the minority. Thus we find that the Hopkins and Whyte map has been drawn to fit the −15 °C at Achnashellach and the −12 °C at Sloy whereas the −12 °C at Ardtalnaig is no less than 9 °C above the map value. It is also worthy of note that the coastal gradients drawn on the Hopkins and Whyte map cannot be expected to apply at high altitudes. The lowest temperature recorded at 900 mb by radiosondes released from Stornoway during the period 1961–70 was −13 °C and this is consistent with the −17 °C and −16 °C observed at Ben Nevis and Cairngorm Chairlift respectively.

3. Quantification of topographic effects

Tabony (1985) found it convenient to distinguish between local and large-scale shelter in his description of the effects of topography on minimum temperature. Local shelter can be interpreted as the height above the valley, and large-scale shelter as the depth of the valley. Although attempts to quantify the effects of large-scale shelter were largely unsuccessful it was found that local shelter could be well represented by the maximum drop in height, h, within a radius of 3 km of the station. This gave an objective representation of the potential for drainage of cold air away from the observation site. A relationship of the form

$$\Delta T = A \exp(-0.0055h) \qquad \ldots \; \ldots \; \ldots \; \ldots \; \ldots \; \ldots \quad (1)$$

was found, where ΔT is the temperature difference between the free atmosphere and the site (in the absence of large-scale shelter) and A is the temperature difference between the free atmosphere and level ground (i.e. $h = 0$). The temperatures ΔT and A are expressed in °C and h in metres.

The exponent describes the way in which the temperature difference increases as h decreases. Thus, three quarters of the difference between the free atmosphere and level ground has occurred when $h = 46$ m. This was the average value of h for the stations used by Tabony and hence may be taken as the value to be attached to a 'standard site'. Half the difference occurs when $h = 120$ m and less than one fifth when $h = 300$ m.

4. Development of a practical scheme

The *Upper-air summaries* (Meteorological Office 1979–81) reveal only small differences across Great Britain in the lowest temperatures experienced in the free atmosphere. The lowest observed values at 900 mb at Crawley and Stornoway for instance, were −12 and −13 °C respectively, with the corresponding figures for 800 mb being −18 and −20 °C. These values are consistent with a standard lapse rate of 6 or 7 °C km^{-1} which may be extrapolated to give a surface temperature of −7 °C. A couple of degrees can be subtracted to convert from the 10-year extremes of the *Upper-air summaries* to the 50-year return period with which we wish to deal. This gives a value of −9 °C for a free atmosphere or summit value at sea level, if this were possible. This is also consistent with the Hopkins and Whyte figures for the west coast. An altitudinal correction of 7 °C km^{-1} can now be applied to give the summit value at any altitude; this yields −18 °C for Ben Nevis which seems reasonable. Therefore the free-atmosphere temperature, T_f, (°C) is given by

$$T_f = -9.0 - 0.007H \qquad \ldots \; \ldots \; \ldots \; \ldots \; \ldots \; \ldots \; \ldots \quad (2)$$

where H is the altitude in metres.

The Hopkins and Whyte map shows that there is not much geographical variation across the United Kingdom in the 50-year minimum screen temperature at topographically similar sites, and a value of −18 °C may be assigned to level ground. This suggests that the temperature difference between the free atmosphere and level ground is 9 °C, and that this is the value of A in equation (1). Tabony found that, averaged over the whole of Great Britain, the value of A associated with a 30-year extreme in a winter month was 6 °C. There are no problems in raising this to 9 °C to cope with 50-year events over the whole year and in changing from a root-mean-square regression which estimates a mean effect to one which errs on the side of caution (i.e. produces estimates which are too low rather than too high).

So far the effect of large-scale shelter has not been taken into account. The lowest temperatures of −27 °C recorded in the Dee and Spey valleys suggest that 18 °C needs to be subtracted from the free-atmosphere value, i.e. double the level-ground correction. Thus the simplest way of including the effect of large-scale shelter is to multiply A in equation (1) by a factor L which ranges from 1 to 2. The value of L will have to be assessed subjectively but, being a function of large-scale rather than small-scale topography, it is capable of being mapped.

Finally, it is necessary to include the effects of lakes and towns. If these are of any size at all they will counteract any influence of large-scale shelter and also diminish the 'level-ground' effect. Values in the centre of London, for instance, are similar to those experienced on the coast. Urban effects are greatest in districts where the area of sky visible is severely curtailed, i.e. where streets are narrowest and buildings tallest. All these factors can be taken into account by multiplying A in equation (1) by a water/building factor, B, which ranges from 0 to 1.

The procedure outlined above leads to the minimum temperature, T_m, (°C) being given by

$$T_m = T_f - LB\Delta T. \qquad \text{(3)}$$

5. Conclusions

If the site is near the coast the Hopkins and Whyte map is adequate. Otherwise the following procedure may be used:

(a) Obtain the site altitude, H, and the maximum drop in height within 3 km, h, both in metres.

(b) Estimate the free-atmosphere temperature, T_f (°C), from equation (2).

(c) Calculate the effect of local shelter from equation (1) with $A = 9.0$ or interpolate from the following table.

h (metres)	0	50	100	200	300
Local-shelter effect (°C)	9.0	6.8	5.2	3.0	1.7

(d) Subjectively estimate the effect of large-scale shelter as lying between 1 and 2, where a value of 1 is appropriate to level ground and 2 to the maximum known effect in Britain. Multiply the local and large-scale shelter effects to get an overall topographic factor ΔT_t. Reduce the topographic factor according to the presence of lakes and towns (deep lakes and towns can eliminate the topographic factor almost entirely).

(e) Estimate the minimum temperature as the free-atmosphere value obtained in (b) minus the topographic factor arrived at in (d) (see equation (3)).

The steps described above become clearer in the examples presented in Table II.

The fact that the minimum temperature observed at Glenmore Lodge in a (broken) 30-year record was only −20.4 °C serves to illustrate the problems in assigning a value to the large-scale shelter factor. Until this quantity is mapped, the recorded extremes at nearby climatological stations, in combination with a knowledge of the data of those extremes and the station values of h, should enable a suitable value to be chosen. In effect, this means that one will be using the drop in height within 3 km to interpolate between the 50-year minima estimated for individual stations in the local area. Many of the recent enquiries for estimates of extreme minima, however, relate to the erection of masts on hills where temperatures are less sensitive to the effects of large-scale shelter, and where the above procedures should enable reliable estimates to be provided.

Table II. *Examples of the procedure used to estimate the minimum temperature for inland sites (for explanation of symbols see text)*

	Glenmore Lodge	Cairngorm Car Park	Cairngorm Summit
Altitude (H)	341 m	663 m	1245 m
Drop in height within 3 km (h)	22 m	325 m	695 m
Free-atmosphere temperature (T_f) $T_f = -9.0 - 0.007H$	−11.4 °C	−13.6 °C	−17.7 °C
Local-shelter effect (ΔT) $\Delta T = 9.0 \exp(-0.0055h)$	8.0 °C	1.5 °C	0.2 °C
Large-scale shelter factor (L)	2.0	1.0	1.0
Water/building factor (B)	1.0	1.0	1.0
Final topographic effect (ΔT_t) $\Delta T_t = LB\Delta T$	16.0 °C	1.5 °C	0.2 °C
Minimum temperature (T_m) $T_m = T_f - \Delta T_t$	−27.4 °C	−15.1 °C	−17.9 °C

References

Hopkins, J.S. and Whyte, K.W. 1975 Extreme temperatures over the United Kingdom for design purposes. *Meteorol Mag*, **104**, 94–102.

Meteorological Office 1979–81 Upper-air summaries 1961–70. Parts 1–6. London, HMSO.

Tabony, R.C. 1985 Relations between minimum temperature and topography in Great Britain. *J Climatol*, **5**, 503–520.

Reviews

Climate, weather and Irish agriculture, edited by T. Keane. 155 mm × 245 mm, pp. xvii + 187, *illus.* Dublin, Mount Salus Press Ltd, 1986. Price Ir. £9.95 (paperback), Ir. £14.95 (hardback).

Weather affects many agricultural operations and it follows that the proper use of weather information should make it possible to use resources more effectively. This book is intended to encourage a greater awareness of the role of weather and climate in agriculture; it is directed at all involved in agriculture but particularly to students at universities and agricultural colleges.

This is not a textbook about meteorology or instruments or the Irish climate, though it necessarily includes chapters on these subjects. It is a book about the relationship between weather and agriculture. The subjects discussed in the book include: weather and crop production; amelioration of climate for horticultural purposes; animals and the environment; pests and diseases of crops and animals; weather and forestry. Separate chapters are devoted to the moisture balance, to the energy balance and to climate and soil management, and there is a review of the potential of the Irish climate for agriculture. Each chapter contains the necessary biological, physiological and scientific information for an understanding of the general principles involved in the processes under discussion, whether it be the use of mulches to conserve water or the effect of weather on lactation in cows.

The book has been written by specialists 'chosen for their knowledge and experience in the interface area between meteorology and agriculture'. The contributors are from the Irish Meteorological Service, from An Foras Talúntais (the Agricultural Institute), from the University Colleges of Galway and Dublin and from the Veterinary Research Laboratory. Each chapter presents a comprehensive survey of all aspects of the topic under consideration, with references to the operational and research work of other countries, including the United Kingdom. Each chapter has a bibliography of standard reference works and recent research papers and, in total, over 500 books and publications, mostly non-meteorological, are listed.

Several references are made in the book to the work of, and papers produced by, the agriculture section of the Meteorological Office. The reference to the joint Meteorological Office–ADAS (Agricultural Development and Advisory Service) plant disease warning scheme is slightly outdated in that net blotch warnings are no longer issued; the warning criteria were developed using 'in-crop' weather data and gave poor results when used with synoptic data. The Office's crop disease environment monitor (CDEM) mentioned as 'currently being evaluated in Britain' was not a conspicuous success; it suffered major problems with the internal battery pack and was unreliable in operation. The system nevertheless demonstrated the value of in-crop weather data and the need is now being met by commercial firms with more efficient data-logging equipment.

Criticisms can be made of this publication, mostly of a minor nature. Some of the chapters attempt to include too much detail, some of which, though relevant, is neither fully researched nor particularly helpful! For instance, in chapter 10 we learn that '...flights of winged ants tend to occur after rain.' That is the entire scholarship on the subject of winged ants. We learn also that eggs and larvae of wire-worm and leather-jackets are prone to dessication, though the authors admit that dessication is unlikely to be a problem in Ireland. Many other bugs receive an honourable mention and not much else.

The attempts to compare the climate of Ireland with the climate of north-west Europe and with New Zealand in terms of the agricultural potential are unsatisfactory. There was never any possibility that this could be done adequately in two and a half pages and the book would not have suffered in any way for the omission of this small section.

The book is well illustrated with line drawings relevant to the text. Some photographs have been included which show meteorological sites or equipment; they are, however, too small and too general to add anything of value to the book. Photographs of the pests and diseases referred to would have added interest for those on the fringes of agriculture.

The index, which runs to over 3000 items, is less than helpful unless the reader knows precisely what to look for. For example, while there is an entry for nematode worms, the four and a half pages on plant nematodes in chapter 10 are not found under that general heading but under their individual titles, e.g. 'potato cyst nematode'. Similarly, potato blight is known as 'late blight' in Ireland and appears in the index under this title, rather than under 'potato blight' or plain 'blight'; the biological index is useful for those knowing the Latin names of biological organisms.

The suggestion that the book will help producers at all levels to maximize their returns is not easy to justify. No attempt has been made to quantify the cost–benefit of meteorology applied to agriculture and little practical guidance is given on how best to apply the information for planning and scheduling operations. Some specific facts and figures on the costs of the damage caused by pests, diseases and poor weather, together with some clear indication of where and how savings are to be made by the wise use of available weather information would have been helpful.

It is, however, difficult to doubt the other claim — that this book is a valuable addition to Irish agricultural literature. It will also find a place in many UK and overseas libraries. This book is to be commended to all meteorologists involved with agriculture, but especially the newcomer to the field of agrometeorology who will find in it a wealth of useful information and a comprehensive overview of agriculture with weather in its proper perspective.

P. Harker

The uncertainty business, by W.J. Maunder. 161 mm × 242 mm, pp. xxviii + 420, *illus*. London, Methuen and Co. Ltd, 1986. Price £45.00.

The uncertainty business appears at first glance a somewhat daunting book; the text is sandwiched between nearly 30 pages of lists, prefaces and acknowledgements, and 90 pages of indices and bibliographies. At second glance too, as further inspection reveals pages full of the abbreviated names of hundreds of committees and organizations, and sentences so long and tortuous that I had to read them several times over to understand them. Alas, the book doesn't invite further reading!

In the initial section, considering the atmosphere as an elite resource, Maunder asserts that the techniques of assessing the impact of the atmosphere on human activities have been badly neglected, and that such impact has significant economic, social and political consequences. He argues that meteorologists should now take their place alongside other disciplines — economics in particular — to guide important decision- and policy-making in all walks of human affairs.

There follows a comprehensive review of the various developments in monitoring and understanding the effect of the atmosphere on the management of resources. The author argues that the real benefits of weather information will come not only when the right information is produced, but also when that information is used efficiently in decision-making processes at all levels. Indeed, until we know the true impact of tomorrow's weather upon human activities, we are not in a good position to assess the importance and value of forecasting it. This is the important central thrust of Maunder's argument.

He goes on to review the major recent studies assessing the effects of weather and climate. The choice of examples, however, taken mostly from Maunder's own researches in New Zealand, gives a rather insular view. That said, there follows an impressive array of tables and graphs demonstrating the benefits of these methods. Here, Maunder goes for quantity in his arguments, heaping example upon example, giving the reader little opportunity to stand back and admire the view; around page 180, statistical indigestion begins to set in.

This is particularly unfortunate, as Maunder has now come to arguably the most significant part of the book — a series of case-studies, assessing the economic impact of weather and climate upon a range of human activities. Not only are the traditional ones here — agriculture, transport, building construction and energy — but also the new market places which are as yet largely undeveloped meteorologically — road construction, manufacturing and retailing. Many good examples and methods of analysis are given; possibly because these are mostly aimed at identifying the relationship between production and climate variables, rather than simply defining climatological indices, this section is more satisfying and convincing. Maunder demonstrates a variety of techniques of analysis, each to some extent determined by the industry concerned. These studies point to the very considerable benefits which would accrue if meteorological information was applied more efficiently and widely. In essence, this section is a primer for organizations which wish to capitalize on these benefits.

Maunder briefly considers the use of statistical models to predict the likely impact of climate. He proposes developments of this work to include the weather-sensitivity analysis of national economic indicators and their subsequent 'weather adjustment'. Such developments, he says, although possibly controversial, would give economists and politicians a much clearer view of underlying economic trends.

Finally, Maunder identifies the major challenges and opportunities in the management of weather-sensitive resources — the rise of carbon dioxide levels, acid rain, and the nuclear winter. These issues are, perhaps wisely, merely indicated; further discussion is left to other forums.

Taken as a whole, this book raises important issues with which many meteorologists will be familiar, but which need to be debated much more fully outside the meteorological community. The application of the study of weather and climate to all walks of life through assessment of its political, social and economic impact, has a potentially vital role. The book's very comprehensiveness lends it undoubted authority, but this same quality, coupled with its failure to highlight clearly the central themes and conclusions, detracts from its value as a persuasive document. The flyleaf describes it as a manifesto; if so, it should have been far shorter, and written with a far wider audience in mind.

F.R. Hayes

The Irish meteorological service: the first fifty years, 1936–86, edited by L. Shields. 208 mm × 296 mm, pp. viii + 107, *illus.* Dublin, The Stationery Office, 1987. Price Ir. £6.00.

'Unto thine own self be true.' Polonius was not always an old fool and, perhaps, here he was not just being moral but also nurturing Laertes's self-confidence. Being true to itself, self-confidence and active up-to-date maturity are three main characteristics of the Irish Meteorological Service which permeate and shine out from this happy book.

Its title summarizes its scope and objective: to review the work and personalities of the Irish Meteorological Service from 1936 to 1986. It does that, and a great deal more. The front cover sets the scene with the first of a number of excellent and sometimes dramatic colour photographs: does any other Meteorological Service have its home in a frustum of a pyramid? A ziggurat? The back cover has a METEOSAT picture of the globe, which would be commonplace if it were not one for St Patrick's Day. This attention to detail must be one factor in making the Irish Meteorological Service worthy of its high international reputation.

Its people must be another. Its first Director was a former Secretary and Treasurer of the Meteorological Office branch of the Institution of Professional Civil Servants. Its second was a Basque who had fought against Franco in the Spanish Civil War. Subsequent staff have all played their individual parts and many of them are recorded here or have contributed an essay.

The humanity of the people who have served meteorology in Ireland, and continue to do so, must be another secret of the Service's ability to serve its many clients in a wide range of weather sensitive activities: its Minister congratulates them 'with a heart and a half'. It is uplifting to see throughout the book the Service's concern for people, an emphasis on the contribution they make and the way in which their nature determines the success of the organization. 'At times Mr Finnegan worried about the small pension he would qualify for when he retired. He need not have worried. The kindly gentle soul departed this life before he qualified'. Like the Service, the book is also based around people; it is made up of a set of essays by a formidable panel of the Service's experts. They cover every aspect of meteorological life in Ireland, both of yesterday and of today: from the truth behind the great potato blight in 1845 to serving the off-shore oil industry in 1986.

The list of meteorologists from Ireland is brilliant with names such as Robert Boyle, Admiral Beaufort, Robinson (of cup anemometer fame), Stokes (Equation and sunshine recorder), Sabine, Tyndall and R.H. Scott (Director of the Meteorological Office). To quote names of the living would be invidious; but it must be said that the forecasting talent brought together at Foynes to support the beginnings of transatlantic air travel can rarely, if ever, have been matched.

Today the Service comes over as up to date, making good use of the data and products it receives, and contributing to meteorology in other countries, not only through participation in the European Centre for Medium Range Weather Forecasts and the usual exchange of World Weather Watch data but also in many other ways. Two instances are the graphics software it has developed in-house and its training programme, both made available through the Voluntary Co-operation Programme of the World Meteorological Organization. In two articles, the book distinguishes carefully between the accuracy of forecasts and their utility: the Service is not only human, it is professional.

Until 1936 the responsibility for meteorology in Ireland lay with the Meteorological Office, so that we may take pride in having a thriving offspring, which has grown to full maturity and continues to have a full and friendly relationship with us. In Hamlet, Laertes dies. In Ireland he has flourished into his second half-century of confident well-balanced maturity and has published a most readable autobiography.

To summarize the book or the history of the Service here might satisfy your curiosity. That would be a shame. You would do better to beg, borrow or even buy — and then enjoy — a copy for yourself.

S.G. Cornford

Landolt-Börnstein: numerical data and functional relationships in science and technology, V/4a, edited by G. Fischer. 200 mm × 277 mm, pp. xii + 491, *illus.* Berlin, Heidelberg, New York, London, Paris, Tokyo, Springer-Verlag, 1987. Price DM 1220.00.

This volume is part of a new series of Landolt-Börnstein books which give exhaustive compilations of numerical constants, tabulated data and functional relationships (i.e. equations etc.) in the physical sciences. At present, these are broadly classified into six groups (e.g. Group I is Nuclear and Particle Physics, Group II is Atomic and Molecular Physics); Volume 4 of Group V (Geophysics and Space Research) deals with meteorology and is split into three subvolumes — the first of which is reviewed here.

As the editor admits in the preface, the choice of material covering the dynamics and thermodynamics of the atmosphere is 'a little problematic'. Furthermore the Landolt-Börnstein philosophy of presenting just tables and figures is transgressed and substantial space is given to theoretical discussion. One can find, for example, a crude scale-analysis of terms in the equations of motion, a review of the Lorenz concept of available potential energy and even a short history of the European Centre for Medium Range Weather Forecasts (ECMWF).

The first section of the book gives a compressed account of the equations of motion in various co-ordinate representations together with some commonly used reduced forms of these equations such as the barotropic and quasi-geostrophic models. I could not find any reference to the important Boussinesq approximation or the semi-geostrophic equations; neither is the concept of potential vorticity given anything more than a brief mention. Although the presentation is clear, much of the material is dated and readily available elsewhere.

The second section, on atmospheric data, provides a wide range of information including tables for the conversion of degrees Fahrenheit to Celsius(!), geostrophic wind speed from isobar spacing, and virtual temperature increments as a function of pressure and temperature. It also contains a thorough treatment of the physical properties of moist air, with many obscure and complicated formulae. I suspect that much of the information given in this section will not be sought after, e.g. tables for the wavelength of the stationary external Rossby wave as a function of latitude and zonal wind speed, and formulae for the vertical structure of polytropic model atmospheres.

Section three, on the general circulation of the atmosphere, forms over one half of the book and contains a collection of time-mean diagnostics derived from 17 years of National Meteorological Center (NMC) analyses. Time-averaging is taken over the four seasons separately for both hemispheres. For instance, one can find maps of the horizontal distribution of temperature at 850, 700, 500, 300, 200, 100 and 10 mb as well as meridional cross-sections of the spectral amplitude (though not phase) of temperature and height (of pressure surfaces) for wave numbers 1, 2 and 3, and various spectral decompositions of the horizontal transport of heat and momentum. Much of the zonally averaged and spectral data are also tabulated even when, as in Table 25e on page 387 (the inter-annual variance of eddy heat transport in wave number 3), all entries in the table are zero! The data of this section will nicely complement existing general circulation statistics (e.g. Oort 1983)*.

Finally, there is a section dealing with meteorological organizations providing, for example, the history and structure of the World Meteorological Organization and an address for virtually all the national meteorological services world-wide.

There is no doubt that the book contains a lot of useful information, but is it really worth £430? Much of the tabulated data is either available in other textbooks, obtainable on magnetic tape from NMC or ECMWF, or easily computed on a pocket calculator.

G. Shutts

Books received

The listing of books under this heading does not preclude a review in the Meteorological Magazine at a later date.

Acidification of freshwaters, by M. Cresser and A. Edwards (Cambridge University Press, 1987. £19.50, US $34.50) examines the numerous interacting physical, chemical and biological processes which regulate acidity in freshwaters. Concepts from many disciplines are brought together in an attempt to make a coherent picture which is understandable to a wide range of people.

Acidic precipitation, Parts 1 and 2, edited by H.C. Martin (Dordrecht, D. Reidel Publishing Company, 1987. £196.00, US $240.00, Dfl.560.00) consists of the proceedings of the international symposium on the subject, held at Muskoka, Ontario, 15–20 September 1985. There are over 200 papers on related subjects, with author and subject indexes.

---

* Oort, A.H.; Global atmospheric circulation statistics, 1958–1973. Washington D.C., NOAA, 1983, Professional Paper 14.

Satellite photograph — 6 April 1987 at 1548 GMT

Throughout the period 5–7 April 1987, a complex depression was situated to the south-west of Ireland and a cold front moved erratically and very slowly north over the British Isles. This front was characterized in the infra-red Meteosat pictures by a distinctive band of cloud with apparently uniform brightness and definite edges. The associated surface weather consisted of rain and drizzle, slowly dying out, with hill and coastal fog, mainly in the east. The accompanying picture, which was taken in the infra-red, shows more detail within the cloud band. From a combination of Meteosat images, the wave-like structures on the northern (anticyclonic) side of the front could be seen to move westwards, each developing differently. The cloud streaming north-west of 46° N, 23° W shows the remains of the crest of the first wave, which had crossed Scotland about 30 hours earlier. The crest of the second wave, at 54° N, 22° W, is beginning to curve forwards while the third wave, at 57° N, 12° W, is 'rolling' backwards.

The areas of showers over the west of England, Wales and southern Ireland are associated with cold pools in a band of cold air which extended from Poland to the Azores. The area of cloud at 42° N, 21° W appears like a PVA (Positive Vorticity Advection) area, which soon became absorbed into the re-invigorating main vortex. The area of cloud over the Bay of Biscay swept northwards and brought extensive moderate to heavy rain over England and Wales from the early hours of April 7.

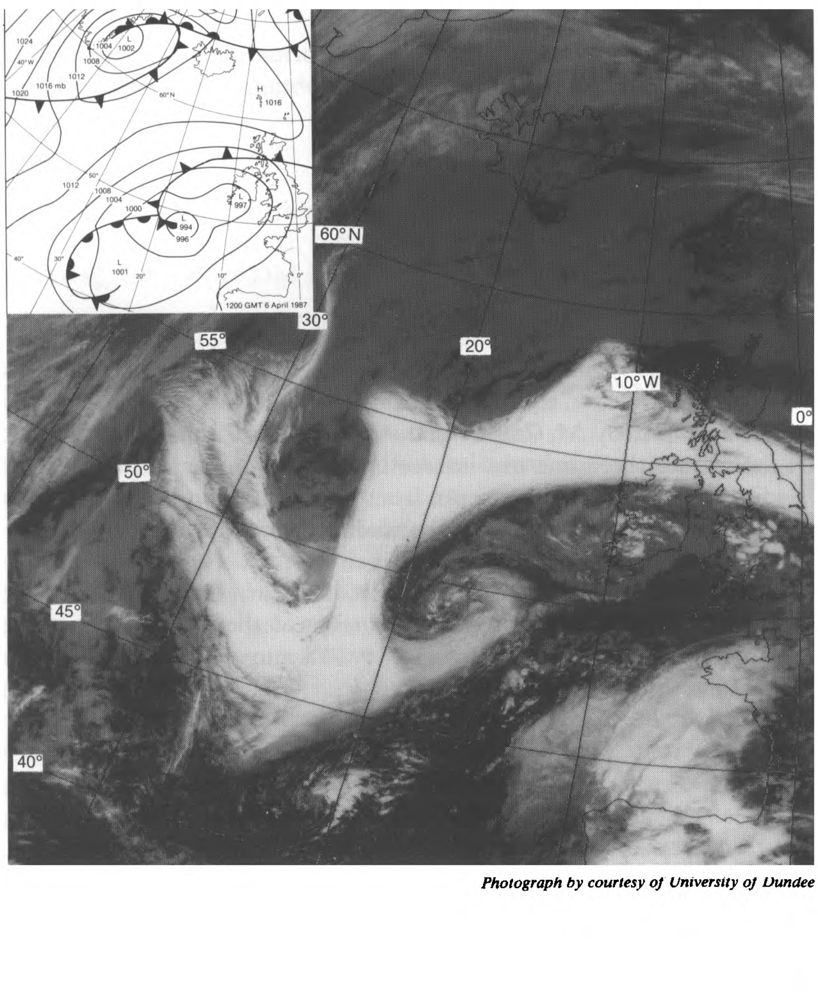

Photograph by courtesy of University of Dundee

Meteorological Magazine

GUIDE TO AUTHORS

Content

Articles on all aspects of meteorology are welcomed, particularly those which describe the results of research in applied meteorology or the development of practical forecasting techniques.

Preparation and submission of articles

Articles for publication and all other communications for the Editor should be addressed to the Director-General, Meteorological Office, London Road, Bracknell, Berkshire RG12 2SZ and marked 'For *Meteorological Magazine*'.

Articles, which must be in English, should be typed, double-spaced with wide margins, on one side only of A4-size paper. Tables, references and figure captions should be typed separately.

Spelling should conform to the preferred spelling in the *Concise Oxford Dictionary*.

References should be made using the Harvard system (author, date) and full details should be given at the end of the text. If a document referred to is unpublished, details must be given of the library where it may be seen. Documents which are not available to enquirers must not be referred to.

Tables should be numbered using roman numerals and provided with headings. We consider vertical and horizontal rules to be unnecessary in a well-designed table; spaces should be used instead.

Mathematical notation should be written with extreme care. Particular care should be taken to differentiate between Greek letters and Roman letters for which they could be mistaken. Double subscripts and superscripts should be avoided, as they are difficult to typeset and difficult to read. Keep notation as simple as possible; this makes typesetting quicker and therefore cheaper, and reduces the possibility of error. Further guidance is given in BS1991: Part 1: 1976 and *Quantities, Units and Symbols* published by the Royal Society.

Illustrations

Diagrams must be supplied either drawn to professional standards or drawn clearly, preferably in ink. They should be about 1½ to 3 times the final printed size and should not contain any unnecessary or irrelevant details. Any symbols and lettering must be large enough to remain legible after reduction. Explanatory text should not appear on the diagram itself but in the caption. Captions should be typed on a separate sheet of paper and should, as far as possible, explain the meanings of the diagrams without the reader having to refer to the text.

Sharp monochrome photographs on glossy paper are preferred: colour prints are acceptable but the use of colour within the magazine is at the Editor's discretion. In either case contrast should be sufficient to ensure satisfactory reproduction.

Units

SI units, or units approved by WMO, should be used.

Copyright

Authors wishing to retain copyright for themselves or for their sponsors should inform the Editor when they submit contributions which will otherwise become UK Crown copyright by right of first publication.

It is the responsibility of authors to obtain clearance for any copyright material they wish to use before submitting it for publication.

Free copies

Three free copies of the magazine are provided for authors of articles published in it. Separate offprints for each article are not provided.

Meteorological Magazine

September 1987

Vol. 116
No. 1382

CONTENTS

Contributions: it is requested that all communications to the Editor and books for review be addressed to the Director-General, Meteorological Office, London Road, Bracknell, Berkshire RG12 2SZ, and marked 'For *Meteorological Magazine*'. Contributors are asked to comply with the guidelines given in the *Guide to authors* which appears on the inside back cover. The responsibility for facts and opinions expressed in the signed articles and letters published in *Meteorological Magazine* rests with their respective authors. Authors wishing to retain copyright for themselves or for their sponsors should inform the Editor when submitting contributions which will otherwise become UK Crown copyright by right of first publication.

Subscriptions: Annual subscription £27.00 including postage; individual copies £2.30 including postage. Applications for postal subscriptions should be made to HMSO, PO Box 276, London SW8 5DT; subscription enquiries 01–211 8667.

Back numbers: Full-size reprints of Vols 1–75 (1866–1940) are available from Johnson Reprint Co. Ltd, 24–28 Oval Road, London NW1 7DX. Complete volumes of *Meteorological Magazine* commencing with volume 54 are available on microfilm from University Microfilms International, 18 Bedford Row, London WC1R 4EJ. Information on microfiche issues is available from Kraus Microfiche, Rte 100, Milwood, NY 10546, USA.

ISBN 0 11 727973 0

ISSN 0026–1149

Printed for HER MAJESTY'S STATIONERY OFFICE
by Delco Printing Co.Ltd. 9/87 Dd 0240021 C14 (40711)

THE METEOROLOGICAL MAGAZINE

HER MAJESTY'S STATIONERY OFFICE

October 1987

Met.O.978 No. 1383 Vol. 116

METEOROLOGICAL OFFICE Met.O.978

THE METEOROLOGICAL MAGAZINE

No. 1383, October 1987, Vol. 116

551.515.827(261.26)

Case study of a persistent mesoscale cold pool

F.F. Hill*

Meteorological Office, Bracknell

K.A. Browning

Deputy Director (Physical Research), Meteorological Office, Bracknell

Summary

A case study is presented of a shallow mesoscale cold pool of diameter 500 km which formed near the southern end of a disrupting upper trough. The cold pool remained within the circulation of a blocking high and survived with a steady-state thickness anomaly for 5 days. During this time it moved first eastwards across southern Britain and then westwards across northern France and the English Channel. Thundery rain occurred close to the centre during its return journey. The cold pool was not easily identifiable on conventional 1000—500 mb thickness charts but was well revealed by analyses of 700–500 mb thickness and, even better, by analyses of isentropic potential vorticity (IPV). A well-defined region of high IPV was associated with subsided stratospheric air immediately above the cold pool and it advected like a passive tracer. During their eastward journey, the cold pool and IPV maximum were associated with a well-marked open wave which, because of the limited extent of cloud, was best revealed by Meteosat water vapour imagery. During the subsequent westward journey, the position of the cold pool was indicated in Meteosat water vapour imagery by an eye-catching swirl of dry air surrounding a moist core.

1. Introduction

Cold pools, otherwise referred to as upper cold lows, cut-off lows, cold-core cyclones, cold vortices or cold domes, have been the subject of study for many years. Early analytical studies by Palmen (1949) and others showed that they form from the cutting off of a pocket of polar air near the southern extremity of a cold trough. Such systems can be over 1000 km in diameter and can last for many days (e.g. Peltonen 1963). Recent studies (e.g. Matsumoto *et al.* 1982) show that they can also occur on the mesoscale when, despite their small size, they give rise to significant precipitation systems. A feature of cold pools discussed by Palmen is the existence of a warm core above them. Matsumoto and Ninomiya (1967) point out that a warm core at tropopause level can provide a good indication of the existence of even a very small cold pool within the troposphere.

Potential vorticity is a particularly useful diagnostic quantity not least because it is often, to a good approximation, advected as a passive tracer along surfaces of constant potential temperature. Potential vorticity is the product of the absolute vorticity and the static stability and, when calculated along isentropic surfaces, is abbreviated to IPV.

* Now at Royal Air Force, High Wycombe.

High values of IPV have been revealed along surfaces which intersect the warm core above a cold pool, implying that this air had descended from the lower stratosphere where such values are commonplace (Eliassen and Kleinschmidt 1957, Degorska 1980). The stratospheric origin of the air in such regions was indicated in studies of tropopause folding by Danielsen (1968) and Danielsen and Mohnen (1977). More recently Hoskins *et al.* (1985), in discussing the general versatility of IPV maps, have suggested that, whereas the low temperature-anomaly of a cold pool may well be important from a purely diagnostic point of view, it can be argued that in terms of cause and effect its importance is secondary by comparison with that of the IPV advection above it. This is because much of the coldness of a cold pool is attributable to the induced temperature field of the IPV maximum above it.

Sumner (1953) carried out a statistical study of cold pools in an area of particular interest to UK forecasters, south of 80° N between 60° W and 30° E. He found that cold pools having at least two closed 1000–500 mb thickness contours (contours drawn at 60 m intervals) persisted on average for 3 days, with no clear relation between the intensity of the cold pool and its duration. Many cold pools were found to occur in association with surface anticyclones and these were found to be accompanied by what was regarded as a surprisingly high occurrence of precipitation.

The purpose of the present paper is to show by means of a case study, using output from the Meteorological Office fine-mesh model together with satellite imagery, that a seemingly anomalous patch of convective showers and thunderstorms within the circulation of an anticyclone was associated with a long-lived mesoscale feature that was manifested in the middle troposphere as a cold pool, and in the upper troposphere and lower stratosphere as a warm region with a pronounced maximum of IPV. The cold pool was a minor feature in conventional 1000–500 mb thickness analyses because the thickness anomaly was small and restricted to a shallow layer. The overall phenomenon, however, of which the thickness anomaly was a part, was more significant when viewed in terms of the IPV anomaly aloft and this feature has been used to backtrack to find the origin of the cold pool before it reached the data-dense region of north-west Europe. At times the influence of the mesoscale feature could be seen to extend over a rather large area when viewed by satellite in terms of the distortion of the upper-tropospheric humidity field.

2. Synoptic setting

The synoptic setting for this event is shown in Figs 1 and 2 which illustrate the situation about half-way through the life cycle of the mesoscale cold pool. Fig. 1 shows the surface analysis and Fig. 2 the 500 mb and 1000–500 mb thickness analyses at 00 GMT on 24 April 1984. The cold pool can just be discerned in the thickness analysis over the English Channel on the southern flank of the anticyclone. The corresponding infra-red imagery from Meteosat (not shown) revealed an isolated patch of cold convective cloud tops associated with the cold pool. Water vapour imagery from Meteosat (Fig. 3) showed a swirl of dry upper-tropospheric air around the moist core associated with the convection at the centre of the cold pool. This swirl in the moisture distribution persisted as an eye-catching feature of the satellite water vapour imagery for the next 2 days and it was this that drew attention to the possibility that, despite the bland appearance of the routine synoptic analyses, the patch of showers at its focus might be other than just a random and inherently unpredictable event.

3. Persistence and movement of the cold pool and associated IPV anomaly

Fig. 4 shows part of the life history of the cold pool by means of a sequence of four analyses of the 700–500 mb layer at 24-hour intervals using a contour interval of 20 m. This layer was chosen rather than the more usual 1000–500 mb because no temperature anomaly could be detected below 700 mb. There are sufficient radiosonde measurements to enable a cold pool to be revealed with closed contours

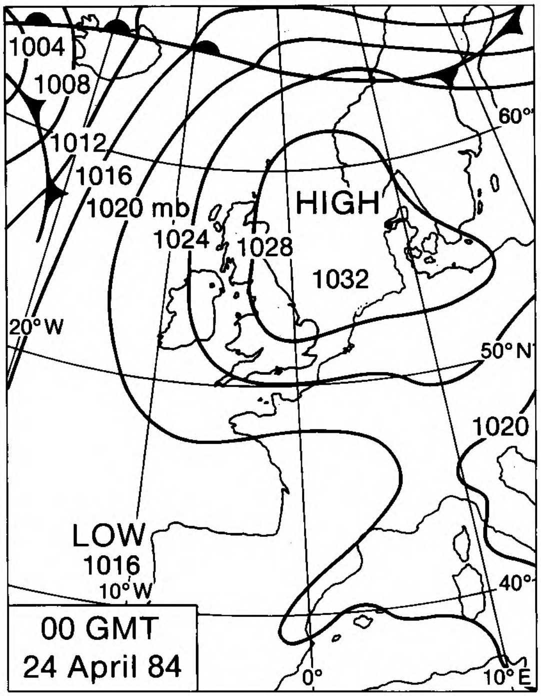

Figure 1. Surface analysis for 00 GMT on 24 April 1984.

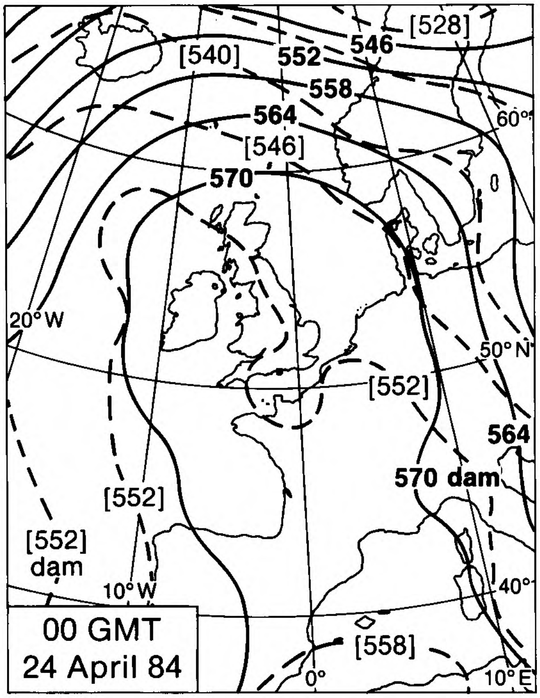

Figure 2. 500 mb contour (solid lines) and 1000–500 mb thickness (dashed lines) analyses for 00 GMT on 24 April 1984.

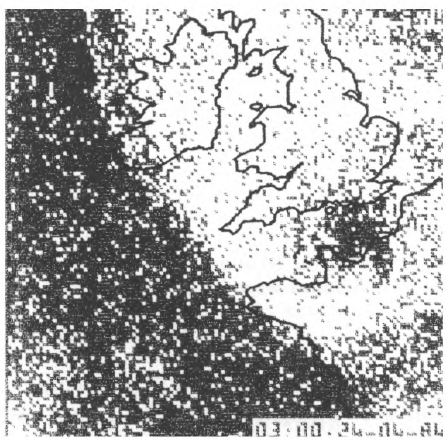

Figure 3. Meteosat water vapour imagery for 03 GMT on 24 April 1984. Areas of high and low humidity in the upper troposphere are shown black and white, respectively. The speckled effect is due to instrumental noise.

throughout the period from 00 GMT on the 22nd to 12 GMT on the 25th and to suggest that the central thickness was close to about 2560 m. For most of the time during which it was well observed, the cold pool remained almost constant in size and depth. The circulation in the 700–500 mb thermal winds extended to 500 km in diameter, although the thickness anomaly was only about 50 m. Because of the smallness of this thickness anomaly, the cold pool was sometimes difficult to identify in UK operational

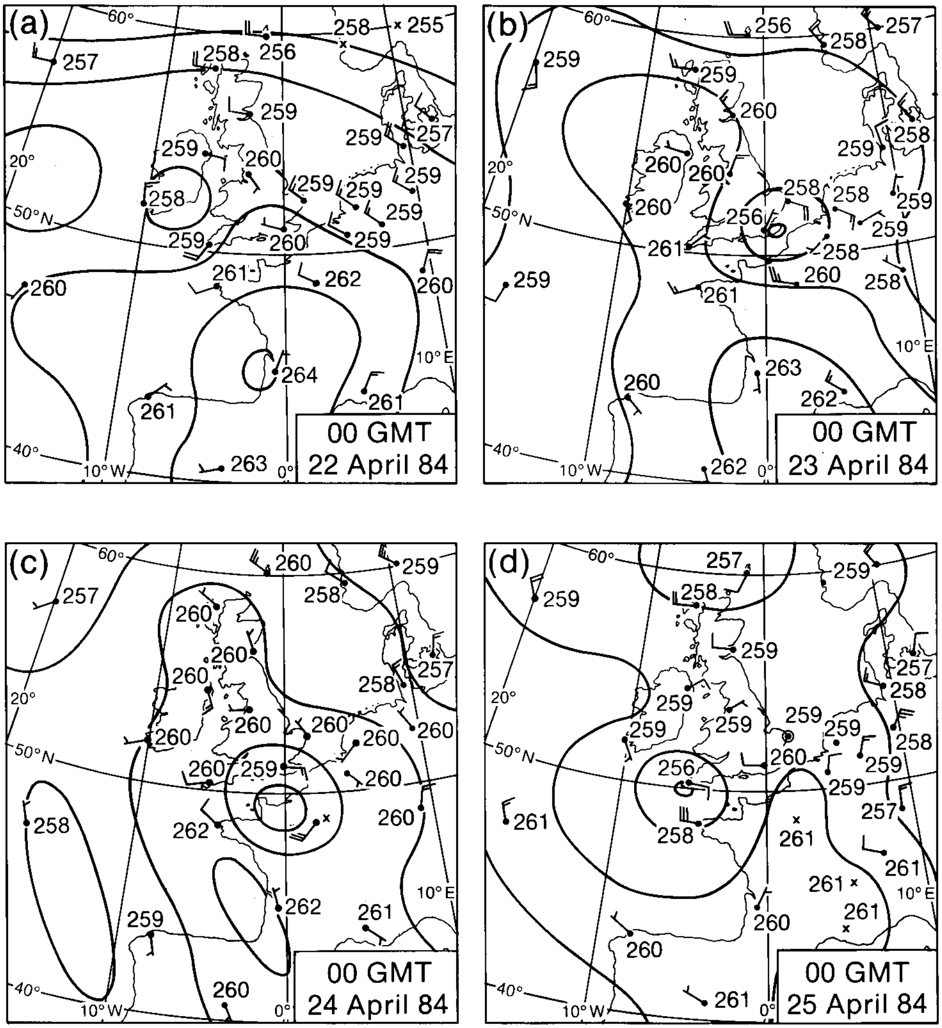

Figure 4. 700–500 mb thickness analyses showing the location of the cold pool at 00 GMT on (a) 22 April, (b) 23 April, (c) 24 April and (d) 25 April 1984. Thickness contours are at 2 dam intervals. Thermal winds and thickness values (dam) are shown for individual radiosonde stations.

thickness charts in which the contours are conventionally drawn at 60 m intervals, although it appears in the 1000–500 mb thickness analyses published by Deutscher Wetterdienst in the *European Meteorological Bulletin* for which the contour interval is 40 m.

The relationship and movement of the cold pool with respect to the 500 mb upper-air pattern is illustrated in Fig. 5. The cold pool, initially on the northern flank of a 500 mb ridge, moved east-north-eastwards towards southern Ireland. The ridge then intensified over Scotland and this caused the upper winds in the vicinity of the cold pool to weaken and veer, resulting in a more south-easterly movement of the cold pool towards northern France. By the morning of 24 April, the upper ridge had become firmly established as a blocking high over Scotland and the North Sea; the cold pool then travelled in a westerly direction around the southern flank of the block. After moving slowly along the English Channel, it

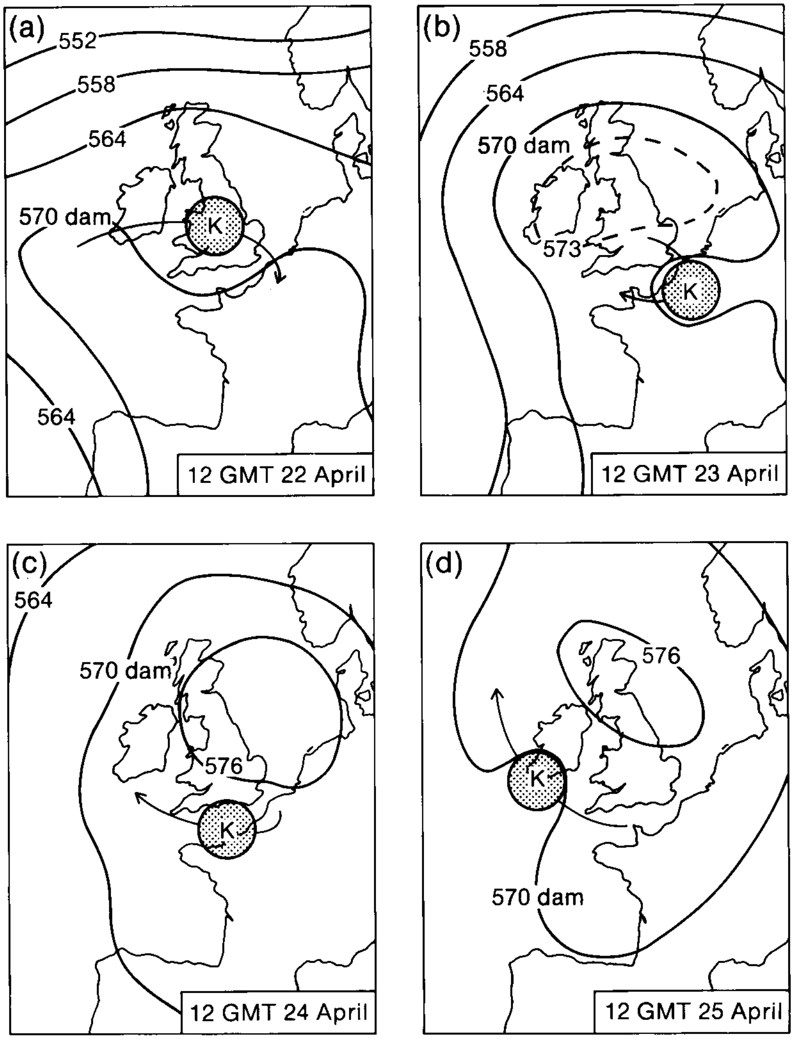

Figure 5. Position (K) of the centre of the cold pool (stippled area), from the 700–500 mb thickness contours of Fig. 4, plotted in relation to the 500 mb contours at 12 GMT on (a) 22 April, (b) 23 April, (c) 24 April and (d) 25 April 1984. Arrows show the movement of the cold pool from H−24 to H+24 in each case.

accelerated as it turned north-westwards towards Ireland. The cold pool probably decayed when it was some 300 km to the north-west of Ireland, early on 26 April.

A well-defined IPV maximum was located above the cold pool throughout its existence. Fig. 6 shows a sequence of nine IPV charts at 12-hour intervals for the 330 K isentropic surface, situated between 250 and 200 mb. These have been calculated using analyses from the Meteorological Office fine-mesh model, the resolution of which is 0.75° latitude by 0.94° longitude. It can be seen from Fig. 6 that the core of high IPV within the 330 K isentropic surface associated with the cold pool was identified fairly consistently in size and intensity from one analysis to the next from 00 GMT on the 22nd until 00 GMT on the 25th. (Before the start of this period it was part of a band of high IPV associated with an upper trough (see section 5), and at the end of this period it merged with the large region of high IPV to the west

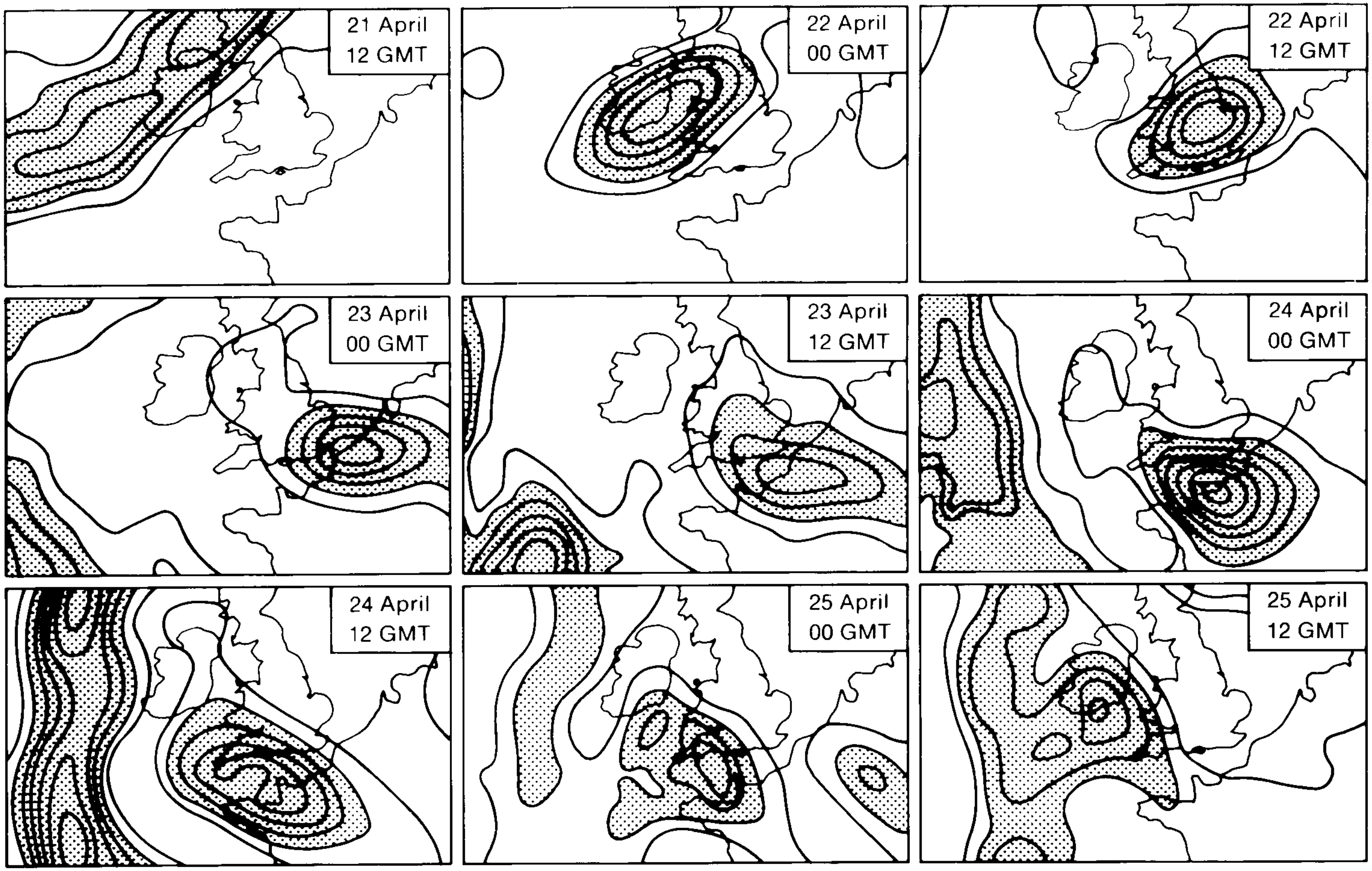

Figure 6. IPV on the 330 K isentropic surface at 12-hour intervals starting at 12 GMT on 21 April 1984. Contours are drawn at intervals of 1 IPV unit corresponding to units of $10^{-6} m^2 K kg^{-1} s^{-1}$ as suggested by Hoskins *et al.* (1985), where one of these units is equivalent to a relative vorticity of zero when the Coriolis parameter is $10^{-4} s^{-1}$ and there is a vertical gradient in θ of 1 K per 10 mb. According to Hoskins *et al.* (1985), a value of 2 or more IPV units (shaded regions) is characteristic of stratospheric air.

of Ireland.) A comparison of Figs 5 and 6 confirms that, as is to be expected, the centre of the region of high IPV moved along a path which coincided with that of the cold pool, effectively acting as a passive tracer.

4. The relationship of the mesoscale cold pool and the IPV maximum

A comparison is made in Fig. 7 between IPV analyses from the Meteorological Office fine-mesh model in the 330 K and the 310 K isentropic surfaces; both IPV values and the pressure height of the isentropic surfaces are shown. The 330 K surface was located just below the tropopause as defined by the lapse rate, whereas the 310 K surface intersected the upper part of the cold pool well within the troposphere. It can be seen that the large IPV values in the 330 K surface did not extend down into the 310 K surface. However, the pressure-height minimum in the 310 K surface, which identifies the centre of the cold pool, was located directly beneath the IPV maximum in the 330 K surface. The diagnostic necessity of a close structural linkage between the cold pool and the overlying IPV maximum is well known (Hoskins *et al.* 1985). The vertical structure as derived from the fine-mesh model is clearly revealed by the cross-section in Fig. 8. The cold pool is identified by the dashed envelope within which the isentropes locally bulge upwards, and the top of the cold pool is at about 330 mb. The IPV maximum, centred near 240 mb, extends down into the middle troposphere and intersects the top of the cold pool.

The effect of the passage of the cold pool on the temperature distribution aloft is clearly brought out by the ascents at two radiosonde stations in southern England (Fig. 9). The cold pool passed south-eastwards across Crawley just before the time of the 00 GMT ascent on 23 April and was approaching Camborne at the time of the 00 GMT ascent on 25 April. Comparing each of these ascents (solid lines in Fig. 9) with corresponding ascents obtained 12 hours earlier (dashed lines in Fig. 9), it can be seen that the air became potentially unstable within the cold pool from 850 to 430 mb as the result of a temperature decrease of around 4 °C in the middle troposphere; at the same time, the air warmed by nearly 5 °C between 400 and 200 mb. Since IPV values exceeding 2 are likely to be associated with stratospheric air, we can deduce from Figs 6 to 9 that the upper tropospheric warming above the cold pool was due to adiabatic warming caused by the descent of air of stratospheric origin. Moreover, according to Hoskins *et al.* (1985) the overrunning high-IPV air probably induced ascent beneath it and this led to the adiabatic cooling that sustained the cold pool in the middle levels.

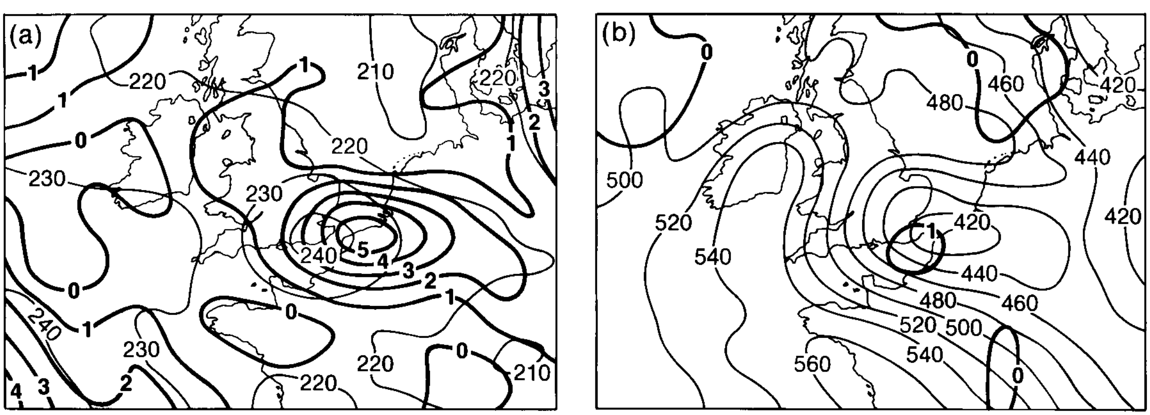

Figure 7. IPV (bold contours labelled in IPV units) and pressure level (fine contours labelled in millibars) of the corresponding isentropic surface at 00 GMT on 23 April 1984 for (a) the 330 K surface and (b) the 310 K surface.

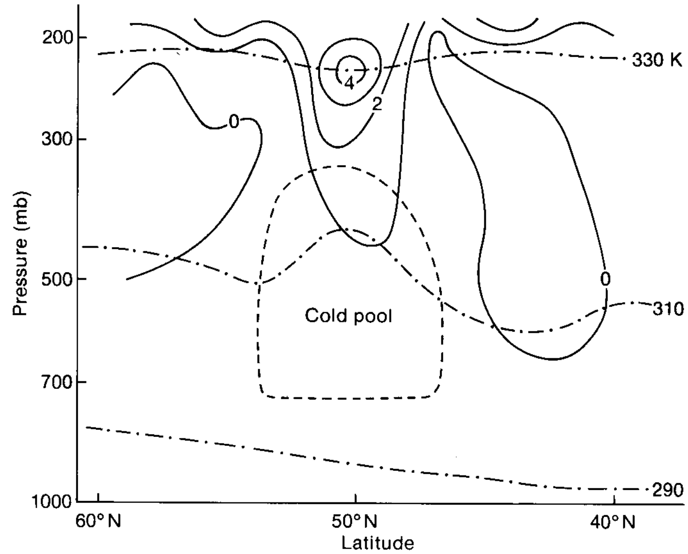

Figure 8. North–south cross-section at 1 ° E through the cold pool at 00 GMT on 23 April 1984 when it was near south-east England. Bold contours show IPV in IPV units. Undulating dash-dot lines show isentropic surfaces. The dashed line outlines the cold pool.

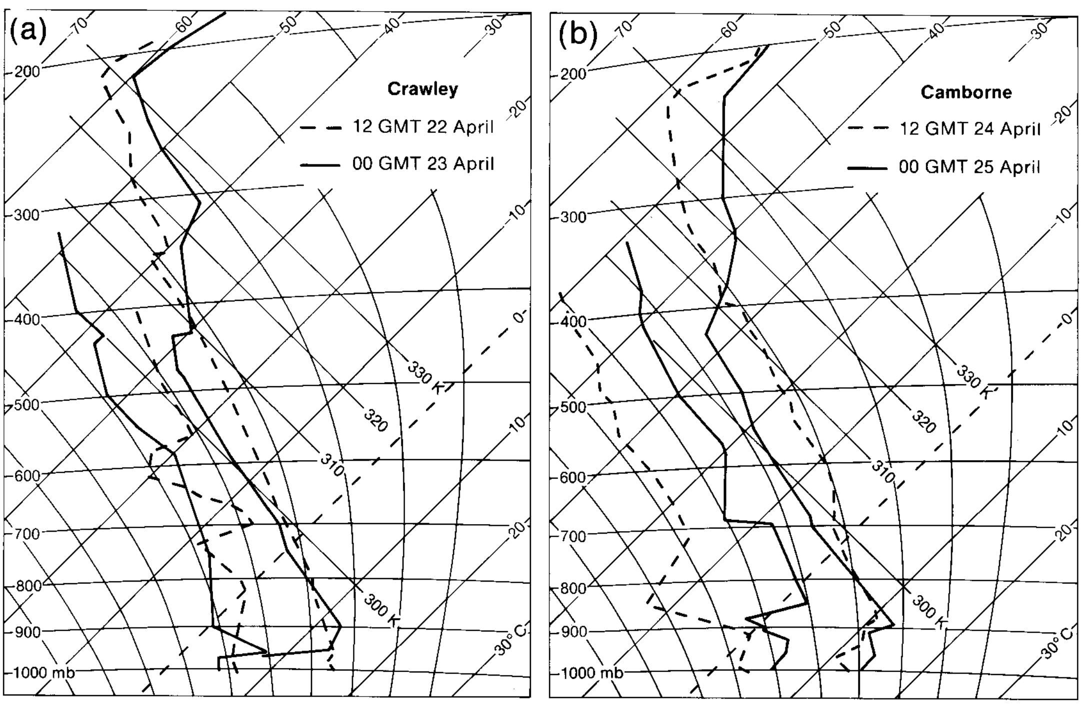

Figure 9. Tephigrams showing radiosonde ascents at (a) Crawley and (b) Camborne close to the centre of the cold pool as it passed overhead (continuous lines) compared with the ascents made at the corresponding stations 12 hours earlier (dashed lines).

5. Initial development of the cold pool

The cold pool developed within a region of high pressure south-west of Ireland on or before 21 April. Because of the dearth of radiosonde stations in this region it was not revealed clearly in the thickness analyses. However, its existence could be inferred from IPV analyses and it was also associated with a characteristic pattern in the satellite imagery, especially the water vapour imagery.

Earlier IPV analyses on 19 April had shown a broad band of high IPV on the 330 K surface extending from south-west to north-east across the Atlantic to the north of the surface fronts. As the upper trough sharpened behind the cold front, so the zone of high IPV extended southwards to 45° N. The forward edge of this zone caught up with the surface cold front during 20 April (Fig. 10(a)). Although the highest values of IPV were associated with the north-eastward-moving depression, a secondary maximum was cut off near 51° N, 30° W between 00 and 12 GMT on 20 April and it moved eastwards towards southern Ireland by 00 GMT on the 22nd (Fig. 10(b)). It is not known from the available data whether the cold pool itself existed on 20 April or developed during the next 24 hours, but it is clear from satellite imagery that the increased cyclonic vorticity in this region had already induced a small wave in the upper cloud at the rear of the cold front early in the morning of 21 April.

By 03 GMT on 22 April the wave was very clearly defined in the infra-red imagery and even more so in the water vapour imagery (Fig. 11(a)). The solid black area over England and Wales in Fig. 11(a) corresponds to upper cloud; the speckled band extending westwards from the wave corresponds to a band of moist upper-tropospheric air which was not producing cloud. The arrow shows the centre of the cold pool. Patches of moist air were found near the centre of the cold pool but much drier upper-tropospheric air (white area in Fig. 11(a)) can be seen around the southern flank of the cold pool. The dry air was associated with the veered flow to the rear of the upper trough (see the wind arrows over south-west Ireland in Fig. 10(b)). As shown in Figs 11(b) and (c), this dry air spread rapidly across southern England and the English Channel as the wave developed. It is this dry air that could be seen swirling around the cold pool during the ensuing days and which led to the eye-catching water vapour image in Fig. 3.

6. Weather associated with the cold pool

The cloud and precipitation associated with the cold pool varied a lot during the 5 days of its existence. Ascent at upper levels ahead of the eastward-moving cold pool caused a broad band of cirrostratus and altostratus to move across southern Ireland on 21 April. This cloud covered most of England and Wales during the night of 21/22 April and had the shape of an open wave in both the infra-red and water vapour imagery (Fig. 11(a)). However, very little rain reached the ground from this extensive area of mainly middle- and upper-level cloud which dispersed as it moved east-north-eastwards during 22 April. Near the centre of the cold pool, bands of altocumulus castellanus gave intermittent rain over central southern England during the afternoon of 22 April. These bands crossed south-east England and dispersed overnight, and by the morning of 23 April, just before the cold pool started returning westwards, there was no cloud near the cold pool.

When the cold pool was returning westwards, areas of thundery rain or showers developed intermittently within it. The location and size of the main areas of convective cloud are illustrated in Fig. 12. A substantial proportion of these areas was occupied by thundery rain which was locally heavy. It can be seen that all the cloud formed within the cold pool as outlined by the 2580 m contour in the 700–500 mb thickness charts. Most of the vigorous convective cloud formed close to the central moist core, while more patchy cloud moved cyclonically around it.

It is apparent from Fig. 9 that air temperatures near the ground of at least 20 °C were required for convection to be initiated by surface heating. Such temperatures were exceeded over northern France

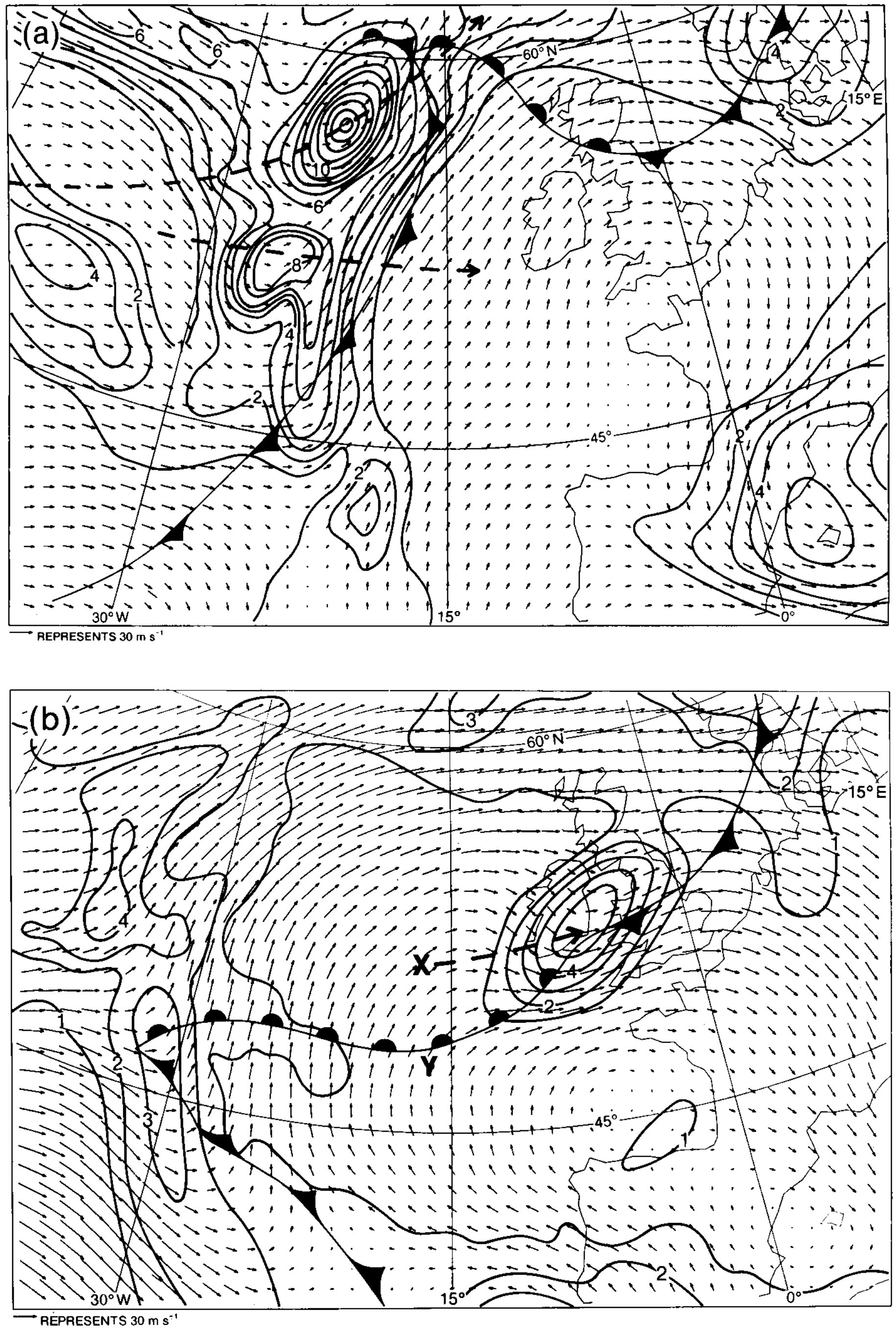

Figure 10. IPV (in IPV units) and flow in the 330 K surface at (a) 12 GMT on 20 April and (b) 00 GMT on 22 April 1984, with surface fronts superimposed. Bold dashed arrows show the direction of travel of the main and secondary IPV maxima. The cold pool was associated with the secondary IPV maximum which travelled in an almost easterly direction from X in (b). 18 hours earlier when the IPV maximum was at X the cold front wave was located to the south of it at Y.

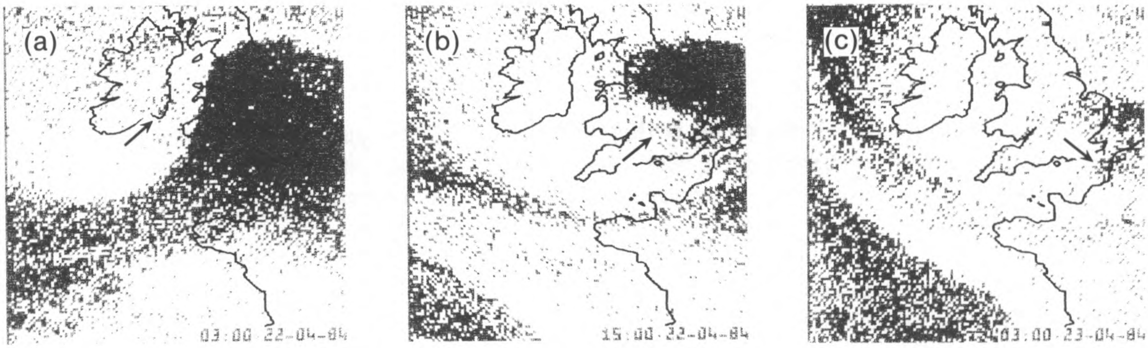

Figure 11. Meteosat water vapour imagery for (a) 03 GMT on 22 April, (b) 15 GMT on 22 April and (c) 03 GMT on 23 April 1984. Areas of high and low humidity in the upper troposphere are shown black and white, respectively, as in Fig. 3. The arrows point to the centre of the 700–500 mb cold pool.

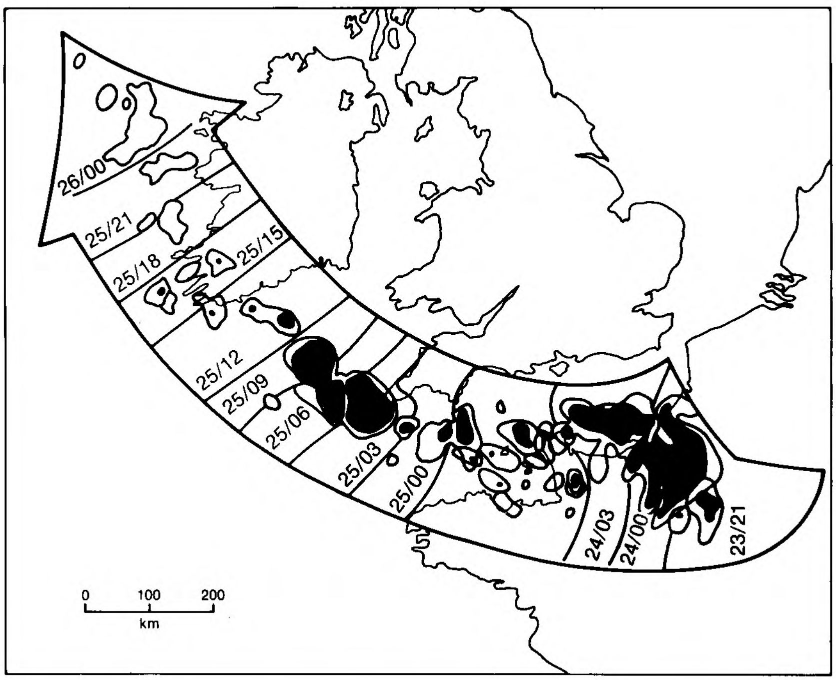

Figure 12. Locations of cumulonimbus (black) and thick altocumulus clouds (outlines) at 3-hour intervals during the period from 21 GMT on 23 April to 00 GMT on 26 April 1984 as inferred mainly from satellite imagery. These convective clouds were closely associated with the centre of the cold pool, whose path is shown by the broad arrow.

during the afternoon of 23 April prior to the development of the storms there. Another warm day occurred on 24 April near the north coast of France; this almost certainly accounts for the small thundery areas which formed briefly to the west of the Cherbourg peninsula early that afternoon. On the other hand, it is clear from the Camborne ascent in Fig. 9(b) that the development, during the night of 24/25 April, of the storm area near Cornwall was not due to local surface heating, since surface air temperatures over the English Channel were only 12 °C. The Camborne ascent shows that there was a layer of potentially unstable warm moist air centred at 850 mb which was enabling the convection to be sustained. This warm moist air appeared to have originated from near the surface over northern France.

7. Concluding remarks

An underlying message of this study is that a mesoscale event can have more organization and persistence than might reasonably have been expected. By carrying out a detailed case study we have obtained a clear description of a non-severe mesoscale event, and determined what kinds of data are suitable for revealing it.

The mesoscale cold pool that we have studied had a circulation extending to 500 km in diameter and, although poorly revealed in conventional 1000–500 mb analyses, its presence was clearly identified by the following three kinds of data:

(a) 700–500 mb thickness, the maximum thickness anomaly in the cold pool being 50 m.

(b) IPV in the 330 K isentropic surface, with a maximum value of typically $8 \times 10^{-6} m^2 K\ kg^{-1} s^{-1}$ occurring directly above the cold pool; the IPV tended to advect like a passive tracer and has been used to backtrack and locate the origin of the cold pool.

(c) Water vapour imagery, with eye-catching patterns that revealed a mass of dry middle- and upper-tropospheric air which invaded and eventually surrounded much of the cold pool.

The cold pool originated within cold air from an upstream trough; the enhanced cooling within the cold pool was consistent with adiabatic cooling owing to local ascent induced when descending stratospheric air with high IPV overran it.

The weather associated with the cold pool in this case study was easy to identify and track because it occurred within a region otherwise dominated by an anticyclone. Thus the cloud and precipitation for the most part was isolated and distinct. The cold pool itself began life as a remnant of an upper trough. Early in its life the cold pool was associated with a well-marked open wave in the satellite infra-red and water vapour imagery. The cloud produced by the wave was limited to the middle and upper troposphere, however, and little precipitation reached the ground. Subsequently this cloud dissipated altogether and a compact area of showers and thunderstorms formed near its centre in association with convection from the surface. Normally the warming due to such convection more than compensates for the combined cooling, due to large-scale adiabatic ascent and long-wave radiation, leading to the demise of a cold pool. However, this cold pool lasted 5 days with a constant thickness anomaly of 50 m. The longevity in this case was perhaps due in part to the limited extent and vigour of the convection because of its location within a region of dry air associated with the surrounding large-scale subsidence. Sumner (1953) in his study of over 200 cold pools found an average diurnal variation of about 20 m in central thickness which he attributed to insolation and the associated convection. In the present study no diurnal variation in thickness could be discerned and this is consistent with the rather limited amount of convection and the lack of diurnal variation in convective activity.

References

Danielsen, E.F. 1968 Stratospheric–tropospheric exchange based on radioactivity, ozone and potential vorticity. *J Atmos Sci*, **25**, 502–518.

Danielsen, E.F. and Mohnen, V.A. 1977 Project Duststorm Report: Ozone transport, in situ measurements and meteorological analyses of tropopause folding. *J Geophys Res*, **82**, 5867–5877.

Degorska, M. 1980 A case study of an upper cut-off cyclone development. *Publ Inst Geophys Pol Acad Sci*, **D-11(141)**, 111–123.

Eliassen, A. and Kleinschmidt, E. 1957 Dynamic meteorology. *In* Bartels, J. (ed.); Handbuch der Physik, Vol. 48. Berlin, Springer-Verlag.

Hoskins, B.J., McIntyre, M.E. and Robertson, A.W. 1985 On the use and significance of isentropic potential vorticity maps. *Q J R Meteorol Soc*, **111**, 877–946.

Matsumoto, S. and Ninomiya, K.	1967	On the mesoscale warm core above the condensation level related to convective activities under the influence of dome shaped cold air. *J Meteorol Soc Jpn*, **45**, 306–314.
Matsumoto, S., Ninomiya, K., Hasagawa, R. and Miki, Y.	1982	The structure and the role of a subsynoptic-scale cold vortex on the heavy precipitation. *J Meteorol Soc Jpn*, **60**, 339–354.
Palmen, E.	1949	Origin and structure of high-level cyclones south of the maximum westerlies. *Tellus*, **1**, 22–31.
Peltonen, T.	1963	A case study of an intense upper cyclone over eastern and northern Europe in November 1959. *Geophysica (Finland)*, **8**, 225–251.
Sumner, E.J.	1953	Cold pools: a statistical and synoptic study. *Meteorol Mag*, **82**, 291–301.

551.553.21:551.577.32(54):551.578.46

Variations in the onset of the summer monsoon over India

I. Subbaramayya and O.S.R.U. Bhanu Kumar

Department of Meteorology and Oceanography, Andhra University, Waltair, India

S. Vivekanandababu

Indian Institute of Technology, New Delhi, India

Summary

The dates of onset of the summer monsoon over India are quite variable. The trend and quasi-periodicity in the onset dates in the years 1956 to 1983 have been investigated. They indicate that the onset date is tending to become delayed all over India and that there are some significant periodic variations in different parts of the country. Increasing trends in the Himalayan, Eurasian and northern hemispheric snow covers and some significant periodic variations in the snow covers have also been found. The onset dates, particularly over Central India, are found to have a positive correlation with the snow cover.

1. Introduction

The start of the summer rains in India, which is known as the onset of the monsoon, is first apparent over the Andaman Islands (commonly called the Bay Islands) in the Bay of Bengal and gradually advances north-westwards. There have been many studies of the normal dates of onset, their variability, the associated upper-air circulation changes and how to forecast them (Maung Tun Yin 1949, Koteswaram 1958, Flohn 1964, Ramamurthi and Keshavamurty 1964, De la Mothe and Wright 1969, Ananthakrishnan 1970, Subbaramayya and Bhanu Kumar 1978, Kung and Sharif 1981). Of particular interest is the pulsatory nature of the advance of the monsoon reported by Subbaramayya *et al.* (1984). South peninsula is covered in one pulse, while north peninsula and parts of central India are covered in the second pulse. In another pulse the monsoon advances westward over a major part of north India (Fig. 1(a)). Considerable variability in the onset dates (Fig. 1(b)) was also found. In this paper the trend and quasi-periodicity of the variability is further examined.

2. Data and analysis

The Indian subcontinent was divided into six regions: south peninsula, north peninsula, north-east India, central north India, north-west India and west central India. These regions were chosen because in each of them the monsoon usually advances in one pulse (see Fig. 1(a)). Five or six stations in each

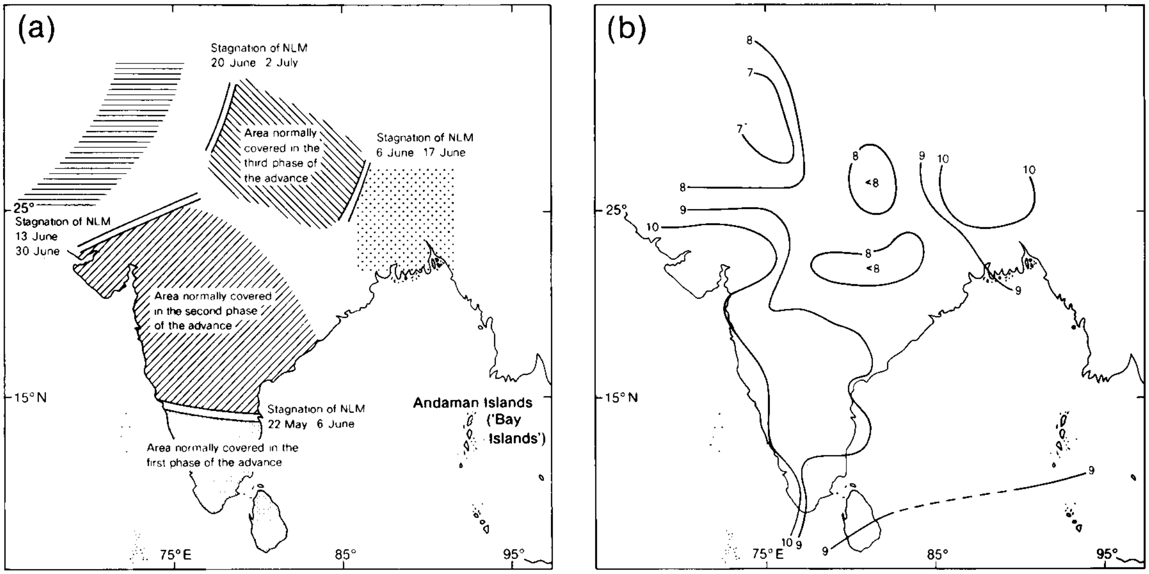

Figure 1. (a) Areas affected and periods of different phases in the advance of the monsoon, and (b) the variability of onset expressed as the standard deviation of the dates of onset. NLM is the northern limit of the monsoon.

region were selected, and the dates of onset at these stations in every year were determined from the northern limit of the monsoon, prepared for every day during the period of advance of the monsoon, for 28 years from 1956 to 1983. This follows the procedure described by Subbaramayya and Bhanu Kumar (1978). The regional averages were then obtained and analysed in the following way:

(a) The trend in the date of monsoon onset for each region was obtained by linear regression. The statistical significance of the trends was determined by Student's *t*-test.

(b) With the trend eliminated, the mean onset dates of each region were subjected to power spectrum analysis following the method described by Maruyama (1968). Power spectra were evaluated using different maximum lags to check the positions of power peaks. Consistent power peaks appeared in all cases; the spectra corresponding to a 16-year maximum lag are presented in this paper. The significance of the power peaks was assessed by the method given by Mitchell *et al.* (1966).

(c) Satellite derived monthly mean snow-cover data over the Himalayas (25–35° N and 60–105° E), Eurasia (5° S–70° N and 10° W–170° E) and the northern hemisphere for the years 1967–80 were obtained from NOAA-NESS. Though the length of the data is short, an attempt was made to examine whether there is any quasi-periodicity besides the trend.

(d) Correlations between monthly mean snow covers over the above three areas in February to May and the onset dates at selected stations were also calculated.

3. Results and discussion

3.1 *Onset dates*

The time series of onset dates for the six regions and the corresponding linear regression equations are presented in Fig. 2. In all six regions there is an increasing trend which means that the onset is getting later each year. The rate of change of onset date in south and north peninsula and north-east and west central India is 5–6 days per decade, while in central north India it is 3.5 days per decade and only 1 day per decade in north-west India. These trends could be only temporary and it cannot be expected that

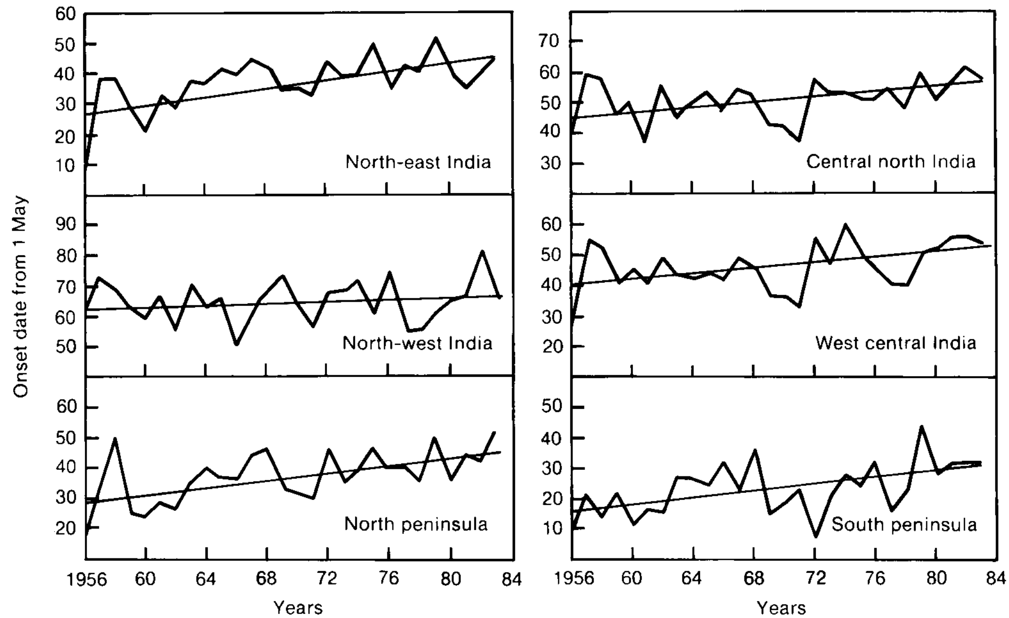

Figure 2. Year to year variations in the dates of onset in different regions of India. The straight line on each graph is the regression line.

such trends could be maintained over long periods. The trends in the first four regions, which are large, are also statistically significant at the 95% level.

In the regions where the trends are small, the rainfall during the onset phase, as well as later, is to some extent accentuated by the westerly troughs, while in the other parts the rainfall entirely depends on the eastern disturbances.

Power spectra of the onset dates for the six regions are presented in Fig. 3. The white-noise null continuum is shown by a horizontal line indicated by NC on each power spectrum. In all the regions there is large power or a peak in the range of 2.0 to 2.5 years. This could be associated with the quasi-biennial oscillation. In north-west India, west central India and central north India prominent power peaks are present in the period 6–8 years. These three regions are contiguous and in the former two the power peaks are significant at the 90% level. In south peninsula there is a peak at 16 years which is also significant at the 90% level. In north-east India and north peninsula there are prominent bands in the range 3–5 years.

3.2 *Snow cover*

The Himalayan, Eurasian and northern hemispheric monthly mean snow covers in the months February to May from 1967 to 1980 and the corresponding linear regressions are presented in Fig. 4. Trends in Eurasian and northern hemispheric snow covers are significant at the 95–99% level, while the Himalayan snow cover trend in May is significant at the 90% level — the trends in other months are not significant. The linear regression indicates an increasing trend of 1–2% of the mean per year in the case of Eurasian and northern hemispheric snow covers, and 0.2–0.9% in the case of Himalayan snow cover. These trends are consistent with the delaying trend in the onset of the summer monsoon over India in view of the accepted fact that heavy snowfall in the western Himalayas in winter has a negative effect on the ensuing monsoon.

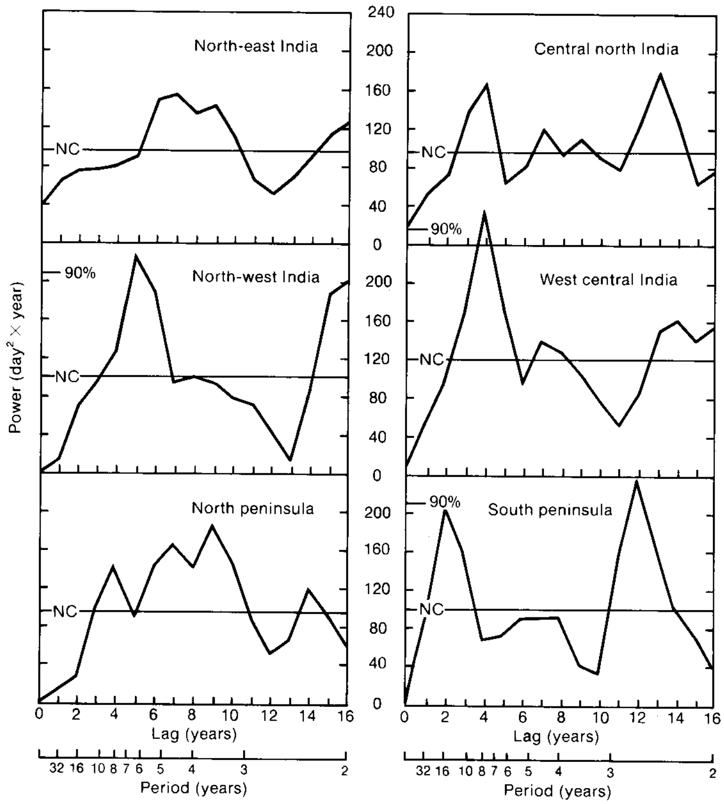

Figure 3. Power spectra of the dates of onset in different regions of India. NC is the null-continuum line. The 90% significant level is indicated where it is relevant.

Power spectra of the snow covers in the 4 months are presented in Fig. 5. All the three regions in February show a significant peak at 5 years. The peak in Himalayan snow cover is significant at the 95% level, while those in the other two are significant at the 90% level. In March and April the spectra are erratic, but in May there is a consistent peak near 2.2 years. It is, however, more pronounced in the northern hemispheric snow cover. A significant peak at 4–5 years is also present in the Himalayan snow in May.

3.3 *Correlations between onset dates and snow covers*

Correlations between onset dates at selected stations and snow covers in different months are presented in Fig. 6. The three snow covers in February show significant positive correlation with onset dates over central India, while in the extreme north-west there is a significant negative correlation. This indicates that the onset tends to be delayed particularly in central India when there is above normal winter snowfall, while it is early over the extreme north-west. In this connection it may be noted that Dey and Bhanu Kumar (1982) found that the period of advance of the monsoon from the southern tip of the Indian subcontinent to the extreme north is smaller in a year in which the Himalayan winter snow cover is large.

In the later spring months the areas of negative and positive correlations shift to the south, and by April and May strong negative correlations are observed in the central parts of the country, especially

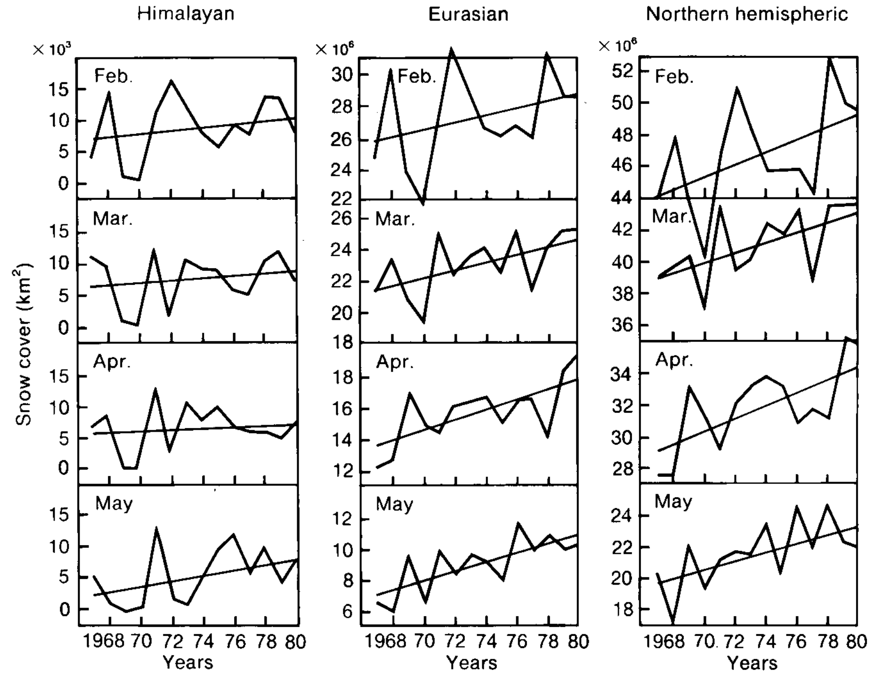

Figure 4. Year to year variations of Himalayan, Eurasian and northern hemispheric snow covers. The straight line on each graph is the regression line.

for the Himalayan snow cover. This indicates that below normal snow cover occurs in April when there is a delayed monsoon. Therefore, there should be rapid snow melt during spring in the years of high snowfall. The correlation between the February snow cover and those in the following months, as well as the snow melts, are given in Table I.

Table 1. *Correlations between February Himalayan snow cover and snow covers in March, April and May. Also the correlations between the February Himalayan snow cover and snow melts from February to March, April and May.*

Snow cover			Snow melt from February to		
March	April	May	March	April	May
0.48	0.28	0.02	0.64	0.70	0.68

The correlations clearly indicate that large snow cover in February is also associated with large snow melt in spring. But the fact remains that large winter snow cover is associated with delayed onset of the monsoon.

It is now known that there has been a warming trend in the northern hemisphere since late nineteenth century till 1940s and cooling thereafter (Budyko 1977, Barnett 1978, Hansen *et al.* 1981, Jones *et al.* 1986a) till early 1970s. Hingane *et al.* (1985) reported a general increasing trend of 0.4 °C per 100 years during 1901–82 in the all-India mean annual temperature. However, their temperature series shows a decrease from early 1950s to early 1970s. These falling trends in temperature in the recent past explain the rising trend in snow covers noted. But the continued rising trend in the snow covers observed in the

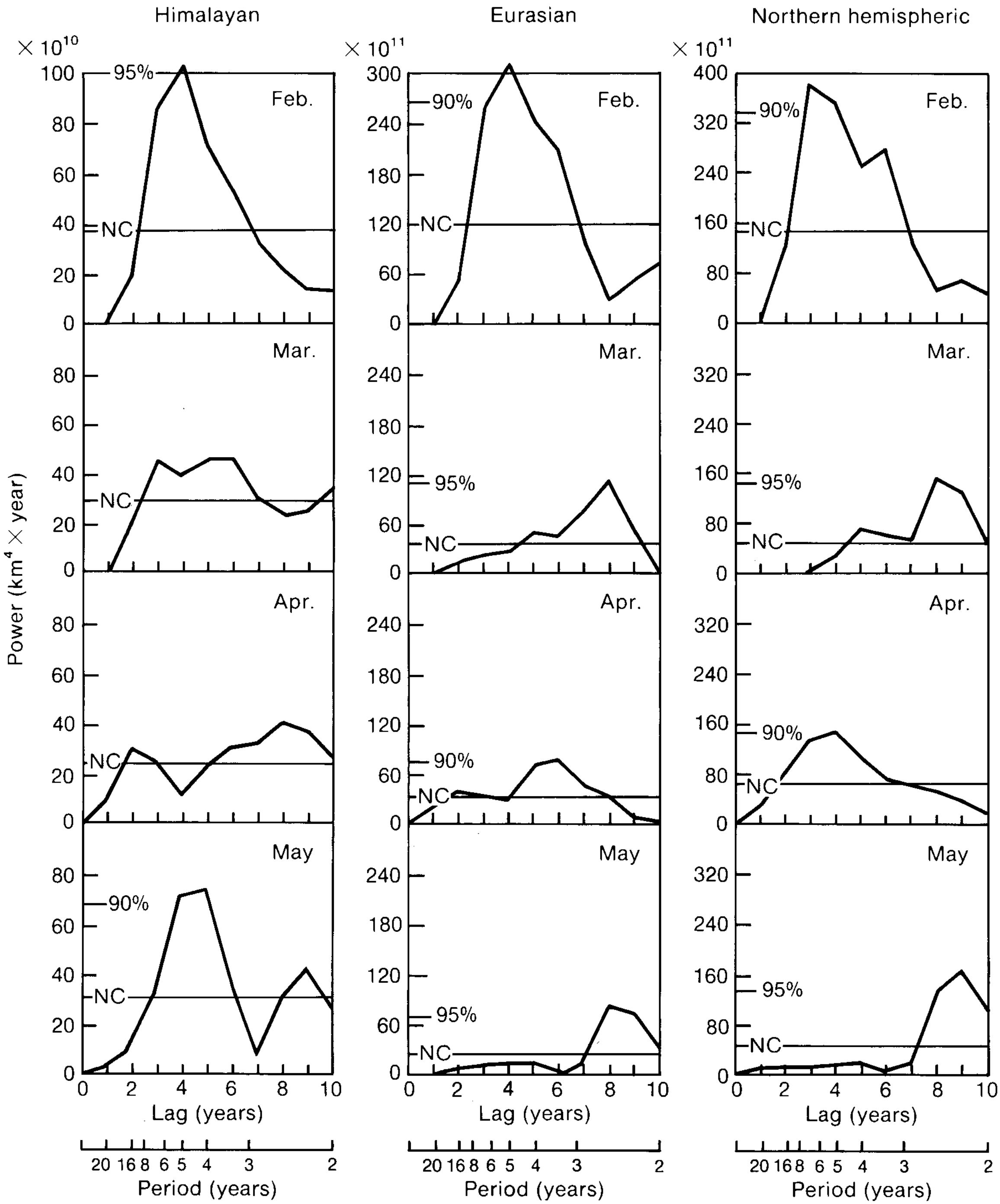

Figure 5. Power spectra of snow covers. NC is the null-continuum line. The 95% and 90% significant levels are indicated where they are relevant.

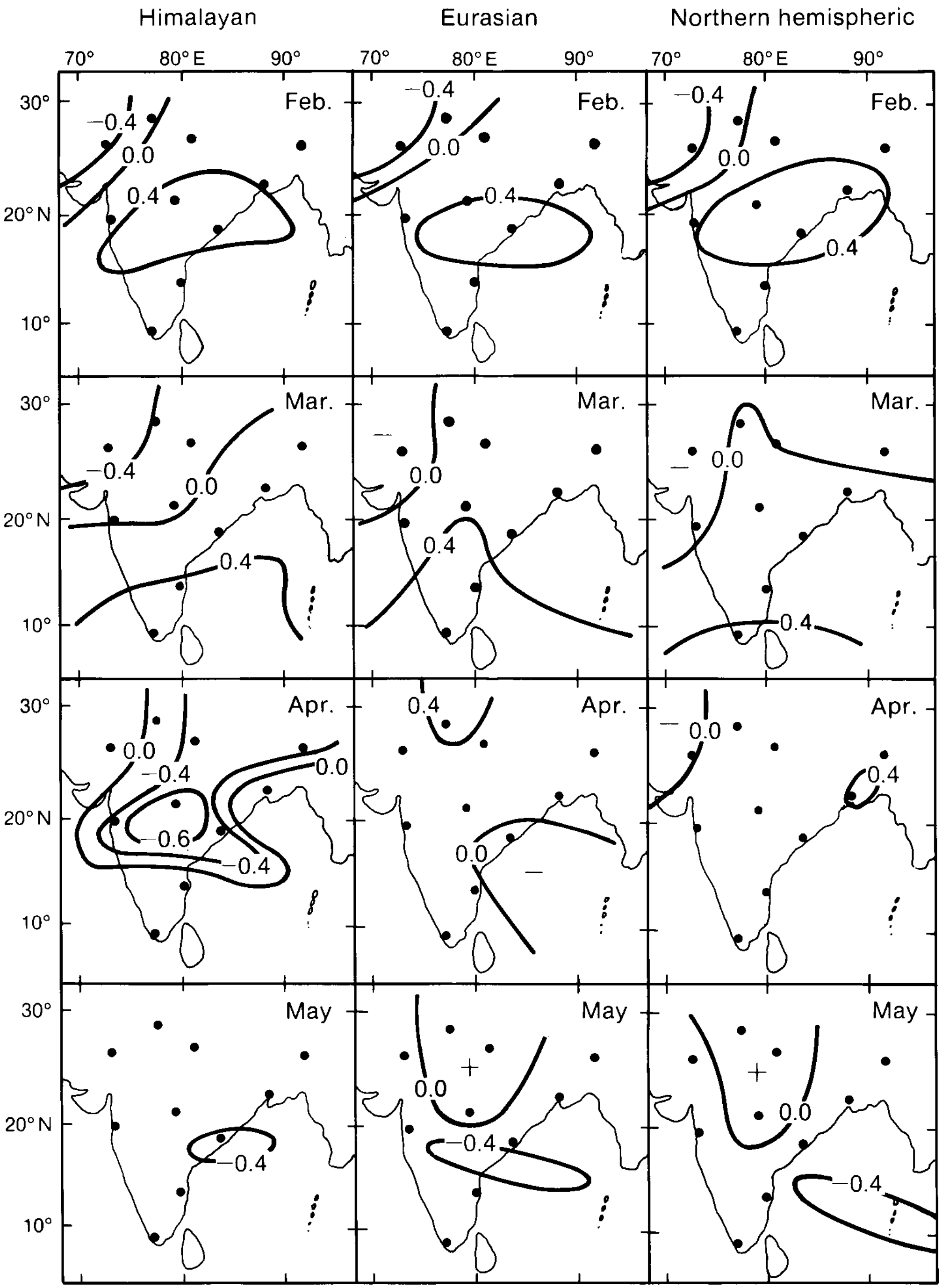

Figure 6. Correlations between Himalayan, Eurasian and northern hemispheric snow covers in different months February to May and the dates of onset at different stations. Locations of the stations are indicated by dots.

present study indicates that it is a more complex phenomenon. Jones *et al.* (1986b) showed that during the cooling phase in the northern hemisphere, i.e. post-1940 period, the temperatures in the southern hemisphere did not have any significant decreasing trend. Also the cooling trend in the northern hemisphere was more in the middle and high latitudes than in the low latitudes. Thus there has been a decreasing trend in the northward temperature gradient. This counteracts the differential heating over south Asia which is responsible for the summer monsoon. Therefore apart from the cooling in the northern hemisphere the differential trends in the northern and southern hemispheres also could be responsible for the delaying trend in the onset of the monsoon.

4. Conclusions

There has been a delaying trend in the onset of the summer monsoon over India during the period 1956–83, and a similar increasing trend in the snow cover over the northern hemisphere, Eurasia and the Himalayas during 1967–80. These trends are consistent with the decreasing trend in temperature of the northern hemisphere as well as India and absence of similar trends in temperature in the southern hemisphere observed by other workers in the recent past.

Power spectra of the onset dates show large power in the 2.0 to 2.5 years which could be associated with the effect of quasi-biennial oscillation. Also, significant power peaks in the 6- to 8-year period in north-west India and the adjoining areas are present, as in a 16-year period in the south peninsula onset dates. For the February snow cover there is a significant period at 5 years.

The snow covers in February show positive correlations with the onset dates, particularly in central India.

References

Ananthakrishnan, R. 1970 The seasonal march of surface pressure gradients across India and the south-west monsoon. *Curr Sci*, **39**, 248–251.

Barnett, T.P. 1978 Estimating variability of surface air temperature in the Northern Hemisphere. *Mon Weather Rev*, **106**, 1353–1367.

Budyko, M.I. 1977 On present-day climatic changes. *Tellus*, **29**, 193–204.

De la Mothe, P.D. and Wright, P.B. 1969 The onset of the Indian south-west monsoon and extratropical 500-mb trough and ridge patterns over Europe and Asia. *Meteorol Mag*, **98**, 145–155.

Dey, B. and Bhanu Kumar, O.S.R.U. 1982 An apparent relationship between Eurasian spring snow cover and the advance period of the Indian Summer Monsoon. *J Appl Meteorol*, **21**, 1929–1932.

Flohn, H. 1964 The tropical easterly jet and other regional anomalies of the tropical circulation. *In* Proceedings of the symposium on tropical meteorology, Rotorua, New Zealand. Wellington, New Zealand Meteorological Service.

Hansen, J., Johnson, D., Lacis, A., Lebedeff, S., Lee, P., Rind, D. and Russel, C. 1981 Climate impact of increasing atmospheric carbon dioxide. *Science*, **213**, 957–966.

Hingane, L.S., Rupa Kumar, K. and Ramana Murty, Bh. V. 1985 Long-term trends of surface air temperature in India. *J Climatol*, **5**, 521–528.

Jones, P.D., Raper, S.C.B., Bradley, R.S., Diaz, H.F. Kelly, P.M. and Wigley, T.M.L. 1986a Northern hemisphere surface air temperature variations: 1851–1984. *J Clim and Appl Meteorol*, **25**, 161–179.

Jones, P.D., Raper, S.C.B. and Wigley, T.M.L. 1986b Southern hemisphere surface air temperature variations: 1851–1984. *J Clim and Appl Meteorol*, **25**, 1213–1230.

Koteswaram, P. 1958 The easterly jet stream in the tropics. *Tellus*, **10**, 43–57.

Kung, E.C. and Sharif, T.A. 1981 Long-range multi-regression forecasting of the Indian summer monsoon onset and rainfall with antecedent upper air pattern and sea surface temperature. *In* International conference on early results of FGGE and large-scale aspects of its monsoon experiments, Tallahassee, Florida. Geneva, WMO.

Maruyama, T.	1968	Time sequence of power spectra of disturbances in the equatorial lower stratosphere in relation to the quasi-biennial oscillation. *J Meteorol Soc Jpn*, **46**, 327–342.
Maung Tun Yin	1949	A synoptic–aerologic study of the onset of the summer monsoon over India and Burma, *J Meteorol Am Meteorol Soc*, **6**, 393–400.
Mitchell, J.M., jun., Dzerdzeevskii, B., Flohn, H., Hofmeyr, W.L., Lamb, H.H., Rao, K.N. and Wallén, E.C.	1966	Climatic change, Technical Note No. 79. Geneva, WMO.
Ramamurthi, K.M. and Keshavamurty, R.N.	1964	Synoptic oscillations of Arabian anticyclones in the transition season. *Ind J Met Geophys*, **15**, 227–234.
Subbaramayya, I. and Bhanu Kumar, O.S.R.U.	1978	The onset and the northern limit of the south-west monsoon over India. *Meteorol Mag*, **107**, 37–48.
Subbaramayya, I., Babu, S V. and Rao, S.S.	1984	Onset of the summer monsoon over India and its variability. *Meteorol Mag*, **113**, 127–135.

551.5:06(b)

Atmospheric research at the University of Manchester Institute of Science and Technology

C.P.R. Saunders

Department of Pure and Applied Physics, University of Manchester Institute of Science and Technology

Summary

This article gives brief descriptions of the research activities being carried out in the Department of Pure and Applied Physics at the University of Manchester Institute of Science and Technology. These include acid-rain studies at our field research station, the development of instrumentation for use in the field and on our instrumented aircraft which has flown in studies of maritime aerosol over South Uist, computer modelling of cloud development, a novel radar technique to discriminate between water and ice in clouds and a long-term investigation of thunderstorm electrification processes.

1. Introduction

The University of Manchester Institute of Science and Technology (UMIST) atmospheric physics group is in its 25th year. Founded by J. Latham, who brought with him from Imperial College, London an interest in thunderstorm electrification, the group now comprises over 40 people and, while the initial interests remain, research is now quite diverse. The group has research facilities in UMIST and at Great Dun Fell (GDF) in Cumbria, and it possesses an instrumented van and aircraft. Although laboratory-based work continues, recent emphasis has been in the field where our own instrument design and development has played an important role. Several members of the group have contributed résumés of their present studies which have been incorporated in this article to give the reader a broad outline of the work in hand. Some of our recent papers are listed in the references and bibliography section at the end.

2. Acid rain

A major experiment to investigate cloud chemical processes and the variation with altitude of wet deposition is being conducted at GDF in collaboration with the Department of Chemistry at UMIST, the Department of Environmental Sciences at the University of East Anglia, the Environmental Sciences Division at the Atomic Energy Research Establishment at Harwell and the Institute of Terrestrial Ecology (ITE) at Penicuik. Great Dun Fell is 847 m above sea level and forms part of the long ridge of the Pennine Hills, which runs from north-west to south-east, and lies to the north-east of the Eden valley. The prevailing south-west winds blow almost at a right angle to the ridge and form a cap cloud which envelops the site for parts of 250 days per year. The experiments performed to date have concentrated on the aqueous-phase oxidation of sulphur dioxide by hydrogen peroxide and ozone and also the deposition by rain-out (by the seeder feeder mechanism) of chemical species incorporated in the cloud droplets by nucleation scavenging or aqueous-phase chemistry. In collaboration with the Central Electricity Research Laboratories a series of experiments is also being conducted in which a plume of sulphur dioxide gas with sulphur hexafluoride tracer is released in the valley bottom and targeted on the summit. Collaboration is also being sought with the Department of Botany at the University of Manchester to investigate the effects of the deposition on the vegetation at GDF.

The experiments are centred on three sites; Fig. 1 shows the deployment of the apparatus. At site 1, the airstream upwind of the cloud is monitored for hydrogen peroxide, sulphur dioxide and ozone in the gas phase; the atmospheric aerosol is captured using an impactor and the size distributions of the hygroscopic particles are measured. Rainfall is measured and collected for chemical analysis. Site 2, the van site, is the mobile laboratory where gas-phase sulphur dioxide and ozone are measured, together with the cloud liquid-water content and droplet size distribution. Cloud water is collected for the continuous monitoring of acidity (pH) and aqueous-phase hydrogen peroxide using a luminol technique; separate samples are stored for later analysis by ion chromatography. An accoustic sounder is located at site 3 (for the remote sensing of the cloud top where entrainment is expected), together with a sonic anemometer for turbulence and occult deposition measurements. All site 2 measurements are repeated at site 3. In addition, cloud-water collectors are positioned at eight other sites on the hillside along with ITE rain-water collectors for hydrogen peroxide measurements and ion chromatography for the major anions and cations. The measurements have shown that when significant concentrations of sulphur dioxide are present in the airstream the hydrogen peroxide dissolved in the cloud water is consumed at a rate consistent with that predicted by recent laboratory studies.

When the cloud is affected by dry air entrainment from aloft, extra hydrogen peroxide is introduced. The results suggest that the concentration of hydrogen peroxide in the free tropospheric air entrained may be several times greater than that in the boundary-layer air in which the cloud forms. The reaction rate data suggest that the hydrogen peroxide–sulphur dioxide reaction is fast and is likely to be oxidant-limited. Consequently in many conditions, when oxidation by hydrogen peroxide is dominant

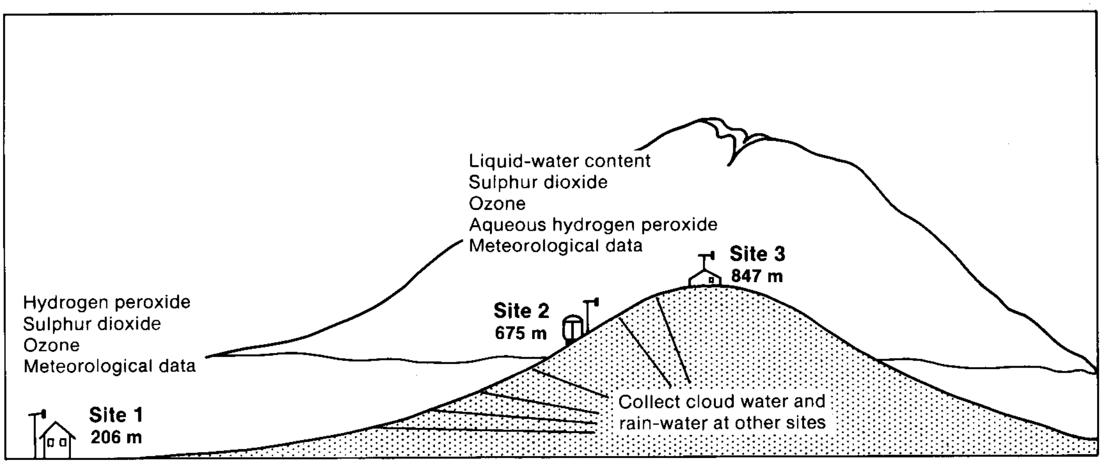

Figure 1. Locations of the three experimental sites on Great Dun Fell showing the elements measured at each.

over ozone due to low cloud-water pH, the rate of sulphate production may be controlled by the rate at which hydrogen peroxide can be entrained into a cloud system.

In the experiments carried out in November 1986 no significant sulphate production was observed. This is consistent with the very low hydrogen peroxide concentrations observed (equivalent to typically around 5 parts per thousand (by volume) in the gas phase), however, during the spring months hydrogen peroxide concentrations typically one hundred times greater than this have been detected using the same instrumentation. In these conditions significant sulphate production is observed.

A marked increase in the concentrations of the major ions in rain is found with altitude. On average, concentrations increase by a factor of two between 250 and 847 m. The increase in rainfall by a similar factor leads to a wet deposition rate of most ions at the summit of four times that at the valley sites. These changes can be accounted for by a quantitative description of the seeder feeder process in which the hygroscopic aerosol particles are incorporated into the feeder cloud droplets by nucleation scavenging and are then efficiently washed out by the raindrops entering the cloud from the seeder cloud above.

3. Instrumentation

The total water mixing ratio is an important parameter in understanding the interaction of a cloud with its environment since it provides information about the origin of air entrained into the cloud. This has provided the stimulus for the development of instruments to measure total water content, and a significant fraction of the group's instrumentation work has recently been directed to this end. Two approaches have been tried. The first uses rapid-response carbon hygristors to monitor cloud air sampled via an evaporator. This provides considerable temporal resolution but, in its most basic form, is subject to the poor long-term stability of this type of sensor. As a consequence the latest versions of this instrument incorporate an automatic re-calibration facility which largely eliminates this problem. The second approach involves a direct capacitive measurement of water vapour content which is potentially capable of faster response than the former technique. The hygristor-based instrument, in addition to its intended use in ground-based cloud evolution studies, has recently been used in the UMIST marine aerosol work to provide dew-point data. Since the sensor is operated at elevated temperatures it is less prone to salt contamination than the cooled-mirror type dew-point instrument used previously. The instrument is also being used on the Natural Environment Research Council HEXOS (Humidity Exchange Over the Sea) marine boundary-layer project to provide information on the vertical transport of water vapour.

4. Research aircraft

The research group operates a Cessna 182 aircraft for studies in cloud physics, atmospheric chemistry, aerosol physics and boundary-layer dynamics. The aircraft is flown with a crew of two and carries an equipment payload of up to 200 kg. Its flight performance permits measurements to be made up to an altitude of 6 km at air speeds in the range 25–27 m s^{-1} and the aircraft can remain airborne for up to 6 hours. To enable a wide range of measurements to be made in flight, certain modifications have been made to the aircraft. All internal equipment is installed on a single removable tray which fills the rear seat and luggage area and facilitates equipment changes. Two attachment points, one under each wing outboard of the propeller, are used to mount particle-sampling probes and other external sensors. Air-sampling intakes on the wing provide an isokinetic supply for a particle-sampling probe, a fast-response humidity sensor and a dew-point hygrometer via an air deceleration system. The electrical power available has been increased by converting the aircraft to 28 V, installing a 95 A alternator and a static inverter to provide 115 V a.c. Other parameters measured include air temperature from both Rosemount and reverse-flow thermometers, pressure altitude, radar altitude and air speed. The aircraft's position is obtained by recording signals from on-board equipment. The computer-based data acquisition system permits in-flight display of any parameter and data are recorded on to industry-standard magnetic tape.

5. Maritime aerosol

Field studies of maritime aerosol particles have been pursued by UMIST since 1979 in an attempt to characterize aerosol over the North Atlantic under a variety of meteorological conditions. Measurements, primarily with particle-sizing instruments covering the radius range 0.1 to 150 μm, have been made for several periods on the coast of South Uist in the Outer Hebrides, which possesses a relatively undisturbed exposure to the prevailing westerly winds. Initial measurements were undertaken in collaboration with a team from the Royal Aircraft Establishment, Farnborough, and other field projects have involved a Dutch team and flights by the Hercules aircraft of the Meteorological Research Flight. These studies have clearly demonstrated the dominant influence of wind speed on particle production at the sea surface and have also illustrated the effects of relative humidity and the depth of the atmospheric mixed layer upon the observed particle concentrations and size distribution (Exton *et al.* 1985). More recently, work has commenced at UMIST on the development of a simple maritime atmospheric boundary-layer model capable of predicting the particle concentrations throughout the mixed layer on the basis of the prevailing meteorological conditions. As a part of this programme, measurements made at South Uist over the past year have involved the UMIST instrumented aircraft as well as ground-based measurements. During August 1986, the aircraft flew for a total of about 50 hours over the sea, gathering data on particle concentrations and meteorological variables to provide vertical and horizontal profiles from 20 m up to cloud base. Also, UMIST had the good fortune (despite the damage sustained to various vehicles and equipment) to be present on the islands during the gales of March 1986 when particulate measurements were obtained with wind speeds approaching 100 m.p.h. Data from these projects are still being analysed.

6. Atmospheric modelling

For the last 10–15 years, fluid problems in plasma and astrophysics have been modelled by simulating a fluid as a collection of incompressible particles of defined radii (Monaghan 1985). However, this Lagrangian element approach (or 'smooth-particle hydrodynamics') has not been applied to fluid-flow atmospheric modelling. Conventional finite difference, spectral or finite element analyses use a Eulerian frame fixed relative to the earth's surface. UMIST research intends to simulate numerically some atmospheric fluid-flow problems by means of this novel technique. It is hoped that, for the case of atmospheric fluid flow, full advantage can be made of the ability to trace the fluid elements around a dynamical system. Water vapour and liquid water are carried around by the fluid elements. The 'blob-like' nature of clouds provides one of the main reasons for using this particular approach. It is also clear that more detailed microphysics could be included into these elements at a later date. However, there are problems with the representation of the thermodynamics in general, and the temperature gradients in particular. In addition the energy is transferred around the system by a series of 'shocks', which produce certain restrictions on the time step and tolerance required. The implicit advantages of using the system of ordinary differential equations, especially when compared with the numerical manipulations involved in obtaining the solutions for partial differential equations, lie in the well-studied stability criteria and error prediction which are available in the current numerical analysis literature. These studies have some similarities to other Lagrangian approaches (Cullen and Purser 1984) which are currently being investigated at other institutions.

At present it is felt that the model is in a suitable state to simulate two-dimensional cumulus cloud development in a 4 km wide box. A stable atmospheric ground state has been achieved, and the current simulation involves gradually increasing the boundary-layer ($<$ 500 m) temperature. It is anticipated, from the previous low-resolution test computations, that convection on different length scales will start to develop. It should be possible to examine, for example, the processes of fluid entrainment. There is a possibility that, if successful, there could be some collaboration with other scientists who are considering an observational programme of the same phenomena. A further long-term plan is to use the model and other numerical techniques to study flow over quasi two-dimensional ridges, using for comparison the measurements from the UMIST field station at GDF.

7. Radar

A new radar technique, using differential reflectivities, makes it possible to distinguish between raindrops and ice particles, to measure the mean size of raindrops and to make more accurate estimates of rainfall by remote sensing. The method was developed by our collaborators at the Rutherford Appleton Laboratory. Observations are made on the 25 m diameter antenna at Chilbolton, Hampshire, which has a beam width of only a quarter of a degree and is the largest steerable meteorological radar in the world. A conventional radar measures the back-scattered power, which is proportional to ND^6 (where N is the concentration of particles of size D) summed over all particle sizes. This power is generally expressed as the radar reflectivity factor, Z, which is the power in decibels (dB) relative to the power which would be scattered by one spherical raindrop of diameter 1 mm per cubic metre (the units of Z are denoted by dBZ). Fig. 2(a) shows values of Z in a vertical section through an active cumulonimbus. The heaviest precipitation is evidently at a range of about 87 km where Z exceeds 60 dBZ (i.e. Z is above 10^6 mm^6 m^{-3}). Various empirical relationships are available to convert Z into a rainfall rate, R, but these are not very accurate because the same rainfall rate can arise from various raindrop-size distributions which would have very different values of ND^6. An additional ambiguity arises because liquid water is a much better microwave scatterer than ice, but from Z alone we have no way of knowing whether the particles are raindrops or frozen hydrometeors.

The differential radar reflectivity measurements, Z_{DR}, can resolve some of these ambiguities. It is defined as $10 \log(Z_H/Z_V)$ where Z_H and Z_V are the radar reflectivity factors measured for horizontally and vertically polarized radiation. The shape of a raindrop is a unique function of its size; if the diameter is less than 1 mm, raindrops are essentially spherical so that Z_{DR} will be zero; larger raindrops are increasingly distorted so that Z_{DR} is positive with a magnitude which is a measure of the mean raindrop size. For ice particles the situation is more complicated, but in convective clouds the graupel particles and hailstones tend to tumble as they fall, so that on average Z_{DR} is zero. These interpretations of the radar signals have been confirmed by direct sampling of the precipitation particles using the Meteorological Research Flight C-130 Hercules aircraft (Bader *et al.* 1987, Cherry *et al.* 1984).

The values of Z_{DR} in Fig. 2(b) were taken simultaneously with Z. The freezing level on this day was at about 3 km; above this height Z_{DR} is essentially zero for all values of Z, suggesting that the particles are all frozen. Positive values are confined to regions below 3 km where the ice has melted to form aspherical raindrops, with a tendency for larger drops where Z is greater. If Z and Z_{DR} measurements are both available, then it is possible to estimate a mean raindrop size from Z_{DR} and, once the size is known, the concentration may be computed from Z. Knowing both the size and concentration of the raindrops leads to greater accuracy in rainfall estimates than those possible from Z alone. Of particular interest in the figure is a narrow region at a range of 87 km where zero values of Z_{DR} extend right down to the ground; it is believed that this is where hailstones are falling to the ground. Any interpretation in terms of small spherical raindrops would require unrealistically large concentrations to give the observed Z, with an equivalent rainfall rate of many millimetres per hour. This method appears to provide the first reliable way of identifying hail by radar, and further observations should show if it is possible to track the movement and development of hail swaths. Observations during the vigorous growth of convective clouds reveal transitory regions containing large supercooled raindrops where the temperature is as low

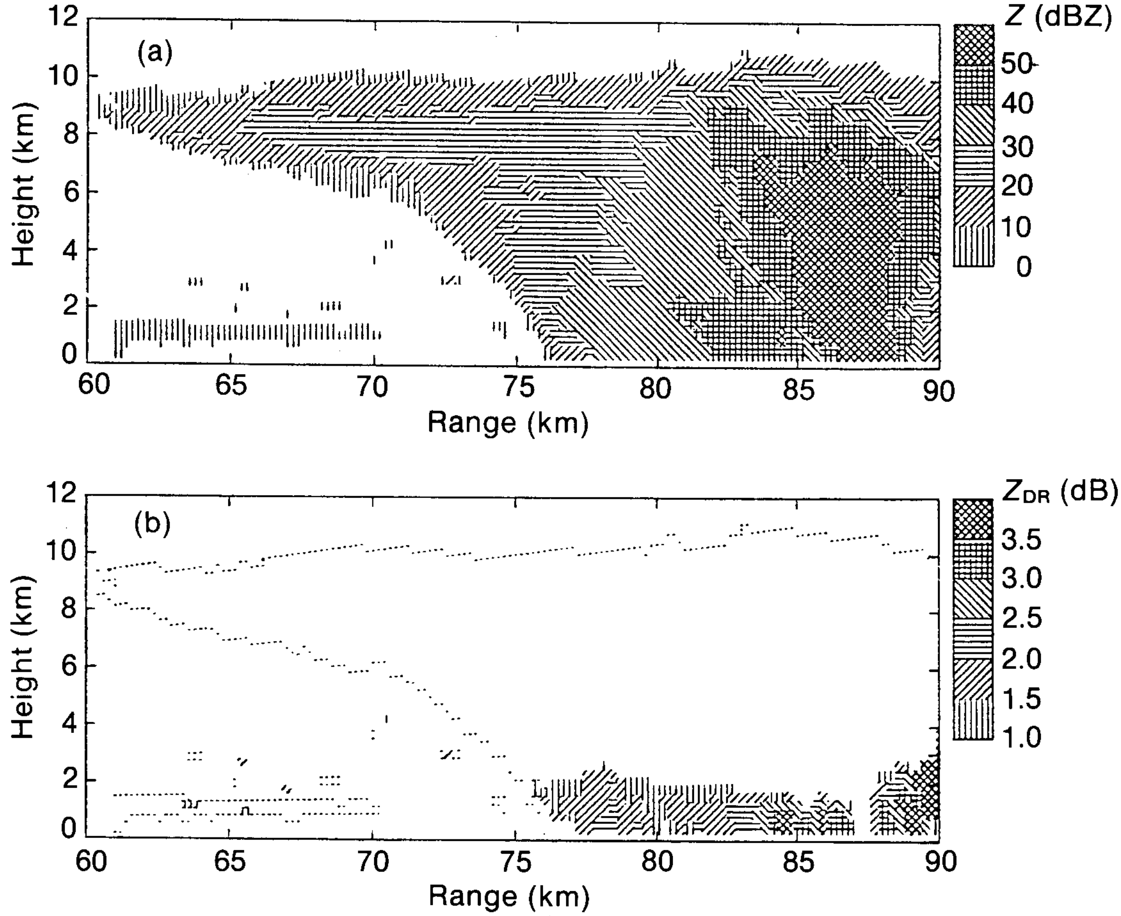

Figure 2. Contour plots of radar reflectivity (Z) and differential reflectivity (Z_{DR}), obtained from a vertical scan through an intense convective storm at 1336 GMT on 6 July 1983. (a) Z values expressed in dBZ above 1 $mm^6\ m^{-3}$. (b) Z_{DR} values in dB. To delineate the extent of the echo, the dotted lines taken from (a) surround the area where Z exceeds 0 dBZ. Hatching is used to denote areas where Z_{DR} exceeds +1 dB. The positive values of Z_{DR} below 2 km altitude are due to large raindrops falling with their horizontal axis larger than the vertical.

as −10 °C. Such regions would be hazardous to sample using an instrumented aircraft. The differential-reflectivity technique works well for water drops because the raindrop shape is a unique function of its size, but problems remain with ice particles which can be of different sizes, shapes, densities and fall modes. Further observations in 1987 with additional polarization parameters should remove some of these ambiguities.

8. Thunderstorm electrification

Laboratory studies of thunderstorm electrification processes have long been a major interest in the group. Over the last few years these have continued with the addition of collaborative field studies in the USA. Using cold rooms, thunderstorm conditions are simulated and ice crystals are made to collide with ice targets which represent soft-hailstones. During the collision and separation events, electrical charge is transferred. Comprehensive experiments covering a wide range of conditions have now shown that the sign and magnitude of the charge transfer is a function of the temperature, the ice crystal size, the impact velocity, the liquid-water content in the cloud and the impurity concentration in the droplets. This wide range of controlling parameters has meant that previous studies which have perhaps ignored some of the variables have produced conflicting results. The present work has now made the measurements reproducible by careful control of all the cloud conditions. In general, the results can be summarized as follows:

(a) adequate charge transfer to explain thunderstorm electrification requires ice crystal/soft-hailstone interactions to take place in the presence of supercooled water (crystals alone separate negligible charge),

(b) at temperatures above about −20 °C the soft-hailstone charges positively, while at lower temperatures it charges negatively, and

(c) the temperature at which the charge sign reversal takes place is controlled by the liquid-water content, so that higher liquid-water contents favour positive charging of the soft hail.

Thus, in a thunderstorm, charge transfer at high levels leads to negatively charged soft hail pellets which fall to form the negative charge region while the positive crystals are carried aloft. At lower levels, with reversed charging, the negative crystals are levitated and contribute to the negative region while the positive soft hail falls to form a lower positive-charge region. Such cloud electrification has been observed and there is increasing evidence that this conceptual model of charges on cloud particles is correct. Remote sensing has shown that lightning is often initiated from the level of charge sign reversal where the negative charges reside in regions of high radar reflectivity (Krehbiel *et al.* 1979). Collaborative flights in the USA have confirmed that charges exist on cloud particles in the boundaries between updraughts and downdraughts where maximum particle collision rates would be expected (Dye *et al.* 1986). However, the mechanism of charge transfer remains to be elucidated; work suggests that the sign is closely controlled by the precise conditions at the surfaces of both the interacting particles. Our aim is to completely resolve this question.

9. Concluding remarks

Over the years the interests of the research group have diversified considerably and no doubt this trend will continue as new questions arise and new interests are aroused. Nevertheless, throughout the group there is a strong unanimity of purpose, which is to help solve some of the outstanding problems in atmospheric physics.

Acknowledgements

The contributors to this article are T.W. Choularton, A. Gadian, M.J. Gay, A.J. Illingworth, C.S. Mill, M.H. Smith and I.M. Stromberg.

References and bibliography

Bader, M.J., Clough, S.A. and Cox, G.P. 1987 Aircraft and dual polarization radar observations of hydrometeors in light stratiform precipitation. *Q J R Meteorol Soc*, **113**, 491–515.

Baker, B., Jayaratne, E.R., Latham, J. and Saunders, C.P.R. (1987) The influence of diffusional growth rates on the charge transfer accompanying rebounding collisions between ice crystals and soft-hailstones. (Submitted to *Q J R Meteorol Soc.*)

Carruthers, D.J. and Choularton, T.W. 1982 Airflow over hills of moderate slope. *Q J R Meteorol Soc*, **108**, 603–624.

1986 The microstructure of hill cap clouds. *Q J R Meteorol Soc*, **112**, 113–129.

Chandler, A.S., Choularton, T.W., Dollard, G.J., Gay, M.J., Hill, T.A., Jones, A., Jones, B.M.R., Morse, A.P., Penkett, S.A. and Tyler, B.J. (1987) A field study of cloud chemistry and cloud microphysics at Great Dun Fell. (Submitted to *Atmos Environ.*)

Cherry, S.M., Goddard, J.W.F. and Ouldridge, M. 1984 Simultaneous measurements of rain by airborne distrometer and dual-polarization radar. *Radio Sci*, **19**, 169–176.
Choularton, T.W., Consterdine, I.E., Gardiner, B.A., Gay, M.J., Hill, M.K., Latham, J. and Stromberg, I.M. 1986 Field studies of the optical and microphysical characteristics of cloud enveloping Great Dun Fell. *Q J R Meteorol Soc*, **112**, 131–148.
Cullen, M.J.P. and Purser, R.J. 1984 An extended Lagrangian theory of semi-geostrophic frontogenesis. *J Atmos Sci*, **41**, 1477–1497.
Dye, J.E., Jones, J.J., Winn, W.P., Cerni, T.A., Gardiner, B., Lamb, D., Pitter, R.L., Hallett, J. and Saunders, C.P.R. 1986 Early electrification and precipitation development in a small, isolated Montana cumulonimbus. *J Geophys Res*, **91**, 1231–1247.
Exton, H.J., Latham, J., Park, P.M., Perry, S.J., Smith, M.H. and Allan, R.R. 1985 The production and dispersal of marine aerosol. *Q J R Meteorol Soc*, **111**, 817–837.
Hill, T.A. and Choularton, T.W. 1985 An airborne study of the microphysical structure of cumulus cloud. *Q J R Meteorol Soc*, **111**, 517–544.
Hill, T.A., Choularton, T.W. and Penkett, S.A. 1986 A model of sulphate production in hill cap cloud and subsequent turbulent deposition onto the hill surface. *Atmos Environ*, **20**, 1763–1773.
Illingworth, A.J., Goddard, J.W.F. and Cherry, S.M. 1987 Polarization radar studies of precipitation development in convective storms. *Q J R Meteorol Soc*, **113**, 469–489.
Jayaratne, E.R., Saunders, C.P.R. and Hallett, J. 1983 Laboratory studies of the charging of soft-hail during ice crystal interactions. *Q J R Meteorol Soc*, **109**, 609–630.
Krehbiel, P.R., Brook, M. and McCrory, R.A. 1979 An analysis of the charge structure of lightning discharges to the ground. *J Geophys Res*, **84**, 2432–2456.
Monaghan, J.J. 1985 Particle method for hydrodynamics. *In* Computer physics reports. Amsterdam, North-Holland Publishing.

An appreciation of the work of Mr D.E. Miller

K.H. Stewart

Director of Research, 1976–82, Meteorological Office, Bracknell

I worked very closely with Derek Miller for over 15 years, so I would like to complement the retirement notice in the last issue of this magazine with my own appreciation of Derek's work.

I first met Derek Miller when in 1959 he came to Kew from forecasting at London (Heathrow) Airport. He was certainly one of the first, perhaps the very first, full-time member of Met O 19 (now the Satellite Meteorology Branch). The task was to devise and construct equipment to measure ozone from the Ariel 2 satellite, within about 3 years, and a rocket version of the equipment had to be made and flown even earlier. The range of topics to be covered, problems to be solved and techniques to be mastered seemed, at times, to cover almost the whole range of classical physics, and the group was so small that everyone had to be aware of and contribute to all aspects. Derek's contributions and the stimulus provided by his keen and enquiring mind were outstanding, but even more important was the speed and thoroughness he showed in translating sketchy ideas into working hardware, with all peculiarities and imperfections explored and understood. His masterpiece was the no-moving-parts spectrometer to scan the spectrum from 250 to 400 n mile by the rotation of the rocket or satellite. In order to complete the detailed optical design of this, he was detached for a few weeks to the optical department of the Imperial College of Science and Technology, London; my impression is that he returned with a better understanding of practical ray-tracing than the staff at the College!

Another essential development was that of the test equipment for photometric measurements in the ultraviolet. This began as a fairly simple piece of commercial equipment but was developed over the next decade or so into an elaborate system of great versatility and, in Derek's hands, high precision, for measurements on a wide range of sensors.

In 1963 the satellite equipment was taken to the USA for 'integration' and testing. Derek spent several lengthy periods there and won considerable respect — not always liking — from the Americans for his thoroughness, his tenacious regard for the requirements of our experiments and the breadth and depth of his knowledge.

Unfortunately, early rocket and satellite experiments fell far short of total success. The main reasons were that the spinning motions of the vehicles were by no means as simple and regular as we had expected and that optical surfaces became contaminated, probably by out-gassing from surrounding materials.

The rest of the 1960s was spent in further rocket experiments (water vapour as well as ozone) in which these difficulties were gradually overcome, and in painstaking analysis of the flawed results of the earlier experiments. Derek's few papers on this work contain some valuable data but are chiefly impressive (in contrast with much other published work) for the completeness with which they analyse and overcome the difficulties and errors of the 'occultation' technique. Derek succeeded in rescuing a considerable amount of ozone data from the satellite experiment but could never be persuaded to publish this, because it had to be based on assumptions which were reasonable but whose validity could not be proved beyond question.

The next development was Derek's work in connection with Meteosat, beginning in the early 1970s. He did valuable work on many committees and working groups but his biggest contribution was to the study that defined the requirement for, and to a large extent the methods to be used by, the Ground Facility for a Geostationary Meteorological Satellite. This study laid the foundations for the effective exploitation of Meteosat data. It was the work of a very small group, including some of the brightest rising stars of the European Meteorological Services. I have the impression that Derek formed closer friendships within this group than within the Office, perhaps because the contacts were occasional and the project free of petty restrictions. Certainly he was, and is, regarded in European Space Agency (ESA) circles with great respect and, I think, affection.

Looking back on Derek's career, it seems to me the constant thread (against a background of first-class physical insight) has been a great thoroughness and a desire to master the details of every task, not in any dull and stodgy sense but with a keen spirit of enquiry that drives him to explore and understand every aspect. In the early days his fault was an unwillingness to delegate work or accept help — he found it quicker to do a job himself than to explain what needed doing. He was also so deeply immersed in his immediate project that he had little time or opportunity to relate it to the wider work of the Office. Over the years he has come to accept that people less bright and dedicated than himself have an essential contribution to make and has taken a steadily increasing interest in the work of the Office as a whole. All this, you might say, is no more than the normal development of a career and a personality, but my impression is that Derek started further back and has travelled further forward than most. He responded with enthusiasm to the increasing opportunities to apply to the mainstream work of the Office the expertise and authority in space matters he had acquired in his earlier work on the fringes of meteorology. In his work with ESA, and later as Assistant Director (Satellite Meteorology), to ensure that data from space were exploited to the full and made available to forecasters in the form best suited to their needs, his advocacy of the wider and fuller use of satellite data was all the stronger for his depth of understanding of the practicalities of the forecasting task.

Although I did not see it at first hand, I know that his horizons continued to expand over the last few years and that the qualities I admired in the early days have been evident in all his tasks.

Reviews

The elements of graphing data, by W.S. Cleveland. 164 mm × 233 mm, pp xii + 323, *illus*. Monterey, California, Wadsworth Advanced Books and Software, 1985. Price £20.85 (paperback).

This book aims to show us how to present data graphically in the clearest possible manner. The author points out that graphs are used in science and technology, both to help analysis and understanding of data, and to communicate the data to others.

Examples are given of badly-designed graphs (including some real howlers) from published papers. Many are reworked to show how they might have been better presented. The range of fields subjected to the author's scrutiny is huge: papers with titles ranging from 'Modulation of atmospheric carbon dioxide by the Southern Oscillation' to 'Transglutaminase-mediated modifications of the rat sperm surface in vitro' figure in the book.

The author goes on to discuss the basic elements of graph construction: tick marks, scales, legends, symbols, labels, etc. He makes the point that even such elementary features are often given insufficient thought, and suggests rules-of-thumb in their use.

The next chapter deals with graphical methods and introduces some ways of displaying data which are astonishingly new — the 'scatterplot matrix' for example was first discussed in the literature in 1983. Other techniques deserving consideration are:

(a) the Tukey sum-difference graph,
(b) Lowess — robust locally weighted regression (a smoothing technique),
(c) the Tukey box graph — indicates variation of measurements more effectively than error bars.

Finally the author deals with graphical perception — how accurately can the brain analyse different methods of representing data magnitudes (distance, area, angle, slope, shading density, colour hue, etc.).

Cleveland deals admirably with these topics, but one unfortunate omission (for us) is that contour maps are not discussed. Moreover, a few minor points he makes are open to question in my mind. Nevertheless, there is much here to provoke thought and encourage high standards of presentation of data.

Ideally, everyone interested in getting the most out of their data or presenting data clearly and concisely should have a copy handy.

T.S. Hills

Remote sensing digital image analysis, by J.A. Richards. 168 mm × 248 mm, pp. xvii + 281, *illus*. Berlin, Heidelberg, New York, London, Paris and Tokyo, Springer-Verlag, 1986. Price DM 138.00.

This book sets out to fill a gap between those texts on remote sensing and its applications, which treat digital analysis methods superficially, and those which are too mathematically detailed for the non-specialist to find of practical use. This gap certainly existed in the past, but this book succeeds in bridging it. It covers most of the topics encountered in remote sensing image analysis in a way which leaves the reader confident of being able to tackle such problems. Part of its success is in assuming little prior knowledge: there are appendices covering satellite orbits, vector and matrix algebra, fundamentals of probability and statistics, and even binary representation of numbers. However, the main reason this book is such a good introduction to the subject is not these useful appendices, but the many examples given throughout the text. In each chapter, a discussion of general principles is followed by numerical examples in sufficient detail that a reader could repeat the calculations and check them at every stage.

Where there are alternative solutions to a problem they are compared in terms of algorithm complexity and quality of results. Between five and ten problems are posed at the end of each chapter and have been selected to permit solutions to be obtained without recourse to a computer. Reference lists are provided for each topic and include a useful preamble comparing and contrasting the value of different references for different applications.

The topics covered include descriptions of specific satellite-borne instruments, error correction and image registration, contrast enhancement and geometric enhancement, multi-spectral transformations, Fourier transformation and several chapters on aspects of classification including supervised and unsupervised techniques, feature reduction, and practical strategies for classifying images. The depth to which each topic is explored is probably sufficient for anyone for whom image analysis is only part of their work. There are sufficient references for those who require more detail and there is advice on which references are most useful. Although the book maintains a good degree of generality there is a tendency to concentrate on the use of LANDSAT data in agricultural/ecological applications. From the point of view of a meteorologist there are a few disappointments about the book. The gross empiricism used in the correction of atmospheric effects and the definition of transmittance that leads to its dependence on zenith angle may offend the purist. The absence of any treatment of pattern matching, as used in cloud tracking, might be expected in an introductory text but the almost synonymous use of 'spectral' space and 'feature' space obscures the use of image properties such as texture as features in classification procedures.

There are a few minor irritations in the presentation of the book. In some chapters the number of typesetting errors is rather high. While this is little more than an annoyance in the text it can be quite serious in equations as in 5.2 where the convolution operation is wrongly defined. The index contains many entries which redirect the reader (e.g. Fourier Transformations, fast — see Fast Fourier transform). It is difficult to understand why publishers do this when it would be simpler to include the page number. For a relatively expensive book (DM 138 = £47.50) printed on very high quality paper the cover is extremely disappointing. In a subject as full of exciting imagery as remote sensing one might expect more than a monochrome representation of an image produced on a line printer! There are, nevertheless, some very good colour images inside.

It is customary to assume that books at this price will be purchased mostly by libraries but in this case that would be a pity. In spite of the cost I would recommend it to researchers and post-graduate students who use image analysis techniques and I am confident that it will quickly take on a well-thumbed appearance.

C. Duncan

Books received

The listing of books under this heading does not preclude a review in the Meteorological Magazine at a later date.

Statistical analysis of spherical data, by N.I. Fisher, T. Lewis and B.J.J. Embleton (Cambridge University Press, 1987. £35.00, US $65.00) aims to present a unified and up-to-date account of the methods of analysis of data in the form of directions in space. The emphasis is on applications of the statistical methods to the many relevant fields.

Satellite photograph — 6 August 1987 at 1359 GMT

The visible image shows the distribution of convective cloud over central and southern Britain on a day when marked sea-breezes were present within a cyclonically-curved, weak, west to north-west airflow.

Over southern England only small cumulus are present, except adjacent to the south coast where, according to surface observations, a sharp sea-breeze front had developed. The convergence line may be inferred from the image as being along the northern limit of the cloud area covering extreme southern England, and lies close to the coast in the west, but well inland over south-east England. Individual convective cells moved downwind (east to east-south-eastwards) towards the English Channel where they dispersed.

In contrast to the cloudiness over south-east England, the coastal strip of north-east France and the Low Countries is generally cloud free. Along these coasts, sea-breeze convergence is absent since the sea-breeze reinforces, rather than opposes, the light onshore wind. Similar cloud-free zones are seen over north-west facing coasts of Britain.

Infra-red data (not shown) indicated that all cloud tops terminated at low or middle levels, and reported precipitation was generally light, however, a waterspout was observed near Yarmouth, Isle of Wight.

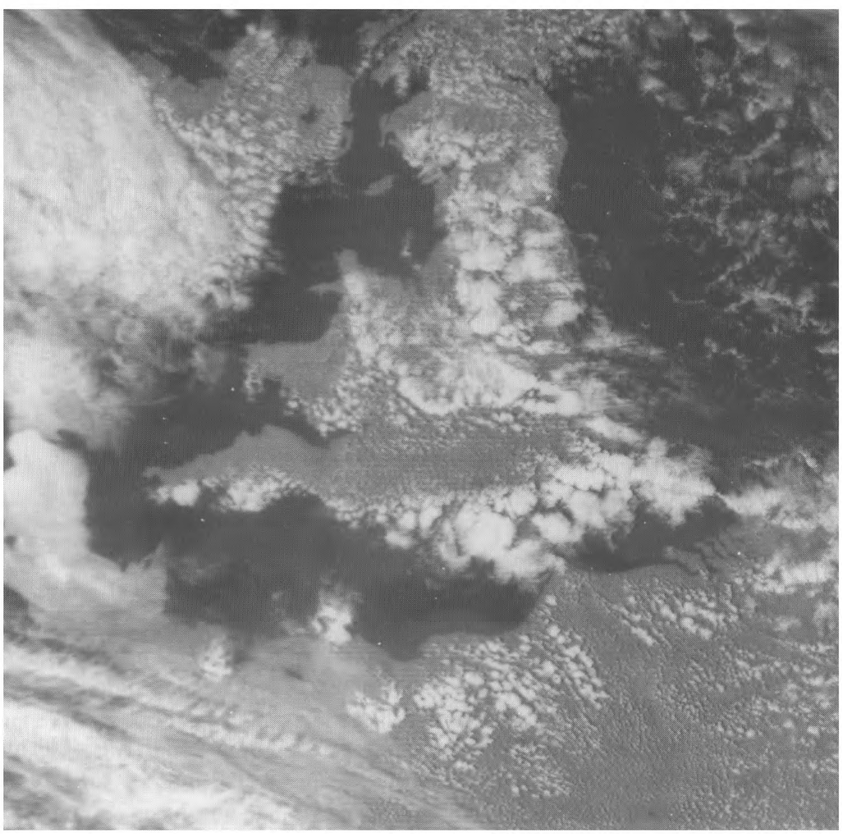

Photograph by courtesy of University of Dundee

Meteorological Magazine

GUIDE TO AUTHORS

Content

Articles on all aspects of meteorology are welcomed, particularly those which describe the results of research in applied meteorology or the development of practical forecasting techniques.

Preparation and submission of articles

Articles for publication and all other communications for the Editor should be addressed to the Director-General, Meteorological Office, London Road, Bracknell, Berkshire RG12 2SZ and marked 'For *Meteorological Magazine*'.

Articles, which must be in English, should be typed, double-spaced with wide margins, on one side only of A4-size paper. Tables, references and figure captions should be typed separately.

Spelling should conform to the preferred spelling in the *Concise Oxford Dictionary*.

References should be made using the Harvard system (author, date) and full details should be given at the end of the text. If a document referred to is unpublished, details must be given of the library where it may be seen. Documents which are not available to enquirers must not be referred to.

Tables should be numbered using roman numerals and provided with headings. We consider vertical and horizontal rules to be unnecessary in a well-designed table; spaces should be used instead.

Mathematical notation should be written with extreme care. Particular care should be taken to differentiate between Greek letters and Roman letters for which they could be mistaken. Double subscripts and superscripts should be avoided, as they are difficult to typeset and difficult to read. Keep notation as simple as possible; this makes typesetting quicker and therefore cheaper, and reduces the possibility of error. Further guidance is given in BS1991: Part 1: 1976 and *Quantities, Units and Symbols* published by the Royal Society.

Illustrations

Diagrams must be supplied either drawn to professional standards or drawn clearly, preferably in ink. They should be about 1½ to 3 times the final printed size and should not contain any unnecessary or irrelevant details. Any symbols and lettering must be large enough to remain legible after reduction. Explanatory text should not appear on the diagram itself but in the caption. Captions should be typed on a separate sheet of paper and should, as far as possible, explain the meanings of the diagrams without the reader having to refer to the text.

Sharp monochrome photographs on glossy paper are preferred: colour prints are acceptable but the use of colour within the magazine is at the Editor's discretion. In either case contrast should be sufficient to ensure satisfactory reproduction.

Units

SI units, or units approved by WMO, should be used.

Copyright

Authors wishing to retain copyright for themselves or for their sponsors should inform the Editor when they submit contributions which will otherwise become UK Crown copyright by right of first publication.

It is the responsibility of authors to obtain clearance for any copyright material they wish to use before submitting it for publication.

Free copies

Three free copies of the magazine are provided for authors of articles published in it. Separate offprints for each article are not provided.

Meteorological Magazine

October 1987

Editor: R.W. Riddaway

Vol. 116
No. 1383

CONTENTS

Contributions: it is requested that all communications to the Editor and books for review be addressed to the Director-General, Meteorological Office, London Road, Bracknell, Berkshire RG12 2SZ, and marked 'For *Meteorological Magazine*'. Contributors are asked to comply with the guidelines given in the *Guide to authors* which appears on the inside back cover. The responsibility for facts and opinions expressed in the signed articles and letters published in *Meteorological Magazine* rests with their respective authors. Authors wishing to retain copyright for themselves or for their sponsors should inform the Editor when submitting contributions which will otherwise become UK Crown copyright by right of first publication.

Subscriptions: Annual subscription £27.00 including postage; individual copies £2.30 including postage. Applications for postal subscriptions should be made to HMSO, PO Box 276, London SW8 5DT; subscription enquiries 01–211 8667.

Back numbers: Full-size reprints of Vols 1–75 (1866–1940) are available from Johnson Reprint Co. Ltd, 24–28 Oval Road, London NW1 7DX. Complete volumes of *Meteorological Magazine* commencing with volume 54 are available on microfilm from University Microfilms International, 18 Bedford Row, London WC1R 4EJ. Information on microfiche issues is available from Kraus Microfiche, Rte 100, Milwood, NY 10546, USA.

ISBN 0 11 727974 9 ISSN 0026–1149

Printed for HER MAJESTY'S STATIONERY OFFICE
Dd 240021 C14 10/87 (40711)

THE METEOROLOGICAL MAGAZINE

HER MAJESTY'S STATIONERY OFFICE

November 1987

Met.O.978 No. 1384 Vol. 116

METEOROLOGICAL OFFICE Met.O.978

THE METEOROLOGICAL MAGAZINE

No. 1384, November 1987, Vol. 116

551.575.1:551.501.796

Observations of the structure of a deep fog

R. Brown
Meteorological Office, Bracknell

Summary

Profiles of temperature, wind, visibility and net radiation through a deep radiation fog are presented. The emergence of an elevated layer in the pattern of echoes from an acoustic sounder is related to the development of a lapse rate within the fog. Significant features of the profiles, such as an elevated maximum in wind shear, are described. The remarkable constancy of the temperature of the fog through the night is discussed but cannot be fully explained without invoking advection.

1. Introduction

Findlater (1985) has presented the results of field investigations to evaluate the use of a low stopping-speed anemometer, a commercially-available acoustic sounder and a mini radiosonde system as aids to forecasting the development and dispersal of radiation fog. The data obtained from these instruments were also used to study the structure and development of radiation fogs. Most of the observations presented were obtained since 1982, however Findlater also considered the development of a radiation fog at Cardington on 17/18 October 1977. This was based upon temperature measurements made from the captive BALTHUM balloon which was used to make routine soundings of the boundary layer. On the same night a second captive balloon was in operation at Cardington during the period 2300–0500 GMT gathering data for studies of fog and stratocumulus by the Cloud Physics Branch of the Meteorological Office. This carried a comprehensive set of instruments and made observations with a much higher spatial and temporal resolution than the BALTHUM balloon.

Regrettably the fog data obtained during these studies has not been as widely published as the stratocumulus data, the latter being given priority because of its importance for both local forecasting and climate studies. Although not new, this data still gives a uniquely-detailed picture of the structure of a mature radiation fog and some of the observations are presented here in order to amplify the description of the fog given by Findlater, especially in the vicinity of the fog top. First,the development of a wet adiabatic lapse rate is described together with the concomitant affect on the acoustic sounder record. The central portion of the paper describes significant features of profiles of the important physical parameters, emphasizing their relationship to the fog top. Finally, using information from the profile data, the near constancy in time of the fog temperature is illustrated and then discussed in relation to the energy budget.

2. The experiment

2.1 *The experimental equipment*

The balloon-borne instrumentation comprised a thermistor, pressure transducer, point visibility meter (PVM), droplet spectrometer, two net-radiometers, two humidity sensors and a Cardington turbulence probe which made high-frequency measurements of temperature and wind. Ascents were made from 20 m above the surface to up to 75 m above the fog top.

A monostatic acoustic sounder was also in operation during the experimental period (not the commercial instrument used by Findlater). Measurements of the surface energy balance were made, comprising the net radiative flux, the soil heat flux and the latent heat flux (evaporation) from a weighing lysimeter. Further details of the instrumentation may be found in Slingo *et al.* (1982) and Caughey *et al.* (1982).

2.2 *Synoptic situation and surface observations*

On 17 October 1977 a stationary anticyclone centred over Europe produced a moist south to south-easterly flow over England. Fog from the previous night had lifted by 1200 GMT into stratus which soon dispersed to produce a warm cloudless afternoon. Surface cooling commenced by 1600 GMT, and by 2000 GMT the surface-based inversion had grown to a depth of 200 m as shown by the BALTHUM ascent. An increase in wind speed in the early part of the evening possibly prevented fog formation, although the visibility declined slowly to reach 2000 m by 2000 GMT. By 2200 GMT the visibility had decreased to 500 m and around 2230 GMT the fog thickened significantly, with the observer reporting 50 m at 2300 GMT. The appearance of a dense fog followed a decrease in surface wind speed after 2100 GMT from 3 to 1 m s^{-1} and also a decrease in dew deposition measured by the lysimeter. This ties in with the suggestion by Roach *et al.* (1976) that when the wind becomes light on a radiation night, turbulent mixing virtually ceases and therefore so does drying of the air by dew deposition. Radiative cooling of the air to the colder ground continues and can eventually lead to direct condensation into the air.

At around 2245 GMT it was still possible to see the fog top beneath the tethered balloon, this places it at about 15 m above the surface. Acquisition of data from the balloon-borne instrumentation commenced at 2300 GMT and by the time of the first ascent, 10 minutes later, the fog was 120 m deep. Thereafter it grew to a maximum height of 280 m by 0340 GMT and when recording ceased at 0500 GMT the fog was still 215 m deep.

3. Development of the temperature profile

The change in the temperature structure of the boundary layer caused by the deep fog, as measured directly and as indicated by the acoustic sounder, is shown in Fig. 1. The strength of the acoustic echoes is mainly determined by temperature fluctuations on the scale of about half the wavelength of the transmitted sound (0.1 m) (Crease *et al.* 1977). Thus the strongest echoes are received from regions experiencing turbulent mixing in the presence of a large temperature gradient. The pre-fog inversion is illustrated by data from the 2000 GMT BALTHUM ascent. At the time of the first ascent of the fully-instrumented balloon (2315 GMT) the fog was already 100 m deep and the pre-fog inversion had been transformed to an isothermal profile. The irregular temperature profile between 100 and 130 m resulted from a few minutes pause in the ascent during which the local fog-top ascended another 40 m. The final transit throughout the fog top is marked on Fig. 1(a) by horizontal bars indicating a visibility of 100 m and 500 m measured by the PVM. Although the evidence presented in section 2 suggested that dense fog may have formed locally at the surface, the dramatic increase in fog depth over a 30-minute period was most likely caused by the advection of a pre-existing fog bank. The other two profiles shown in Fig. 1(a) (0020 and 0230 GMT) illustrate the upward growth of the fog and the transition from an isothermal to a wet adiabatic lapse rate within the fog.

The transition to a wet adiabatic lapse rate produced a dramatic change in the pattern of echoes from the acoustic sounder, as shown in Figs 1(b), 1(c) and 1(d). At the start of the observational period (2245–2320 GMT) a continuous zone of echoes extended from the surface to around 200 m (Fig. 1(b)). Such a pattern is typical of the stable boundary layer, and the echo region coincides with the surface-based inversion and the region of significant wind shear as measured by the BALTHUM earlier. Before 2250 GMT the fog was too shallow to affect the structure of the inversion, however we know that by about 2315 GMT the rapid deepening of the fog locally was associated with an isothermal profile below 100 m. This transformation had little affect on the echo pattern although a slight weakening of the echo below 100 m may be discernible. One hour later (Fig. 1(c)) the echo strengths below 130 m have decreased noticeably, whilst between 170 m and 200 m they have increased, the net effect being the emergence of an elevated echo layer. (This process is partly obscured by a permanent-echo layer between 130 and 150 m caused by spurious returns from a nearby building; this is also seen on Fig. 1(d).) Since the fog top was found to be at about 150 m at 0020 GMT, it lay beneath the developing elevated echo layer. The top of this layer still coincided with the top of the pre-fog inversion. By 0200 GMT the elevated echo layer was clearly defined with few echoes being received from the body of the fog (Fig. 1(d)). At 0235 GMT the fog top was found at 215 m, within the elevated echo layer. As shown later, this relationship persisted to the end of the observational period. The environment leading to the generation of small-scale temperature fluctuations in the vicinity of the fog top is described in detail in section 4; basically this is a region where an elevated inversion coincided with enhanced wind shear and strong radiative cooling.

4. The profile data

Examples of profiles of the basic physical parameters are shown in Figs 2(a), 2(b) and 2(c). The plotted points are instantaneous values sampled at 10-second intervals. Allowance has been made for the vertical separation of the instruments on the balloon cable which totalled 8 m. The point visibility meter measures extinction coefficient (σ) and this has been plotted against height. The visibility (V) is related to the extinction coefficient by Koschmeider's formula $V = 3.0/\sigma$. Using this relationship a scale of visibility has also been included on Figs 2(a), 2(b) and 2(c). The position of the elevated echo layer has also been delineated. The profiles have many similarities and also some interesting differences, not all of which can be explained.

4.1 *Visibility*

The first interesting feature to note is that this fog did not exhibit a marked or consistent decrease of visibility with increasing height, as has been reported by others, e.g. Pinnick *et al.* (1978). Of course it is apparent to the casual observer that the density of fog exhibits small-scale fluctuations. Features such as the minimum in visibility around 100 m in Fig. 2(b) are probably indicative of such fluctuations, rather than of the mean vertical profile. However most profiles show no trend in visibility with height, or a region of increasing visibility as in Fig. 2(b). Two of the ten profiles showed a slight decrease of visibility with height and one of these is reproduced in Fig. 2(a). The visibility has also been calculated from the fog droplet size distributions, these profiles (not illustrated) show a similar trend with height to the PVM data. Visibility profiles obtained in several other fogs at Cardington were similar to those shown here. Since the profiles terminated at 20 m above the surface it is possible that a gradient in visibility existed beneath this. The observer consistently reported a greater visibility than measured by the PVM on this night but it is dangerous to read too much into this because we do not know how comparable the two estimates are.

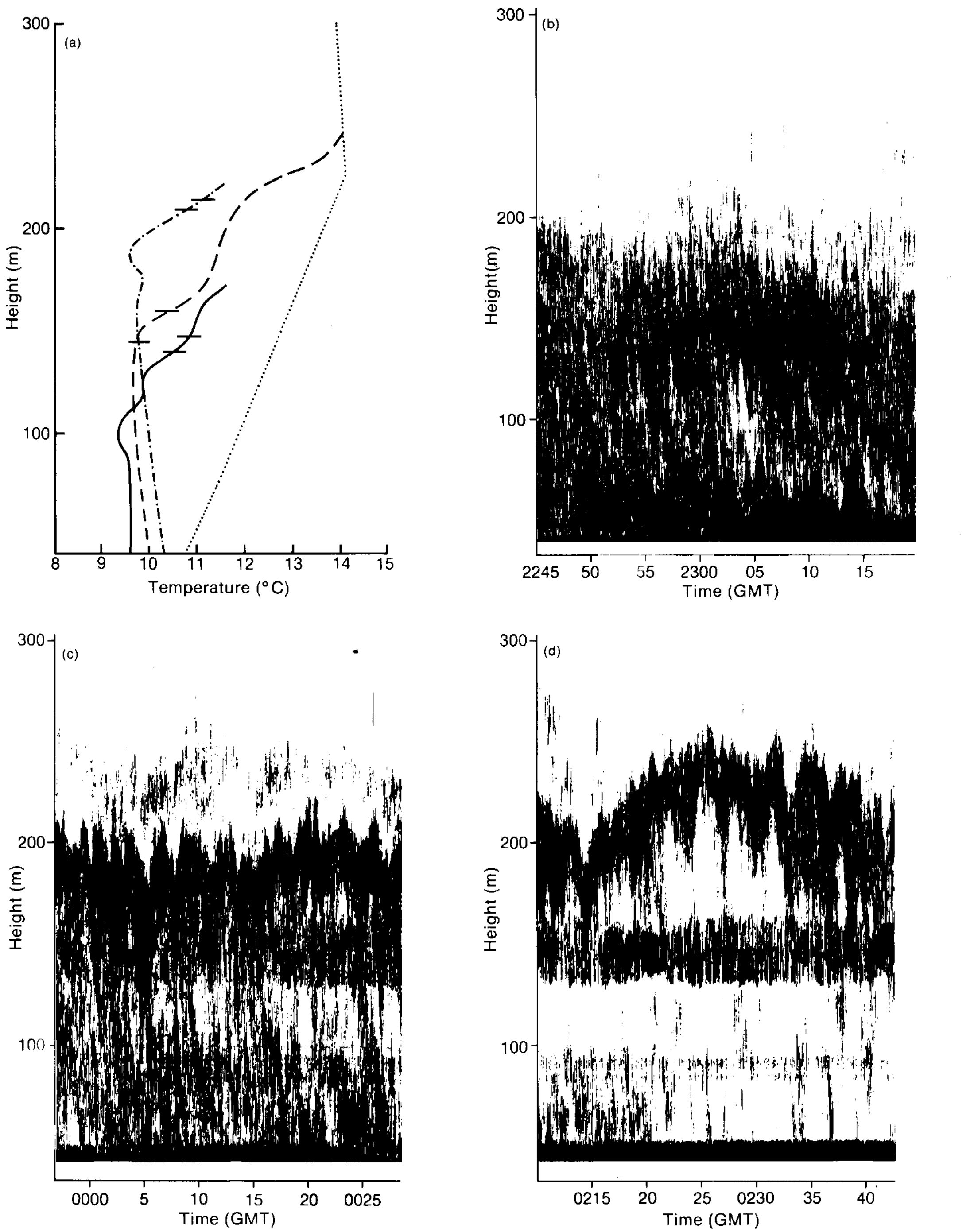

Figure 1. (a) Temperature soundings for 17/18 October 1977 at 2000 GMT(dotted line) (BALTHUM), 2315 GMT(solid line), 0020 GMT(dashed line) and 0230 GMT(dot-dash line); horizontal bars indicate visibilities of 500 m (upper bar) and 100 m (lower bar) measured by the point visibility meter. (b), (c), (d) Acoustic sounder records for the period in which the soundings in (a) were made.

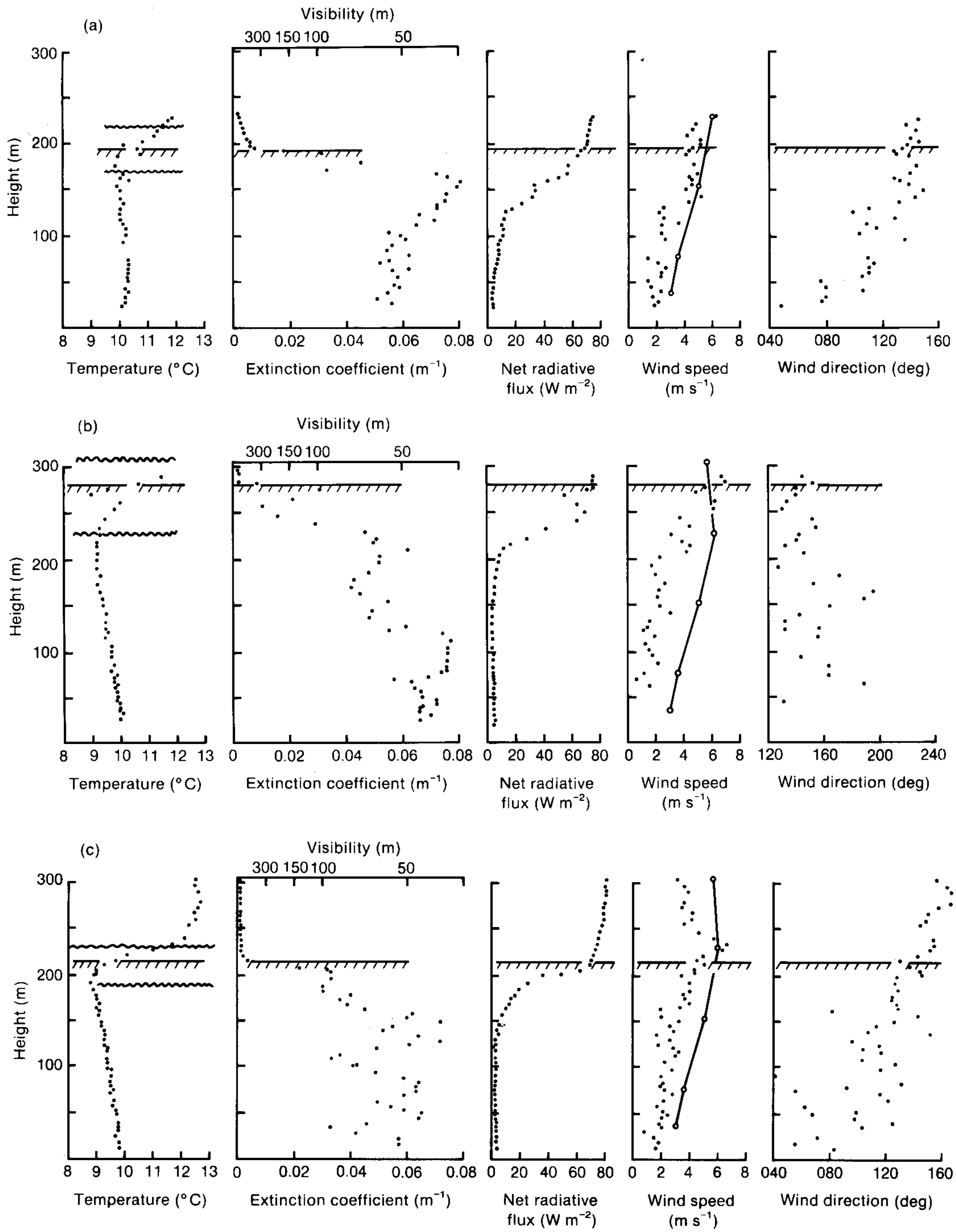

Figure 2. Profiles of temperature, extinction coefficient, net radiation and wind for (a) 0042–0047 GMT, (b) 0347–0355 GMT and (c) 0451–0500 GMT on 18 October 1977. The position of the elevated acoustic echo is marked and the fog top. The wind-speed profile from the 1700 GMT BALTHUM ascent is shown as .

4.2 *Fog top*

In discussing the other profiles the obvious reference point is the fog top. A complication now arises because the meteorological definition of fog, visibility less than 1000 m (extinction coefficient >0.003 m^{-1}), is not relevant to the physical processes responsible for the changes in the boundary-layer temperature structure. In particular unless the visibility is less than 200–300 m the fog liquid water content will be too low to produce significant radiative cooling. Therefore in the rest of the discussion 'fog top' will refer to the top of the dense fog. This has been marked on Figs 2(a), 2(b) and 2(c) as the height where the visibility rises above 300 m (extinction coefficient falls below 0.01 m^{-1}).

As noted by Findlater (1985), the fog-top inversion extended into the fog. The high-resolution profiles show that sometimes the inversion base was well-defined and located close to the fog top, as in Fig. 2(c). Other profiles show the inversion merging into an isothermal layer, up to 40 m beneath the fog top, as in Fig. 2(b). On average the fog top was 25 m (standard deviation 15 m) above the inversion base. This is half the distance quoted by Findlater for the same fog. It is very likely that the difference arises from the poorer resolution of the BALTHUM ascents used by Findlater. Another factor may be the 10-minute sampling time used by the BALTHUM at every level; the fog top can fluctuate by a few tens of metres over this period. Even the continuous ascents presented here were affected by fluctuations in the fog-top height. For example the profiles illustrated in Fig. 2(b) were obtained whilst the balloon was descending. As the instruments entered the fog, the temperature fell to 9 °C and the net radiative flux also started to decrease. However at 270 m the instruments started to emerge from the fog, the temperature rose by 1 °C and the net radiative flux increased again. Either a detached patch of cold, thick fog was blown past the instruments at 280 m or the fog top descended faster than the instrument package locally.

Figs 2(a), 2(b) and 2(c) show that the elevated echo-layer coincided with the fog-top inversion and that the fog top lay within the echo layer. On average the fog top lay 25 m (standard deviation 13 m) beneath the top of the elevated echo-layer and was always contained within it. When interpreting this statistic it should be noted that the resolution of the acoustic sounder was 8 m on this occasion. (As mentioned earlier, before the emergence of the elevated echo-layer the fog top was not closely associated with the top of the echo layer.)

4.3 *Net radiative flux*

The net radiative flux profiles show that there was a net radiative loss from the fog top of about 70 W m^{-2}. The radiative cooling rate is proportional to the vertical gradient of the net radiative flux. It can be seen from Figs 2(a), 2(b) and 2(c) that the largest radiative cooling is found beneath the fog top (as defined earlier), within a layer about 70 m thick. The value is typically 3 °C h^{-1}, averaged over this layer.

A less obvious but still significant factor is the small gradient of net flux above the top of the dense fog. This indicates radiative cooling of the air above the fog to the colder fog top. The gradients in Figs 2(a) and 2(c) represent cooling rates of 0.35 and 0.55 °C h^{-1} respectively. This cooling is analogous to the radiative cooling of the air to the colder ground which can initiate fog formation at the surface. When the relative humidity above the fog is high, radiative cooling can lead to condensation and hence the deepening of the fog.

4.4 *Wind speed and direction*

The wind speed profiles show a marked shear beneath, and sometimes through, the fog top. Inspection of all the profiles reveals a tendency for three types to occur. Sometimes there is a sharp discontinuity in wind speed a few tens of metres beneath the fog top, as in Fig. 2(a). In other profiles the shear extends over a greater depth, as in Fig. 2(b), but is still contained within the thick fog. Finally the shear can extend through the fog top, as in Fig. 2(c). This profile is atypical, however, in that it is the only one in which the wind speed decreases markedly above the fog. Also plotted on Figs 2(a), 2(b) and 2(c) is the wind speed profile from the 1700 GMT BALTHUM (no winds are available from the 2000 GMT ascent). It can be seen that the maximum wind speed varies little through the night but relative to the 1700 GMT profile a deficit develops within the body of the fog, leading to the elevated shear-layer. The reason for this is discussed later. The wind direction was around 140° above the fog, backing to 080° towards the surface. The directional shear tended to decrease through the night, occasionally almost disappearing as in Fig. 2(b). This change cannot be explained at present. As with the wind speed some profiles show a marked change in direction a few metres beneath the fog top (e.g. Fig. 2(a)). Other profiles show a more gradual change, sometimes extending through the fog top (e.g. Fig. 2(c)). This profile also shows a marked decrease in the variability of wind direction above 160 m, which is indicative of a decrease in turbulent mixing in the capping stable-layer.

Brown (1980) has shown that a one-dimensional numerical fog model can reproduce the observed behaviour of the wind field within a mature fog. The model indicated that increased mixing within the fog (relative to the fog-free case) led to enhanced transfer of momentum to the surface. At the same time transfer of momentum from above was inhibited by the fog-top inversion. This caused a reduction in wind speed within the body of the fog (up to the top of the adiabatic region) and enhanced shear through the elevated inversion.

5. Constancy of fog temperature with time

Despite the radiative loss from the fog-top, the temperature of the fog changed little during the observational period. This is shown in more detail in Fig. 3 where the fog-top height and the temperature at several levels, including the base of the elevated inversion, have been plotted as a function of time. Unfortunately there is a gap from 0100 to 0230 GMT because of an instrument failure. From 2300 to 0100 GMT there was a rise in temperature of about 0.5 °C. The fall in temperature at 140 m was caused by the fog growing through this level between 2330 and 2350 GMT. From 0230 to 0500 GMT the temperature fell by 0.5–0.7 °C. The net result is that the temperature within the body of the fog was virtually the same at 0500 and 2300 GMT. The temperature at the inversion base fell by about 0.6 °C between these times as a result of the upward growth of the fog and the wet adiabatic lapse rate within it.

To understand this remarkable constancy of temperature we must consider the energy budget of the fog. It must be admitted at the outset that it is not possible to explain fully the observed temperature trend since advective changes appear to be important. If we consider first the cooling of a layer 200 m deep due to the observed radiative loss from the fog top and only offset by the soil heat flux (which in this case was very small, around 10 W m^{-2}), then this amounts to 0.9 °C h^{-1}. If we make the reasonable assumption that the fog-laden air is saturated, so that any cooling leads to further condensation and the release of latent heat, then the cooling rate is reduced to just under 0.4 °C h^{-1}. This is still much larger than observed, implying a cooling of 2.5 °C between 2300 and 0500 GMT.

An important factor is missing from this calculation. As the fog grows upwards, warm air from above the fog is incorporated into the body of the fog. Therefore part of the radiative cooling must be utilized in cooling this air to the temperature of the fog. In terms of the energy budget, the mixing of warm air into the fog can be represented as a downward heat flux through the fog top. The magnitude of this depends upon the temperature difference between the fog and the air above and also how fast the fog grows upwards (assuming negligible subsidence). This suggests that in order for the fog temperature to remain constant or increase it must continue to grow upwards, once growth ceases cooling should commence, which will be observed locally if advective effects are negligible. There is some support for this in Fig. 3, although cooling appears to set in before 0400 GMT whilst the fog is still deepening locally. If we assume that the fog grows upwards at 30 m h^{-1} (the mean local rate between 2330 and 0330 GMT) and the fog-top temperature difference is 2 °C, then the fog would cool at between 0.14 and 0.25 °C h^{-1}. The

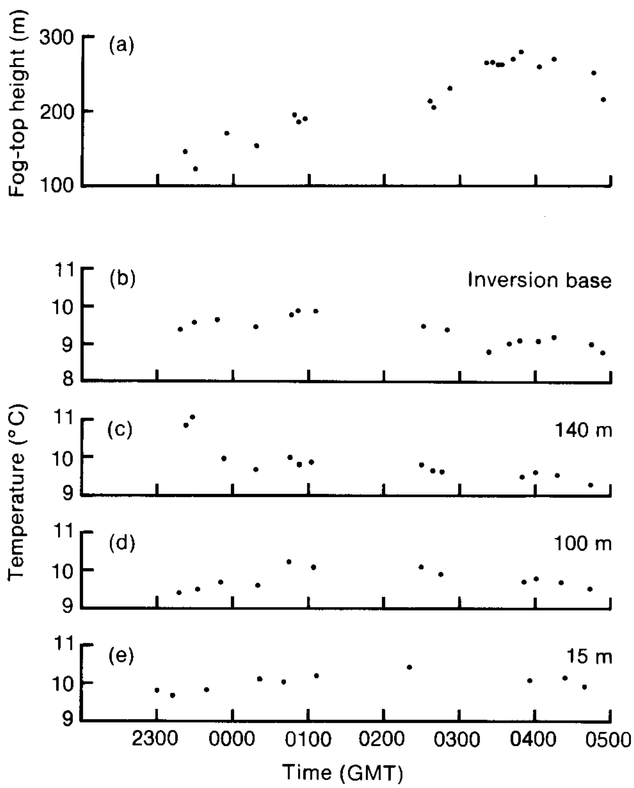

Figure 3. (a) Fog-top height as a function of time. Temperature as a function of time at (b) the inversion base, (c) 140 m, (d) 100 m and (e) 15 m above ground level.

range of values arises from the uncertainty in the measurement of the fog-top step in humidity mixing ratio. Thus the local rate of growth cannot account for the observed temperature rise until 0130 GMT and one must invoke warm advection to explain the difference. Assuming a wind speed of 4 m s^{-1} a temperature gradient of about 3 °C 100 km^{-1} would be required. There is no indication of a gradient of this magnitude from the synoptic reports upwind and downwind of Cardington, and to resolve the discrepancy further would require detailed ascents to have been made at another one or more stations.

6. Conclusions

The structure of the mature fog is best summarized by dividing the temperature profile into three regions as shown in Fig. 4.

Region A : The portion of the inversion above the top of the dense fog. Radiative cooling to the cold fog-top can lead to condensation here and hence the upward growth of the fog. The base of this region is also a source of strong acoustic-sounder echoes.

Region B : The portion of the inversion containing the dense fog. The radiative cooling rate was several degrees per hour here, yet locally the temperature changed little. Factors which can have offset the cooling include the mixing in of warmer air from above the fog, release of latent heat, and weak convective transport of heat from below. Bennetts *et al.* (1986) have described a similar situation at the top of nocturnal stratocumulus. There the radiatively-cooled air at the cloud top descends as cold downdraughts, entraining warmer air from above the cloud and also inducing compensating warm updraughts. However, there is a difficulty in applying this picture to explain the constancy of the fog-top temperature. Within stratocumulus the adiabatic layer (region C) extends close to the cloud top with the inversion laying mainly above the cloud. However, the definition of region B reflects the fact that the inversion extends tens of metres into the fog. It is difficult to understand how radiatively-cooled air can sink through this environment. It seems likely that transport is effected by small-scale turbulence generated by the wind shear which is most pronounced within this region. This would also generate the temperature fluctuations necessary to produce the strong acoustic echoes observed from region B.

Region C : A well-mixed region as a result of weak convection generated by warming at the surface and radiative cooling at the top. The latter results from the fact that significant radiative cooling often extended beneath region B. The absence of acoustic sounder echoes from much of this region indicates negligible small-scale temperature fluctuations, despite the convection. Ascending and descending air parcels tend to follow a wet adiabat and so deviate little from the 'local' temperature. In other radiation fogs well-marked acoustic echoes, associated with convective plumes, have been observed to extend upwards from the surface (e.g. Plate III, Crease *et al.* 1977). However on this night the soil heat flux and hence the surface warming were atypically low. Occasionally, weak surface-based echoes can be seen (e.g. Fig. 1(d)) around 0215 GMT.

Although we now have some understanding of the evolution of the above structure (see for example Fig. 1, Findlater 1985), the method by which the fog grows upwards is not fully understood, nor the factors which limit the depth to which a fog can grow. For example, upward growth could be halted if the fog encountered a very dry layer. Although the humidity measurements were of poor quality in this case, there was no evidence of a very dry layer above the fog as generally encountered above stratocumulus, and the relative humidity within 50 m of the fog top probably exceeded 95%. In the numerical model referenced earlier (Brown 1980), upward growth of the fog is mainly caused by radiative cooling in region A leading to condensation. However, the model consistently underestimates

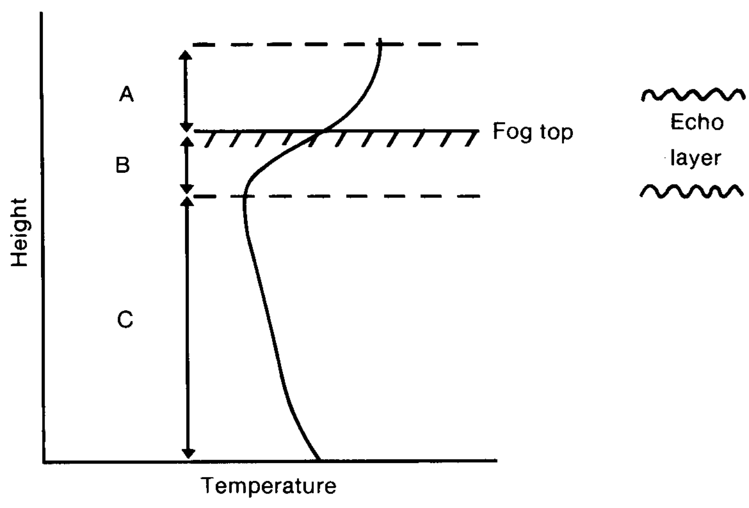

Figure 4. Idealized model of the structure of the fog.

the growth rate, for example in simulations of this case the model took 6 hours to grow the fog to a depth of 80 m. This suggests that turbulent mixing also plays an important role in the upward growth (which the model appears to underestimate).

It is possible to envisage a feedback mechanism whereby turbulence could be maintained through the fog-top inversion by the elevated maximum in wind shear. Suppose the turbulence in regions A and B decayed because the effect of stability predominated. Without the mixing in of warm air from above the fog or transport from beneath, region B would be cooled radiatively and hence region C would start to grow closer to the fog top. Upward growth of the fog would also be slowed by the cessation of turbulence. Hence the temperature gradient and wind shear aloft would tend to increase, since the changes in temperature and wind would occur over a smaller vertical distance. The flow will become turbulent again when the Richardson Number (*Ri*) falls below a critical value. *Ri* may be written in its gradient form as

$$Ri = \frac{g}{\theta}\frac{\Delta\theta\,\Delta z}{(\Delta V)^2} \qquad \ldots \ldots \ldots \ldots \ldots \ldots \quad (1)$$

where g is the acceleration due to gravity, θ the potential temperature and $\Delta\theta$, ΔV the differences in potential temperature and wind across layer depth Δz. Equation (1) shows that if the differences in temperature and wind remain constant but Δz decreases, then *Ri* decreases. Once it falls below a critical value turbulence will ensue, enhancing the upward growth of the fog and increasing Δz again. It is also likely that the presence of gravity waves in the stable layer (a probable cause of the undulating nature of the elevated echo layer) will result in the shear being enhanced periodically. Further measurements are required to confirm these suggestions.

Acknowledgements

The author wishes to express thanks to Dr S.J. Caughey for providing the acoustic sounder record and to Mr J. Turton for the model results. Thanks are also due to all those members of the Cloud Physics and Boundary Layer Branches of the Meteorological Office who developed the instrument package and participated in the field experiment.

References

Bennetts, D.A., McCallum, E., Nicholls, S. and Grant, J.R.	1986	Stratocumulus: an introductory account. *Meteorol Mag*, **115**, 65–76.
Brown, R.	1980	Some field observations of radiation fog and their interpretation. *In* Communications à la VIIIème conférence internationale sur la physique des nuages, Clermont-Ferrand, 15–19 juillet 1980, Vol. II. Clermont-Ferrand, UGGI.
Caughey, S.J., Crease, B.A. and Roach, W.T.	1982	A field study of nocturnal stratocumulus. II. Turbulence structure and entrainment. *Q J R Meteorol Soc*, **108**, 125–144.
Crease, B.A., Caughey, S.J. and Tribble, D.T.	1977	Information on the thermal structure of the atmospheric boundary layer from acoustic sounding. *Meteorol Mag*, **106**, 42–52.
Findlater, J.	1985	Field investigations of radiation fog formation at outstations. *Meteorol Mag*, **114**, 187–201.
Pinnick, R.G., Hoihjelle, D.L., Fernandez, G., Stenmark, E.B., Lindberg, J.D. and Hoidale, G.B.	1978	Vertical structure in atmospheric fog and haze and its effects on visible and infrared extinction. *J Atmos Sci*, **35**, 2020–2032.
Roach, W.T., Brown, R., Caughey, S.J.,Garland, J.A. and Readings, C.J.	1976	The physics of radiation fog: I — a field study. *Q J R Meteorol Soc*, **102**, 313–333.
Slingo, A., Brown, R. and Wrench, C.L.	1982	A field study of nocturnal stratocumulus; III. High resolution radiative and microphysical observations. *Q J R Meteorol Soc*, **108**, 145–165.

551.515.1:551.507.362.2

The development of an extraordinary depression — a satellite perspective

J.N. Ricketts
Meteorological Office, Bracknell

Summary

Data from the Advanced Very High Resolution Radiometer (AVHRR) on the American TIROS-N series of spacecraft provide high-resolution imagery of cloud tops and the earth's surface. Considerable detail can be observed in an AVHRR picture, but a further dimension is given to the study of atmospheric developments by the examination of a series of pictures. This article describes the evolution of cloud systems associated with the development of the deepest extra-tropical Atlantic depression ever recorded. The work took advantage of the availability of four daily passes over the area, from the combination of NOAA-9 and NOAA-10 satellites in orbit. Movie-loops of Meteosat images were also used to study the movement of cloud within the associated fronts as they crossed the British Isles.

1. Introduction

The period from late afternoon on 13 December to midnight on 15 December 1986 saw the generation of the deepest depression analysed over the North Atlantic (Burt 1987). This rapid development was followed by equally rapid decay over the next 24 hours. The depression originated from the merging of two lows; one started as a wave and was centred about 300 n mile south-south-east of Newfoundland at 1800 GMT on 13 December, while the other was a small low situated about 600 n mile to the north-east of the wave. The wave moved north-eastwards at an average speed of 75 kn over the next 12 hours, merging with the other low during the morning of the 14th. The central surface pressure of the wave fell 30 mb in the 12 hours to 0600 GMT on 14 December, followed by explosive development with a fall of 26 mb over the next 6 hours. The lowest analysed surface pressure was 916 mb at 60° N, 35° W on the midnight chart of 15 December.

Satellites are uniquely situated to provide an overall view of such developments (Schwalb 1978). NOAA-10 had been launched in September 1986 so, with NOAA-9, there are now two polar-orbiting satellites from which four Advanced Very High Resolution Radiometer (AVHRR) images can be taken each day. It was decided to make a detailed study of a series of these images so that important features might be revealed which may be common to similar such intense developments.

2. Image processing

The Satellite Meteorology Branch of the Meteorological Office uses the HERMES system (Turner *et al.* 1985) to convert raw data from meteorological satellites into useful imagery. A processed image can then be examined to identify features of a weather system, such as size, shape or cloud-top temperatures. An image is made up of pixels, rather like the dots which go to make up a newspaper photograph. Each pixel can have any one of 256 possible colours, normally represented by grey shades between white and black. In the case of an image from an infra-red sensor, this represents 256 possible temperature values. It is customary to select the colours such that the lowest temperature appears white and the highest black.

The HERMES system is capable of replacing the black and white shading with a range of colours. This is sometimes quite pretty to look at, but is of limited use. A better technique is selective colour enhancement. This involves replacing specified ranges of grey shading by a selected colour, while the other ranges stay unchanged. The colours are made up of combinations of the primaries red, green and blue. Figs 1 to 8 are pictures taken during passes over the centre of the depression throughout most of its lifetime by NOAA-9 and NOAA-10 satellites. The palette chosen for the colour enhancement was designed both for its appearance (white, coldest; purple, warmer) and for good contrast between neighbouring colours. Each picture was calibrated automatically such that 203 K (−70 °C) was white and 303 K (+30 °C) was black, giving approximately 0.4 K between each grey shade. The temperature ranges of the colours are shown in Table I. All temperatures are calculated from measurements of the radiation emitted by the earth's surface and by cloud tops. However, water vapour absorbs radiation, thereby affecting the apparent temperature of the earth's surface and low-level clouds. These temperatures may be in error by several degrees, particularly in the tropics. At high levels, there is little water vapour outside cloud, hence satellite measurements of cloud-top temperatures at these levels are quite accurate.

Table I. *Upper and lower temperature limits (°C) of colour ranges*

Limit	White	Blue	Yellow	Green	Purple	Grey
Upper	−61.0	−53.2	−44.9	−37.9	−29.3	+30.0
Lower	−70.0	−60.6	−52.8	−44.6	−37.5	−28.9

3. The sequence of satellite pictures

The main features found in each satellite picture will now be considered (note that the times given for each picture are only approximate, due to the movement of the satellite).

In Fig. 1 there appears to be two main cloud systems; a fairly thick mass in the south, associated with the frontal wave, and an area with lower tops to the north exhibiting a hook shape which partially surrounds the centre of the more northerly depression.

By the morning of 14 December, although it appears from surface charts that the two lows have almost merged, Fig. 2 shows that the two cloud systems remain separate. The more northerly has developed extensively and has thickened into a large cloud-shield with a definite edge on the cold-air boundary. The hook feature has become detached and is now a relatively insignificant cloud area south of Cape Farewell. The more southerly cloud area, which was associated with the frontal wave, has changed little in size, although temperature values indicate that the cloud tops are at a lower height than in the previous picture. The surface centre of the wave has also become separated from the frontal cloud area.

In Fig. 3 the two cloud areas still retain their separate identify and both are now developing vigorously, each with a large shield of high-level cloud, though the cloud areas are still relatively compact in shape. The more northerly cloud mass is showing the appearance of an occlusion. The cold front associated with the more southerly cloud mass appears very weak with the higher-level cloud having moved ahead of the surface front, particularly near the triple point.

Further development of the two cloud masses has taken place by the time of the photograph shown in Fig. 4. The speckled appearance within the occlusion over south-west Iceland is of interest, perhaps indicating embedded deep convection within the frontal cloud. This may be contrasted with the more uniform appearance of the thick cloud area approaching Ireland. The surface occlusion and cold front are situated near the rear edge of the lower-level cloud-band which curves north then north-westerly from 55° N, 24° W. The two cloud masses have separated at higher levels since the previous pass, with only a narrow link remaining well ahead of the triple point.

In Fig. 5 there is continued development in the area of cloud crossing the British Isles. The occlusion has expanded in size with development now occurring preferentially to the north-west of the vortex. The surface fronts around the triple point appear to have nearly caught up with the main cloud area, while a tongue of high cloud has moved northwards. Ahead of the cold front, three distinct levels of cloud are evident at increasing heights moving away from the front. Cold air is becoming drawn into the vortex, and convective cloud to the south is showing higher tops, implying increasing depth of cold air. The central surface-pressure of the low is approaching its minimum.

In Fig. 6 the depression is now past its maximum development. There is a large area of very cold cloud near the tip of the occlusion, over and to the west of Greenland. The vortex is becoming separated from the main cloud mass and is composed of quite-thin low- and medium-level cloud with some associated convection.

Less than five hours have passed since the last image was taken, but in Fig. 7 the appearance of the system is already less organized. Much of the frontal cloud is becoming broken, with the edge more ragged and higher-level cloud dissipating, apart from the large area around Greenland. The swirl of the vortex is less compact and the cloud more convective as cold air becomes absorbed. Deep, convective cloud has swept round the depression and is showing signs of greater concentration west of the British Isles.

Although the surface pressure at the centre of the low is still about 941 mb, the well-broken and disorganized cloud pattern shown in Fig. 8 indicates a system in an advanced state of decay. Higher-level cloud is patchy and dissipating, and the vortex is now more or less composed of convective elements. Convection in the cold air has become further concentrated showing the development of troughs with cumulonimbus activity. The 'wave' shapes in the cloud edge north of Iceland indicate minor ripples in the occlusion where baroclinic instability may be enhanced.

4. Synoptic developments

Conventional analyses of surface pressure, 500 mb and 250 mb contours and 1000–500 mb thickness contours were examined in an attempt to relate them to features on each image. Chart and image times are not coincident and interpolation is difficult, in particular because movement and development of the depression were so rapid.

At midnight on 14 December there was an intense thermal gradient between very cold air north of Newfoundland and warm air over the Atlantic to the south-east. During the following 12 hours there was an intense drive of cold air south-eastwards behind the depression and marked warm advection to the north-east ahead of it. The strong thermal advection was, perhaps, accentuated by there being two systems which extended the northerly and southerly flows at low levels before they merged. The 500 mb pattern at midnight on 14 December showed a trough with its axis extending approximately southwards across Newfoundland. This accelerated, though it did not intensify, and by midday was situated immediately behind the occlusion. At 250 mb, there was a broad flow in excess of 100 kn. The jet stream was unusually strong (about 200 kn) but the depression only reached the left exit region, favourable for cyclonic development, at about midday on 14 December, by which time considerable development had already taken place. The strongest winds passed through the cloud shields, so the definite edges do not mark the location of a jet stream, as might be expected. Instead, they probably indicate mass descent on the edges of areas of powerful ascent. It seems that the initial impetus for development of the system was thermodynamic. As the morning of 14 December progressed, the effect of dynamic influences increased and became predominant in maintaining the deepening of the system during the afternoon.

5. Conveyor belts associated with the developing system

The image taken at 0558 GMT on 14 December (Fig. 2) was timed close to a main synoptic hour, which allowed comparison of synoptic and image features. The surface analysis was available for this time and 500 mb and 250 mb patterns could be interpolated from the 0000 GMT and 1200 GMT

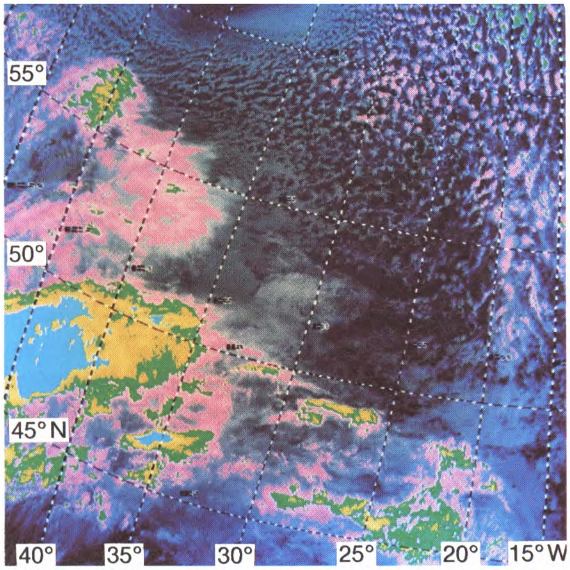

Figure 1. NOAA-10 infra-red image at 2046 GMT on 13 December 1986.

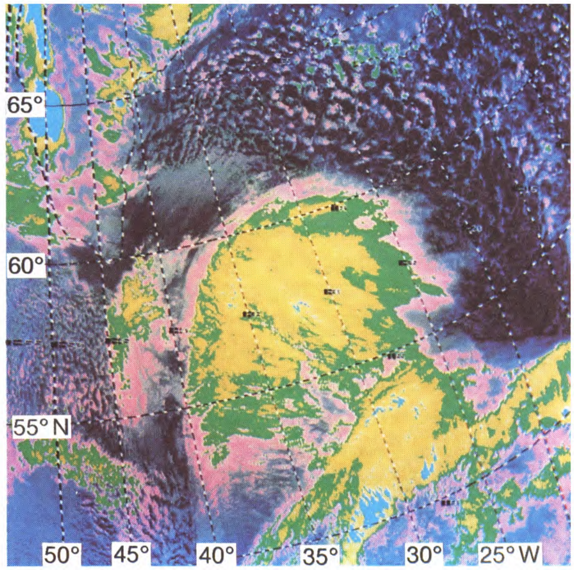

Figure 2. NOAA-9 infra-red image at 0558 GMT on 14 December 1986.

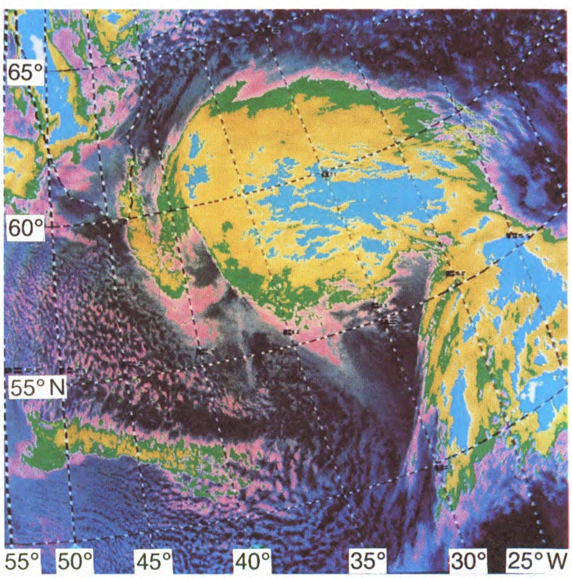

Figure 3. NOAA-10 infra-red image at 1036 GMT on 14 December 1986.

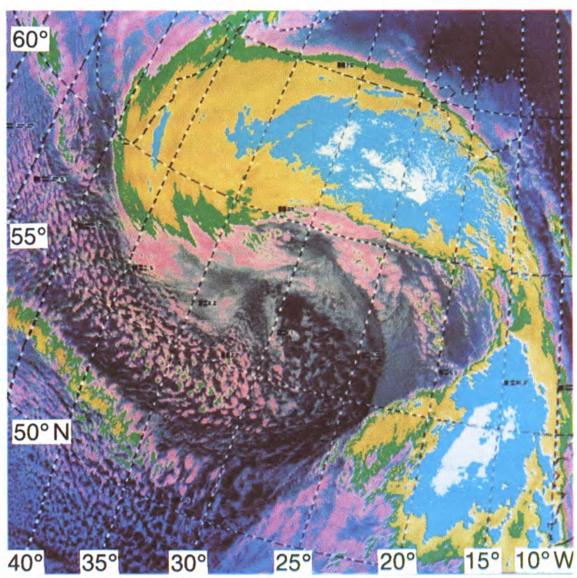

Figure 4. NOAA-9 infra-red image at 1554 GMT on 14 December 1986.

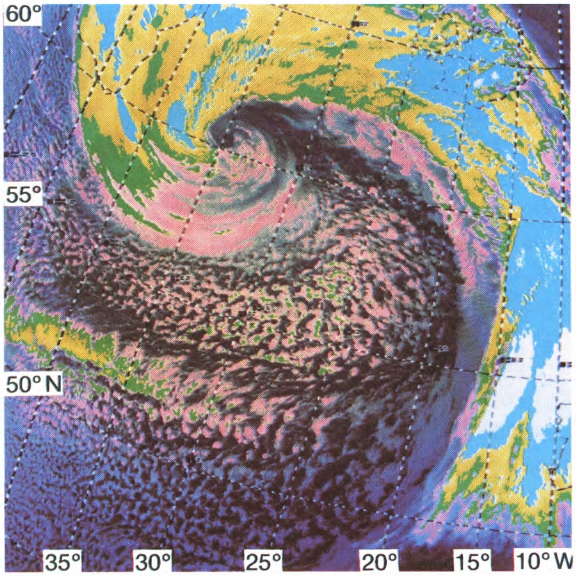

Figure 5. NOAA-10 infra-red image at 2025 GMT on 14 December 1986.

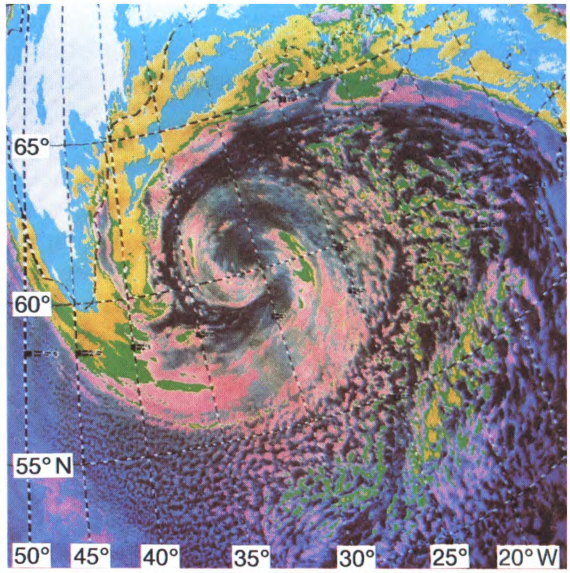

Figure 6. NOAA-9 infra-red image at 0547 GMT on 15 December 1986.

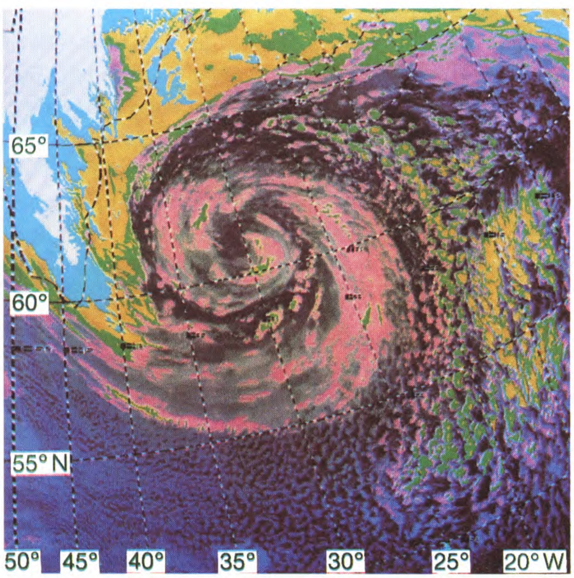

Figure 7. NOAA-10 infra-red image at 1013 GMT on 15 December 1986.

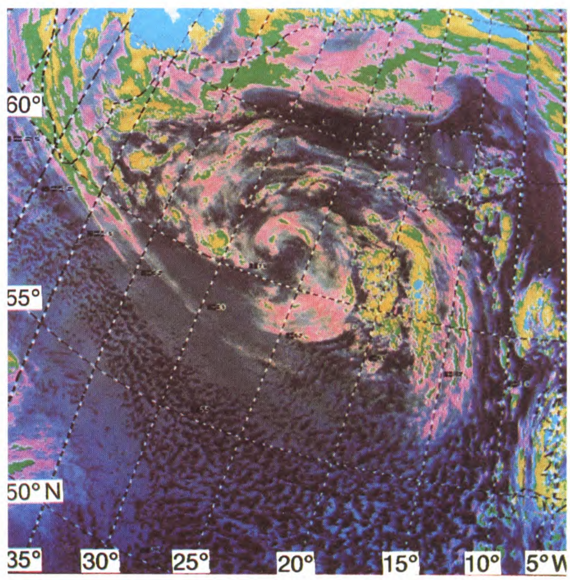

Figure 8. NOAA-10 infra-red image at 2005 GMT on 15 December 1986.

analyses. At this time, considerable development was taking place and estimations were made of the relative flows within the depression and compared with the image to see how they appeared.

The three-dimensional flow within a frontal system has been described by Browning (1985) using the concept of conveyor belts (Harrold 1973) as a means of transporting heat and moisture between different levels. The direction and velocity of the depression at this time was calculated as 200° 65 kn. The assessments of the relative flow at different levels around the depression produced the pattern as in Fig. 9, which includes an outline of the cloud distribution. It shows an ascending conveyor belt across and to the south of the triple point, turning southwards as it reaches the forward cloud edge. The picture shows that there may be two or more parallel conveyors, each ascending into the more southerly cloud area. Ahead of the warm front and occlusion, there is a low-level conveyor belt moving in towards the system, then quickly turning north as it ascends into the more northerly cloud shield. The ribbon of cloud at the rear of the system indicates a descending conveyor moving southwards towards the cold front. As the depression turned towards the north and slowed down during the day, the direction of the descending conveyor belt to the rear of the centre became closer to the ground-relative flow pattern. The diffuse nature of the forward edge of the cloud masses is consistent with marked descent ahead of the system, where the relative motions turn southwards.

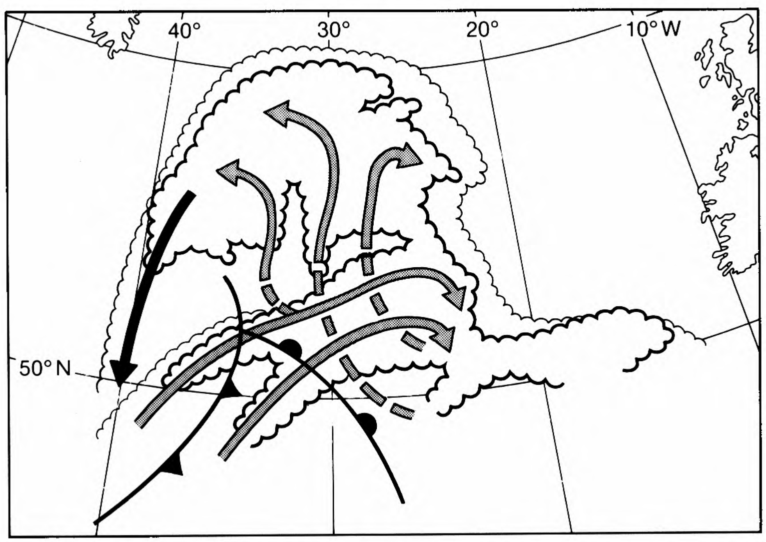

Figure 9. Relative flows within the deepening depression at 0600 GMT on 14 December 1986. The stippled arrows represent 'conveyor belt' motions with ascent occurring within the cloud masses, and the solid arrow represents descent to the rear and near the cloud edge. The bold outline represents thicker cloud while the thinner outline indicates the boundary of more fibrous cloud.

6. Relative motion within the fronts

At midnight on 15 December the position of the surface occlusion was almost vertically beneath the rear edge of its associated cloud mass. Wet-bulb potential temperature (θ_w) is an indicator for defining air mass, and should be conservative for motion within the frontal band. The system relative motions computed for an appropriate θ_w should give an idea of the conveyor belt motions. Just ahead of the surface occlusion are a number of radiosonde stations at points along much of its length. The ascents from each of these stations were plotted and the levels of θ_w of 283 K, 285 K and 288 K were assessed. The winds relative to the front were calculated from the resultant of the winds at these levels and the velocity of the front. In each case, frontal velocity was taken from that part of the front nearest the station.

Fig. 10 shows the flow of air within the system on the 283 K, 285 K and 288 K isentropic surfaces. The warm, moist air ascends quite steeply from 700 mb at Valentia, initially parallel to the front. The flow diverges from the front further north and at Thorshavn it turns away towards the east at 330 mb. The cooler air initially moves in towards the front, particularly at the lower level, with the 285 K surface ascending at a steeper angle than the 283 K surface. The flow becomes parallel to the front over Iceland and diverges from it over Greenland.

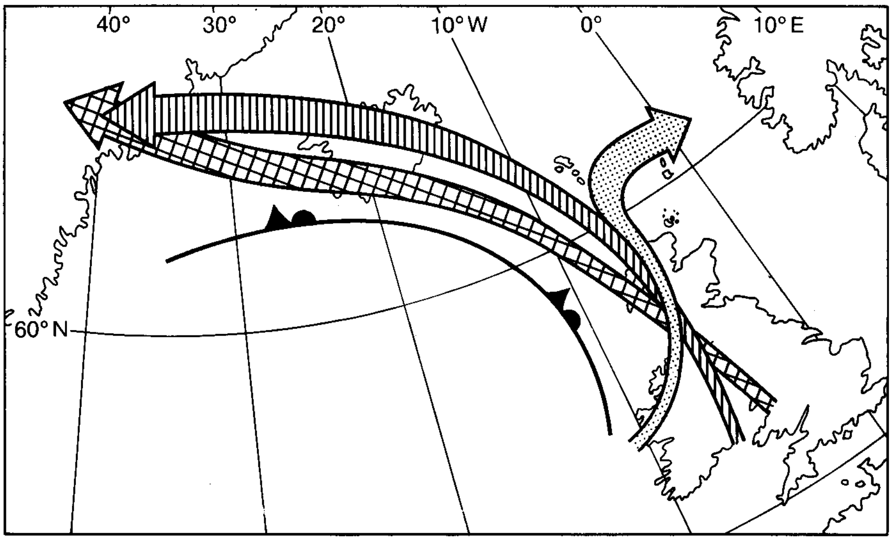

Figure 10 Schematic representation of the flow on the 283 K (hatched arrow), 285 K (shaded arrow) and 288 K (stippled arrow) isentropic surfaces ahead of the occluded front as it approached the British Isles at 0000 GMT on 15 December 1986.

In an attempt to verify these motions within the frontal system as it crossed the British Isles, a movie-loop was made of 31 half-hourly Meteosat images from 1400 GMT on 14 December to 0500 GMT on 15 December. This showed cloud at relatively low levels near to the occlusion moving northwards parallel to it. Cloud at higher levels appeared to move in 'surges', initially parallel to, and slightly ahead of, the cold front and occlusion. The three levels of cloud that can be detected ahead of the cold front in Fig. 5 are probably areas where surges are taking place. One surge pushed well to the north, but later surges made less northward progress and sank away southwards as they reached the forward cloud edge. The dissipation of cirrus and lower-level cumulus ahead of the main frontal cloud showed evidence of marked descent in the downstream ridge. Later in the loop, cloud at higher levels north of the triple point began to become more broken.

7. Conclusions

Enhancement techniques can be used effectively on satellite imagery to accentuate interesting features. They have been used in this case to show how the associated frontal cloud developed and decayed throughout the lifetime of this extraordinary depression. The series of pictures also shows how the intense development rapidly produced large areas of cloud. The depression grew from the convergence of a fast moving wave with an initially small low. The cloud masses associated with the two systems always remained separate and developed equally rapidly, the more northerly becoming part of the occlusion. The area between the two cloud masses was of interest in that it showed the structure of lower-level cloud. The higher-level cloud associated with the cold front and triple point moved well ahead of the corresponding surface features, indicating that most precipitation might be expected near the warm front. This is confirmed by the surface observations. As the depression matured, cold air became increasingly drawn in to the system. Maximum development coincided with cold air reaching the vortex. Once the depression had begun to fill, cloud soon became broken and less organized, even though the surface pressure remained relatively low.

The existence of conveyor belts within the system, which had been inferred from synoptic data, was verified to some extent, particularly where lower-level cloud was visible. The 'surge-like' motions within the frontal cloud evident from the Meteosat movie-loop were of particular interest.

References

Browning, K.A.	1985	Conceptual models of precipitation systems. *Meteorol Mag*, **114**, 293–319.
Burt, S.D.	1987	A new North Atlantic low pressure record. *Weather*, **42**, 53–56.
Harrold, T.W.	1973	Mechanisms influencing the distribution of precipitation within baroclinic disturbances. *Q J R Meteorol Soc*, **99**, 232–251.
Schwalb, A.	1978	The TIROS-N/NOAA A–G satellite series. Washington, NOAA, Tech. Memo. No. NESS 95.
Turner, J., Eyre, J.R., Jerrett, D. and McCallum, E.	1985	The HERMES system. *Meteorol Mag*, **114**, 161–173.

551.508.824:551.585.7(412)

Weather observations on Cairn Gorm summit 1979–86

J.S. Barton

Department of Physics, Heriot-Watt University, Edinburgh

Summary

An automatic weather station specifically designed for a mountain environment is described, together with a short account of its operation, data dissemination and observations of temperature and wind speed on the summit of Cairn Gorm, Scotland, for the period 1979–86.

1. Introduction

Weather observations on high ground in Britain have never been plentiful, because of the difficulties imposed by a severe climate and the lack of a strong commercial stimulus, in contrast to the development of marine or aviation meteorology. Taylor (1976) reviewing upland climate data wrote of '... the extreme paucity of primary information on our upland climates which necessitates the substitution of crude and unavoidable upslope extrapolation from lowland stations'. There is a limited but growing demand for data on British mountain climates relating to hydrology, forestry, design and siting of wind turbines and communication aerials, skiing developments and forecasting for the large number of recreational hill-walkers and imate data wrote of '... the extreme paucity of primary information on our upland climates which necessitates the substitution of crude and unavoidable upslope extrapolation from lowland stations'. There is a limited but growclimbers throughout the year. For example, Davison (1987) describes the problems of assessing snow-lie in the Scottish Highlands in planning ski developments. This paper gives a short account of a specialized automatic weather station (AWS) situated on an exposed mountain summit, and a brief survey of its observations.

2. Historical background

No survey of mountain weather should omit mention of the manned observatory on Ben Nevis summit (1883–1904), which even now is the largest British observational record of all weather elements in such an environment (Roy 1983). Apart from Ben Nevis, most other sites with significant data are on hill tops carrying radio mast installations such as Lowther Hill and Great Dun Fell (Fig. 1). A few small-scale and necessarily shorter-term studies have been made by enthusiasts such as Baird in the Cairngorms (Baird 1957) and Pedgley in Snowdonia (Pedgley 1974).

In 1971 the deaths from exposure of six young people hill-walking on the Cairngorm plateau led to an examination of improved forecasting for such areas. The outcome of a meeting of the Advisory Committee for Meteorology in Scotland in 1975 was a research proposal by the Heriot-Watt Physics Department, in collaboration with the Institute of Hydrology and the Meteorological Office, to the Natural Environment Research Council for development of an AWS station capable of functioning throughout the year on Cairn Gorm summit. This was a uniquely-favourable site in that, although Britain's fifth highest mountain (1245 m), it already boasted a small stone-built hut with mains power supply, housing radio relay equipment for mountain rescue co-ordination. A skiing development on the northern slopes provided relatively easy access by road and chairlift to within 1 km of the summit.

The problems faced were heavy icing and strong winds in the lengthy winter season which prevented unattended operation of normal instruments. A manned observatory on the Ben Nevis pattern would have been far too costly, while even once-daily visits by staff from the ski area could not guarantee continuity of readings. The Heriot-Watt solution was to place normal instruments inside a heated housing from which they could be automatically deployed to sample the weather. The concept was tested by building a prototype which was installed in March 1976 (Curran *et al.* 1977). The research grant led to construction of a better-engineered Mark 2 version which was mounted on a gantry on the hut roof on 12 March 1977 (Fig. 2). This AWS is still operating without any major design changes. The Institute of Hydrology have developed a separate AWS, continuously exposed and actively de-iced (Strangeways 1985).

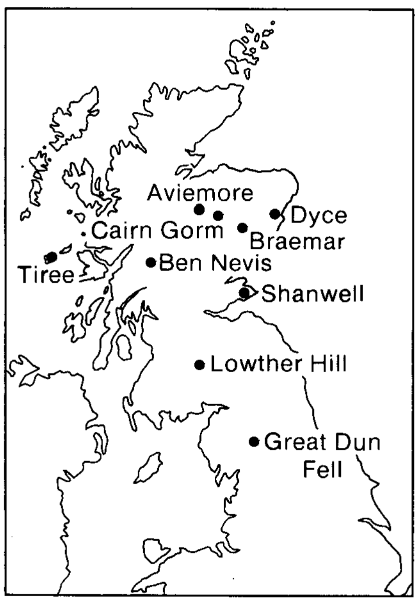

Figure 1. Location of sites mentioned in the text.

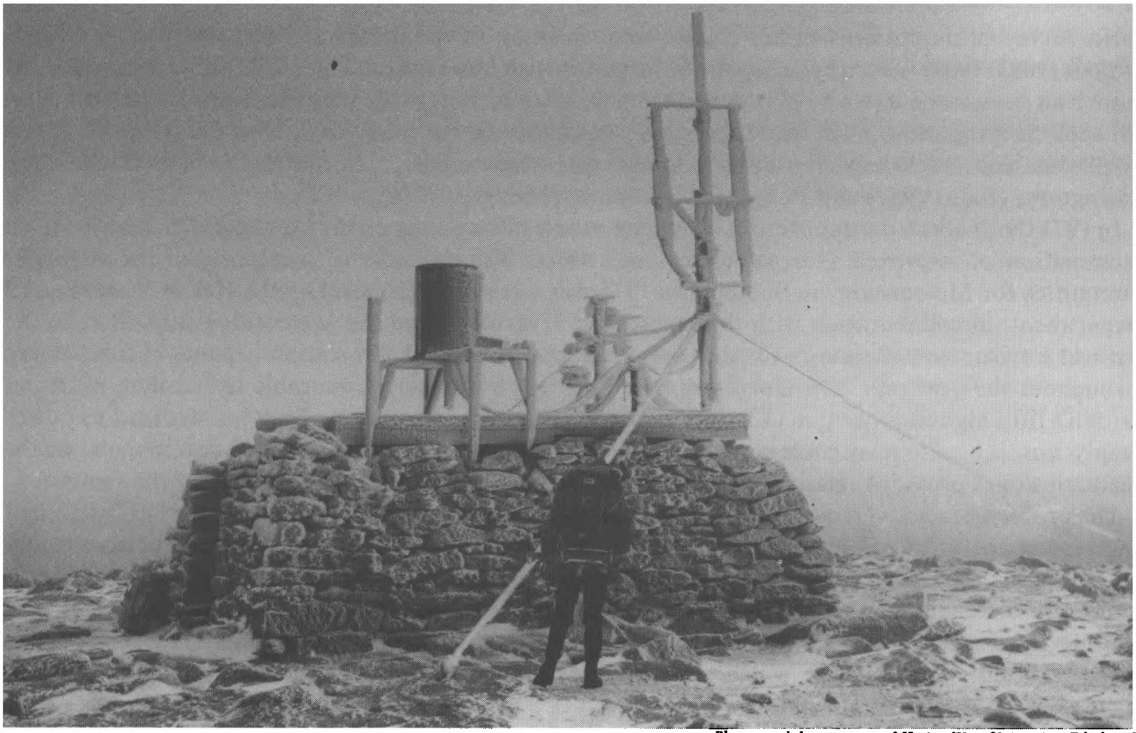

Photograph by courtesy of Heriot-Watt University, Edinburgh

Figure 2. Photograph of Cairn Gorm summit looking south. The AWS is the black cylinder, here shown in the closed position. To the right is a conventional AWS that was temporarily installed for comparison purposes.

3. AWS design

The body of the AWS is cylindrical, 0.63 m in diameter and 0.95 m high, formed from three removable fibreglass panels on an aluminium framework. The sensor platform is normally retracted inside the cylinder and sealed by its lid until the AWS is opened automatically by a 150 W electric motor driving a screw mechanism. The instruments are deployed for 3 minutes every half hour, kept ice-free by thermostatically-controlled heaters (700 W total) inside the housing. After logging the data the AWS closes until the next observation is due. The control and data-logging electronics are within the hut, linked to the AWS by multicore cable.

The instruments are relatively conventional; two dry-bulb platinum-resistance thermometers, a Porton anemometer and wind vane. One thermometer is passively shielded against moisture and radiation, the other is force-ventilated. The 3-cup anemometer is rated to 75 m s^{-1}, with an accuracy of ±2%, and is mounted with cups downward on the underside of the lid, being 4 m above the ground when deployed. The wind vane is mounted vertically below the anemometer, reading to an accuracy of ±3°, smoothed by a 30-second time constant. Data logged every 30 minutes are temperature, 2½-minute mean wind speed and 3-second maximum gust and direction.

It is not possible to use wet-bulb thermometers with any reliability in sub-zero temperatures, while a thin-film humidity sensor has not proved stable enough for long-term operation, possibly due to condensation and thermal cycling in deployment. Precipitation measurement has not been attempted, partly through difficulty of ensuring sufficient accuracy in a short sampling time, and partly because of the problems of collecting rain or snow in high winds. Further details of the AWS are given by Baker *et al.* (1979) and Barton (1984).

4. AWS operation

Although the fundamental mechanical design has not been changed, some detail improvements have contributed to reliability and ease of maintenance. The station has made more than 146 000 open–close cycles since installation. The AWS was removed to Heriot-Watt for refurbishing from May to July 1982, followed by an intercomparison with standard instruments at Eskdalemuir Observatory from July to August. Only two serious breakdowns have led to prolonged gaps in the data; from August to October 1978 after the AWS was struck by lightning, and from December 1983 to March 1984 caused by mechanical trouble with the screw mechanism.

Routine visits are made at about 6-week intervals to change the logger tape and check calibrations; annual maintenance is performed each summer. Winter (i.e. November to April) brings the hazards of cold, wind and 'white-out' visibility if full snow cover is combined with hill fog and perhaps blowing snow also. The summit path-marker cairns and posts can become rime-covered and invisible, and careful navigation is sometimes required simply to find the AWS. Access becomes impossible in severe winter storms, when conditions on the summits can only be guessed from the AWS observations and by extrapolation from personal experience in uncomfortable but less extreme weather.

5. Data dissemination

The data dissemination has evolved from simple on-site data-logging on cassette to VHF telemetry based on a Meteorological Office system, which is received by several independent base stations (Fig. 3).

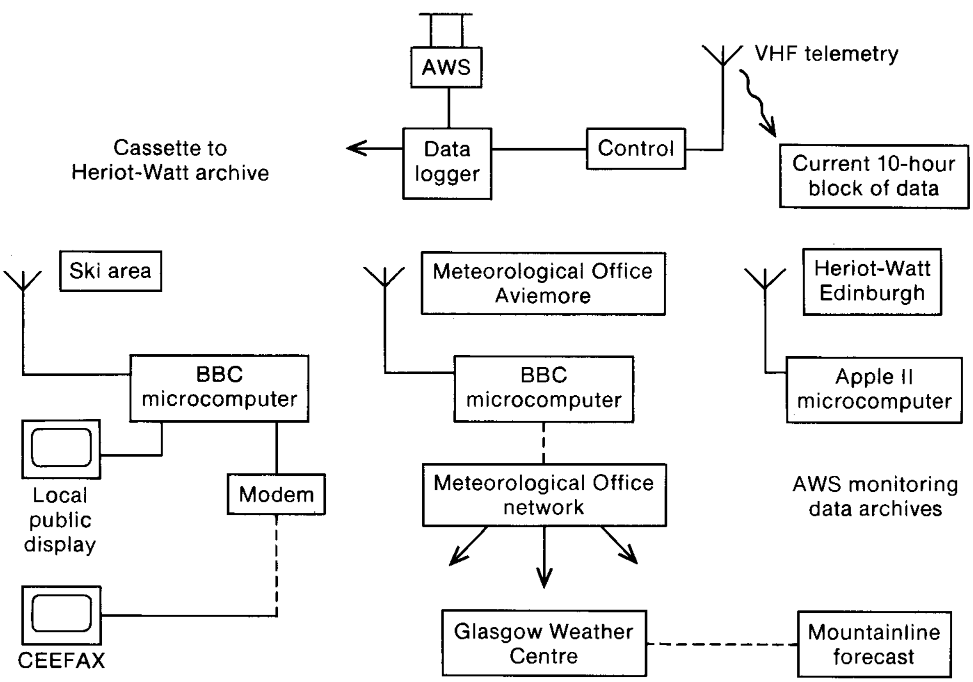

Figure 3. Block diagram of the data dissemination system.

Real-time data transmission is vital for forecasting and important in monitoring the AWS so that faults can be speedily rectified. The Heriot-Watt receiving station uses an Apple II microcomputer while the two more recent stations are based on BBC machines. A local public display at the Cairngorm Ski Area has been supplemented since January 1987 by CEEFAX information pages which include summit observations and a local forecast. Data received at Aviemore Meteorological Office, about 16 km from the summit, are quality checked by the duty observer and telephoned in coded form to Lossiemouth for onward transmission to Bracknell. AWS observations (usually 0400 and 1600 hrs) are included in the Mountainline telephone forecast issued twice daily by Glasgow Weather Centre, which covers popular Scottish mountain areas. Cassette data are quality controlled and archived as daily and monthly summaries at Heriot-Watt University.

6. Brief survey of observations 1979–1986

Data from October 1978 to December 1982 have been archived and analysed by the University of Edinburgh Meteorology Department (Borthwick 1983). No gust observations were made prior to October 1978 and the 1977/78 data have not been analysed in detail. The Edinburgh and Heriot-Watt archives form a data set used as the basis for this survey, covering complete years 1979–86 inclusive.

It should be emphasized that the observations are site-specific, and some caution should be exercised in interpretation and in extrapolation to other mountain areas. An example is the influence of topography on wind speed; summit wind observations may have little relevance to ridge or corrie sites only 1 or 2 km away. Cairn Gorm has a rounded summit, and although there are valleys and cliffs in the surrounding area, the exposure is much more symmetrical than that of Ben Nevis summit, where the proximity of a 550 m cliff strongly affects winds except from the south-east sector.The AWS temperature and wind speed observations 1979–86 for Cairn Gorm are summarized in Tables I and II.

6.1 *Temperature statistics*

The temperature data are based on 48 half-hourly observations reduced to daily and monthly statistics. Data for 1982 are incomplete as the AWS was out of service from mid-May to September, so 1982 has been excluded as being unrepresentative. The overall mean annual temperature (1979–86 excluding 1982) of +0.9 °C can be compared with the Ben Nevis mean (1884–1903) of −0.3 °C (Roy 1983). As Ben Nevis is approximately 100 m higher than Cairn Gorm, on simple lapse rate grounds one might expect the difference in means to be approximately 0.6 °C, i.e. half the observed difference, but the sample is too short to allow firm conclusions to be drawn.

The maximum monthly mean tends to occur in mid to late summer, while the highest individual temperatures are sometimes observed on hot days in May. The minimum month and overall minimum temperature tend to occur closer together in February or March. In cold weather there is a distinction between inversions and relatively uniform lapse-rate conditions. For example, very low minima were observed at valley sites in January 1982 (−26.8 °C at Grantown-on-Spey on the 8th and −27.2 °C at Braemar on the 10th), while the Cairn Gorm minimum was −12.6 °C on the 8th. The author recalls visiting the AWS on 7 and 8 January in conditions of extreme clarity and sunshine above valley-level haze in the inversion layer about 100 m deep.

The lowest summit-temperatures have been observed in easterly winds in polar continental air with a high lapse rate. For example, the lowest minimum of −16.5 °C occurred on 12 January 1987 in south-east winds of 7–15 m s^{-1}. There was no significant diurnal variation, with a maximum of −15.0 °C and a daily mean of −15.9 °C. The Shanwell radiosonde ascent at 1200 GMT gave a lapse rate between 5 m and 1603 m of 9.4 °C km^{-1}, quite close to the dry adiabatic value. Comparison with low-level stations at Dyce (Aberdeen) and Aviemore is interesting since the Dyce temperatures were almost

Table I. *Cairn Gorm summit temperature statistics (°C) 1979–86 inclusive*

Year	1979	1980	1981	1982*	1983	1984	1985	1986	1979–86†
% data	49	74	83	52	90	67	99	85	
Overall maximum	18.6	18.0	16.2	12.0	21.6	18.3	18.0	22.8	22.8
Date	18 June	16 May	12 May	14 May	22 July	22 Aug.	3 June	28 June	28 June 86
Maximum monthly mean	6.2	6.2	6.8	3.1	10.6	9.1	7.2	7.2	10.6
Month	June	Aug.	Aug.	Sept.	July	Aug.	July	June	July 83
Annual mean	−1.0	0.3	1.1	—	1.9	2.9	1.0	−0.2	0.9
Minimum monthly mean	−9.1	−4.6	−4.2	−3.7	−4.3	−5.2	−5.1	−7.6	−9.1
Month	Feb.	Jan.	Dec.	Mar.	Feb.	Mar.	Jan.	Feb.	Feb. 79
Overall minimum	−15.3	−11.4	−11.4	−12.6	−11.7	−9.3	−12.0	−12.0	−15.3‡
Date	14, 15 Feb.	31 Jan. 1 Feb.	22 Mar.	8 Jan.	10 Feb.	31 Mar.	12 Feb.	1 Mar.	14, 15 Feb 79

* AWS overhaul and calibration mid-May to end of August
† Excluding 1982
‡ Lowest minimum −16.5 on 12 Jan. 87

Table II. *Cairn Gorm summit wind observations (m s^{-1}) 1979–86 inclusive*

Year	1979	1980	1981	1982*	1983	1984	1985	1986	1979–86†
% data	47	83	88	51	88	66	98	85	
Annual mean	12.3	12.9	13.4	15.9	13.3	12.6	12.9	14.9	13.3
Maximum monthly mean	15.5	20.2	20.3	17.9	24.5	17.4	16.0	19.1	24.5
Month	Nov.	Dec.	Jan.	Nov.	Jan.	Dec.	Feb.	Nov.	Jan. 83
Maximum daily mean	25.9	30.3	31.4	33.9	37.3	39.8	35.6	34.7	39.8
Direction	SW	W	NW	W	W	SE	SE	S	
Date	4 Dec.	18 Apr.	6 Feb.	19 Nov.	5 Mar.	23 Mar.	9 Feb.	15 Mar.	23 Mar. 84
Maximum 2½-minute mean	39.5	41.1	47.5	45.9	55.6	57.8	46.6	51.4	57.8
Direction	S	W	S	S	NW	SE	SE	S, NW	
Date	12 Dec.	29 Dec.	13 Dec.	26 Oct.	17 Jan.	24 Mar.	8 Feb.	15 Mar., 30 Oct.	24 Mar. 84
Maximum 3-second gust	49.1	56.4	54.0	52.3	65.2	65.1	54.6	76.3	76.3
Direction	SW	W	S	SW	W	SE	W	SE	
Date	4 Dec.	29 Dec.	13 Dec.	12 Feb.	25 Oct.	24 Mar.	31 Jan.	20 Mar.	20 Mar. 86

* AWS overhaul and calibration mid-May to end of August
† Excluding 1982

constant at −5.5 °C throughout the day, while Aviemore showed marked diurnal variation. Winds at Aviemore were lighter, and temperatures ranged from −15.7 °C at 0600 GMT to −6.9 °C at 1400 GMT. This illustrates well the local variations possible between valley and summit.

The lowest minimum on Ben Nevis summit was −17.4 °C on 6 January 1894, following a period of easterly winds. The corresponding observation at Fort William, near sea level, was −5.5 °C giving a lapse rate of 8.9 °C km^{-1}.

Borthwick (1983) has compared AWS monthly mean temperatures with 850 mb temperatures from the Shanwell radiosonde ascents for 1980. Allowing for the height of the 850 mb surface (about 1380–1500 m) by applying an average lapse rate of 6 °C km^{-1}, AWS temperatures are generally within 0.6 °C of the free-air values, but over 1 °C below in February and April. Clearly a more detailed analysis of the full data set would be required to reveal any systematic effects.

6.2 *Wind statistics*

The wind statistics in Table II reflect the exposed nature of the site. The overall annual mean (1979–86, excluding 1982 as unrepresentative) of 13.3 m s^{-1} can be compared with 7.9 m s^{-1} (1961–70 average) for Tiree, an exposed coastal site (Shellard 1976) and with 6.4 m s^{-1} (1895–1904 average) for Ben Nevis summit (Borthwick 1983). This latter figure shows the sheltering effect of the Ben Nevis topography.

Extremes for averaging times ranging from 2½ minutes to 1 month are listed, together with the relevant wind direction to the nearest 45°. Not surprisingly, the strongest winds occur in the autumn and winter months either as westerlies or between south and south-east. Some noteworthy examples of westerly gales occurred on 29 December 1980 (cold front), 17 January 1983 (cold front), 25 October 1983 (warm front) and 30 October 1986 (cold front); the front named being that associated with the strongest winds during the episode. Very strong winds, often in cold air, also occur if fronts are aligned roughly north–south over Britain in a strong south or south-easterly flow. Examples of this situation were observed on 6–7 December 1978, 21 January 1984 (a storm resulting in the exposure deaths of five mountaineers in the area and widespread blockage of roads), 23–24 March 1984 and 15 and 20 March 1986.

The high average and extreme speeds suggest that the mountain's topography may be causing an acceleration of the free atmosphere wind, particularly if stable layers constrict the flow vertically. This possibility is supported by Borthwick (1983) who compared Cairn Gorm and upper-air winds. Using monthly mean winds for 1980, the ratio for Cairn Gorm summit to the Shanwell 850 mb value was 1.21 ±0.13 averaged over 12 months. Further analysis of individual case studies would be of interest in understanding how the atmosphere flows over a mountainous area.

Because the AWS samples only two 2½-minute periods each hour, the gusts recorded are clearly not necessarily the maximum for the hour, as would be obtained from a continuously exposed instrument. The AWS gust is the maximum of 50 contiguous 3-second measurements during the 2½-minute wind-averaging time, therefore the timing of the gust with respect to the 3-second periods is also significant. Overall, the observed ratio of gust to 2½-minute mean speed is approximately 1.25. Gusts over 100 m.p.h. (approximately 45 m s^{-1}) have occurred every winter to date. Not included in Table II is the second highest recorded gust of 66.0 m s^{-1} in a south-easterly gale on 7 December 1978.

The highest gust of 76.3 m s^{-1} was observed at 0049 GMT on 20 March 1986 (mean speed 45.0 m s^{-1}, direction 168°, temperature −5.4 °C) preceded by a gust of 61.0 m s^{-1} half an hour earlier. A deep depression was moving north-east across northern Scotland with an occluded front passing the Cairn Gorm area around 1000 GMT. Winds then veered rapidly to the north-west and increased in the afternoon. Gusts exceeded 45 m s^{-1} from 1119 to 1719 GMT inclusive with a maximum of 67.5 m s^{-1}

(mean speed 49.8 m s^{-1}, direction 306° and temperature −4.5 °C) at 1449 GMT. Winds decreased later in the day as the pressure gradient eased.

7. Conclusions

The Cairn Gorm observations constitute a limited but useful data set relating to climatic conditions of exposed summits in the Scottish Highlands. Comparison with the Ben Nevis observations reveals a broadly similar temperature regime, but a much higher mean wind speed reflecting the different exposures of the two summits. Extreme winds with gusts exceeding 60 m s^{-1} have been observed on several occasions, in agreement with the Ben Nevis observers' estimates.

Data are being used in real time as an aid in the difficult task of forecasting for the mountains in the area, and it is hoped that the AWS will continue operation in order to build up a climatologically significant set of observations of this interestingly severe climate.

Acknowledgements

The author gratefully acknowledges the Meteorology Department of the University of Edinburgh and A.S. Borthwick for permission to use his thesis; Miss M.G. Roy, Edinburgh Meteorological Office for supplying and analysing both contemporary comparison data and Ben Nevis statistics, and A.J. Quinn, Heriot-Watt University, for maintaining the AWS.

References

Baird, P.D. 1957 Weather and snow on Ben Macdui. *Cairngorm Club J*, **17**, 147–149.

Baker, B., Curran, J.C., Harrison, F., Peckham, G.E. and Smith, S.D. 1979 An automatic weather station for operation in severe icing climates. *J Phys E: Sci Instrum*, **12**, 734–738.

Barton, J.S. 1984 Observing mountain weather using an automatic station. *Weather*, **39**, 140–145.

Borthwick, A.S. 1983 Mountain weather in Scotland (thesis). (Unpublished, copy available in University of Edinburgh.)

Curran, J.C., Peckham, G.E., Smith, D., Thom, A.S., McCulloch, J.S.G. and Strangeways, I.C. 1977 Cairngorm Summit automatic weather station. *Weather*, **32**, 60–63.

Davison, R.W. 1987 The supply of snow in the eastern Highlands of Scotland: 1954–5 to 1983–4. *Weather*, **42**, 42–50.

Pedgley, D.E. 1974 Field studies of mountain weather in Snowdonia. *Weather*, **29**, 284–297.

Roy, M.G. 1983 The Ben Nevis meteorological observatory 1883–1904. Part 1. Historical background, methods of observation and published data. *Meteorol Mag*, **112**, 318–329.

Shellard, H.C. 1976 *In* Chandler, T.J. and Gregory, S. (eds); The climate of the British Isles. London, New York, Longman.

Strangeways, I.C. 1985 A cold regions automatic weather station. *J Hydrol*, **79**, 323–332.

Taylor, J.A. 1976 *In* Chandler, T.J. and Gregory, S. (eds); The climate of the British Isles. London, New York, Longman.

551.501.9(458.2):551.5(09):355.48

The Meteorological Office, Valletta, Malta 1942–45

T.A. FitzPatrick

Glasgow*

Summary

An account of activity at Air Headquarters, Malta from October 1942 until May 1945 is given, based entirely on the author's memory of events during that period.

1. October 1942–July 1943

1.1 *The Meteorological Office in Valletta*

I was posted to Air Headquarters (AHQ) Malta from Sullom Voe in the Shetlands in July 1942, and given a Civilian Component commission in the RAF with the rank of Flight-Lieutenant. (At a later date Meteorological Officers were re-commissioned in the RAFVR.) After a short interim posting to Abbotsinch, I eventually reached Malta towards the end of October, along with two other Meteorological Branch officers, Flt Lt J.R. Scott and Flt Lt A.M. Lewis. We travelled out on HMS *Welshman*, a vessel built for laying mines in enemy waters and one of the fastest ships in the Navy. On our outward journey we were held up for about three weeks in Gibraltar while the invasion of North Africa began, and were able to spend a little time at the Meteorological Office there.

The Meteorological Office in Valletta was located in (and later on) the St. John Cavalier, a massive building which was part of the medieval fortifications built by the Knights of Malta during the Great Siege of 1565. It was situated at the highest part of the small peninsula on which Valletta stands, with a commanding view over Malta's two magnificent natural harbours, the Grand Harbour and Sliema Harbour, and over the surrounding sea to north and east. It consisted of a truncated pyramid on a square base, which had served the Knights as a fort, a look-out point and a stable for horses. There was a large internal chamber (see Fig. 1) at the centre of the base which originally had been the stable. A sloping tunnel leading from the entrance at ground level ended in a flight of steps which gave access to the flat top of the building. Here had stood a solid structure built of the distinctive Malta stone, which had been occupied by the Meteorological Office in peace-time. It had had ample space to accommodate forecasting and ancillary meteorological staff, wireless operators, deciphering staff and runners — the latter a necessary element in the wartime situation — and their equipment. However, the office had been severely damaged by enemy action, and at the time of our arrival all its work was being carried out in the tunnel.

If memory serves, the layout there was somewhat as is indicated in Fig. 1; the wireless telegraphy (W/T) section, consisting usually of two or three operators on watch at any time, occupied the first part, seated along the wall of the tunnel one behind the other. Next to them were the 'cipherines' (C) — Maltese girls, to whom the messages received were passed for decoding and then passed on to the meteorological assistants (A), most of whom were Maltese civilians with a few service personnel in addition, who plotted the charts and carried out the observations which of course had to be encoded before being transmitted by W/T. The charts were then taken over to be analysed and drawn up by the duty forecasters (F). Elsewhere in the tunnel, space had to be found for the administrative staff.

*Formerly of the Meteorological Office

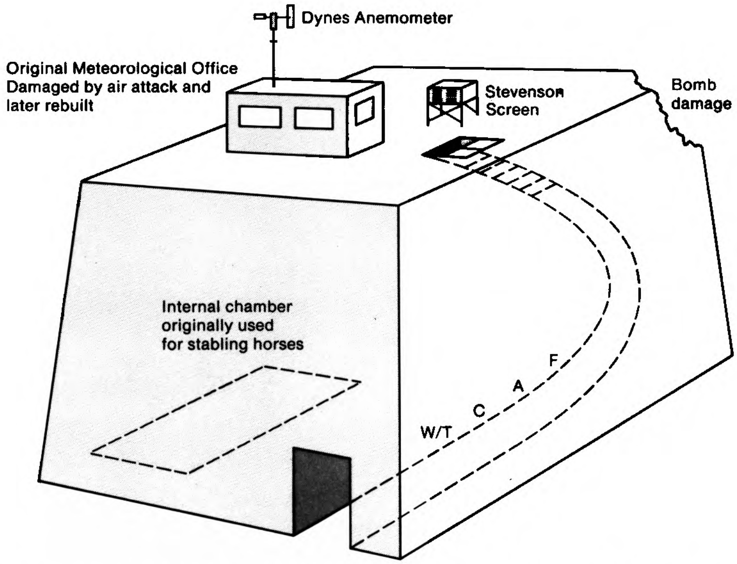

Figure 1. The St. John Cavalier, part of the fortifications of Valletta showing the position of the peacetime meteorological office and the tunnel in which the staff were located following bomb damage. The positions shown are the duty forecaster (F), the meteorological assistant (A), the cipherines (C) and the wireless operators (W/T).

In October 1942 the Senior Meteorological Officer was Sqn Ldr J.H. Brazell, with whom I had worked as a trainee in Invergordon in the spring of 1940, and whom I had met again briefly at Wick. On the staff were Flt Lt McCaffrey and one or two others whose names I cannot now recall, whom we had come to relieve, and Lt W. Eccles, RNVR, the Naval Liaison Officer. I recall also Flt Lt 'Johnny' Johnson, a Canadian officer, who was on the staff with me for a considerable period. Administration was in the hands of Fg Off May and Mr Angelo Ghigo, a local man with considerable length of service, whose prime task was to look after the arrangements for the Maltese personnel. Fg Off Allan Logan (eventually posted to a Mobile Meteorological Unit in the Western Desert) and Fg Off Edward Pyrah were also recent arrivals. Both were posted to the airfield at Luqa, the principal operational base on the island. There were also operational bases at Hal Far (Fleet Air Arm) and Ta'Qali (Fighter Command) and a flying-boat base at Kalafrana at the south end of the island. The Meteorological Office staff in 1943 are shown in Fig. 2.

1.2 *The needs of the RAF, Royal Navy and the Army*

At this time Malta was still in a state of siege. Although victory at Alamein was achieved by about the first week of November 1942, full relief had to wait until the Eighth Army had reached Tripoli, which it did in February 1943. The routine at AHQ Malta was extremely heavy. The Meteorological Office had responsibility for coverage of the central Mediterranean from 5° to 15° E, with no specific limit to the south or to the north, and the area of interest stretched northwards across France to the United Kingdom and southwards into the Western Desert, as well as including all neighbouring parts of the Mediterranean theatre. Weather information had to be supplied to the RAF, Royal Navy and the Army. The demands were enormous.

The needs of the RAF were perhaps self-explanatory; they did include however the broadcast, daily at a fixed-time, of landing conditions at Malta for an aircraft which took off from Gibraltar to run the gauntlet to Malta, and which listened out for this forecast before reaching its point of no return

Figure 2. Some of the Meteorological Office staff, Valletta 1943. Back row — Maltese airmen, W/T operators and meteorological assistants, middle row — Maltese airmen (runners), 5 cipherines, and meteorological assistants and front row (seated left to right) Mr Naudi, Fg Off Rushton, Fg Off May, Flt Lt Johnstone, Flt Lt Scott, Sqn Ldr Brazell, Lt Randall, Flt Lt FitzPatrick, Fg Off Logan, and Mr Ghigo (senior Maltese assistant).

somewhere over Tunisia. A striking force of bombers operated from the island in support of the armies in North Africa, and various transport flights were made to the east and to the west over enemy-occupied territory. When, later, conditions improved as a result of military successes, first in North Africa and the Western Desert and later over Sicily, Italy and Europe generally, weather information had to be provided for flights south and west to North Africa and Gibraltar, east to points in the Middle East, and over occupied France to the United Kingdom, as well as around the central Mediterranean generally. A Photographic Reconnaissance Unit operated from Malta over targets in the Western Desert, Libya, Tripolitania and Tunisia as well as Sicily and southern Italy.

For the Army, the Office issued details of upper-air temperatures and winds for the anti-aircraft batteries, and when the First and Eighth Armies entered our area in North Africa, forecasts of weather conditions in the Western Desert were issued to Army and Air Command. It was rarely possible to check on the accuracy of these, but I believe it to be the case that, on occasion, warnings which AHQ Malta was able to give of rising sand in the desert were of considerable value to RAF and Army units. Co-operation with the Army in Malta was always good. Once the state of supply of ammunition allowed it, an ack-ack (anti-aircraft) battery would, on request, fire smoke shells to burst at a predetermined height, usually 20 000 or 25 000 ft, so that the upper wind could be determined by observation of the movement of the smoke-puffs by theodolite. This gave more accurate results than the nephoscope, and in any case could be used on occasions of cloudless skies, a fairly frequent occurrence, when the nephoscope of course was of no help.

The Navy was interested primarily in the state of sea and visibility throughout the central Mediterranean, without ever divulging the particular operations of submarines or surface craft that might have been making use of the information. The Fleet Air Arm at Hal Far also depended on AHQ Malta for weather information.

1.3 *Observations and forecasts*

All weather observations were received in code by radio. Broadcasts from the United Kingdom, Almaza (Middle East) and Gibraltar formed the basis of the synoptic chart. In addition we listened to broadcasts from enemy-occupied territory in North Africa, mainly Tunisia and Algiers. Within the meteorological staff a remarkable degree of expertise in breaking enemy codes had developed. I can well recall my own astonishment when I arrived there at the speed with which a change in the code-books being used by the enemy was overcome, and wondering if I would ever be able to make any worthwhile contribution to the exercise, but with experience it became remarkably simple.

The forecasters faced problems that were probably unique because of the island situation and the fact that the nearest land areas were in enemy hands. An additional difficulty arose from the shortage of aviation fuel, so that air sorties had to be strictly controlled and the amount of weather information coming from that source, or from sea-borne operations, was limited and irregular. The processing of weather information also raised problems. The observations which we received had first been put into the international weather code, then recoded into a number code, broadcast, received, deciphered (by which stage they had returned to international weather code form) and then plotted. At every stage errors could occur. When reception was poor or broadcasts were being jammed, plotted reports had to be treated with caution. Even with all the information thus collected, the chart usually remained remarkably free of solid up-to-date information over a vast area surrounding the island, extending south into the Western Desert and north, west and east over Sicily, Italy, Spain, France, the Balkans, Greece and the eastern Mediterranean.

In addition to the problem of lack of hard information, the forecaster had to be able to judge the accuracy or otherwise of the information which had passed through so many processes before reaching him. One illustration of this which comes to mind may be of interest. There was an occasion, probably about late September 1943, when the general state of the atmosphere pointed to the likelihood of an outbreak of thunder. The problem was the obvious one of predicting the time it would occur and giving adequate warning. Observations from Tunisia throughout the day recorded clear skies and a light wind; then in the late evening one report, from the Cape Bon area, showed a change in wind direction from south-east to north-west with some increase in strength. Small amounts of upper cloud were also reported. On the strength of this slender, unsupported and possibly erroneous evidence a storm was forecast, which duly arrived at Malta in all its terrifying glory around 0900 hrs the following morning.

The heavy routine at AHQ was not made less onerous by the requirement that the duty Meteorological Officer had to brief the Air Officer Commanding (AOC) at 0800 hrs every morning, as the culmination of his exhausting night watch. At this time the AOC was Air Vice-Marshall Sir Keith Park, who had already made history, not only by his part as strategist in the Battle of Britain, but also by the spectacular success of his first encounter with the enemy in the Mediterranean, when he used the element of surprise in a most dramatic way. Spitfires, not hitherto seen on the island, took off from an aircraft carrier off the Cape Bon Peninsula and carried out a devastating attack 'out of the blue' on enemy bombers engaged in an unopposed raid on Malta, and then landed on the island. Giving the daily weather briefing to the AOC was particularly exacting, not only because of the paucity of information and the difficulties inherent in the island situation, but also because of the incisive questioning from this very lively-minded Air Officer.

2. Major operational events

Of great interest are the major operational events for which weather information had to be supplied. These were the invasion of Sicily in July 1943, and the Yalta Conference in 1945, for which the principal participants on the Allied side, Churchill and Roosevelt, came together in Malta for their joint preparation, and flew from there to Yalta. Besides these historic events the other onerous responsibilities of the weathermen, which included forecasting for flights over enemy-occupied territory to the United Kingdom as well as operational flights in support of the Army in North Africa, tended to pale into insignificance. The brief accounts which follow are based entirely on memory.

2.1 *Invasion of Sicily*

By June 1943 the German and Italian forces had been driven out of Africa, but had withdrawn only as far as Sicily. Land, sea and air forces congregated at Malta in preparation for the invasion which began on 10 July 1943. Weather information was required for naval forces, which included a vast array of tank landing-craft, and aircraft which included troop carriers, gliders and towing machines as well as fighters and bombers. In my recollection the weather map was remarkably devoid of information from Malta northwards as far as the United Kingdom. There were observations from Gibraltar, from North Africa from west to east, from the neighbouring islands of Linosa, Lampedusa and Pantelleria (I think; but these observations may not have begun till later), but nothing from Sicily, Italy, France or the Balkans. However the general synoptic situation seemed to suggest that a mistral-type situation had been prevailing in the south of France, with the consequent probability of a depression forming in the Gulf of Lions. The difficulty was to time its genesis and predict its intensity and subsequent speed of movement. A depression did in fact develop and move south into the Tyrrhenian Sea, with the result that the invasion had to take place in the teeth of a wind from the north-west of Force 7, to the great discomfort of many who were making the long sea crossing. One helpful factor for them was the fact that because of the wind direction, the sea conditions moderated as the ships approached the Sicilian coast. Some gliders had an unfortunate experience. Insufficient attention had been paid to the information given about the strength of adverse upper winds above 10 000 ft and some were released too soon and failed to reach the Sicilian coast.

Sicily was soon taken, and thereafter the position in Malta markedly improved. In due time it became possible to send personnel to Sicily for leave, to the rest camps which had been established on Mount Etna and at Taormina. Aerial activity from Malta however continued at an intense level, with increasing numbers of transport and other aircraft flying between the central Mediterranean, the Middle East and the United Kingdom.

2.2 *The Yalta Conference*

This historic event took place in February 1945. For some weeks before, activity at the Meteorological Office at AHQ had increased to a level of intensity which had never previously been reached. Sqn Ldr (now Wing-Commander) Brazell had been posted to Iraq, without replacement. To help meet the increased work-load, and to provide someone with experience of conditions and provision of information in the Black Sea area, Sqn Ldr Chambers was posted temporarily to Malta from Almaza. This addition to the staff, welcome as it was, scarcely stood comparison with the corps of US meteorologists, consisting as it did of a Colonel, two Majors and sundry other junior officers and other ranks, who arrived to oversee the American involvement.

A major problem was the collecting, deciphering and decoding of Russian weather broadcasts from the Black Sea area. The amount of work for the W/T operators more than doubled, and to help out the hard-pressed ciphering staff everyone had to lend a hand. In my recollection, a period of several weeks — perhaps three to four — went past, during which this effort had to be made round the clock, and the weather scanned for a possible trip to Yalta, with particular attention to reasonable landing conditions at Yalta as well as safety *en route*. At this time of the year snow was still liable to occur in the Yalta area, with consequent high risks to aircraft at the limit of their endurance. At the same time the routine work greatly expanded because of the increased coming and going from the United Kingdom by high-ranking personnel.

When Churchill and Roosevelt eventually set off on a more than normally hazardous journey, AHQ Malta had to co-operate in the provision of weather information for the flights.

The aircraft carrying the principal parties would have a point of no return somewhere in the eastern Mediterranean. To provide fighter protection as far as this was possible, the route would be overflown by a number of Mosquitoes, some flying from Naples and landing at Almaza, others moving in the reverse direction. A Sunderland seaplane would fly the route behind the main body to be ready to pick up survivors from any machine that might be forced into the sea from whatever cause. For all of these, AHQ Malta had to co-operate in the provision of flight forecasts and landing forecasts, and assist in the briefing of aircrew. Needless to say, the responsibilities were shared with the US staff. In all, it was an exciting, exhausting and interesting exercise in international co-operation.

3. Some general points

For forecasters whose practical experience had been gained in higher latitudes open to oceanic influence, transition to the Mediterranean area demanded considerable intellectual adjustment. Because of the land-locked nature of the Mediterranean basin, the high relief of much of its coastal zones and the influence of the vast land mass of Africa and the Sahara, the weather tends to develop in ways not readily described in the clear-cut terms of frontal analysis that work well over the sea in higher latitudes. Phenomena of particular interest to the wartime meteorologist included rising sand and sandstorms in the Western Desert associated with atmospheric instability and intense surface heating, violent thunderstorms, poor visibility, low stratus and sea fog over vast sea areas when all available observations (over land) reported clear skies and excellent visibility, conditions of exceptional visibility (e.g. when the summit of Mount Etna could be seen from Valletta) and violent turbulence at low levels in cloudless conditions. On one such occasion aircraft on escort duty could not maintain station at 2000 ft, although there was no cloud in the sky, but found smooth flying conditions at a mere 4000 ft.

It has to be remembered that, at the time to which these notes refer, aircraft were propellor-driven and limited in range and operational height. Flights made from Malta over occupied France to the United Kingdom frequently had to operate in conditions when icing constituted a high risk. Navigational aids were at an early stage of development and upper-air data limited. When the siege conditions lifted, Malta began its own meteorological flight — a vertical ascent by a Hurricane fighter. Attempts were made to locate thunderstorms over the sea using W/T direction-finding techniques, and to gain information about upper winds by tracking, in the same way, pilot balloons covered with tin foil.

4. Conclusion

I was posted back to the United Kingdom shortly after VE Day, to HQ 18 Group at Pitreavie. It was then expected by many that Transport Command would soon be making big demands on meteorological personnel, but all such speculations were brought to a close by the sudden and horrific ending of the conflict in the Pacific.

Correction

Meteorological Magazine, September 1987, p. 279. The correct title of the article by D. Offiler is 'Wind measurements from the European remote-sensing satellite, ERS-1'.

Satellite photograph — 25 August 1987 at 0400 GMT

This NOAA-9 infra-red image was taken during a period when heavy rainfall and severe thunderstorms affected large areas of western and central Europe. Most apparent is the large comma-shape in the cold-cloud top. This resulted from the merging of cloud bands associated with a cold-front wave (Low E) which had developed ahead of a sharp upper trough, and bands generated chiefly through positive vorticity advection (PVA) closer to the axis of the upper trough (located near 4° E over central France at 0400 GMT). Within the cold-frontal band, in the comma tail, a large shield of anvil cirrus resulting from the combined outflows from numerous cumulonimbus cells covers north-east Italy and Alpine regions of Switzerland and Austria. Flash-floods from these storms caused extensive damage and loss of life. Developing cells can also be seen over central Italy. Within other parts of the comma, especially towards the head, deep convection on a smaller scale can be identified, generated within bands extending across the North Sea, with the resulting anvils shearing northwards in the strong flow aloft. Some other features of interest in the image include the bands of dense cirrus within a region of strong wind shear over central Britain and the circulation associated with an old tropical storm (Low A) situated near 46° N, 17° W.

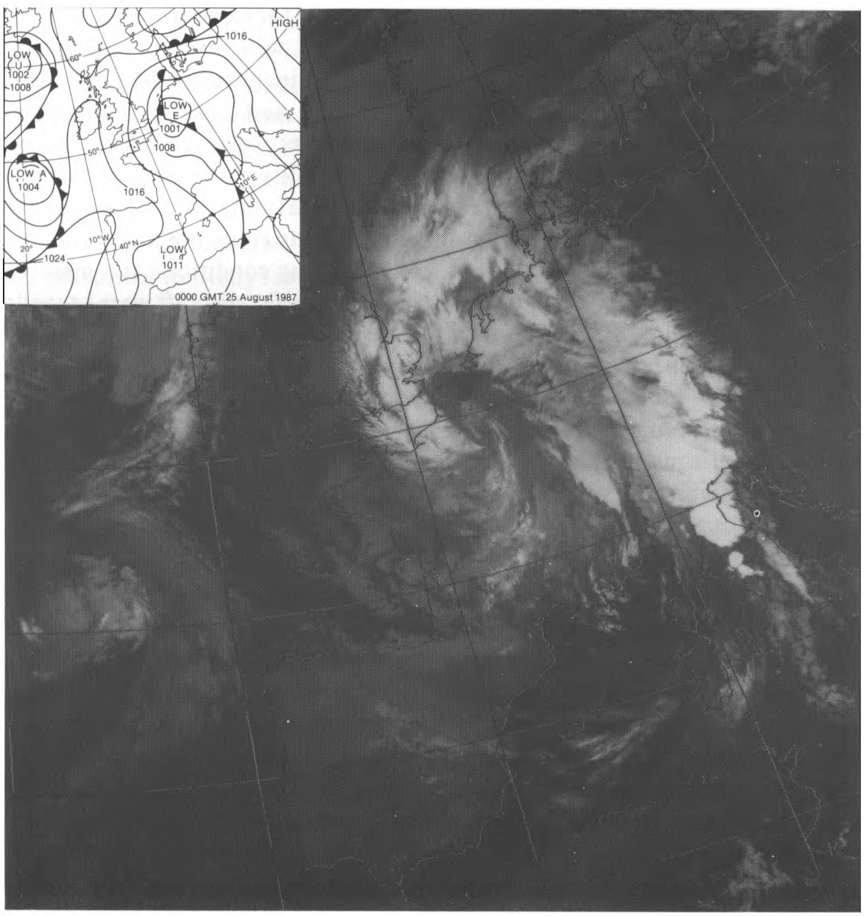

Photograph by courtesy of University of Dundee

Meteorological Magazine

GUIDE TO AUTHORS

Content

Articles on all aspects of meteorology are welcomed, particularly those which describe the results of research in applied meteorology or the development of practical forecasting techniques.

Preparation and submission of articles

Articles for publication and all other communications for the Editor should be addressed to the Director-General, Meteorological Office, London Road, Bracknell, Berkshire RG12 2SZ and marked 'For *Meteorological Magazine*'.

Articles, which must be in English, should be typed, double-spaced with wide margins, on one side only of A4-size paper. Tables, references and figure captions should be typed separately.

Spelling should conform to the preferred spelling in the *Concise Oxford Dictionary*.

References should be made using the Harvard system (author, date) and full details should be given at the end of the text. If a document referred to is unpublished, details must be given of the library where it may be seen. Documents which are not available to enquirers must not be referred to.

Tables should be numbered using roman numerals and provided with headings. We consider vertical and horizontal rules to be unnecessary in a well-designed table; spaces should be used instead.

Mathematical notation should be written with extreme care. Particular care should be taken to differentiate between Greek letters and Roman letters for which they could be mistaken. Double subscripts and superscripts should be avoided, as they are difficult to typeset and difficult to read. Keep notation as simple as possible; this makes typesetting quicker and therefore cheaper, and reduces the possibility of error. Further guidance is given in BS1991: Part 1: 1976 and *Quantities, Units and Symbols* published by the Royal Society.

Illustrations

Diagrams must be supplied either drawn to professional standards or drawn clearly, preferably in ink. They should be about 1½ to 3 times the final printed size and should not contain any unnecessary or irrelevant details. Any symbols and lettering must be large enough to remain legible after reduction. Explanatory text should not appear on the diagram itself but in the caption. Captions should be typed on a separate sheet of paper and should, as far as possible, explain the meanings of the diagrams without the reader having to refer to the text.

Sharp monochrome photographs on glossy paper are preferred: colour prints are acceptable but the use of colour within the magazine is at the Editor's discretion. In either case contrast should be sufficient to ensure satisfactory reproduction.

Units

SI units, or units approved by WMO, should be used.

Copyright

Authors wishing to retain copyright for themselves or for their sponsors should inform the Editor when they submit contributions which will otherwise become UK Crown copyright by right of first publication.

It is the responsibility of authors to obtain clearance for any copyright material they wish to use before submitting it for publication.

Free copies

Three free copies of the magazine are provided for authors of articles published in it. Separate offprints for each article are not provided.

Meteorological Magazine

November 1987

Vol. 116
No. 1384

CONTENTS

Contributions: it is requested that all communications to the Editor and books for review be addressed to the Director-General, Meteorological Office, London Road, Bracknell, Berkshire RG12 2SZ, and marked 'For *Meteorological Magazine*'. Contributors are asked to comply with the guidelines given in the *Guide to authors* which appears on the inside back cover. The responsibility for facts and opinions expressed in the signed articles and letters published in *Meteorological Magazine* rests with their respective authors. Authors wishing to retain copyright for themselves or for their sponsors should inform the Editor when submitting contributions which will otherwise become UK Crown copyright by right of first publication.

Subscriptions: Annual subscription £27.00 including postage; individual copies £2.30 including postage. Applications for postal subscriptions should be made to HMSO, PO Box 276, London SW8 5DT; subscription enquiries 01–211 8667.

Back numbers: Full-size reprints of Vols 1–75 (1866–1940) are available from Johnson Reprint Co. Ltd, 24–28 Oval Road, London NW1 7DX. Complete volumes of *Meteorological Magazine* commencing with volume 54 are available on microfilm from University Microfilms International, 18 Bedford Row, London WC1R 4EJ. Information on microfiche issues is available from Kraus Microfiche, Rte 100, Milwood, NY 10546, USA.

ISBN 0 11 727975 7

ISSN 0026–1149

Printed in the United Kingdom by Her Majesty's Stationery Office
Dd 0240021 10/87 C15 93379/1 (40711)

THE METEOROLOGICAL MAGAZINE

HER MAJESTY'S STATIONERY OFFICE

December 1987

Met.O.978 No. 1385 Vol. 116

METEOROLOGICAL OFFICE Met.O.978

THE METEOROLOGICAL MAGAZINE

No. 1385, December 1987, Vol. 116

551.583:551.588:551.510.4

Simulation of climate change due to increased atmospheric carbon dioxide

J.F.B. Mitchell
Meteorological Office, Bracknell

Summary

Increases in the atmospheric concentration of carbon dioxide and other trace gases are expected to produce changes in climate with potential economic and social consequences. The use of numerical models to determine the likely changes in climate is reviewed, with the emphasis on the physical mechanisms producing the simulated changes in climate. The problems of detecting climate change are discussed briefly.

1. Introduction

Atmospheric carbon dioxide (CO_2) is, to a first approximation, well mixed throughout the troposphere and lower stratosphere. Measurements made at Mauna Loa, Hawaii indicate that the concentration of atmospheric CO_2 has risen from 316 parts per million by volume (ppmv) in 1958 to 342 ppmv in 1985 (Fig. 1), and was probably about 300 ppmv at the turn of the century (see Oeschger and Stauffer (1986)). This change is attributed mainly to the increased emission from fossil fuels (Fig. 2). It has been estimated that the concentration of atmospheric CO_2 could exceed 600 ppmv by the end of the next century, but this estimate is subject to the uncertainties in forecasting the future use of fossil fuels, and predicting the response of the natural carbon cycle. These topics are considered further in a recent review by US Department of Energy (1985a) and references therein. A comprehensive assessment of the natural carbon cycle is given by International Council of Scientific Unions (1979).

The possibility that artificially produced CO_2 might affect climate was first considered by Callendar (1938). However it is only over the last 15 years that the advent of numerical models of climate and confirmation of the accelerating increase in observed CO_2 concentrations has stimulated widespread interest in 'the CO_2 problem' (see, for example, US Department of Energy (1985a,b,c,d) and International Council of Scientific Unions (1986)). The modelling of the climatic effects of CO_2 has been pioneered by Manabe and colleagues at the Geophysical Fluid Dynamics Laboratory (GFDL) in Princeton and much of that work has been reviewed recently (Manabe 1983).

Here the emphasis will be on the understanding of the physical mechanisms relevant to CO_2-induced climate change as the state of the art is not yet adequate to make detailed quantitative predictions of climate change. In doing so, reference has been made to typical results rather than trying to give a comprehensive review of numerical studies of the effect of increased CO_2 on climate. (A more detailed survey of recent work is given in Schlesinger and Mitchell (1987).)

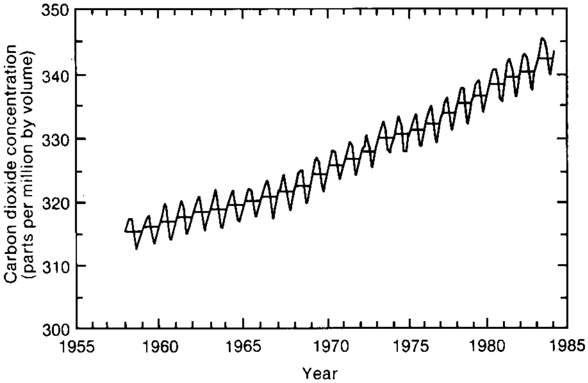

Figure 1. Concentration of atmospheric CO_2 at Mauna Loa Observatory, Hawaii. The horizontal bars represent annual averages and the diagram is reproduced from US Department of Energy (1985a).

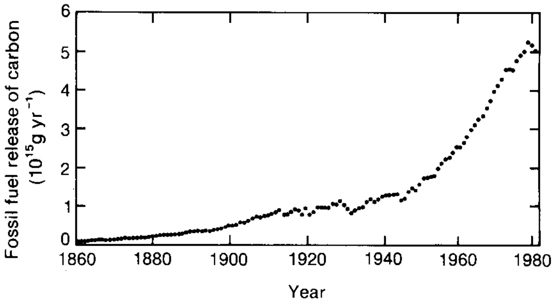

Figure 2. Fossil fuel emissions of carbon (from CO_2) from 1860 to 1982, from Marland and Rotty (1984) and reproduced in US Department of Energy (1985a).

The main concern will be with the effects of enhanced CO_2 from the beginning of the industrial revolution (about 100 years ago) until the end of the next century. In other words, we are interested in time-scales of up to a few centuries at most. We define a thermal response time to be the e-folding time to equilibrium (i.e. the time taken to reach 63% of the equilibrium temperature change due to a change in thermal forcing). As can be seen from Table I, the thermal response times of the atmosphere, land surface and upper ocean lie well within this time-scale, and that of the deep ocean partly so; hence these systems must be represented in our numerical models. On the other hand, the continental ice sheets have a much longer thermal response time, and hence it is assumed that, on the time-scale of interest, they will remain substantially unchanged.

Table I. *Thermal response times of various components of the climate system*

Component	Approximate response time (years)
Troposphere	0.05
Lower stratosphere	0.2–0.5
Land surface	0.2–1.0
Upper ocean	5–10
Deep ocean	100–1000
Continental ice sheets	≈ 10 000

2. Radiative forcing and simple feedback mechanisms

2.1 *Radiative effects*

The earth–atmosphere system is heated at a rate $(1-\alpha)S_0/4$ by solar (short-wave) radiation, where S_0 is the solar constant, α is the fraction of radiation reflected by the earth and atmosphere (currently about 0.33) and the factor of 4 allows for the spherical shape of the earth. This must be balanced by long-wave (thermal or infra-red) cooling to space. For a perfect emitter for example the earth's surface or thick cloud, the rate of long-wave cooling is given by σT^4, where T is the temperature of the emitter and σ is Stefan's constant. If the earth had no atmosphere, and α were unchanged, the surface temperature of the earth, T, would be given by

$$(1-\alpha)\,S_0/4 = \sigma T^4 \qquad \ldots \ldots \ldots \ldots \ldots \ldots \quad (1)$$

which gives an approximate value of T of 255 K (−18 °C). Certain gases (water vapour, carbon dioxide, ozone) absorb solar radiation weakly but strongly absorb and emit long-wave radiation. The (increased) downward long-wave radiation from these gases is responsible for the earth's surface temperature being 288 K (15 °C), some 33 K warmer than expected according to equation (1), a phenomenon often referred to as the 'greenhouse' effect.

Most of the radiation emitted to space emanates from the atmospheric gases rather than the surface. The effective emitting temperature of 255 K given by equation (1) corresponds to a height of about 6 kilometres. By increasing the concentration of an atmospheric absorber such as CO_2, the mean level from which radiation escapes to space moves to a higher, and therefore colder, level (see Fig. 3). The long-wave cooling to space is reduced and the earth–atmosphere system warms until the long-wave cooling again balances the incoming solar radiation.

The global mean temperature in the stratosphere is close to radiative equilibrium, but this is not true in the troposphere. If the temperature in the troposphere was controlled by radiation alone, the decrease in temperature with height (or lapse rate) would be much greater than observed (Manabe and Wetherald 1967). In regions where dense air overlies less dense air, the atmosphere produces overturning (mixing in the vertical, or convection) until the lapse rate is reduced to the stable value, which is 9.8 K km^{-1} for dry air. If moisture is present, rising air may cool sufficiently to become supersaturated, so that condensation occurs and latent heat is released. This further reduces the lapse rate, so the global mean value is about 6.5 K km^{-1}. To summarize, the equilibrium temperature of the troposphere is dependent on the balance between radiative cooling to space and the convective transfer of heat from the surface. Conversely, the surface is heated radiatively, and cooled by the loss of sensible and latent heat to the atmosphere. Both these processes must be represented in any model which is to be used to study the surface and tropospheric response to increased CO_2.

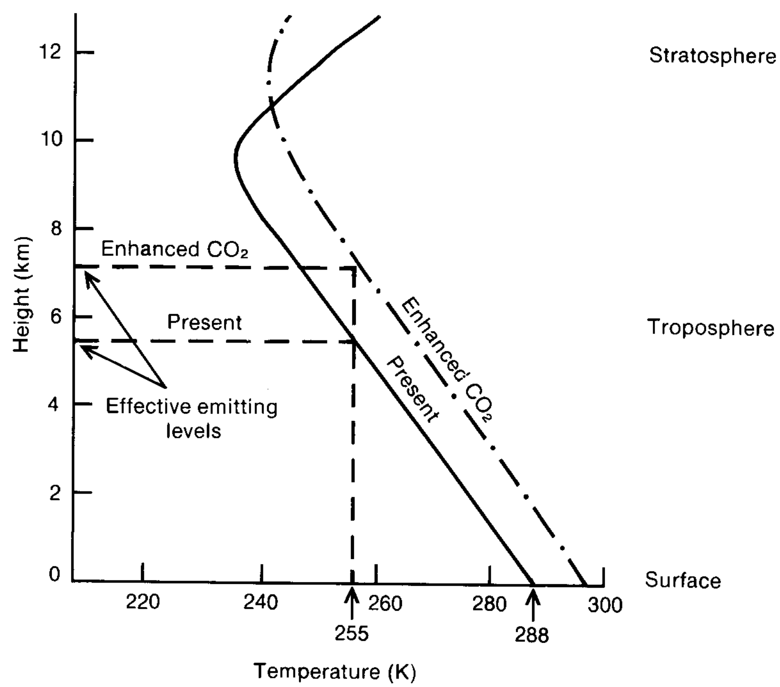

Figure 3. The effect of increasing CO_2 on the vertical profile of temperature (schematic representation).

2.2 *Some climate feedbacks*

Any model used to investigate the effect of increased CO_2 on the climate must be able to represent the important climate feedbacks; these are due to water vapour, sea-ice/snow, cloud cover and cloud optical properties.

(i) *Water vapour.* Increasing temperature by 1 K from 288 K increases the saturation vapour pressure of water by about 7%. Thus, it is to be expected that the atmospheric water vapour content will increase with temperature. Manabe and Wetherald (1967), on the basis of the observed seasonal variation of atmospheric humidity, concluded that relative humidity (the percentage of saturation) was approximately constant. This being the case, an increase in atmospheric temperature will be accompanied by an enhancement of atmospheric water vapour which increases the opacity of the atmosphere to long-wave radiation and thus enhances the warming of the atmosphere and earth's surface.

(ii) *Sea-ice/snow.* An increase in atmospheric temperature will tend to reduce highly reflective snow and sea-ice cover, leading to increased absorption of insolation and further warming. Clearly, the strength of this feedback will depend on the areal cover of snow and sea-ice, and hence the temperature of the unperturbed simulation. In general, the colder the simulation the greater the sensitivity of the model. Removal of sea-ice greatly increases the thermal inertia of the surface and reduces the amplitude of the annual cycle — this will enhance a warming in winter and reduce it in summer.

(iii) *Cloud-cover.* Clouds reflect solar radiation and absorb and emit infra-red radiation. A decrease in cloud cover reduces both the reflection of solar radiation, producing a surface warming, and the emission of long-wave radiation, producing a cooling. Current evidence suggests that the former effect is dominant at most latitudes where insolation is significant. The long-wave effects may be more important for high, thin cirrus. In addition, an increase in cloud height will also tend to warm the surface because radiation from the cloud top is emitted to space at a lower temperature.

Simulations with increased CO_2 using three-dimensional climate models show a consistent decrease in middle- and upper-tropospheric cloud at most latitudes, with increases in cloud in the lower stratosphere, particularly in middle and high latitudes (Schlesinger and Mitchell 1987). Similar changes have been found in an experiment using a version of the Meteorological Office 11-layer model in which CO_2 amounts were doubled (Wilson and Mitchell 1987b). These changes are consistent with an increase in the height of the tropopause. The observed tropopause is highest in low latitudes and in summer when insolation is strongest; thus there is at least circumstantial observational evidence that the model's response to tropospheric warming is physically correct.

The details of the above changes are obviously sensitive to the parametrization of radiation, particularly with respect to water vapour, and the vertical transport of water. The vertical resolution of most models is poor near the tropopause (generally there are three layers above 250 mb though the Meteorological Office model has four) and the vertical extent of cloud is usually limited; for example, in the Meteorological Office model used here it is confined below 60 mb.

(iv) *Cloud optical properties.* The parametrization of cloud has to date been based on relative humidity, although attempts have been made to devise a parametrization of cloud liquid water. This approach has the advantage that cloud optical properties can be related in a consistent manner to the liquid water content but, as yet, such liquid-water content parametrizations are fairly arbitrary. A general increase in atmospheric specific humidity might be expected to lead to an increase in cloud liquid-water content and hence the reflectivity of cloud. Stephens (1978) has derived simple parametrizations of the relation between cloud optical properties and cloud liquid-water content, based on observational data. He found a gradual increase in cloud reflectivity (albedo) with cloud liquid-water content, although the long-wave emissivity of thin cloud (e.g. cirrus) may also increase significantly. An increase in albedo would cool the surface; an increase in the long-wave emissivity of high cloud would have the opposite effect. It is by no means clear how one can relate cloud liquid-water content to large-scale model variables (e.g. temperature, humidity, etc.). Nevertheless, Somerville and Remer (1984) have attempted to do this by relating cloud liquid-water content to temperature, and find that the resulting negative feedback is sufficient to counteract all the positive feedbacks described earlier. In view of the uncertainties in their parametrization, the magnitude of cloud optical feedback is also extremely uncertain, and is a priority for future research.

3. Equilibrium studies using general circulation models

3.1 *Introduction*

Some aspects of climate change can be investigated economically using inexpensive one-dimensional models (for example, the initial study of water-vapour feedback made by Manabe and Wetherald (1967)). However, many factors such as horizontal transport, land–sea contrasts and the effects of orography are treated inadequately or omitted altogether. Furthermore, one-dimensional models cannot provide the regional variations which are needed to assess the possible impacts of climate changes, so there has been an enormous effort to develop and use the considerably more expensive three-dimensional models of climate.

The atmospheric component of a three-dimensional climate model can be regarded as a numerical prediction model which has been designed for long integrations. (Most of the physical parametrizations in the Meteorological Office forecast model have been taken from the Office's climate model with only minor modifications.) However, although general circulation models simulate the passage of individual disturbances, it is the behaviour of the model over long periods which is of interest. The philosophy for carrying out model 'experiments' is as follows. Firstly, the model is run for a long period, usually between several years and several decades, with present-day boundary conditions (in this case, present CO_2 concentrations). The length of simulation is chosen so that the long-term statistics (for example, monthly mean surface temperatures and inter-annual variances) are well defined and independent of the initial conditions. Then an anomaly simulation with enhanced CO_2 is made, and the difference in the statistics of the two simulations is examined to assess the impact of the changes.

As noted in section 1, atmospheric CO_2 and trace gases are increasing on a time-scale of decades to centuries, and hence changes in ocean temperatures and sea-ice must be taken into account. Due to the large thermal inertia of the deep oceans, it has not been practical to integrate a detailed climate model with a deep ocean to equilibrium, though this is now possible if the seasonal cycle of solar radiation is ignored. Hence, most work to date has involved models with grossly simplified representations of the ocean.

3.2 *An early study*

In the earliest study (Manabe and Wetherald 1975), oceanic heat storage and transport were ignored, and sea surface temperatures were determined diagnostically such that the net heat flux across the air–sea interface was zero. Sea-ice was predicted where the ocean temperature fell below the freezing-point of sea water. This representation of the ocean is often referred to as as 'swamp' ocean. The diurnal and seasonal variation of incoming solar radiation must be ignored in view of the neglect of the ocean's heat capacity. Manabe and Wetherald also limited the computational domain to a sector covering approximately one-sixth of the globe, used an idealized land–sea distribution and ignored the effects of topography.

The simulated equilibrium change in atmospheric temperature due to doubling CO_2 (Fig. 4) varies considerably with latitude. In low latitudes, the warming is about 2 K near the surface and increases to over 3 K at upper levels of the troposphere. As noted earlier, in the tropical atmosphere the vertical gradient of temperature tends to the moist adiabatic lapse rate which becomes smaller as temperature increases, leading to enhanced warming at upper levels. Conversely, in high latitudes, the surface warming is enhanced because the inherent stable stratification inhibits the transfer of heat to upper levels. Two further mechanisms contribute to the enhanced surface warming in high latitudes. Firstly, the increase in temperature will reduce the extent of highly reflective snow and sea-ice cover, leading to increased absorption of insolation and further warming (temperature–albedo feedback). Secondly, the atmospheric water content is greater in the warmer atmosphere, leading to a larger poleward transport of moisture and enhanced latent heat release in high latitudes. The areal mean warming on doubling CO_2 is 2.9 K.

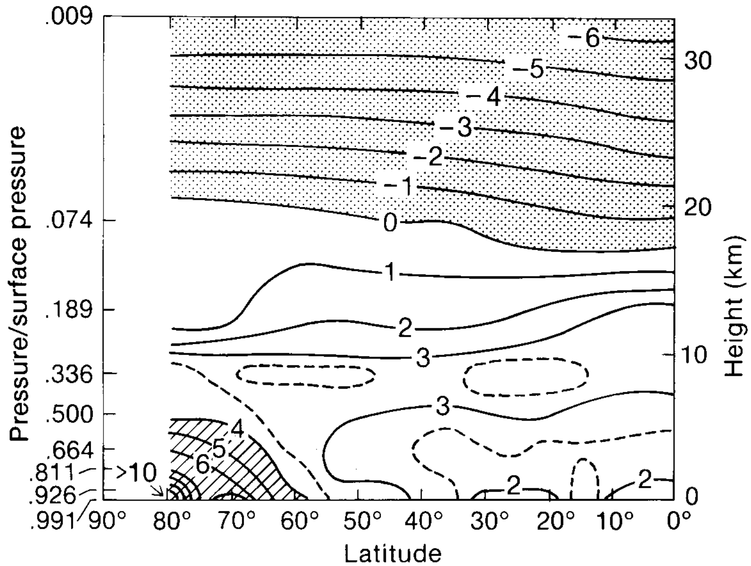

Figure 4. Height–latitude diagram of zonally averaged temperature changes (K) due to doubling CO_2 in an idealized climate model, from Manabe and Wetherald (1975). Changes greater than 4 K are shaded and less than zero stippled.

3.3 *A detailed study with prescribed cloud cover*

Useful as Manabe and Wetherald's study is for illustrating some of the physical mechanisms which contribute to changes in climate, it gives no guidance on the seasonal and regional changes which, for example, are necessary for the assessment of the likely social and economic effects of increased CO_2. To do so, one must use a model which includes the annual cycle of insolation. This has been attempted using two differing but complementary approaches.

In the first approach, the ocean is represented by a static pool with the depth (typically 50–70 metres) chosen to provide reasonable simulation of the annual cycle of sea surface temperatures over most of the oceans. A simple representation of sea-ice is also included. This approach allows the sea surface temperatures and sea-ice extents to interact with the atmosphere as it responds to the increase in CO_2 concentrations. It has the disadvantage that errors in the atmospheric model, and the crudeness of the ocean model, lead to errors in the simulation of present-day climate which may distort the response of the model to small perturbations.

Manabe and Stouffer (1980) investigated the effect of quadrupling CO_2 amounts in such a model with realistic geography and orography, and using prescribed zonally averaged cloud cover. The global mean surface temperature increased by 4.1 K. In the tropics, the warming is less than 3 K near the surface (Fig. 5) and increases to over 4 K in the upper troposphere, whereas in high latitudes in winter, especially over the Arctic, the warming is a maximum near the surface and decreases rapidly with height, in qualitative agreement with Manabe and Wetherald (1975). However, in high latitudes in summer, the lower atmosphere is not inherently stable in the unperturbed integration, and so the warming is more uniformly distributed in the troposphere. In the Arctic in summer, the near-surface warming is small for reasons discussed below.

In the $4 \times CO_2$ integration, the areal extent of highly reflective sea-ice is substantially reduced leading to enhanced absorption of solar radiation by the high-latitude oceans, particularly in summer (sea-ice

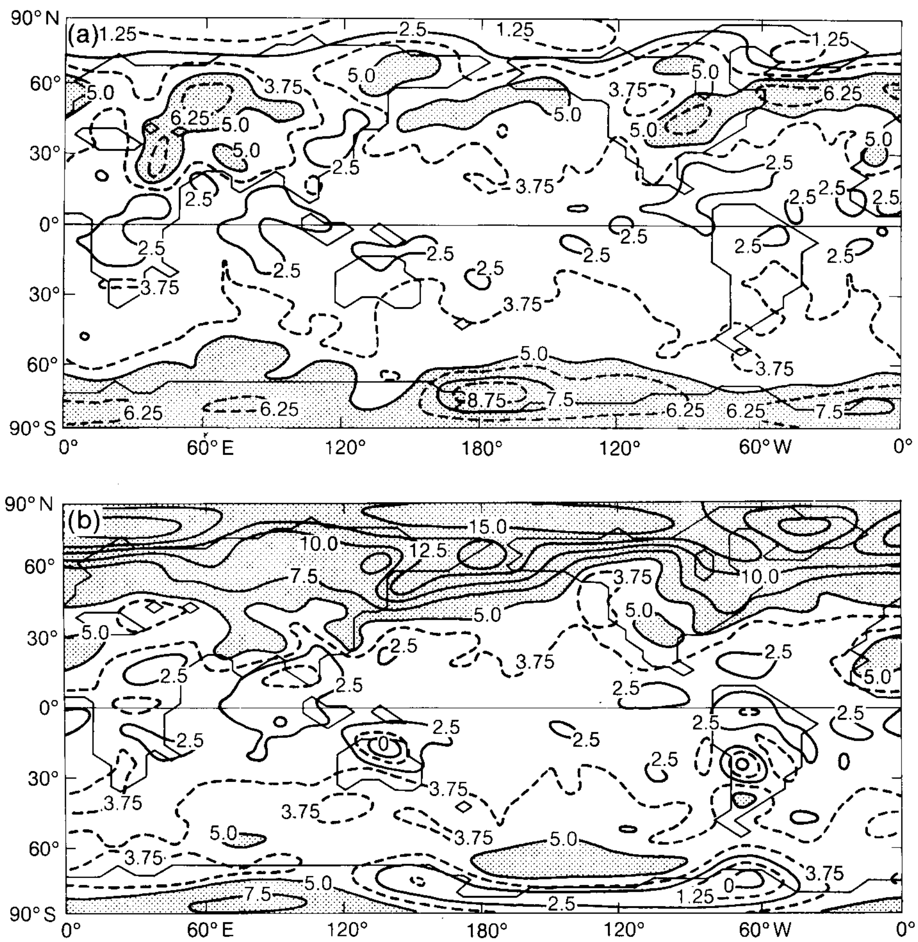

Figure 5. Average changes in surface air temperature (K) due to quadrupling CO_2 in a low-resolution climate model with prescribed cloud (Manabe and Stouffer 1980) from (a) June to August and (b) December to February. The areas with changes greater than 5 K are stippled.

disappears from the Arctic in summer and is absent from the Antarctic during most of the year). The enhanced ocean heat storage delays the formation of ice in autumn, leading to thinner ice in winter and consequently earlier melting of ice in spring. In the Arctic, the delay in the formation of sea-ice and the consequent reduction in the insulation of the atmosphere from the relatively warm mixed-layer surface leads to a maximum warming in autumn. In winter, there is still a substantial increase in surface air temperature since the atmosphere is inherently stable and the warming is confined to the lowest model layer as found by Manabe and Wetherald (1975). In summer, however, the warming is a minimum, despite increases of up 50 W m^{-2} in solar heating, because the large thermal inertia of the mixed layer prevents temperatures rising much above 271 K, the melting point of sea-ice. Around Antarctica, the seasonal variation in the temperature change is smaller, probably because the seasonal variation in the control integration is smaller than in the Arctic. The mean warming is also smaller, perhaps because the sea-ice in the control integration is thinner and less extensive than in the northern hemisphere (and less than the observed thicknesses).

Temperature changes over the northern hemisphere continents are generally similar to those over neighbouring oceans. In April, there is a secondary maximum warming near 60° N associated with the earlier removal of highly reflective snow cover in the $4 \times CO_2$ integration. Over Antarctica, the temperature–albedo feedback is much weaker, as throughout the year in the control integration the surface temperatures are substantially lower than the threshold above which albedo varies. This is largely a result of the height of the Antarctic plateau.

It should be noted that Manabe and Stouffer used a low-resolution (15 spectral waves) model which is inadequate to represent the weak baroclinic disturbances which are characteristic of the northern hemisphere mid-latitude summer circulation, and which on the western side of continents are associated with much of the summer precipitation. Furthermore, the neglect of the oceanic circulation leads to errors in the distribution of sea surface temperatures and sea-ice, which may distort the response of their model to enhanced CO_2. The errors in the sea-ice distribution in Manabe and Stouffer's control integration have already been noted. Even where atmospheric models have been coupled to a dynamical model of the ocean (Manabe *et al.* 1979, Washington *et al.* 1980, Gates *et al.* 1985) there are substantial errors in the simulated sea surface temperatures and sea-ice extents. Hence, some studies carried out in the Meteorological Office have followed a different strategy, which will now be described.

3.4 *Studies with prescribed cloud cover carried out at the Meteorological Office*

In the control integration used by the Meteorological Office, sea surface temperatures are prescribed from climatology. Since the changes due to CO_2 are sufficiently small to be regarded as a perturbation, the changes in sea surface temperature are prescribed on the basis of a succession of perturbation experiments which approximate equilibrium with increasing accuracy. The advantages of this approach are that the simulated control climate is not distorted by errors in sea surface temperatures and sea-ice, and the simulations attain equilibrium after about 1 year as opposed to 10 or more years needed with a 'slab' ocean. In the Meteorological Office, the consequent saving in computer time has allowed the use of high-resolution atmospheric models which are capable of representing baroclinic disturbances throughout the year. The disadvantage of the method is that the prescribed changes (particularly of sea-ice extent) are only approximately in equilibrium, and hence may influence other aspects of the model's response.

In the first Meteorological Office study (Mitchell 1983) the response of the ocean was ignored. In the second, also described by Mitchell (1983), the ocean temperature increase was assumed to be the same everywhere. In the third (Mitchell and Lupton 1984), the ocean temperature changes were prescribed as a function of latitude on the basis of the previous two experiments, assuming that the sea surface temperatures respond locally and linearly to changes in the surface heat balance. The specified changes in sea surface temperature in the tropics and subtropics were similar to those found by Manabe and Stouffer (1980), but in high latitudes the method proved unreliable and so changes were based on the GFDL experiments. Analysis of the experiments has concentrated on the changes in the hydrological cycle since the temperature change over most of the earth's surface is prescribed.

The warming of the atmosphere is accompanied by an increase in atmospheric moisture, which in the absence of marked changes in circulation leads to increased precipitation (or more accurately, precipitation minus evaporation) in the main regions of low-level atmospheric convergence. Thus, the flux of moisture into high latitudes in winter is enhanced leading to increased precipitation, soil moisture and run off. The equatorward moisture flux associated with the lower branch of the main Hadley cell (the trade winds in the winter hemisphere) is also enhanced, giving enhanced moisture divergence in the winter subtropics where there is a tendency to reduced precipitation. These changes are reflected in the geographical distribution of precipitation; the precipitation increases in the main regions of atmospheric convergence including the mid-latitude depression tracks, especially in winter, and along the intertropical convergence zone and its extension into the continents. Thus precipitation increases over the southern United States, the Sahel and south-east Asia during the northern summer (Fig. 6 (a)) and in eastern South America, South Africa and eastern Australia during the southern summer (Fig. 6 (b)). Precipitation tends to decrease in the regions of enhanced divergence in the subtropics. The pattern of the changes in precipitation is broadly similar to that in the earlier experiment with a uniform increase in sea surface temperatures (Mitchell 1983); this suggests that changes in precipitation are not critically dependent on the detailed structure of changes in sea surface temperature.

Most studies to date have concentrated on the mean changes in climate. The changes in variability may be of greater economic and social importance. Wilson and Mitchell (1987a) analysed changes in variability over western Europe in the third Meteorological Office experiment. They found, for example, that the general reduction in precipitation over southern Europe during the northern summer is the result of both fewer precipitation events and reduced precipitation per event.

3.5 *Detailed studies with simulated cloud*

The earlier GFDL and Meteorological Office experiments used prescribed zonally averaged cloudiness. The parametrization of cloud in climate models is extremely crude, being based on grid-box relative humidity or, in the case of convective cloud, the occurrence of moist convection. Nevertheless, several studies have included model-generated cloud cover (e.g. Hansen *et al.* (1984), Washington and Meehl (1984)). The role of changes in cloudiness in CO_2 experiments has been reviewed by Wetherald and Manabe (1986), and results from a recent Meteorological Office experiment using a low-resolution atmospheric model coupled to a mixed-layer ocean are fairly typical. Cloud amounts increase at upper levels near the model tropopause, due to deeper convection and vertical motion, and decrease in the upper and middle troposphere, particularly in the equatorial mid-latitude convection zones. In effect, the height of the model tropopause is increased. In addition, Wetherald and Manabe (1986) note an increase in low stratus cloud in regions where the atmosphere is inherently stable (e.g. over the winter continents and in the marine boundary layer under the subtropical anticyclones). This they attribute to enhanced evaporation which increases the flux of moisture into the boundary layer where it is trapped under the climatological inversion.

The changes in cloudiness produce a substantial increase in the sensitivity of climate to thermal forcing (Hansen *et al.* 1984). The reduction in total cloud noted in most experiments will warm the surface and troposphere, as noted in section 2.2. Where high cloud is increased at the expense of more highly reflective low cloud, the loss of solar radiation to space is reduced and, because the effective cloud height is also increased, the emission of long-wave radiation to space is also reduced. Hence the warming

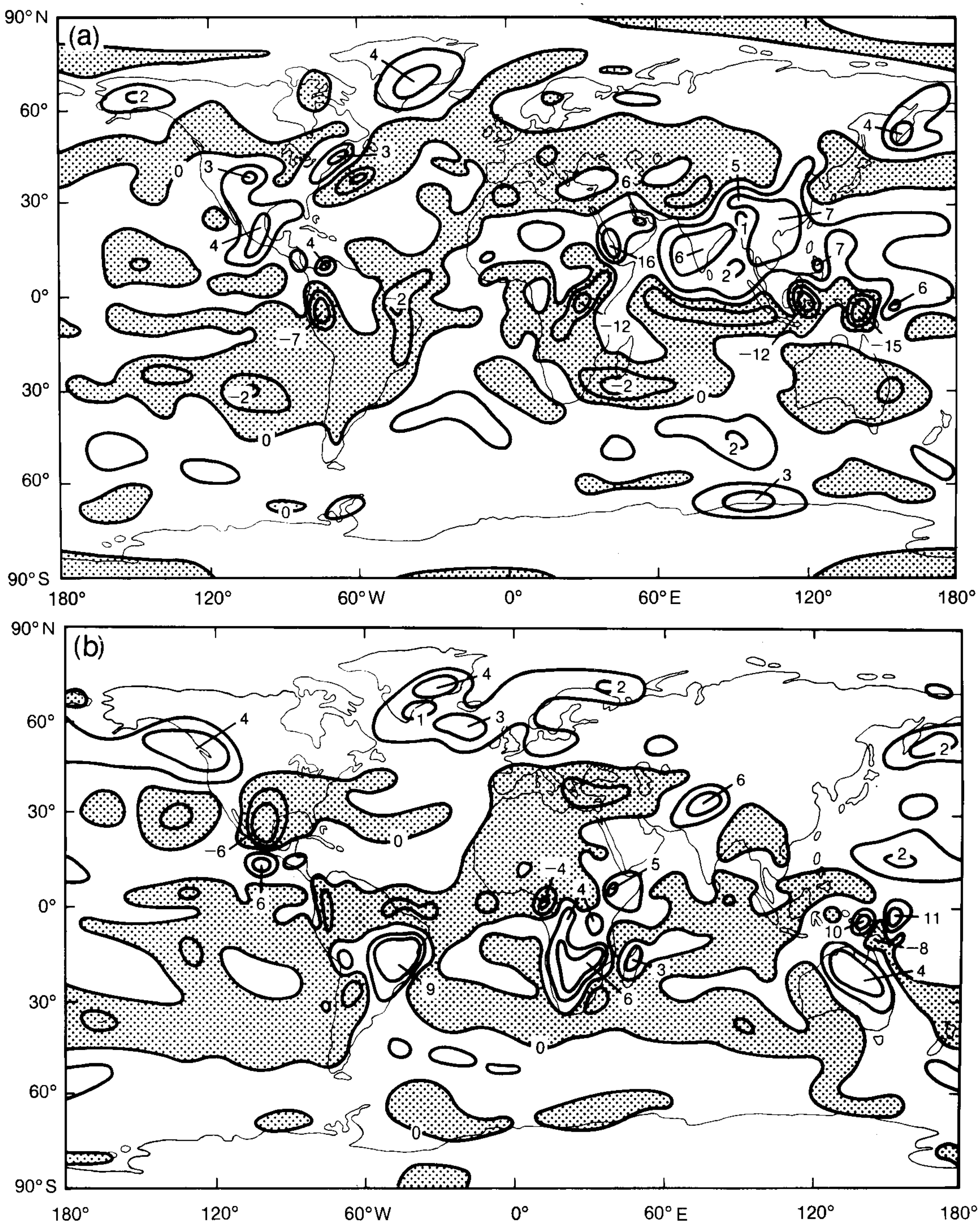

Figure 6. Average changes in precipitation (mm d^{-1}) in the $4 \times CO_2$ experiment with climatological cloud and prescribed changes in the sea surface temperature (Mitchell and Lupton 1984) from (a) June to August and (b) December to February. The areas of decrease are stippled.

of the troposphere and surface is further augmented by enhanced solar heating and reduced long-wave cooling.

The effect of the cloud feedback is such that the global mean temperature changes due to doubling CO_2 is as large as that due to quadrupling CO_2 in a model with fixed cloud (Manabe and Wetherald 1986). The patterns of temperature change in the GFDL $4 \times CO_2$ fixed and $2 \times CO_2$ variable cloud experiments are remarkably similar except in the Antarctic periphery, particularly in the southern summer, where the warming in the $4 \times CO_2$ experiment is smaller, perhaps owing to the underestimation of Antarctic sea-ice extents in the earlier control integration.

A similar though less-marked correspondence exists between the changes in precipitation in the Meteorological Office $4 \times CO_2$ experiment with prescribed cloud (Fig. 6) and a $2 \times CO_2$ experiment with variable cloud (Fig. 7). In both experiments, precipitation increases along the depression tracks

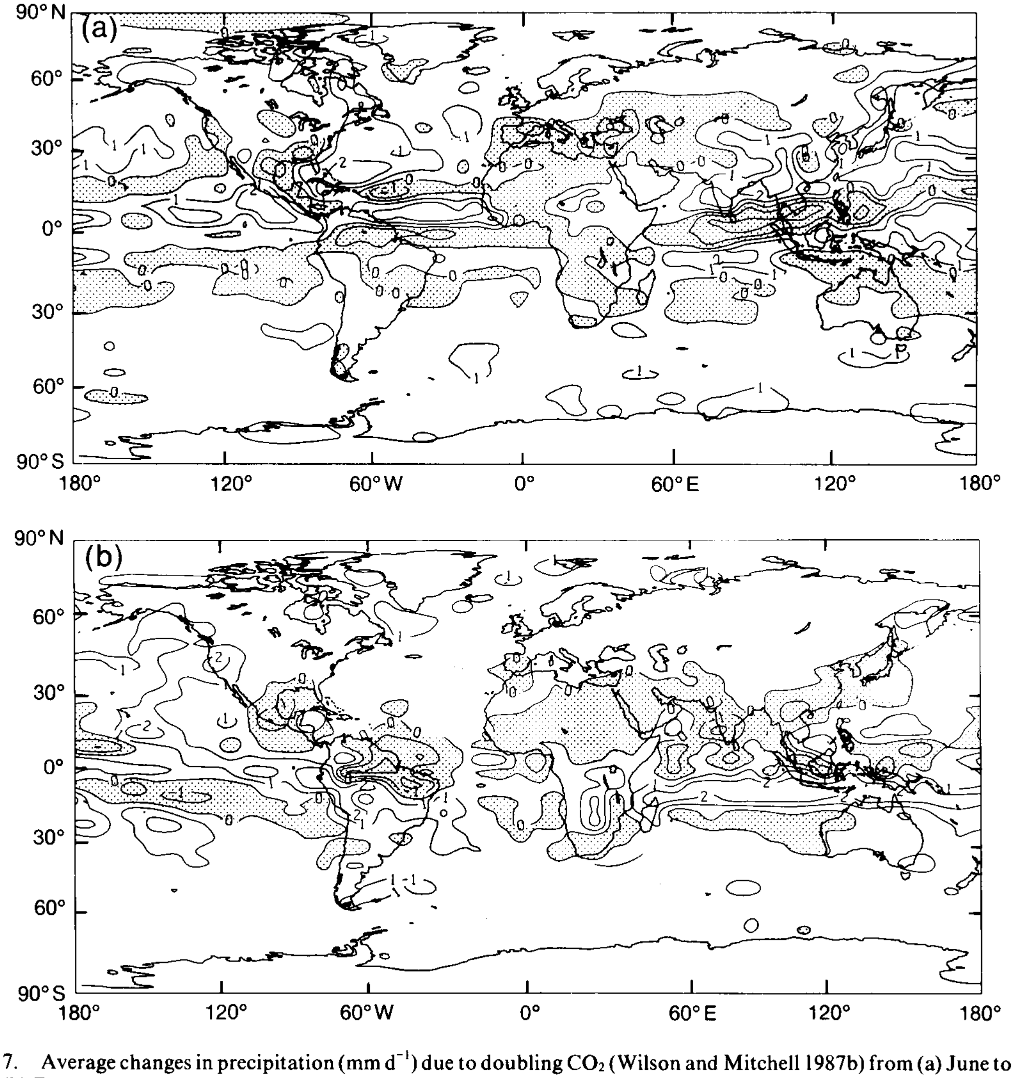

Figure 7. Average changes in precipitation (mm d^{-1}) due to doubling CO_2 (Wilson and Mitchell 1987b) from (a) June to August and (b) December to February. The areas of decrease are stippled.

and in the summer monsoon regions, and changes little or tends to decrease in the subtropics. In general there is a greater tendency for precipitation to increase over the oceans in the $2 \times CO_2$ experiment; since there were considerable differences in the atmospheric models used in the two experiments, this discrepancy is not necessarily due to the differences in the prescription of cloud or sea surface temperature. The problem of model dependence of results is discussed in more detail by Mitchell *et al.* (1987). Note the tendency in the $2 \times CO_2$ experiment for the intertropical convergence zone to shift polewards in the summer hemisphere. (In general, the distribution of changes in precipitation in simulations with increased CO_2 agree less well than the distribution of changes in temperature (Schlesinger and Mitchell 1987). This is largely due to the greater temporal and spatial variability of precipitation and to the large variation in precipitation patterns in control simulations from different models.)

In general, changes in soil moisture are more stable, particularly outside the tropics. As noted earlier, there is a general tendency in the GFDL and Meteorological Office experiments for the land surface in the middle and high latitudes of the northern hemisphere to become drier during summer in the enhanced CO_2 simulations. This is particularly true in studies with model-generated cloud (see Manabe and Wetherald (1986), Wilson and Mitchell (1987b)). One may speculate that the reduction in evaporation associated with the drier surface may reduce boundary-layer cloud, producing a further drying of the surface and so forth.

3.6 *Oceanic effects*

The use of three-dimensional coupled ocean–atmosphere models to study the effects of CO_2 has largely been limited to low-resolution simulations using annually averaged insolation and idealized geography (Spelman and Manabe 1984, Manabe and Bryan 1985). Manabe and Bryan performed six experiments with CO_2 concentrations ranging from 150 to 2400 ppmv. Equilibrium was reached using the acceleration techniques, including those described by Bryan (1984). The zonal mean temperature changes in the upper ocean due to a fourfold increase in CO_2 (Fig. 8) follow those in the atmosphere, with smallest changes in low latitudes due to the effects of moist convection, and the greatest warming in high latitudes due to sea-ice albedo feedback and the weakening of the surface inversion. The large surface warming in high latitudes is propagated into the deep ocean where it is advected equatorwards. Manabe and Bryan comment that the intensity of the model's oceanic meridional circulation changes little for CO_2 concentrations above 300 ppmv. The coefficient of expansion of sea water increases sharply with temperature. Hence, the greater warming in high latitudes is largely compensated by the larger coefficient of thermal expansion in low latitudes and the meridional density gradient is changed little.

3.7 *The transient response*

So far, we have considered only the equilibrium response of climate to enhanced atmospheric CO_2 concentrations. The time-dependent response of climate to an increase in CO_2 concentrations is likely to be slowed by the large thermal inertia of the oceans. Since the effective thermal inertia of the oceans is dependent on the ocean circulation and varies with latitude, it is possible, as suggested by Schneider and Thompson (1981), that the transient response of the climate to enhanced atmospheric CO_2 could differ substantially from the equilibrium response. Spelman and Manabe (1984) investigated the effect of 'switching on' a fourfold increase in CO_2 using synchronous coupling between the ocean and atmosphere (that is, the devices to accelerate convergence to equilibrium were removed) and compared the response with that at equilibrium. After 25 years, the fractional response in the upper atmosphere and surface layer of the ocean was generally uniform with latitude (Fig. 9). The greatest penetration of the warming

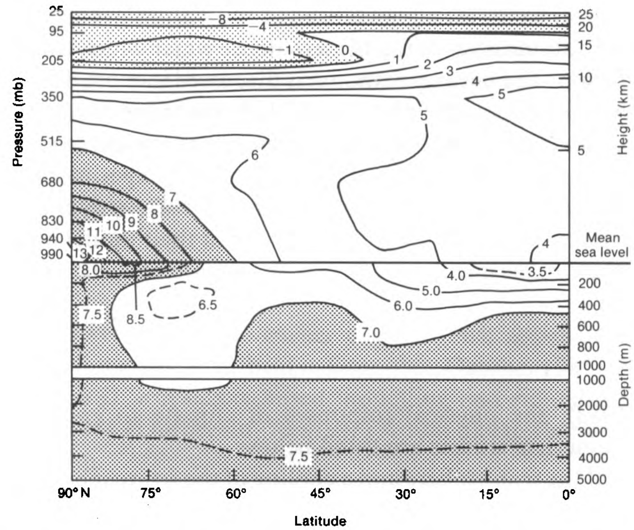

Figure 8. Height–latitude diagram of zonally averaged equilibrium changes in temperature (K) due to quadrupling CO_2 in an idealized coupled ocean–atmosphere model (Spelman and Manabe 1984). Increases of greater than 7 K and decreases are separately delineated.

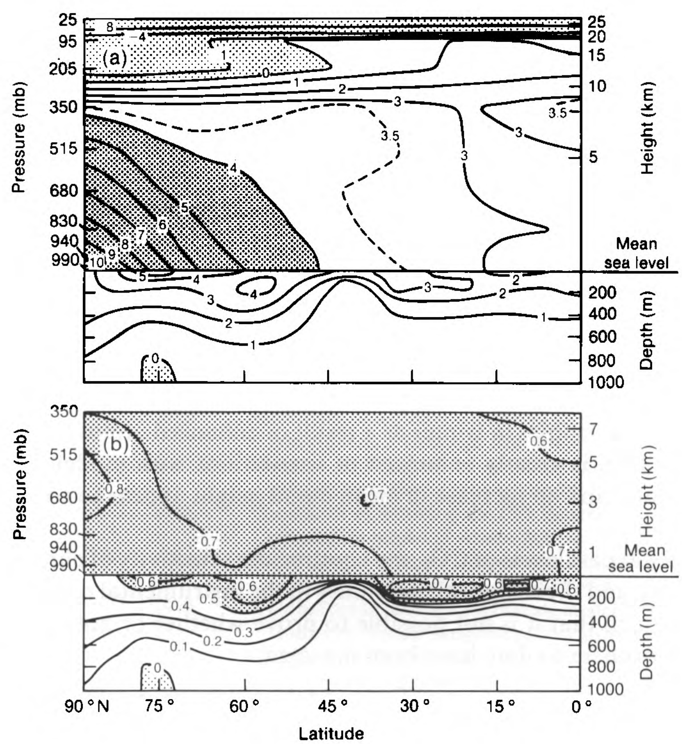

Figure 9. Height–latitude diagram of zonally averaged changes in temperature (a) 25 years after quadrupling CO_2 amounts in an idealized coupled ocean–atmosphere model and (b) fraction of equilibrium response (Spelman and Manabe 1984). Various significant areas are delineated.

in the deep ocean occurred near 55° N. At higher latitudes, the warming is largely confined to the surface layer, due to the presence of a stable layer of fresher less-dense water which was the result of the excess of precipitation over evaporation. The oceanic response is discussed in more detail by Bryan and Spelman (1985). Spelman and Manabe suggest that, provided the time constant for increasing CO_2 concentrations is greater than 25 years, the transient response of zonally averaged temperature should resemble the equilibrium response. The ocean model used in their experiments is highly idealized, does not resolve mesoscale eddies and substantially underestimates the strength of the meridional circulation. As Spelman and Manabe point out, the transient behaviour of their model needs to be verified against observational data and their experiment repeated with a more realistic model before we can have confidence in these results.

4. Concluding remarks

Following Manabe (1983), the physical responses of climate to enhanced CO_2 concentrations determined from recent numerical studies are listed below:

(a) There is a warming of the troposphere and a cooling of the stratosphere because the enhancement of atmospheric CO_2 concentrations increases the opacity of the atmosphere to long-wave radiation, and raises the effective emitting level of the atmosphere.

(b) The annual mean surface warming is largest in high latitudes because of sea-ice and snow–albedo feedbacks, the inherent low-level stability in high latitudes, and perhaps the enhanced advection of latent heat from lower latitudes.

(c) Over the Arctic Ocean and surrounding regions the warming has a large seasonal dependence, and is a minimum in summer. There is little seasonal dependence in temperature changes in low latitudes.

(d) Global mean rates of evaporation and precipitation increase. This is due to enhanced radiative heating at the surface in the warmer, moister, CO_2-enriched atmosphere.

(e) The snow-melt season begins earlier.

(f) Sea-ice is less extensive (and thinner, at least in those studies from which such information is available).

(g) Precipitation and (where reported) run off increase in high latitudes because of the enhanced poleward transport of moisture in the warmer, moister atmosphere.

(h) In most studies to date, soil moisture is reduced over much of the middle- and high-latitude continents of the northern hemisphere in summer. This change is due to one or more of the following factors: earlier snow melt, enhanced evaporation and reduced precipitation. Soil moisture also decreases in northern subtropics in winter as a result of enhanced atmospheric moisture divergence.

(i) The response to CO_2 is greatly enhanced in simulations with model-generated cloud. Both a reduction in total cloud and an increase in mean cloud height appear to contribute to the enhanced surface warming.

(j) The uncertainties in past levels of CO_2, the equilibrium sensitivity of climate to CO_2, the transient response of the ocean, and the temporal variability in the instrumental record of temperature during the last century are such that it is not possible to prove whether or not the climatic effects of CO_2 increases in the atmosphere to date have been detected.

Recent work has demonstrated that simplified models, although invaluable for identifying physical mechanisms, can produce misleading results since they may omit processes relevant to climate change, or they may not weight competing mechanisms correctly. In the same way, it must be recognized that the most sophisticated models in use at present contain many simplifications and approximations which may distort the simulated response to enhanced CO_2. In particular, the horizontal resolution employed in most climate models to date is inadequate to provide an accurate simulation of present-day regional climate, and so such models are unlikely to provide reliable guidance on regional climate change.

Many disciplines are involved in assessing the human consequences of increases in atmospheric CO_2. To do so, they require accurate predictions of potential changes in climate. Numerical models of climate provide the most promising means of making those predictions. Since, unlike those involved in numerical weather prediction, we cannot verify the detailed behaviour of these models using case histories, our confidence in the model's performance must depend on the degree to which it is based on physical principles.

Acknowledgements

This paper is a shortened version of two earlier papers which appeared in the Proceedings of the NATO Workshop 'Abrupt climatic change' held in Grenoble, October 1985 (Dordrecht, Reidel) and the Proceedings of the NATO ASI 'Physically-based modelling and simulation of climate and climatic change' held in Erice, May 1986 (Dordrecht, Reidel). I would like to thank Dr R.W. Riddaway for his help in producing this version.

References

Bryan, K. 1984 Accelerating the convergence to equilibrium of ocean–climate models. *J Phys Oceanogr*, **14**, 666–673.

Bryan, K. and Spelman, M.J. 1985 The ocean's response to a CO_2-induced warming. *J Geophys Res*, **90**, 11679–11688.

Callendar, G.S. 1938 The artificial production of carbon dioxide and its influence on temperature. *Q J R Meteorol Soc*, **64**, 223–240.

Gates, W.L., Han, Y.-J. and Schlesinger, M.E. 1985 The global climate simulated by a coupled atmosphere–ocean general circulation model, preliminary results. *In* Nihoul, J.C.J.(ed); Coupled ocean–atmosphere models. New York, Elsevier.

Hansen, J., Lacis, A., Rind, D., Russell, G., Stone, P., Fung, I., Ruedy, R. and Lerner, J. 1984 Climate sensitivity and analysis of feedback mechanisms. *In* Hansen, J.E. and Takahashi, T. (eds); Climate processes and climate sensitivity. Washington DC, American Geophysical Union.

International Council of Scientific Unions 1979 The global carbon cycle, SCOPE 13. Bolin, B., Degens, E.T., Kempe, S. and Ketner, P. (eds). Chichester, Wiley.

1986 The greenhouse effect, climatic change and ecosystems SCOPE 29. Bolin, B., Döös, B.R., Jäger, J. and Warwick, R.A. (eds). Chichester, Wiley.

Manabe, S. 1983 Carbon dioxide and climatic change. *Adv Geophys*, **25**, 39–82.

Manabe, S. and Bryan, K. 1985 CO_2-induced change in a coupled ocean–atmosphere model and its paleoclimatic implications. *J Geophys Res*, **90**, 11689–11707.

Manabe, S. and Stouffer, R.J. 1980 Sensitivity of a global climate to an increase of CO_2 concentration in the atmosphere. *J Geophys Res*, **85**, 5529–5554.

Manabe, S. and Wetherald, R.T. 1967 Thermal equilibrium of the atmosphere with a given distribution of relative humidity. *J Atmos Sci*, **24**, 241–259.

1975 The effects of doubling the CO_2 concentration on the climate of a general circulation model. *J Atmos Sci*, **32**, 3–15.

1986 Reduction in summer soil wetness induced by an increase in atmospheric carbon dioxide. *Science*, **232**, 626–628.

Manabe, S., Bryan, K. and Spelman, M.J. 1979 A global ocean atmosphere climate model with seasonal variation for future studies of climate sensitivity. *Dyn Atmos and Oceans*, **3**, 393–426.

Marland, G. and Rotty, R.M. 1984 Carbon dioxide emissions from fossil fuels: a procedure for estimation and results for 1950–82. *Tellus*, **36B**, 232–261.

Mitchell, J.F.B. 1983 The seasonal response of a general circulation model to changes in CO_2 and sea temperatures. *Q J R Meteorol Soc*, **109**, 113–152.

Mitchell, J.F.B. and Lupton, G. 1984 A $4 \times CO_2$ integration with prescribed changes in sea temperatures. *Prog Biometeorol*, **3**, 353–374.

Mitchell, J.F.B., Wilson, C.A. and Cunnington, W.M. 1987 On CO_2 climate sensitivity and model dependence results. *Q J R Meteorol Soc*, **113**, 293–322.

Oeschger, H. and Stauffer, B. 1986 Review of the history of atmospheric CO_2 recorded in ice cores. *In* Trabalka, J.R. and Reichle, D.E. (eds); The changing carbon cycle: a global analysis. New York, Springer-Verlag.
Schlesinger, M.E. and Mitchell, J.F.B. 1987 Model projections of equilibrium climatic response to increased CO_2 concentration. *Rev Geophys Space Phys*, **25**, 760–798.
Schneider, S.H. and Thompson, S.L. 1981 Atmospheric CO_2 and climate: importance of the transient response. *J Geophys Res*, **86**, 3135–3147.
Somerville, R.C.J. and Remer, L.A. 1984 Cloud optical thickness feedbacks in the CO_2 climate problem. *J Geophys Res*, **89**, 9668–9672.
Spelman, M.J. and Manabe, S. 1984 Influence of oceanic heat transport upon the sensitivity of a model climate. *J Geophys Res*, **89**, 571–586.
Stephens, G.L. 1978 Radiation profiles in extended water clouds. II: Parameterization schemes. *J Atmos Sci*, **35**, 2123–2132.
US Department of Energy 1985a Atmospheric carbon dioxide and the global carbon cycle. Report No. DOE/ER-0239. Washington DC, US Dept of Energy.
1985b Projecting the climatic effects of increasing carbon dioxide. Report No. DOE/ER-0237. Washington DC, US Dept of Energy.
1985c Detecting the climatic effects of increasing carbon dioxide. Report No. DOE/ER-0235. Washington DC, US Dept of Energy.
1985d Direct effects of increasing carbon dioxide on vegetation. Report No. DOE/ER-0238. Washington DC, US Dept of Energy.
Washington, W.M. and Meehl, G.A. 1984 Seasonal cycle experiment on the climate sensitivity due to a doubling of CO_2 with an atmospheric general circulation model coupled to a simple mixed-layer ocean model. *J Geophys Res*, **89**, 9475–9503.
Washington, W.M., Semtner, A.J. jun., Meehl, G.A., Knight, D.J. and Mayer, T.A. 1980 A general circulation experiment with a coupled atmosphere, ocean and sea ice model. *J Phys Oceanogr*, **10**, 1887–1908.
Wetherald, R.T. and *Manabe, S.* 1986 An investigation of cloud cover change in response to thermal forcing. *Clim Change*, **8**, 5–23.
Wilson, C.A. and Mitchell, J.F.B. 1987a Simulated climate and CO_2-induced climate change over western Europe. *Clim Change*, **10**, 11–42.
(1987b) A $2 \times CO_2$ climate sensitivity experiment with a global climate model including a simple ocean. (To appear in *J Geophys Res.*)

551.524.37(412):551.507.362.2

Satellite images of the distribution of extremely low temperatures in the Scottish Highlands

J. McClatchey, A.M.E. Runacres* and P. Collier

Department of Geography, Portsmouth Polytechnic

Summary

Temperatures below −20 °C have been recorded at stations in the Scottish Highlands on a number of occasions in the last six years. This paper describes the use of data from the Advanced Very High Resolution Radiometer on board the NOAA series of satellites to investigate the distribution of such low temperatures in the Highlands, and shows that even lower temperatures may have occurred than were recorded at any climatological stations.

1. Introduction

In three out of the last five winters since the UK extreme minimum screen temperature of −27.2 °C was last equalled on 10 January 1982 at Braemar, minima below −20 °C have been recorded at one or more stations in the Scottish Highlands. This paper examines the use of data from the Advanced Very

* Now at University College, Swansea

Met.O.978

THE METEOROLOGICAL MAGAZINE

1987 Volume 116

INDEX

	Pages		Pages
January	1–28	July	197–228
February	29–60	August	229–260
March	61–96	September	261–296
April	97–128	October	297–328
May	129–160	November	329–360
June	161–196	December	361–392

The responsibility for facts and opinions expressed in the signed articles and letters published in this magazine rests with their respective authors.

Published for the Meteorological Office by Her Majesty's Stationery Office

High Resolution Radiometer (AVHRR) on board the NOAA series of satellites to investigate the distribution of such low temperatures, and to determine whether even lower values are likely to have occurred at places where no climatological station is sited.

2. Problems in data analysis

2.1 *Satellite thermal imagery*

The AVHRR data consist of radiance values for each of five channels with a nadir instantaneous field of view of 1.1 km × 1.1 km and, although this spatial resolution is not as high as that available from Landsat for example, the temporal resolution is much greater with two satellite overpasses per 24 hours as compared to Landsat's one in 16 days. The thermal infra-red imagery is split into three channels (Channels 3, 4 and 5) of which Channels 4 and 5 are of most use in estimating surface temperatures. The spectral characteristics of the NOAA AVHRR are given by Lauritson *et al.* (1979).

An archive of AVHRR data is held by the Department of Electrical Engineering and Electronics at the University of Dundee from whom a computer tape of the digital information for a particular date can be obtained.

The radiance values from each channel come in the form of a 10-bit count giving a range of values from 0 to 1023. Using the method of Lauritson *et al.* (1979), these can be converted to equivalent black-body temperatures termed brightness temperatures. These brightness temperatures differ from actual surface temperatures by a variable amount which depends on, in particular, the effects of atmospheric attenuation and the values of surface emissivity. Also, as clouds effectively act as black bodies for terrestrial wavelengths, only cloud-free pixels (the approximately 1.1 km × 1.1 km picture elements) can be used in determining surface temperatures. Despite these problems, AVHRR data have been successfully used to estimate sea surface temperatures (Singh and Warren 1983). Also Pescod *et al.* (1986) reported that the operational use of AVHRR data in the production of maps of sea surface temperature is being investigated at the Meteorological Office.

2.2 *Surface emissivity*

The use of AVHRR imagery for determining the temperature of water surfaces is simplified by the fact that a constant emissivity can be assumed. Unfortunately, the same is not true for land surfaces and, although Kalma *et al.* (1986) felt justified in assuming a constant emissivity across their study area in New South Wales, Cooper and Petersen (1985) working in New Mexico estimated that an error of 2 °C or more was introduced as a result of emissivity changes across their images. This problem does not exist in areas with a permanent snow cover as the emissivity can again be assumed to be constant. Thermal imagery has therefore been successfully used in areas such as the Antarctic (Thomas and D'Aguanno 1985).

Although snow cover in the Scottish Highlands is certainly not permanent, the dates with minima below −20 °C investigated in this study all occurred during periods of widespread snow cover with depths of at least 20 cm and often more than 30 cm recorded at all the climatological stations in the study area (except on 27 February 1986 when one station at the fringe of the area recorded only 14 cm of lying snow). The assumption was therefore made that emissivity would be constant across the study area.

The value of snow-surface emissivity suggested by various authors ranges from 0.97 to 1.00 with a value of 0.99 being the most frequently quoted (e.g. Aguado 1985 or Müller 1985). Roach and Brownscombe (1984) suggested, however, that an emissivity of unity was a good approximation for snow surfaces and, as one of the dates in this study (10 January 1982) is the same as that investigated by them, an emissivity of 1.00 was also used in this study to enable a direct comparison to be made with their results.

An emissivity of less than 1.00 will reduce the brightness temperature calculated from the AVHRR radiance value and therefore will suggest a surface temperature somewhat lower than the true value. If the snow-surface emissivity was taken as 0.99 this would decrease the apparent surface temperatures recorded by the radiometer by about 0.6 °C (at temperatures of the order of −20 °C). The results quoted later are therefore unlikely to be greatly affected by the use of an emissivity of 1.00 rather than 0.99.

2.3 *Atmospheric attenuation*

Cloud cover obviously presents the greatest problem in using AVHRR data to determine surface temperatures, but even when clouds are not present attenuation of the transmitted radiation occurs principally due to infra-red absorption bands of water vapour. It is possible to calculate the amount of attenuation for a given scene, but this requires a knowledge of the structure of the atmosphere at the place and time of observation. A number of techniques are available to overcome this problem, the most commonly used being multi-spectral scanning and the calibration of the satellite data with *in situ* observations.

Multi-spectral scanning makes use of two or more channels to estimate attenuation as each channel will be affected to a different degree by the same attenuating conditions. Various algorithms have been published, for example those by Robinson (1985), and a number of these were used in this study.

Calibration with *in situ* observations makes use of measurements of temperatures at a series of points on the image to determine differences between the brightness temperatures and observed temperature at the surface. These differences indicate the amount of attenuation by the atmosphere, and the average attenuation can then be used to estimate surface temperatures in parts of the scene where no surface observations were taken. Such *in situ* data are usually used in conjunction with multi-spectral scanning and are generally considered essential to validate algorithms (Callison and Cracknell 1982).

2.4 *Earth location*

The location of any pixel in the scene can be computed from the satellite navigation data. The predicted position of the satellite above the earth can, however, have an along-track error of over 10 km (Pescod *et al.* 1986) which results in some location error. Roach and Brownscombe (1984), for example, reported that the NOAA-7 image taken at 0417 GMT on 10 January 1982 appeared to have about a 2 km mismatch between the navigation data location and topography in the Spey Valley (on the assumption that the coldest air was in the valleys). Pescod *et al.* (1986) corrected for such errors by computing a coastline and comparing that with the actual coastline on the image, the location information then being recomputed to include the offsets between the two coastlines (coastlines are used as the contrast between land and water surfaces makes them easy to identify). Such a procedure is obviously only possible when there is at least some cloud-free coast within the image, but in the present study this was not a problem as virtually the whole of northern and eastern Scotland was cloud free in each of the four cases. In fact, it was also possible to use a number of the Scottish lochs (notably Loch Ness, Loch Laggan and Loch Ericht) which provided clear linear features on the images and, together with the coastlines, these greatly aided accurate registration. Given their clarity, these features were used in preference to the satellite navigation data for determining pixel locations. It should be noted, however, that if the image is towards the edges of the large swath of information produced by the satellite then considerable distortions occur as a result of the earth's curvature (the pixel size is increased too); therefore pixels can only be effectively located in this way if they are from images in the centre of the swath.

3. Results

3.1 *Dates of investigation*

Four dates on which low minima were recorded in the Scottish Highlands were included in the investigation. There were a few other dates on which similarly low minima were recorded but these were rejected either because of cloud contamination found by inspection of the image, or because the area under study was distorted due to its being towards the edge of the image swath. It can, however, be difficult to discriminate between low cloud or fog and a cloud-free snow surface at night, and therefore the weather and cloud-amount reports recorded at stations in the area were also examined to confirm that cloud and fog were not present. The dates finally chosen have the advantage of being completely independent as they are all from different years. The dates and the screen minimum temperatures observed at climatological stations within the area are given in Table I.

Table I. *Dates of satellite images and screen minima (°C) for those dates recorded at stations within the study area*

	10 Jan. 1982	20 Jan. 1984	25 Jan. 1985	27 Feb. 1986
Station		Screen minimum temperatures		
Aviemore*		−20.6	−18.9	−19.5
Braemar	−27.2	−21.3	−20.1	−18.2
Dalwhinnie	−18.0	−19.1	−16.4	−14.4
Grantown-on-Spey	−25.7	−23.6	−20.1	−21.2
Lagganlia	−24.1	−23.5	−22.0	−20.6

*Aviemore synoptic station was not opened until after January 1982.

3.2 *AVHRR estimated temperatures*

The images for the four dates were processed to produce brightness temperatures; this processing included the non-linearity correction suggested by Lauritson *et al.* (1979). The brightness temperatures for each of the pixels in which the climatological stations were sited were then compared with the screen minima recorded at these stations. The screen minima were used even though the grass minima would be more likely to be closer to the radiative skin temperatures measured by the satellite. This decision was made because an examination of the climatological records suggested that there may have been some inconsistency in the exposure of the grass minimum thermometers at the various stations.

The brightness temperatures differ from the screen minima for a number of reasons:

(a) Atmospheric attenuation affects the recorded radiance values.

(b) The satellite overpass time does not necessarily correspond with the time of screen minimum.

(c) The satellite sensor averages the radiance value over a 1.1 km × 1.1 km pixel whereas the screen minimum is a point value.

(d) Surface temperatures may not be the same as screen minima recorded at 1.2 m.

(e) There may be an error in the location of the station on the image.

(f) Noise and other errors in the measurement systems.

The calculated brightness temperatures for AVHRR Channels 3, 4 and 5 were all higher than the recorded screen minima, which is rather unusual as in most studies the brightness temperatures are lower than *in situ* observations. This discrepancy probably arises for two reasons. Firstly, the time of the satellite overpass was either before or after the time the screen minima were reached (as the 0900 GMT dry-bulb temperatures were all higher than the minima, the screen minima probably occurred before

0900 GMT) and secondly, atmospheric attenuation was small as all occasions had low values of precipitable water (as recorded by the midnight radiosonde ascent at Shanwell). Since attenuation was small, the main difference was almost certainly as a result of the time of overpass not coinciding with the time of screen minimum, a conclusion which tends to be confirmed by the lowest mean offset value for Channel 4 (the mean difference between recorded screen minima and brightness temperatures) being found on 25 January 1985 when the satellite overpass was at 0841 GMT. This overpass was less than 30 minutes after sunrise and probably not much more than this after screen minima were recorded. It should also be noted that Channel 4 is the least likely to be affected by attenuation by any variation in the amount of water vapour as its waveband range lies within the range of the minimum values of the effective mass-absorption coefficients for water vapour (Ramsey *et al.* 1982).

The differences between the screen minima and the computed Channel 4 brightness temperatures, the offsets, are given in Table II along with the root-mean-square (r.m.s.) value of the variations from this mean (following Bowers *et al.* (1982)).

Table II. *Offsets between AVHRR Channel 4 brightness temperatures and recorded screen minima (°C) for the same dates as Table I*

	10 Jan. 1982	20 Jan. 1984	25 Jan. 1985	27 Feb. 1986
Satellite	NOAA-6	NOAA-7	NOAA-6	NOAA-9
Time (GMT) of overpass	0925	0450	0841	0410
Station				
Aviemore*		1.0	0.7	1.0
Braemar	2.5	1.5	0.0	1.9
Dalwhinnie	2.2	1.5	0.4	1.4
Grantown-on-Spey	2.2	1.1	0.0	0.8
Lagganlia	3.4	2.4	0.6	3.9
Mean offset	2.6	1.5	0.3	1.8
r.m.s. error	0.49	0.49	0.30	1.12
Mean offset (excluding Lagganlia)	2.3	1.3	0.3	1.3
r.m.s. error	0.14	0.23	0.30	0.42

*Aviemore synoptic station was not opened until after January 1982.

The mean offsets are given with and without the values from Lagganlia as the Lagganlia offsets were noticeably higher than the other stations, particularly on 27 February 1986. This difference is almost certainly the result of local site conditions and visits to the stations suggest that there is greater local shelter at Lagganlia than at the other sites.

The mean offsets were then subtracted from the Channel 4 brightness temperatures for each pixel to create a map of the distribution of minimum temperatures for each of the four dates. Although it made little difference on three of the dates, the offsets used were those excluding Lagganlia, as not using that offset gave a substantial improvement in the r.m.s. error on 27 February 1986.

Various published multi-spectral attenuation algorithms for calculating surface temperatures were also used to see if it was possible to obtain better results as measured by the r.m.s. error from the observed screen minima; see for example Robinson (1985) or Bowers *et al.* (1982). No multi-spectral imagery was available on 25 January 1985 due to an error on Channel 3 and the algorithms which included Channel 5 brightness temperatures could not be used on 10 January 1982 as NOAA-6 does not have a separate Channel 5. However, of the 11 different algorithms tested, even the best of them had r.m.s. errors more than twice as large as those obtained by simple subtraction of a mean offset from the Channel 4 brightness temperatures (even those with the Lagganlia values included). This was not an unexpected result as the multi-spectral algorithms are normally derived for typical mid-latitude or global maritime atmospheric conditions but it did confirm that such algorithms are of little use during conditions of extreme cold.

3.3 *Density slicing*

The calculated pixel values were then density sliced using the image-processing system for a Sirius microcomputer with Pluto colour board written at the Department of Geography, Portsmouth Polytechnic. This density slicing allows a range of pixel-count values to be assigned a single intensity value. A careful choice of intensity values enables a detailed thermal map to be produced with an uncertainty as measured by the r.m.s. errors of less than 0.5 °C. It was therefore felt valid to density slice at 0.5 °C intervals but this would have caused overcomplication over the whole image as it is difficult to assign more than 30 separate colours which can be clearly distinguished. However, as the study was concerned with the distribution of very cold temperatures, an uneven density slice was carried out with the 0.5 °C intervals used only for temperatures below −20 °C.

Although the map of temperature distribution was very detailed, an isotherm interval of 5.0 °C was chosen for the printed maps. This interval provided a good summary of the overall pattern, demonstrating the match with topography, and it was also the interval used by Roach and Brownscombe (1984) in their investigation of minimum temperatures on 10 January 1982.

3.4 *Errors*

Despite the detail available by density slicing, it is important to make some estimate of the reliability of the derived temperature distribution. Errors can arise from each stage of the processing so that there are *in situ* observational uncertainties depending on the instruments used and their exposure, uncertainties introduced in locating the ground stations on the image and errors arising from the radiometric measurements.

As far as the *in situ* observations are concerned, the instruments and their exposure were all standardized so any error is likely to be small, and less than 0.1 °C. Location errors, however, are not so easy to quantify but, following the example of Cooper and Petersen (1985), average differences were calculated between the pixels containing the climatological stations, and their eight adjacent neighbours. This error was 0.5 °C. Errors which arise from the radiometric measurements include:

(a) Instrument calibration and precision (quoted as 0.31 °C by Lauritson *et al.* (1979)).
(b) Errors in the offset values (r.m.s. errors were found to be less than 0.5 °C).
(c) Emissivity errors (spatial variations were assumed to be negligible in this study).
(d) Atmosphere attenuation (spatial variations assumed negligible).

A measure of the total uncertainty can be obtained by the root sum square method used by Cooper and Petersen (1985) which takes the square root of the sum of squares of the error terms. In this study the root sum square value was 0.78 °C and therefore isotherms as drawn should be correct to within 1.0 °C.

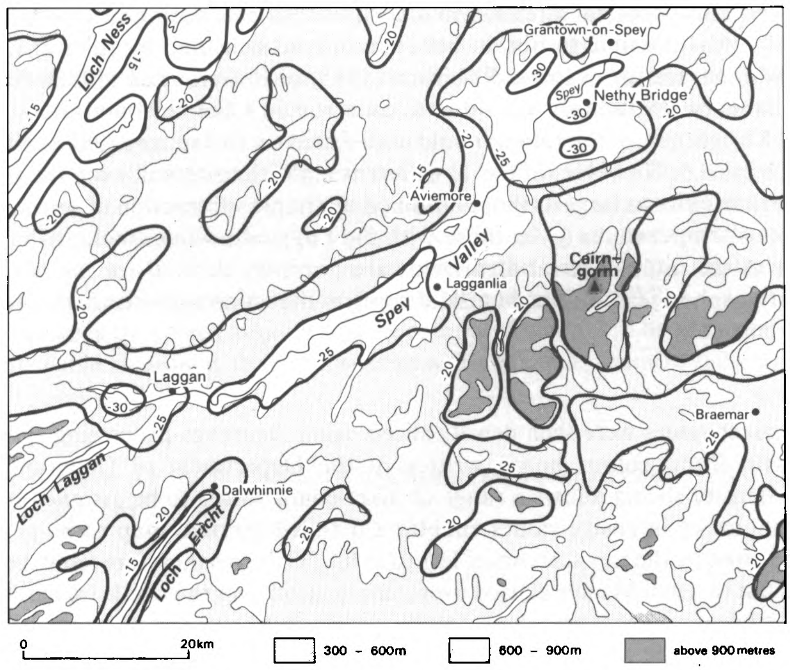

Figure 1. Isotherms (°C) showing the distribution of temperature in the Scottish Highlands on 10 January 1982 derived from NOAA-6 AVHRR data (0925 GMT overpass).

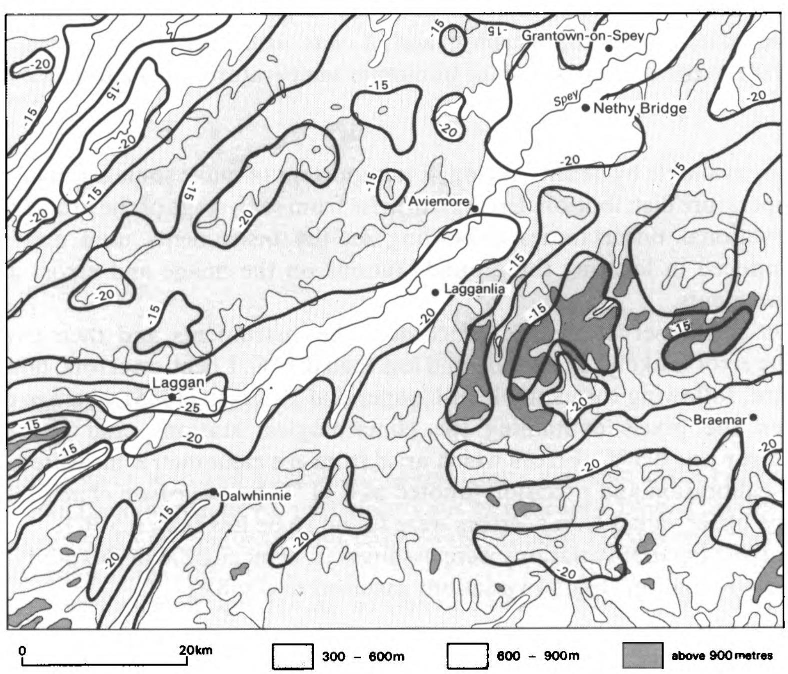

Figure 2. Isotherms (°C) showing the distribution of temperature in the Scottish Highlands on 20 January 1984 derived from NOAA-7 AVHRR data (0450 GMT overpass).

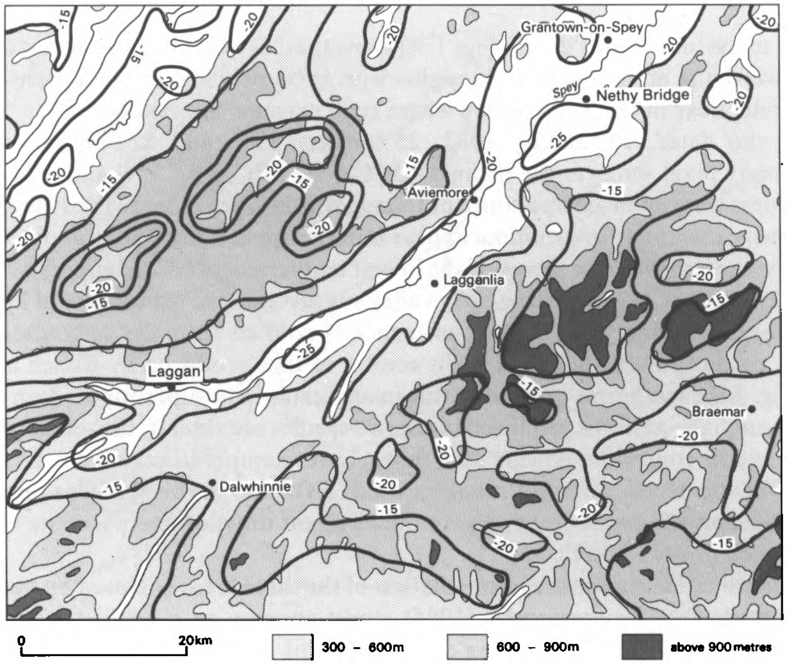

Figure 3. Isotherms (°C) showing the distribution of temperature in the Scottish Highlands on 25 January 1985 derived from NOAA-6 AVHRR data (0841 GMT overpass).

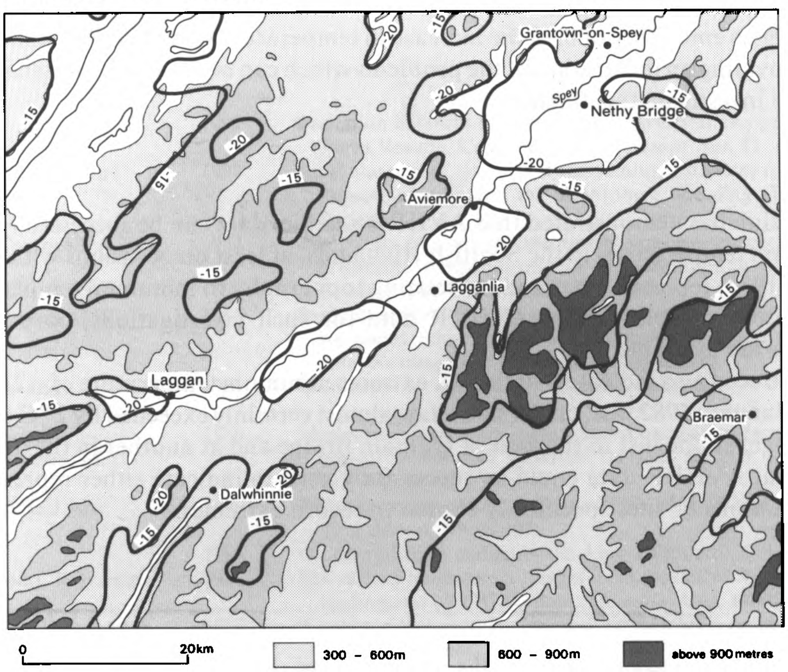

Figure 4. Isotherms (°C) showing the distribution of temperature in the Scottish Highlands on 27 February 1986 derived from NOAA-9 AVHRR data (0410 GMT overpass).

3.5 *Isotherm maps*

The isotherm maps for the four dates (Figs 1–4) show that, as expected, the lowest temperatures were found in the lower-lying areas and that on nights with extremely low minima there do appear to be a number of discrete areas in the Spey Valley where such extreme minima occur.

On three of the dates, 10 January 1982, 25 January 1985 and 27 February 1986, the lowest temperatures in any pixel were (to the nearest 0.5 °C) −31.5 °C, −25.5 °C and −24.0 °C respectively. These temperatures were all in an area south of Grantown-on-Spey close to the village of Nethy Bridge. Another area where extremely low minima appear is in the upper Spey Valley about 4 km to the west of Laggan. That area appears to have recorded the lowest temperatures on 20 January 1984 (−26.0 °C) and 10 January 1982 (−30.5 °C). Visits to the Spey valley suggest that the occurrence of low temperatures at these two locations is probably due to the confluence of cold air from the surrounding areas.

The isotherm pattern for 10 January 1982 is similar to that produced by Roach and Brownscombe (1984) and in Fig. 5 the isotherms created in this investigation are superimposed on top of those from their study. Although the patterns produced in the two studies are similar, the temperatures estimated in this investigation are somewhat lower, and those lower temperatures cover a larger area. These differences may be due to the different satellites used (NOAA-6 in this study as opposed to NOAA-7 data used by Roach and Brownscombe) and to the different times of overpass (their calculations were based on data taken at 0417 GMT).

One particularly interesting feature is the smallest of the three areas enclosed by the −30 °C isotherm which in the Roach and Brownscombe (1984) study appears as a small tongue of cold air (the intersection is shown by the cross-hatching on Fig. 5). This area appears to be centred on Abernethy Forest which might not be expected to record the lowest temperatures.

However, Henderson-Sellers and Robinson (1986) quote an infra-red emissivity of 0.88 for snow-covered vegetation which would give a temperature 7 °C warmer than that estimated using an emissivity of 1.0. Even with an emissivity of 0.95 the increase in temperature would be 3 °C and it may be that this small area is providing an illustration of the problems which can be created if emissivity is not constant. It is intended to investigate this further.

4. Conclusions

The investigation has demonstrated that AVHRR satellite data can be successfully used to produce maps of minimum temperatures in the Scottish Highlands, at least on occasions with widespread snow cover. Tabony (1985) reported a method for relating topography to minimum temperatures but it may prove rather easier to make use of AVHRR data for such investigations, particularly if suitable emissivity values are available.

The maps produced also indicate that the UK extreme minimum temperature of −27.2 °C recorded at Braemar on 10 January 1982 was, on the same day, almost certainly exceeded by 2 °C or more at one site near Nethy Bridge, at one just to the west of Dulnain Bridge and at another in the upper Spey Valley. This suggests that AVHRR data could be successfully used to indicate either representative sites for climatological stations or sites specifically chosen to record extremes.

Acknowledgements

The authors would like to thank R. Reynolds of the Department of Meteorology, University of Reading for his helpful comments and the Cartographic Unit of the Department of Geography, Portsmouth Polytechnic for drawing the maps.

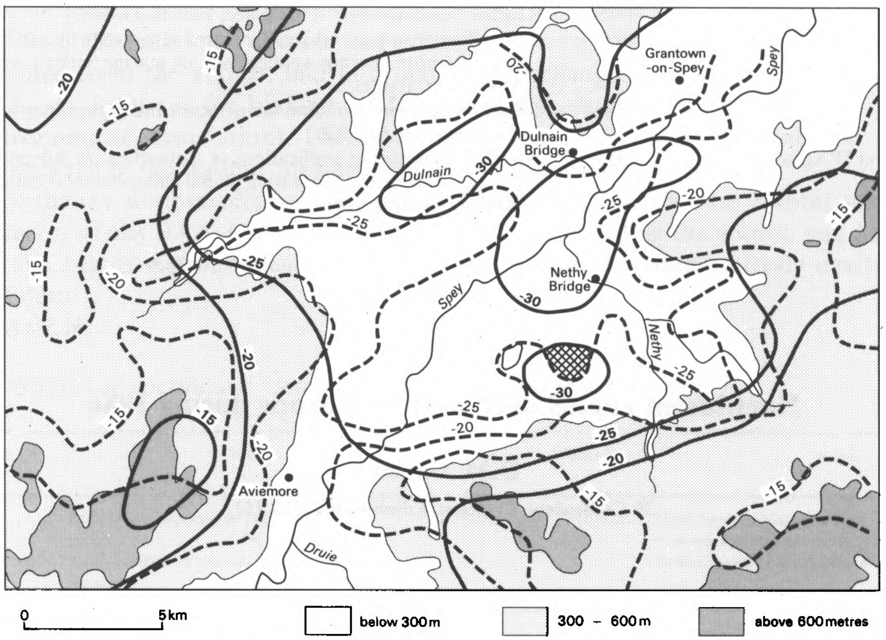

Figure 5. Isotherms (°C) for part of the Spey Valley on 10 January 1982. Dashed isotherms are those given by Roach and Brownscombe (1984) and solid isotherms are those produced in this study. The cross-hatching is an area of interest discussed in the text.

References

Aguado, E. 1985 Radiation balances of melting snow covers at an open site in the Central Sierra Nevada, California. *Water Resour Res*, **21**, 1649–1654.

Bowers, D.G., Crook, P.J.E. and Simpson, J.H. 1982 An evaluation of sea surface temperature estimates from the AVHRR. *In* Remote sensing and the atmosphere. Reading, The Remote Sensing Society.

Callison, R.D. and Cracknell, A.P. 1982 The results of some calculations of atmospheric corrections to AVHRR brightness temperatures. *In* Remote sensing and the atmosphere. Reading, The Remote Sensing Society.

Cooper, D.I. and Petersen, G.W. 1985 Evaluation of AVHRR sensor for monitoring land surface temperatures. *In* Advanced technology for monitoring and processing global environmental data. Reading, The Remote Sensing Society.

Henderson-Sellers, A. and Robinson, P.J. 1986 Contemporary climatology. Harlow, Longman.

Kalma, J.D., Laughlin, G.P., Green, A.A. and O'Brien, M.T. 1986 Minimum temperature surveys based on near-surface air temperature measurements and airborne thermal scanner data. *J Climatol*, **6**, 413–430.

Lauritson, L., Nelson, G.J. and Porto, F.W. 1979 Data extraction and calibration of TIROS-N/NOAA radiometers. NOAA, *Tech Memo*, NESS 107.

Müller, H. 1985 On the radiation budget in the Alps. *J Climatol*, **5**, 445–462.

Pescod, R.W., Saunders, R.W. and Eyre, J.R. 1986 Sea surface temperature images from Advanced Very High Resolution Radiometer (AVHRR) data. *Meteorol Mag*, **115**, 318–325.

Ramsay, J.W., Chiang, H.D. and Goldstein, R.J. 1982 A study of the incoming longwave atmospheric radiation from a clear sky. *J Appl Meteorol*, **21**, 566–578.

Roach, W.T. and Brownscombe, J.L. 1984 Possible causes of the extreme cold during winter 1981–82. *Weather*, **39**, 362–372.

Robinson, I.S.	1985	Satellite oceanography. Chichester, Ellis Horwood.
Singh, S.M. and Warren, D.E.	1983	Sea surface temperatures from infrared measurements. *In* Cracknell, A.P. (ed); Remote sensing applications in marine science and technology. Dordrecht, Reidel.
Tabony, R.C.	1985	Relations between minimum temperature and topography in Great Britain. *J Climatol*, 5, 503–520.
Thomas, I.L. and D'Aguanno, J.A.	1985	AVHRR monitoring applications in Antarctica. *In* Advanced technology for monitoring and processing global environmental data. Reading, The Remote Sensing Society.

551.593.653(4):551.506.1

Noctilucent clouds over western Europe during 1986

D.M. Gavine

29 Coillesdene Crescent, Edinburgh EH15 2JJ

Summary

The sightings of noctilucent clouds reported to the Aurora Section of the British Astronomical Association during 1986 are presented.

Table I summarizes the noctilucent cloud (NLC) reported to the Aurora Section of the British Astronomical Association (BAA) during 1986. The times (UT) are of reported sightings, not necessarily the duration of a display. Hourly sky reports are no longer received from meteorological stations; consequently negative nights are now based on the judgement of two or more experienced observers with clear or nearly clear sky, watching throughout the whole period during which NLC is likely to occur, and in the case of Britain, north of 54° N. Table II lists those nights adjudged to be negative.

The large number of sightings, despite a summer beset with tropospheric cloud in Britain, suggests a high incidence of the phenomenon in 1986. The network of observers has been extended, both geographically and in numbers. British data came from 26 amateur astronomers and other individuals, and 12 meteorological stations. The Finnish network now comprises 20 single observers and 6 teams, covering latitudes 60–65° N, longitudes 21–30° E. They employ data storage systems and produce a detailed annual report. The Danish group of 5 is co-ordinated by Mr J. Østergaard Olesen at Rønne in Bornholm. Mr Olesen and Mr Holger Andersen continue to submit reports which are models of clarity, and their outstanding colour photographs, especially of panoramic views of NLC, have been exhibited at the BAA and other meetings.

We are very pleased to welcome to the survey the Royal Netherlands Meteorological Institute, who contributed NLC sightings from 21 stations. Photographs of the 1986 displays have already been published (Zwart 1986). In addition, NLC reports have been received from two Canadian observers, Mr Brown and Mr Zalcik; these are briefly mentioned for comparison. Following a popular article (McConnell 1987) several amateur observers in Canada have expressed a desire to participate, and the development of a North American network seems likely.

Thirty-four definite NLC were observed in Finland, 29 in Britain, 17 in Denmark and 5 in the Netherlands. Parallactic photography was achieved on the spectacular display of 23/24 July using fixed cameras at Milngavie (Dr Simmons), Edinburgh (Dr Gavine) and Aberdeen (Dr Gadsden). Dr Gadsden also carried out time-lapse photography and TV polarimetry.

Because of the greatly increased volume of data for 1986 it has been found necessary to omit from the summary of NLC the individual altitude and azimuth observations. Full data on individual displays may be obtained from the author, and information is exchanged between the Finnish and British networks. The co-ordinator for Finland is Mr Veikko Mäkelä, Tähtitieteellinen yhdistys URSA ry (URSA Astronomical Association), Laivanvarustajankatu 3, SF-00140 Helsinki 14. All data are ultimately preserved in the Balfour Stewart Archive, University of Aberdeen.

The author thanks all observers for their efforts, Dr Michael Gadsden for helpful advice, Mr Ron Livesey, Director of the BAA Aurora Section, for hard work behind the scenes, and Mr Neil Bone, Director of the Junior Astronomical Society Aurora Section, for making freely available his own collection of data.

Table I. *Displays of noctilucent clouds over western Europe during 1986*

Date — night of	Times UT	Notes
28/29 Apr.	2010	Faint billow suspected at Tapiola, Finland.
28/29 May	2130–0000	Small, rather faint veil and bands at Turku and Helsinki.
6/7 June	2310–0200	Faint bands and billows, mostly in tropospheric cloud, Scotland and N England.
10/11	2330	Faint NLC up to zenith at Wick.
13/14	2030–0225	Moderately bright display, all forms, seen throughout Britain down to Worcester, Denmark and Netherlands. Strong billow structure photographed by Mr Andersen at Vildbjerg.
14/15	0000–0100	Faint band at Wick; no NLC at Aberdeen 2200–2305.
15/16	2240	Very faint NLC visible through binoculars at Rønne.
16/17	2100–2145	Very faint NLC visible through binoculars at Rønne.
18/19	2100–0200	Bright display well into the southern sky in S Finland, observed in Estonia. Faint bands visible in Britain to 53.5° N and Deventer, Netherlands.
19/20	2140–2323	Faint NLC at Helsinki, maximum altitude 75° at 2302. Faint bands at Castleford (Yorks) and Rønne.
21/22	2110	Bands in broken cloud at Rønne.
22/23	2125–2320	Faint bands at Helsinki. NLC suspected in cloud gaps at Sale (Manchester) but negative at Stirling.
23/24	2119–0200	Faint bands in zenith and SW sky at Helsinki. Magnificent display, all forms, bright, over Denmark. Faint NLC at Rotterdam. Billows up to 10° at Edmonton, Canada.
24/25	2150–0045	Faint bands in tropospheric cloud gaps, Edinburgh; faint NLC in Denmark. Small faint band and billow display at Vantaa (Finland) after 0130 local time. Bands and billows to 7° at Edmonton.
25/26	2155–2345	Small, diminishing and fading bands and billows in Britain, visible down to 52° N.
26/27 June	2145–0015	Faint; bands at Morpeth, Northumberland, billows at Bornholm. Veil, bands and billows east of Helsinki, increasing towards dawn.
27/28	0012–0050	Faint NLC patch suspected in zenith at Wick, very faint bands and billows at Vildbjerg. Faint billows at Edmonton.
28/29	2100–0250	Large bright display, all forms, in England and Denmark, observed in tropospheric cloud in Scotland. Reported at 11 Netherlands stations. In Helsinki one NLC area in zenith and S sky, another low in N with strong billows in W. Bright at Morpeth with billows and whirls but became fainter from 2350.
29/30	2215–0200	Bright bands seen at Todmorden (Yorks), widespread display overhead in haze at Aberdeen. Faint blue-green patch at Rønne, faint bands at Helsinki after 0100 local time.
1/2 July	2120–0255	Moderately bright, extensive display, bands and some billows, observed from 10 British and 2 Danish stations, also Fishery Protection Vessel *Jura* at 59° N, 5.5° W. Faint forms seen S of zenith near dawn at Bedford. Small faint patches at Tapiola and Vantaa, Finland.
2/3	2309–0215	Faint bands and a few billows in cloud gaps in N England.
3/4		Bands and billows up to 15° at Edmonton, Canada.
5/6	2230–0232	Faint NLC, mainly bands, N Britain. Suspect bands at Tapiola.
6/7	2320–0240	Faint bands at Bornholm and in N Britain. Bright NLC in cloud gaps at Turku.
7/8	2115–2300	Bands at Todmorden. Bright widespread display at Helsinki and Turku, all forms in E sky from horizon to zenith.
8/9	2115–0240	Faint bands reported at Todmorden but no NLC visible at Aberdeen at 2230. Small faint NLC in S Finland.

Date — night of	Times UT	Notes
10/11 July	2130–0100	No NLC at Stirling 2300 but NLC in cloud gaps, Linton-on-Ouse (Yorks) 0100. NLC in cloud gaps, Denmark. Faint widespread NLC at Kustavi, SW Finland.
11/12	2100–0154	Bright display, all forms, Denmark and Twenthe (Netherlands).
12/13	2135–0130	Small bands in Orkney. Bright display, all forms, in S Finland and Kuopio area. NLC at Fort McMurray, Canada.
13/14	2155–0030	Bright bands and billows at Bornholm. Faint bands at Fort McMurray.
15/16	2110–2315	Widespread and bright display in Finland, all forms. Up to zenith at Helsinki, all-sky at Rautalampi and Kuopio.
16/17	2210–0204	Faint to moderate NLC over Britain down to Yorkshire, mainly bands, some billows and whirl structure. Small faint veil in S Finland after 0030 local time.
17/18	2100–0230	Negative at Aberdeen 2315 but faint veil suspected overhead at Todmorden 2135–2159, and definite NLC in cloud gaps 0215–0230. Small bright NLC in E Finland.
18/19	0240–0315	Faint NLC patch suspected overhead at Todmorden.
19/20	2125–0240	Moderate display, all forms, in cloud gaps at Morpeth, faint bands at Vildbjerg. Small faint to moderate NLC in Finland at 62°N. Bands at Fort McMurray.
20/21	2110–2230	Bands in cloud gaps at Todmorden. Moderately bright display, all forms, by 7 observers in Finland.
21/22	2200–0030	Very faint bands visible through binoculars, Morpeth. Large bright display in N Finland.
22/23	2108–0045	Bands and billows in tropospheric cloud gaps in Orkney and Shetland. Bright and extensive display in Finland, all forms, dense brown–yellow structures described in eastern sky.
23/24 July	2130–0300	Very bright and extensive display, the best for many years, seen by 30 observers and meteorological stations throughout Britain on a clear night. NLC seen in cloud gaps in Finland. In Scotland large curved bands gave way to intensely bright whirls and knots near local midnight, then to strong billows high in NE towards dawn.
24/25		Billows up to 40° at Edmonton.
25/26	2100–2300	Small NLC at Kutunjärvi, Finland.
26/27	2100–2200	Faint bands and veil overhead at Todmorden. Bright NLC, all forms, observed throughout Finland and at Västerås, Sweden.
27/28	2045–2145	Faint veil suspected at Tampere but negative reports from several Finnish stations.
29/30	2130–2145	Doubtful. Possible small faint NLC at Kuopio but other Finnish stations negative. No NLC at Morpeth but faint band suspected at 2° at Swansea (Wales).
30/31	2000–2330	Faint display with bright individual structures, all forms, widely observed in Finland.
31 July/1 Aug.	2210–2245	Small faint NLC at Turku.
1/2	2315–0000	Bright, all forms, at Liminka, N Finland. Stations in S Finland negative.
2/3	2040–0300	Faint bands and billows in cloud gaps at Morpeth, suspect NLC in zenith at Todmorden. Small medium NLC in Finland.
3/4	2055–2300	Moderately bright bands and billows, S Finland.
4/5	2110–0050	Bands and billows, Orkney and Shetland; moderately bright bands, Kuopio and Illo, Finland.
7/8	2015–2330	Bright NLC, all forms, at Kuopio, Illo, Tampere and Joensuu. Described as fast-changing.
9/10	0010	Small medium NLC, veil and bands, at Kemiö, Finland.

Table II. *Nights in Finland and in Great Britain north of 54° N judged to have negative sightings of NLC*

Britain: May 8/9, 15/16, 21/22, 27/28; June 1/2, 3/4, 4/5, 7/8, 9/10, 11/12, 15/16; July 4/5, 9/10, 31/Aug. 1.

Finland: May 3/4, 4/5, 5/6, 6/7, 8/9, 9/10, 15/16, 31/June 1; June 9/10, 10/11, 11/12, 14/15, 15/16, 16/17, 17/18, 21/22, 25/26; July 2/3, 9/10, 13/14, 14/15, 18/19, 28/29; Aug. 6/7, 10/11, 14/15, 19/20, 25/26.

References

McConnell, D. 1987 Clouds of the twilight. *Astronomy*, **15**, 42–47.

Zwart, B. 1986 Lichtende nachtwolken. *Zenit*, **13**, 378–382.

551.553.8(420)

Exceptionally strong winds of 16 October 1987 over the south of England

Advisory Services Branch
Meteorological Office, Bracknell

Summary

A brief description is given of the exceptionally strong winds which occurred over the south of England on 16 October 1987.

On the evening of 15 October 1987 there was a depression with a central pressure of 972 mb in the vicinity of East Anglia. A front lying over the south of England linked this depression with another deep depression over the western entrance of the English Channel. To the north of the front there were cool, light to moderate north-easterly winds, whereas to the south there were stronger winds from the south-west.

By midnight the depression in the English Channel was centred over the south coast of Cornwall and had deepened to less than 958 mb. The associated front was moving quickly northward over the south of England and brought a band of heavy rain to the region. Behind the front there were strong winds with gusts of over 40 kn being reported over inland areas.

As the depression tracked north-eastwards into the North Sea the winds strengthened, with the strongest winds occurring over southern England between 0200 and 0600 GMT. Of particular note are the gusts of 80 kn or more between 0300 and 0500 GMT over the area south-east of a line from London to the Isle of Wight (see Fig. 1). By 0600 GMT a broad band of very strong winds covered most of

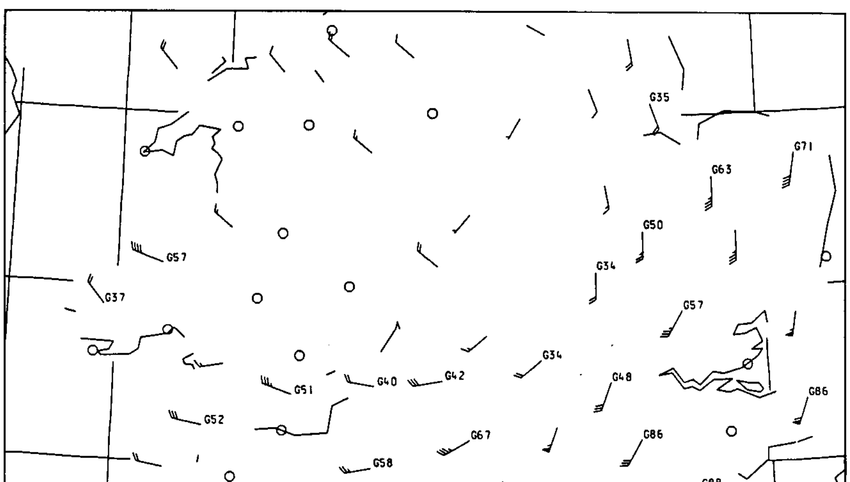

Figure 1. Mean wind speeds and gusts reported at 0500 GMT on 16 October 1987.

England south of a line from the Severn Estuary to the Wash, but by 0900 GMT the winds had decreased in strength over most areas except the north of East Anglia.

It is interesting to consider how unusual the winds were on 16 October 1987. Provided that sufficient long-term records are available from stations with sophisticated wind-recording equipment, it is possible by statistical methods to estimate the average interval in years between wind speeds of a given strength (the return period). However, it must be stressed that the return period is only an average interval so in reality extreme winds could occur more frequently. Table I gives the 19 sites with their highest mean speeds and/or gusts recorded on 16 October together with an indication of the approximate return period where available.

As yet the data have not been subjected to the usual careful scrutiny so the values quoted may be revised in the light of later examination.

Table I. *19 sites with their highest mean speeds and/or highest gusts recorded on 16 October 1987 between 0000 and 1300 GMT with an indication of the approximate return periods where available*

	Mean speed kn	Approximate return period years	Maximum gust kn	Approximate return period years
Brize Norton	25	Less than 10	50	Less than 10
Oxford Airport	35	Not available	62	Not available
Boscombe Down (Salisbury)	36	Less than 10	70	20
Hurn (Bournemouth)	37	10	62	10
Southampton	48	Not available	75	Not available
St Catherines (Isle of Wight)	58	Not available	90	Not available
Jersey	55	10	85	15
Herstmonceux (Eastbourne)	60	Not available	90	Not available
Langdon Bay (Dover)	62	Not available	90	Not available
Manston (Margate)	61	Over 500	86	Over 200
East Malling	37	Not available	74	Not available
Gravesend	34	Not available	74	Not available
Gatwick Airport	34	Less than 10	86	Over 300
London (Heathrow) Airport	39	20	66	40
London Weather Centre	44	200	82	120
Stansted Airport	34	10	65	20
Shoeburyness	55	Over 500	87	Over 500
Wattisham (Stowmarket)	48	45	72	10
Hemsby (Great Yarmouth)	45	Not available	78	Not available

In some areas the winds were not exceptional, having return periods of 20 years or less. However, in a few cases the return periods appear to be in excess of 200 years and possibly as long as 500 years in one or two cases. These figures suggest that in some areas the winds recorded on 16 October were exceptionally strong. Elsewhere in Britain, especially in western and coastal areas (and over mountains), such wind speeds occur much more frequently.

Review

Antarctic science, edited by D.W.H. Walton. 225 mm × 282 mm, pp. viii + 280, *illus*. Cambridge University Press, 1987. Price £25.00, US $39.50.

This book is a celebration and assessment of international co-operation since the signing of the Antarctic Treaty 25 years ago. After an introduction by Sir Vivian Fuchs, the first section concerns itself naturally with the history of the exploration, and there are some fine pictures of the sailing ships used in the rugged surroundings and descriptions of the toll these surroundings took. One may learn that Captain Cook was unimpressed with Antarctica and prophesied that it would be of no use – an early forecast gone astray! Also, it is rather worrying to think that no less a person than Gauss had miscalculated the magnetic South Pole by several hundred miles.

Subsequently there are sections on earth sciences, politics, biology and atmospheric science. Although I am a non-expert in all these subjects the authors are all experts from the British Antarctic Survey and they have all provided excellent text, bibliographies and index. There are many photographs, plenty in colour, and the diagrams are simple but instructive, reminiscent of Reihl's *Tropical Meteorology*. However, there are some rather gory photographs about whaling and one of a fish with its entrails hanging out with the distraught expression of one who has come round from the anaesthetic too early.

Some indication of the difficulty in observing the weather in the Antarctic can be gleaned from the fact that there were only 12 permanently manned weather stations in operation south of 55° S as late as 1955. However, the International Geophysical Year during 1957/58 made a considerable improvement.

Interestingly, there aren't any thunderstorms and hardly any rain in Antarctica, though fronds of ferns do appear on rocks (the result of a tropical climate many million years ago). The tectonic development of the area is described in chapter 13.

A fine bi-polar diagram of the earth's albedo reveals just how much of the surface is highly absorbent. Incidentally, the diagrams and photographs are unnumbered which leaves them less cluttered but makes the exact textual reference to them harder to find. This all leads on to space exploration and rocketry and a picture (novel to me) of an X-ray aurora from a satellite.

Looking to the way the future of exploration will unfold, chapter 18 contains the idea of science used as a tool for political defusion. The Antarctic Treaty is printed out in Appendix I, a useful reminder, and the whole book is written in non-technical terms as far as possible (not an equation in sight). Priced at £25, it sounds a lot to anyone over 50 years old, but there's plenty in it for many people, not only Antarctic buffs, and it is an excellent broadening-of-knowledge experience for anyone.

S.H. Barker

Books received

The listing of books under this heading does not preclude a review in the Meteorological Magazine at a later date.

Weather radar and flood forecasting, edited by V.K. Collinge and C. Kirby (Chichester, New York, Brisbane, Toronto, Singapore, John Wiley and Sons, 1987. £39.00) is based on a symposium held in the University of Lancaster, and examines the capabilities of weather radar with emphasis on operational experience in the United Kingdom. Hydrological aspects of flood forecasting, with specific real-time problems, are also discussed.

Satellite photograph — 2 September 1987 at 1550 GMT

This NOAA-9 visible image shows the cloud associated with a north-eastward moving Atlantic depression, with a central pressure of 973 mb. The cloud structure associated with the frontal zone is particularly well illustrated, due mainly to the general absence of an upper-cloud shield. South of 57° N, the front may be inferred to be a classical cold front with rearward-sloping ascent* since dense low and medium cloud terminates at a sharp forward boundary (close to the position of the surface cold front), whilst semi-transparent cirrus (where present) marks a sharp rearward boundary.

North and west of 57° N, where the front is probably occluded, a zone of low-level layered cloud, with embedded convection (as suggested by the 'lumpy' texture) terminates at a sharp rear edge. Cirrus, where present, lies within the forward portion of the front, with anticyclonically curved filaments defining a 'saw tooth' appearance to the forward limit of the cloud. This structure is characteristc of a split front where, due to forward-sloping ascent*, the front at upper levels (marked by the termination of upper cloud) has advanced ahead of that at lower levels (marked by the rearward edge of the lower cloud).

Within the circulation of the depression, extensive open cellular convection is present, except immediately behind the front where cloud formation is probably suppressed due to post-frontal subsidence.

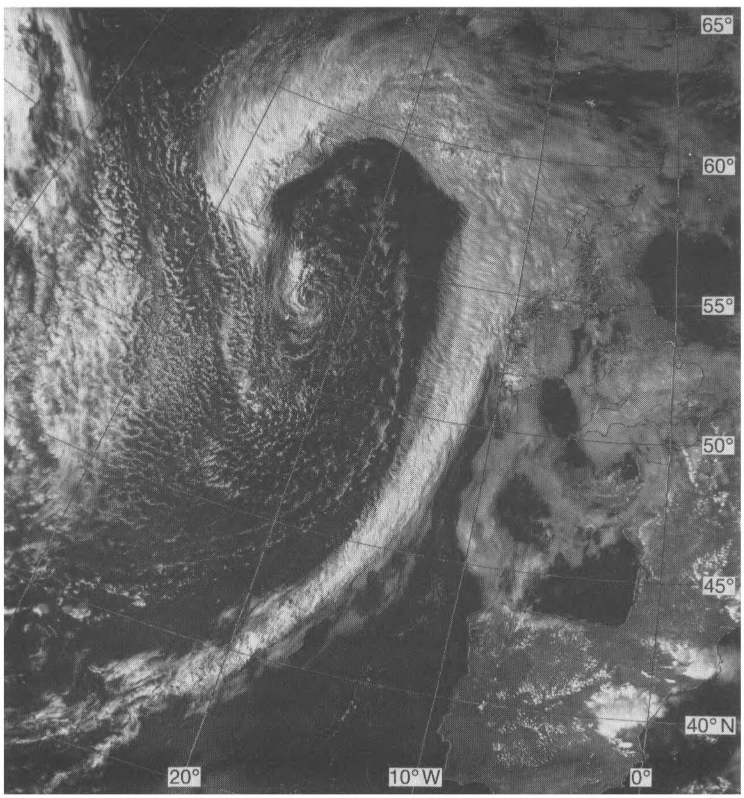

Photograph by courtesy of University of Dundee

* Browning, K.A.; Conceptual models of precipitation systems. *Meteorol Mag*, **114**, 1985, 293–319.

Meteorological Magazine

GUIDE TO AUTHORS

Content

Articles on all aspects of meteorology are welcomed, particularly those which describe the results of research in applied meteorology or the development of practical forecasting techniques.

Preparation and submission of articles

Articles for publication and all other communications for the Editor should be addressed to the Director-General, Meteorological Office, London Road, Bracknell, Berkshire RG12 2SZ and marked 'For *Meteorological Magazine*'.

Articles, which must be in English, should be typed, double-spaced with wide margins, on one side only of A4-size paper. Tables, references and figure captions should be typed separately.

Spelling should conform to the preferred spelling in the *Concise Oxford Dictionary*.

References should be made using the Harvard system (author, date) and full details should be given at the end of the text. If a document referred to is unpublished, details must be given of the library where it may be seen. Documents which are not available to enquirers must not be referred to.

Tables should be numbered using roman numerals and provided with headings. We consider vertical and horizontal rules to be unnecessary in a well-designed table; spaces should be used instead.

Mathematical notation should be written with extreme care. Particular care should be taken to differentiate between Greek letters and Roman letters for which they could be mistaken. Double subscripts and superscripts should be avoided, as they are difficult to typeset and difficult to read. Keep notation as simple as possible; this makes typesetting quicker and therefore cheaper, and reduces the possibility of error. Further guidance is given in BS1991: Part 1: 1976 and *Quantities, Units and Symbols* published by the Royal Society.

Illustrations

Diagrams must be supplied either drawn to professional standards or drawn clearly, preferably in ink. They should be about 1½ to 3 times the final printed size and should not contain any unnecessary or irrelevant details. Any symbols and lettering must be large enough to remain legible after reduction. Explanatory text should not appear on the diagram itself but in the caption. Captions should be typed on a separate sheet of paper and should, as far as possible, explain the meanings of the diagrams without the reader having to refer to the text.

Sharp monochrome photographs on glossy paper are preferred: colour prints are acceptable but the use of colour within the magazine is at the Editor's discretion. In either case contrast should be sufficient to ensure satisfactory reproduction.

Units

SI units, or units approved by WMO, should be used.

Copyright

Authors wishing to retain copyright for themselves or for their sponsors should inform the Editor when they submit contributions which will otherwise become UK Crown copyright by right of first publication.

It is the responsibility of authors to obtain clearance for any copyright material they wish to use before submitting it for publication.

Free copies

Three free copies of the magazine are provided for authors of articles published in it. Separate offprints for each article are not provided.

Meteorological Magazine

December 1987

Vol. 116
No. 1385

CONTENTS

Contributions: it is requested that all communications to the Editor and books for review be addressed to the Director-General, Meteorological Office, London Road, Bracknell, Berkshire RG12 2SZ, and marked 'For *Meteorological Magazine*'. Contributors are asked to comply with the guidelines given in the *Guide to authors* which appears on the inside back cover. The responsibility for facts and opinions expressed in the signed articles and letters published in *Meteorological Magazine* rests with their respective authors. Authors wishing to retain copyright for themselves or for their sponsors should inform the Editor when submitting contributions which will otherwise become UK Crown copyright by right of first publication.

Subscriptions: Annual subscription £27.00 including postage; individual copies £2.30 including postage. Applications for postal subscriptions should be made to HMSO, PO Box 276, London SW8 5DT; subscription enquiries 01–211 8667.

Back numbers: Full-size reprints of Vols 1–75 (1866–1940) are available from Johnson Reprint Co. Ltd, 24–28 Oval Road, London NW1 7DX. Complete volumes of *Meteorological Magazine* commencing with volume 54 are available on microfilm from University Microfilms International, 18 Bedford Row, London WC1R 4EJ. Information on microfiche issues is available from Kraus Microfiche, Rte 100, Milwood, NY 10546, USA.

ISBN 0 11 727976 5

ISSN 0026–1149

Printed for HER MAJESTY'S STATIONERY OFFICE
Dd 240020 C14 11/87